Proceedings of the Third ENIGMA Meeting

Jerisjärvi, Finland - April 25-28, 2004

The 3rd ENIGMA meeting was organized by Tuorla Observatory team of Leo O. Takalo

The European Network for the Investigation of Galactic nuclei through Multifrequency Analysis (ENIGMA) is a Research Training Network funded within the FP5 program of the European Community

Network Coordinator: Stefan J. Wagner

Final programme

9:00 Leo Takalo: Welcome by LOC
9:10 Stefan Wagner: Status of the Project
9:40 Overview of 0716 ENIGMA campaign
9:50 Gamma/X-ray observations
10:00 Luisa Ostorero: Optical/NIR observations
10:10 Thomas Krichbaum: mm/radio observations

10:20 Coffee

10:50 Niall Smith: Task I - Introduction
11:00 Kari Nilsson: The influence of the host galaxy
11:20 Alan Giltinan: The use of L3CCDs in HTR obs.
11:40 Marcus Hauser: The robotic telescope ATOM

Task II: Intrinsic & Extrinsic IDV

14:10 Introduction (SW)

14: 25 Mirko Tröller: Host galaxies of CSS sources

14:45 Stefano Ciprini: Optical variations of 0735+178

15:05 Luisa Ostorero: Optical IDV in 0716+714

15:20 Thomas Krichbaum : Summary ISS meeting

15:40 Ivan Agudo: Polarimetric monitoring with PV

16:00 Coffee

16:30 Emmanouil Angelakis: Foreground in CBI fields

16:50 Anne Lähteenmäki: AGN variability for Planck

17:10 Task III: HE radiation processes: Introduction

17: 20 Krzysztof Katarzynski: X-ray/TeV correlations

17:40 Dimitrios Emmanoulopoulos: Flares with XTE

18:00 Peter Strub: Determinations of Doppler factors

Tuesday, April 27

Task IV: Variations of source struture and flux

9:00 Silke Britzen: Introduction

9:20 Thomas Krichbaum: The 0716 campaign

9:40 Simone Friedrichs: 0954+65 with space VLBI

10:00 Tuomas Savolainen : VLBA campaign studies

10:20 Task V: Overview (Apostolos Mastichiadis)

10:25 Coffee

10:55 Task VI: Introduction (Gabriele Ghisellini)

11:00 Gabriele Ghisellini: Structured Jets

11:20 Dimitrios Emmanoulopoulos: Beamed TeV jets

Group picture

11:40 Young Researchers Session

Working groups

14:30 Working groups I
High precision photometry
Variability and the sub-mm/mm background

16:00 coffee

16:30 Working groups (ctd.) || Team leaders meeting
The ENIGMA archive

Wednesday, April 28

9:00 Jean-Paul Berhault: Research Training Networks

9:40 Jose Gracia: Jet formation from MHD flows

9:45 Gino Tosti: AO0235+164 campaign update

9:55 Leo Takalo: 3C66A campaign update

10:15 Luisa Ostorero: 0716 campaign update

10:30 Anne Lähteenmäki: Metsähovi campaign studies

10:45 Coffee

11:15 Team leaders session

12:00 Leo Takalo: The CCI time application

Wednesday, April 28

14:30 Young researchers session

15:15 All: Future campaigns,

New Opportunities, and Science Perspectives

16:00 Coffee

16:30 Discussions: WG reports

Working group Blazars & GRBs

Exchange programme of young researchers

The mid-term review meeting

Future network meetings/schools

3rd ENIGMA network meeting

Welcome to Jerisjärvi!

- especially -

Welcome to the new young researchers in the ENIGMA network (Ivan Agudo, Stefano Ciprini, Jose Gracia, Krysztof Kataczynski), bringing the total of young researchers in the network to nine, close to the total - this should be reached by the next meeting.

Welcome to new members

Welcome to Alan Marscher

ENIGMA

E uropean
N etwork for the
I nvestigation of
G alactic nuclei through
M ultifrequency
A nalysis

ENIGMA

One of three Astrophysics Programs in 2nd round

Eight teams from six countries:

(LSW, MPIfR, TU, HUT, OAT, OAB, IASA, CIT)

and several associated teams and members.

Objectives: Training, research, and networking

Added value beyond existing collaborations

http://www.lsw.uni-heidelberg.de/enigma.html

Six scientific themes (sessions 1-6 at this meeting)

Research

- Six topical themes (tasks):
- toward automated, fast, and accurate photometry
- Separating intrinsic and extrinsic intraday variab.
- Variations of source structure and flux.
- Radiation processes at high energies.
- Particle acceleration in MHD outflows.
- The power of jets.

Programme:

- revised revised programme
- the six science themes (talks & discussions)
- workshop (working groups)
- young researchers' session (moving this?)
- team leaders' session
- past, ongoing, and future campaigns
- scientific strategies

Status of ENIGMA

- 9 / 12 young researchers hired
- 3 / 8 network meetings organized
- 1 / 2 schools held
- 1st year report pending
- 4 / n (n >> 4) papers written
- 4 campaigns finished
- 3 campaigns ongoing
- 12000 hits (webpage) [improving]

To be done:

Training:

implementing secondments

Research:

getting the most out of campaigns

focus future campaigns on science questions

be creative

Networking:

linking activities in different teams

talks & discussion !

working-group activities

sharpening the profile of science themes

The ENIGMA campaign on 0716+714

Main motivations:

Understand high-energy radiation mechanisms

Test unconventional ideas concerning IDV

Investigate intrinsic/extrinsic variability

Search for fast structural variations

Set-Up (campaign and results)

INTEGRAL pointing (November 2003)
Organized MWL campaign
(cm, mm, sub-mm, IR, opt., X-ray, gamma-rays)

Bright phase – early start
campaign proper
extended bright state – extended campaign
TOO trigger of XTE observations
TOO trigger of additional INTEGRAL time

Set-Up (campaign and results)

Several talks will present first results.

To get an overview and put these results into perspective we will start with three short introductions:

Gamma-ray/X-rays (SW)
optical/IR (Luisa Ostorero)
mm/radio (Thomas Krichbaum)

Gamma-ray observations

INTEGRAL AO1 proposal

original proposal 1 Msec on 0716+714/0836+71
500 ksec granted (A/B)
largest open time proposal on AGN (cf. HDF)
amalgamated with Mrk 3 proposal

SPI not available
ENIGMA campaign

Additional HE observations

November 2003: MAGIC none (not ready)

High state (2004):
TOO trigger with XTE (PCA)

TOO trigger of AO2 proposal (Pian et al.)
trigger delayed wrt to optical outburst.
Meeting extended campaign

Gamma-ray observations

VERY late data delivery (03/04)

OSM data taken
JEM-X monitoring data taken
IBIS data taken
no analysis to date -
to be continued at next meeting.

ENIGMA CAMPAIGN ON S5 0716+71:

UPDATE ON OPTICAL-NIR OBSERVATIONS

Luisa Ostorero(*) & Stefan Wagner(*)

on behalf of the 0716 optical-IR collaboration

(*) Landessternwarte Heidelberg, Germany

3rd ENIGMA Meeting - Jerisjärvi (Finland), April 26-28, 2004

Organization of the optical-infrared campaign

- ***INTEGRAL pointing*** ***Nov 10 – Nov 18, 2003***
- ***Core campaign:*** ***Nov 06 - Nov 20***
- ***Extended campaign:*** ***Oct 08 - Nov 05 ; Nov 20 - Dec 20***
- ***Further extension:*** ***Until the end of May 2004***

Telescopes involved

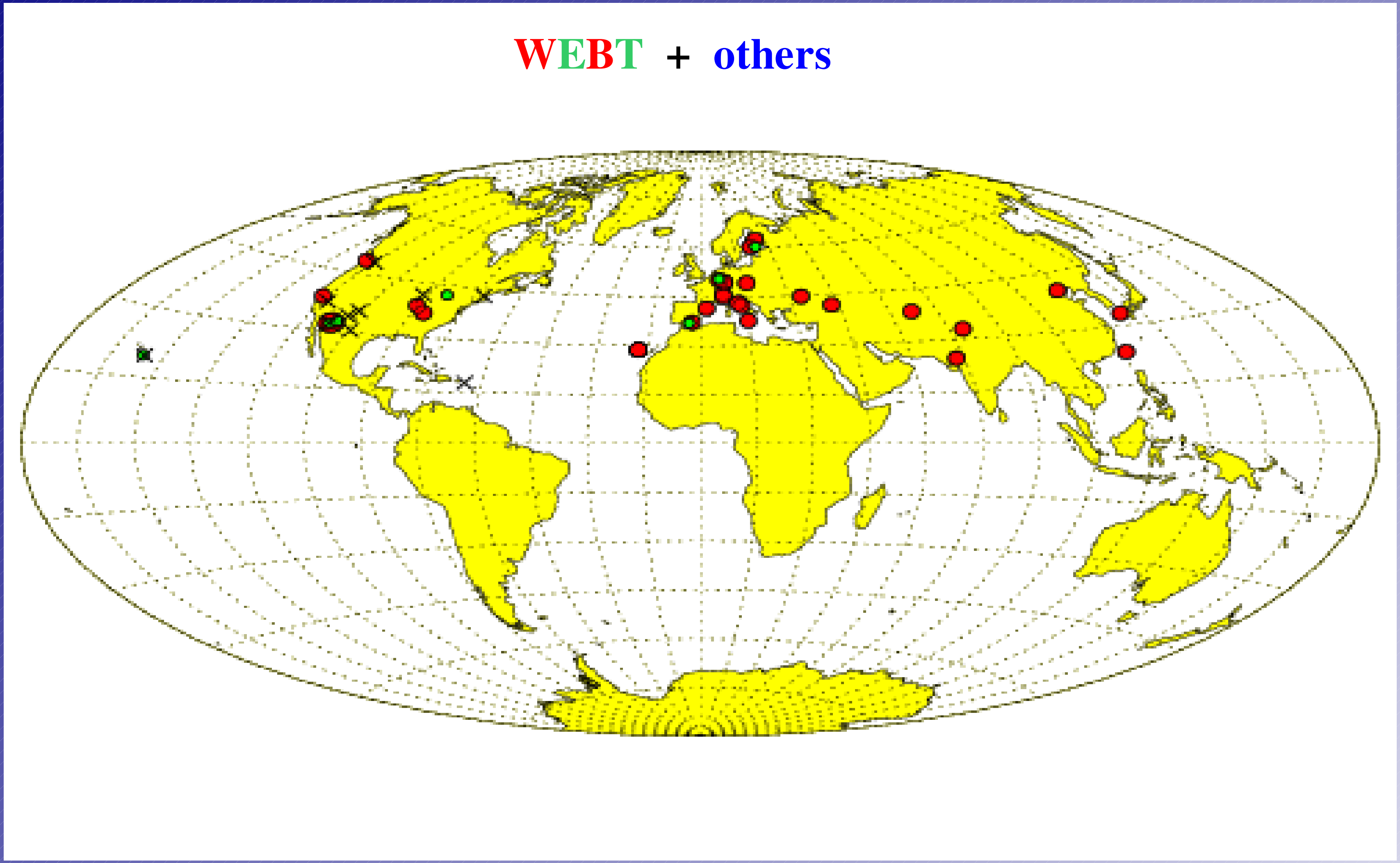

● Optical/IR telescopes (34; 28 cm – 2.5 m)
● Radio/mm/submm telescopes (8)
X VLBA antennas

lon = -123.22   128.46

http://www.lsw.uni-heidelberg.de/users/lostorer/0716-nov2003.html

Optical-NIR Telescope list (W ⇒E)

W

Lon	*Lat*	*Tel.*	*(Observers)*
-123.22	+48.25	CL	Climenhaga Observatory, Victoria, Canada (Robb)
-121.5	+38.38	CH	Coyote Hill, California, USA (Pullen)
-111.615	+31.9533	RCT	Arizona, USA (Mattox)
-111.6	+35.3	LO	Lowell, Arizona, USA (?) (Carini)
-111.5947	+31.7862	WY	WYIN , Kitt Peak, Arizona, USA (Rector)
-110.7908	+32.2674	ML	Mt. Lemmon, Arizona (Sohn,...)
-90.30833	+38.70555	SL	St Louis, Schwartz Obs., Missouri (Wilking,Tartar)
-86.6111	+36.9197	BE	Bell Farm, Kentucky (Carini)
-17.8761	+28.7594	ULT	ULTRACAM- La Palma, Spain (Smith,...)
-17.8761	+28.7594	KVA	La Palma, Spain (Takalo,Nilsson,Lindfors)
-17.8761	+28.7594	NOT	La Palma, Spain (Pursimo)
-2.54625	+37.2236	CA	Calar Alto, Spain (Kurtanidze)
+2.0914	+41.5511	SA	Agrupacio Astronomica de Sabadell, Spain (Ros)
+6.85	+50.1633	HL	Hoher List , Bonn, Germany (Bach,...)
+7.775	+45.038	TO	Torino, Italy (Villata, Crapanzano)
+7.79167	+45.9844	TI	TIRGO, Gornergrat, Switzerland (Tozzi)
+8.4114	+49.7356	TR	Trebur, Germany (Ohlert)
+8.7210	+49.3986	HD	Heidelberg, Germany (Strub,Hauser,Ostorero,Tapken,Kachel, Emmanoulopolous)

E

Optical-NIR Telescope list (W ⇒E)

Lon	*Lat*	*Tel. (Observers)*	
+12.3916	+43.1122	PG	Perugia, Italy (Tosti,Ciprini,Nucciarelli)
+13.5625	+ 42.2285	CI	Campo Imperatore, Italy (Larionov)
+14.973	+37.692	CT	Catania, Italy (Frasca,...)
+16.58394	+49.204139	MB	MonteBoo, Czech Republic (Hroch,...)
+22.17	+60.27	TU	Tuorla, Finland (Takalo,Lindfors,Nilsson,...)
+25.5130	+62.34233	NY	Nyrölä, Finland (Oksanen)
+29.996944	+62.7275	JA	Jakokoski, Finland (Pääkkönen,Karppanen,Itkonen)
+34.0125	+44.7266	CR	Crimean Obs., Ukraine, FSU (Larionov,....)
+42.8	+41.8	AB	Abastumani, Georgia (Kurtanidze, Nikolashvili)
+66.8964	+38.6733	MD	Mt. Maidanak, Uzbekistan, FSU (Ibrahimov)
+72.71	+24.6	ABU	GIRT, Mt. Abu, India (Baliyan)
+78.95	+32.7833	HA	Himalayan Chandra Tel.Hanle, Ladakh, India (Shastri, Baliyan)
+117.5750	+40.3933	XI	Xinglong station, China, 2 tel. (Peng, Jiang)
+120.8736	+23.4686	LU	Lulin Observatory, Taiwan (Chen,...)
+128.4576	+32.9344	SO	Mt Sobaek, Korea (Sohn,....)

W

E

Data reduction

- ***When possible: collected reduced frames***

- ***When not possible: data collected as instrumental mags of the source and comparison stars***
  --> application of the same analysis and calibration procedures to all datasets

Suggested data format:

JD-2452000	0716+71	1	2	....
950.62357	13.042 0.004	10.630 0.001	11.121 0.002	....

http://www.lsw.uni-heidelberg.de/users/lostorer/0716-nov2003.html

Rc band:

~2900 frames collected up to now for Nov 2003

W

NOV-R	1	2	3	4	5	6	7	8	9	10	11	12	13	14	15	16	17	18	19	20	21	22	23	24	25	26	27	28	29	30
CL																				117										
CH											73																			
RCT															2	3	14													
LO																														
WY																														
ML																														
ST																			3											
BE																				3				3						
ULT																														
KVA										12		5	7				24	10									6			
CA												141	111	172																
SAB																														
HL										24			18																	
TO	2	4	2							1							17	2												
TR				-30	-20	-25				-10			-10																	
HD						74	61						30		33					110										
PG			1		3	1				2	2		1	1															1	1
CI																														
CT																														
MB											22	40																		
TU								63				39																		
NY																														
CO			1			2								1									1		2				21	
AB			139	140	109	181					49		10		189	110	20					176	151	30			2		4	
MD																		2					5			5	5			
ABU																														
HA												*	*	*																
XI-n																														
XI								6J																						
LU										44	3	17	11	55			12	11												
SO																														

⇓

E

INTEGRAL POINTING (Nov 10-17,2003)

Preliminary optical light curves

- o *Catania (Italy)*
- o *Perugia (Italy)*
- o *Nyrola (Finland)*
- o *Torino (Italy)*
- * *Sabadell (Spain)*
- o *Mt Boo (Czech Rep.)*
- o *KVA (La Palma)*
- ◊ *Tuorla*
- ◊ *NOT (La Palma)*
- ◊ *Lulin (Taiwan)*
- ◊ *Coyote Hill (California)*

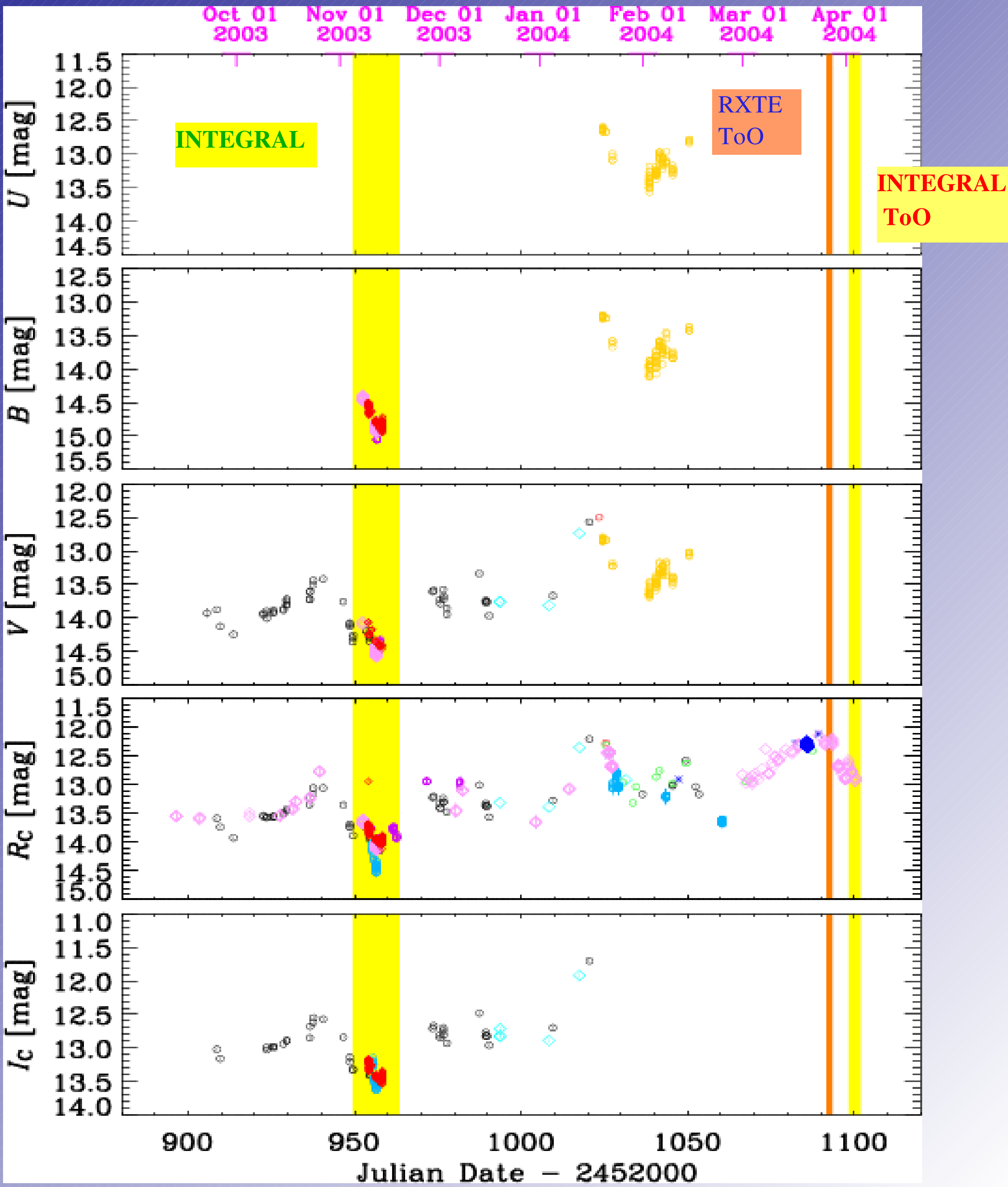

Some Calibrated datasets...

Optical (B band) - photometer

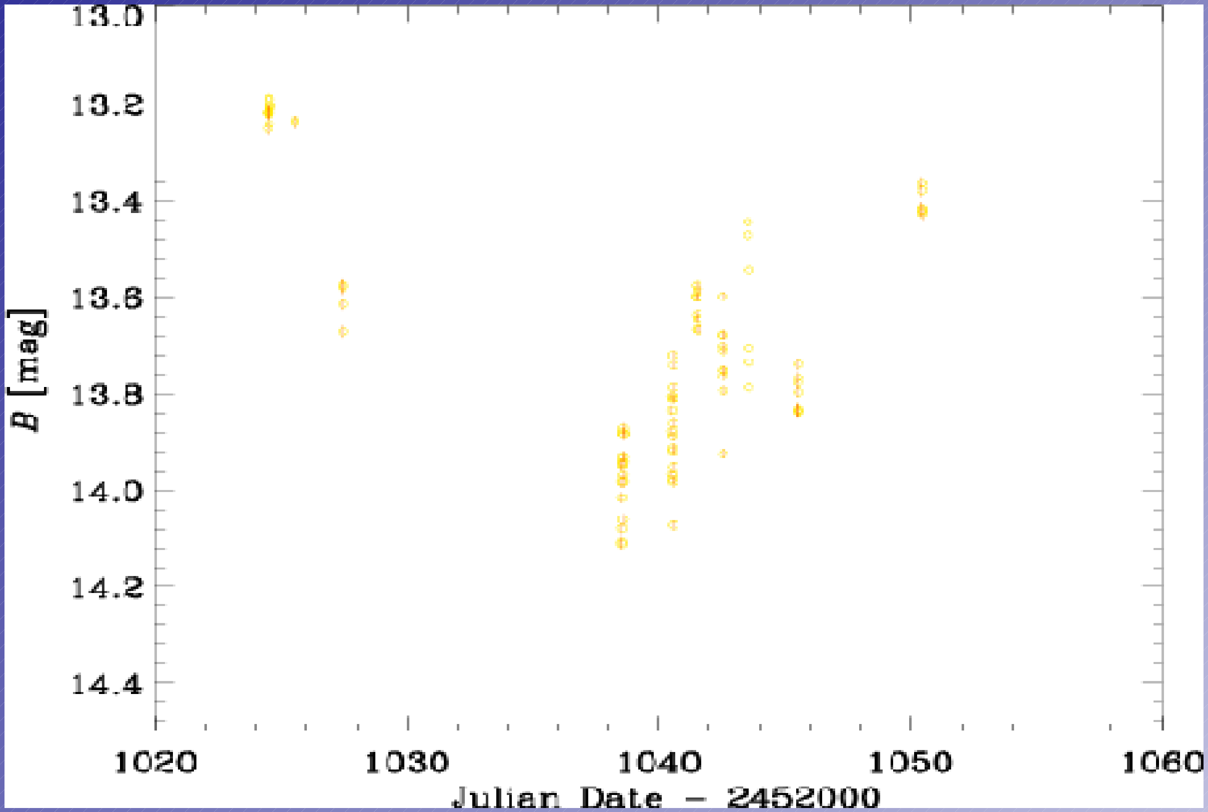

Data by A.Frasca (Catania Observatory, Italy)

...No instrumental mags available

Some Calibrated datasets...

Optical (B band), intranight - photometer

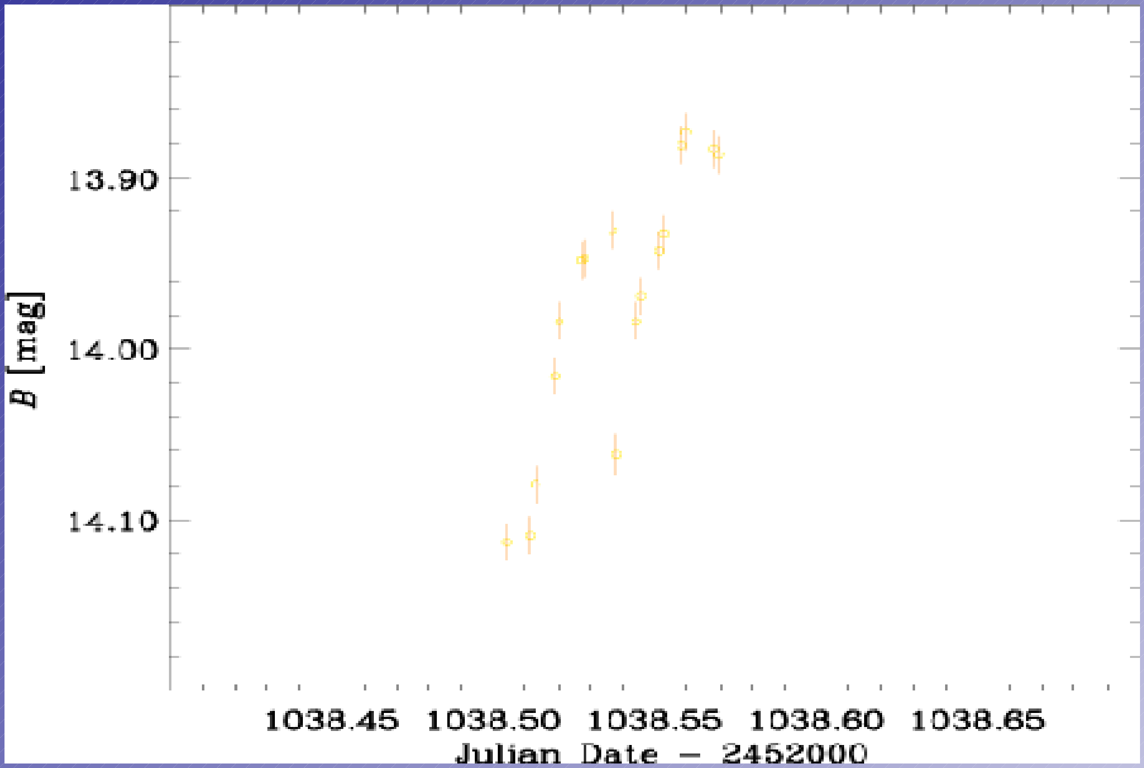

Data by A.Frasca (Catania Observatory, Italy)

...No instrumental mags available

Some Calibrated datasets...

Optical (Rc) obs. during the historical maximum of S5 0716+71 (March 2004) and the RXTE and INTEGRAL ToOs

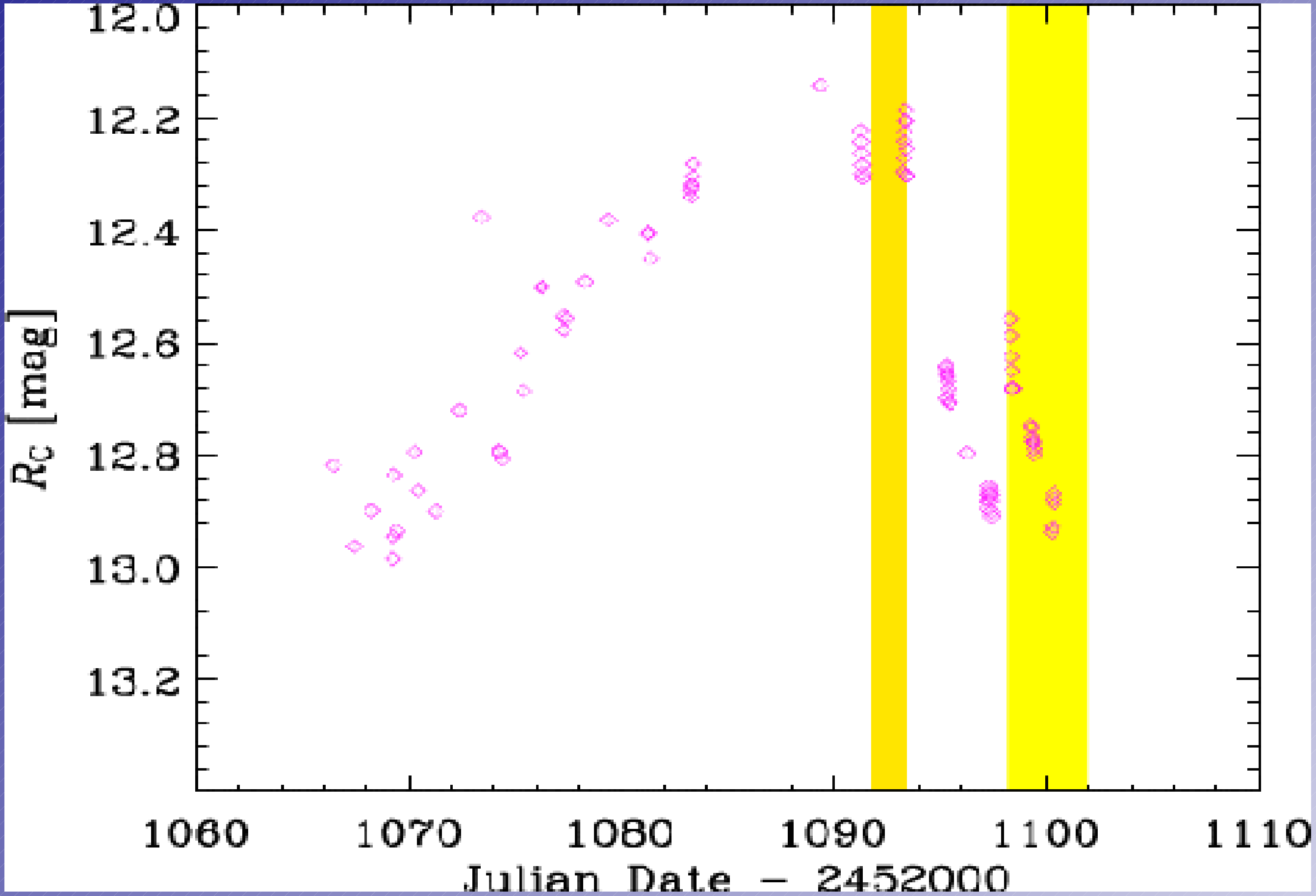

Data by Kari Nilsson (Tuorla Observatory, Finland)

...Instrumental mags available

Some Calibrated datasets...

Zoom (INTEGRAL ToO)

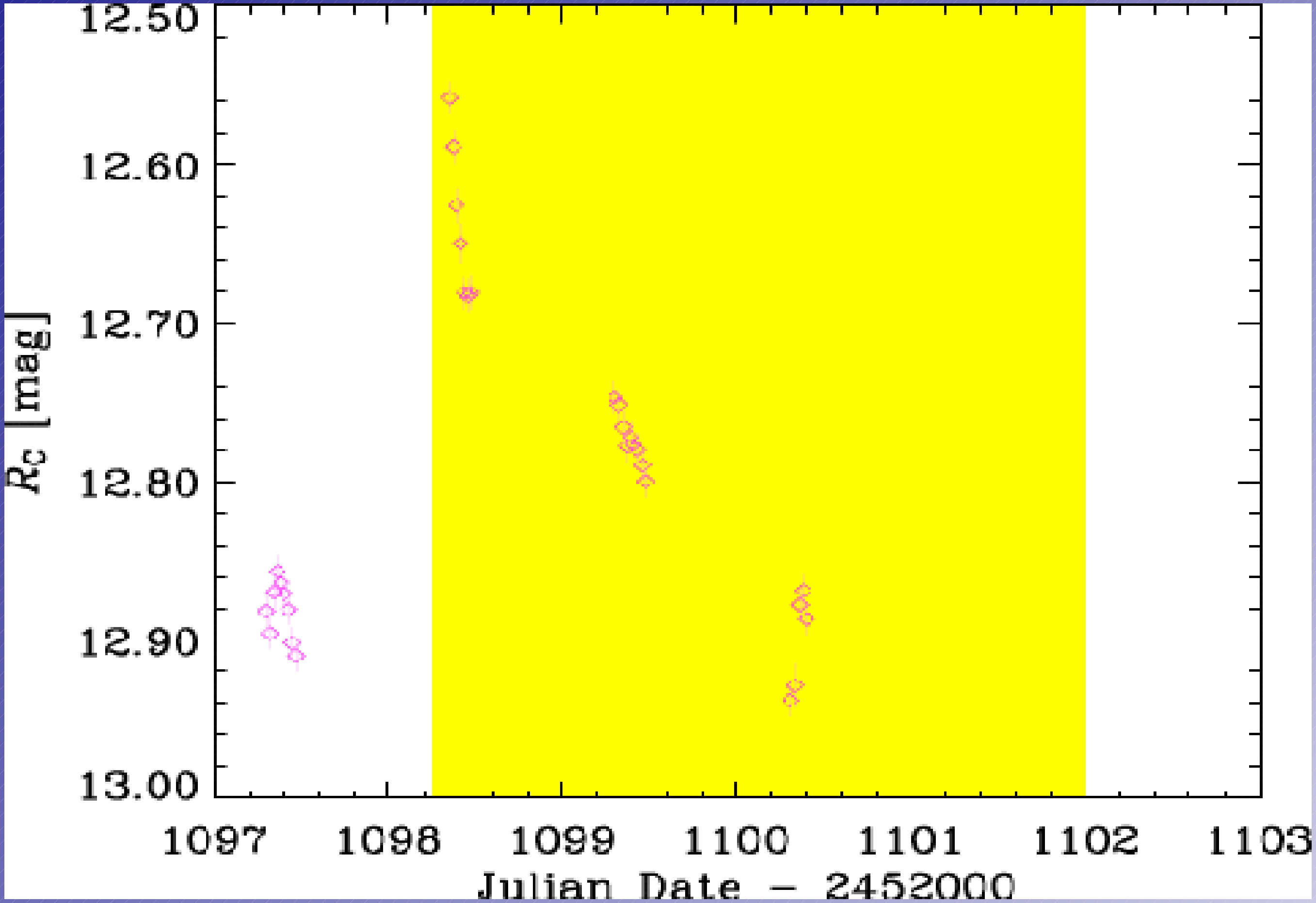

Data by Kari Nilsson (Tuorla Observatory, Finland)

...Instrumental mags available

Many uncalibrated datasets...

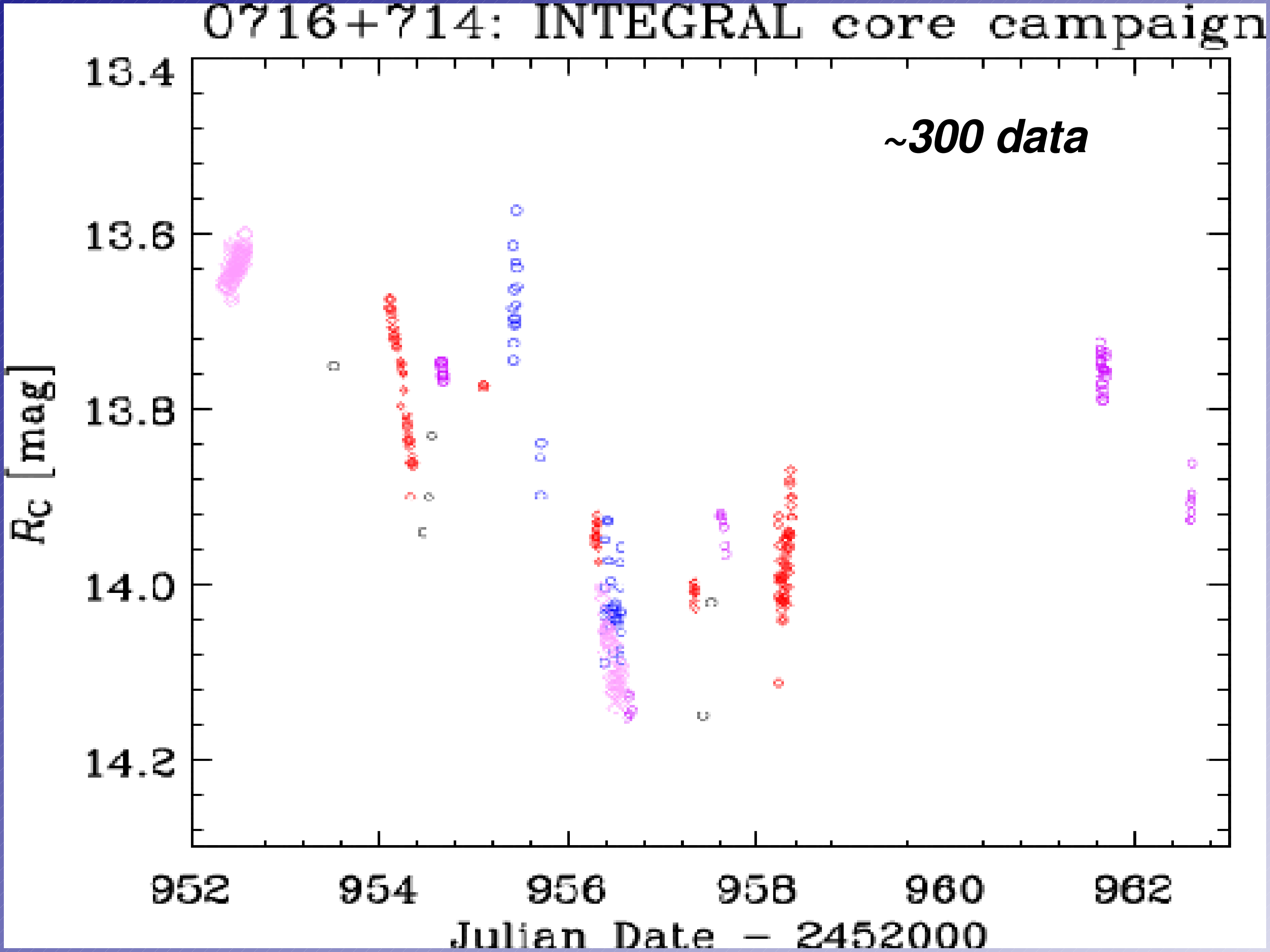

Expected >3000 Rc data points for the core campaign (Nov 06-20)

Calibrations - I

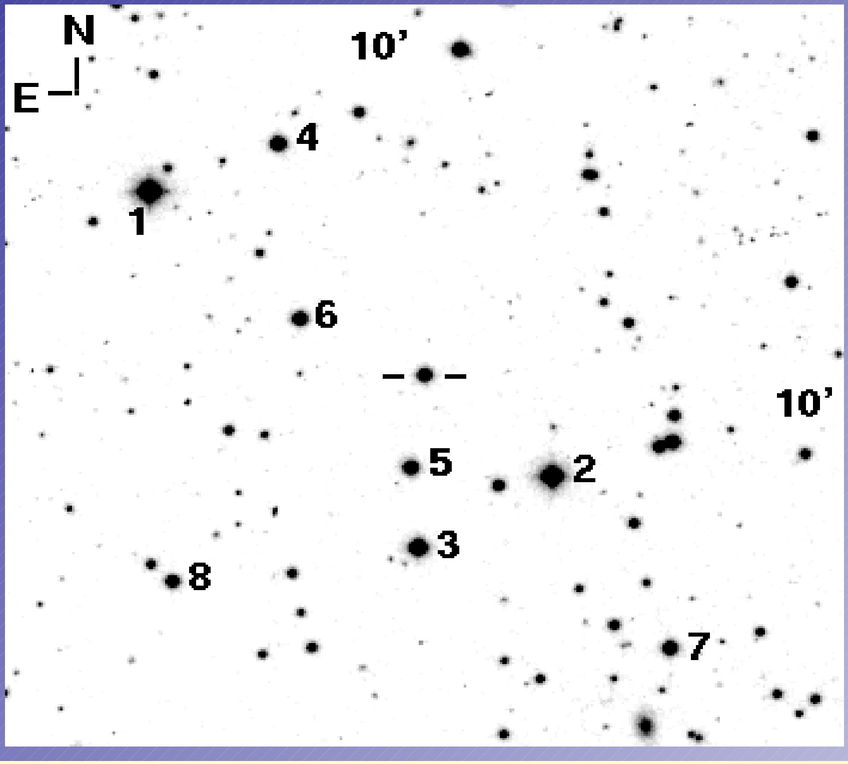

Star	U	B	V	R	I
1	--	11.54 (0.01)	10.99 (0.02)	10.63 (0.01)	--
2	12.089 (0.005)	12.02 (0.01)	11.46 (0.01)	11.12 (0.01)	10.92 (0.04)
3	13.199 (0.007)	13.04 (0.01)	12.43 (0.02)	12.06 (0.01)	11.79 (0.05)
4	13.629 (0.006)	13.66 (0.01)	13.19 (0.02)	12.89 (0.01)	12.656 (0.001)
5	14.246 (0.003)	14.15 (0.01)	13.55 (0.02)	13.18 (0.01)	12.85 (0.05)
6	14.360 (0.004)	14.24 (0.01)	13.63 (0.02)	13.26 (0.01)	12.79 (0.04)
7	15.002 (0.021)	14.55 (0.01)	13.74 (0.02)	13.32 (0.01)	13.306 (0.038)
8	14.804 (0.004)	14.70 (0.01)	14.10 (0.02)	13.79 (0.01)	13.419 (0.007)

B,V,R Villata et al., 1998, A&AS, 130, 305
I Ghisellini et al., 1997, A&A, 327, 61
U,I Gonzáles-Pérez et al. 2001, AJ, 122, 2055

Calibrations - II

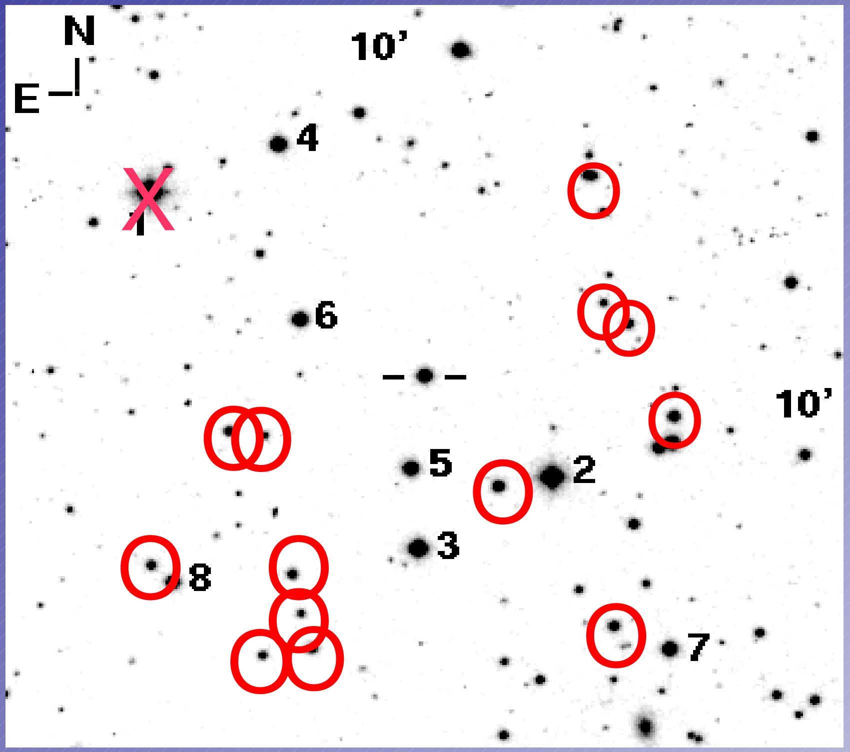

Gonzáles-Pérez et al. 2001, AJ, 122, 2055

20 comparison stars (13 new):

* Field "not well observed" by the authors
* Agreement: 2-3 % with Villata et al. 1998

Any suggestions?

Future work

- ***Assembling the total optical light curve***
    - *Analysis of the optical frames*
    - *Calibration of the reduced datasets*
    - *Determination of the offsets between different datasets*
- ***Analysis of the INTEGRAL data***
- ***Data availability within the ENIGMA Network***
    - *Proper data format for the archive:*

      JD, instrumental mags & errors / calibrated mags & errors (procedure, offset table?) / fluxes & errors (procedure?)...
    - *Definition of a data publication policy*

A broad band flux density monitoring of 0716+714 -

Data and first Results

T.P. Krichbaum on behalf of the observing teams

Max-Planck-Institut für Radioastronomie, Bonn, Germany

tkrichbaum@mpifr-bonn.mpg.de

Involved Scientists at MPIfR:

I. Agudo, M. Angelakis, U. Bach, T. Beckert, S. Britzen,

S. Friedrichs, L. Fuhrmann, V. Impellizzeri,

M. Kadler, J. Klare, E. Körding, A. Kraus, T.P. Krichbaum,

A. Pagels, B.W. Sohn, A. Witzel, J.A. Zensus

Partners:

most participants in this workshop, plus

H. Ungerechts, M. Grewing (IRAM)

A. Apponi, B. Vila-Vilaro, P. Strittmatter, L. Ziurys (Steward Obs.)

R. Strom (ASTRON)

H. Teräsranta (Metsähovi)

H. & M. Aller (Michigan)

Participating observatories

Radio:

Effelsberg (5 GHz I+P, 10.7 GHz I+P, 32 GHz I),

Michigan (5, 8, 15 GHz, I+P)

Westerbork (1.4 & 2.2 GHz, I),

Metsähovi (22 & 37 GHz, I)

VLBA (6 x 8 hrs, 1.6 - 43 GHz, dual pol.)

Millimeter:

Pico Veleta (90 & 230 GHz), Kitt Peak (90 GHz),

Heinrich-Hertz (345 GHz), JCMT (345 GHz, Merja)

Optical: WEBT (more than 30 optical telescopes)

High Energies: INTEGRAL (optical, X-ray, Gamma-ray)

The Jet of the BL Lac S5 0716+714

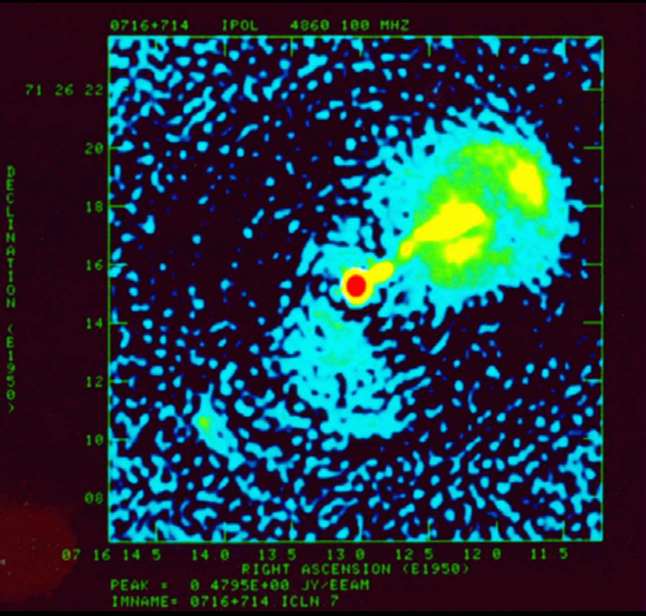

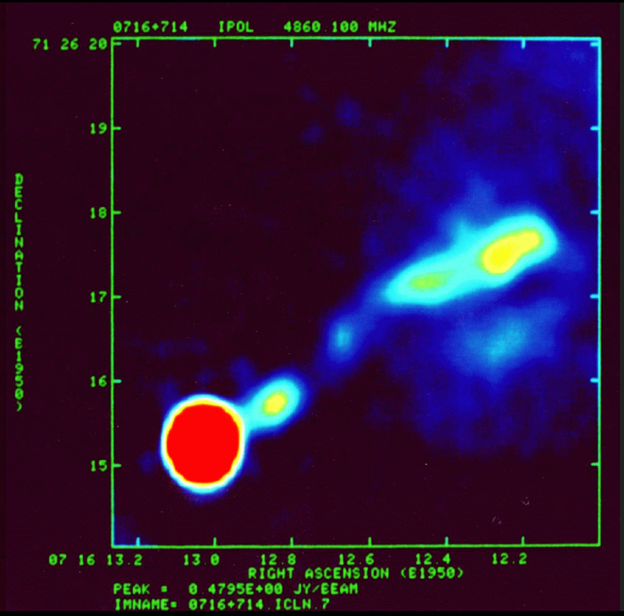

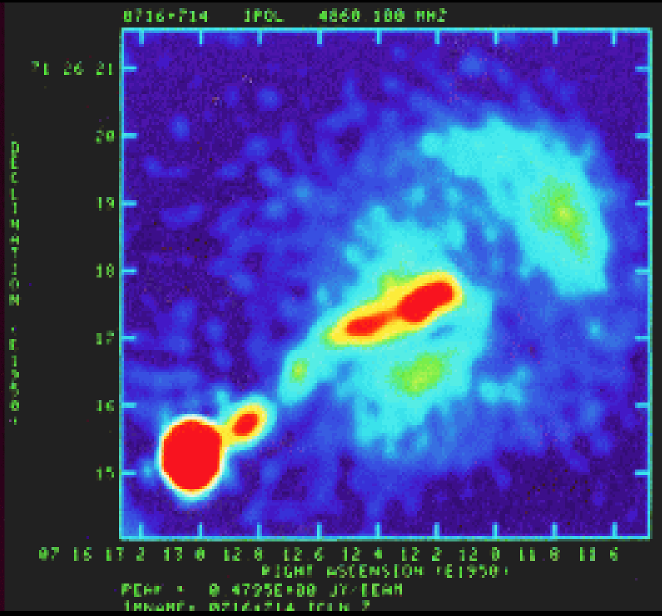

Slow

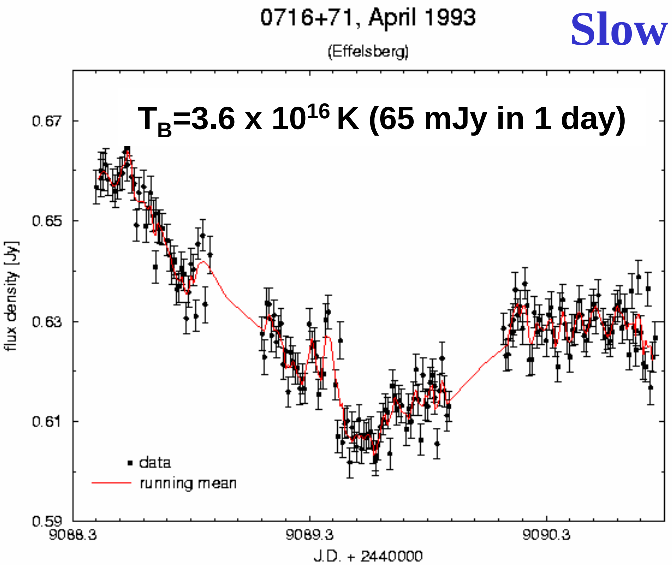

Fast

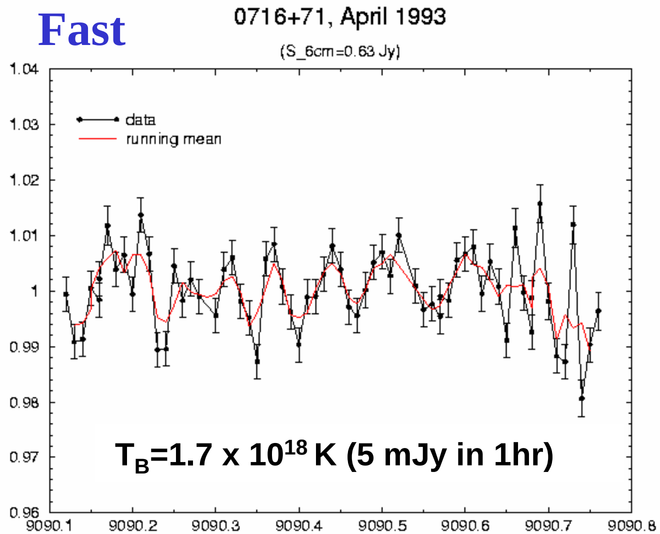

IDV in 0716+714

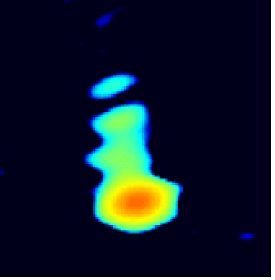

0716+714 on different scales

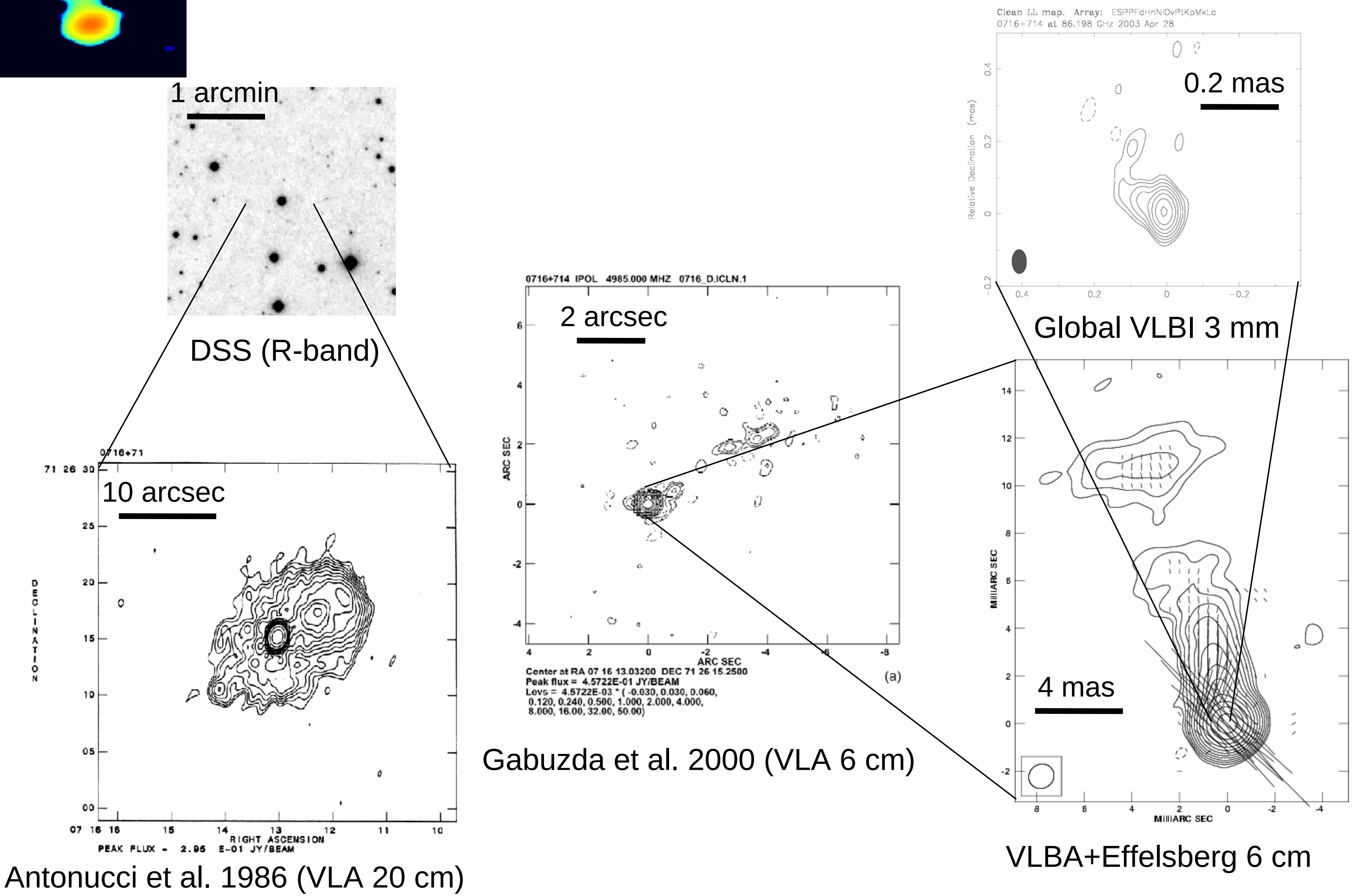

XMM-Newton observations of 0716+714

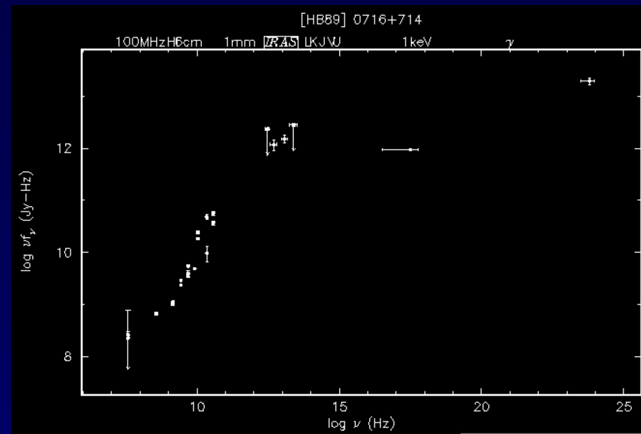

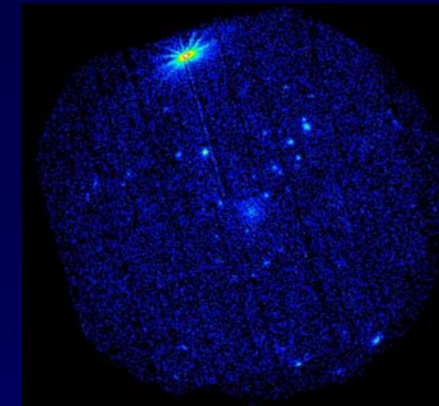

- Two distinct spectral components (synchrotron, IC)
- Tentative Iron K α line detection: z = 0.1 (blue shifted or distance measure?)

- Pronounced and rapid (500 sec) X-ray variability in March 2002
- Soft Lag of ~150s
  ⇒ Cooling

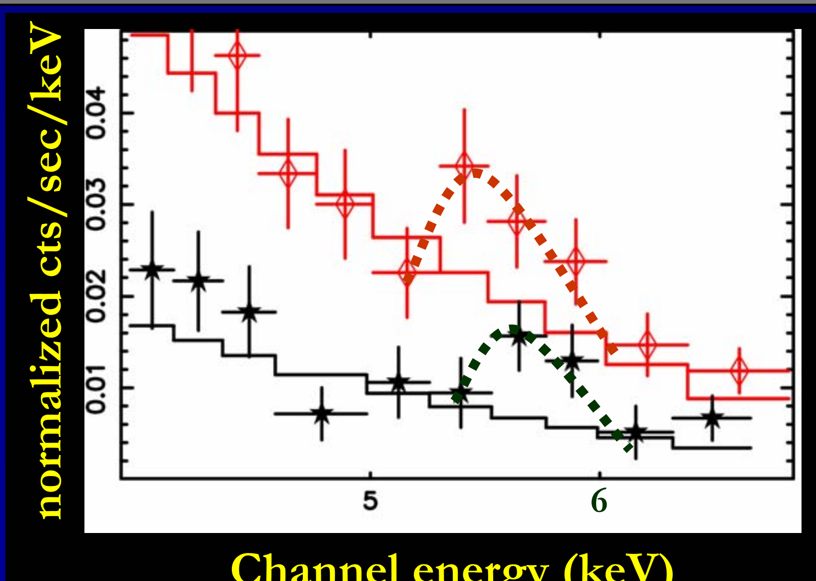

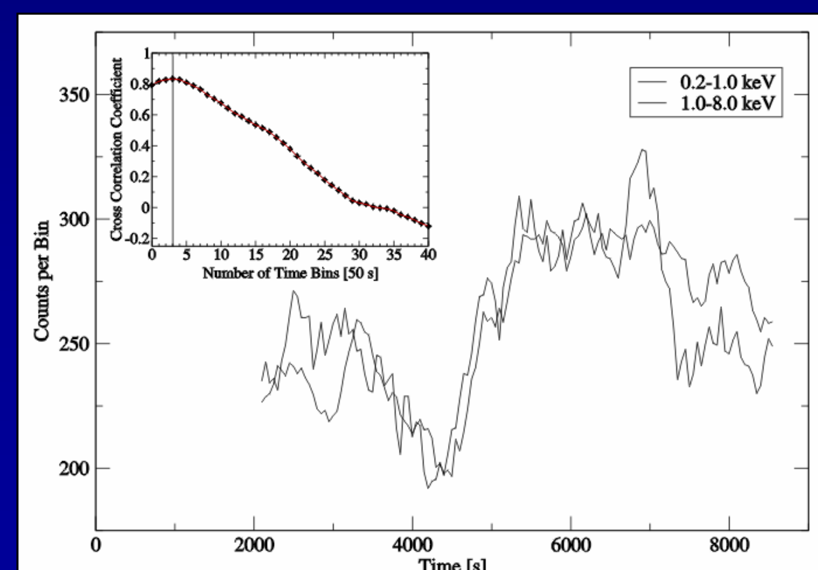

Kadler, Kerp, & Krichbaum 2004, A&A, submitted

0716+714 – A Hard Nut to Crack

Improved knowledge on kinematics:

Witzel et al. (1988), Gabuzda et al. (1998):	Subluminal source
Jorstad et al. (2001):	0.9-1.2 mas/yr
Bach et al. (2003)	0.3-0.9 mas/yr
Kellermann et al. (2004, ApJ, in press):	~0.5 or ~0.3 mas/yr

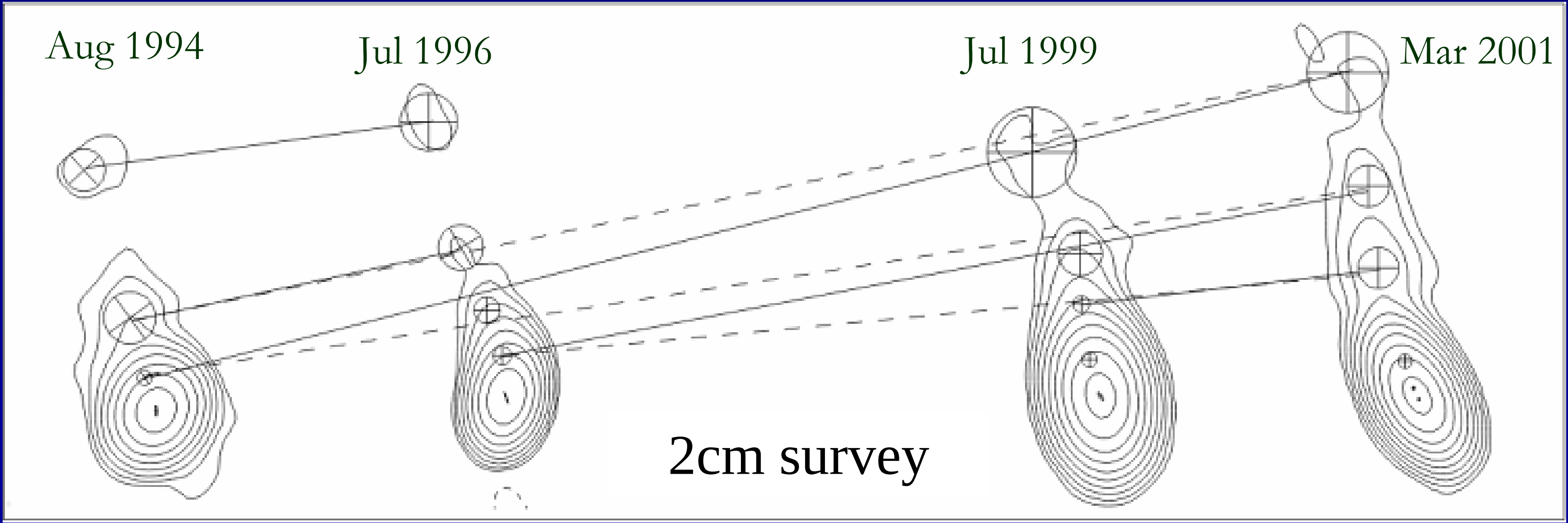

0716+714: 10 yrs of VLBI monitoring

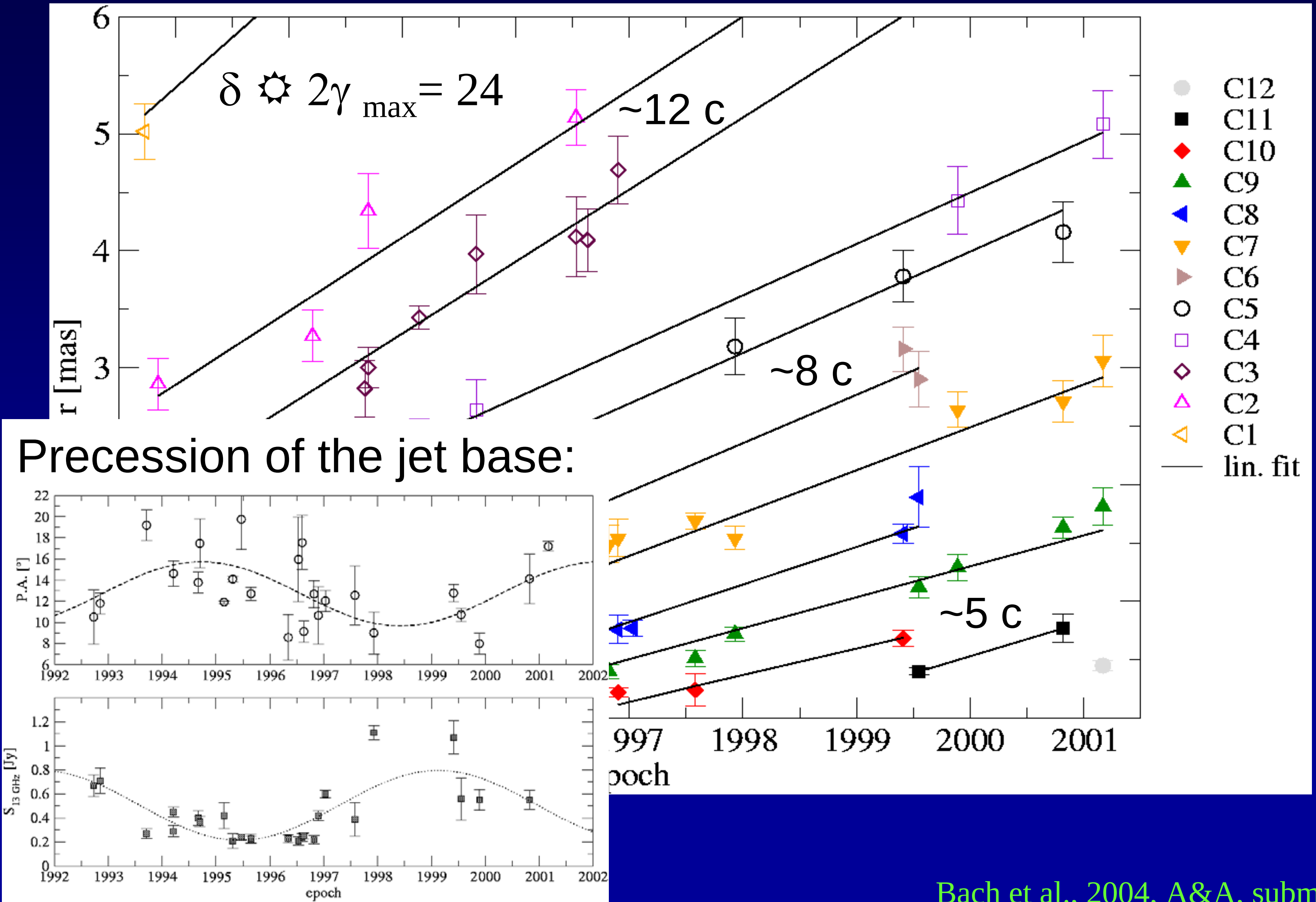

Bach et al., 2004, A&A, submitted

New 7mm and 3mm maps of 0716+714

On 0.2 mas scales the jet direction is misaligned with mas-jet

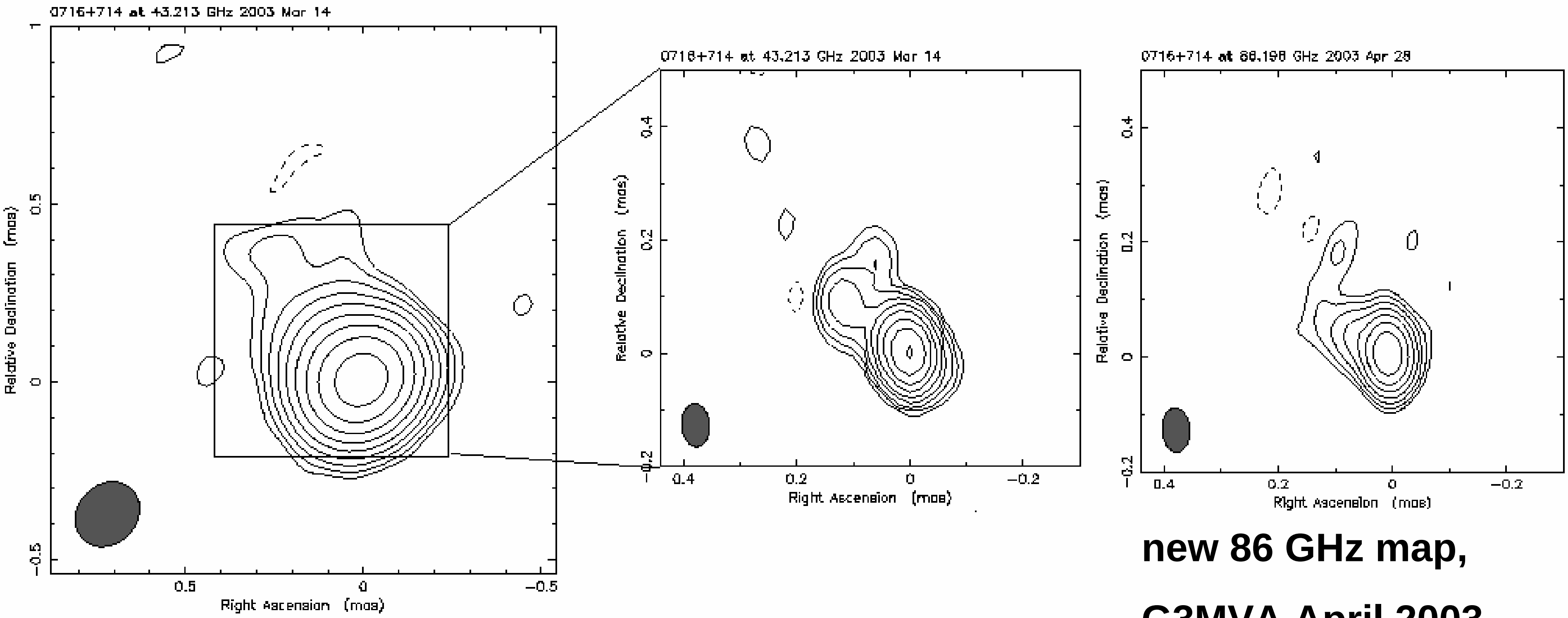

new 86 GHz map,

G3MVA April 2003

U. Bach et al.

Polarisation and total Intensity are strongly correlated

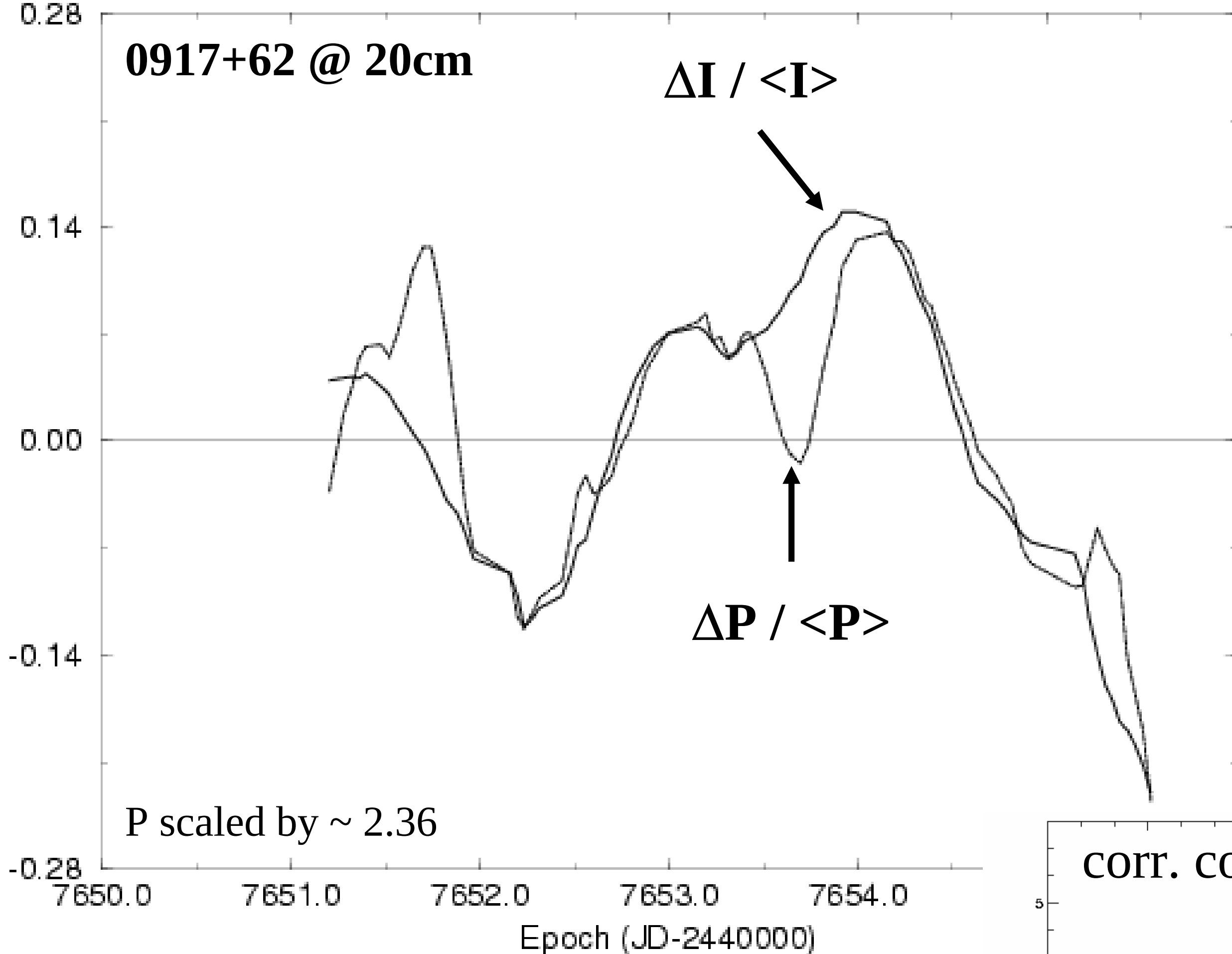

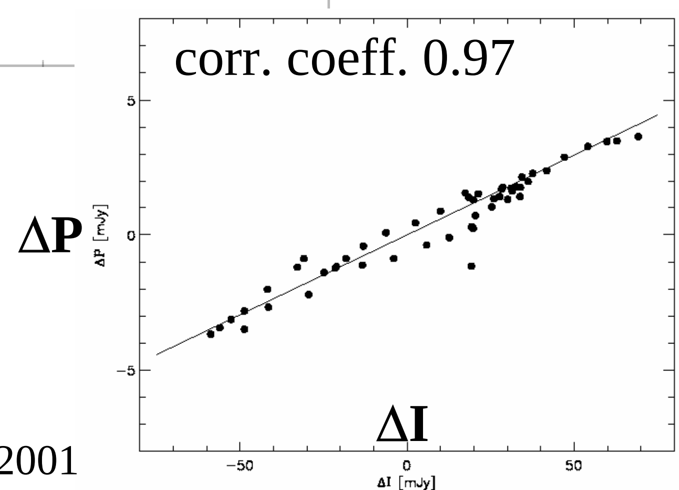

This proportionality implies that RISS might be at work. At shorter wavelength, however, we see correlations and anti-correlations between I & P !

Qian et al. 2001

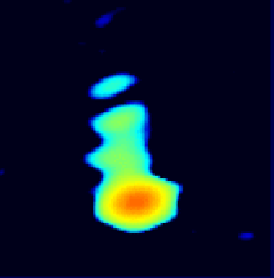

Space-VLBI of 0716+714

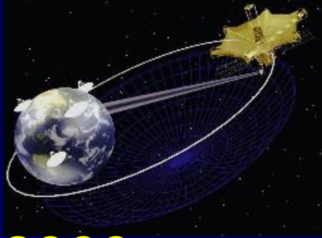

29. Sep. 2000 4. Oct. 2000 5. Oct. 2000

I

P

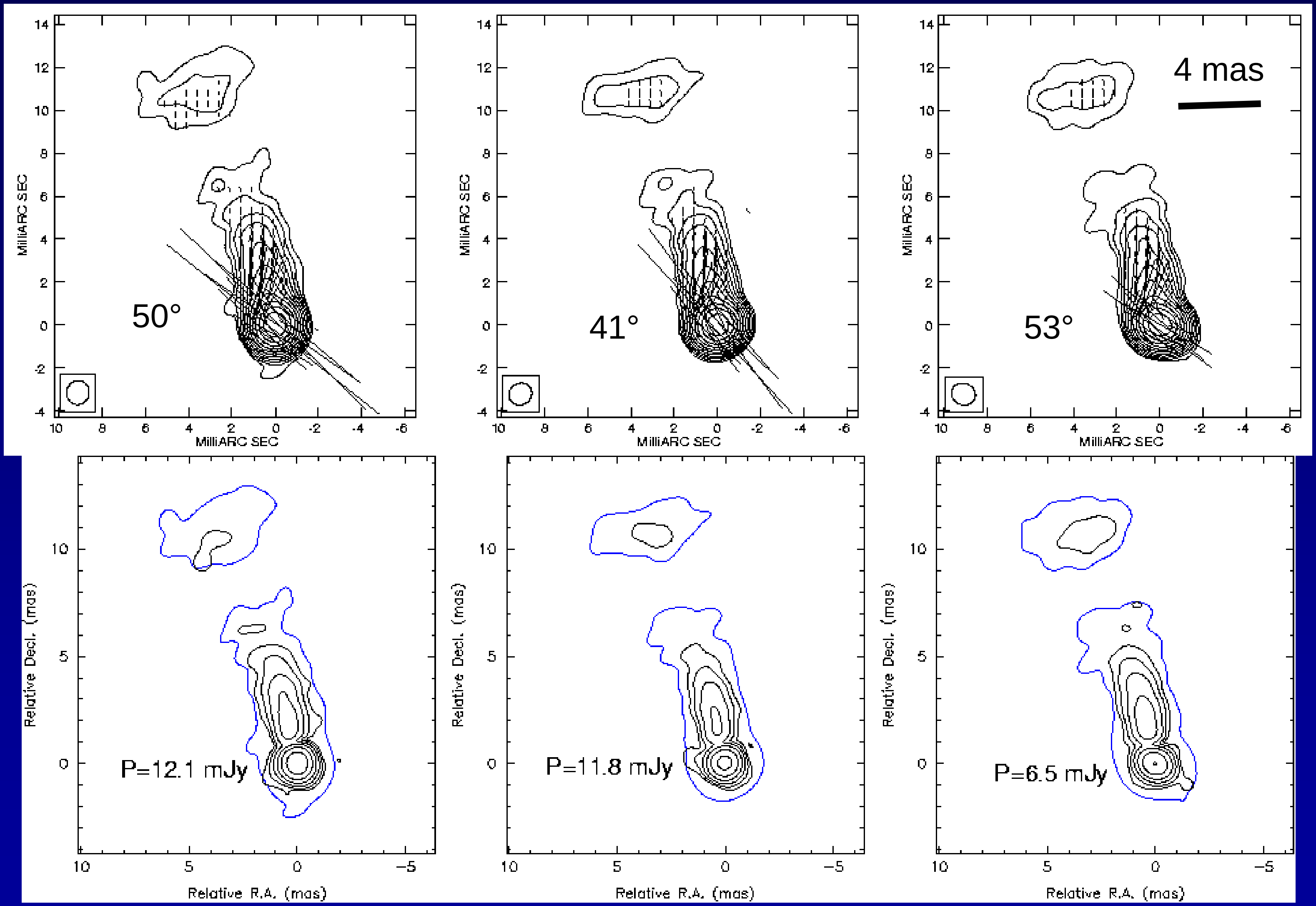

Bach et al., 2004

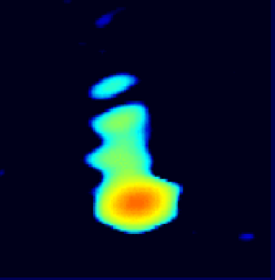

Intraday Variations of the VLBI core

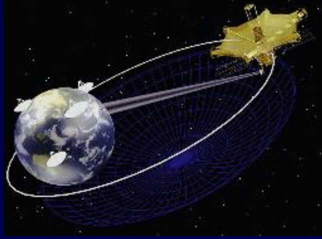

Array	Part	I [mJy]	P [mJy]	χ [°]
		29 Sep 2000		
VLBI	Core	520.3 ± 26.9	12.1 ± 1.3	49.4 ± 4.1
	Jet	56.0 ± 4.7	7.4 ± 0.8	-10.8 ± 5.6
Eb		763.2 ± 6.9	21.4 ± 2.6	23.4 ± 2.1
		4 Oct 2000		
VLBI	Core	499.3 ± 26.1	11.8 ± 1.3	40.7 ± 4.0
	Jet	54.8 ± 6.3	7.3 ± 0.8	-11.2 ± 7.8
Eb		735.7 ± 16.2	21.6 ± 2.6	18.6 ± 2.2
		5 Oct 2000		
VLBI	Core	503.9 ± 25.4	6.5 ± 1.1	52.7 ± 5.2
	Jet	54.7 ± 6.0	7.5 ± 0.8	-9.5 ± 7.4
Eb		740.2 ± 14.6	15.7 ± 1.1	13.3 ± 2.5

Bach et al., 2004

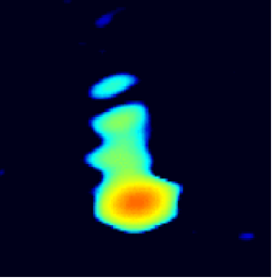

Variability on October 4

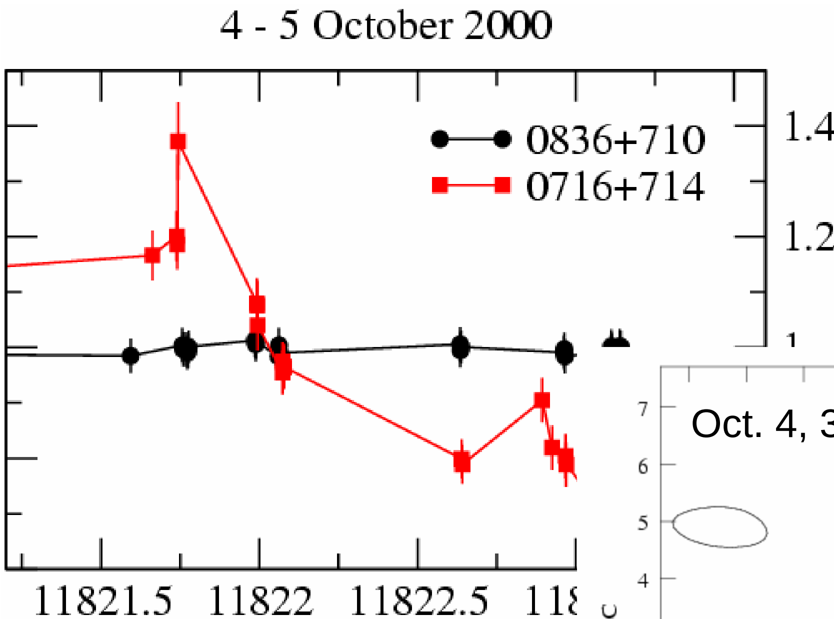

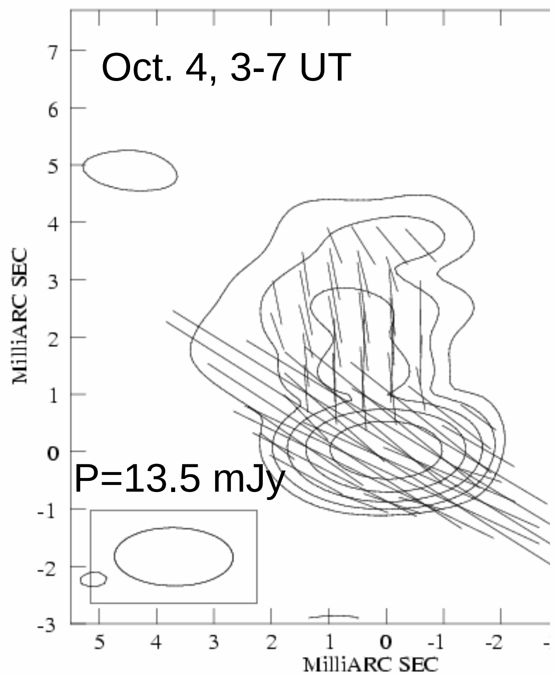

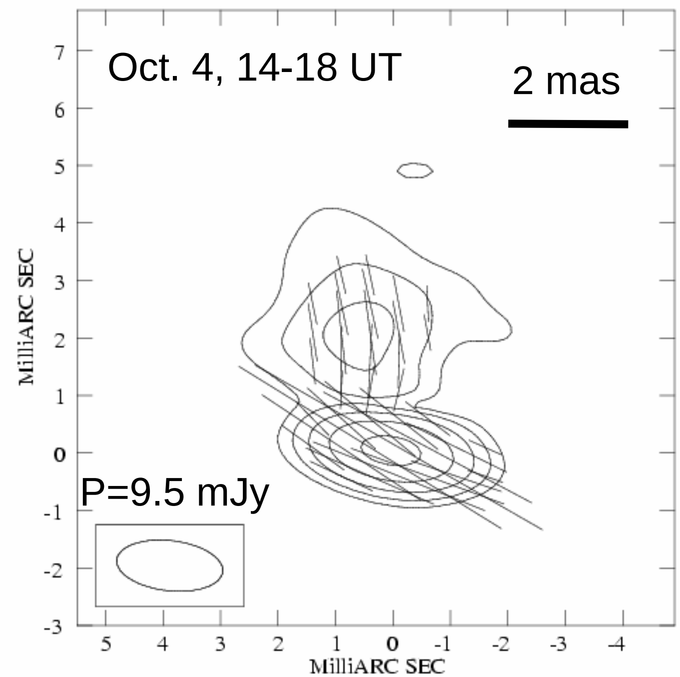

Bach et al., 2004

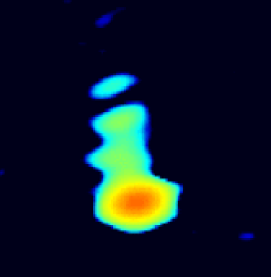

Brightness Temperature

$$T_{\rm b} = 1.86 \times 10^4 \; S \; \left(\frac{d_{\rm L}}{\nu \; t_\nu \; (1+z)^2} \right)^2$$

with

$$t_\nu = \frac{<S>}{\Delta S} \frac{\Delta t}{(1+z)},$$

- Between October 4th and 5th ($<S> = 10.2\,$mJy, $\Delta S = 3.2\,$mJy and $\Delta t = 24\,$h $= 0.0027\,$yr):

$$T_{\rm b} \approx \mathbf{3} \times \mathbf{10^{15}}\,\mathrm{K}.$$

- On October 4th ($<S> = 11.5\,$mJy, $\Delta S = 2.8\,$mJy and $\Delta t = 10\,$h $= 0.0011\,$yr):

$$T_{\rm b} \approx \mathbf{10^{16}}\,\mathrm{K},$$

- Doppler factor of 14 to 22 are needed to reduce these values to the inverse-Compton limit of $10^{12}\,$K.

A coordinated multi-frequency flux monitoring campaign of 0716+714 (INTEGRAL + ground telescopes)

Nov. 11 – 18 , 2003

(500 ksec)

OMC V-band

JEM-X 3 – 35 keV

IBIS 15 keV – 10 MeV

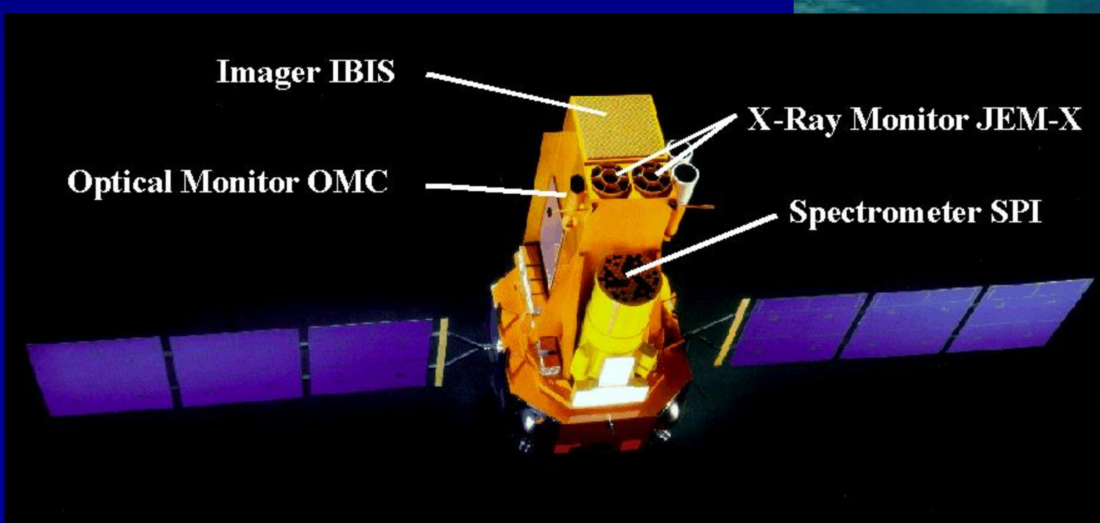

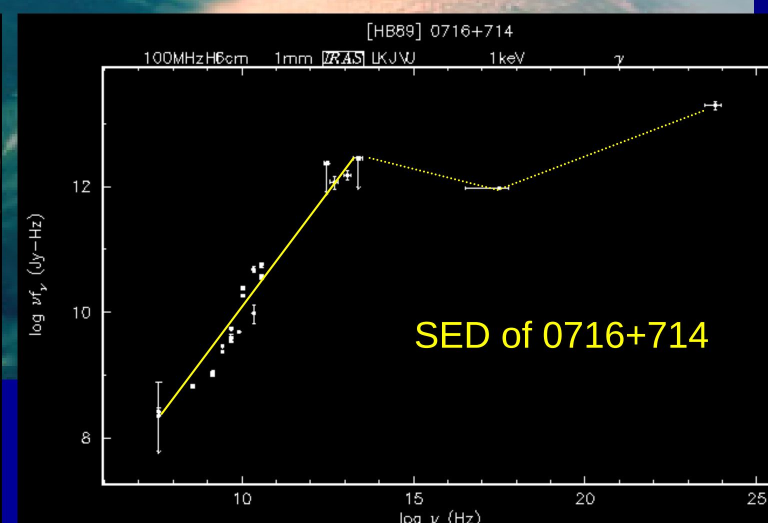

Motivation for the INTEGRAL campaign

- disentangle between extrinsic and source intrinsic contributions to IDV
- violation of IC limit in radio bands should cause enhanced X-ray and Gamma-ray emission (Compton catastrophe)
- search for correlated variability from radio to Gamma-rays
- search for frequency dependence of the Doppler-factor
- search for electron/positron plasma

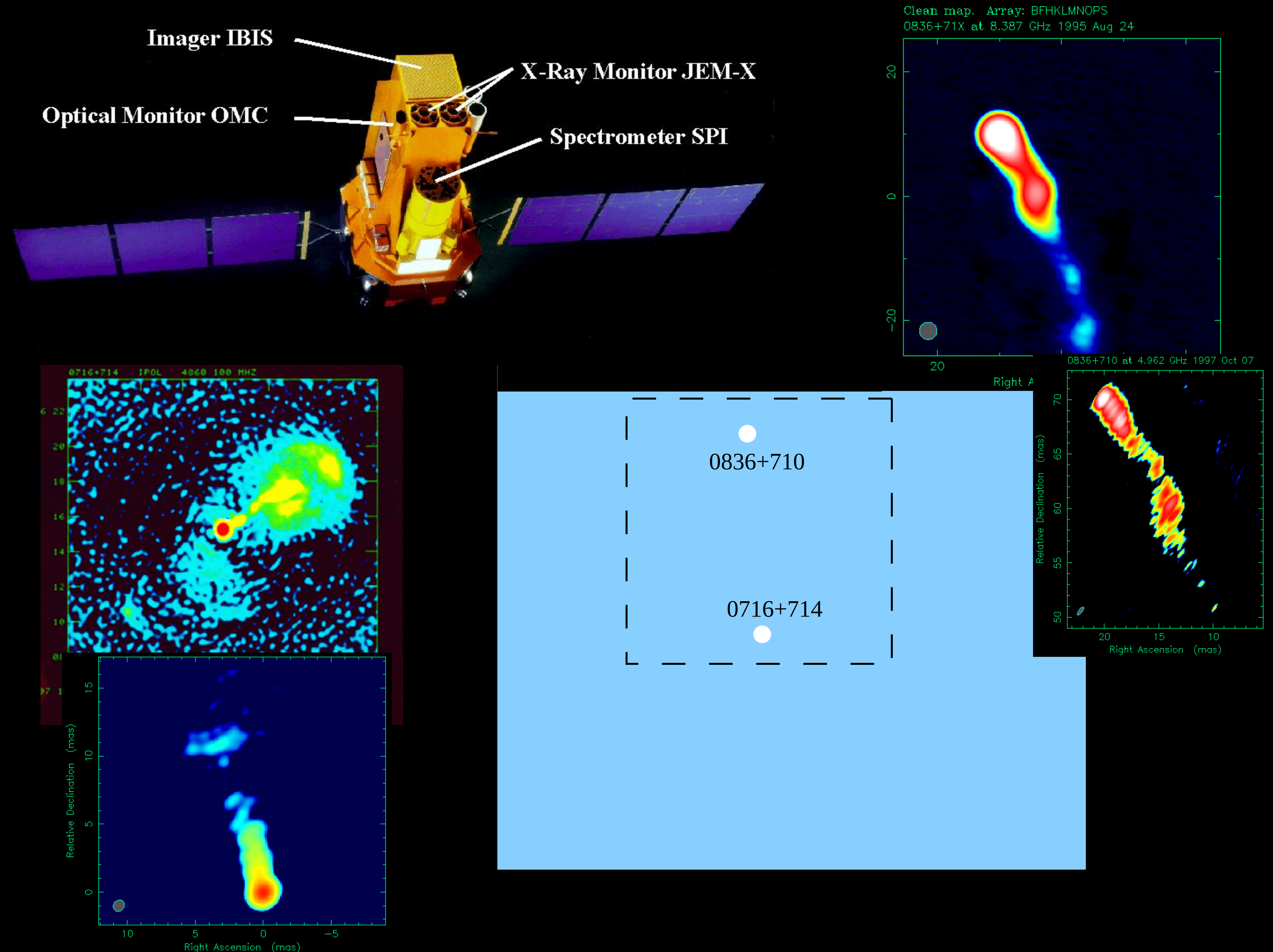
Imager IBIS
X-Ray Monitor JEM-X
Optical Monitor OMC
Spectrometer SPI
Clean map. Array: BFHKLMNOPS
0836+71X at 8.387 GHz 1995 Aug 24
0836+710 at 4.962 GHz 1997 Oct 07
Relative Declination (mas)
Right Ascension (mas)
0716+714 IPOL 4860.100 MHZ
0836+710
0716+714
Relative Declination (mas)
Right Ascension (mas)

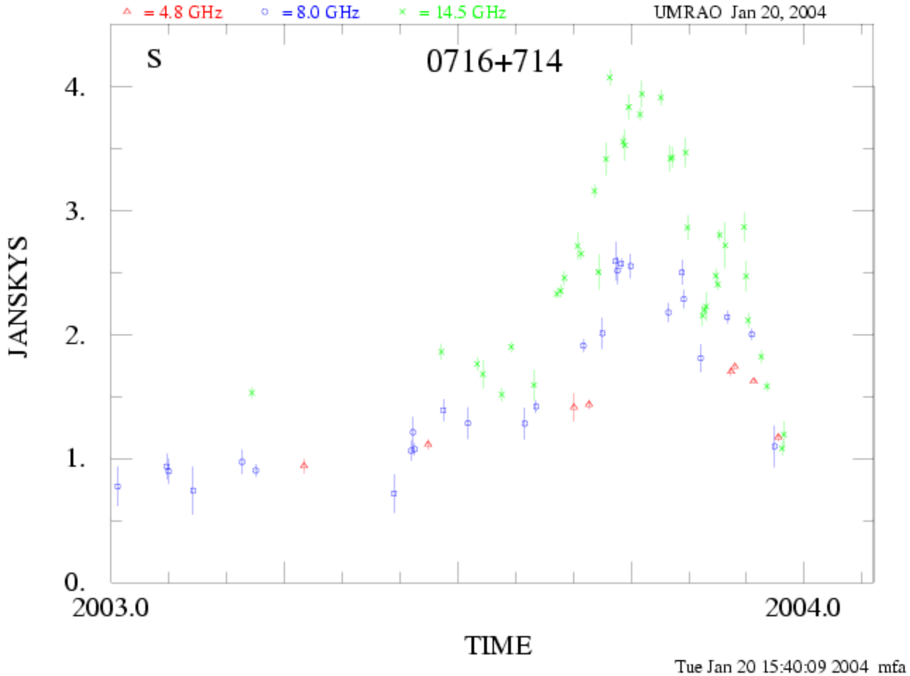
= 4.8 GHz
= 8.0 GHz
= 14.5 GHz
UMRAO Jan 20, 2004
S
0716+714
JANSKYS
4.
3.
2.
1.
0.
2003.0
2004.0
TIME
Tue Jan 20 15:40:09 2004 mfa

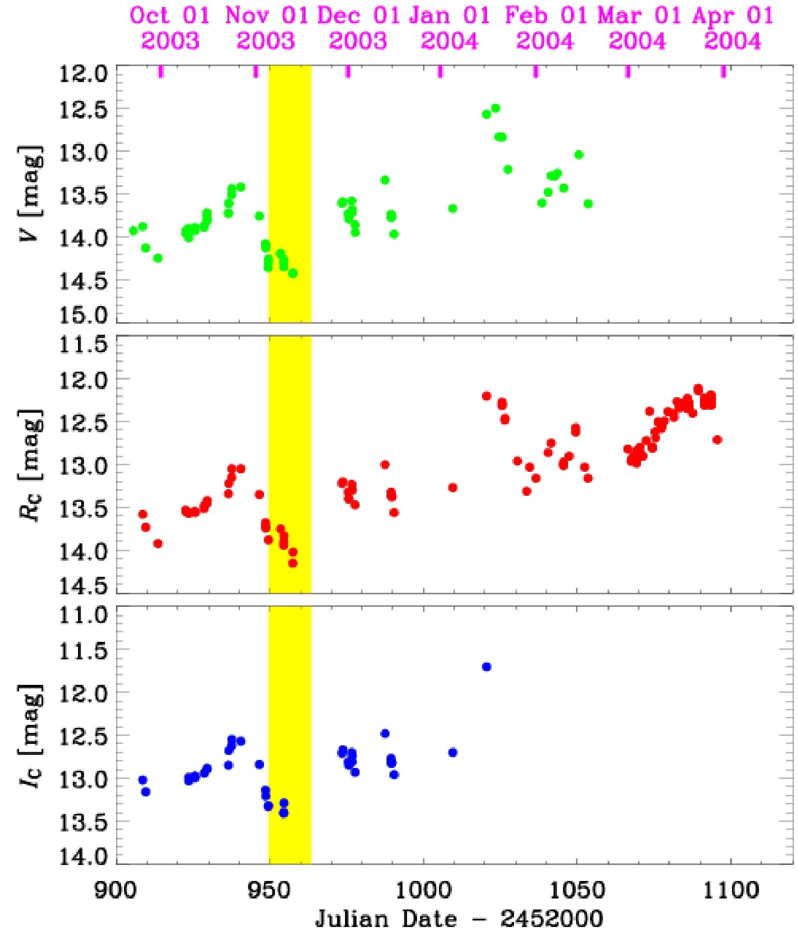
Oct 01 2003
Nov 01 2003
Dec 01 2003
Jan 01 2004
Feb 01 2004
Mar 01 2004
Apr 01 2004
V [mag]
R_C [mag]
I_C [mag]
900
950
1000
1050
1100
Julian Date − 2452000

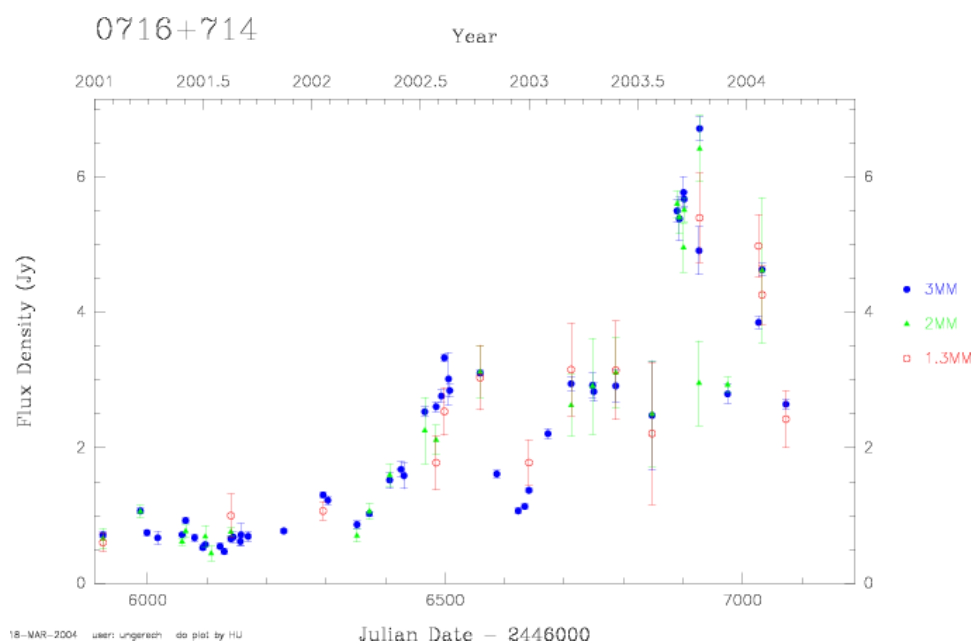
0716+714
Year
2001
2001.5
2002
2002.5
2003
2003.5
2004
Flux Density (Jy)
3MM
2MM
1.3MM
6000
6500
7000
Julian Date − 2446000
18-MAR-2004 user: ungerech do plot by HU

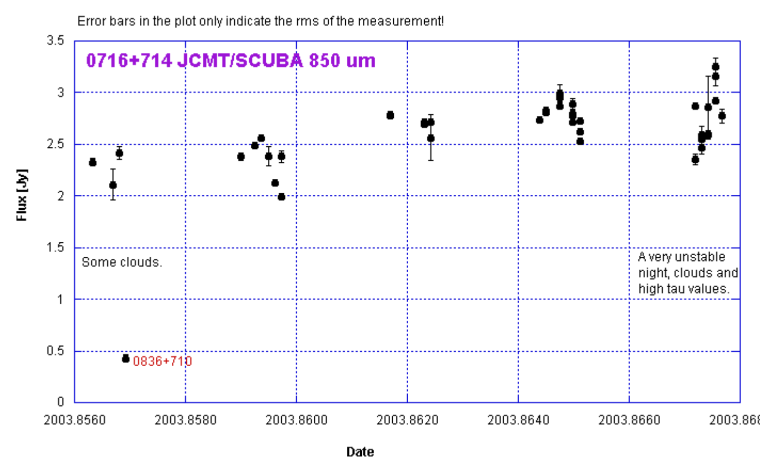
Error bars in the plot only indicate the rms of the measurement!
0716+714 JCMT/SCUBA 850 um
Flux [Jy]
Some clouds.
A very unstable night, clouds and high tau values.
0836+710
2003.8560
2003.8580
2003.8600
2003.8620
2003.8640
2003.8660
2003.8680
Date

The 100m radio telescope of the MPIfR in Effelsberg

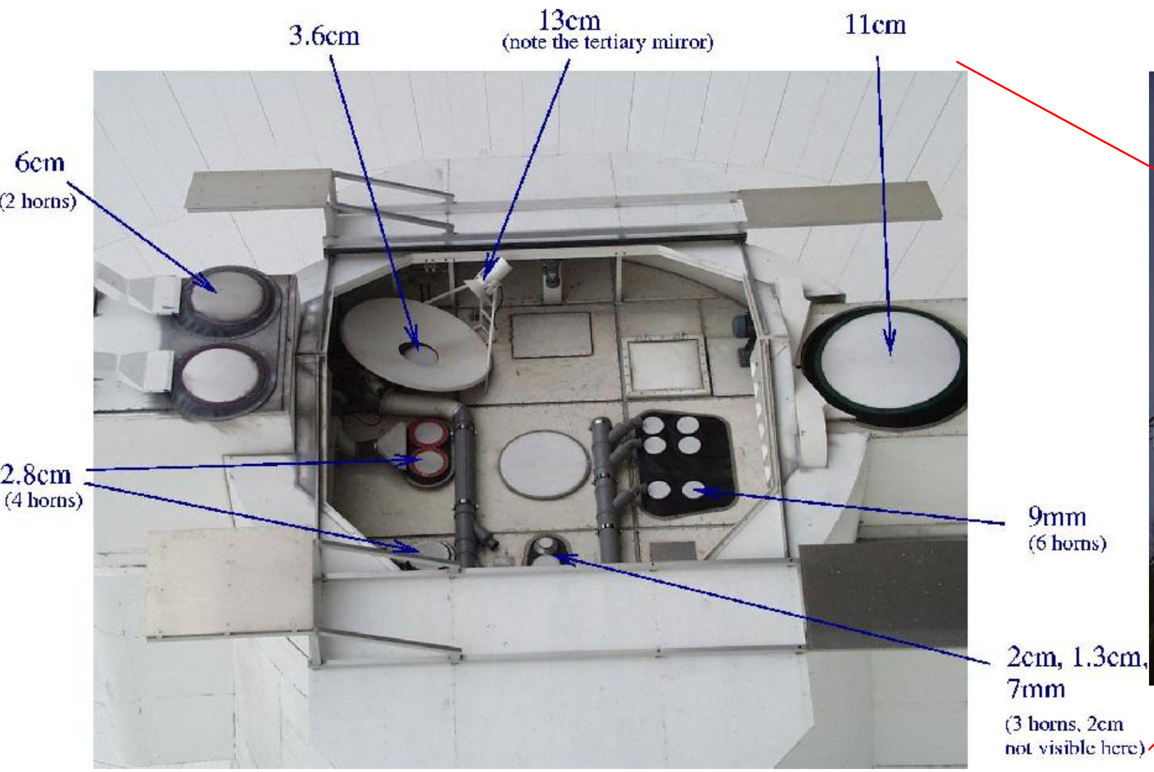

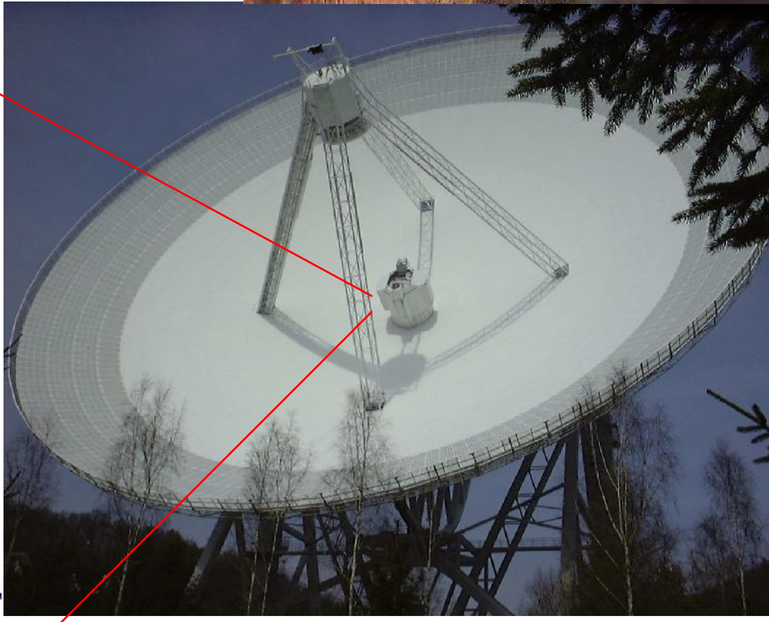

Effelsberg 6cm 2.8cm

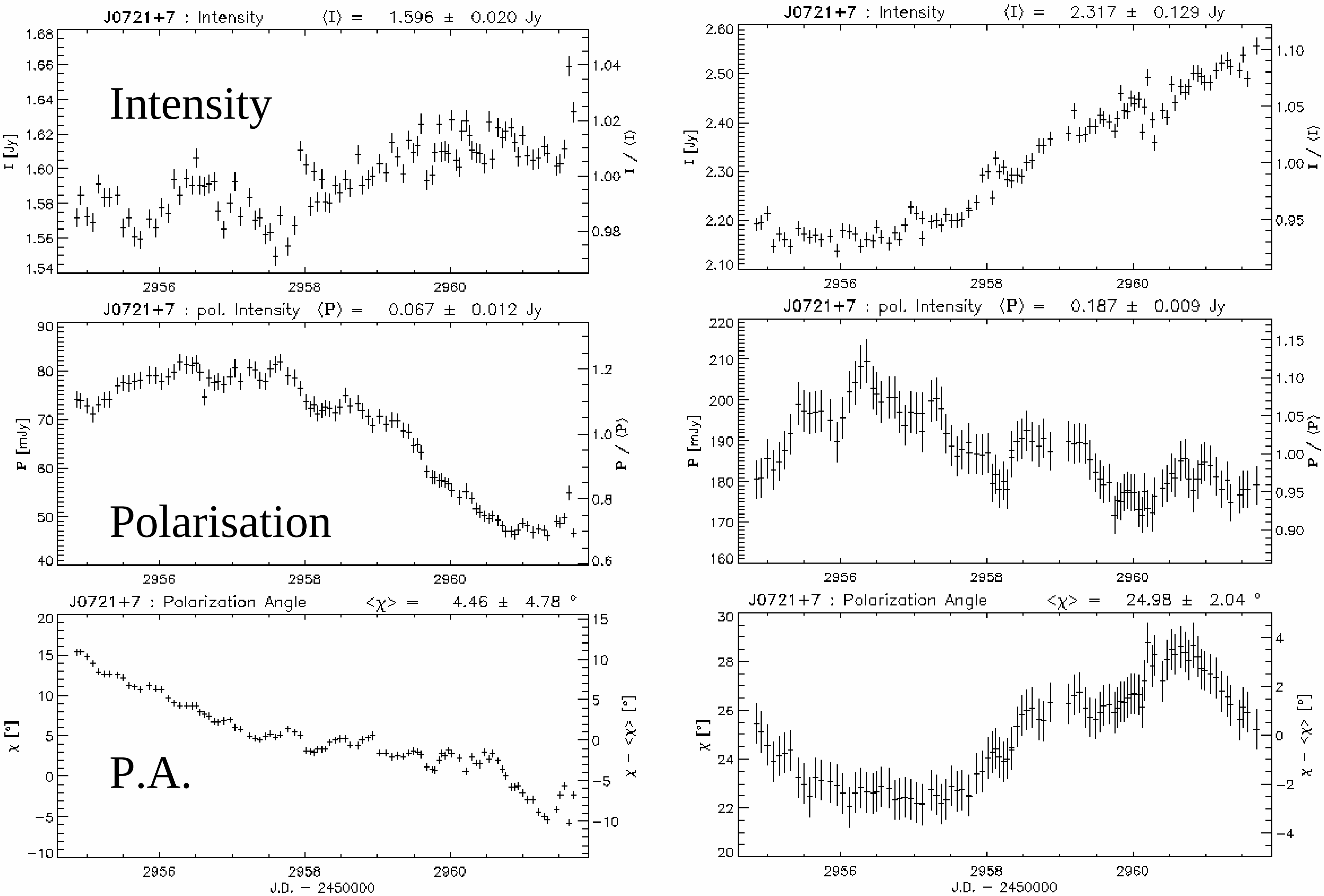

analysis: Impellizzeri, Friedrichs, Kraus et al.

Effelsberg 6cm 2.8cm

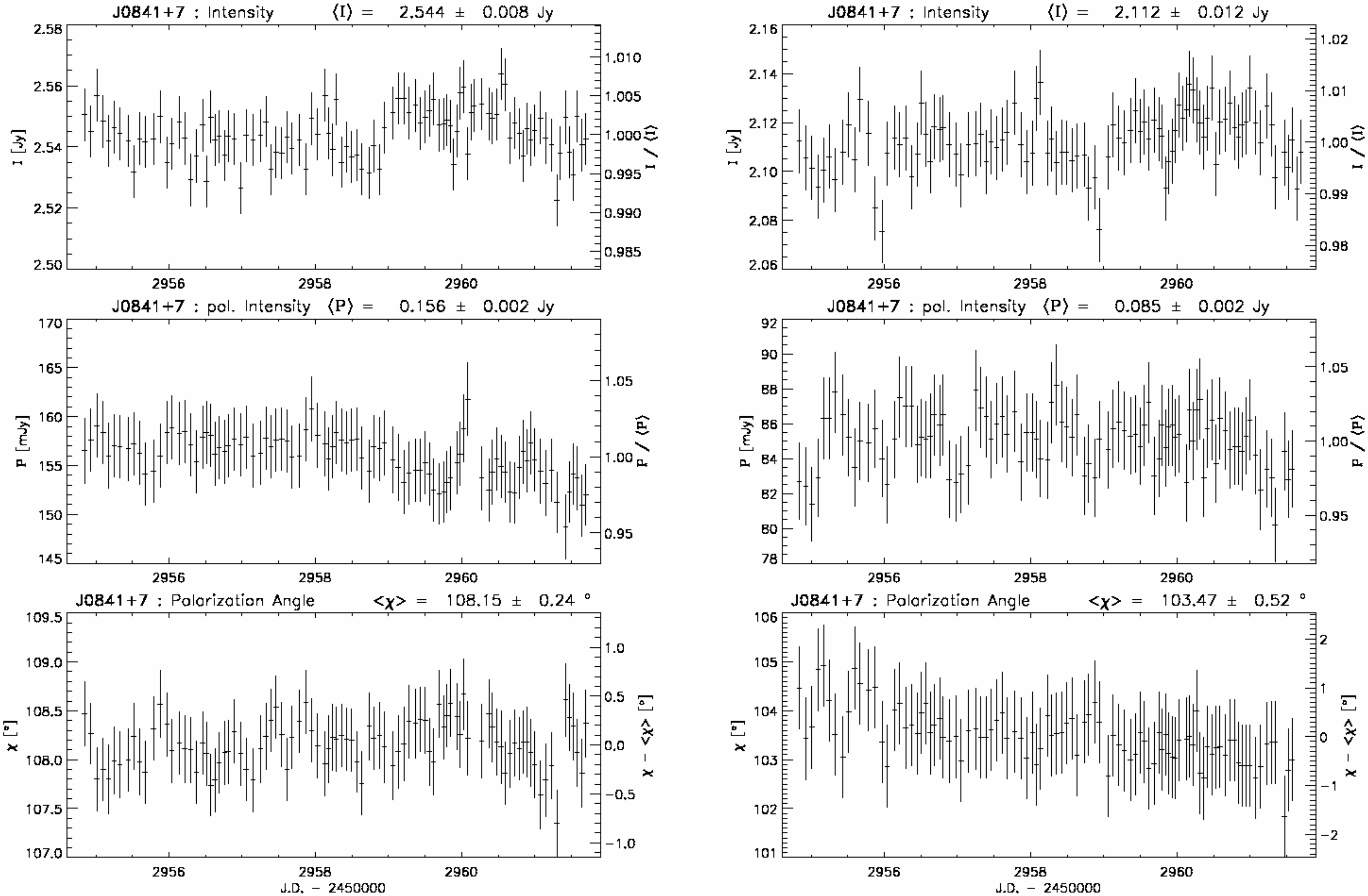

0836+71 used as secondary calibrator

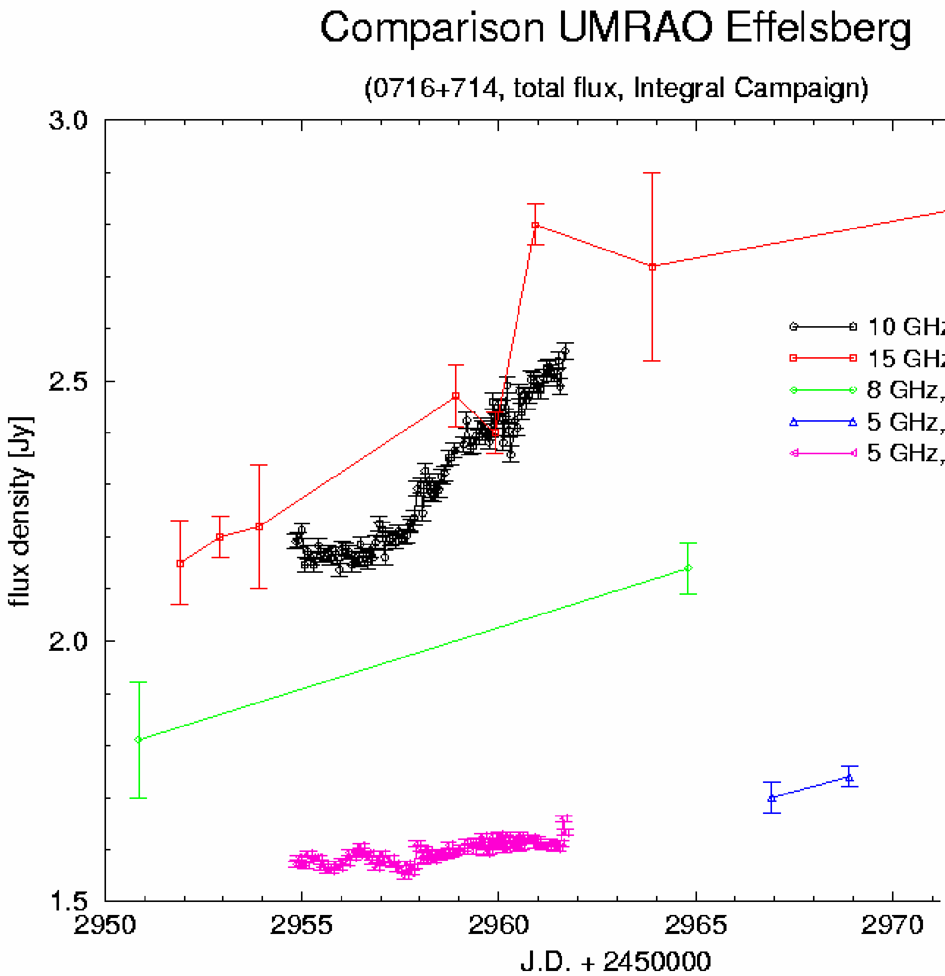

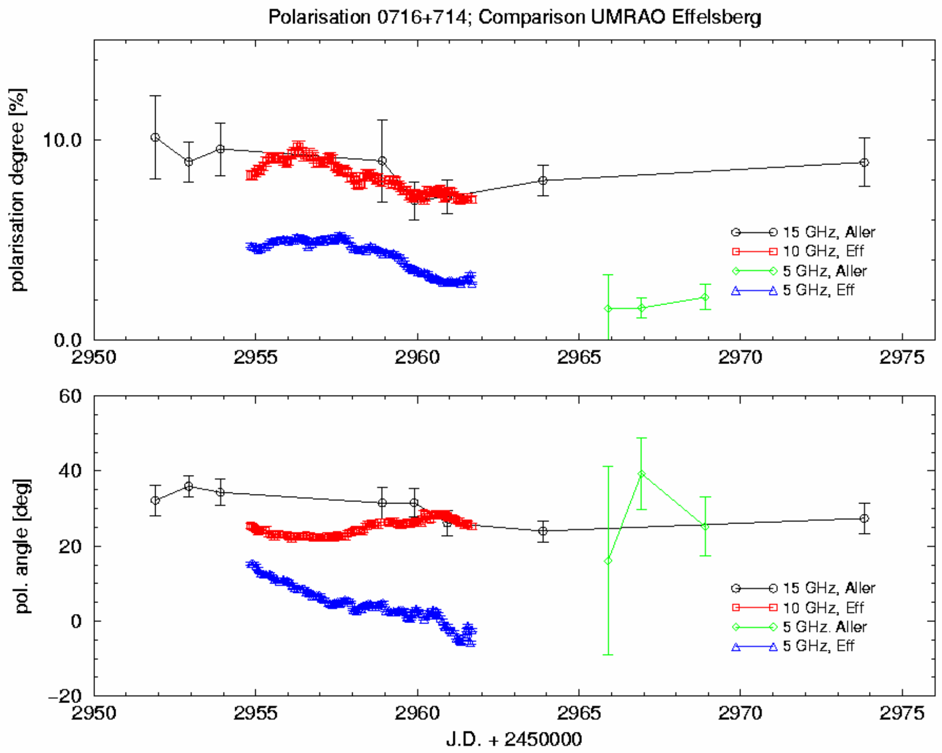

note the change of the EVPA

30m MRT Pico Veleta - 90 GHz

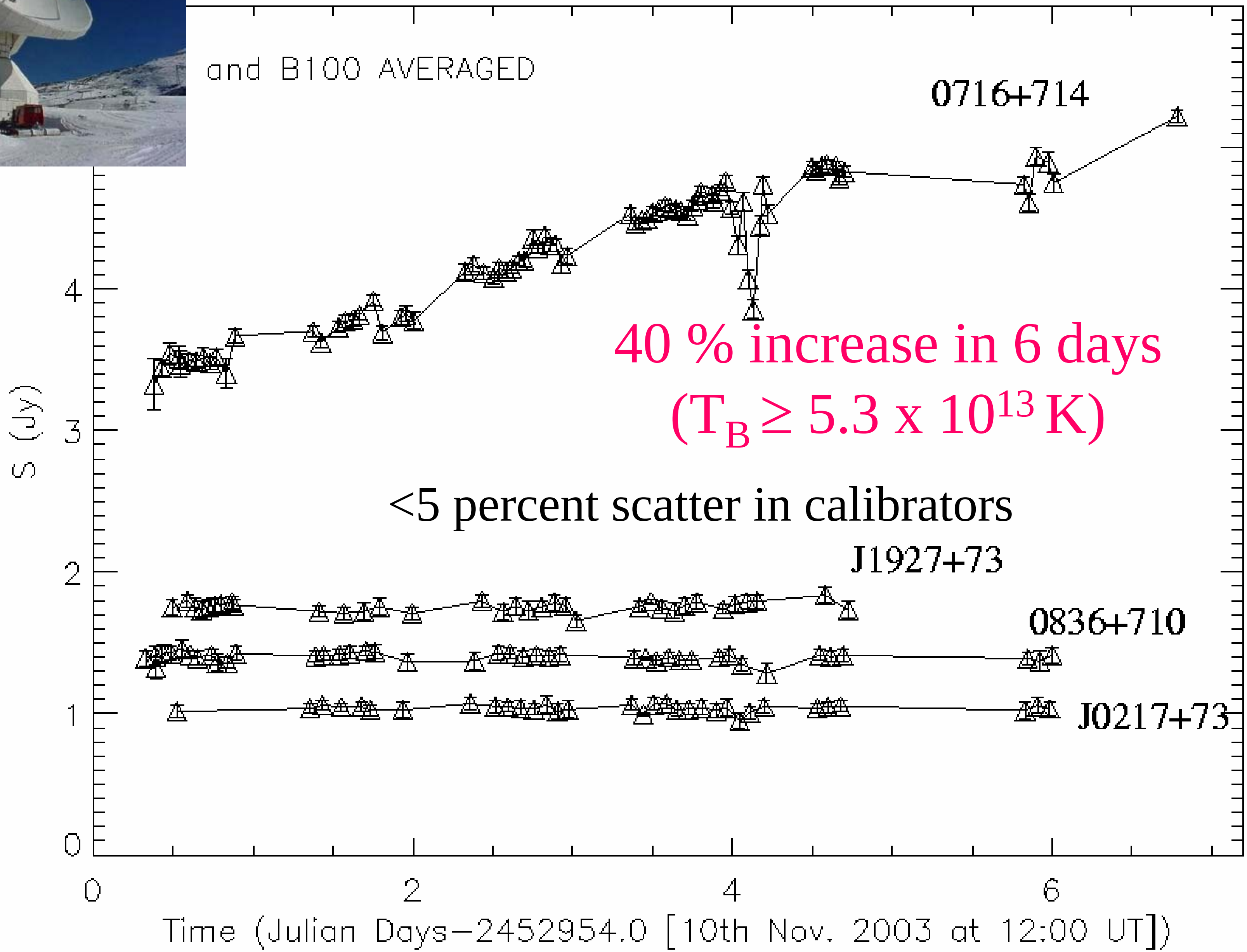

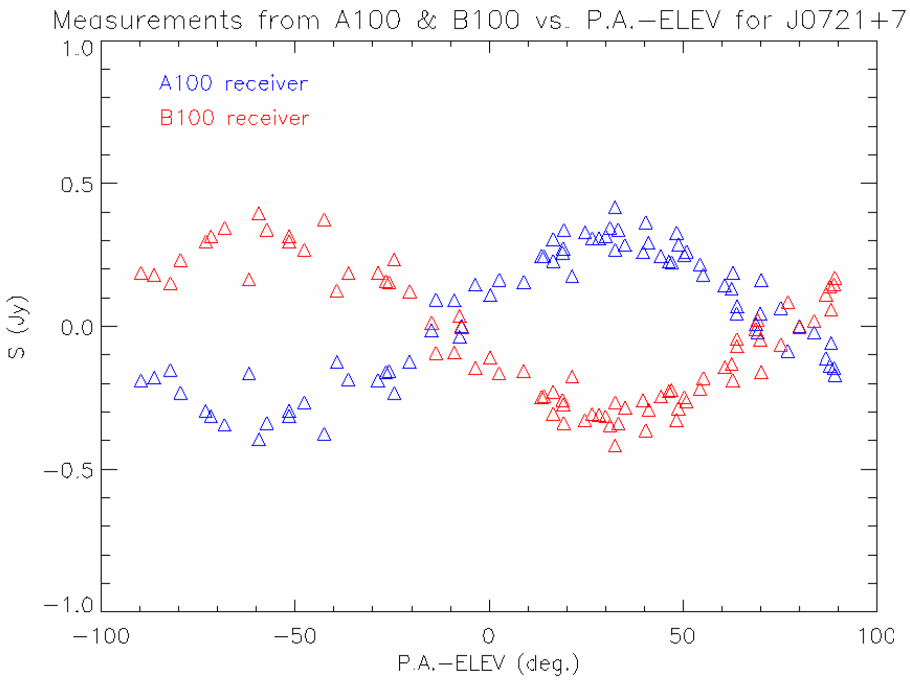

A, B: receivers with orthogonal linear feeds

→ parallactic rotation of signal

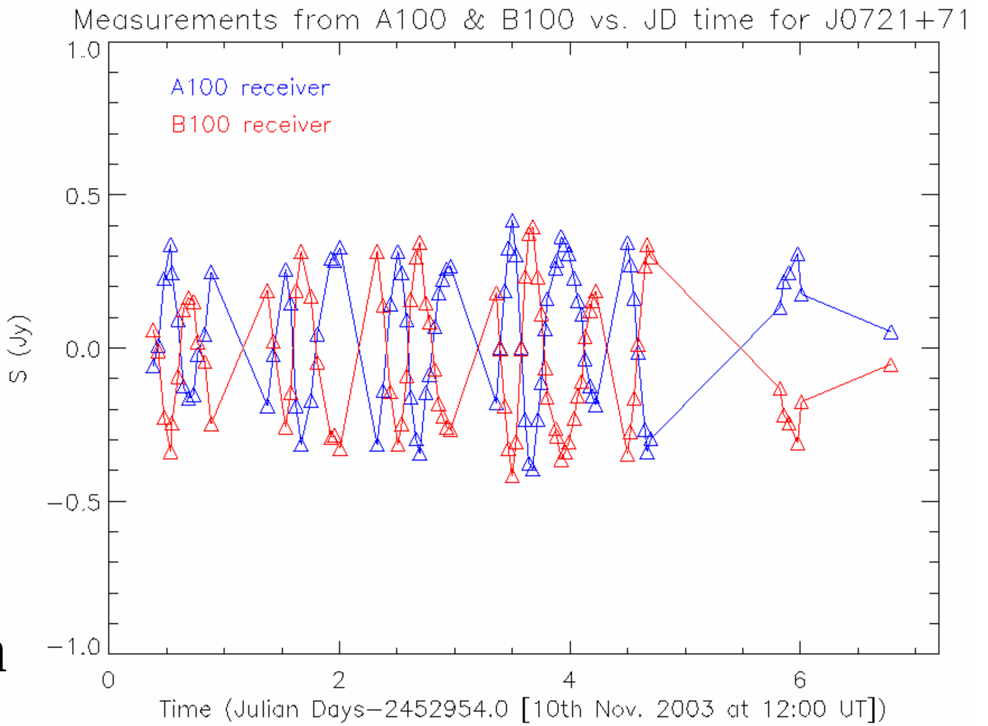

ΔP = 0.8 Jy → P/S = 10 %

still need to check if polarisation is constant with time

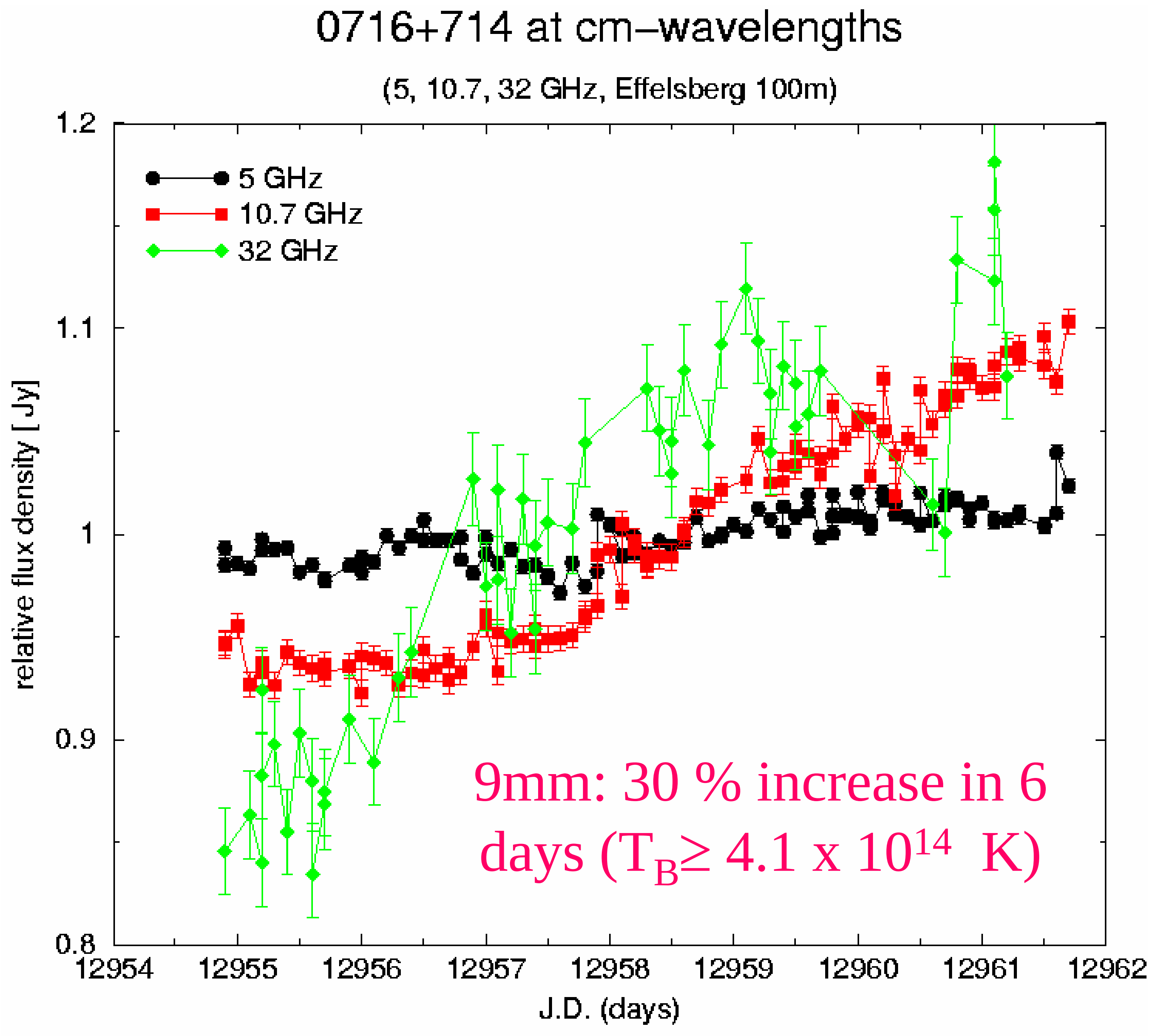
0716+714 at cm–wavelengths
(5, 10.7, 32 GHz, Effelsberg 100m)
5 GHz
10.7 GHz
32 GHz
relative flux density [Jy]
J.D. (days)
1.2
1.1
1
0.9
0.8
12954
12955
12956
12957
12958
12959
12960
12961
12962
9mm: 30 % increase in 6 days ($T_B \geq 4.1 \times 10^{14}$ K)

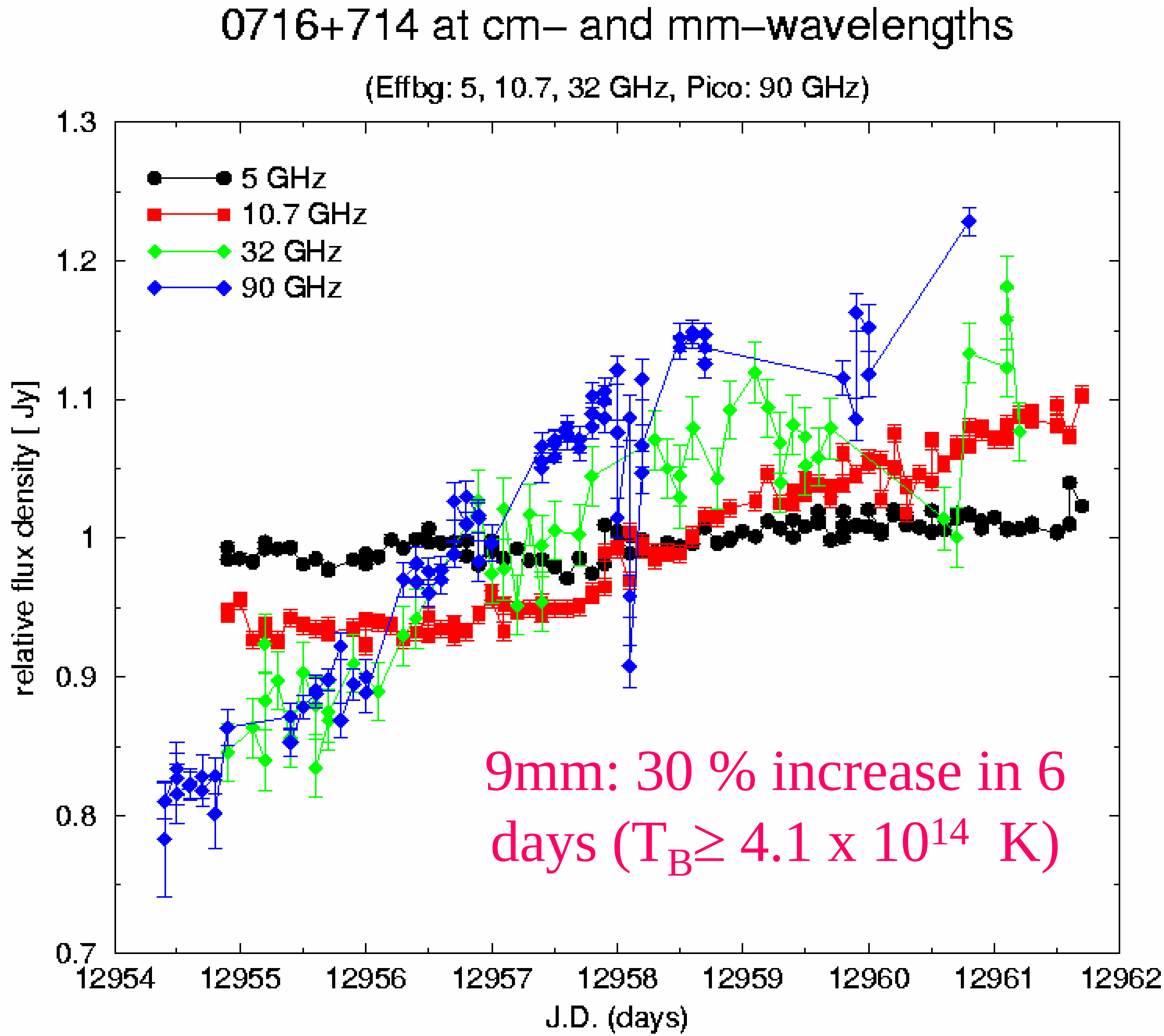

0716+714 at cm– and mm–wavelengths
(Effbg: 5, 10.7, 32 GHz, Pico: 90 GHz)
5 GHz
10.7 GHz
32 GHz
90 GHz
relative flux density [Jy]
J.D. (days)
1.3
1.2
1.1
1
0.9
0.8
0.7
12954
12955
12956
12957
12958
12959
12960
12961
12962
9mm: 30 % increase in 6 days ($T_B \geq 4.1 \times 10^{14}$ K)

3mm Monitoring at Kitt Peak (NRAO 12m)

Observer: B.W. Sohn, A. Pagels

Observing Summary

10th –18th Nov 2003, data obtained during 14th – 18th

Frequency : 86.852 GHz, bandwidth : 600MHz (SSB)

two orthogonal polarizations (channel1:elv., channel 2: azi)

T_{sys} ~ 270 K, Kelvin/Volt ~ 25 (slowly time varying)

Calibration

Calibrators : 0836+71, J1927+73, J2005+77

Observing cycle : 0716+71 - 0836+71 - J1927+73 - J2005+77

Channel offset correction : ch1/0.881, ch2/1.000 wrt J1927+73

Time variable gain correction : wrt 0836+71

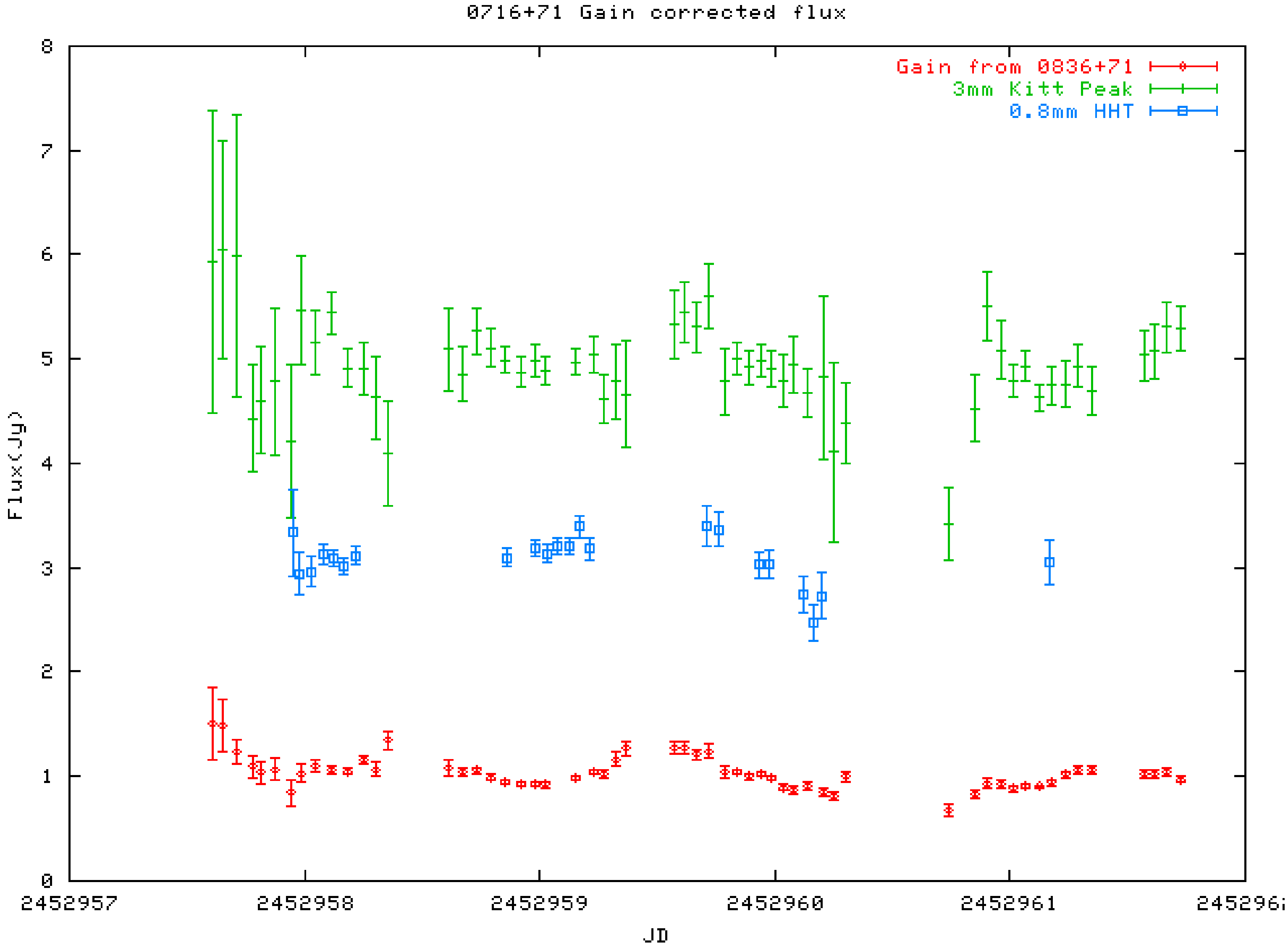

analysis: B.W. Sohn et al.

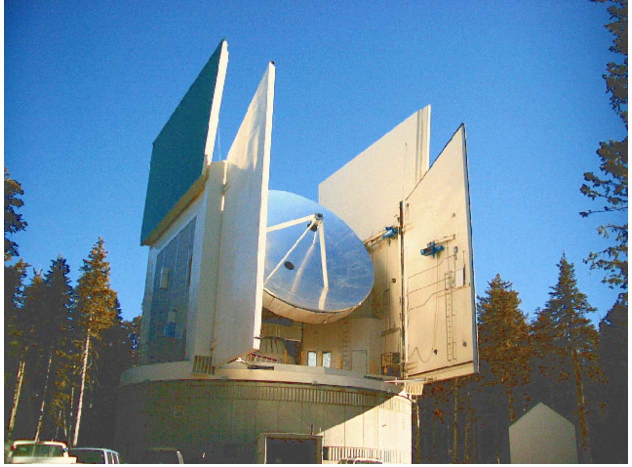

0.8 mm monitoring with the Heinrich Hertz Telescope on Mt. Graham (HHT 10m)

observing dates :

November 14, 15, 16, 17

19 channel bolometer,

on - off measurements

time sampling:

1 measurement every

1.5 - 2 hrs

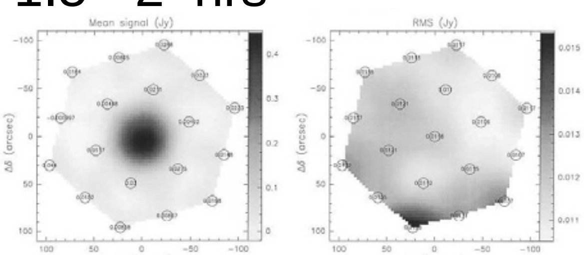

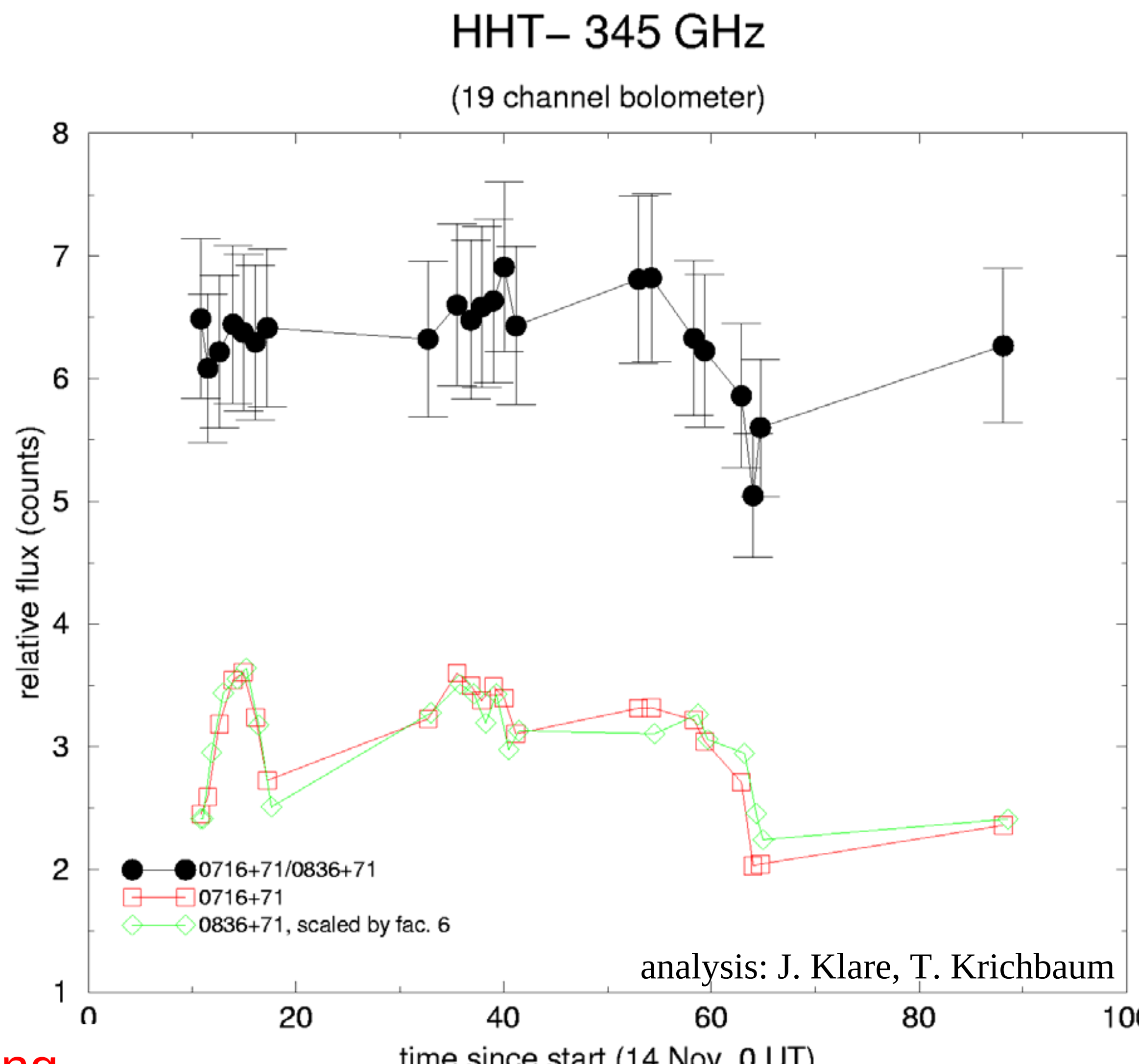

Observer: J. Klare, E. Körding

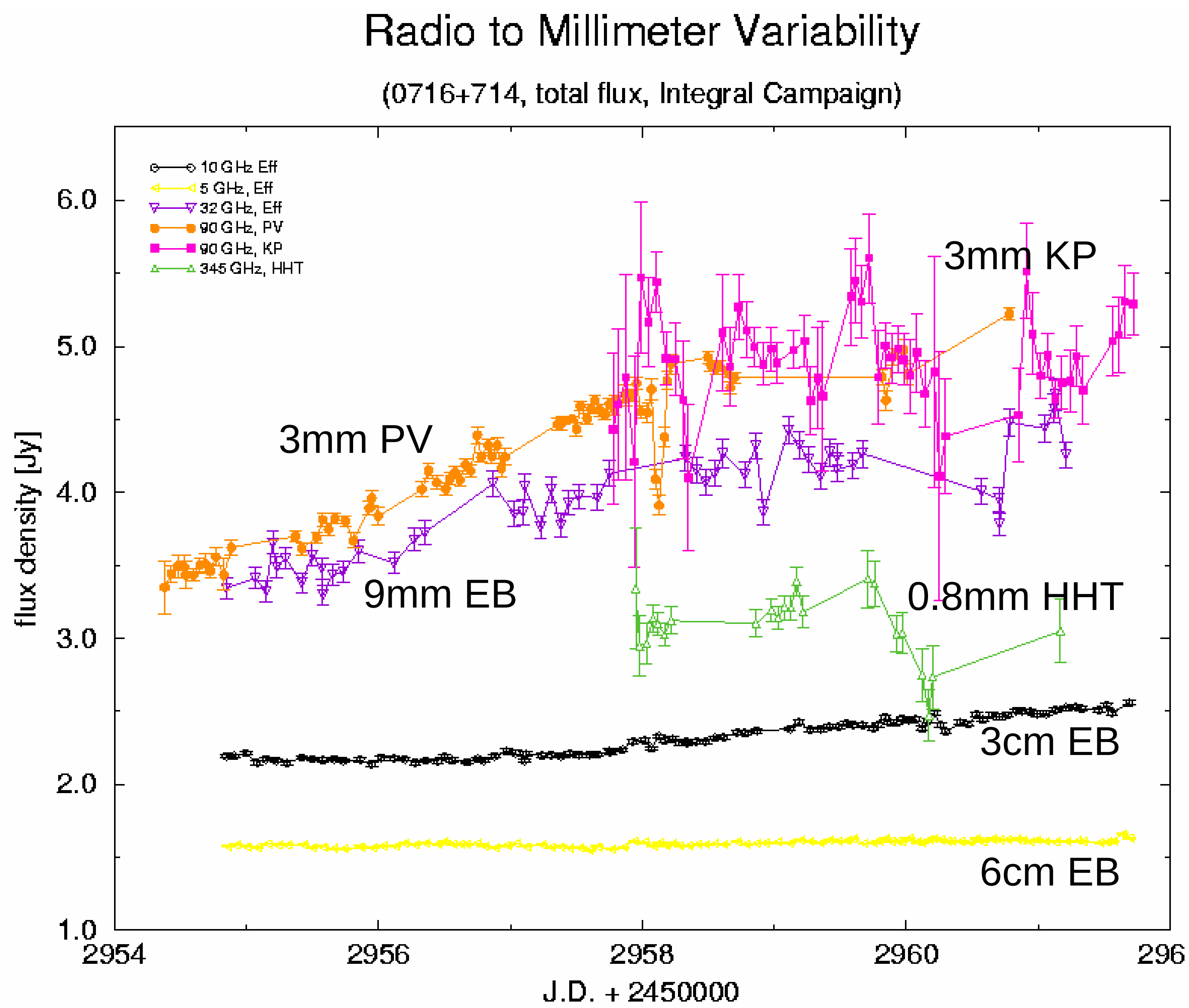

Radio to Millimeter Variability
(0716+714, total flux, Integral Campaign)
10 GHz Eff
5 GHz, Eff
32 GHz, Eff
90 GHz, PV
90 GHz, KP
345 GHz, HHT
3mm KP
3mm PV
9mm EB
0.8mm HHT
3cm EB
6cm EB
flux density [Jy]
J.D. + 2450000
6.0
5.0
4.0
3.0
2.0
1.0
2954
2956
2958
2960
296

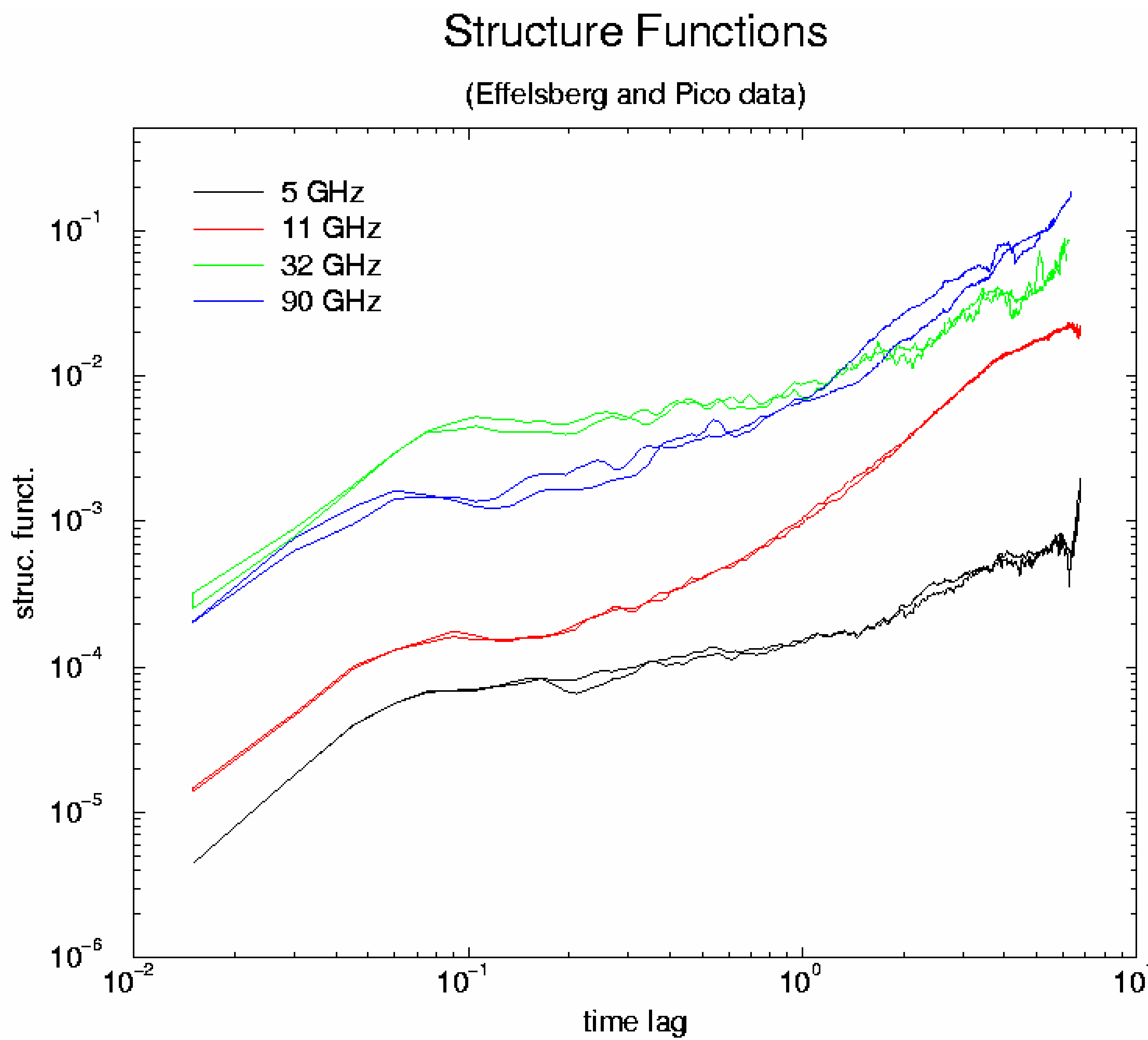

Structure Functions
(Effelsberg and Pico data)
5 GHz
11 GHz
32 GHz
90 GHz
struc. funct.
time lag
10^{-1}
10^{-2}
10^{-3}
10^{-4}
10^{-5}
10^{-6}
10^{-2}
10^{-1}
10^{0}
10^{1}

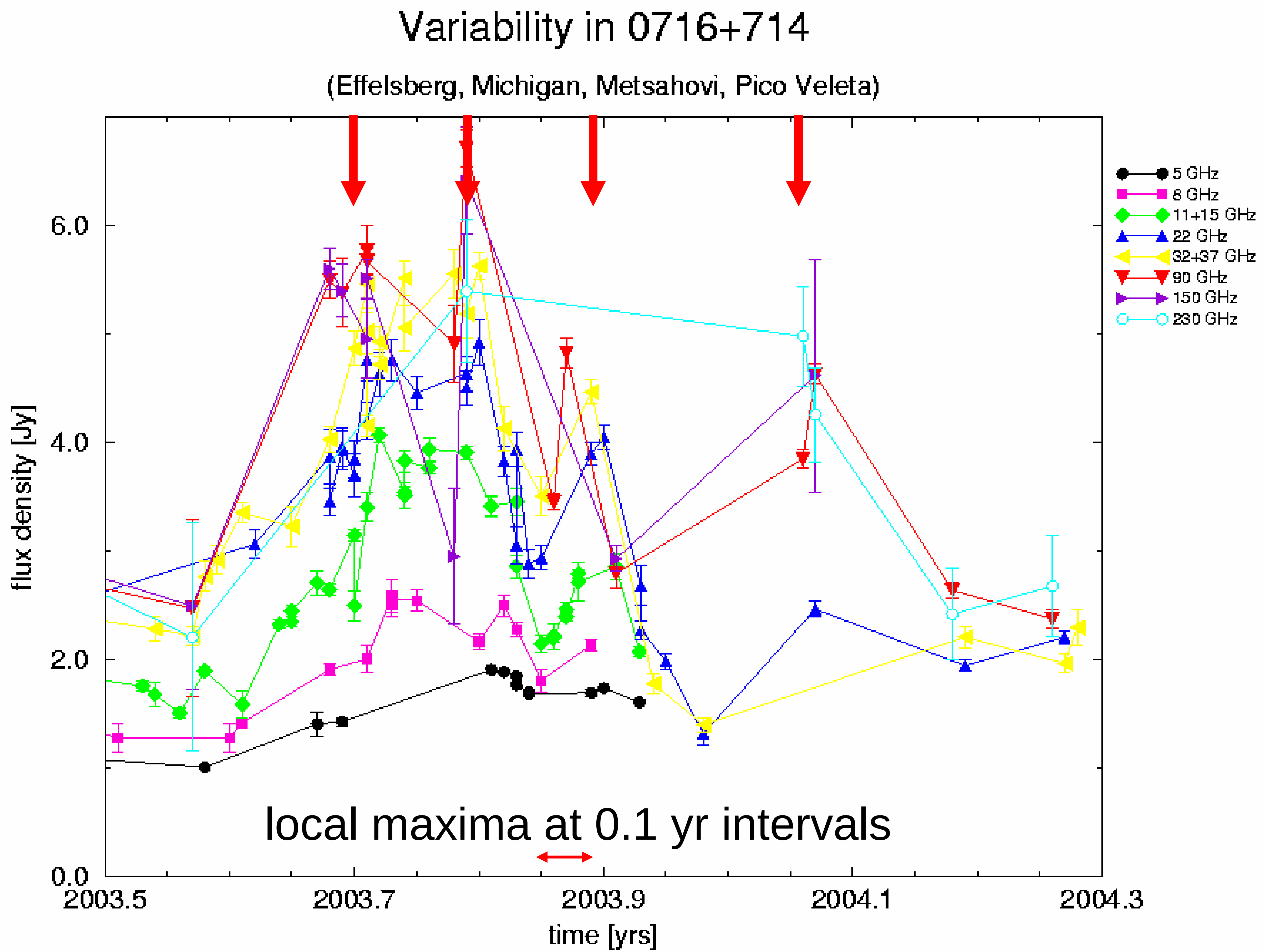
Variability in 0716+714
(Effelsberg, Michigan, Metsahovi, Pico Veleta)
flux density [Jy]
6.0
4.0
2.0
0.0
2003.5
2003.7
2003.9
2004.1
2004.3
time [yrs]
5 GHz
8 GHz
11+15 GHz
22 GHz
32+37 GHz
90 GHz
150 GHz
230 GHz
local maxima at 0.1 yr intervals

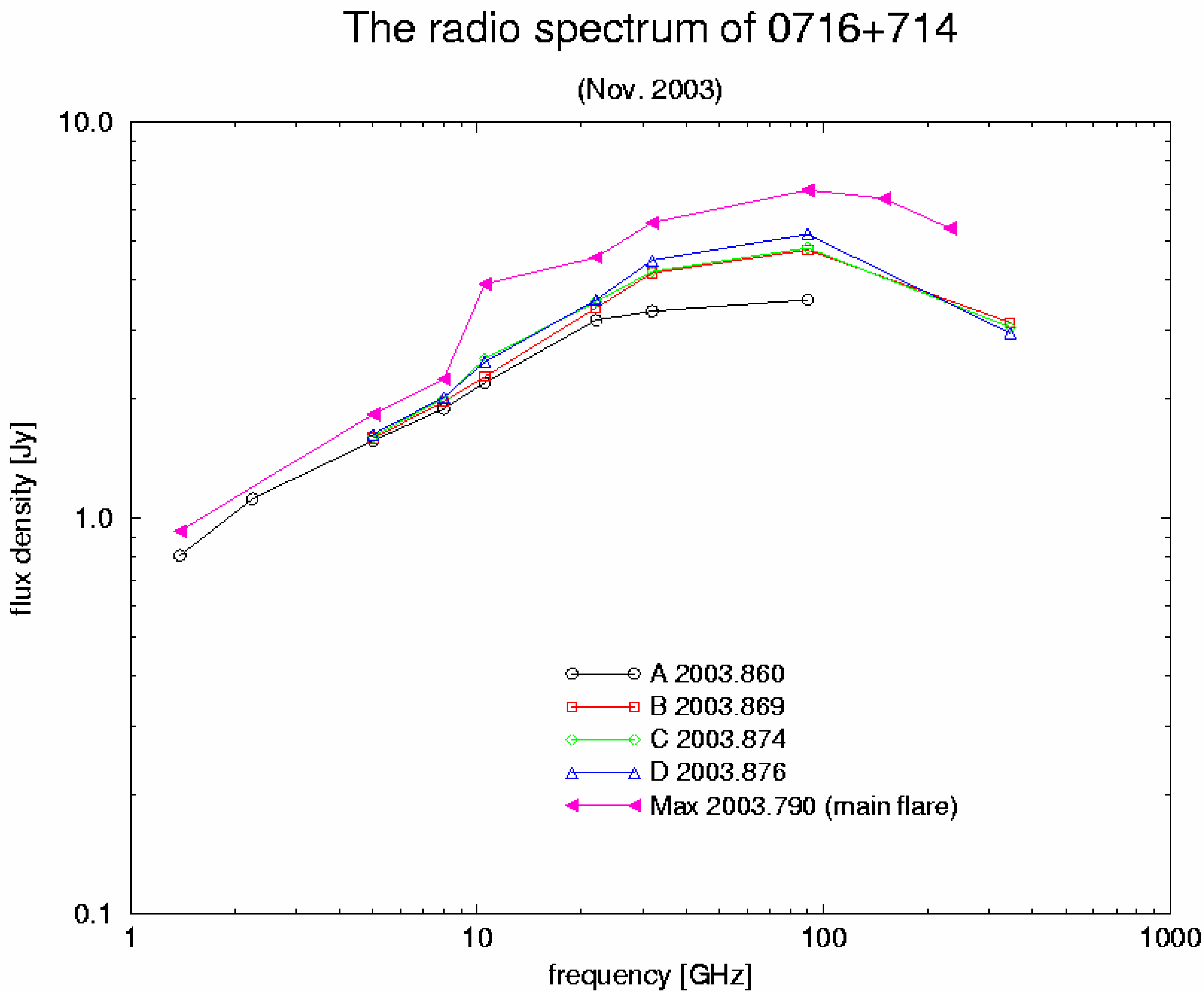

The radio spectrum of 0716+714
(Nov. 2003)
flux density [Jy]
10.0
1.0
0.1
1
10
100
1000
frequency [GHz]
A 2003.860
B 2003.869
C 2003.874
D 2003.876
Max 2003.790 (main flare)

Conclusion

- 0716+714 varied in the radio to mm-bands on time scales of days
- only mild IDV was detected at cm-wavelengths
- at mm-wavelengths the source is highly (~10%) polarized
- first detection of $T_B > 10^{12}$ K at mm-wavelengths, consistent with superluminal motion and normal (δ=10-20) Doppler-factors
- the radio spectrum peaks near 100 GHz
- two periodicity time scales in the long term light curve

We now need to combine all this with the data from the optical and from INTEGRAL.

Reaching ENIGMAtic Milestones – the Key to Success

Task 1

<u>Original Milestones</u>

1a: A better understanding of the parameters that affect the quality of differential photometry of point sources. (Achieved by end of year 3.)

1b: Implementation of programs that allow measurements close to the photon flux limit (or as close as modern CCD technology allows). (Achieved by end of year 3.)

1c: Assessment of the technical requirements for robotic telescopes. (Achieved by end of year 2.)

1d: Practical implementation of a network of robotic telescopes operated by members of the network. (Achieved by end of year 4.)

Additional Milestones – Even More Key?

Additional Milestones

1aa: A better understanding of the parameters that affect photometry in blazars with resolved host galaxies – the TeV problem. (Achieved by end of year 3.)

1e: Assessment of definitive empirical tests of competing theories. (Achieved by end of year 4.)

Task 1

The influence of the host galaxy in differential photometry

K. Nilsson
Tuorla Observatory

The host galaxy

- Adds extra flux in the optical/IR bands.
- The increase depends on aperture size and seeing.

The host galaxy

- Adds extra flux in the optical/IR bands.
- The increase depends on aperture size and seeing.

Mrk 501 SED (Katarzyński et al. 2001)

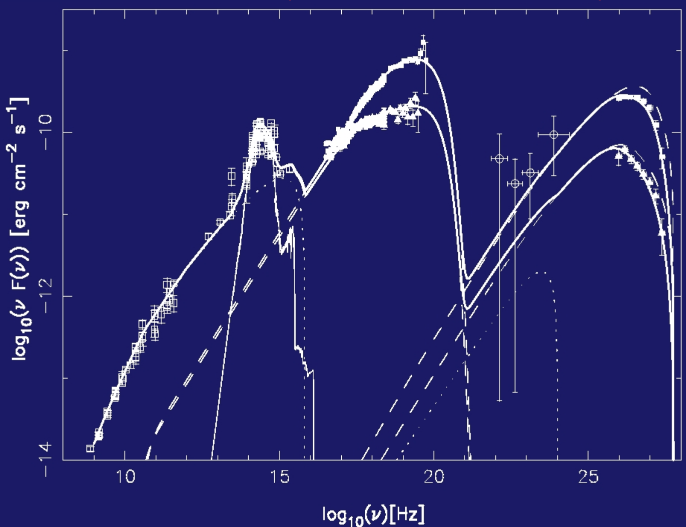

NOT R-band

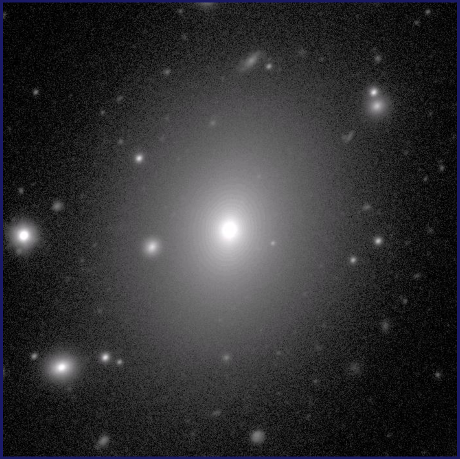

Host galaxies of radio-loud AGN

$z < 0.3$:

RLQ (e.g. Kukula et al. 2001, Dunlop et al.2003) :

- Bulge-dominated, $<M_R>$ = -23.7, $<r_{\rm eff}>$ = 12 kpc

BL Lacs (e.g. Urry et al. 2000, Nilsson et al. 2003) :

- Bulge-dominated, $<M_R>$ = -23.8, $<r_{\rm eff}>$ = 13 kpc

Host galaxies of radio-loud AGN

$z < 0.3$:

RLQ (e.g. Kukula et al. 2001, Dunlop et al.2003) :

- Bulge-dominated, $<M_{\rm R}>$ = -23.7, $<r_{\rm eff}>$ = 12 kpc

BL Lacs (e.g. Urry et al. 2000, Nilsson et al. 2003) :

- Bulge-dominated, $<M_{\rm R}>$ = -23.8, $<r_{\rm eff}>$ = 13 kpc

$z = 0.3...1.5$:

RLQ & BL Lacs : luminosities consistent with a single formation epoch at $z \approx 5$ and passive evolution thereafter (e.g. Dunlop 2003, Heidt et al. 2004).

Aim of this study

Measure the host galaxy contribution as a function of aperture size and seeing in differential aperture photometry.

→ A nucleus/host galaxy decomposition required.

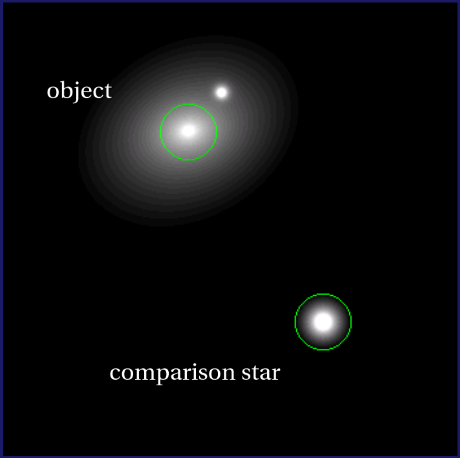

Separating the nucleus from the host

2-dim. model fitting :

Object = nucleus + host galaxy

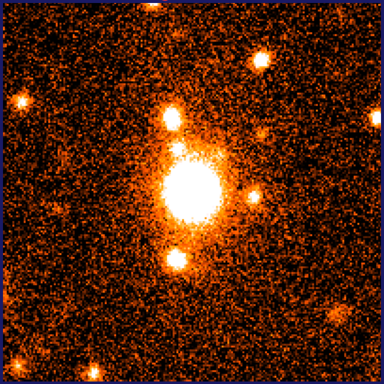

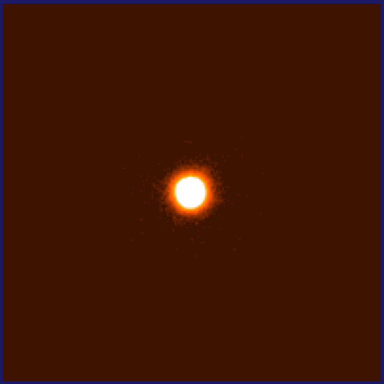

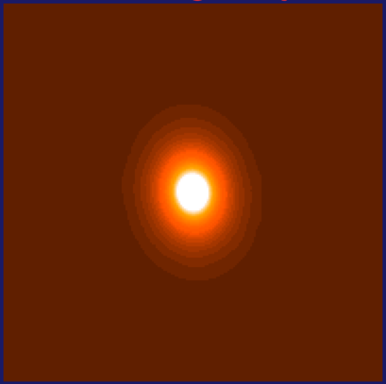

Separating the nucleus from the host

2-dim. model fitting :

Object = nucleus + host galaxy

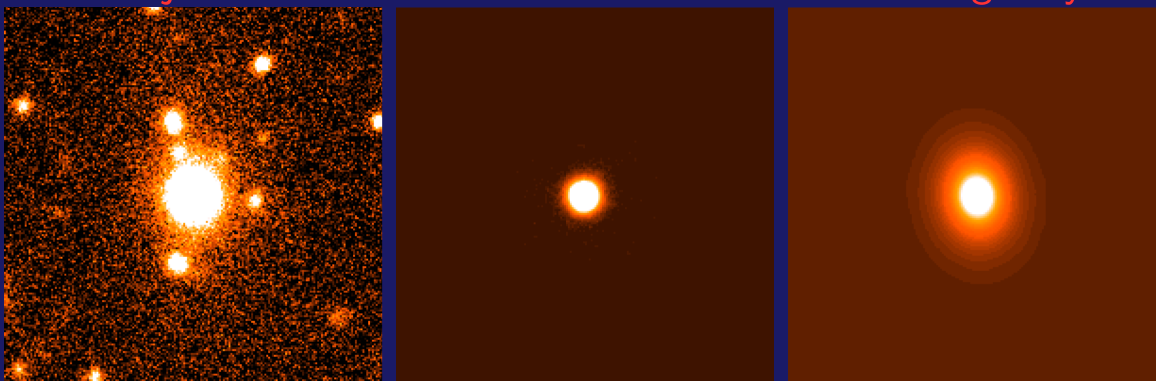

free parameters : core : x_c, y_c, m_c

host : x_g, y_g, m_g, r_{eff}, ϵ, PA, β

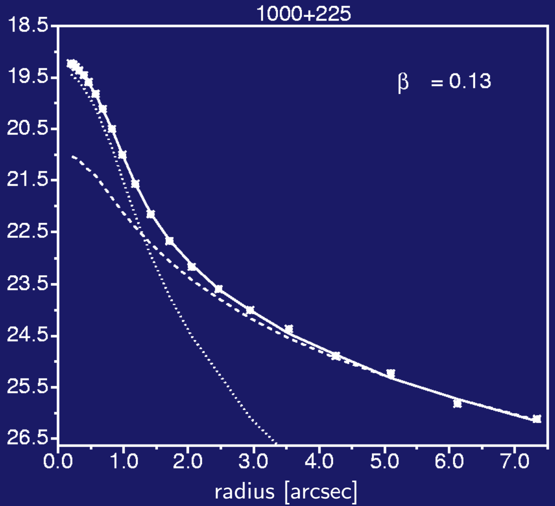
1000+225
β = 0.13
18.5
19.5
20.5
21.5
22.5
23.5
24.5
25.5
26.5
0.0
1.0
2.0
3.0
4.0
5.0
6.0
7.0
radius [arcsec]

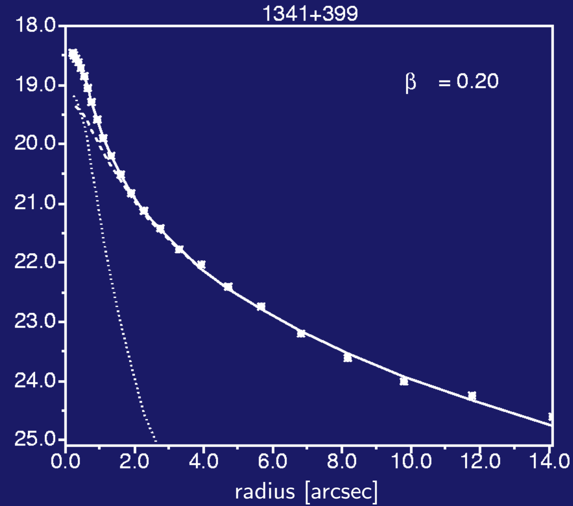
1341+399
β = 0.20
18.0
19.0
20.0
21.0
22.0
23.0
24.0
25.0
0.0
2.0
4.0
6.0
8.0
10.0
12.0
14.0
radius [arcsec]

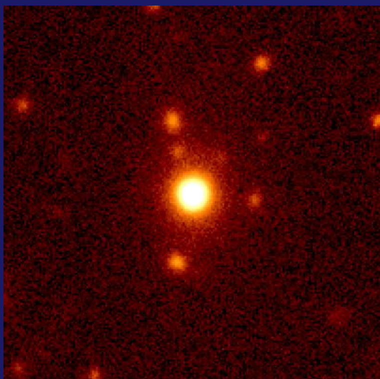

obs. image

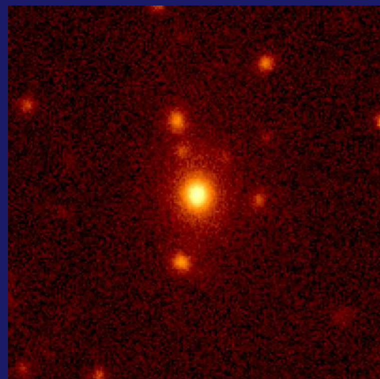

core subtracted

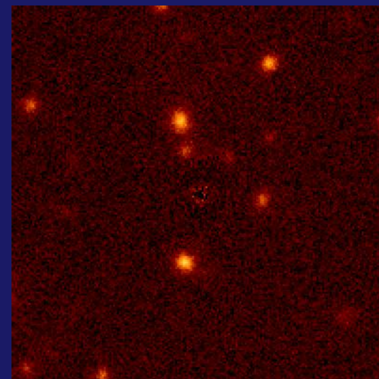

core + host subtracted

Studied objects

Object	R_{core}	R_{host}	$\frac{F_{core}}{F_{host}}$	r_{eff} [″]	β
Mrk 421	12.9	13.2	1.3	8.2	0.36
Mrk 501	14.4	11.9	0.1	45	0.10
1ES 1959+650	15.2	14.8	0.7	9.5	0.41
1ES 2344+514	16.6	13.8	0.08	11	0.19

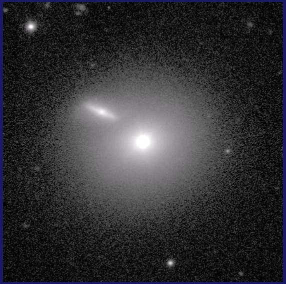
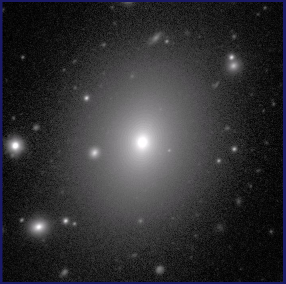
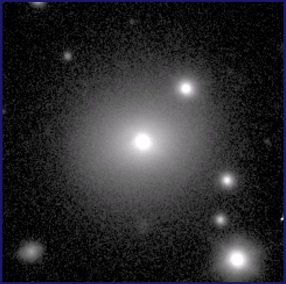
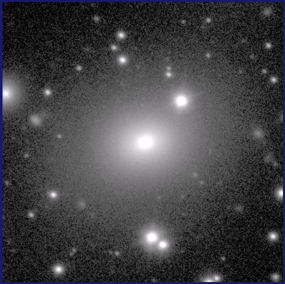

The method

1) Fit the object with a 2-dim model
$\longrightarrow$ position and proper scaling of the nucleus,
model image for the host galaxy light distribution.

2) a) Subtract nuclear component or
b) use the model galaxy image directly.

3) Convolve to the desired seeing
(convolving kernel: Moffat function, $\beta_{\mathrm{M}} = 2.3$).

4) Measure comp. star & object fluxes.

Repeat steps 3) and 4) over a range of seeing values.

observed image - core

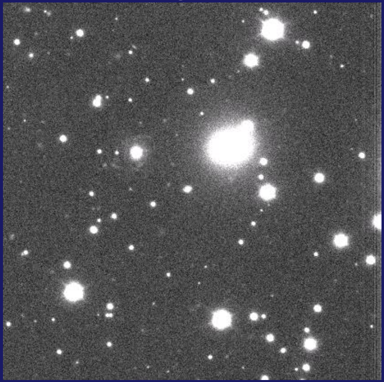

2" FWHM

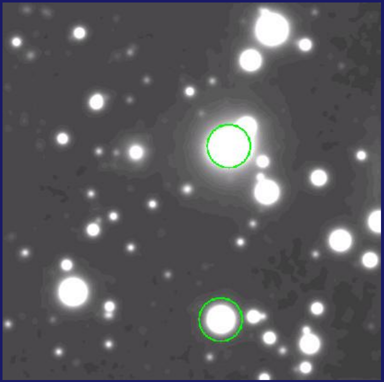

5" FWHM

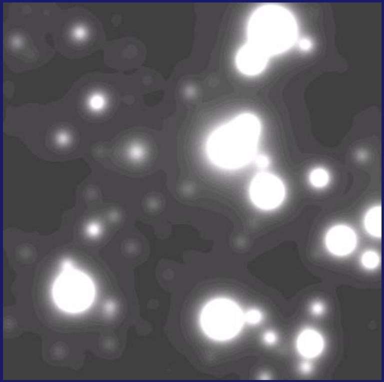

model galaxy

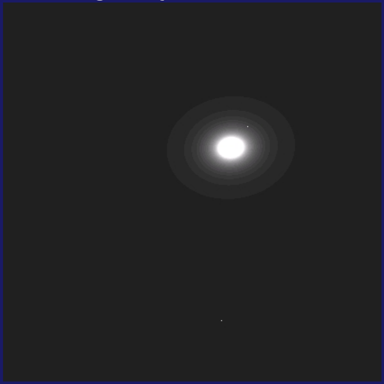

2" FWHM

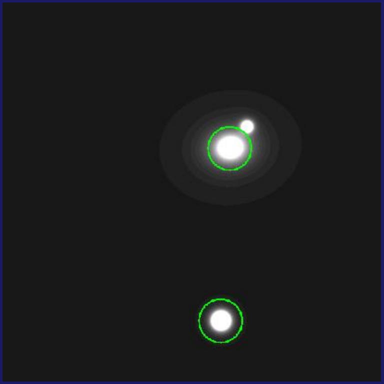

5" FWHM

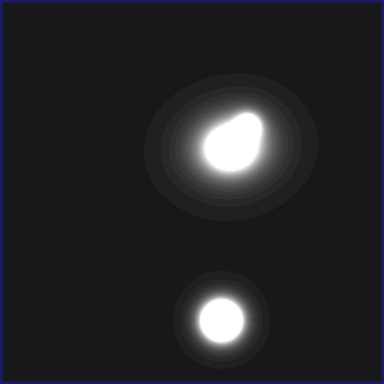

Mrk 501 host galaxy & comparison star, instrumental magnitudes

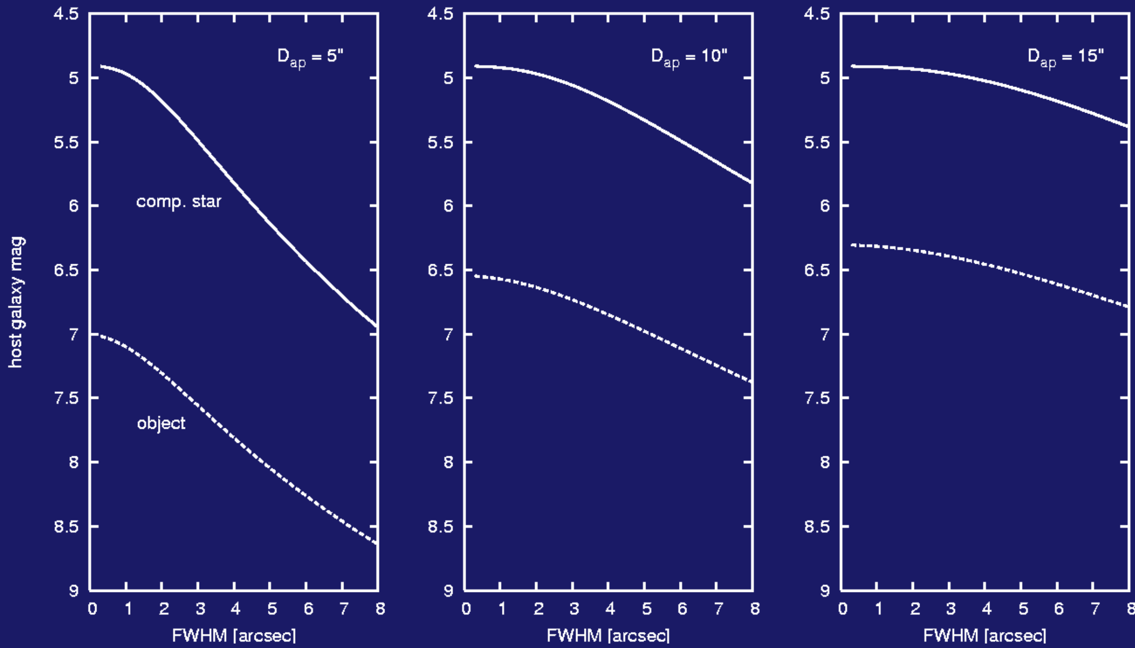

Mrk 501 host galaxy, differential magnitudes

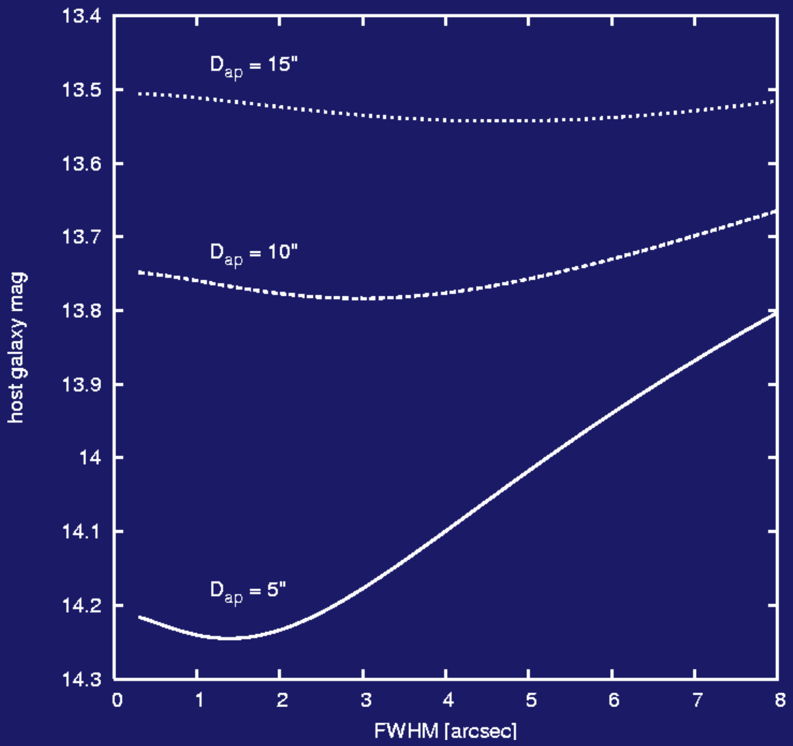

Host galaxy magnitudes, $D_{AP} = 15''$

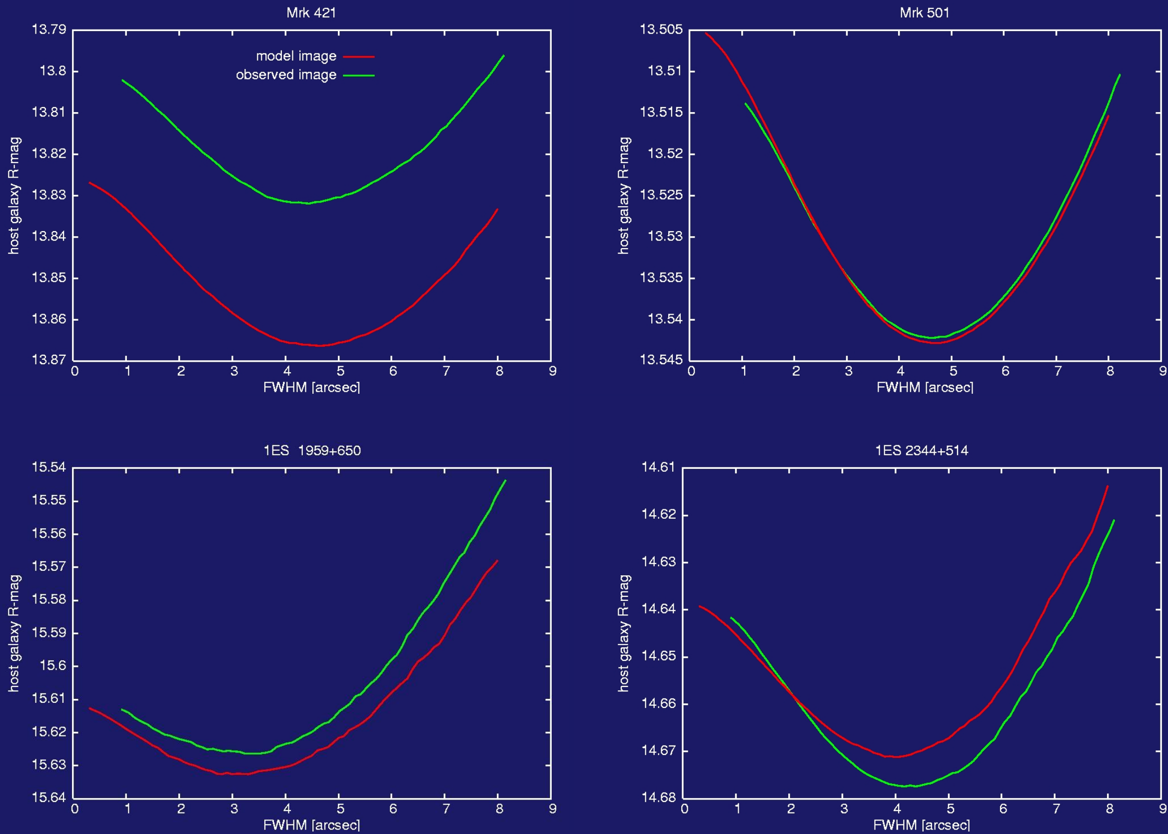

Dependence on PSF shape (1ES 2344+514) :

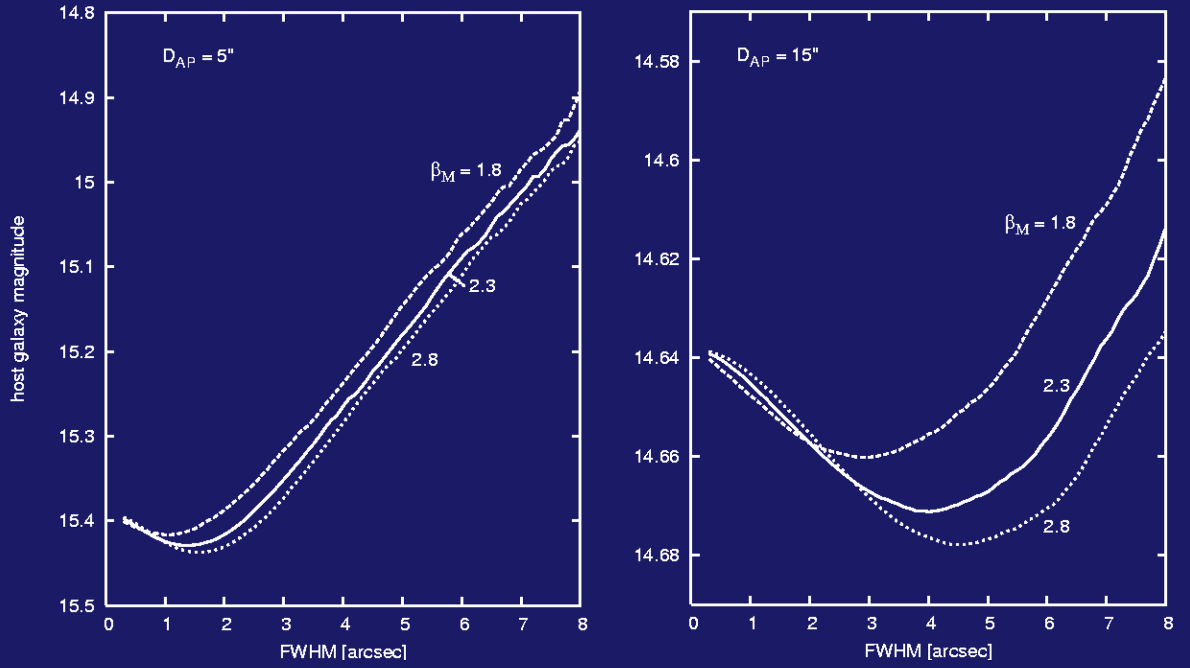

Comparison with observed data ($D_{AP} = 15''$) :

1ES 1959+650

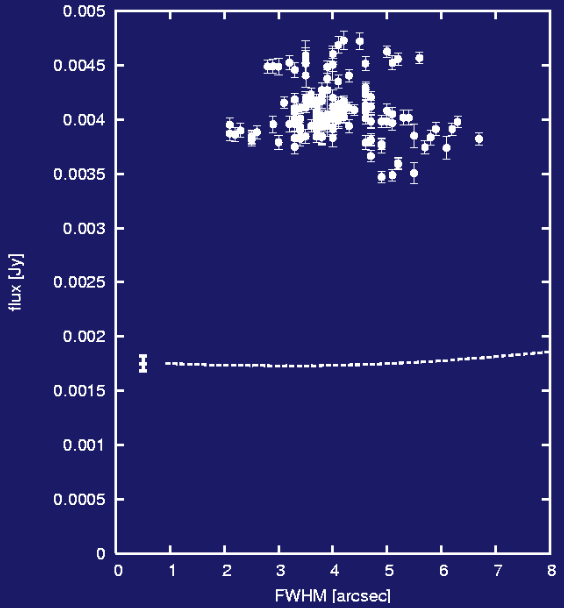

1ES 2344+514

Comparison with observed data ($D_{AP} = 15''$) :

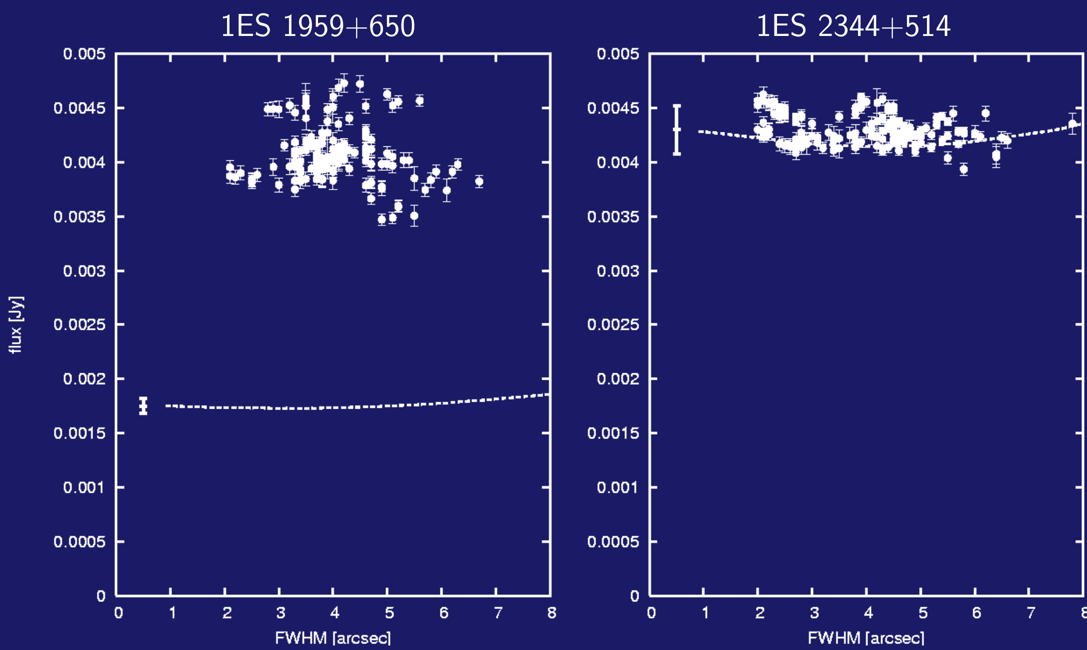

Summary

- 2-dim. model fitting has been used to determine the influence of the host galaxy in differential aperture photometry.
- Both model images and observed images can be used for this task.
- Host galaxy magnitude is a strong function of aperture size, but depends very little on seeing.
- The accuracy is mainly limited by the accuracy of the comparison star magnitudes and calibration of the host images.

Summary

- 2-dim. model fitting has been used to determine the influence of the host galaxy in differential aperture photometry.
- Both model images and observed images can be used for this task.
- Host galaxy magnitude is a strong function of aperture size, but depends very little on seeing.
- The accuracy is mainly limited by the accuracy of the comparison star magnitudes and calibration of the host images.

TBD : more objects, more work on the influence of the PSF shape and fitting errors, better calibration of the comparison stars.

The use of L3 CCD's in High Time Resolved Observations of Blazars

Enigma Meeting
Jerisjärvi, Finland
April 2004

The Teams

EMSSG, CIT:
Alan Giltinan
Niall Smith
Aidan O' Connor
Stephen O' Driscoll
John Howard

Heidelberg:
Stefan Wagner
Marcus Hauser

Overview

- L3 CCD Technology
- Storage
- Reduction pipeline
- Instrument examination
- Variability / Imaging
- Effects on photometry

L3 CCD's (Low Light Level CCD)

Architecture of both conventional and L3 CCD

- Same Photosensitive area
- Same CCD Readout register
- Same output Node

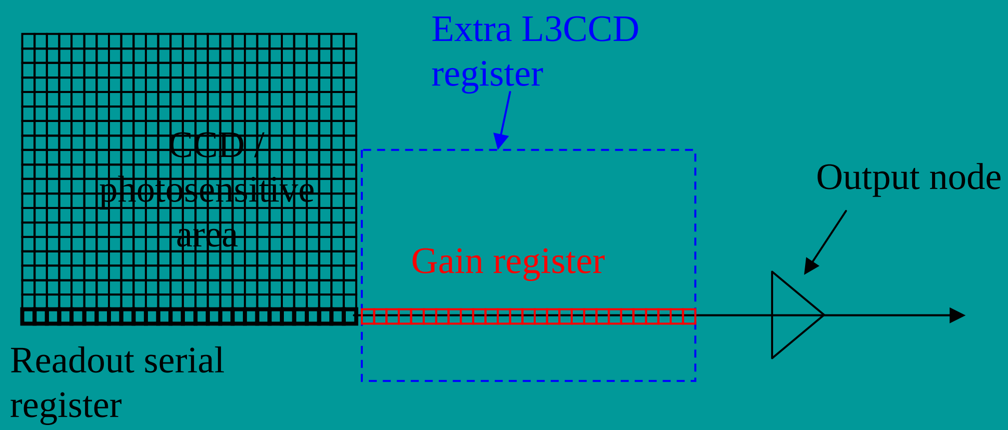

Figure 1. CCD schematic (conventional and L3).

Conventional CCD Readout

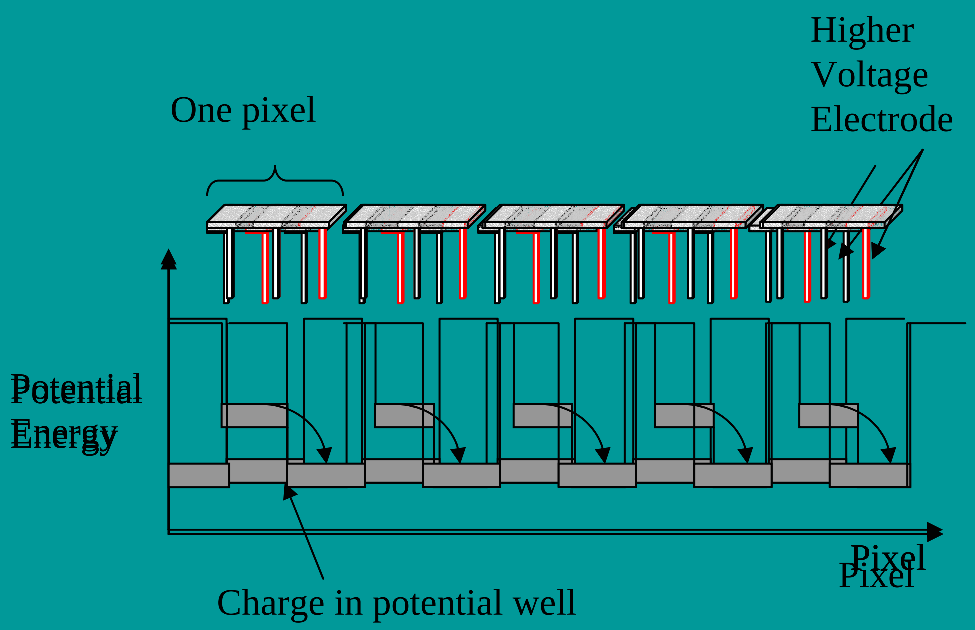

- CCD Readout in sequential manner by inverting voltages
- Electrode potential used to move and contain charge
- Same potential differences used throughout CCD

L3 CCD Gain Register

- Extra electrode held at low dc voltage
- High voltage differences accelerates charge carrier

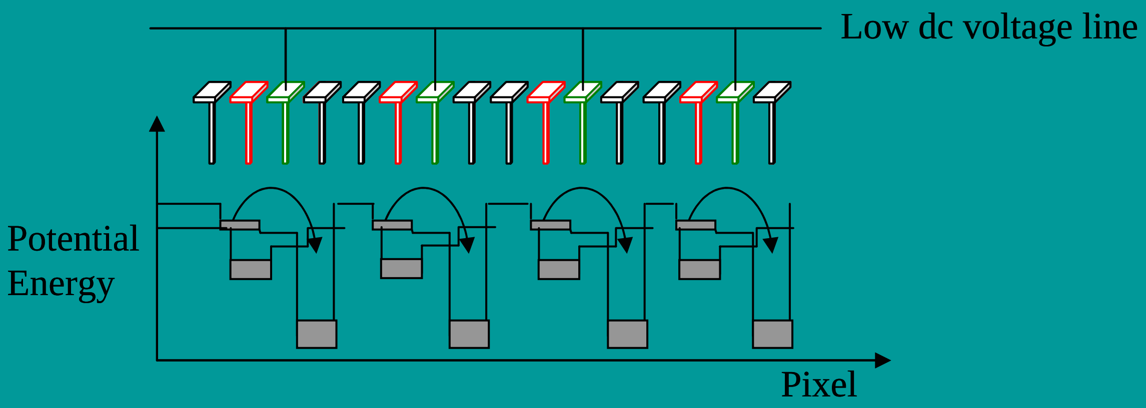

- Impact ionisation frees new charge carriers
- Voltage stability is crucial to gain stability
- Voltage difference controls level of gain

- Probability of multiplication per charge carrier per pixel is small (~1 - 1.5%)

- large number of pixels means the overall gain can be large since

  Total Gain, $M = g^N$

  where, g is (1 + probability)

  N is the total number of pixels

- e.g. with p = 1 and N = 536 (as in E2V CCD87)

  M = 207

  with p = 1.5 and N = 536

  M = 2292

Effects of Multiplication Gain

$$\sigma_{eff} = \sqrt{\left[\mathbf{F}^2\left(S + S_{dark}\right) + \frac{\sigma^2_{readout}}{\mathbf{M}^2}\right]}$$

Where σ_{eff} is the effective image noise

$\sigma_{readout}$ is the readout noise and

M is the total gain

- Making the total gain M large, reduces effect of readout noise
- Amplifying signal prior to readout
- S/N very high prior to readout noise introduction
- Low noise characteristics at high frame rates
- Multiplication Noise effects exist

Cooling the L3 CCD

• Gain value can be affected by temperature variations

• CCD noise can be amplified by gain if

proper cooling is not adhered to

• Effects of cooling can be seen in the following Dark current frames

(Colin Coates, Andor Technology)

-80°C   30 ms dark exposure

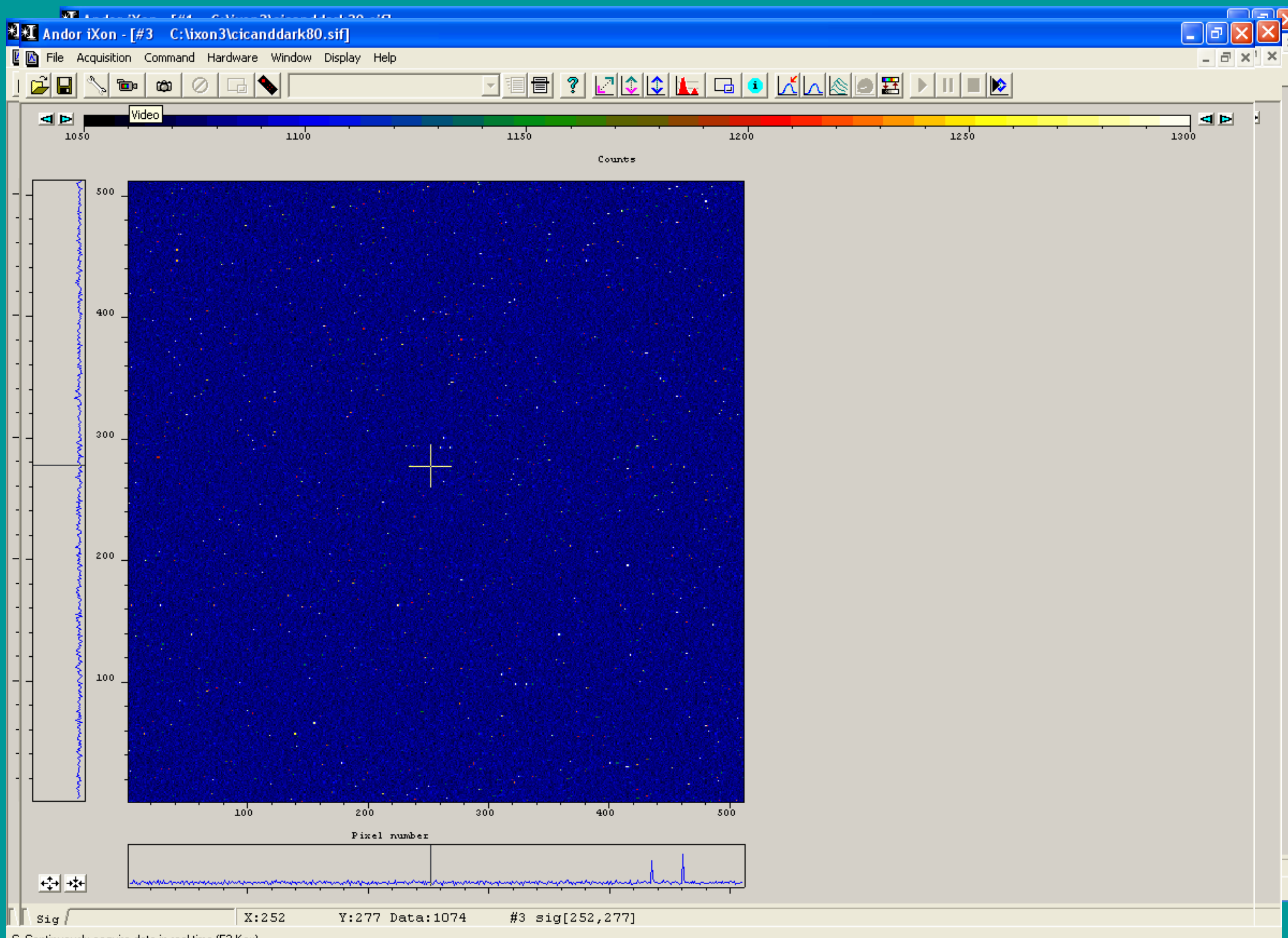

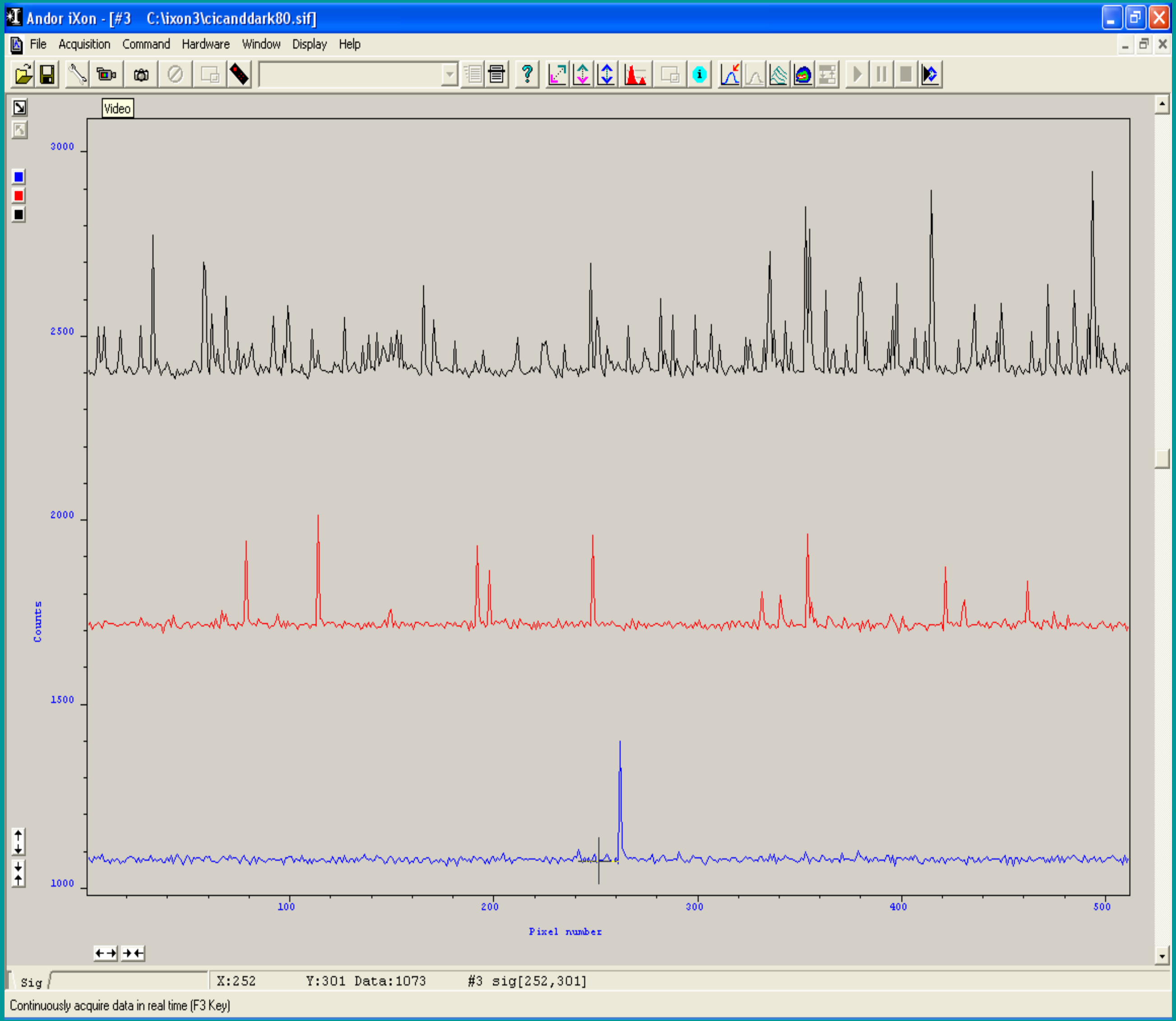

-30 ^{0}C

-50 ^{0}C

-80 ^{0}C

Cooling the L3 CCD

• Gain value can be affected by temperature variations

• CCD noise can be amplified by gain if

proper cooling is not adhered to

• Effects of cooling can be seen in the following Dark current frames

(Colin Coates, Andor Technology)

• Cooling greatly reduces the number of thermal electrons generated

• Stable cooling essential for accurate gain values

STORAGE:

High frame rates with low noise

Large volumes of data

e.g. L3CCD run @ max 32 fps (full frame single mode)

720 GB per night (10 hour night)

Compare to Ultracam (130GB per 10 hour night)

Difficult to store all images in one place

Solution:

Automated reduction

Reduction process

Combination of Linux and Windows based software packages

Step 1: Iraf (Linux)

FITS conversion

↓

CCDPROC (zero & flat)

↓

Selectrefs (star selection)

↓

DOPHOT (magnitude generation)

↓

PREPRESULTS (output file for next stage)

Step 2: Q-Var (Windows)

Center each star and quasar value about zero

↓

Average all centered values for stars (R_{AV})

↓

Generate Q- R_{AV}

↓

Statistical tests

↓

Final Lightcurves

Camera evaluation set-up

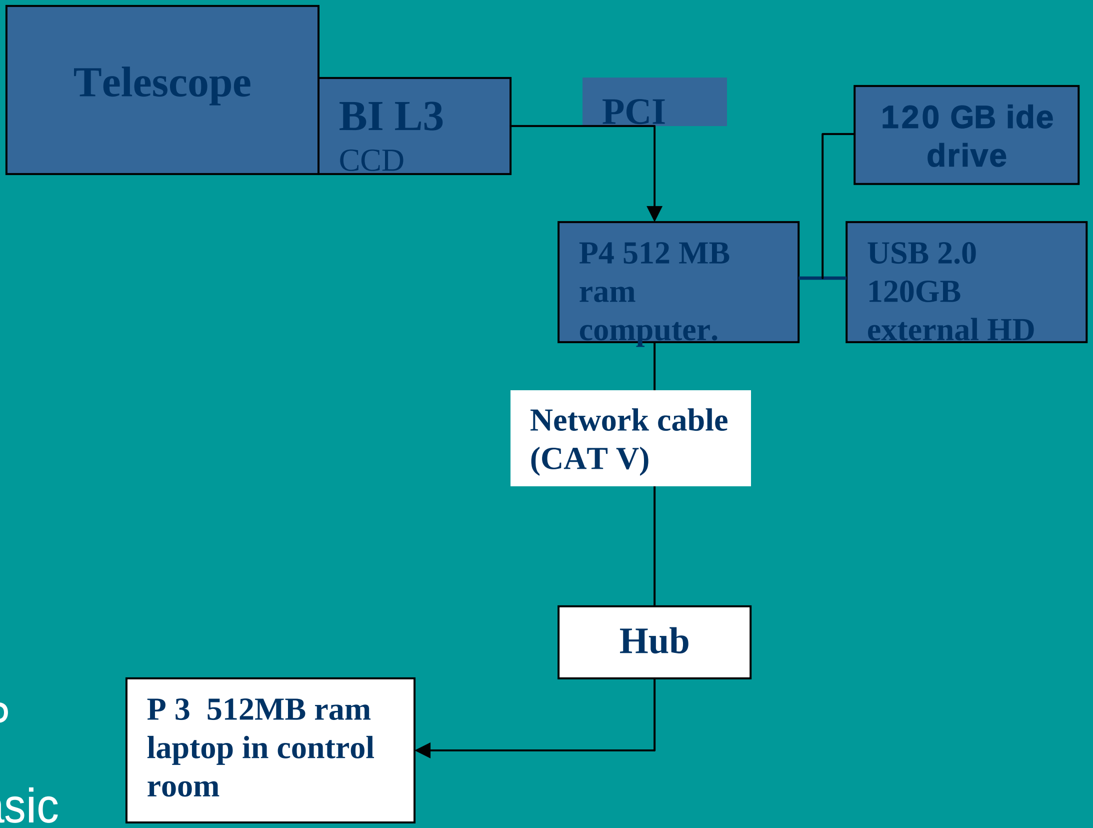

Win XP

Andor Basic

Camera Control

Scriptable Language for basic functions (Andor Basic)

• 2 modes

Single imaging

Kinetics (Stacked) imaging

• Max fps ~10

windowed for storage maximisation

Single windowing only

Results

340,000 frames

230GB.

0716+71 Raw Data (60s averages)

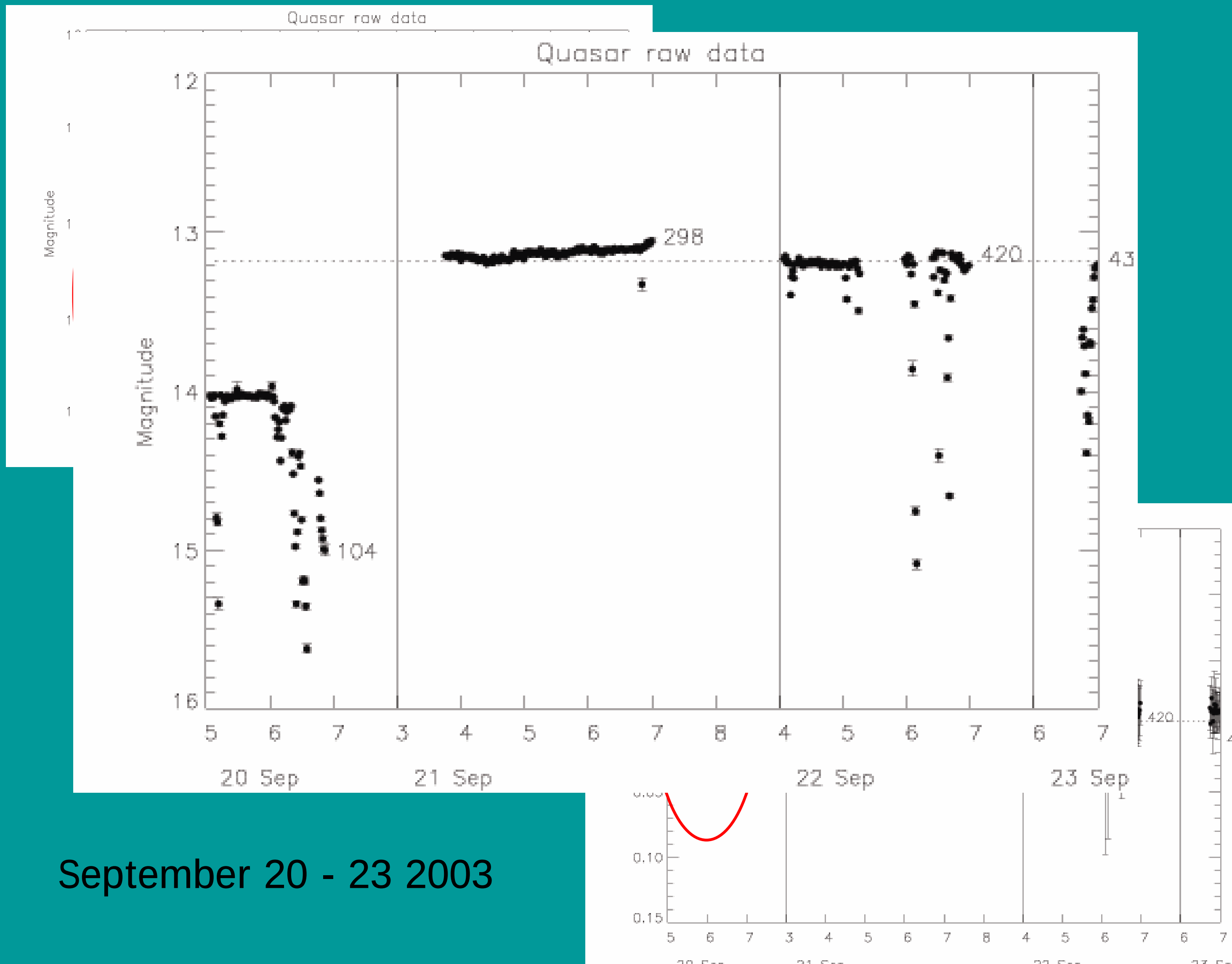

September 20 - 23 2003

0716+71

98345 Frames (60s average)

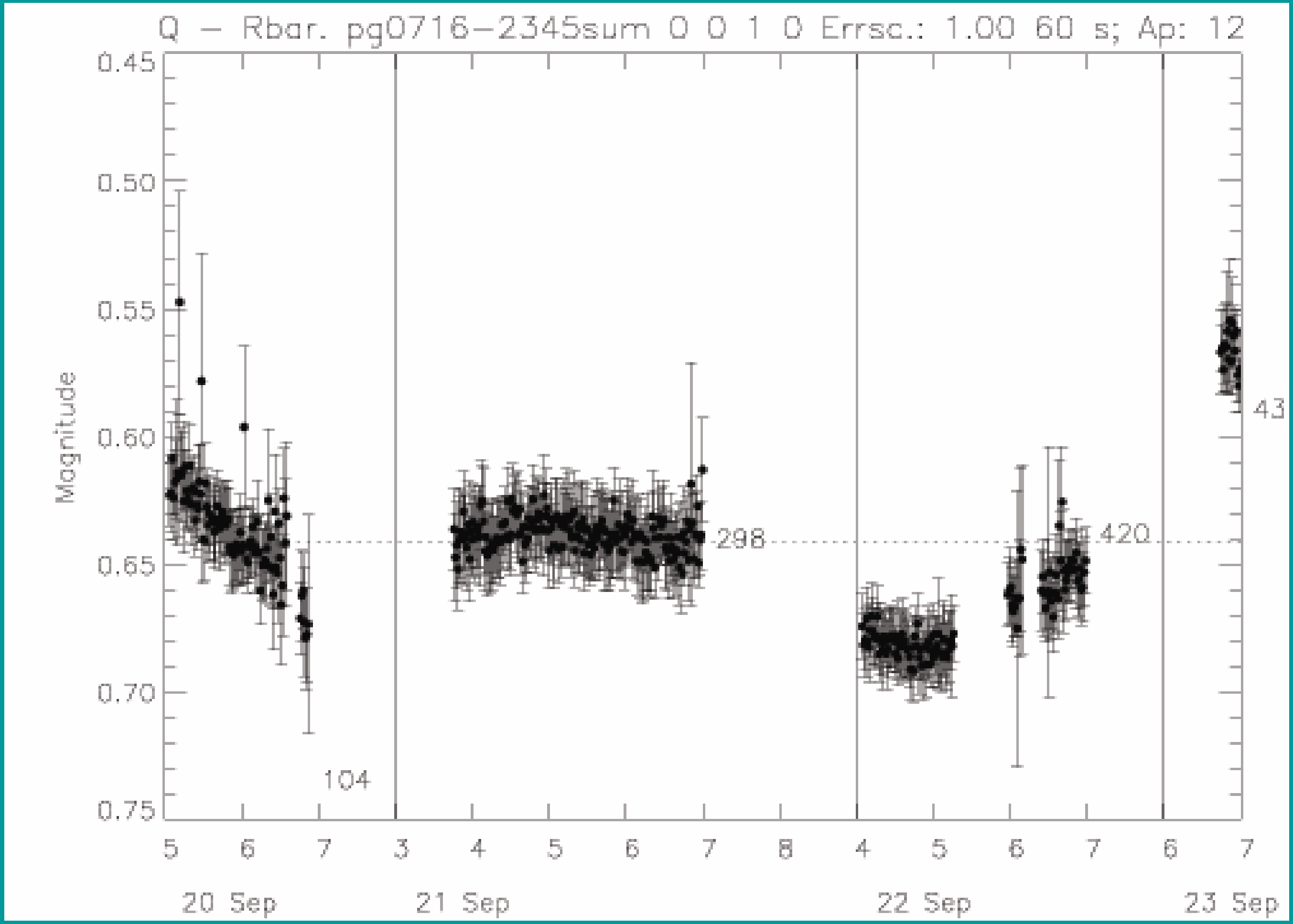

0716+71

35456 FRAMES (Night 1)

60s average

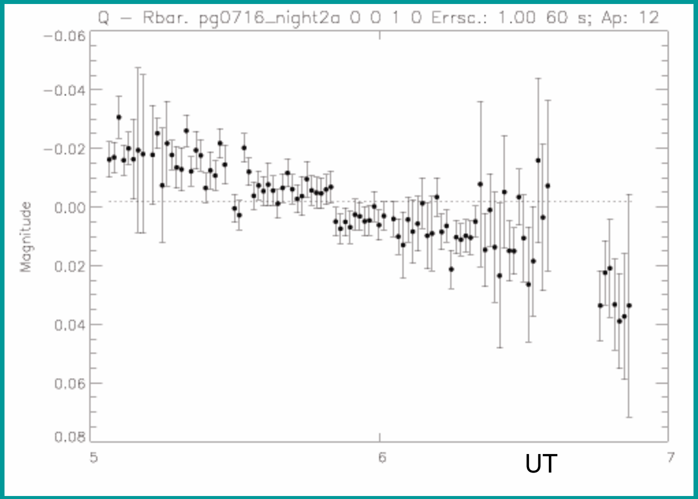

240s average

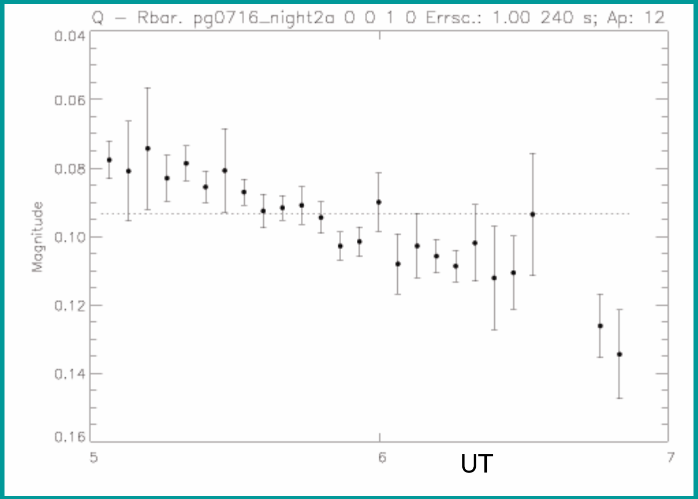

600s average

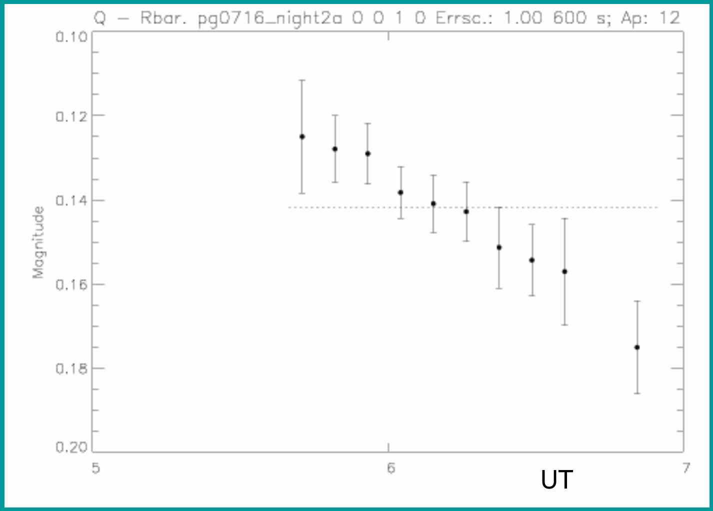

0716+71

36456 FRAMES (Night 3)

60s average

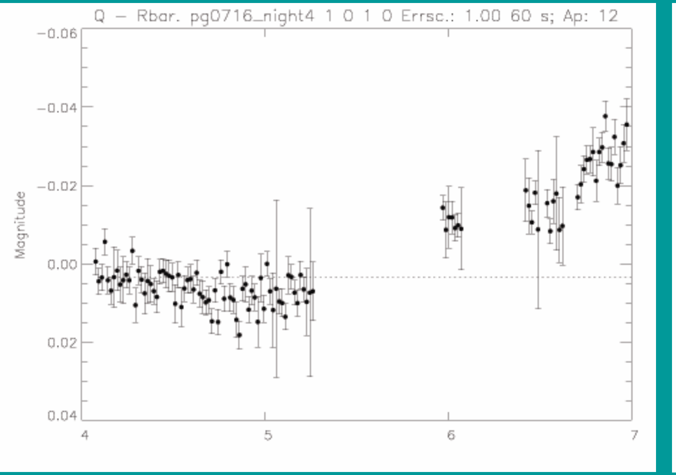

240s average

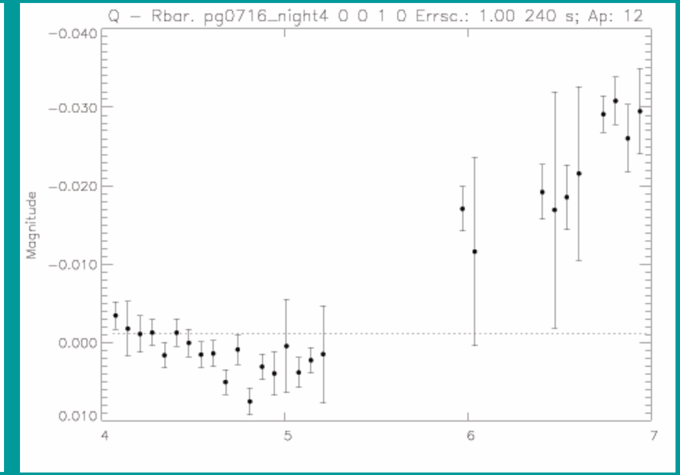

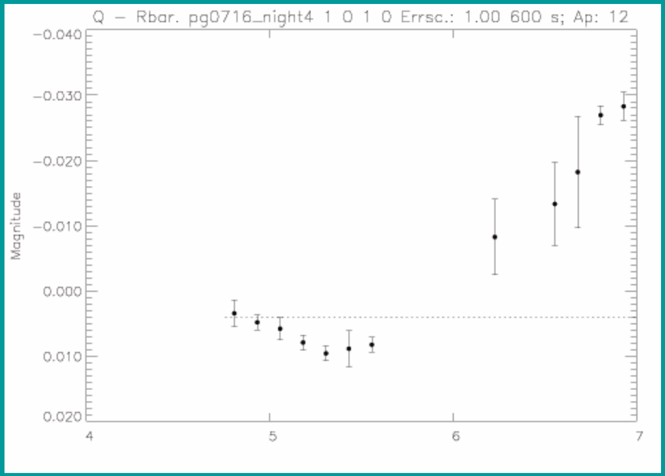

600s average

Effects on photometry

Summed Image of the field of 0716+71

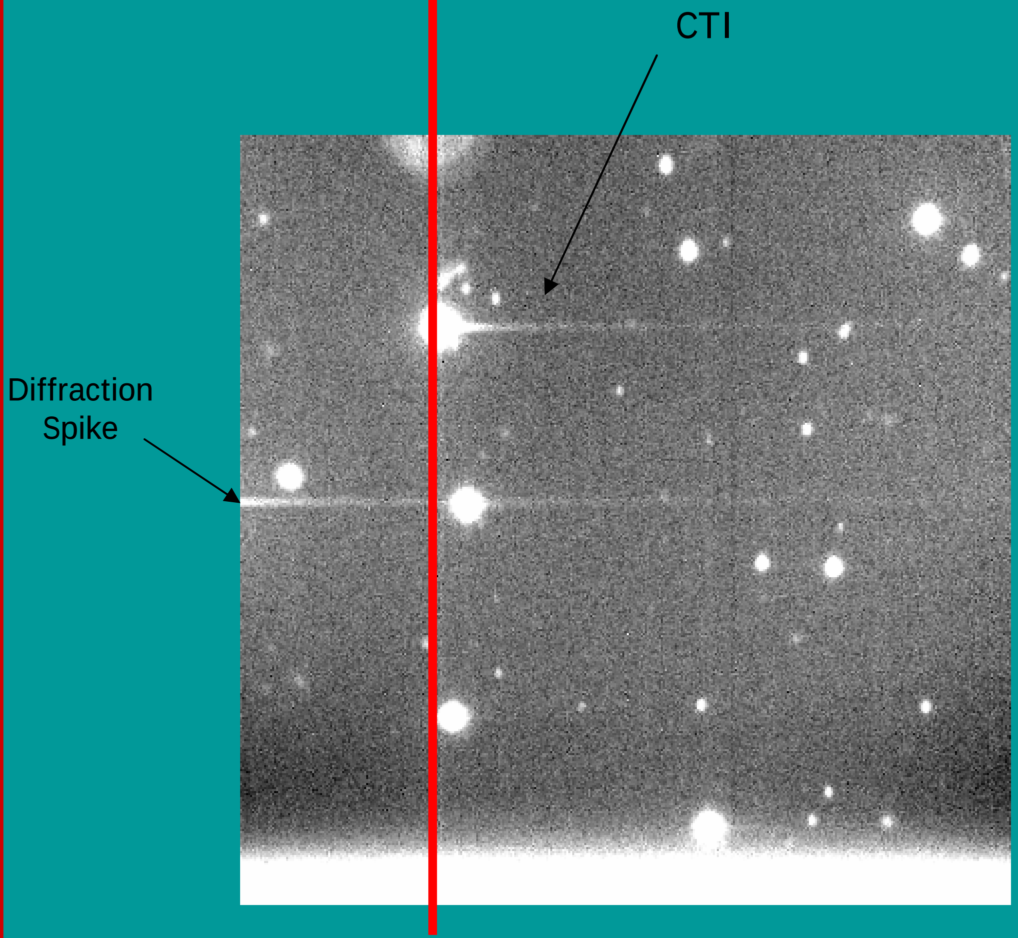

0716+71 sequence

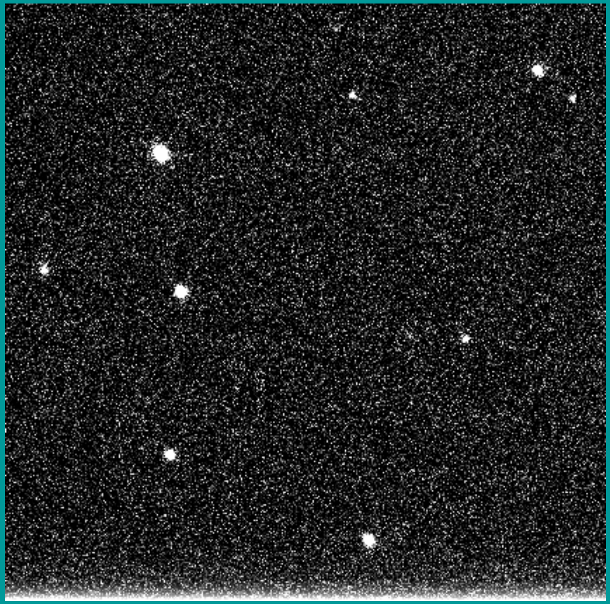

4572
frames

Serial/Gain
Register?

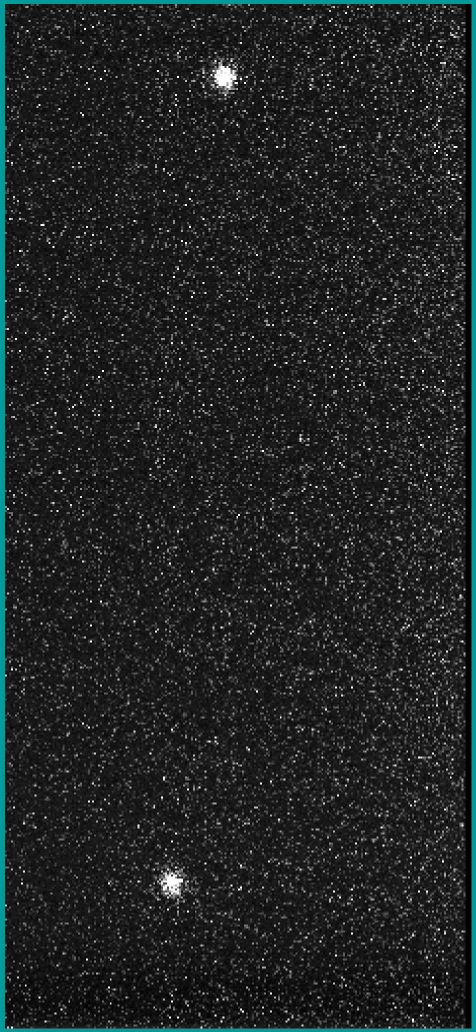

0716+71 real-time imaging

Conclusion

High frame rates

Very large data sets

Standardised online reduction pipeline

Photometric accuracy limited by

Atmospheric effects

Is it the best CCD?

Application

Low light levels

Photon counting

The robotic telescope ATOM

ENIGMA meeting April 2004

M. Hauser, C. Möllenhoff, G. Pühlhofer, L. Schäffner, S. Wagner
Landessternwarte Heidelberg, Germany

H. Hagen, M. Knoll
Sternwarte Hamburg, Germany

Overview of ATOM

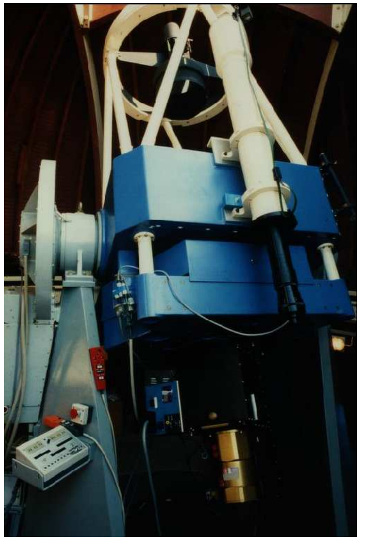

The telescope

- 76 cm main mirror, Ritchey-Chrétien type
- Zeiss prototype for AltAz mounting, ≈ 25 years old
- Still at Landessternwarte, preparations for robotic mode finished, dismantled and waiting for transport to Hamburg

Overview of ATOM

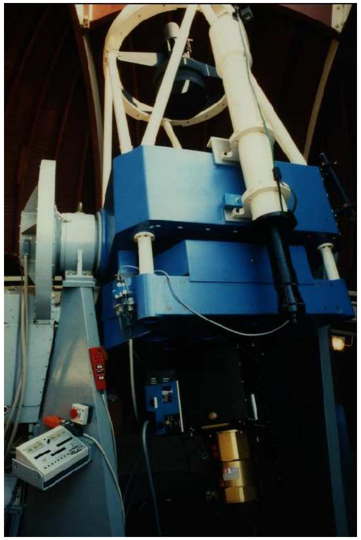

The telescope

- 76 cm main mirror, Ritchey-Chrétien type
- Zeiss prototype for AltAz mounting, $\approx$ 25 years old
- Still at Landessternwarte, preparations for robotic mode finished, dismantled and waiting for transport to Hamburg

Goal

- fully robotic telescope @ H.E.S.S. site
- first stage: only contemporaneous observations with H.E.S.S., later (hopefully): extension to moon time

Overview of ATOM

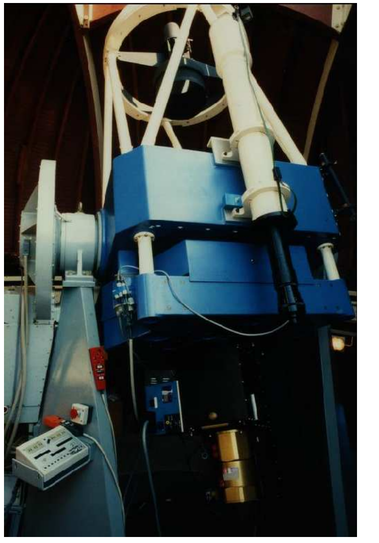

The telescope

- 76 cm main mirror, Ritchey-Chrétien type
- Zeiss prototype for AltAz mounting, $\approx$ 25 years old
- Still at Landessternwarte, preparations for robotic mode finished, dismantled and waiting for transport to Hamburg

Goal

- fully robotic telescope @ H.E.S.S. site
- first stage: only contemporaneous observations with H.E.S.S., later (hopefully): extension to moon time

Science

- AGN monitoring
- runs in H.E.S.S. slave mode whenever requested
- atmospheric monitoring

Overview of ATOM - continued

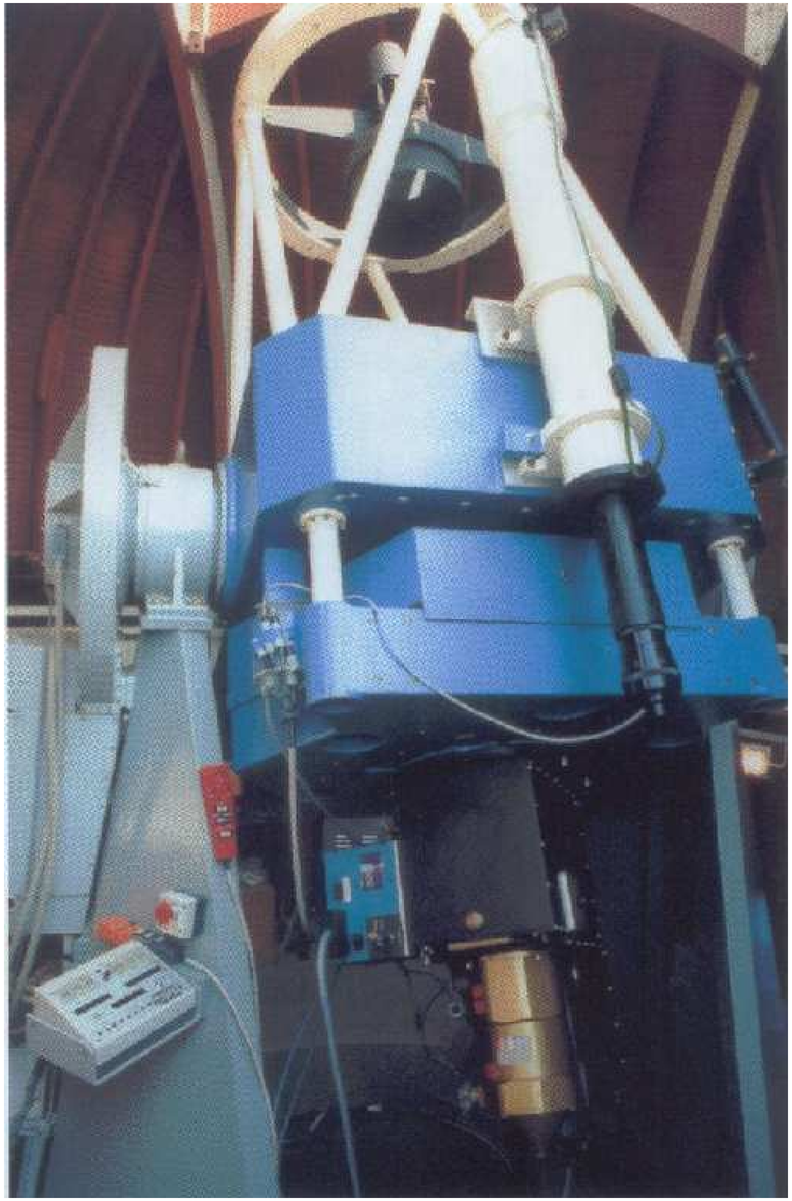

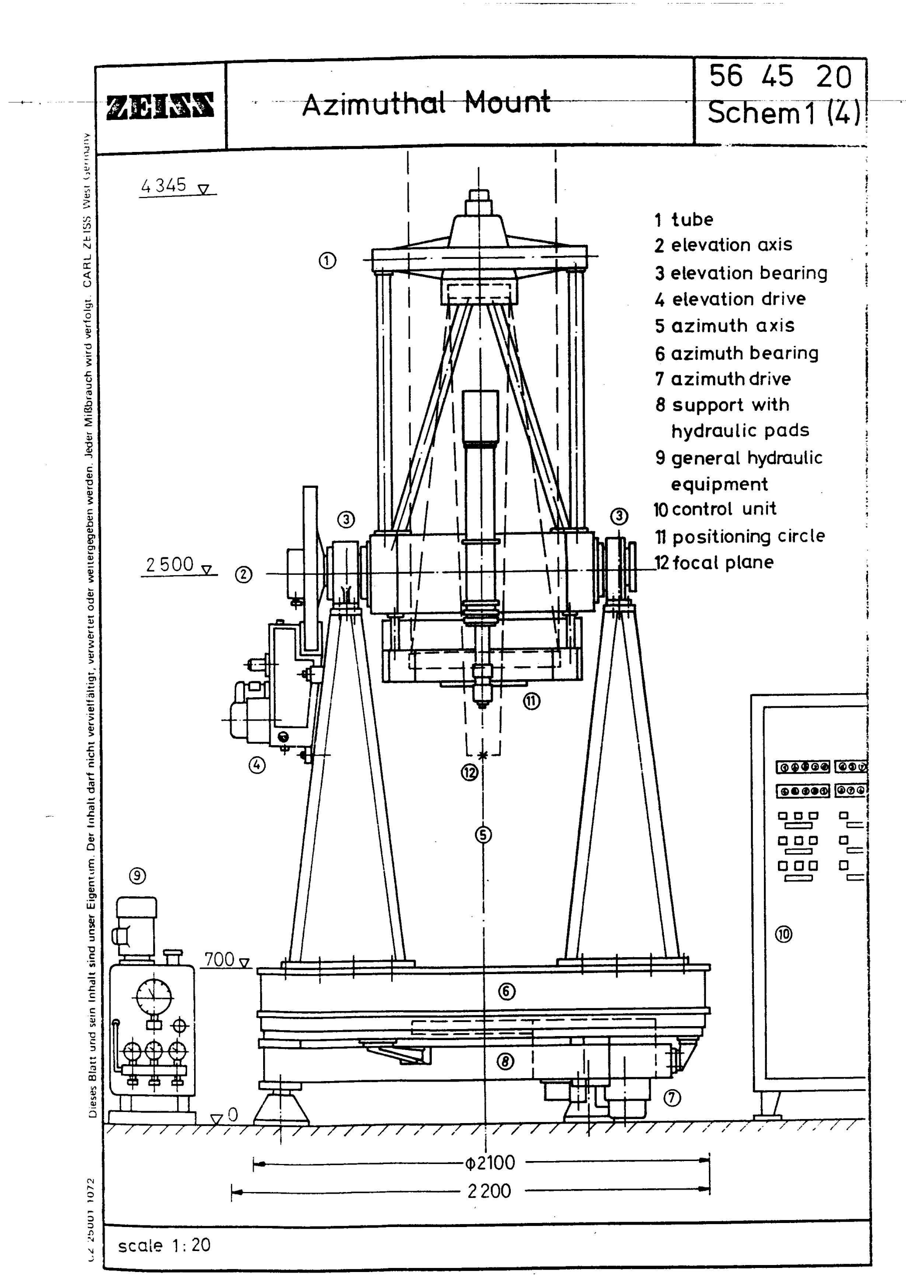

Rough timeline

@ Heidelberg (HD)	@ Hamburg (HH)	@ Namibia
components check, some automatisation	steering software	
preparation of disassembly	assembly of tel control hardware	
Software development		site decision
(robotic mode, instrument, data analysis)		
dome decision + basement plans		negotiation with NEC
tests of possible science cameras	STELLA leaves Sternwarte HH	about building
move telescope to Hamburg		
decision for science camera	recoating of mirrors	construction of
instrument / analysis software	assembly of telescope	basement and
order dome	electronics + motors tests	building walls
buy + test science CCD camera	software / DAQ tests	
	(preliminary camera)	
move telescope to Namibia		
		dome assembly
		telescope assembly
		testing

Future location of ATOM (H.E.S.S. - Site, Namibia)

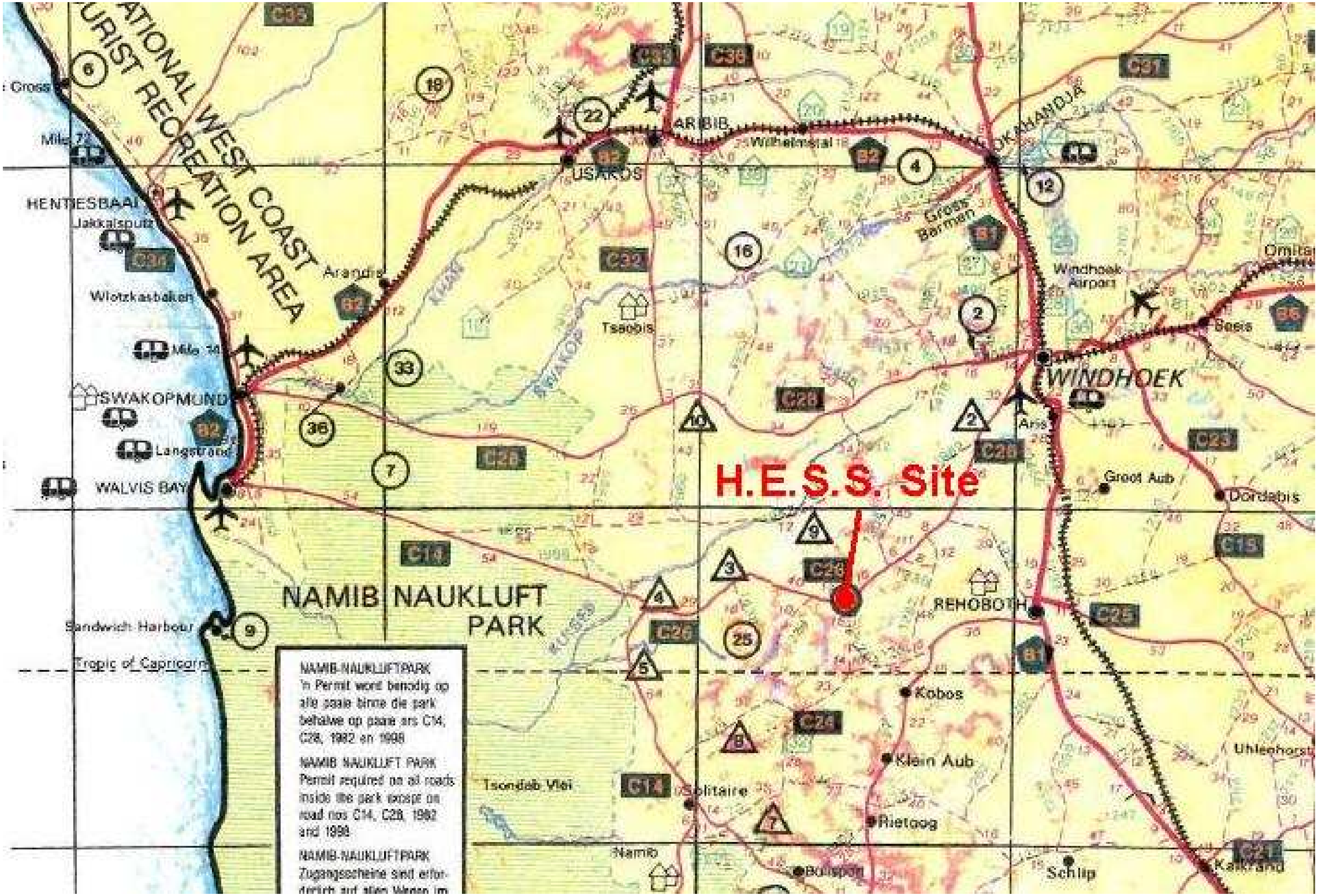

The H.E.S.S. Experiment

- Array of four Cherenkov telescopes
- each dish has a diameter of 13m
- total mirror area: 108m^2 each

Component tests+replacements/automatisation @ HD

- telescope motors + hydraulics tested and working
- motorized mirror cover tested and ready
- new shaft encoders bought, one in HH for system development, one already assembled
- focus motor: tested and working

Mirror cover

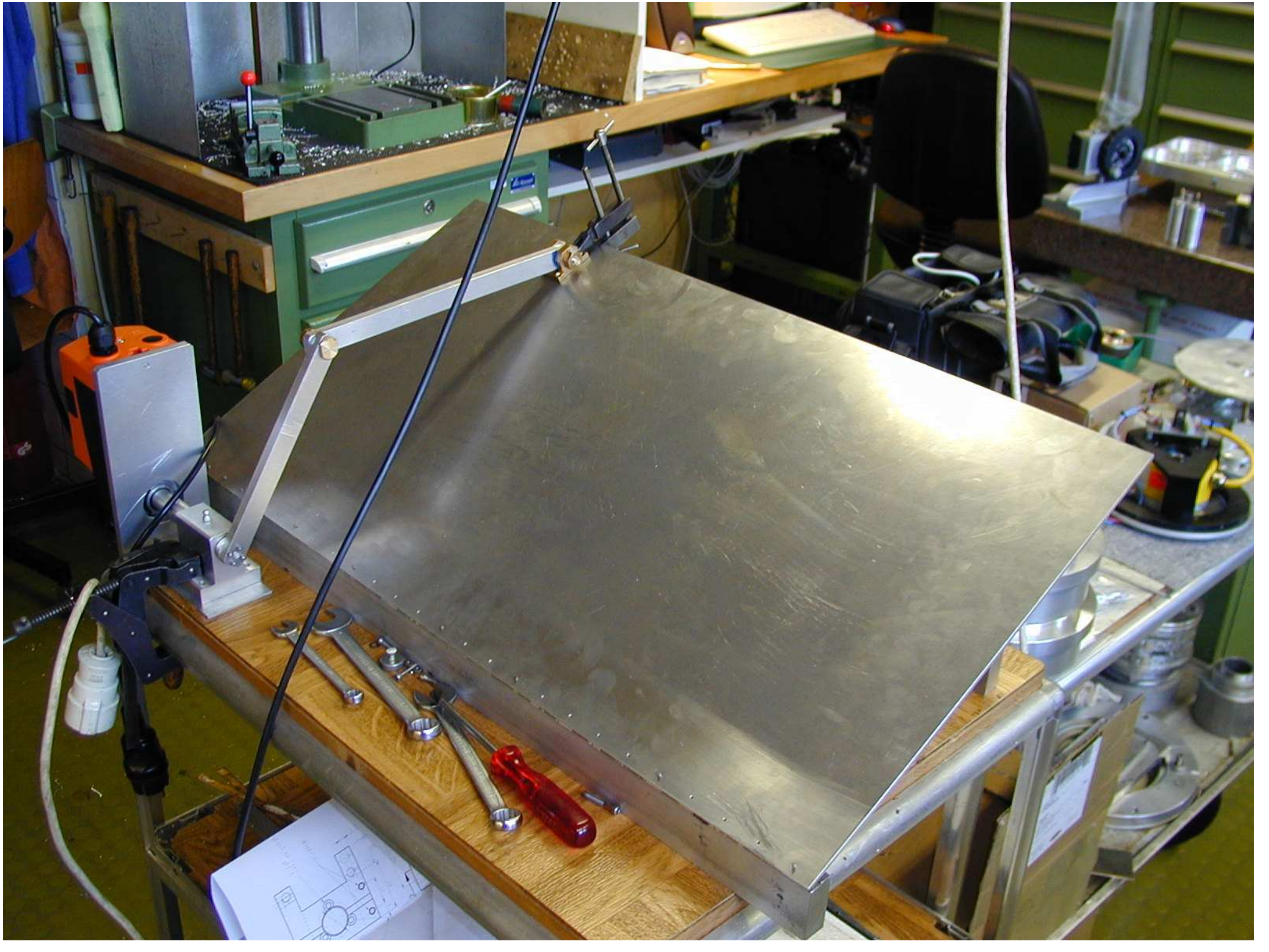

Disassembly of the main mirror

Status @ HH

H. Hagen, M. Knoll

- group experienced in robotisation of existing telescopes
- Software module for telescope steering interface written, needs to be tested
- Control cabinet: all parts delivered, assembly nearly finished
- waiting for STELLA to leave the "dome" where ATOM will be tested (scheduled for next week)

Telescope building ("dome")

- blueprint: Tarot container
- drawings @ HD refined
- contact with NEC (Namibia) in November 2003
- not affordable

Pro Dome 15

- HomeDome,
  Gaithersburg, Maryland, US
- d = 4.34m
- slit width = 1.21m
- cost about 16kEuro

Pro Dome 15

- HomeDome, Gaithersburg, Maryland, US
- d = 4.34m
- slit width = 1.21m
- cost about 16kEuro

Software, Science camera

Software

- layout settled
- software components being tested
- still major work
- concerning data analysis: hope to profit from ENIGMA photometry-workgroup

Software, Science camera

Software

- layout settled
- software components being tested
- still major work
- concerning data analysis: hope to profit from ENIGMA photometry-workgroup

Science CCD camera

- must be Peltier-cooled CCD
- serious camera test in june (Andor iXon L3, see previous talk by A. Giltinan)
- final decision (hopefully) soon

Steps to be done (conclusion)

- Site decision √
- finish movable parts, disassembly of mount in HD √
- transport to Hamburg next week, (re-)assembly
- test phase in Hamburg
- Dome, basement building
- transport to Namibia, assembly
- test phase

- **have a fully robotic telescope in Namibia**

If you have any suggestions for this project, please tell me!

special points of interest at this moment are

- cheap domes
- filter wheels
- astrometric software (to check the pointing)

Separating intrinsic and extrinsic IDV

Stefan J. Wagner
Landessternwarte
Heidelberg
Germany

Jerisjärvi 3[nd] ENIGMA meeting April 26, 2004

Intra-Day Variability (IDV)

IDV: Variations on time-scales of 100 000 sec.

Radio-IDV at face value implies r ~ $\mathcal{D}$ 200 AU, and thus very high photon densities.

Photon densities <=> brightness temperatures

$$T_B \propto D^2 \frac{S}{\nu^2} \left[\frac{1}{\Delta t_{obs}(1+z)} \right]^2 < T_{IC}$$

Limit to photon densities

Efficient particle acceleration leads to high u_{rad}, and thus to efficient IC scattering.

Self regulation through IC catastrophe

$$\frac{L_C}{L_S} = 0.5\left(\frac{T}{10^{12}}\right)^5 \nu \quad \left[1 + 0.5\left(\frac{T}{10^{12}}\right)^5 \nu\right]$$

Variability implies high photon-density/compactness.

Maximum value: log T ~ 12

The IDV problem

IDV: Variations on time-scales of 100 000 sec.

$z \sim 1$, $S \sim 0.1$ Jy, $\nu \sim 5$ GHz

$$T_B \propto D^2 \frac{S}{\nu^2} \left[\frac{1}{\Delta t_{obs}(1+z)} \right]^2 < T_{IC}$$

Inferred brightness temperatures up to 10^{17} K,
i.e. >100000 above IC limit!

Possible solutions

$$T_B \propto D^2 \frac{S}{\nu^2} \left[\frac{1}{\Delta t_{obs}(1+z)} \right]^2 < T_{IC}$$

Concept wrong

Distances wrong
Fluxes wrong
Diameters wrong
Limit invalid
Limit wrong

Extrinsic mechanisms

Non-cosmological redshifts
Relativistic amplification
Geometry
Ongoing IC catastrophes
Radiation mechanism

Interstellar Szintillation

Unavoidable as atmospheric szintillation

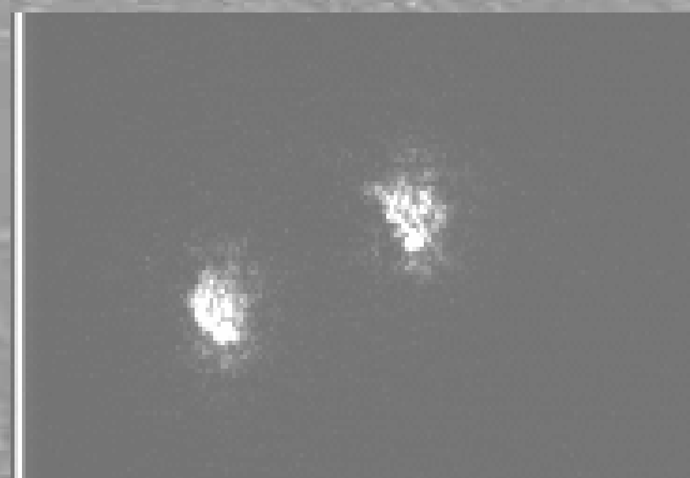

Intrinsic variability?

Radio-optical IDV

Highly significant correlations:

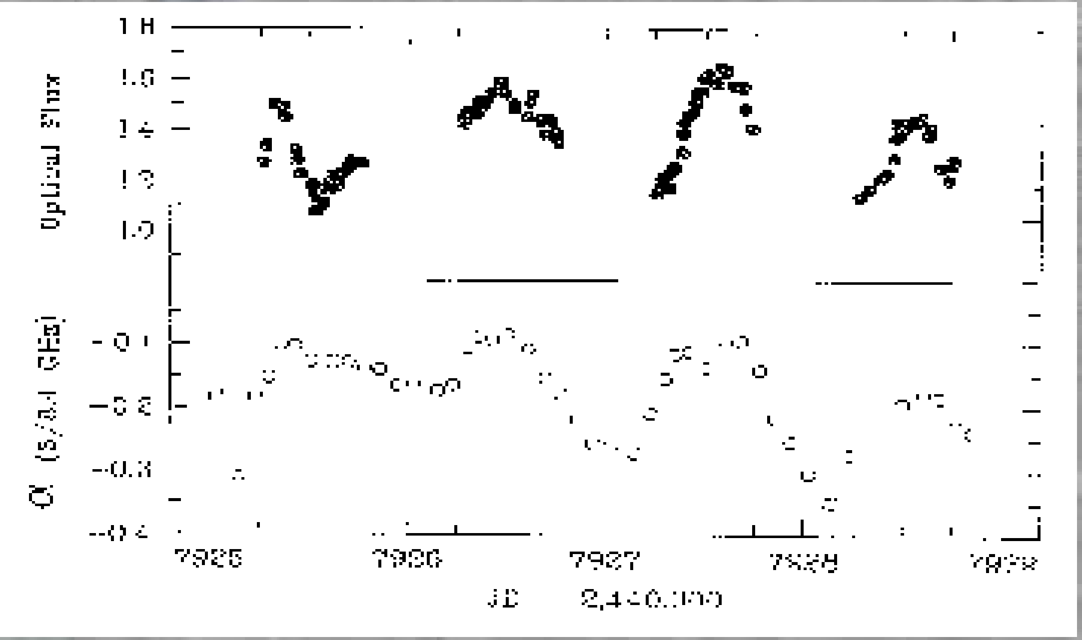

Is this a chance coincidence (not always correlated)?

Time-scales of variability

Structure functions: $P = kt^N$
with break on time-scale
t ~ 100 ksec (~1 day)
over a wide frequency range
in many sources

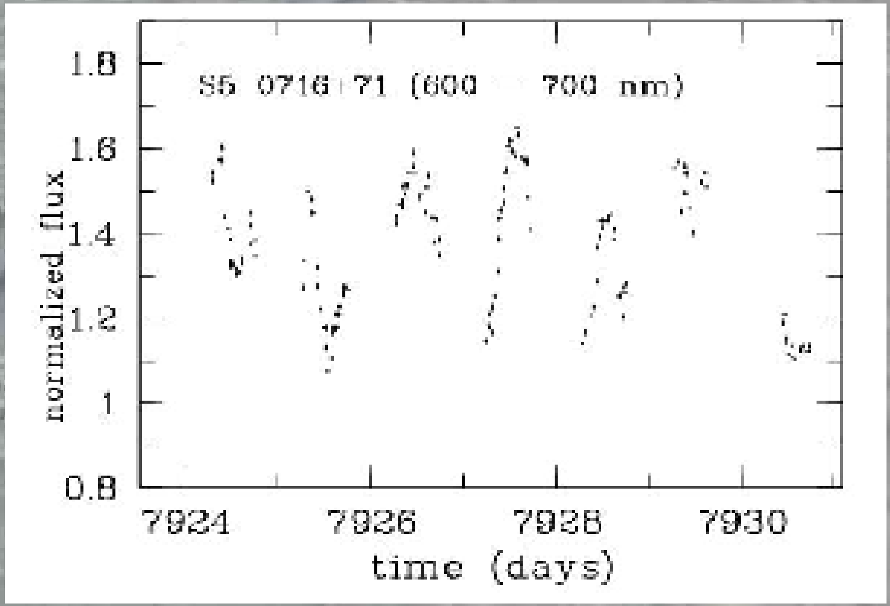

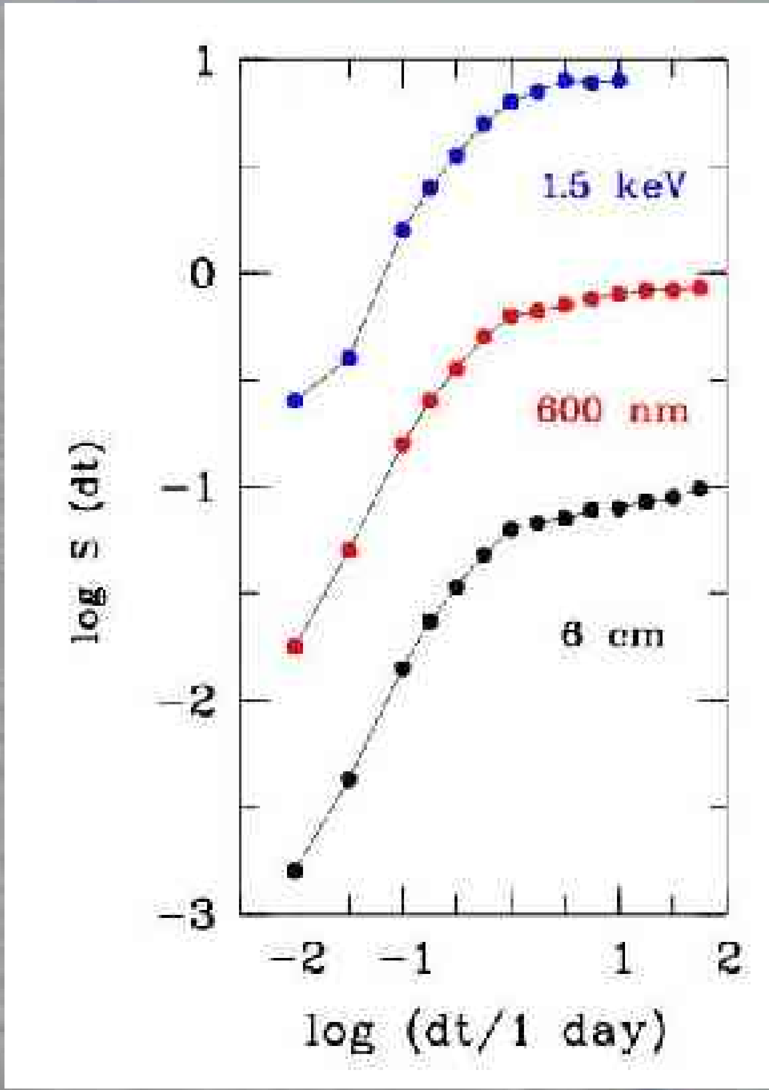

Intrinsic IDV dominates ?

Intrinsic IDV has similar characteristics throughout EM spectrum

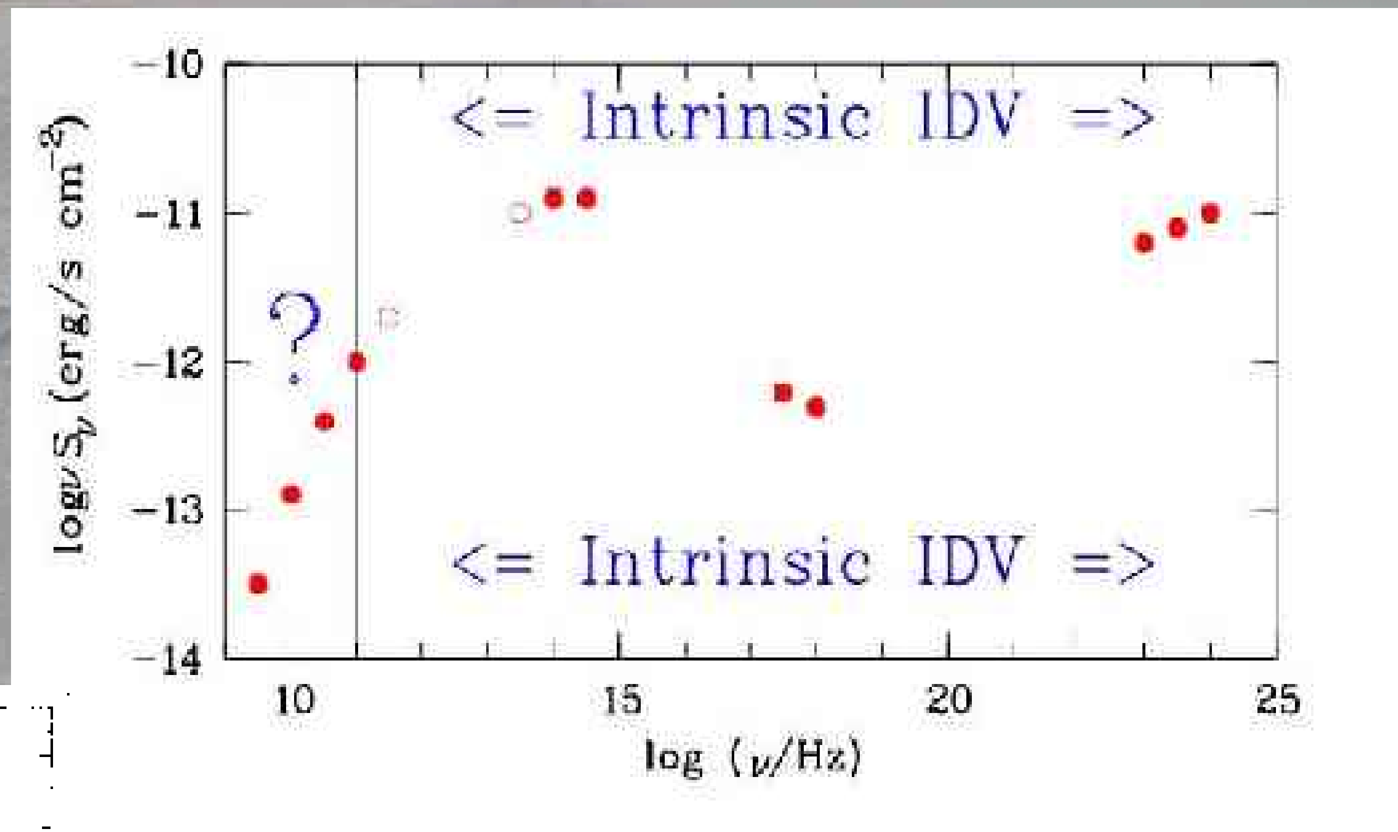

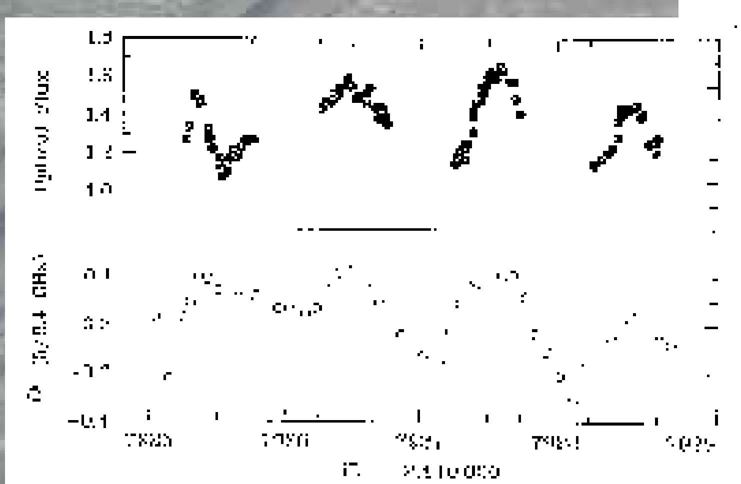

Can intrinsic radio IDV be avoided?

Host Galaxies of Compact Steep Spectrum Radio Sources

Mirko Tröller
Metsähovi Radio Observatory

ENIGMA Meeting
April 26th 2004
Jerisjärvi, Finland

in collab. with
Merja Tornikoski, Metsähovi
Esko Valtaoja, Tuorla Observatory

Outline

Introduction

Observation / the sample

Analysis / aim of the work

Preliminary results

Introduction

Powerful radio source population

I. compact gigahertz peaked spectrum (**GPS**) sources

radio sizes smaller than 1kpc (NLR size scale)

II. compact steep spectrum (**CSS**) sources

radio sizes of ≤15kpc, subgalactic proportions

III. large scale Fanaroff-Riley II (**FR II)** galaxies

radio structure expanded beyond the host galaxy

Properties of CSS Radio Sources

- compact, small intrinsic size ≤ 15 kpc
- high luminosity (like 3CR doubles)
- steep spectra $\alpha \leq 0.5$
- peaked around 100MHz
- turnover frequency varies with size $\nu \propto l^{-0.65}$
- low polarisation
- superluminal motion appears to be rare

Evolution Scenarios

Why are GPS/CSS radio sources small?

The long time riddle of GPS/CSS radio sources:
young vs. ***frustrated***

young:

- hot spot velocity
- radiative age
- radio luminosity evolution

frustrated:

- too many
- suppressed by unusal ISM (density/turbulence/merger)
- alignment effect @ all z

youth scenario is most likely

Evolution of Radio Loud AGN

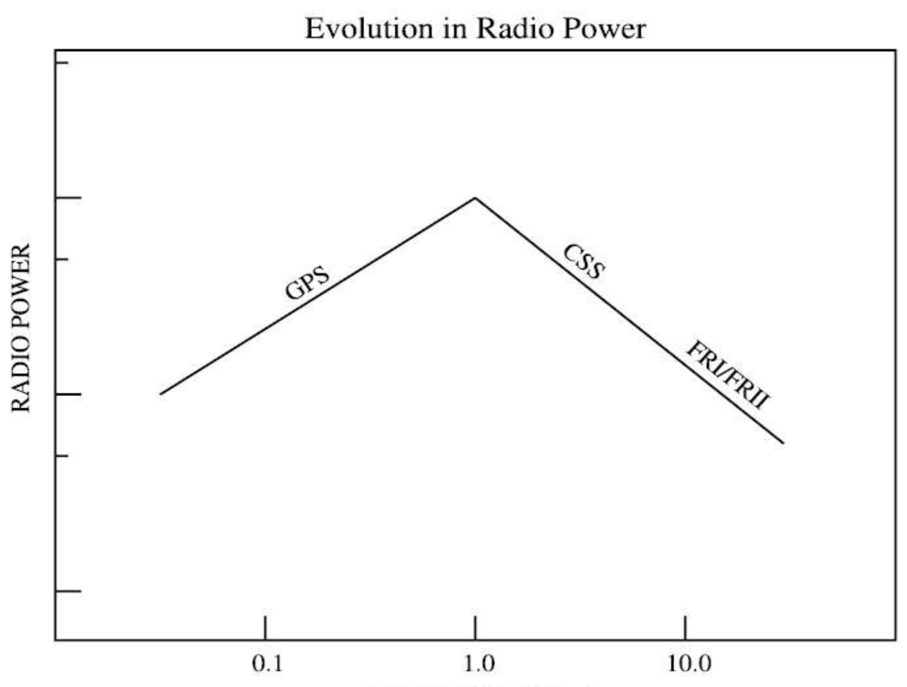

Snellen et al 2000

Evolution of radio power as a function of linear size

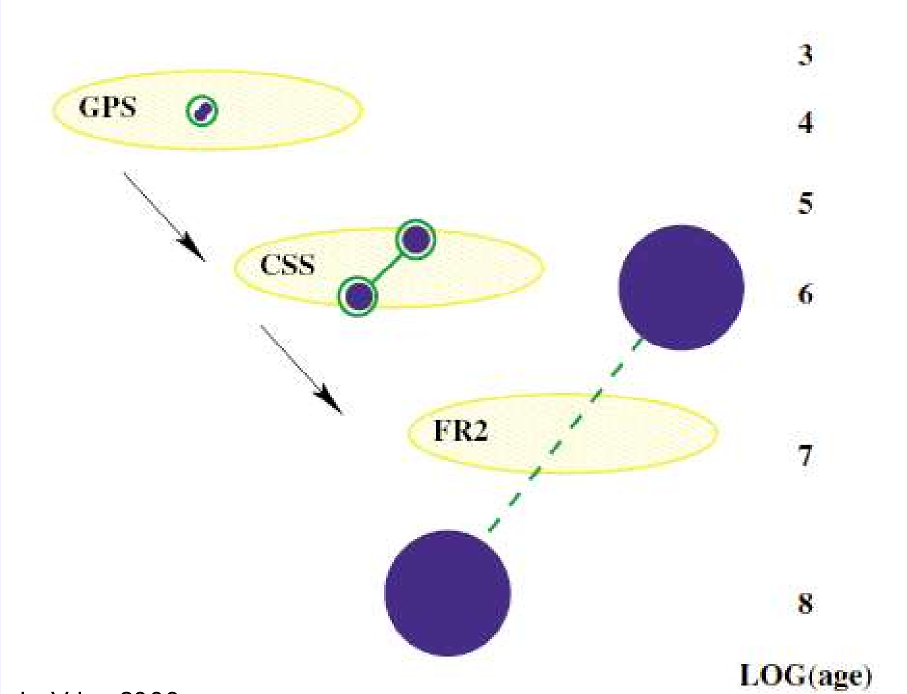

de Vries 2003

Radio source evolution:
the GPS - CSS - FRII sequence

Observation / The Sample

Complete sample of 55 CSS sources from 3CR

28 galaxies, 27 QSOs

broad-band images in R and V

t_{int} = 600 - 1800 sec

observed at the NOT

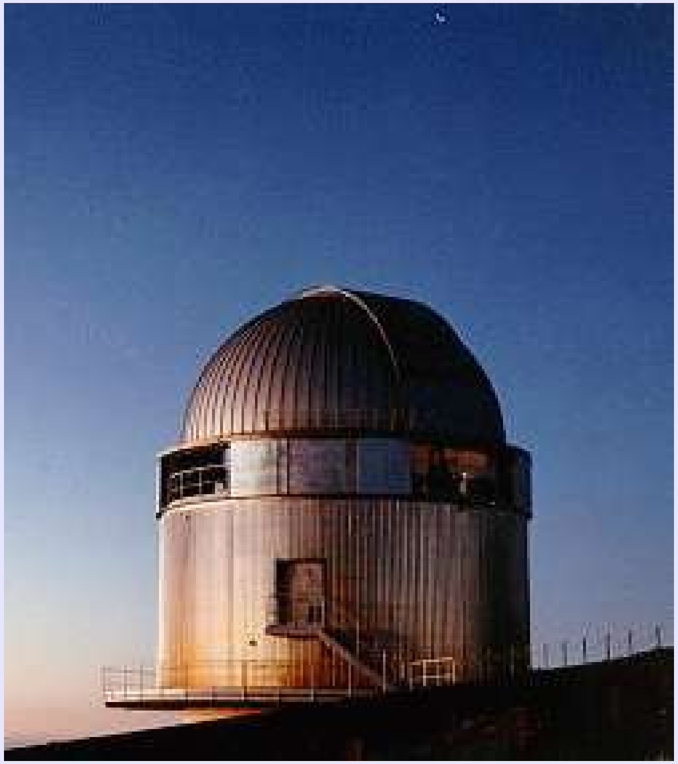

NOT, La Palma, Spain
d = 2.5m, Alfosc 2k x 2k

The Sample

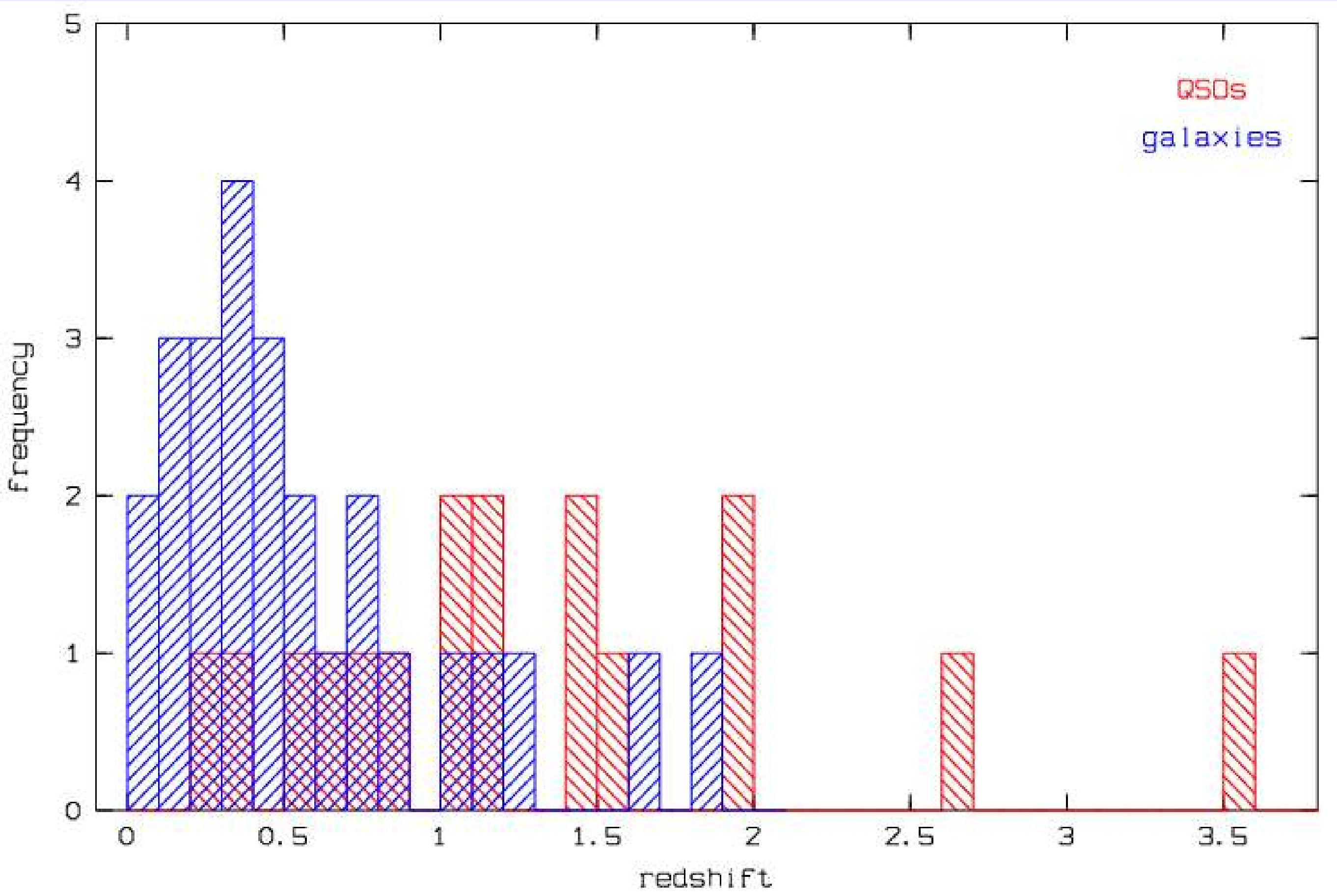

Redshift distribution : galaxies - QSOs
only 4 galaxies at redshifts greater than 1

Aim of the Work

- Identifying interacting/merging systems by searching for distributed optical morphology
- Estimating the local galaxy density
- Detailed comparison between the radio and the optical morphology
- Determining V-R colours to constrain the age of the stellar population
  - probing the evolution scenarios
  - alignment between radio and optical
  - study environment properties of the hosts

Optical/Radio

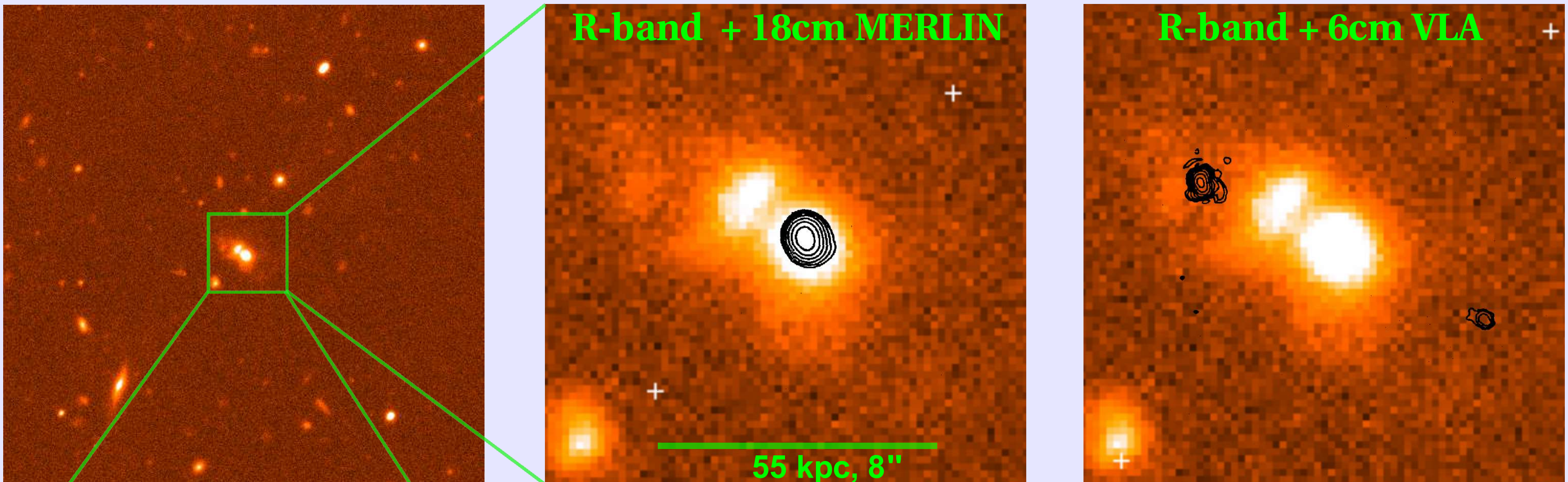

(MERLIN,VLA Spencer et. al)

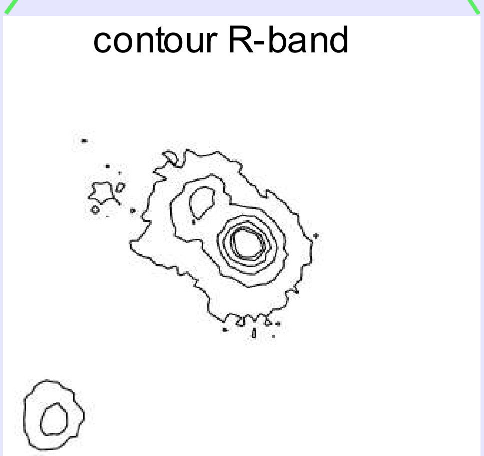

3C299 galaxy @ z=0.37
- distributed optical morphology
- close companions
- alignment radio and optical

Mirko Tröller
Metsähovi Radio Observatory

Optical/Radio

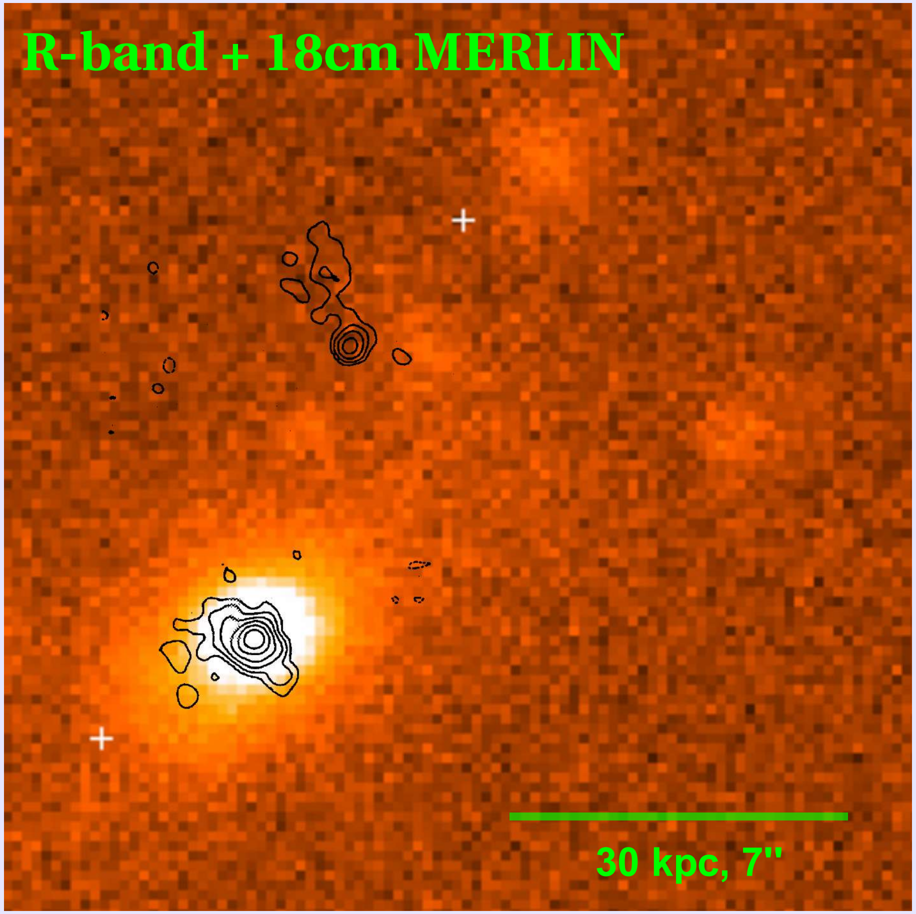

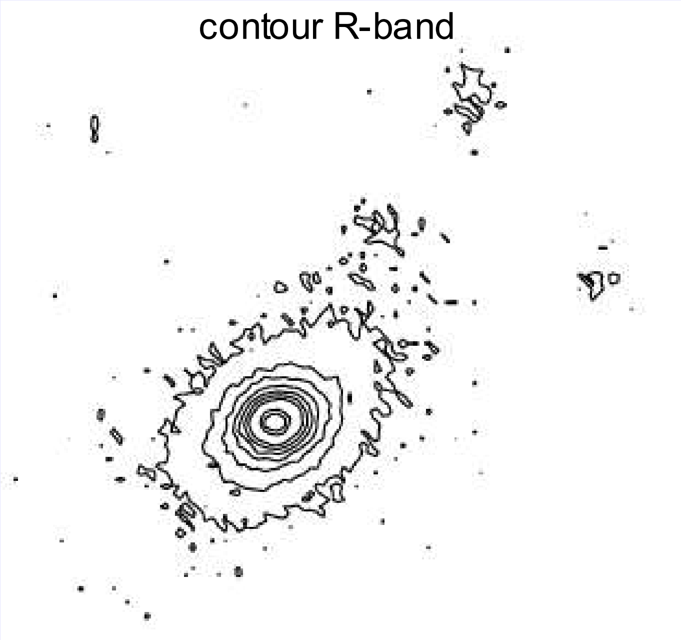

3C213.1 galaxy @ z=0.2

some faint componets NW

alignment between opt.-radio

Preliminary Results

22/55 objects show distributed optical morphologies

16/55 objects have close companions (<5")

16/55 show evidence of a poor cluster environment

Mirko Tröller
Metsähovi Radio Observatory

To Do

- going on with the analysis
- determine local galaxy density
- photometry of the hosts

Thanks for your attention

Stefano Ciprini
Tuorla Astronomical Observatory
University of Turku
Piikkiö, Finland

S. Ciprini, L.O. Takalo, G. Tosti, C. M. Raiteri, M. Villata

Optical Variability of the Blazar PKS 0735+178.

(Very) Preliminary Notes.

III ENIGMA Meeting
April 25-28, 2004 - Jerisjärvi (Lappland), Finland

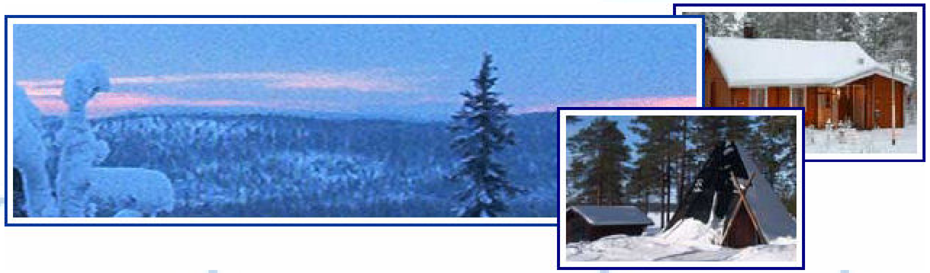

PKS 0735+178 Characteristics

• Radio source PKS 0735+178 (z=0.424, Parkes radio catalog, other most used names: S3 0735+17, OI 158, DA 237, VRO 17.07.02, PG 0735+17, RGB J0738+177, 1Jy 0735+17, RX J0738.1+1742, 3EG J0737+1721) was classified as a classical BL Lac object by Carswell et al. (1974).

• This object is both radio (Kuhr et al. 1981) and X-ray selected (Elvis et al. 1992).

• Optical data spans over about 100 years!, and about over 20 years in the near-IR (Lin & Fan 1998, Fan & Lin 1999). This is one of the older and fair sampled blazar at Metsähovi radio observatory (data from 1980). The University of Michigan UMRAO observatory monitor regularly this blazar starting from 1977. The source seems to vary quite slow in the radio.

• Several possible periods for the optical light curves of PKS 0735+178 were claimed: 1.2 and 4.8 years (Smith et al. 1987,Webb et al. 1988,Smith & Nair 1995); 14.2 and 28.7 years (Fan et al. 1997), 8.6, 13.8, 19.8, 37.8 years (Qian & Tao 2004).

PKS 0735+178 Characteristics

• The optical spectrum shows the absorption line due to an intervening system identified with Mg II and this gives z>0.424. Imaging was presented by Bregman et al. (1981) Hutchings et al. (1988), Stickel et al. (1993), Scarpa et al. (2000), Falomo & Ulrich (2000), Pursimo et al. (2002) and other, but the host galaxy remain unresolved. On the other hand the companion galaxies are well resolved. The nearby environment has been shown recently in Pursimo et al. (1999).

• The source has shown very different levels of optical polarization percentage in the past years, from around 1% to more than 30% (Tommasi et al. 2001).

• PKS 0735+178 is also known as an optical and infrared intraday variable blazar (Massaro et al. 1995; Heidt & Wagner 1996; Bai et al. 1998).

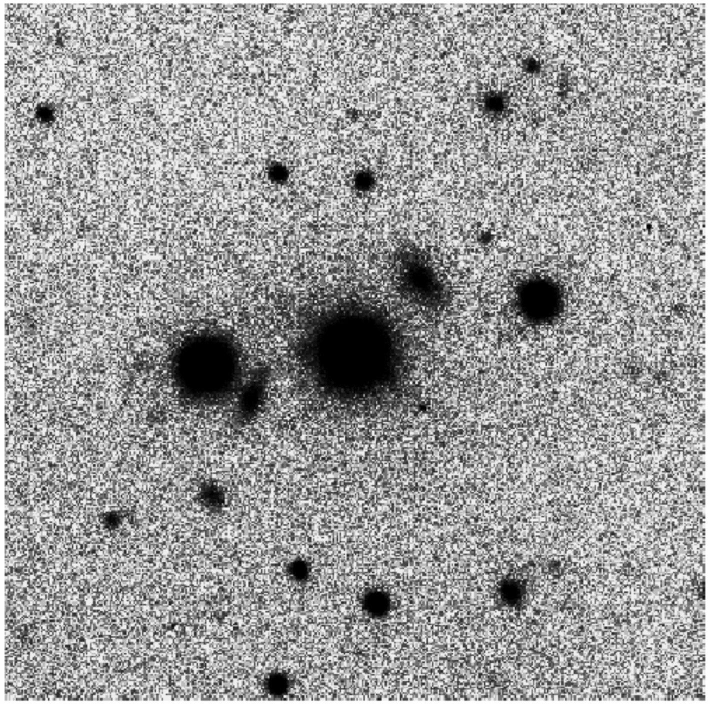

Fig. 4. The BL Lac object PKS 0735+17 (brightest object in the center) imaged by NTT+SUSI (R filter). The two bright objects at both sides of 0735+17 are stars. Field shown is 52 arcsec and North-East is at the top-left side.

Falomo & Ulrich 2000

PKS 0735+178 Characteristics

- PKS 0735+178 has been extensively studied in the radio range and several moving components have been detected using VLBI.

- PKS 0735+178 has one of the most bent jets on the mas scale (Gabuzda et al. 1994). Multi-epoch VLBA images confirm the presence of a twisted jet with two sharp apparent bends of 90° within the inner 2 mas from the core, resembling a helix in projection. This was interpreted as the result of a precession of the jet or produced by pressure gradients in the external medium (Gòmez et al. 2001). A scenario in which the plasma of the jet is traveling inside a slowly moving curved funnel is suggested (Agudo et al. 2002).

- The unusual morphology is also described and interpreted by Kellermann et al. (1998), Gòmez et al. (1999), Homan et al.(2002) .

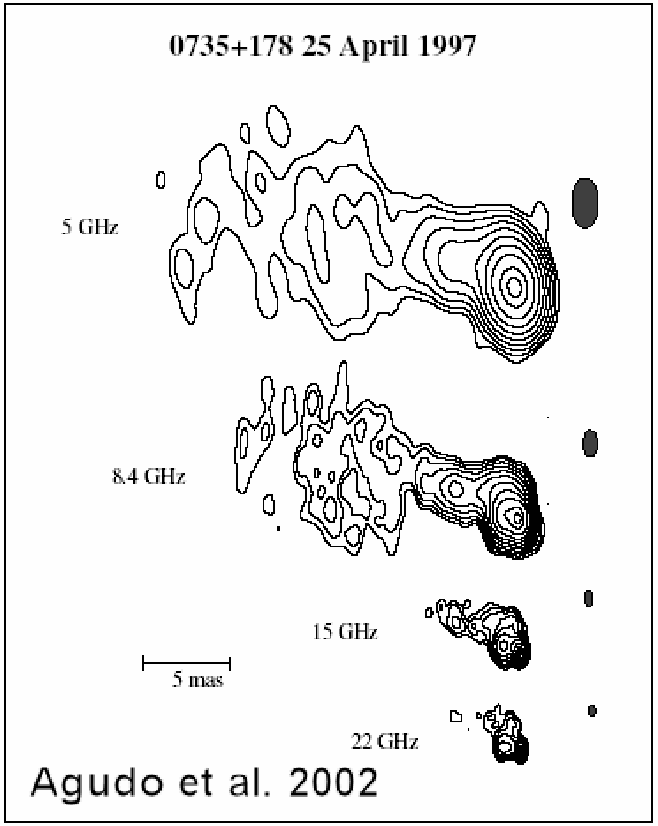

Fig. 1. 5, 8.4, 15 and 22 GHz (from top to bottom) VLBA images of 0735+178 in 25 April 1997. Contour levels increment by factor of 2 (plus 90 per cent contour). From top to bottom images, levels start at: 0.25%, 0.125%, 0.5% and 1% of the peak intensity of 0.684, 0.487, 0.445 and 0.321 Jy/beam. In the same order, convolving beams (shown as filled ellipses) are 2.55×1.38, 1.44×0.79, 0.85×0.46 and 0.58×0.32 mas, at position angles of 1.8°, 0.6°, -0.3° and -3.0°,respectively.

PKS 0735+178 Characteristics

- VLBI total intensity and linear polarization images at 6cm and 2cm shown a path of the jet appreciably different at the two wavelengths (Gabuzda et al. 2001).

- In the twisted jet, the magnetic field appears to smoothly follow one of the bends in the jet, suggesting that this structure may be the result of a precessing nozzle in the jet (Gòmez et al. 1999).

- A large outburst observed in the radio a few years ago (Aller et al. 1999).

- Einstein, ROSAT, ASCA X-ray observations. X-ray emission was suggested early to be inverse Compton emission operating in one of the VLBI radio components (Madejski & Schwartz 1988).

- EGRET positive detection (source 3EG J0737+1721).

New Calibration of Comparison Stars

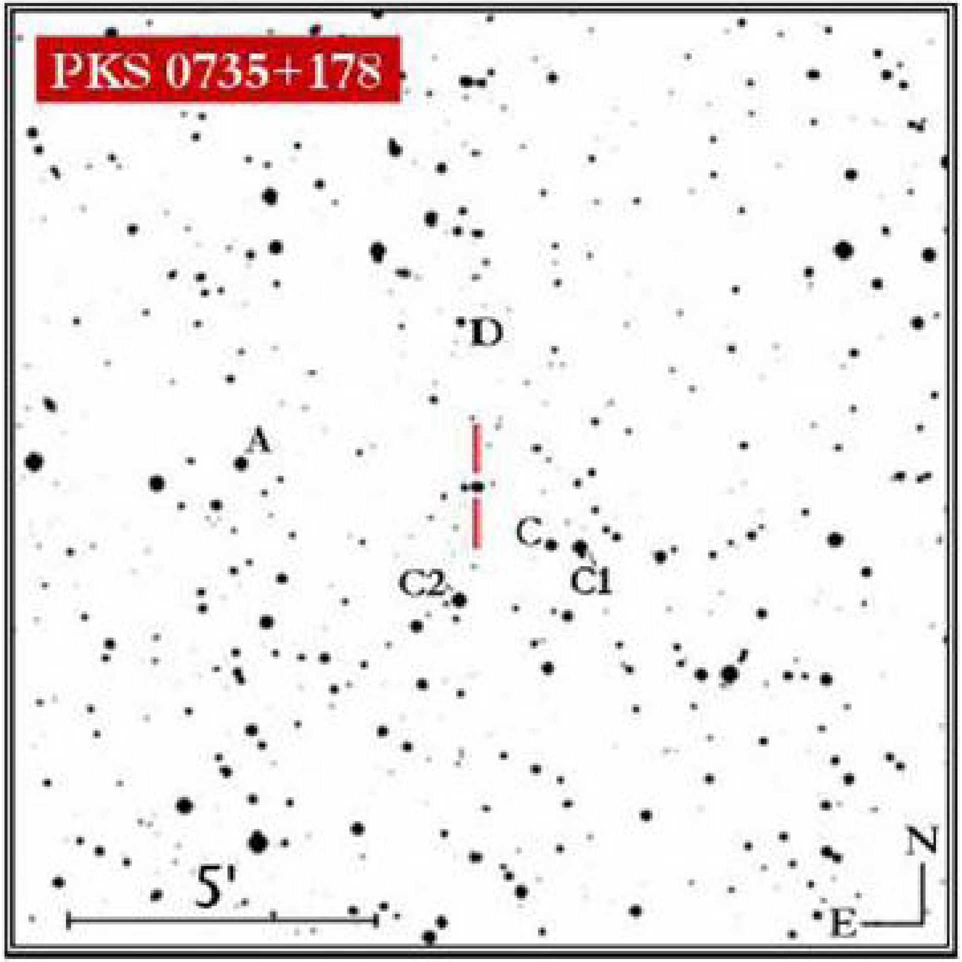

• Source Magnitude by differential photometry with respect to comparison stars in the same field. (Johnson-Cousins photometric system, see, e.g. Bessel 1979)

• New unpublished *VRI* calibration of comparison stars in the field of PKS 0735+178 (C1, C, D, C2).

• A C D stars belong also to the photometric sequence calibrated by Smith et al. (1985).
There is not any other recent photometric calibration of comparison stars in this filed (see, e.g. Gonzalez-Perez 2001) .

New Calibration of Comparison Stars

• Calibrations derived from several photometric nights at the Perugia Univ. Obs., using Landolt standards. (for observing and reduction details see e.g. Fiorucci & Tosti (1996), Fiorucci et al. (1998)).

Table 1. The new VR_cI_c Johnson-Cousins photometric calibration of comparison stars C1, C, D, C2, in the field of PKS 0735+178. A, C, D, stars were previously calibrated by Smith et al. (1985). C and D star magnitudes are in agreement within the uncertainties.

star	R.A. (J2000.0)	Dec. (J2000.0)	$U^{(\dagger)}$ [mag]	$B^{(\dagger)}$ [mag]	V [mag]	R_c [mag]	I_c [mag]
C1	07 38 00.5	+17 41 19.9	...	...	13.24 ± 0.06	12.91 ± 0.04	12.59 ± 0.07
C	07 38 02.4	+17 41 22.2	16.26 ± 0.08	15.48 ± 0.05	14.44 ± 0.05	13.84 ± 0.04	13.33 ± 0.06
D	07 38 08.3	+17 44 59.7	16.65 ± 0.12	16.48 ± 0.10	15.88 ± 0.05	15.44 ± 0.04	15.08 ± 0.04
C2	07 38 08.5	+17 40 29.2	...	...	13.30 ± 0.07	12.81 ± 0.05	12.37 ± 0.07

$^{(\dagger)}$ U, B values by Smith et al. (1985).

Ten Years Optical Monitoring

• Optical long-term data:
10 years of optical monitoring (BVRI bands).
Data from Perugia University Observatory (Italy), INAF-Torino Observatory (Italy), Turku Univ. Tuorla Observatory (Finland). Optical data from Qian & Tao (2004) are also added to improve the analysis. Perugia and Torino Obs. data are unpublished, some Tuorla data was just published in Katajainen et al. 2000.

Table 2. The number of photometric $UBVR_cI_c$ data points of GC 0109+224 obtained by each observatory,

DATA POINTS PER OBSERVATORY						
Obs.	B	V	R	I	Tot.	Period
Perugia	0	226	490	282	998	Feb1993-Feb2004
Torino	75	38	150	0	263	Dec1994-Apr2002
Tuorla	0	55	0	0	55	Oct1995-Feb2001
Shanghai	0	115	52	138	305	Jan1995-Dec2001
Total	75	434	692	420	1621	

10 Years BVRI Light Curves

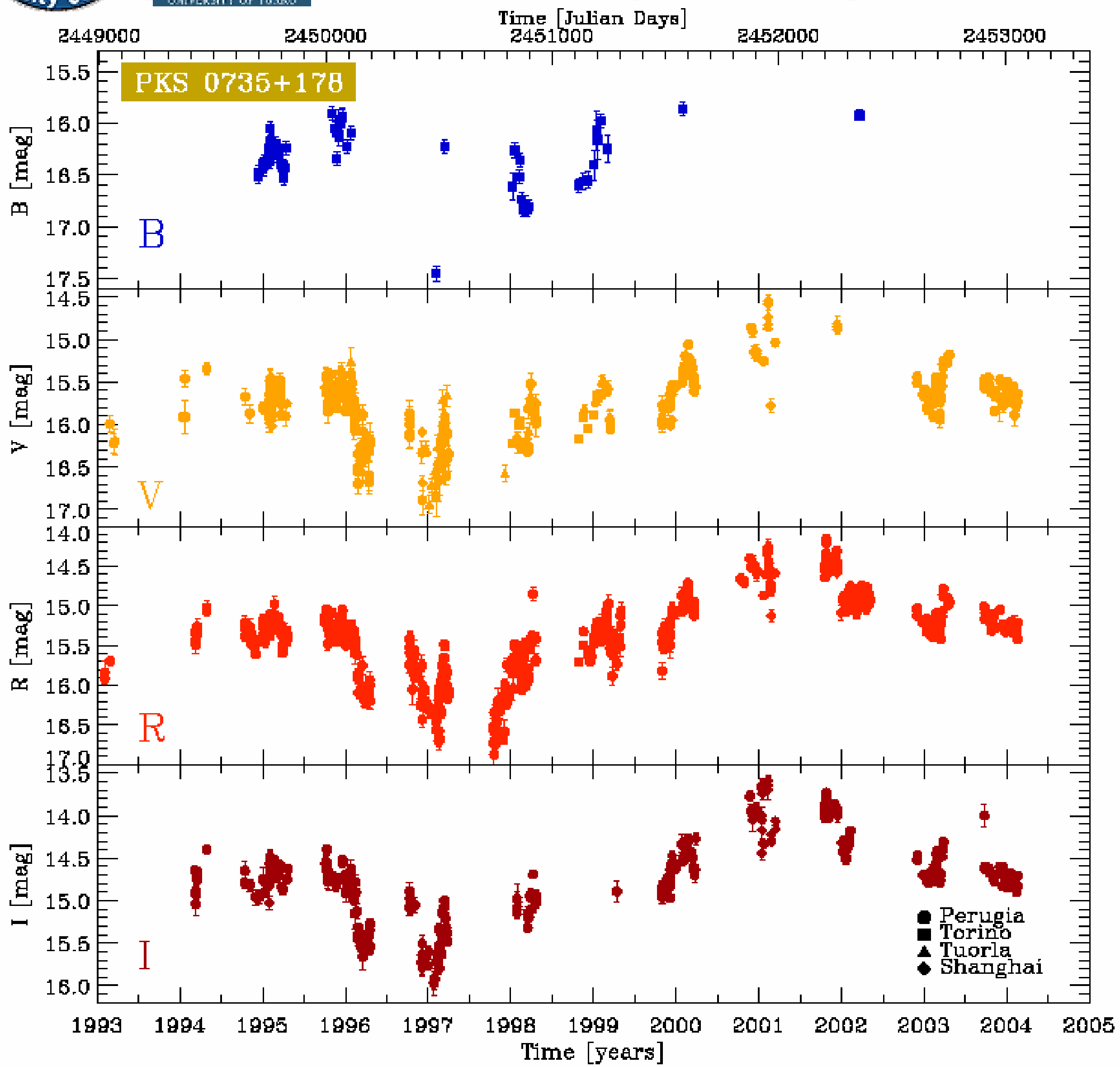

Fig. 2. *BVRI* magnitude light curves of PKS 0735+178 from 1993 to beginning of 2004. Data cames from our ten-years observing monitoring. Published observations from Shanghai Observatory (Qian & Tao 2004) are added in order to improve the sampling. Data sets of different observatories are in agreement within the uncertainties.

- Data from different observatories are completely in agreement within the uncertainties.
- PKS 0735+178 showed rapid optical variations connected to slow base level variations (as appear in the radio flux light curves). R the best sampled band.
- 11 observing seasons, 10 years light curves, 1621 photometric data points.
- Our improved sampling recorded also the larger (and faster) optical flares.

Optical Historical Light Curve

Historical optical data starting from 1905 (Almost 100 years of data!).
Good sampling (with respect to the usual <u>optical</u> and <u>historical</u> light curves!) starting from 1970 (more than 30 years of data), → sufficient level of confidence in the analysis results.

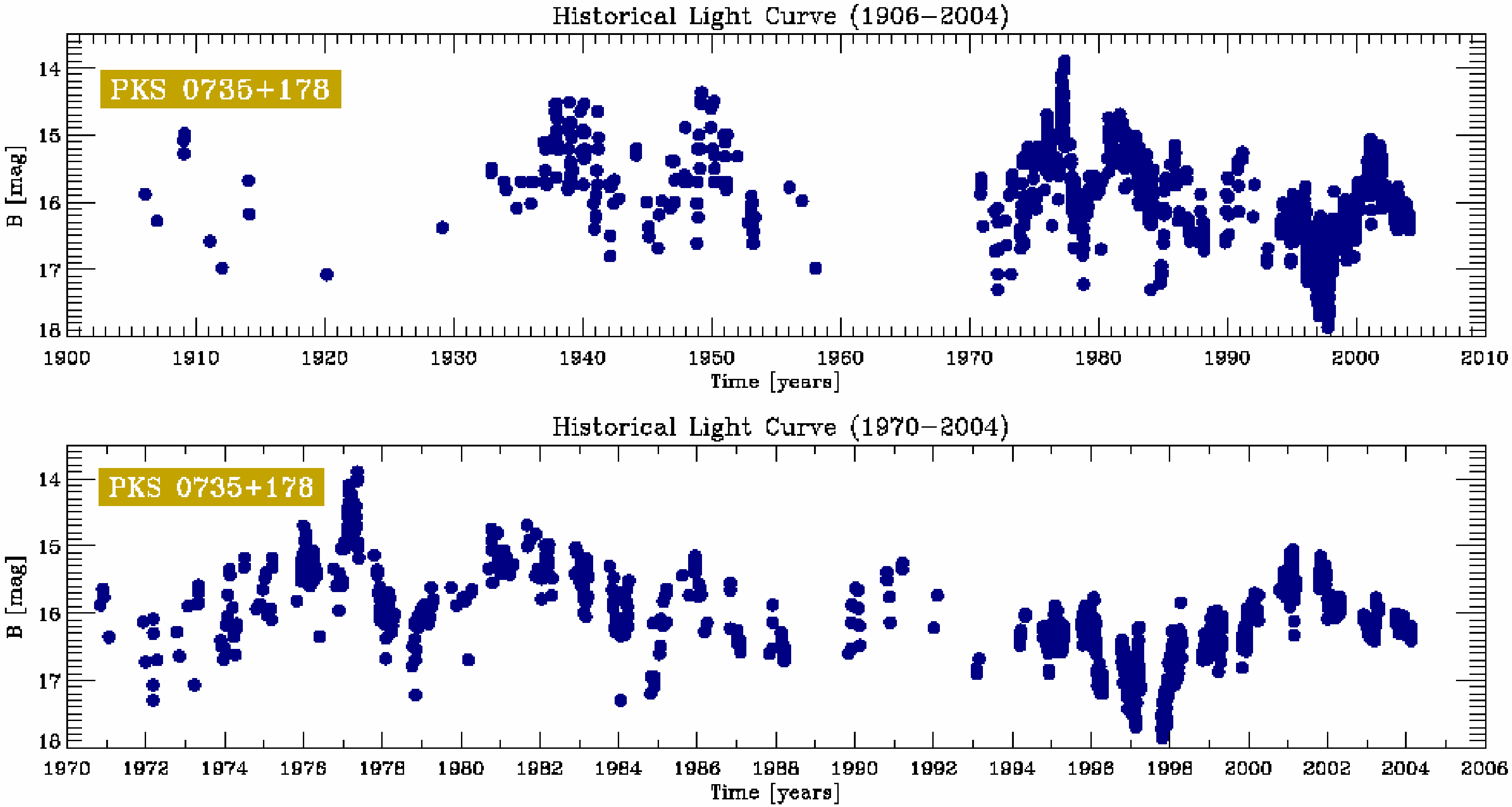

Fig. 3. The historical light curve of PKS 0735+178 in B band reconstructed from literature (data mainly from Qian & Tao 2004) and with our original B and R data added (magnitudes derived using mean colour index $B - R = 0.993$ for data sets homogeneity Fan et al. 1997; Qian & Tao 2004). The time series so obtained is composed of 1725 data

III E

(Very) Preliminary Analysis

PKS 0735+178

1970-2004 light curve

• Standard methods optimized for unevenly sampled datasets used in order to give a quantitative statistical description of the optical time variability: first order structure function (SF), discrete correlation function (DCF), and discrete Fourier transform in the Lomb-Scargle implementation (periodogram).

• First hints of recurrent time scales of variability, (in particular a possible period of about 8.4-8.6 years) appears by the preliminary analysis.

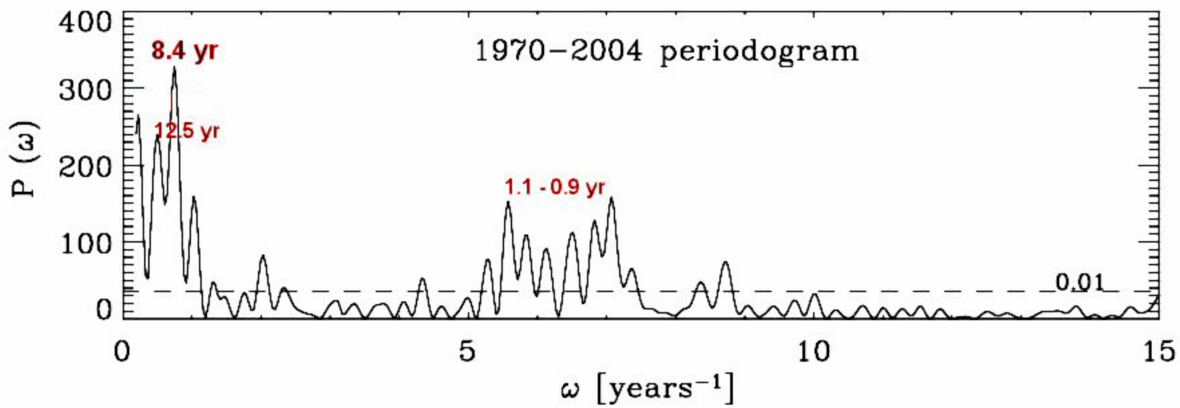

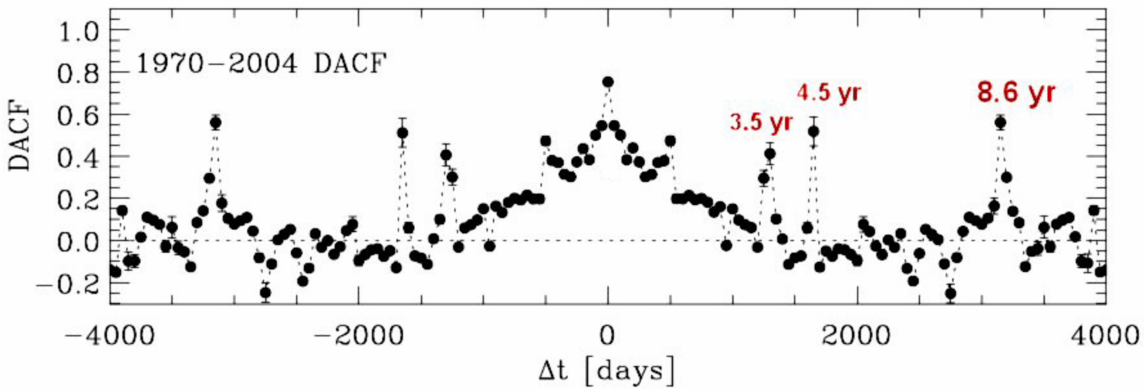

(Very) Preliminary Analysis

Example of cubic spline interpolation over the light curve binned at around 1.6 years.

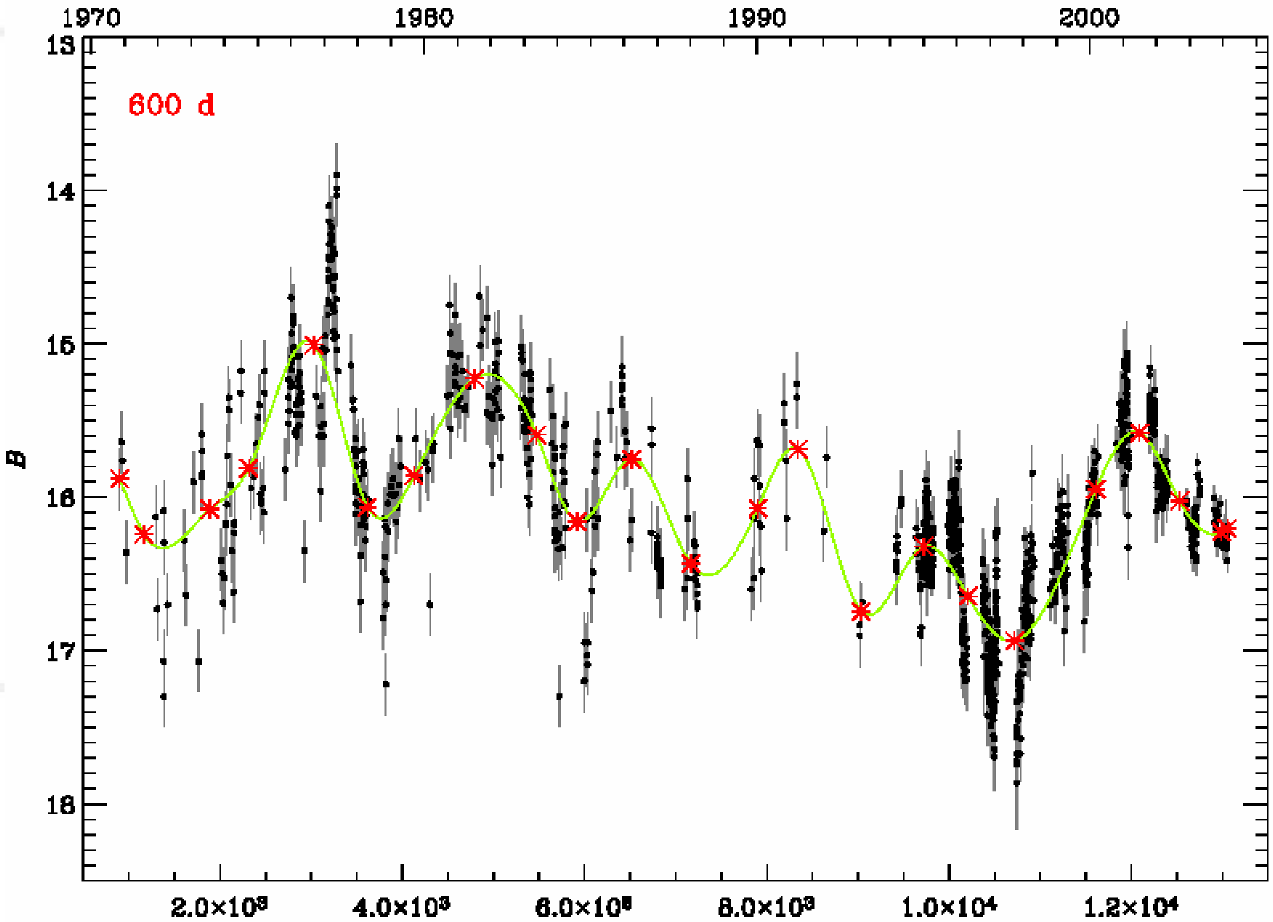

Preliminary SED

EGRET source. Synchrotron peak in the Near IR-optical bands. X-ray emission is likely inverse Compton emission.

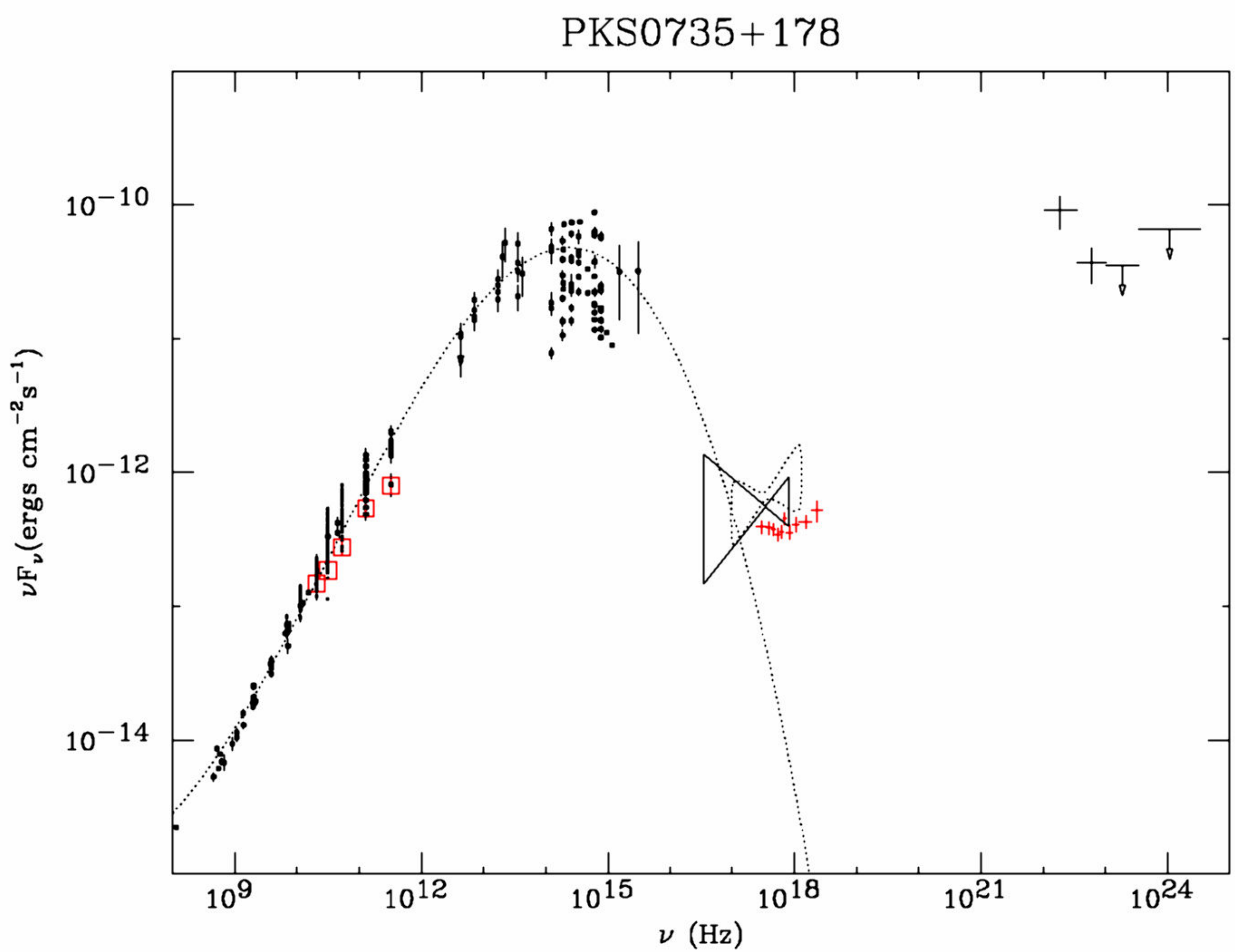

OPTICAL INTRADAY VARIABILITY OBSERVED in S5 0716+71 DURING THE ENIGMA CAMPAIGN

Luisa Ostorero(*) *& Stefan Wagner* (*)
on behalf of the 0716 optical collaboration

(*) *Landessternwarte Heidelberg, Germany*

3rd ENIGMA Meeting - Jerisjärvi (Finland), April 26-28, 2004

Astronomical observatories

CORE CAMPAIGN (Nov 06-20, 2003)

Optical observations simultaneous to the INTEGRAL pointing

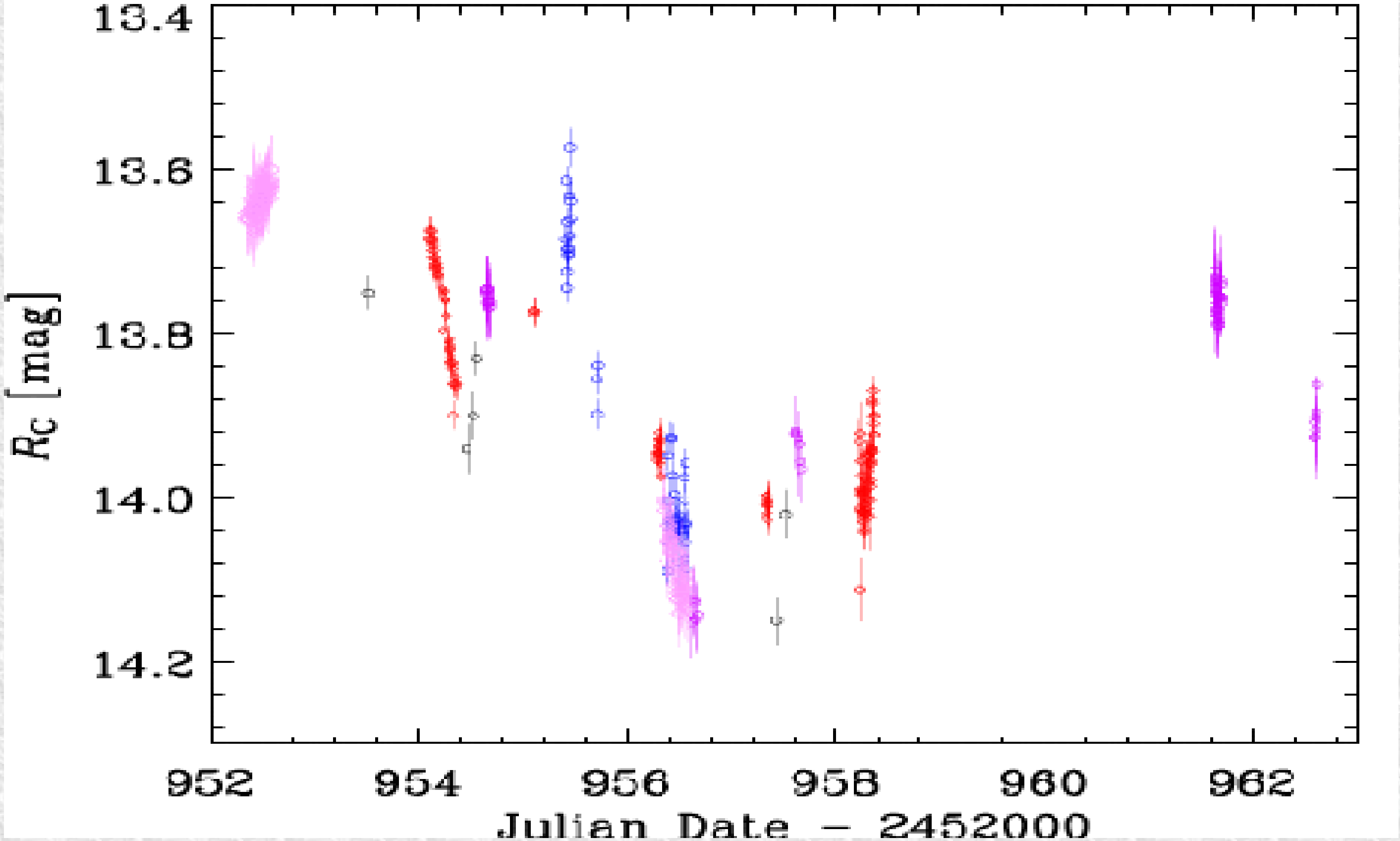

o *Mt Boo (Czech Rep.)*
o *KVA (La Palma, Spain)*
◊ *Lulin (Taiwan)*
◊ *Tuorla (Finland)*
o *Perugia (Italy)*

CORE CAMPAIGN (Nov 06-20, 2003)

Optical observations simultaneous to the INTEGRAL pointing

Intranight variations

Abastumani Observatory (Georgia, FSU)

O. Kurtanizde, M. Nikolashvili

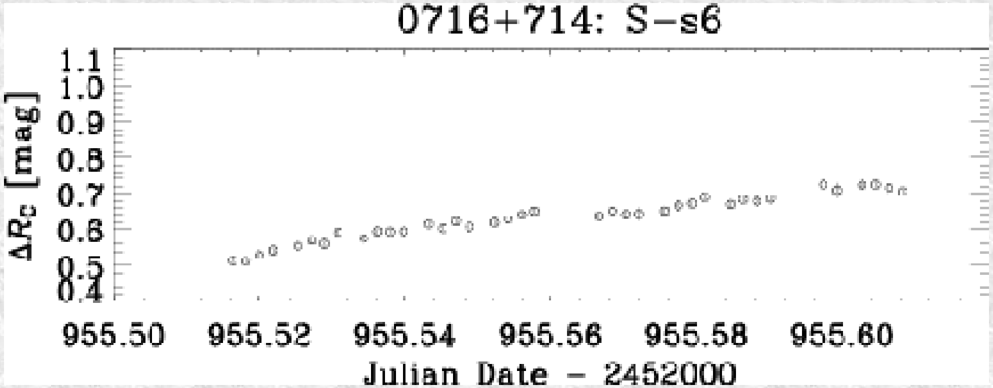

Δ R~0.2 in Δ t=2h 30m

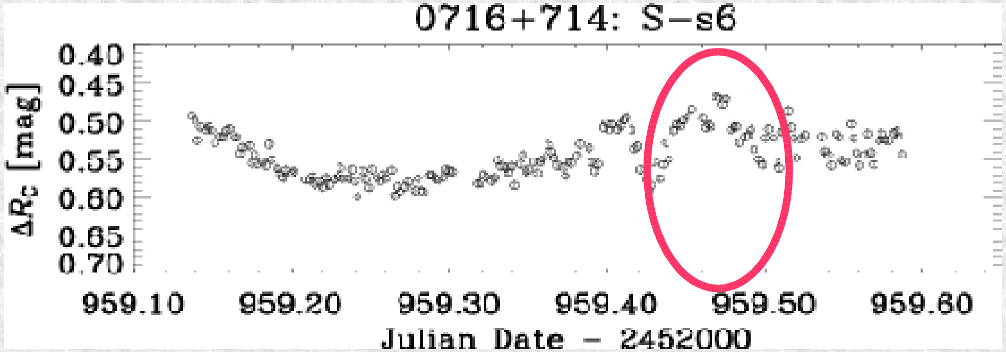

Δ R~0.15 in Δ t~1h 30m

Amateur observatories:

remarkable contribution, mainly during the high-energy pointings!

Coyote Hill Observatory, California

- C. Pullen -

ΔR~0.1

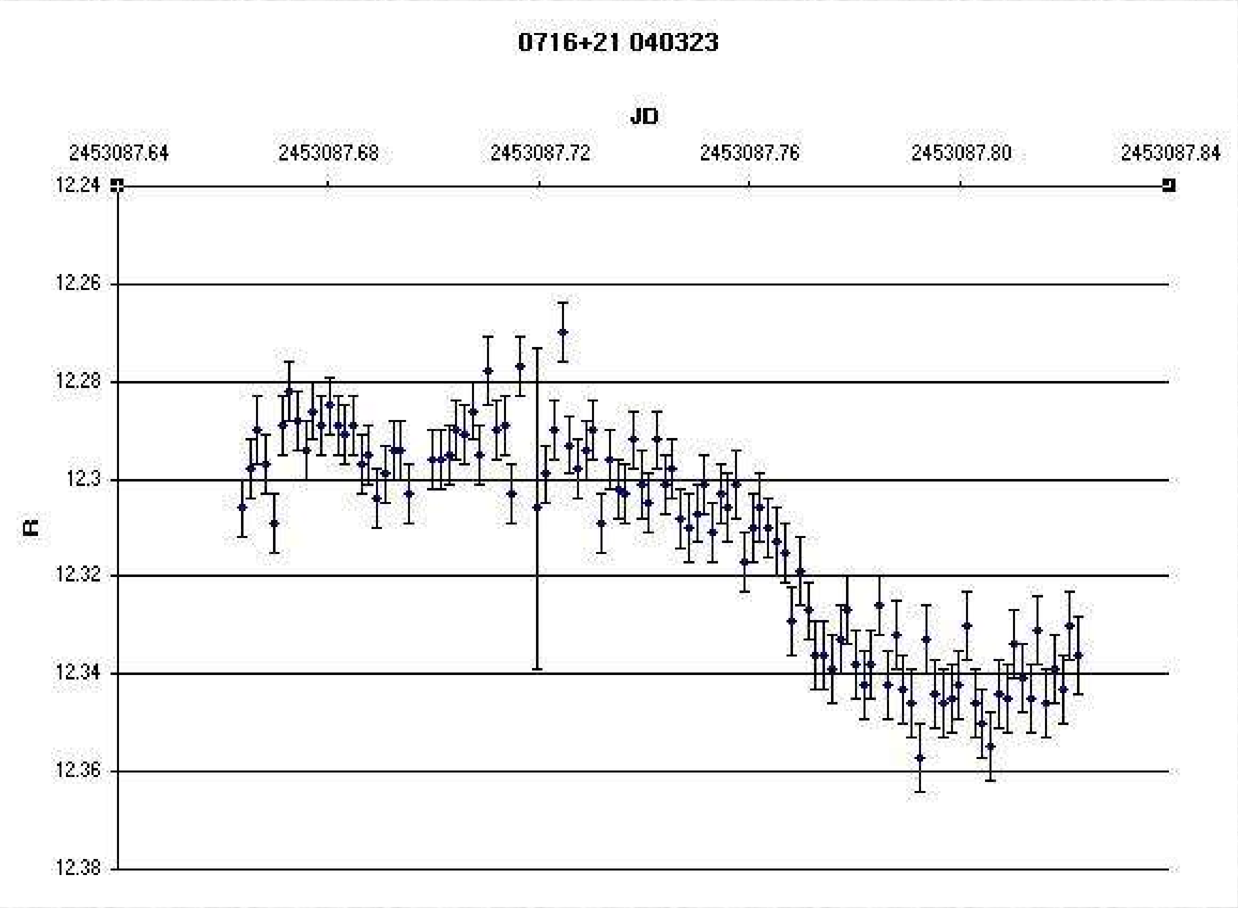

Intranight Mar 22, 2004

> 100 frames in <5h

Δt~2 h

Nyrölä Observatory (Finland)

- A. Oksanen -

Optical - RXTE simultaneous observations

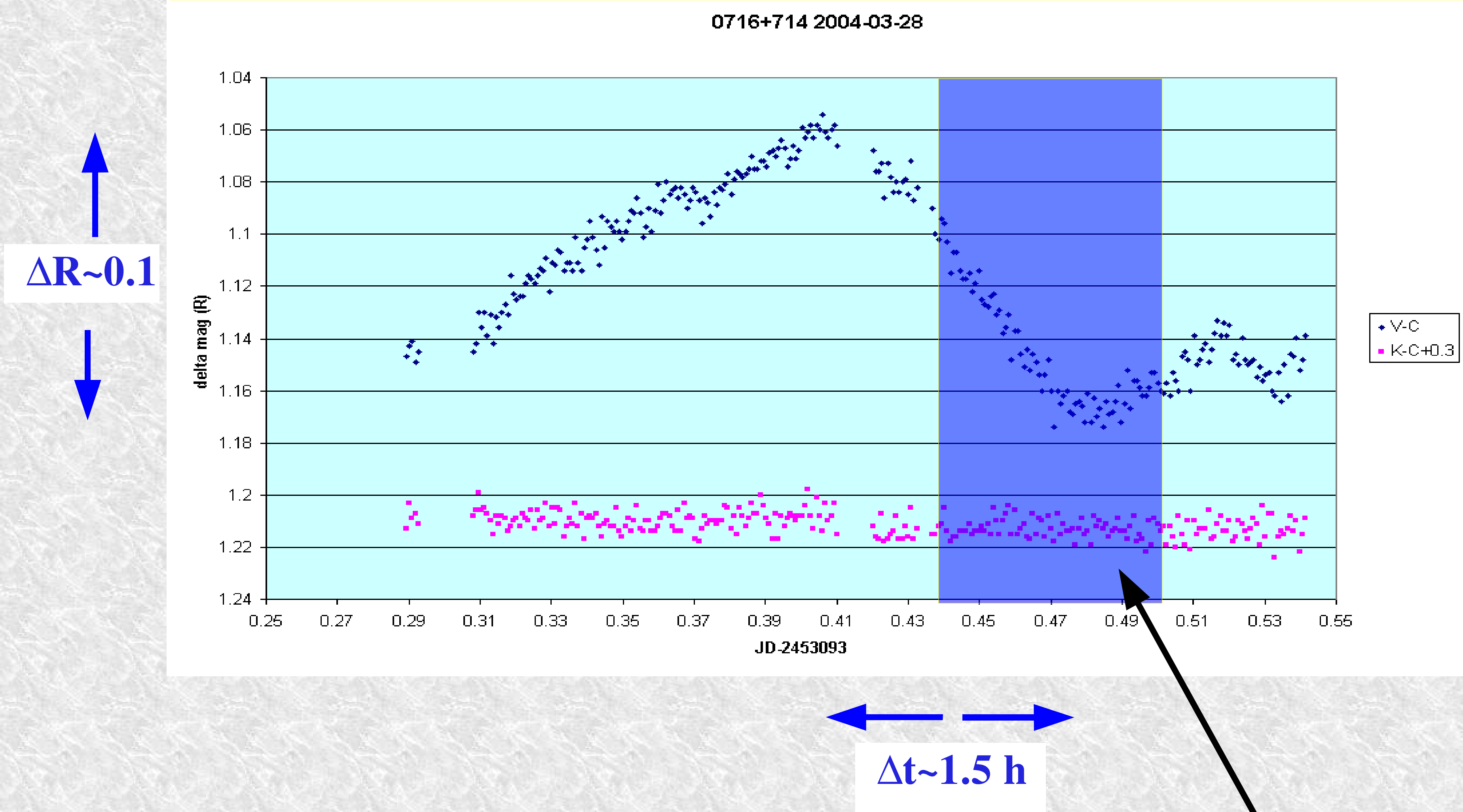

RXTE ToO observation - March 28, 22:25 ÷ March 29, 00:20

Nyrölä Observatory (Finland)

- A. Oksanen -

Optical - RXTE simultaneous observations

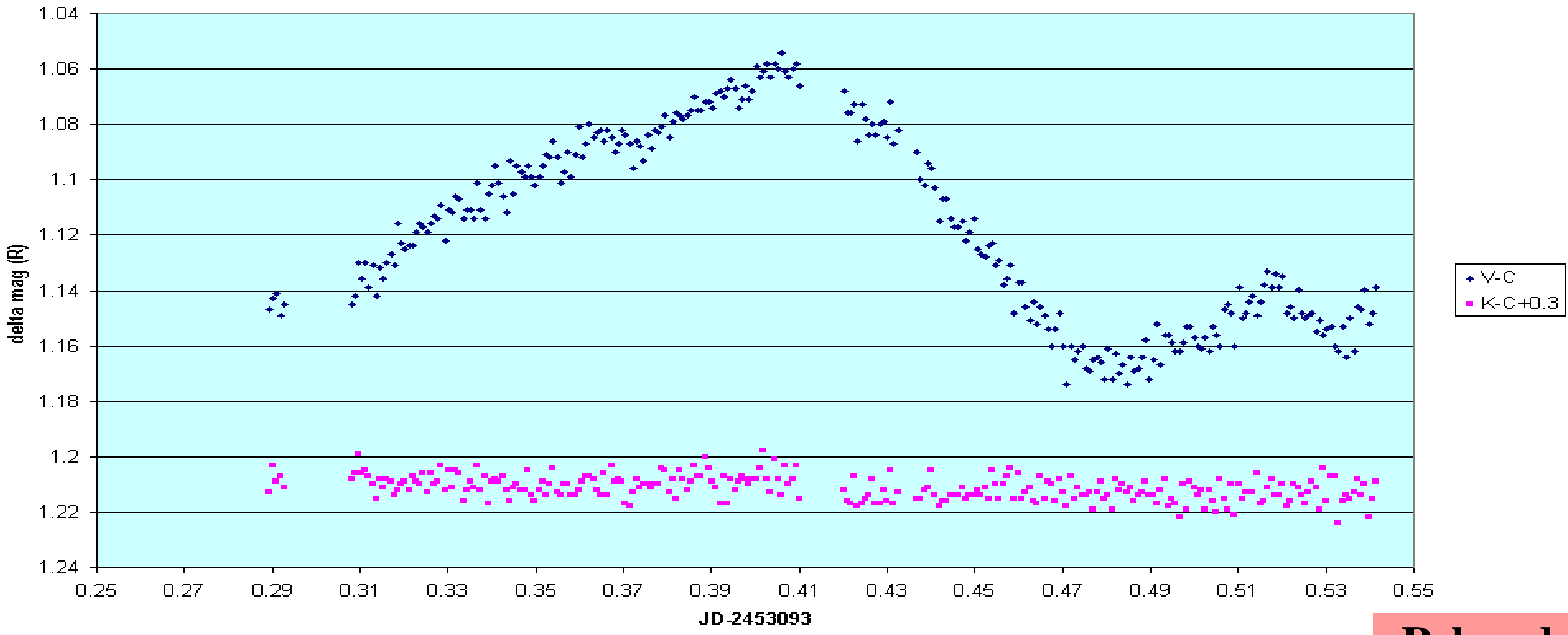

R-band data by A. Oksanen

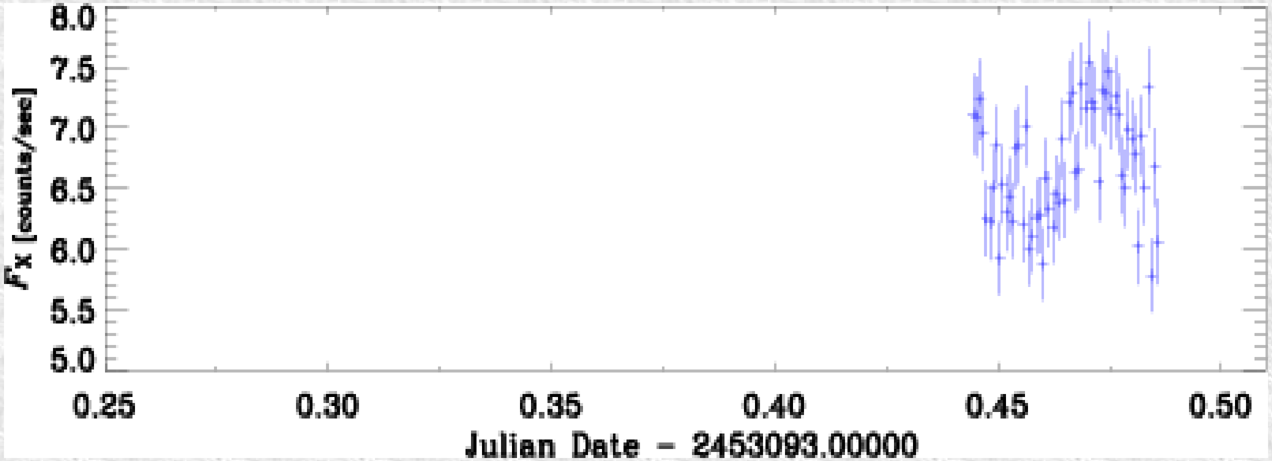

Preliminary RXTE analysis by D.Emmanoulopolous

Nyrölä Observatory (Finland)

- A. Oksanen -

Optical (R) – RXTE - INTEGRAL simultaneous observations

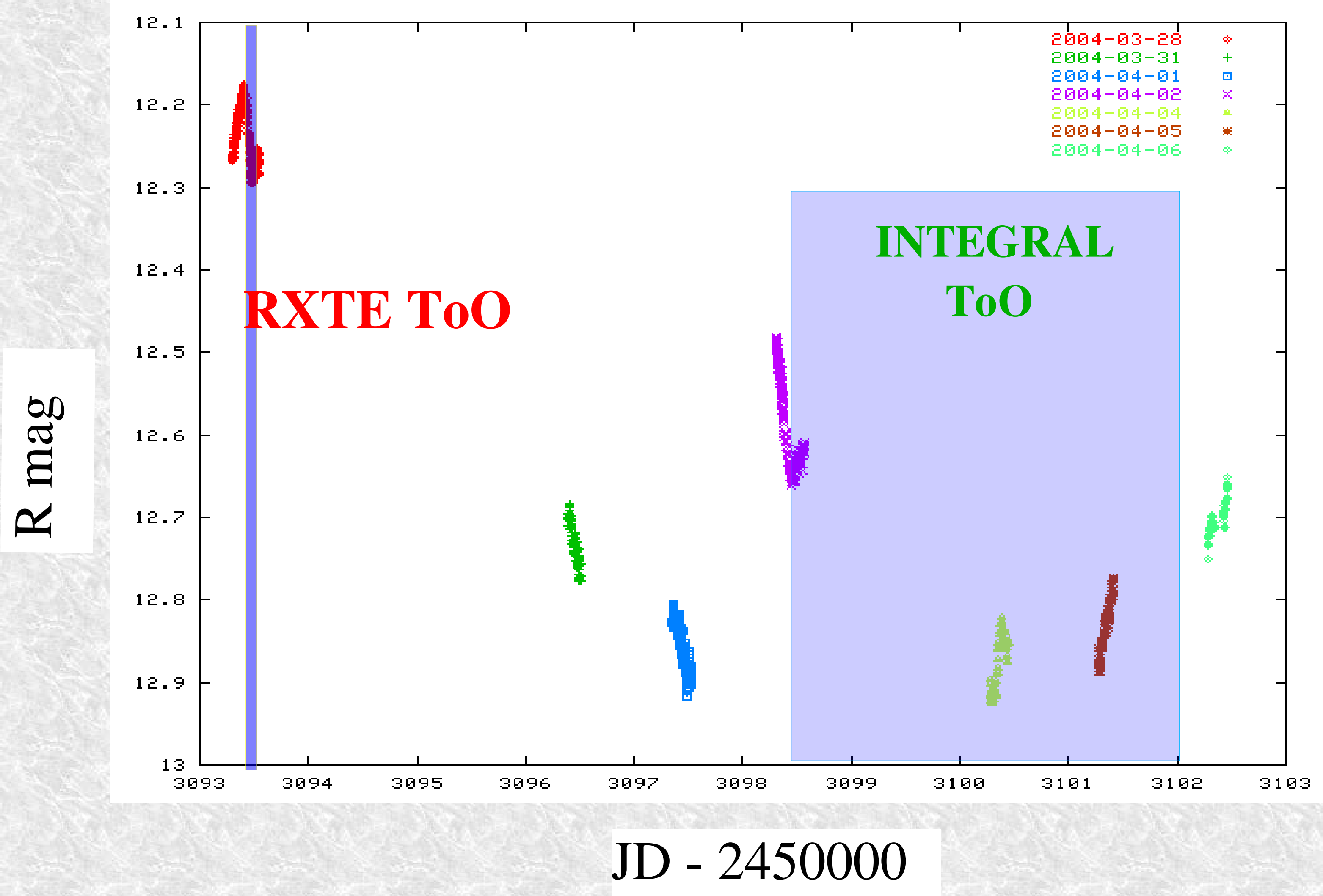

Nyrölä Observatory (Finland)

- A. Oksanen -

Optical (V) – INTEGRAL simultaneous observations

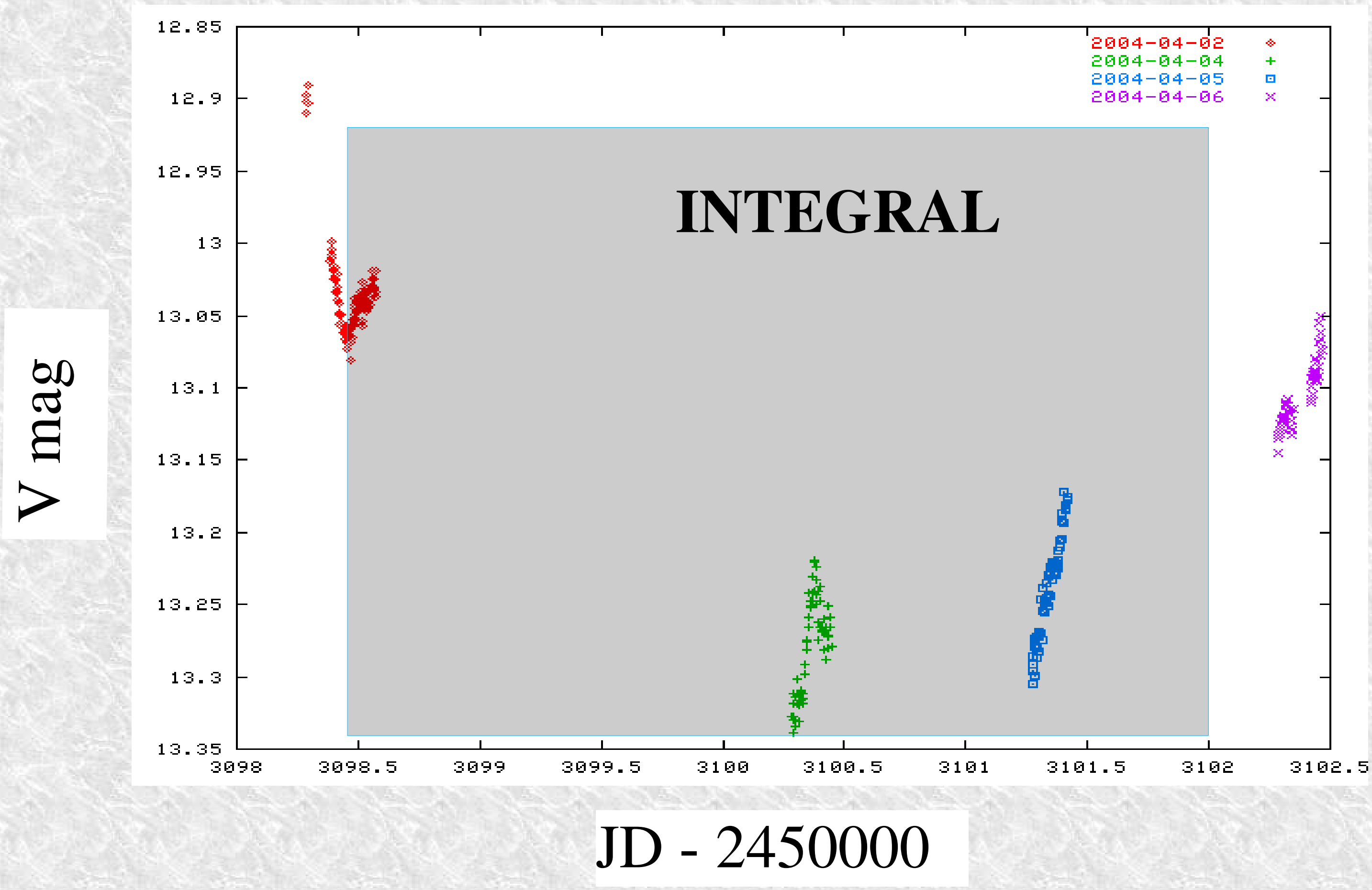

Nyrölä Obs. (Finland) - *A. Oksanen*

Jakokoski Obs. (Finland) - *P. Pääkkönen*

Optical (V,R,I) - INTEGRAL simultaneous observations

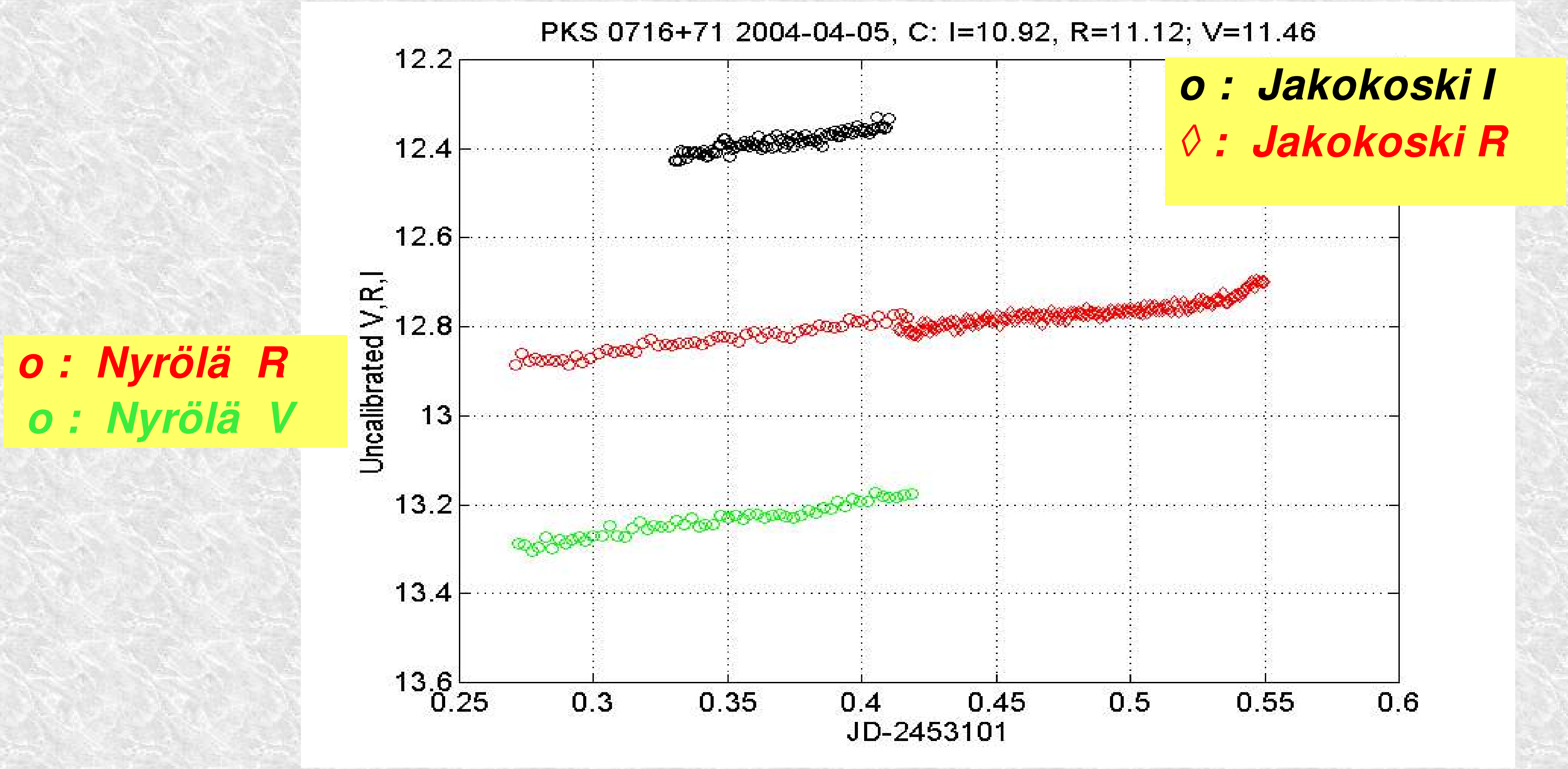

Δt = 60-90 sec

ΔR~ 0.2 mag
~ 7 h monitoring

IDV meeting on interstellar scintillation of extragalactic radio sources

Dwingeloo, ASTRON

April 5-7, 2004

Participants:

B. Rickett, G.de Bruyn, C. Gwinn, S. Kulkarni, R. Wijers, L. Gurvits, J. Marquart, J. Cordes, M. Walker, D. Jauncey, J. Lovell, R. Ohja, Cimo, T. Beckert, T. Krichbaum, L.Fuhrmann; V. Impellizzeri, et al.

All overlays taken from the Web-page of the IDV workshop at ASTRON in Dwingeloo !

www.astron.nl

Setting the Scintillating Scene

Barney Rickett
U. C. San Diego

ASTRON/JIVE Workshop on
Interstellar Scintillation of Extragalactic Radio Sources

ISS and Source Diameter

Plot Source diameter θ_{so} vs frequency
Dashed lines at constant T_b/S_{Jy}

Typical ISS at 45 deg Galactic latitude
Typical ISS timescale at right

Weak ISS if $\theta_{so} < \theta_{weak}$
Intra-Day Variation IDV

Diffractive ISS if $\theta_{so} < \theta_{diss}$
Pulsars only

Refractive ISS if $\theta_{so} < \theta_{riss}$
Low Freq Variables LFV

Note GRB 970508

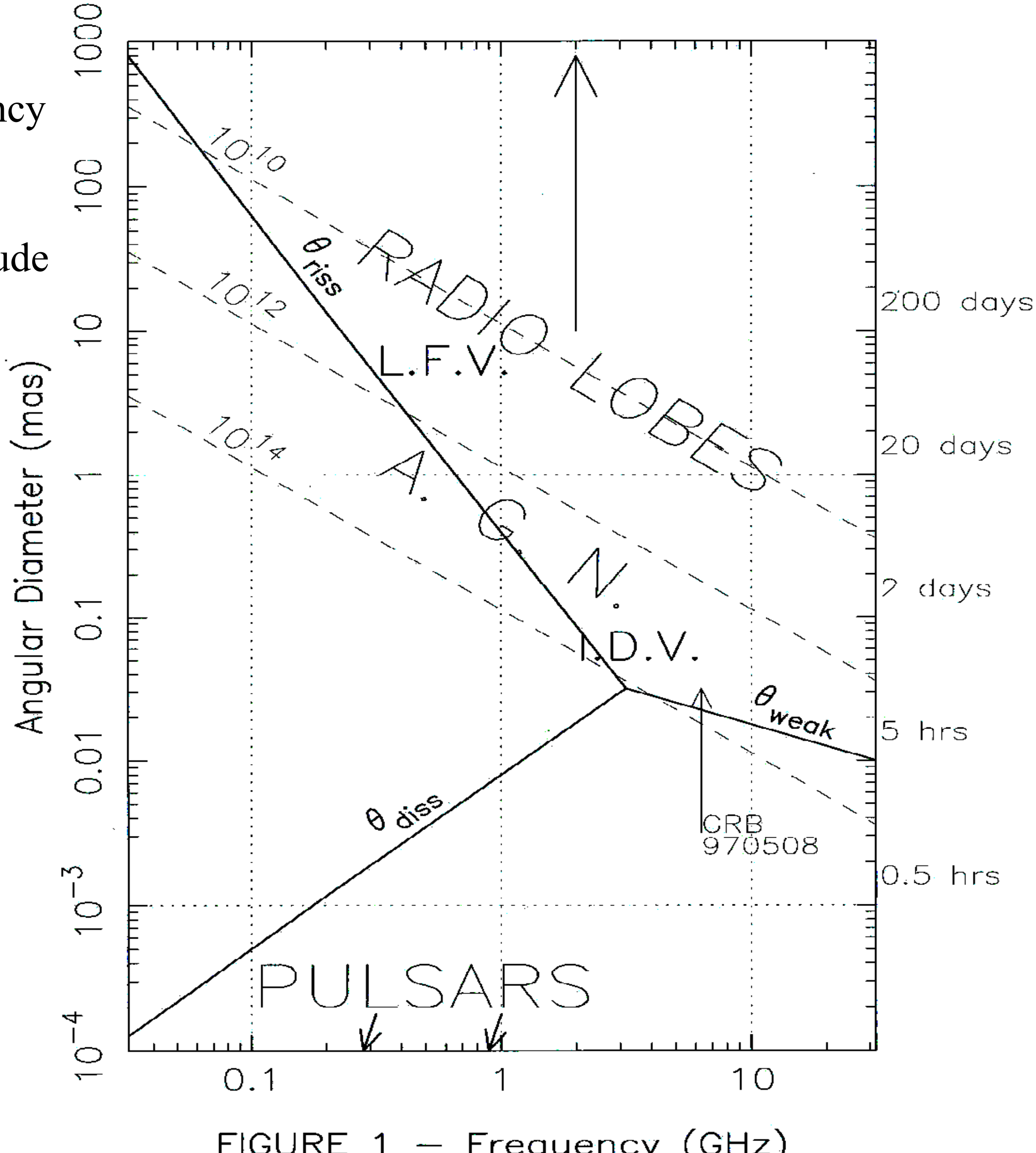

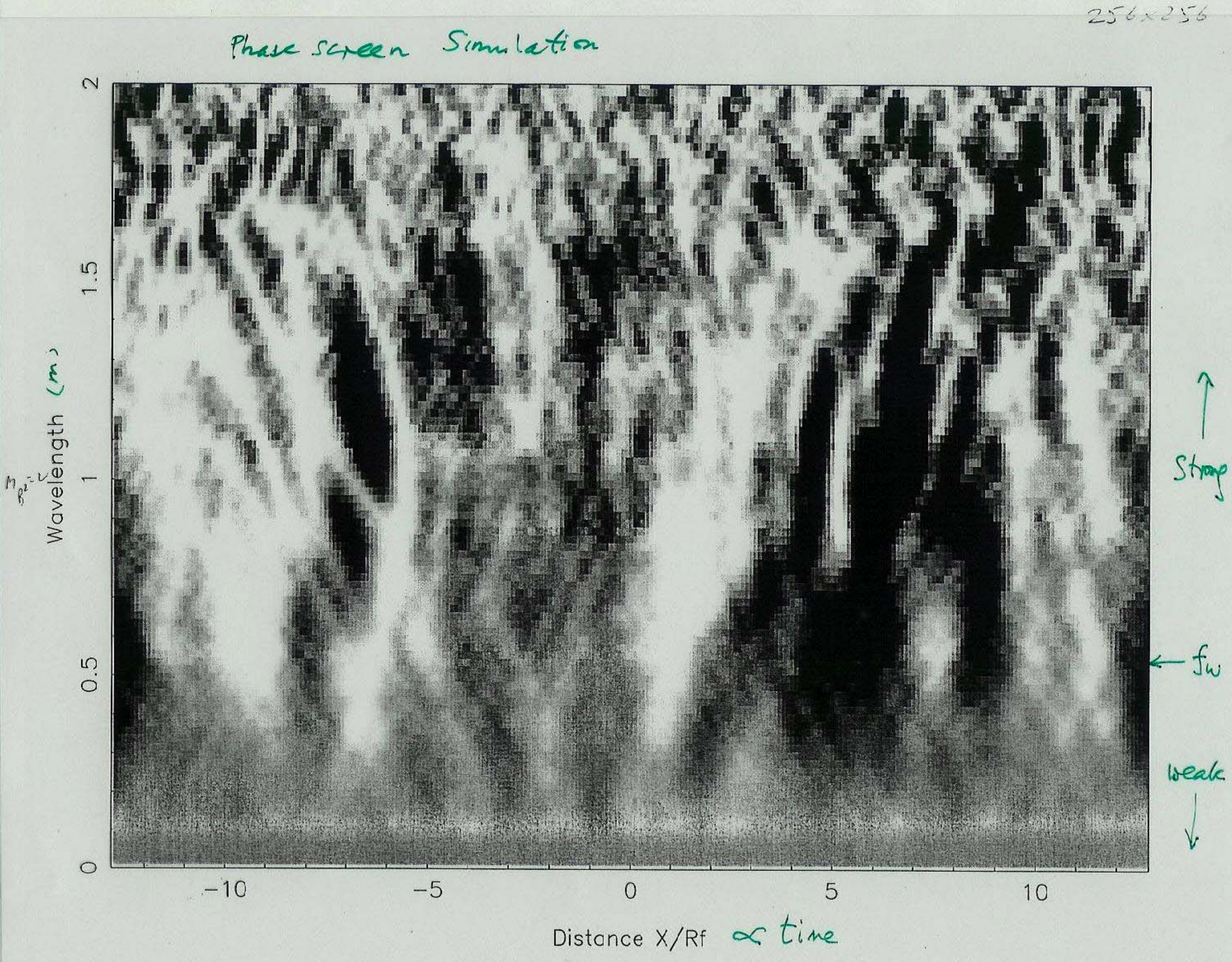

256x256
Phase screen Simulation
Wavelength (m)
2
1.5
1
0.5
0
−10
−5
0
5
10
Distance X/Rf ∝ time
Strong
← fw
weak

ISS of PKS B0405-385 observed with ATCA

Rickett, Kedziora-Chudczer & Jauncey (ApJ 2002)

Source Dia / Screen Dist trade-off

8.6 GHz:

modulation index

$0.08 < m_c < 0.37$

and time scale

$0.31\text{hr} < \tau_c < 0.51\text{hr}$

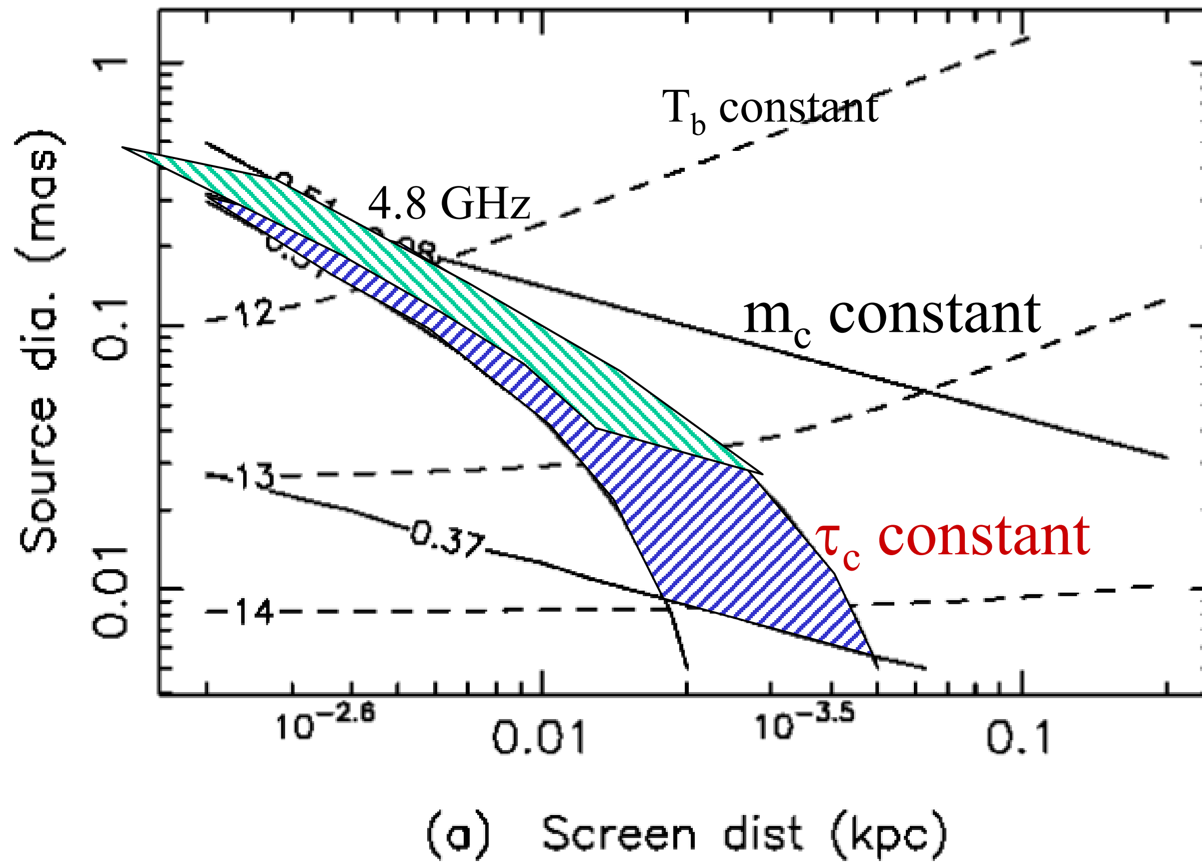

Key Topics in Theory and Analysis

- Theory for extended source scattered by an extended medium
- Simulation methods between weak and strong scint => scales intermediate between diffractive and refractive
- Anisotropic scattering
- Use more observables together in the interpretation
  - ie scint index and full power spectrum at one or more frequencies, cross-spectra (or correlation), ISM mode & multi-component source models

J1819+3845: modulations, evolution, polarization and other properties

Ger de Bruyn

ASTRON-Dwingeloo & Kapteyn Institute-Groningen

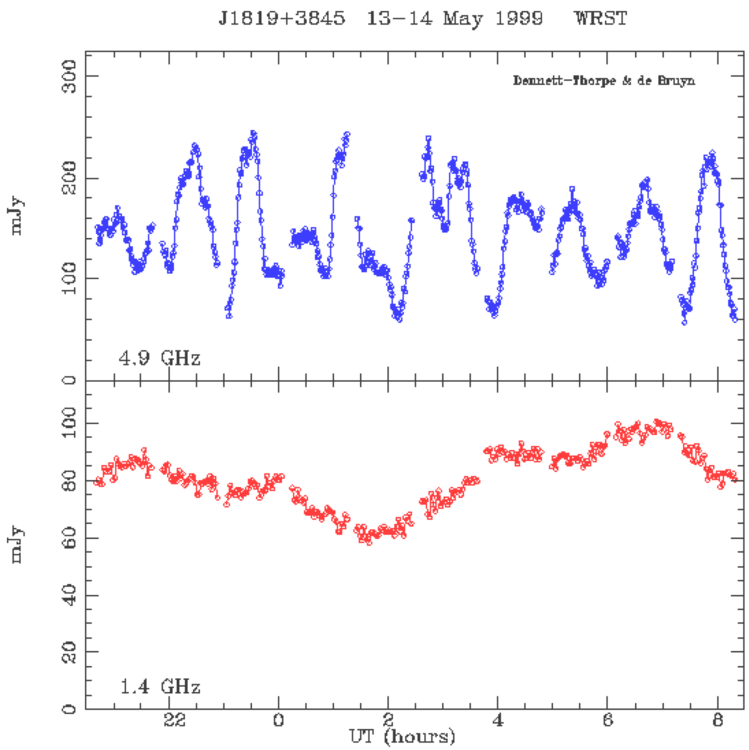

Collaborators:

J-P Macquart (Kapteyn Institute)
Jane Dennett-Thorpe
Barney Rickett (UCSD)

Rapid IDV of Quasar J1819+38

WSRT data from G de Bruyn & J Dennett-Thorpe

- Quasar J1819+38 exhibits ISS with a pronounced annual cycle in its characteristic timescale

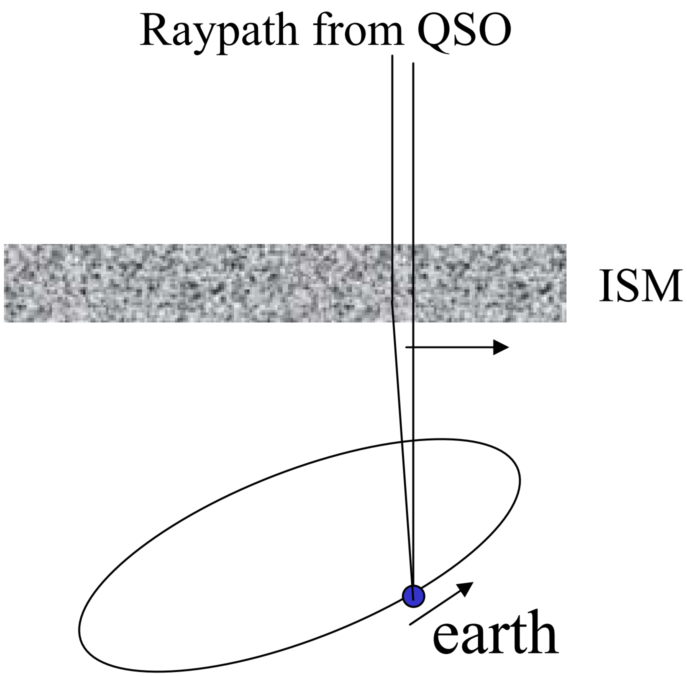

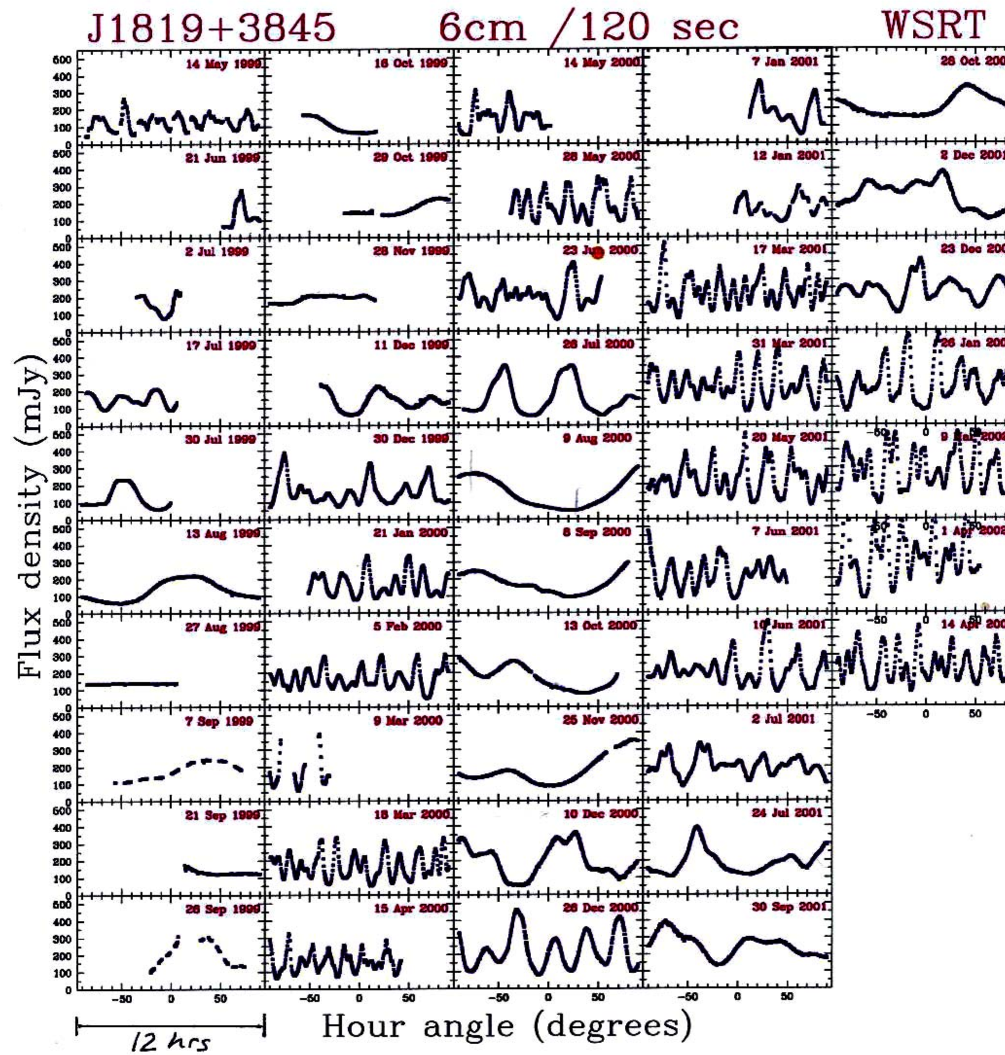

Annual change in timescale of J1819+38 (J Dennett-Thorpe and G de Bruyn 2003)

- Observed timescale for two years (6cm)
- Model is slice through an ellipse at angle of the effective Earth Velocity
- Effective velocity of scattering plasma relative to the Sun
- Best fit by adjusting ellipse parameters and the V_α and V_δ of the plasma relative to LSR.
- Ellipse represents anisotropy due to source or medium

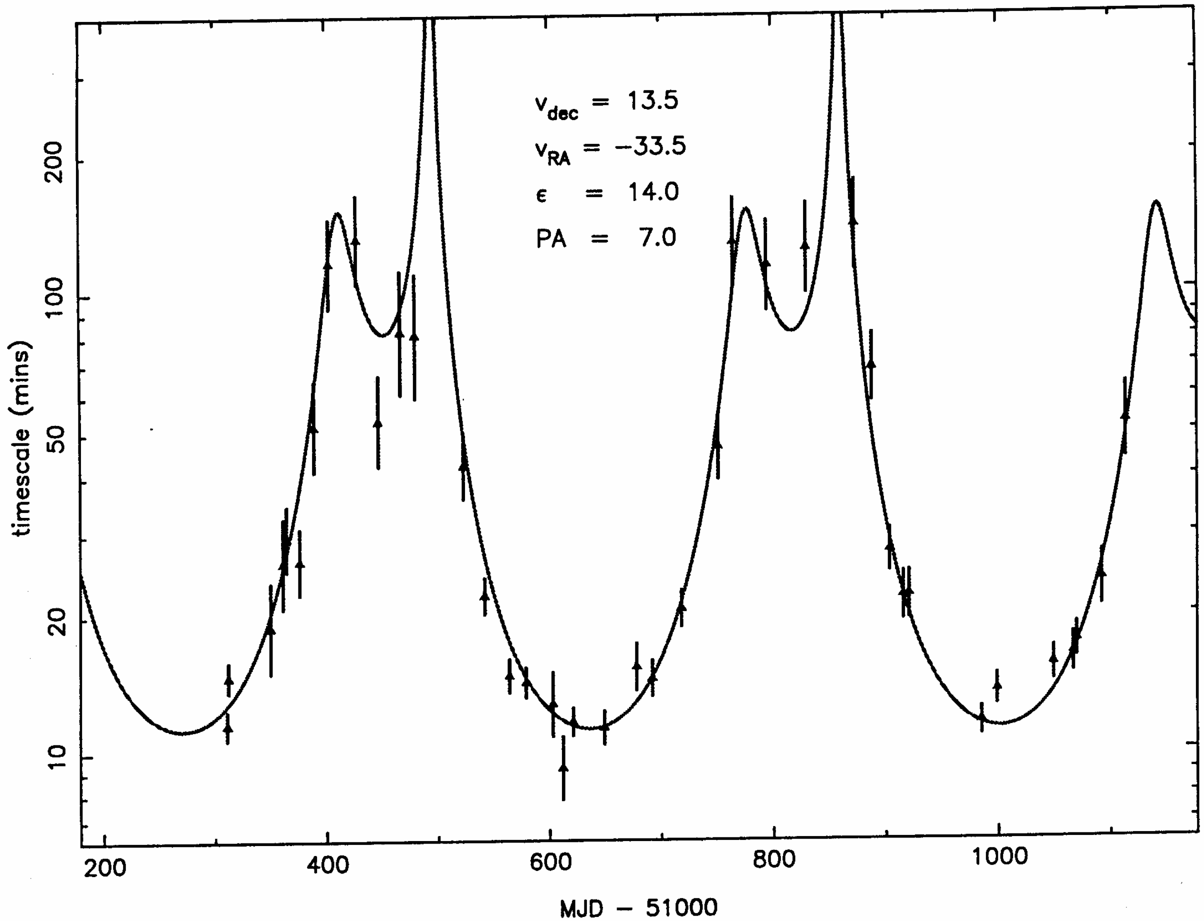

6cm scintillations are broad band

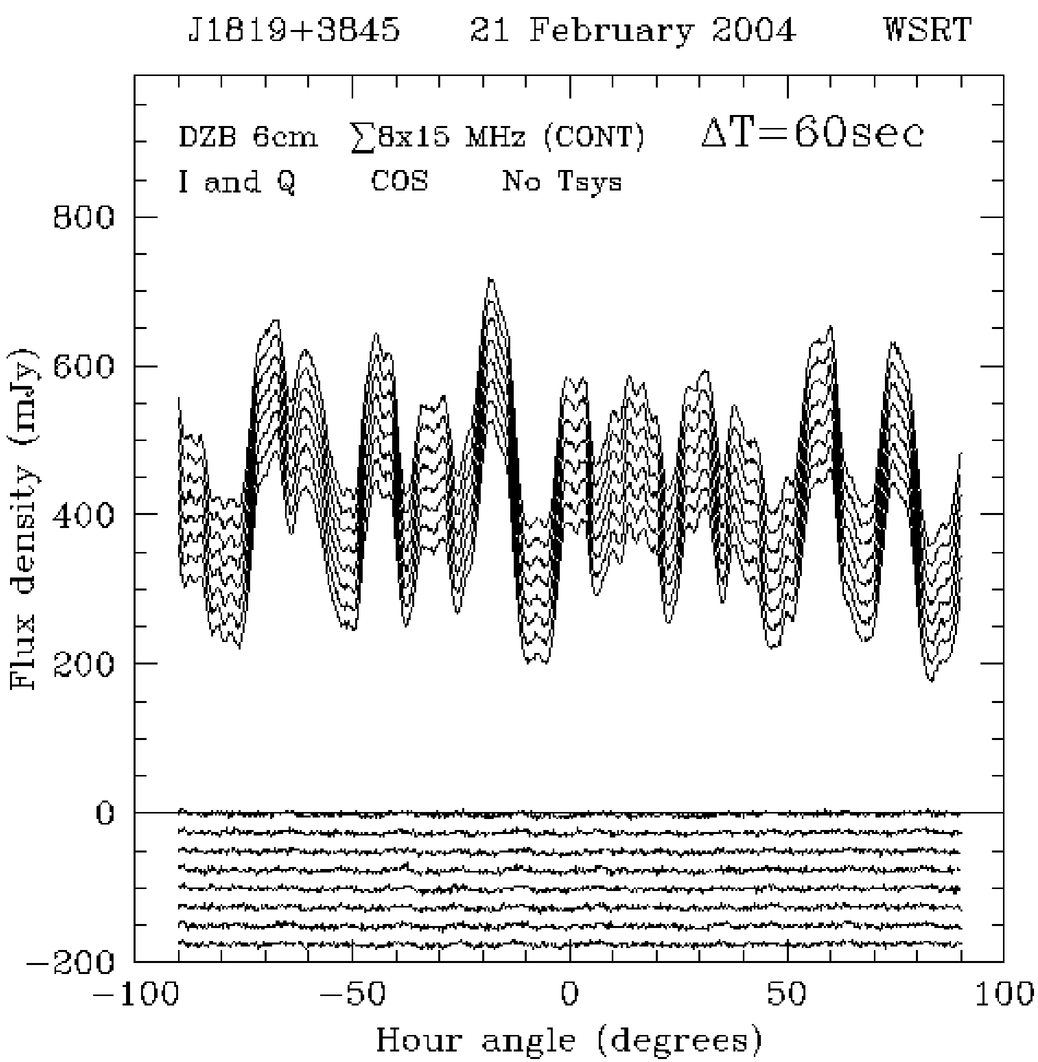

If you thought J1819+3845 was fast.

If 15min x 50 km/s ~ Fresnel scale → d ~ 1 pc !?

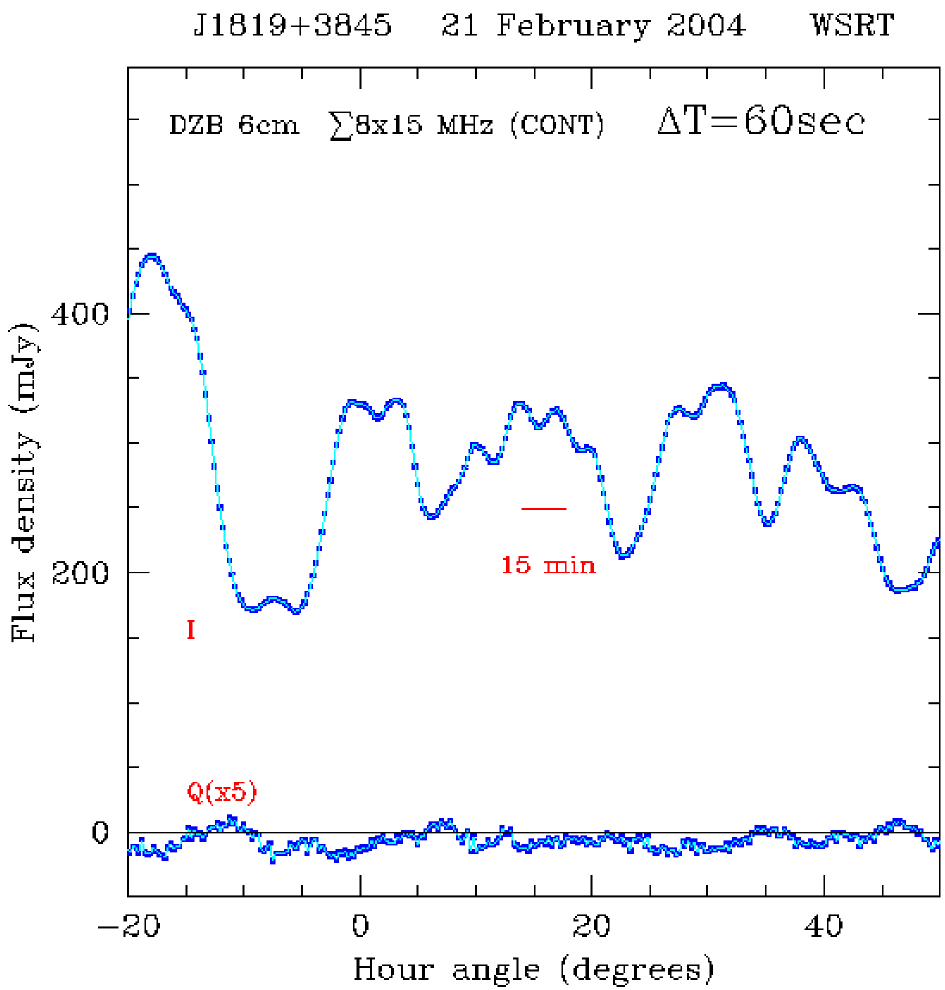

J1819+3845: what did it teach us?

- **Screen properties**

- Distance 5 - 10 pc
- Probably thin

- Anisotropic turbulence
- V_{trans} ~ 30 km/sec

- **AGN properties**

- 6cm size ~ 100 marcsec
- $T_b \sim 10^{12}$ K
- $V_{exp} < 0.25$ c
- Elongated source
- Complex polarized jet
- Multiple pol features , slowly moving (if at all)
- New component in 2004: $< R_f$

PKS 1257-326: time delays, annual cycles and μas-scale evolution

Hayley Bignall (JIVE)
Jean-Pierre Macquart (Kapteyn Institute, Groningen)
Dave Jauncey, Jim Lovell, Tasso Tzioumis (ATNF)
Lucyna Kedziora-Chudczer (U. Sydney)

Time delay, May 13-14 2002

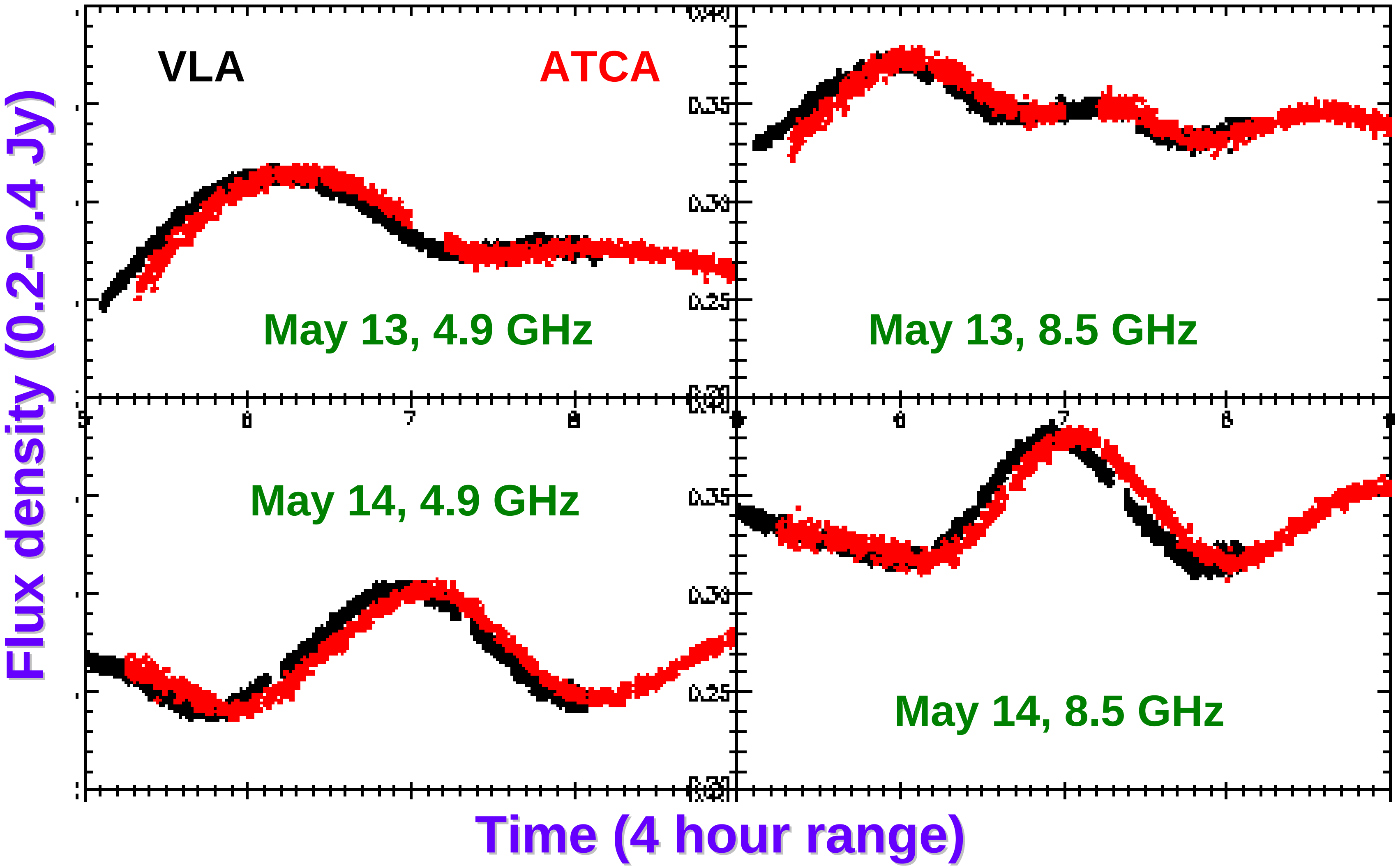

Time delay, Jan 10 2003

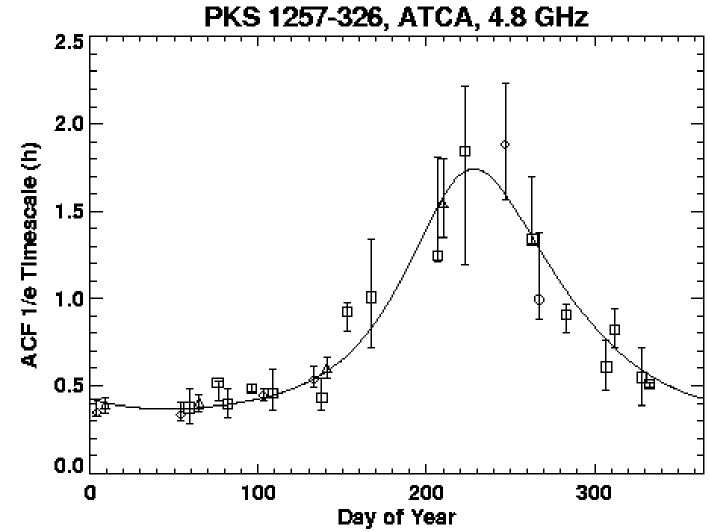

Flux density (0.2-0.4 Jy)

Jan 10, 4.9 GHz

Jan 10, 8.5 GHz

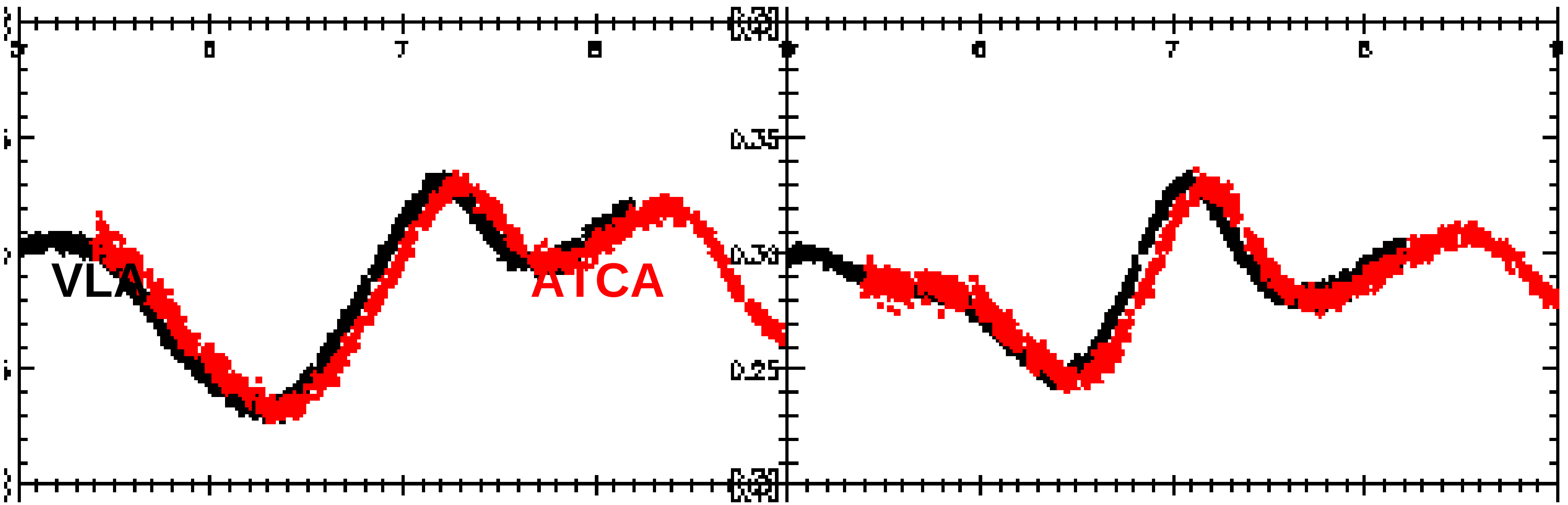

Time (4 hour range)

Time delay varies throughout the year: 300 - 450 sec

Rapid polarisation variability in the core of 0716+714

Uwe Bach
Max-Planck-Institut für Radioastronomie Bonn, Germany

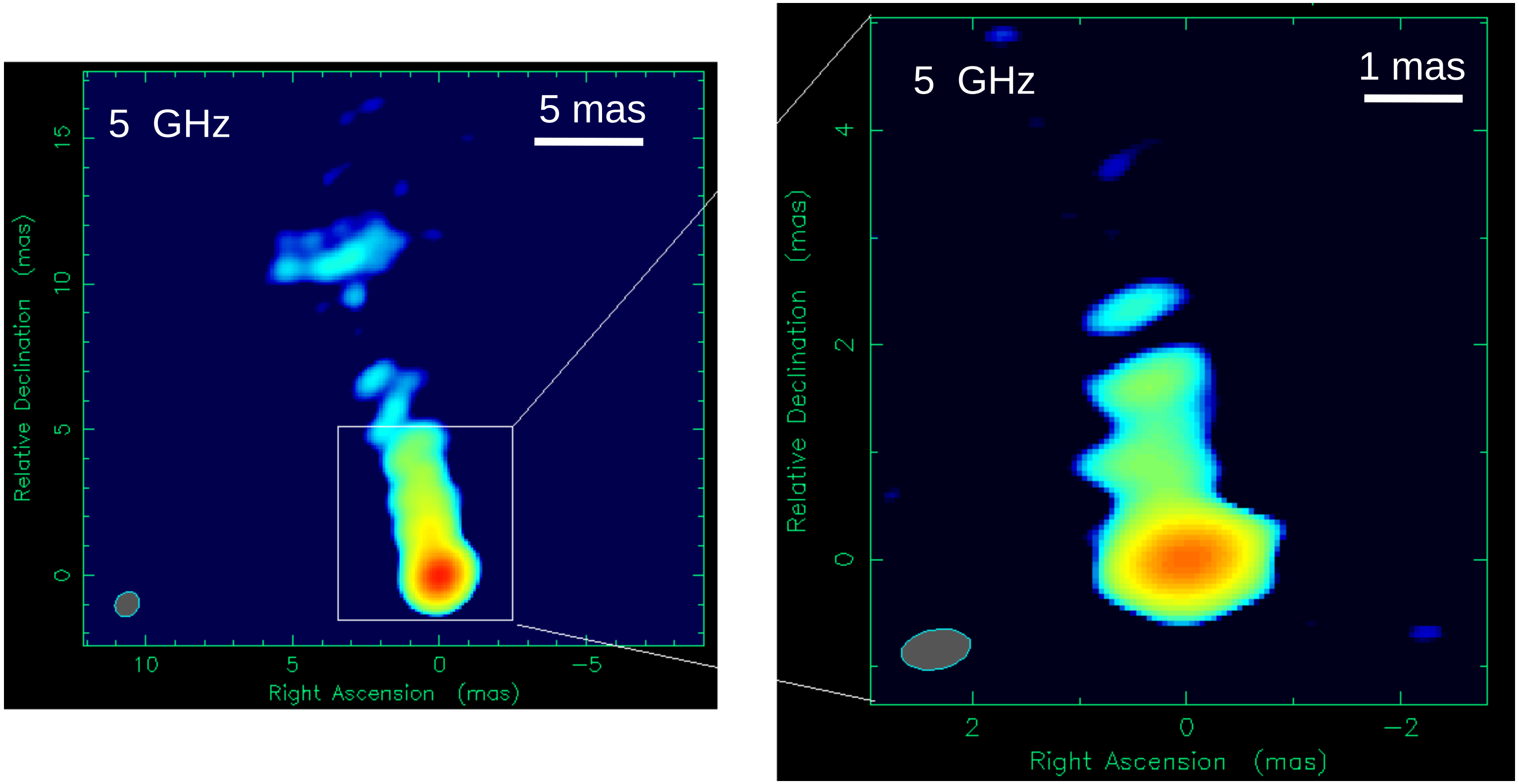

in collaboration with:
T.P. Krichbaum, E. Ros, A. Kraus, S. Britzen, A. Witzel and J.A. Zensus

Search for the Scattering Screen in Front of IDV Blazar Cores

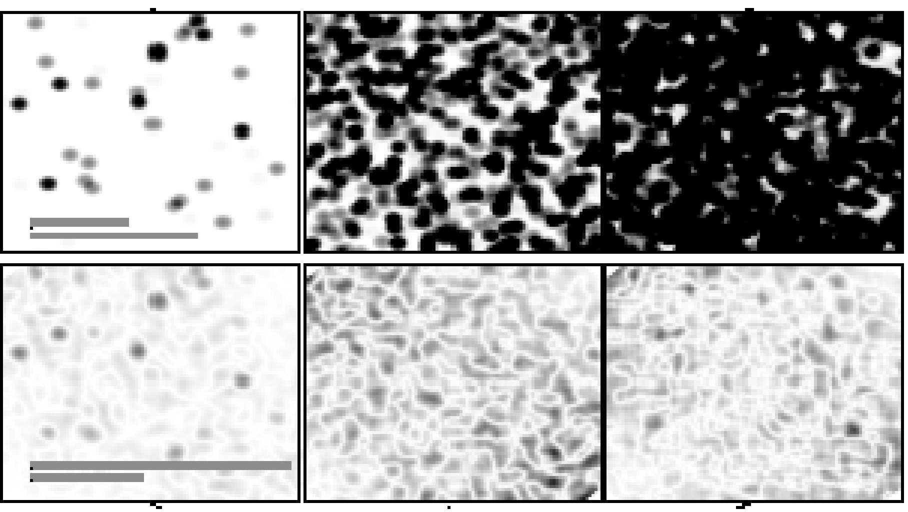

Lars Fuhrmann

T.P. Krichbaum, T. Beckert, G. Cimò, A. Kraus, A. Witzel, J. A. Zensus

Max-Planck-Institut für Radioastronomie, Bonn

Max-Planck-Institut für Radioastronomie

First Spectral Line Observations

2. CO observations with the HHT:

- good correlation of IDV positions with dust and CO
- May 2002:
- ^{12}CO (2-1) observations @ 230 GHz towards 0954+658

  detection of a CO-cloud in the direction of an IDV source

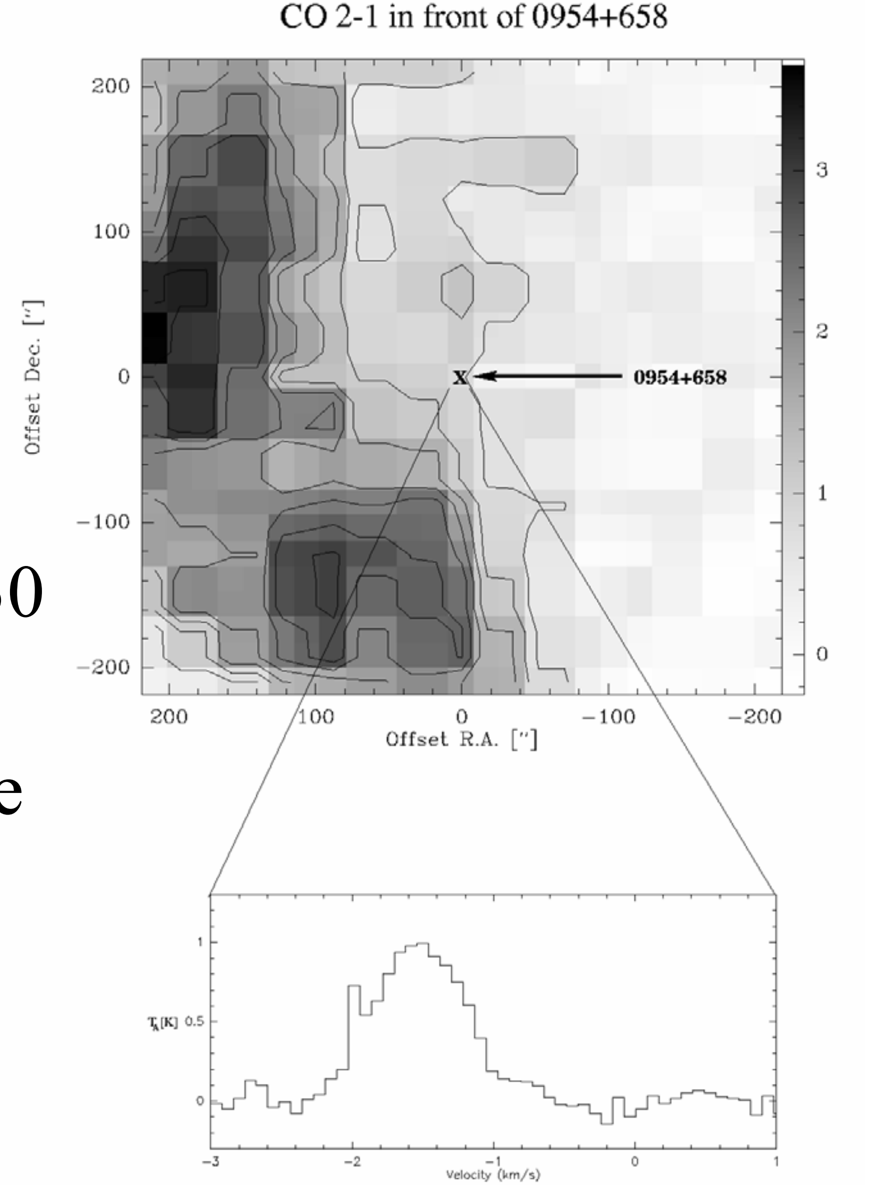

Fuhrmann et al. 2002

HLCs as Origin of Scattering Material for IDVs?

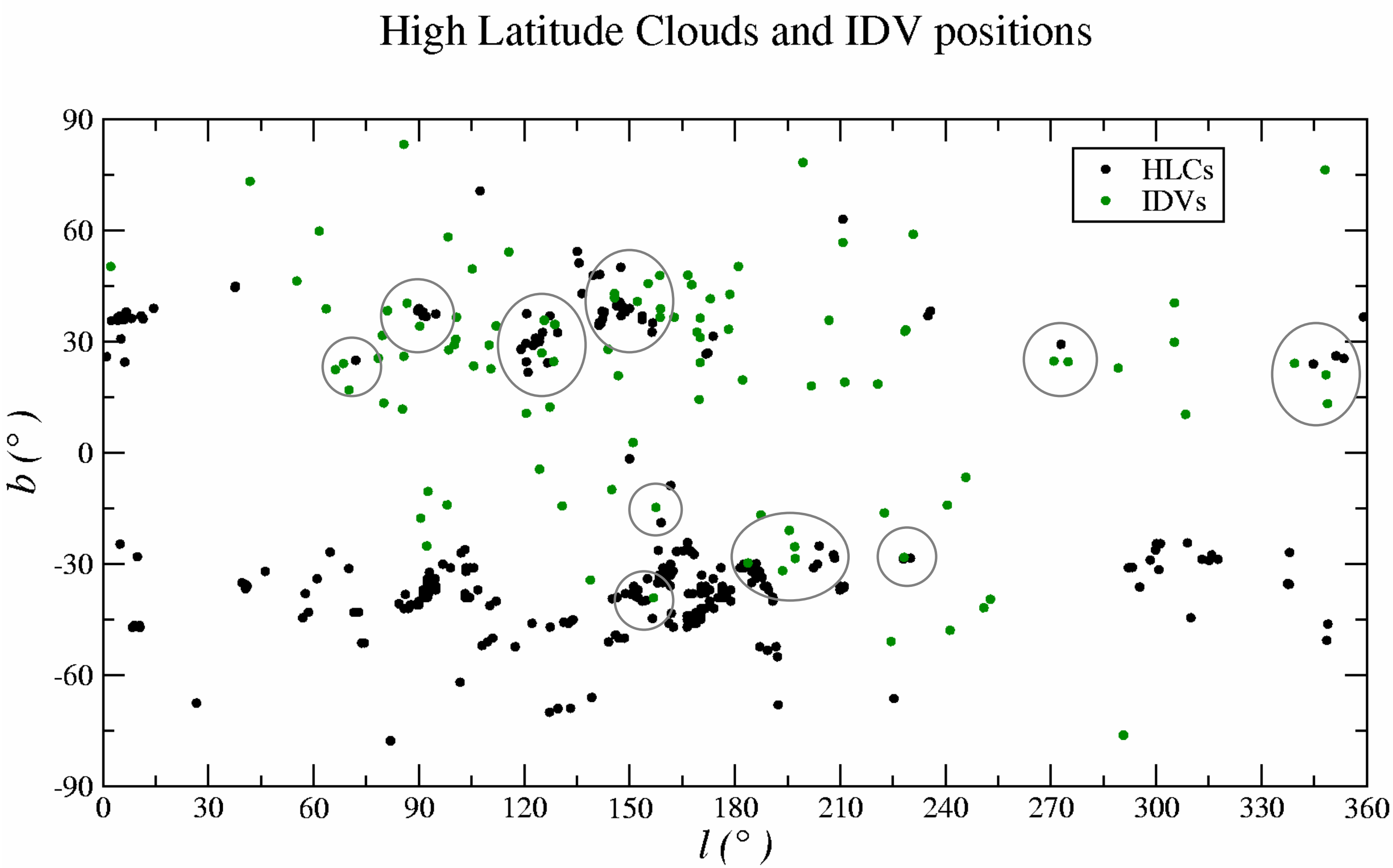

IDV from Subimages

Carl Gwinn

UC Santa Barbara

Outline:

- IDV has some seemingly paradoxical properties
  - ✓Quasi-sinusoidal intensity variation
  - ✓Nearby scattering screen
    (tricky to explain via selection effects)
- Scintillations of PSR J0437-471 show:
  - ✓Large decorrelation bandwidth ⇒small scattering angle
  - ✓Fine substructure
- Subimages can give rise to substructure
- Subimaging of IDV sources can explain some paradoxes:
  - ✓Sinusoidal intensity variation
  - ✓Selects nearby scatterers
- SKA and LOFAR can observe subimages directly

Substructure in Scintillation Spectrum of PSR J0437-4715

- The fine structure visible in the scintillation spectrum is *really there*.
- Such substructure is not uncommon in pulsar dynamic spectra (Stinebring et al. 2001, Hill et al. 2003).
- We see characteristic bandwidth $\Delta\nu \approx 0.5$ MHz.
- All* previous measurements for PSR J0437-4715 found decorrelation bandwidth near this narrowband value.

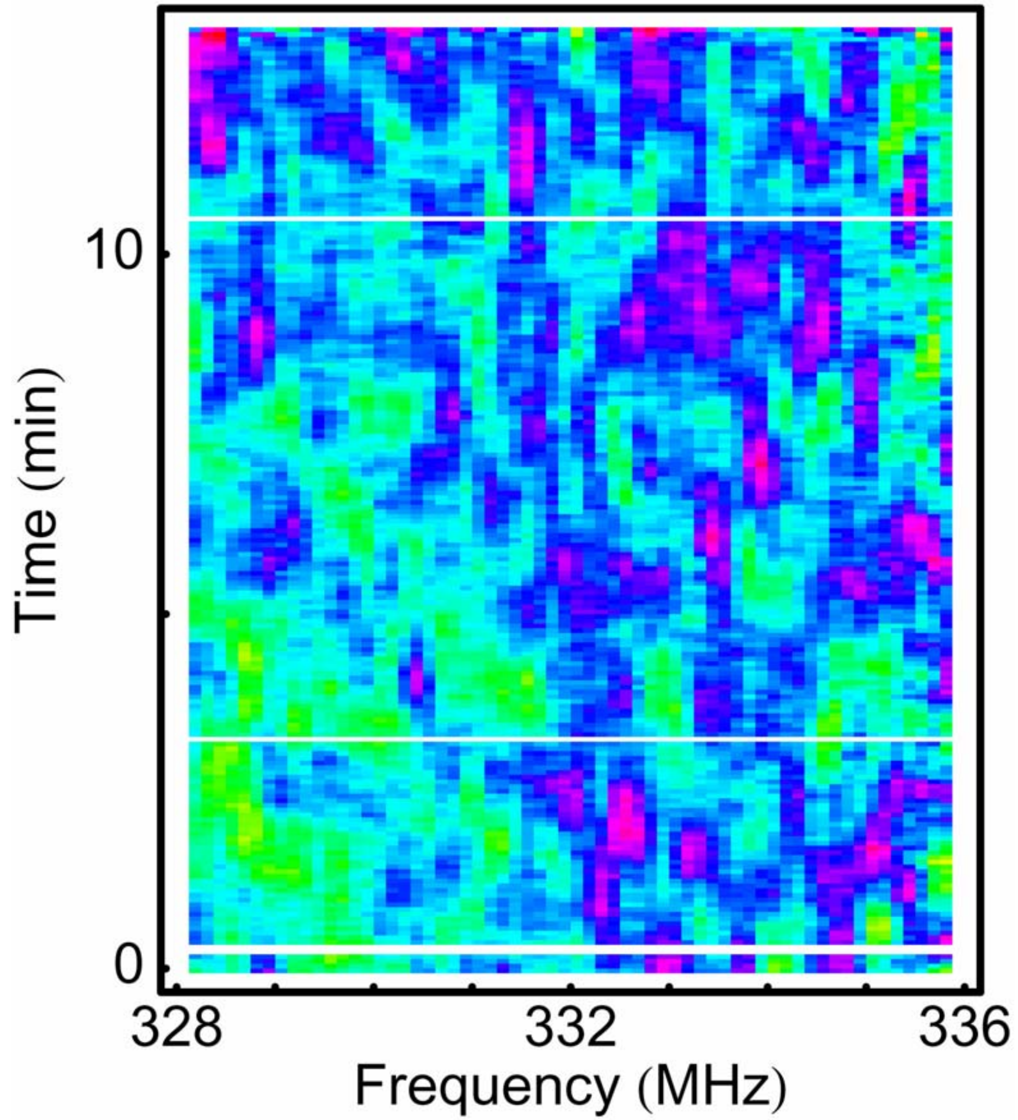

From Hirano PhD thesis 2001

* Except for Issur 2000.

Stinebring et al. (2001) propose: Subimages create substructure.

The subimages interfere with the primary scattered image.

In effect, subimage-primary image pairs act as interferometers, to create a fringe pattern in the observer plane. The fringes are sinusoidal.

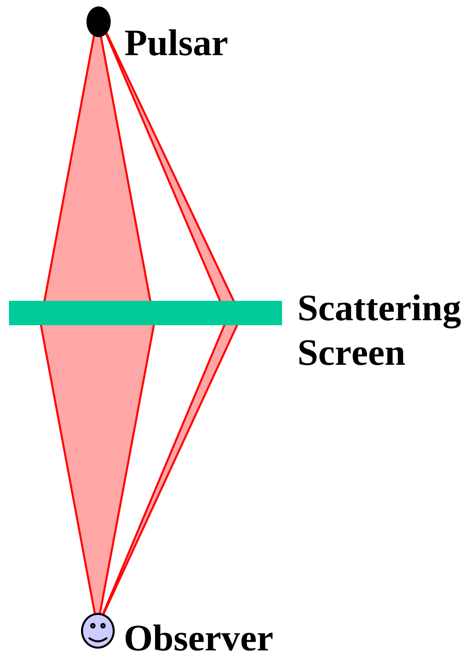

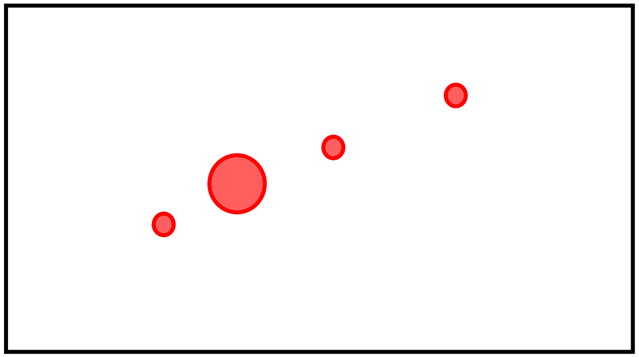

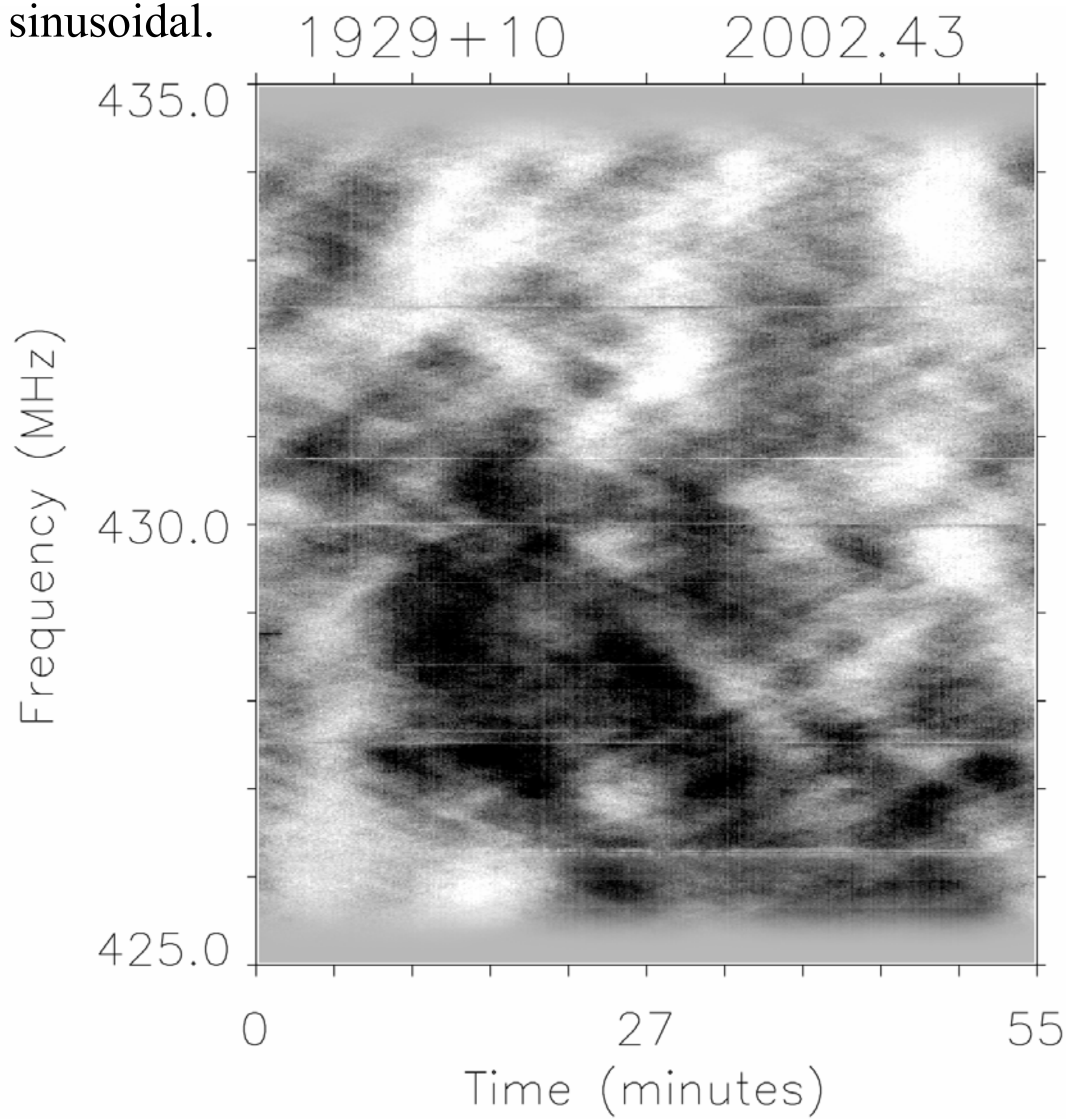

From Hill et al. 2003

S. Kulkarnies summary of what we know about GRBs

- GRBs are highly collimated explosions and possess central engines which drive the explosion
- Long duration GRBs are deaths of massive stars (SN Ib/c connection)
- There is growing evidence of underenergetic GRBs (e.g. 980425, 030329, 031203) with engines outputing a mix of ejecta: ultra-relativistic (Γ >100), relativistic(Γ >10) and mildly relativistic (Γ >2) ejecta
- The fraction of nearby Ib/c supernovae with features indicative of a central engine is small, less than 10%.

GRB Energetics: Tiger becomes Lamb

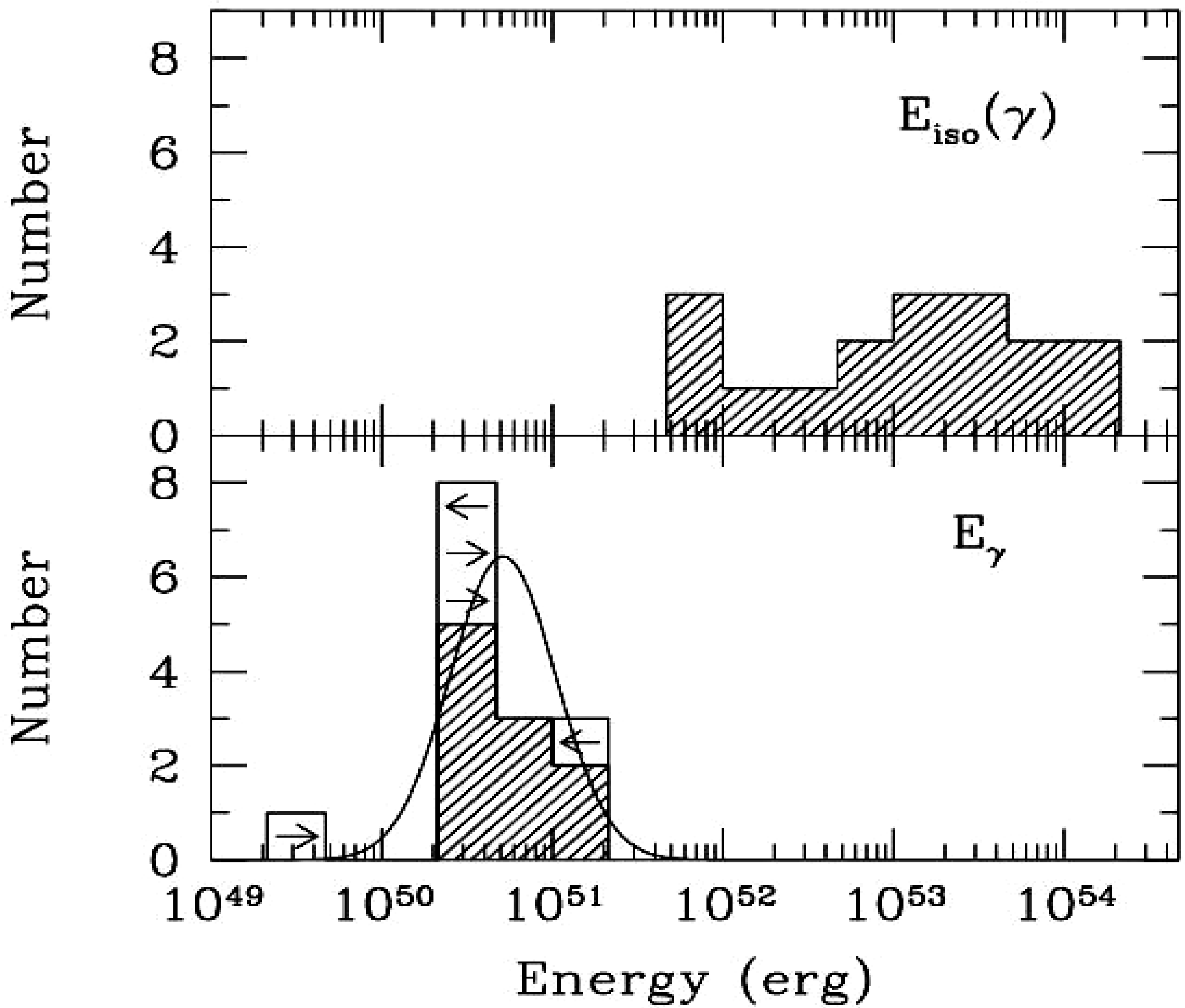

Before the beaming correction (isotropic)

After the beaming correction

(Frail et al.)

and the latest ….

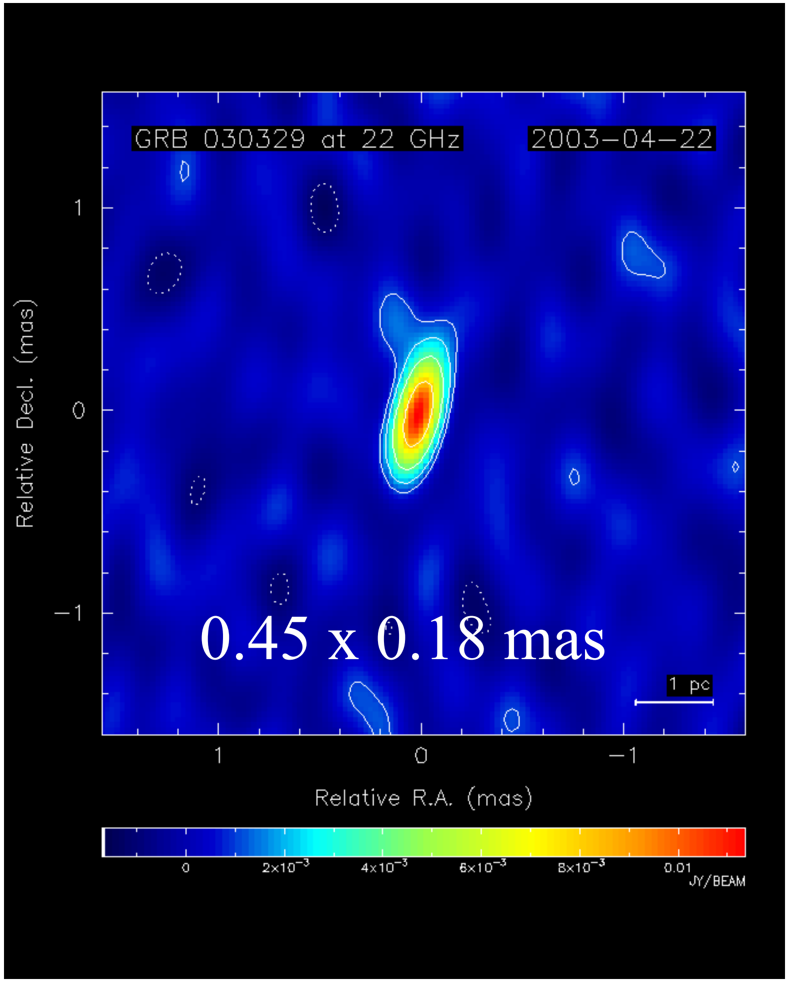

- GRB 030329, 24 days after the burst
  - VLBA+Bonn at 22 GHz
- Marginally resolved at 0.08 milliarcsec
- In line with expectations from the fireball model
  - superluminal expansion (5c)

Taylor et al.

Galactic Electron Density Models and Constraints on Scattering in the IGM

Jim Cordes
Cornell University

- NE2001 = Galactic Electron Density Model
  - n_e and δn_e (as C_n^2)
  - Relationship to TC93
  - Input Data
  - Structure of Model
  - Implications
  - Availability
- New Pulse Broadening Times
- New Parallaxes
- Constraints on the IGM
- New Pulsars

Model Components

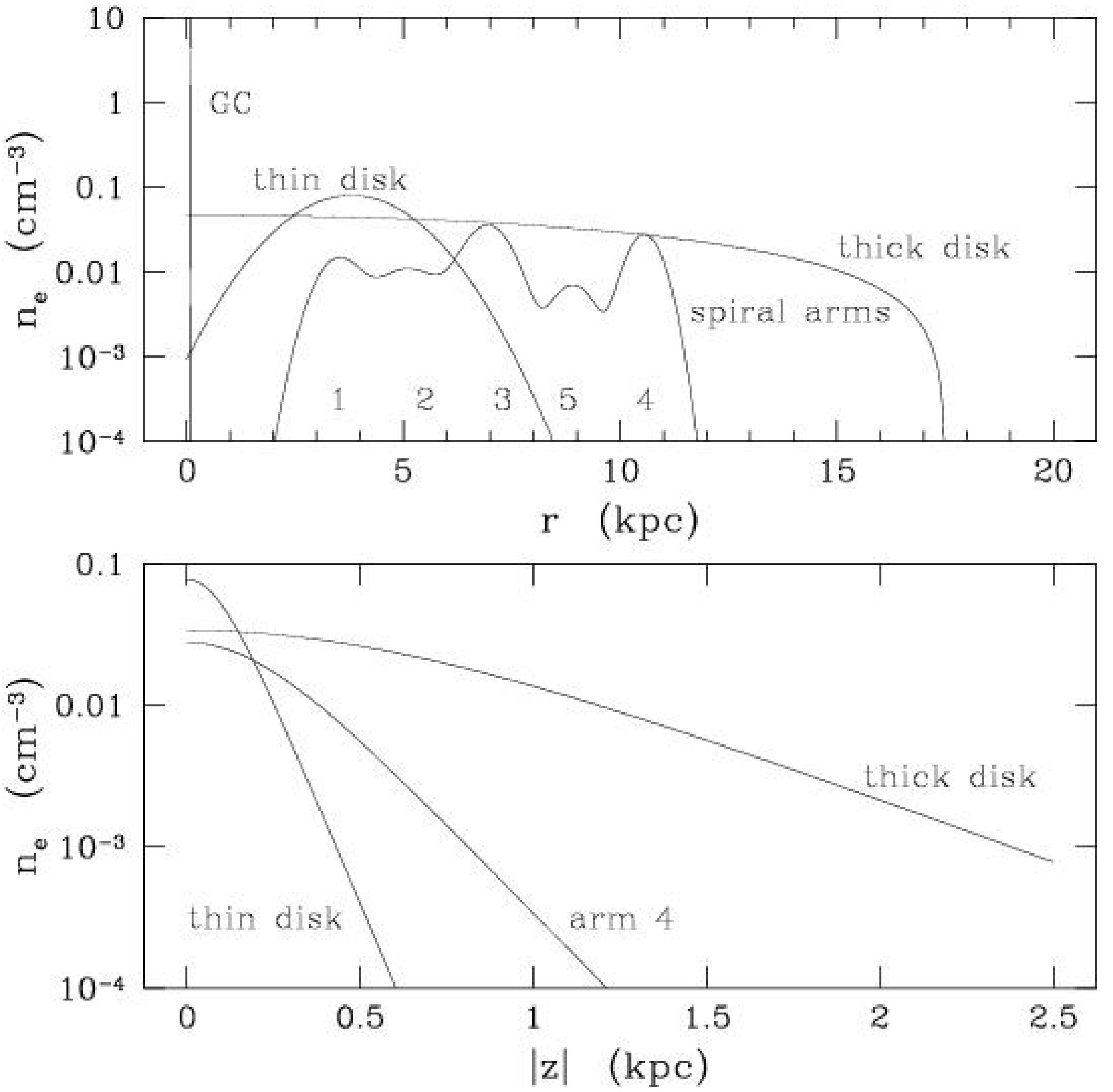

NE2001

- x2 more lines of sight (D,DM,SM)

  [114 with D/DM, 471 with SM/D or DM] (excludes Parkes MB obj.)
- Local ISM component (new) (relies on new VLBI parallaxes)

  [12 parameters]
- Thin & thick disk components (as in TC93)

  [8 parameters]
- Spiral arms (revised from TC93)

  [21 parameters]
- Galactic center component (new)

  [3 parameters] (+auxiliary VLA/VLBA data ; Lazio & Cordes 1998)
- Individual clumps/voids of enhanced dDM/dSM (new)

  [3 parameters x 20 LOS]
- Improved fitting method (iterative likelihood analysis)

  penalty if distance or SM is not predicted to within the errors

J.P. Marquart, DISS in J1819+38

Acrobat-Dokument

IDV scattering screens: clues from pulsar spectroscopy

Mark Walker
(Sydney Uni)
[& Don Melrose & Dan Stinebring]

More “anomalies” …

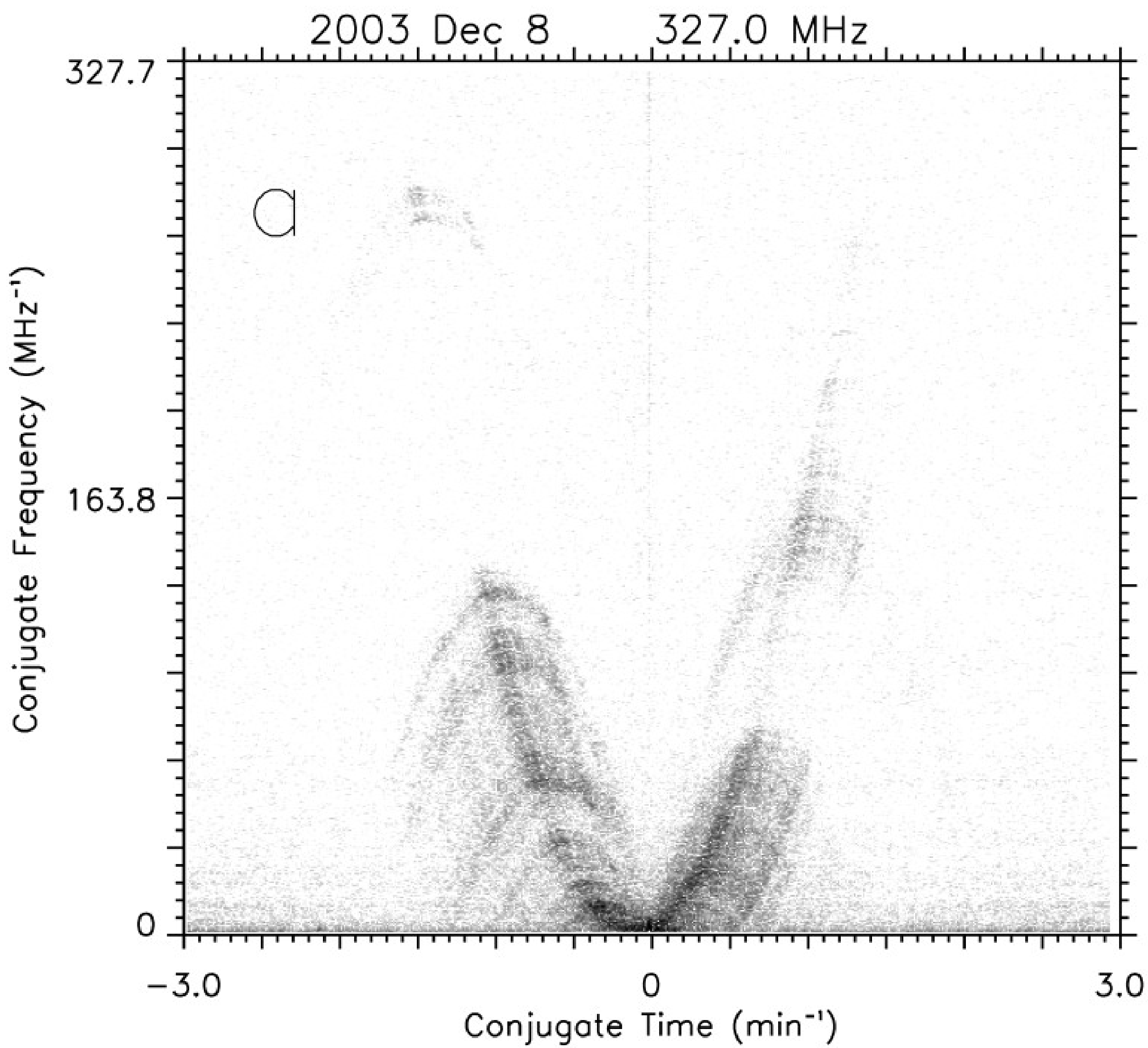

B0834+06

Arecibo data showing arclets whose apexes follow a parabola

Courtesy Dan Stinebring

Implications

- Patchy illumination --> power concentrations on scales < 0.15 AU (0834+06)
- Power concentrations may be diffractive (localised scattering) or refractive (lens-like)
- Scattering angles comparable to what is expected from IDV screens
- V_{scr} not large compared with V_{psr}

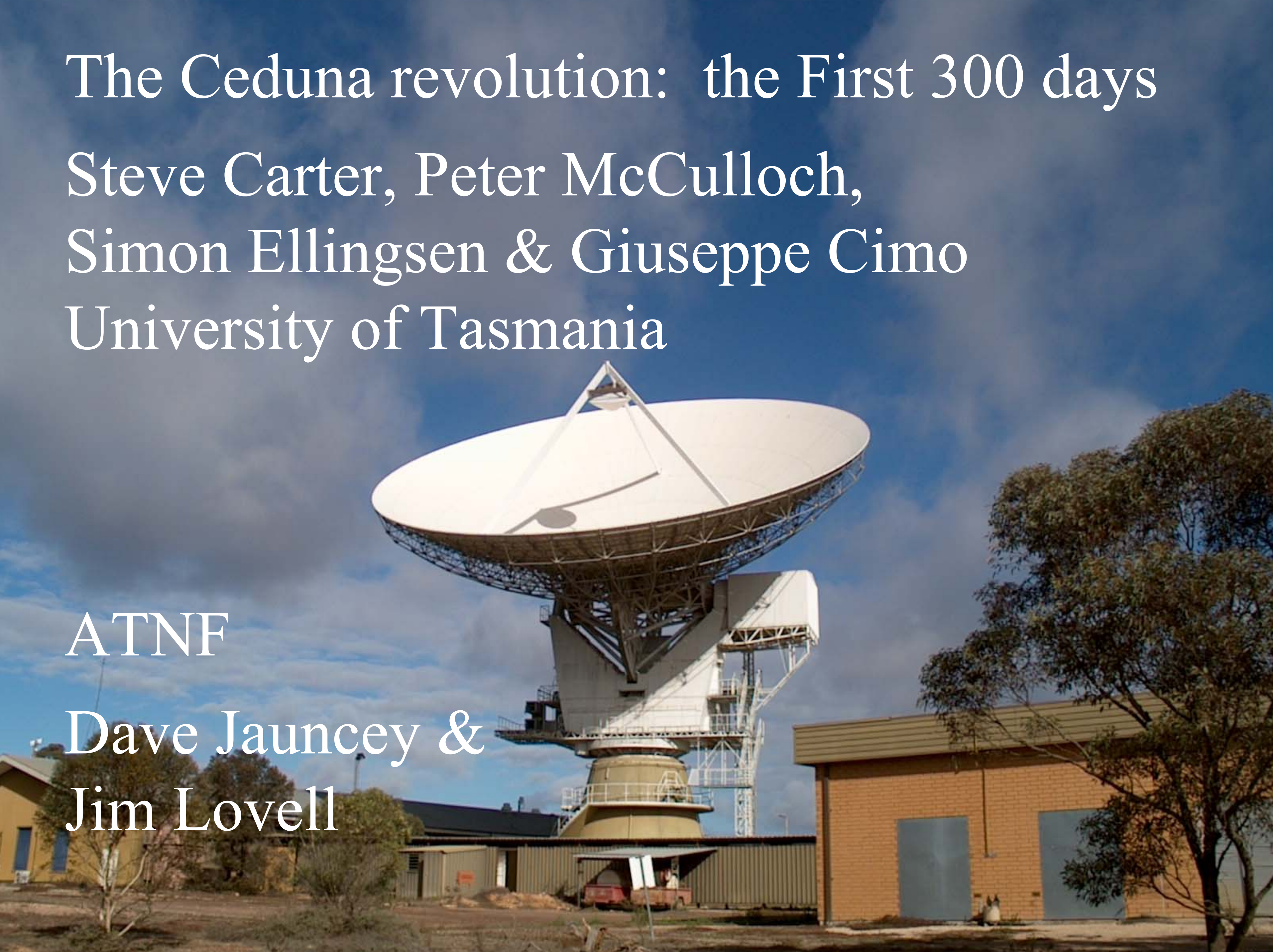
The Ceduna revolution: the First 300 days
Steve Carter, Peter McCulloch,
Simon Ellingsen & Giuseppe Cimo
University of Tasmania
ATNF
Dave Jauncey &
Jim Lovell

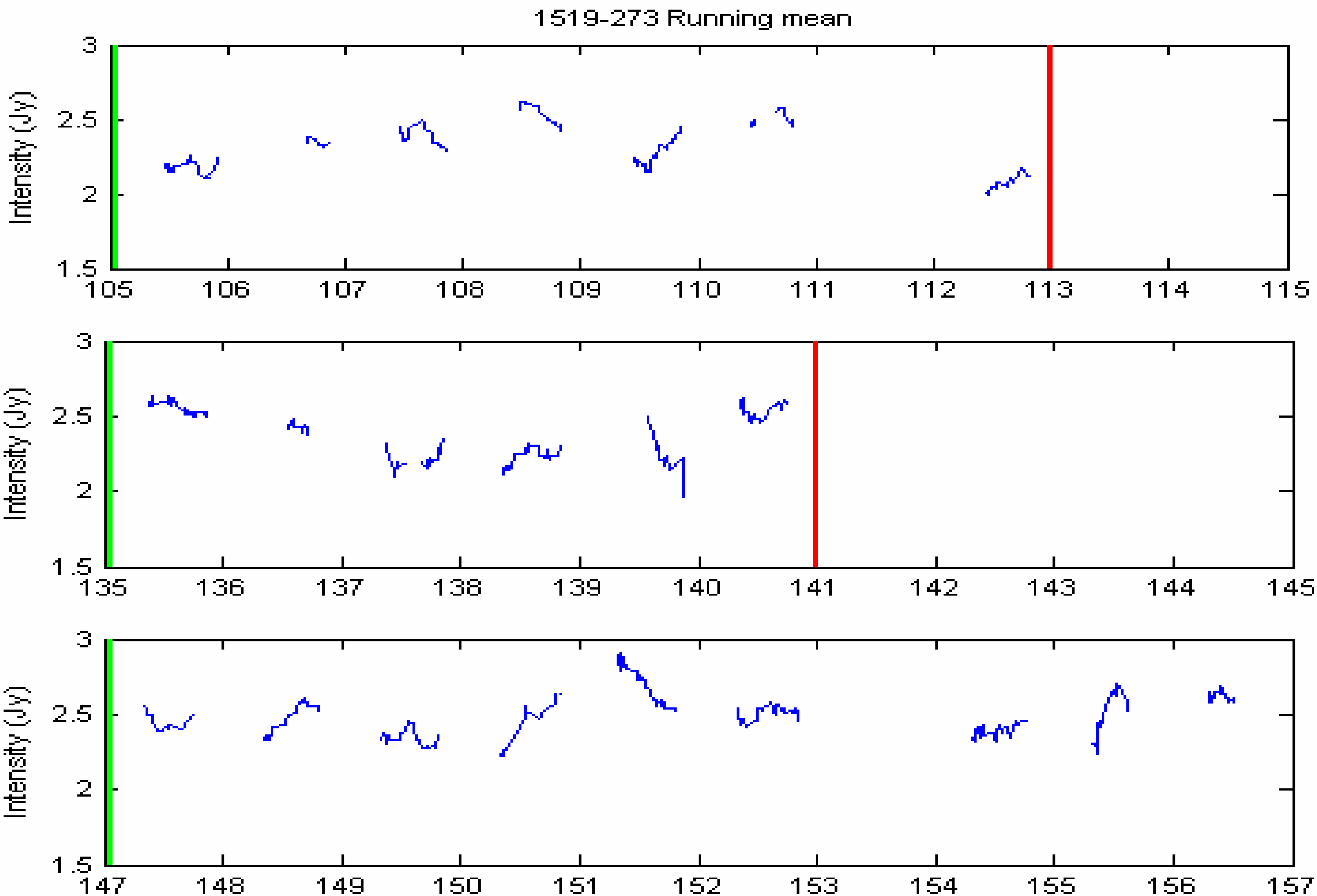
1519-273 Running mean
Intensity (Jy)
3
2.5
2
1.5
105
106
107
108
109
110
111
112
113
114
115
135
136
137
138
139
140
141
142
143
144
145
147
148
149
150
151
152
153
154
155
156
157

Variability annual cycle

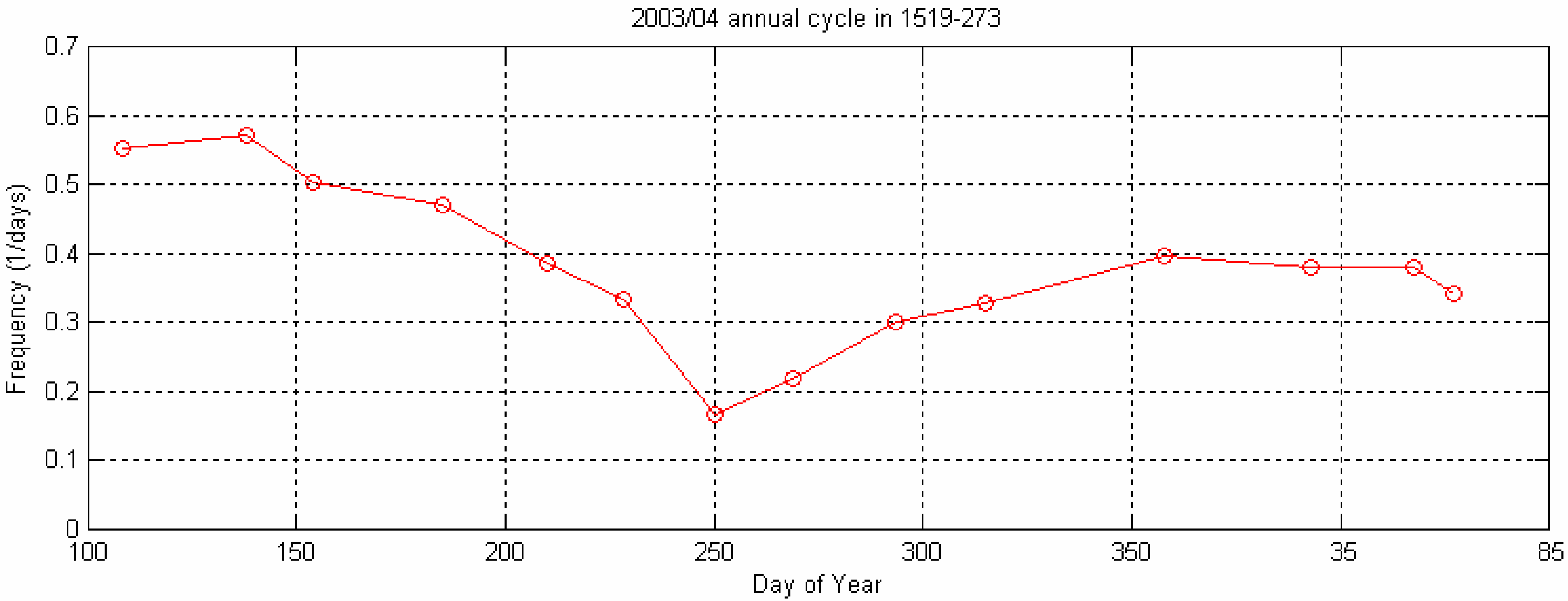

Where to next?

We are exploring several possibilities for continuous 24-hour coverage:

GAVRT,
Yamaguchi
and PARI.

MASIV: The Micro-Arcsecond Scintillation-Induced Variability survey

Jim Lovell[1], Dave Jauncey[1], Hayley Bignall[2], Lucyna Kedziora-Chudczer[3], J-P Macquart[4], Barney Rickett[5], Tasso Tzioumis[1]

1 ATNF
2 JIVE
3 Sydney Uni
4 Kapteyn Institute, Netherlands
5 Uni California San Diego

Current Status

- Observations complete
- First results published
  - 85 of 710 variable
  - $T_B < 10^{12}$K
  - "Top 29" sources listed

Lovell et al. 2003, AJ 126, 1699

- All 4 epochs now reduced
  - Analysis underway
  - Polarisation still to do

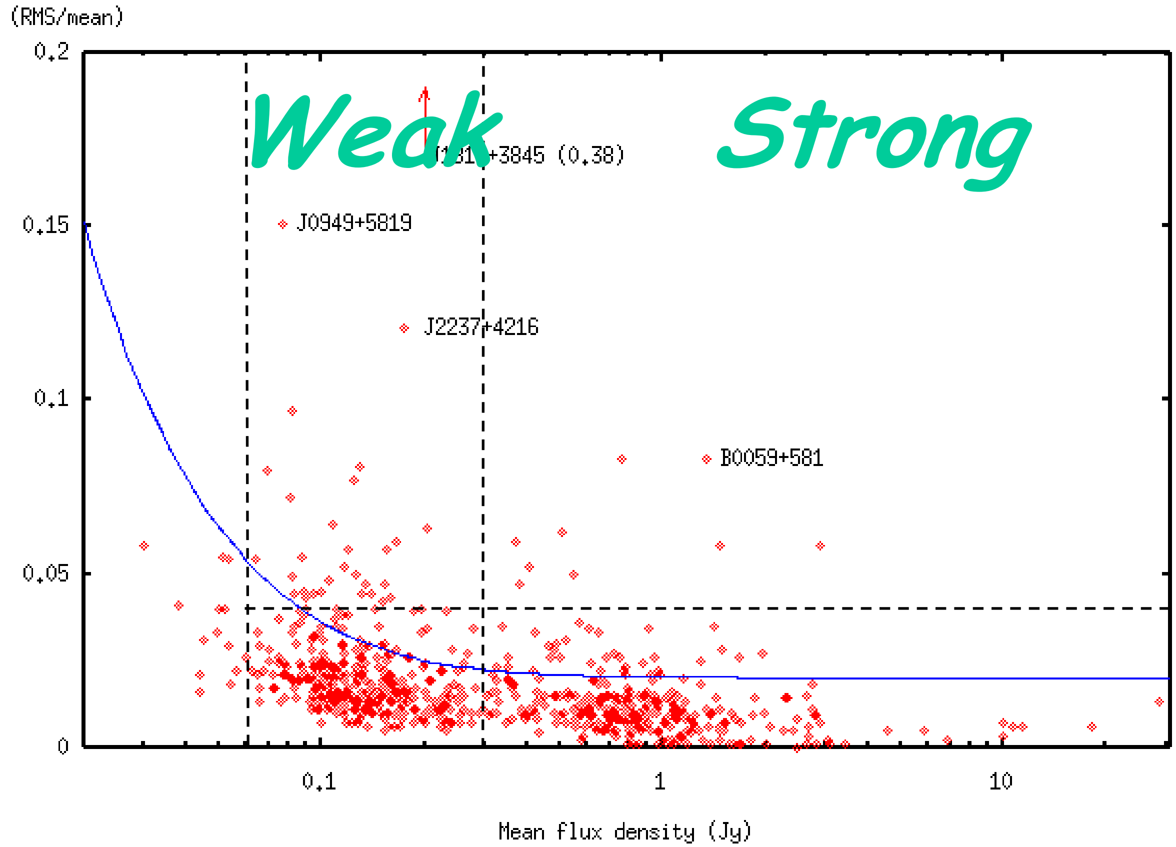

- Extreme variables are rare
- More high modulation index sources in the weaker sample. Difference in mas-scale structure? See Roopesh’s talk.

Intensive polarimetric 3mm monitoring of 0716+714 with the Pico Veleta telescope

Iván Agudo
Max-Planck-Institut für Radioastronomie

T. P. Krichbaum, H. Ungerechts, E. Angelakis, A. Witzel

Overview of the Talk:

- Introduction
- Data reduction procedure
  - Point to point calibration and editing
  - Systematic effects correction
- Results
- Future work

Introduction

- Pico Velela (IRAM-30m) observations part of the 0716+714 ENIGMA campaign
- They started the 10th Nov 2003 with good weather conditions for 3mm observations
- During more than 4 days these conditions were maintained
- The 15th we should stop the observation due to fast winds and a storm. Only a few (non regular) measurements were obtained after that.
- In addition to planets and Galactic calibrators we measured a set of extragalactic calibrators close to **0716+714**. The duty cycle:

0716+714
J0217+73
J0639+73
0836+710
0716+714
J1642+68
J1800+78

0716+714 was measured every ½ hour

Extragalactic calibrators were measured every hour

Introduction

One of the 1.3 mm receivers (A230) was much less sensitive and we loose SNR even for the strong sources

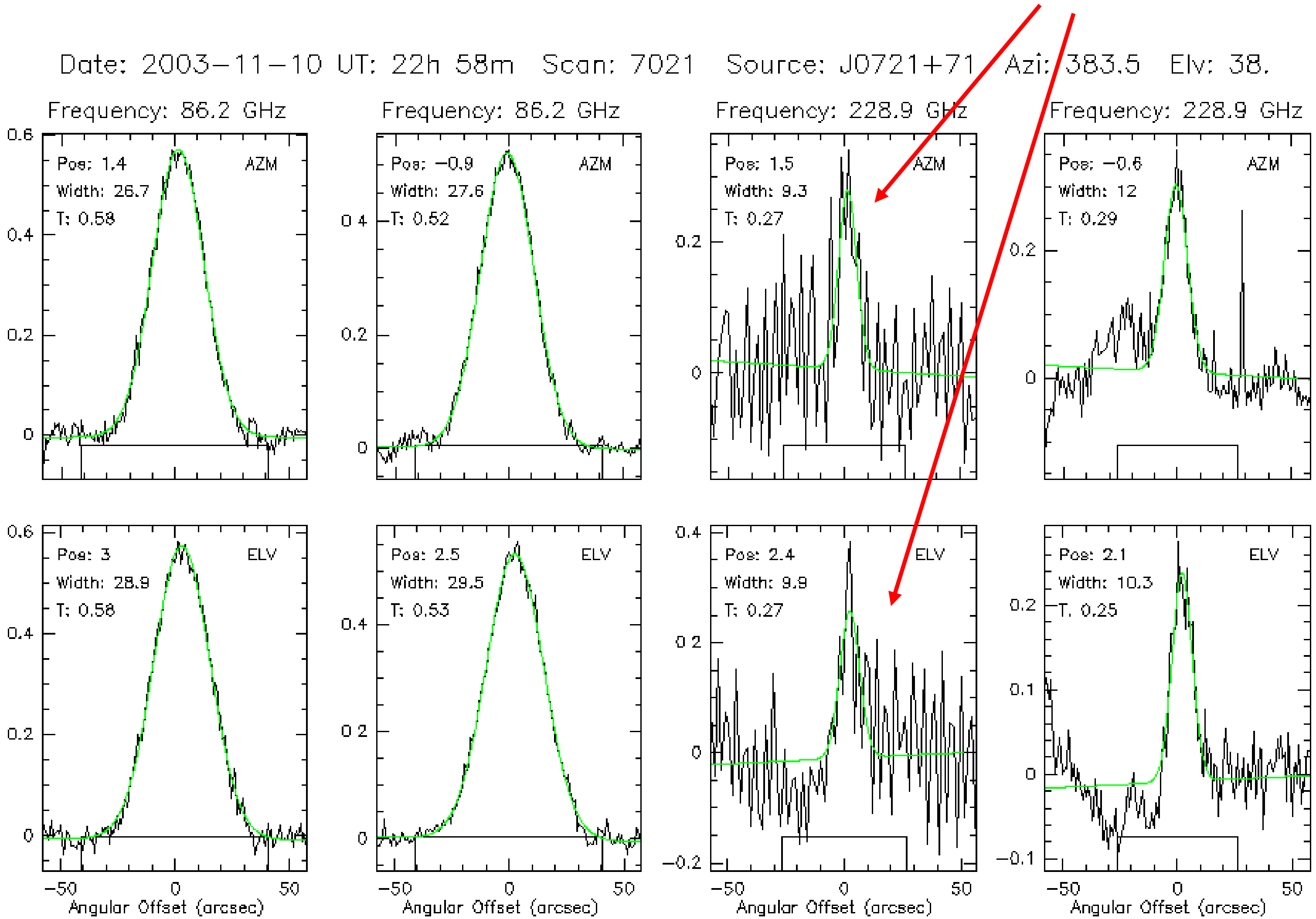

Introduction

We observed simultaneously with 4 different receivers at 3mm (A100, B100) and 1.3mm (A230 and B230)

For each frequency, each receiver recorded relative orthogonal linear polarizations

Measurements were preformed by cross scans (scanning the source position in AZI and ELV)

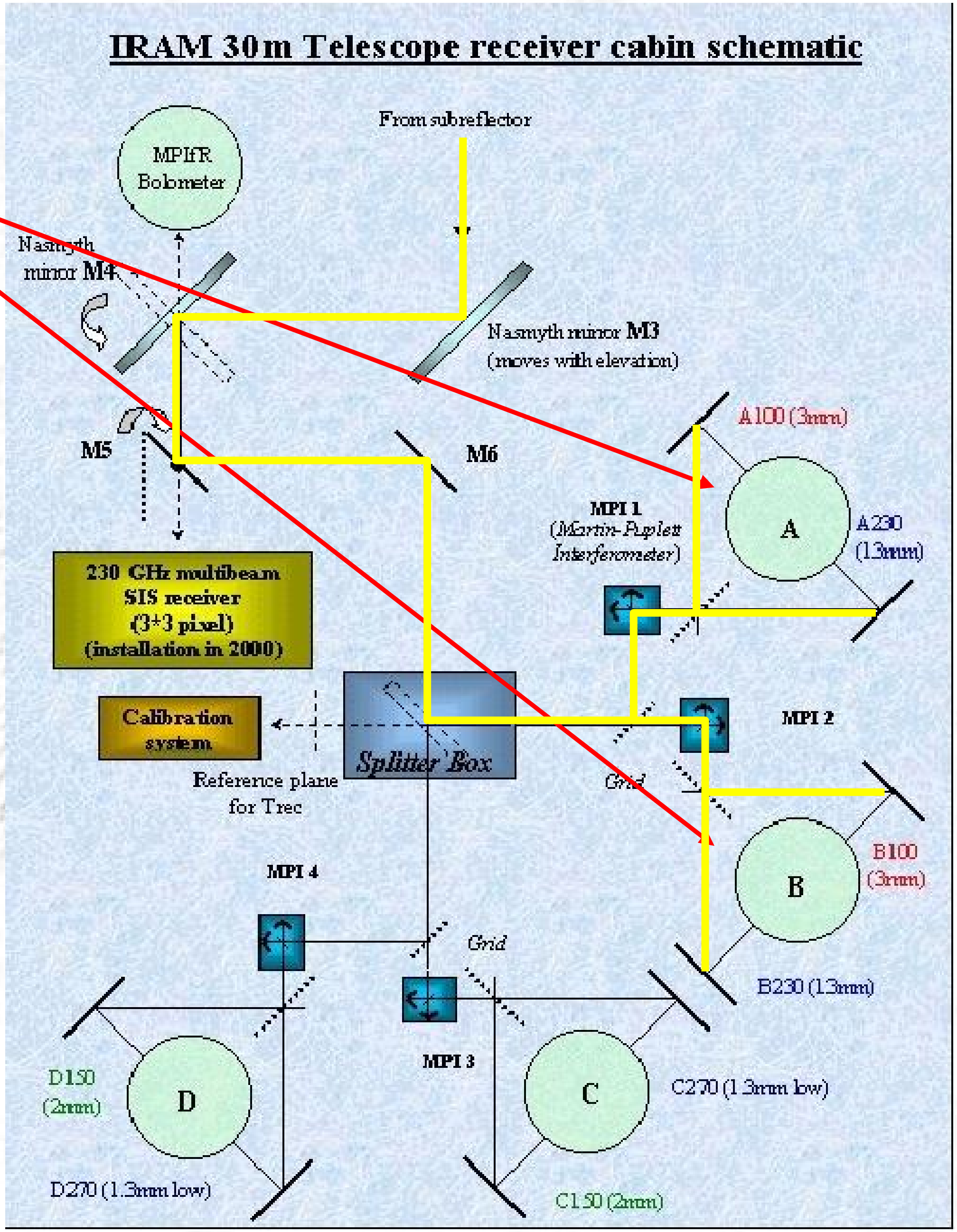

Introduction

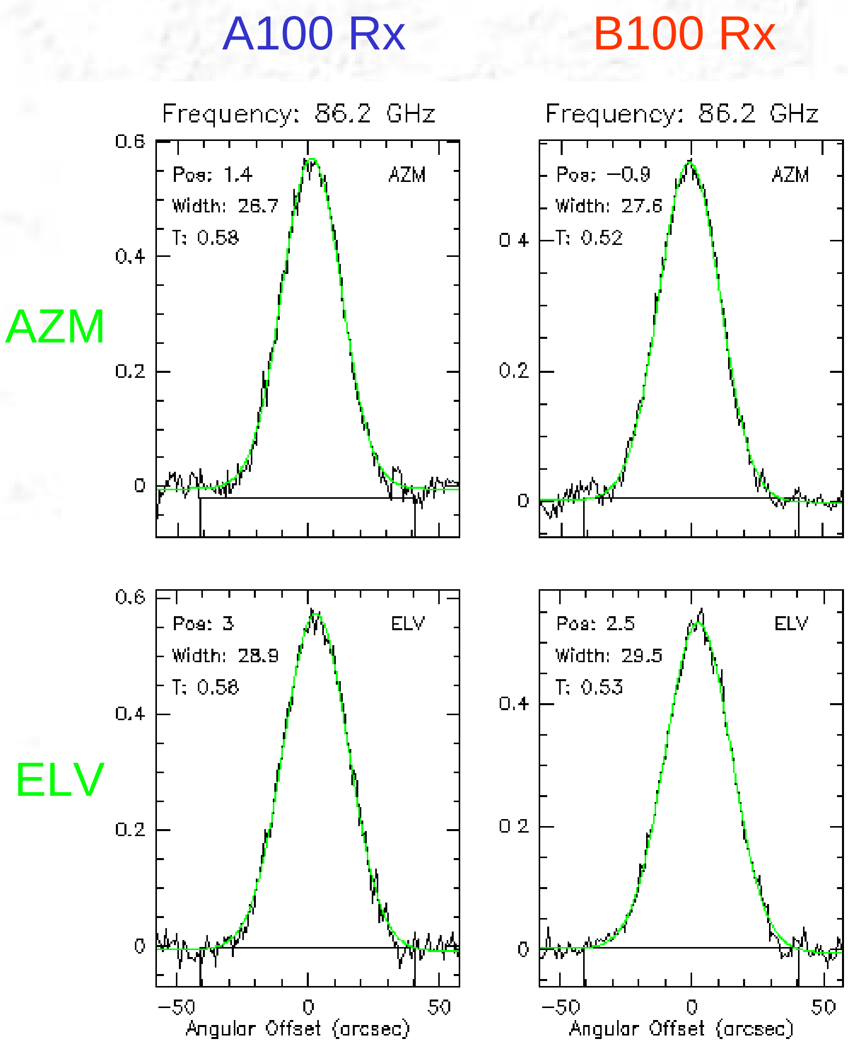

- We first concentrate on the 3mm data reduction
- The most difficult 1.3 mm data reduction will be performed later

Data reduction: Point to point calibration and editing

- Initial calibration using the telescope (CLASS, GILDAS) software:
  - Opacity correction
  - Conversion from counts to T_A^* [K]

- Average the sub-scans for each measurement (AZI and ELV separately)

- Fit the results to Gaussians scan by scan (AZI and ELV separately)

- Correction of the errors introduced by pointing offsets, typically less than 3” (FWHM of telescope beam 28” at 3mm)

- Average the measured flux densities in the AZI and ELV orientations

- Data editing. Removing bad measurements

Data reduction: Point to point calibration and editing

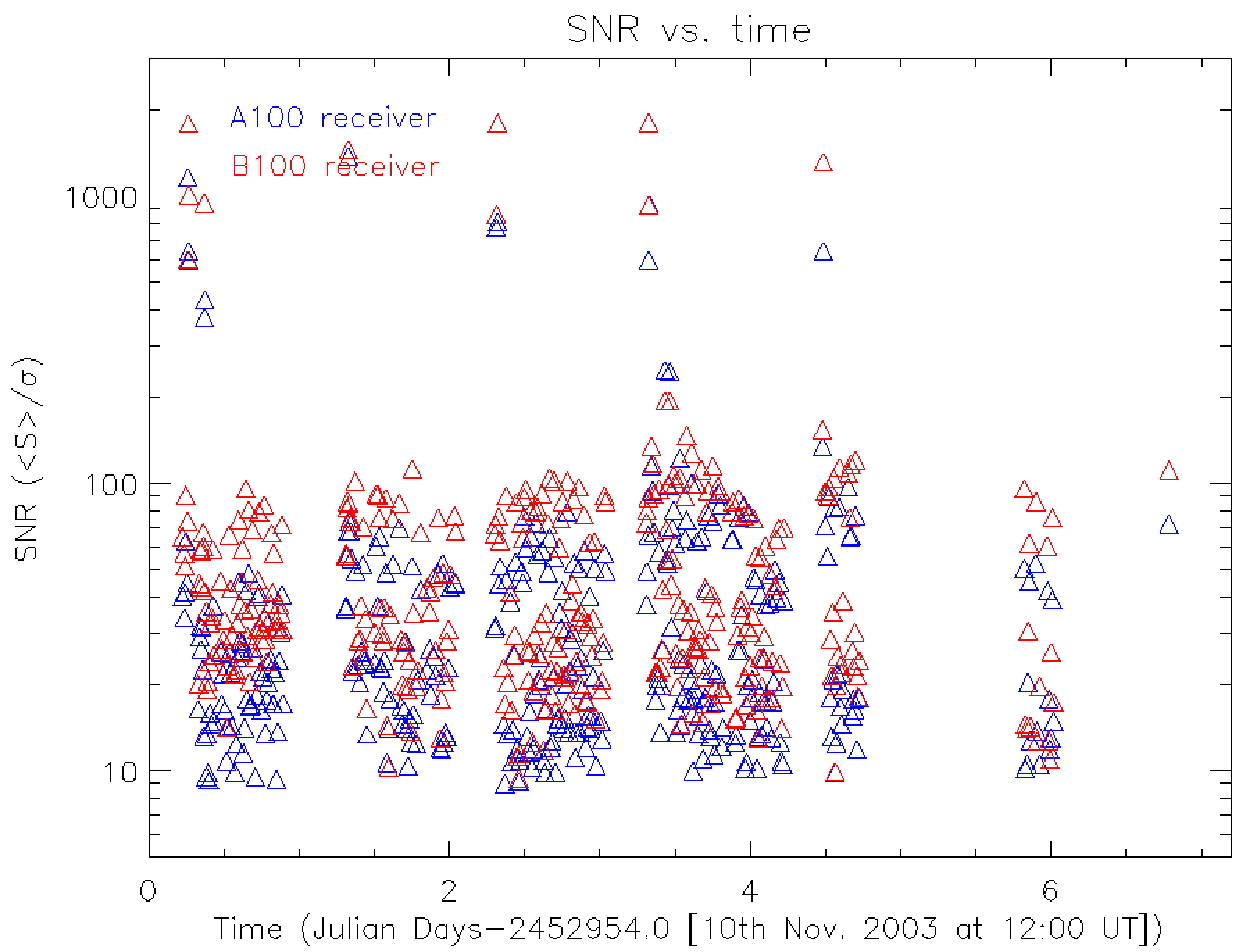

SNR always larger than 8

Data reduction: Systematic effects correction

- Apply the elevation dependent gain curve (Greve et al. 1998) for the 30-m telescope

- It accounts for the elevation dependence of the beam pattern due to gravitational deformation of the dish

- We have completed the STANDARD DATA REDUCTION (except for the absolute S calibration)

- But we need better accuracy than 5%. We look for further possible corrections

Data reduction: Systematic effects correction

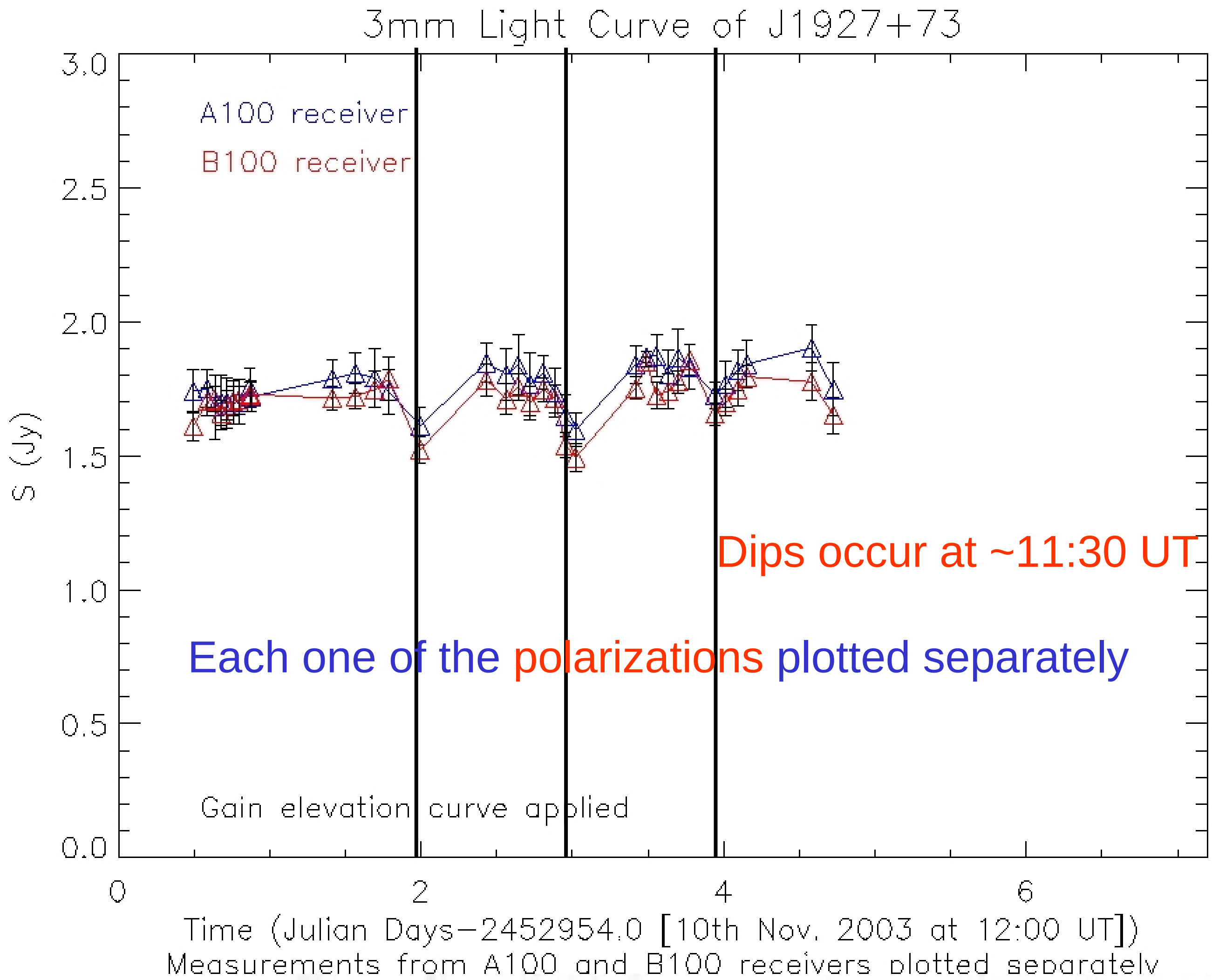

Data reduction: Systematic effects correction

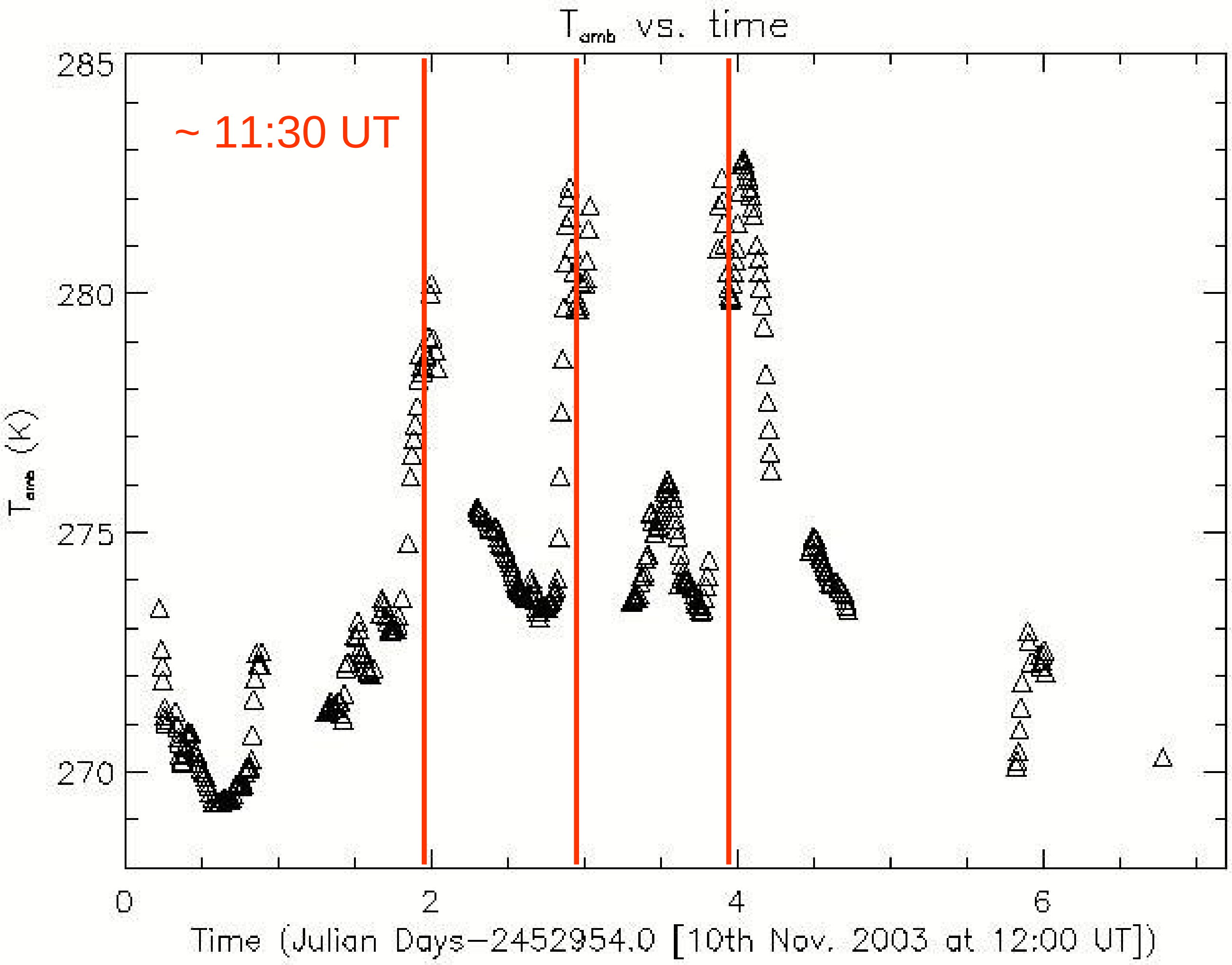

Data reduction: Systematic effects correction

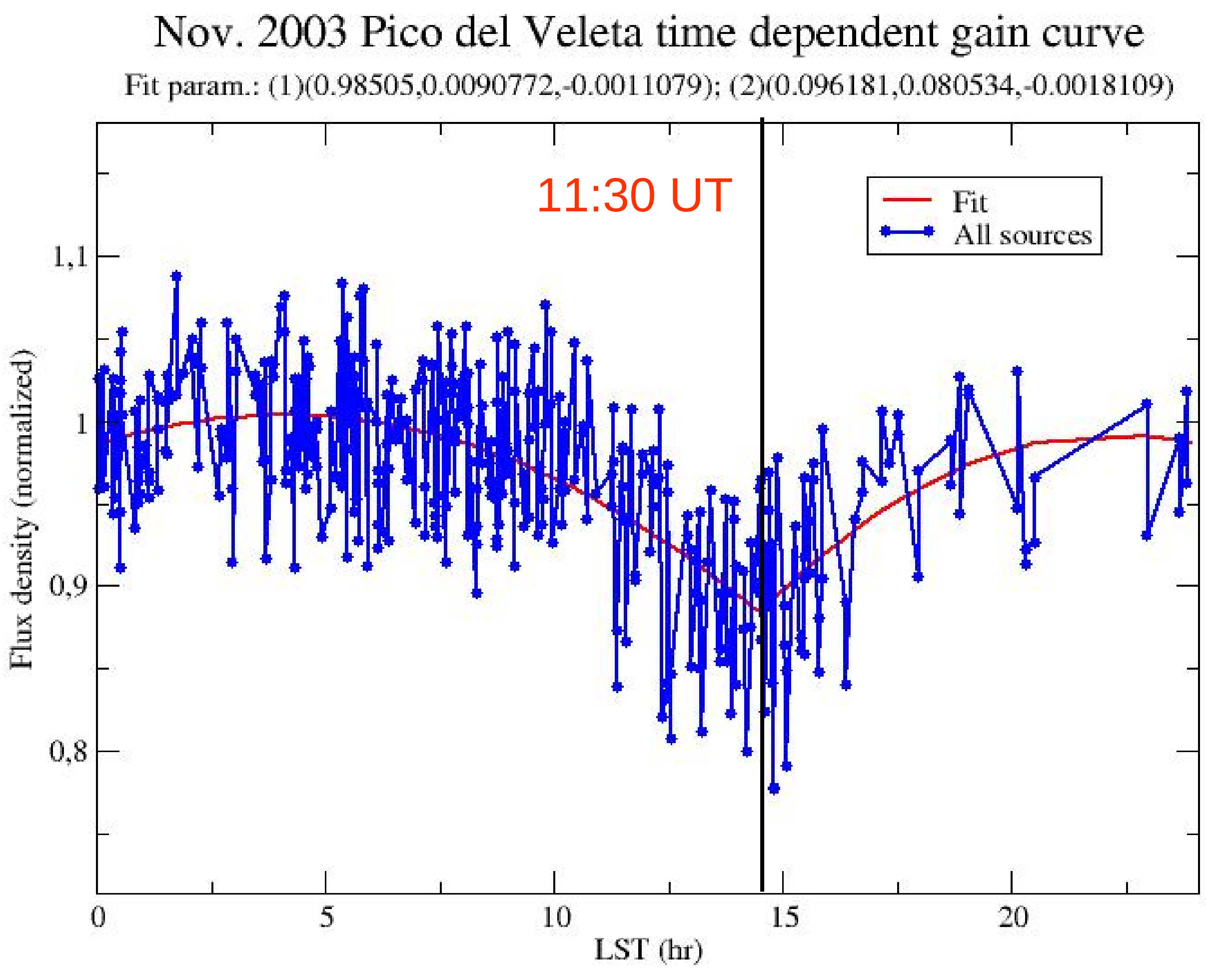

Data from all the observing time span folded in 24 hr (LST)

Data reduction: Systematic effects correction

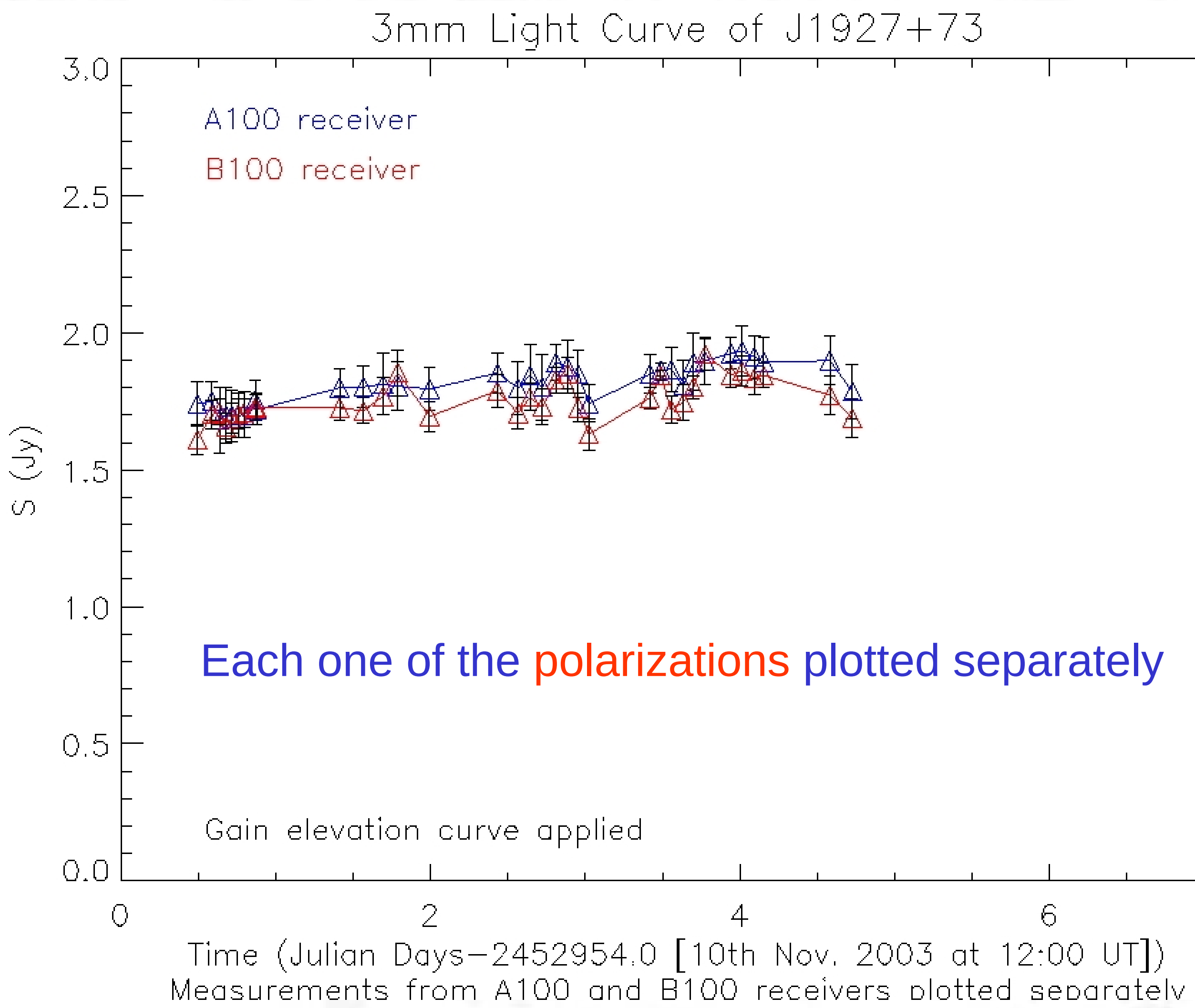

Data reduction: Systematic effects correction

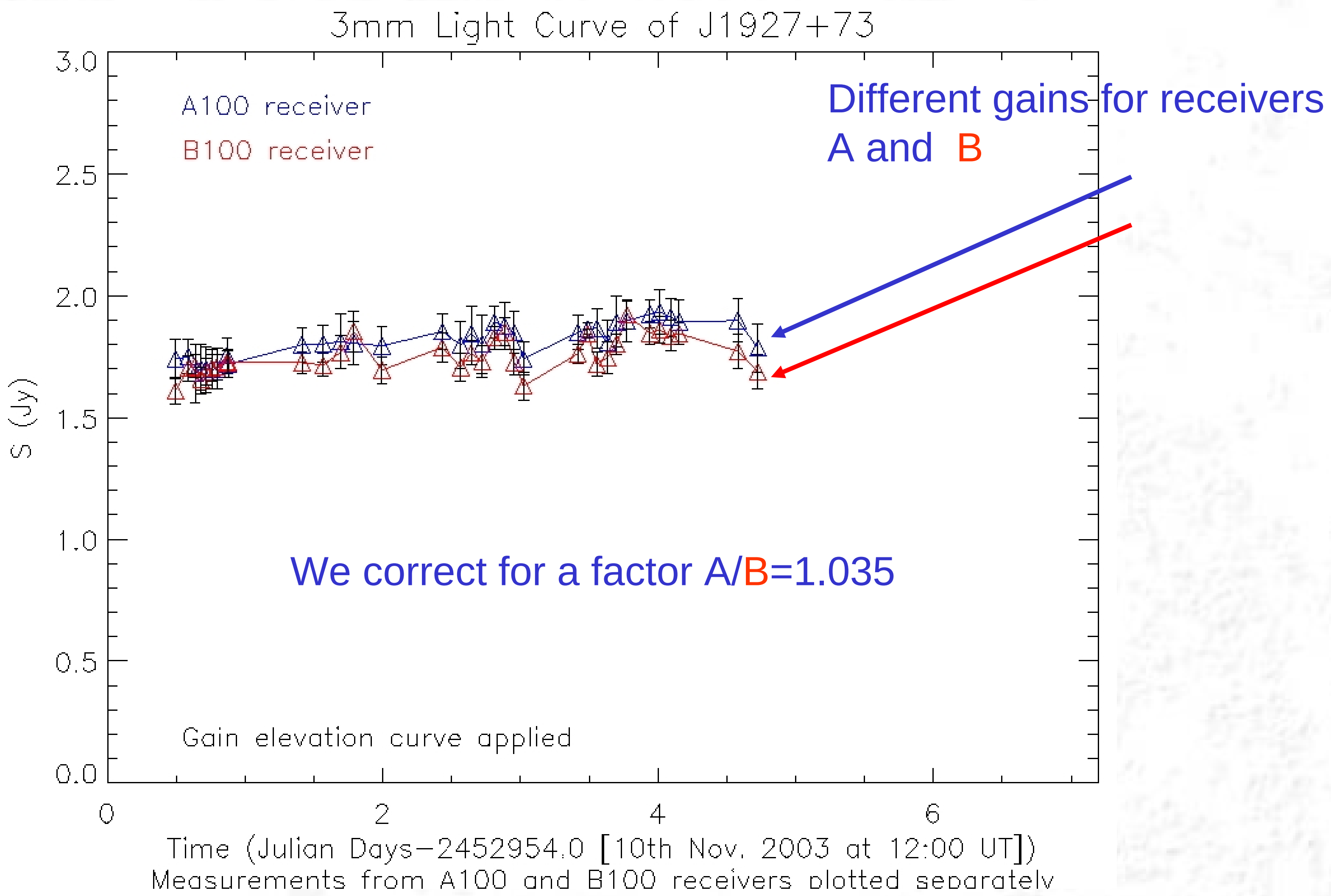

Data reduction: Systematic effects correction

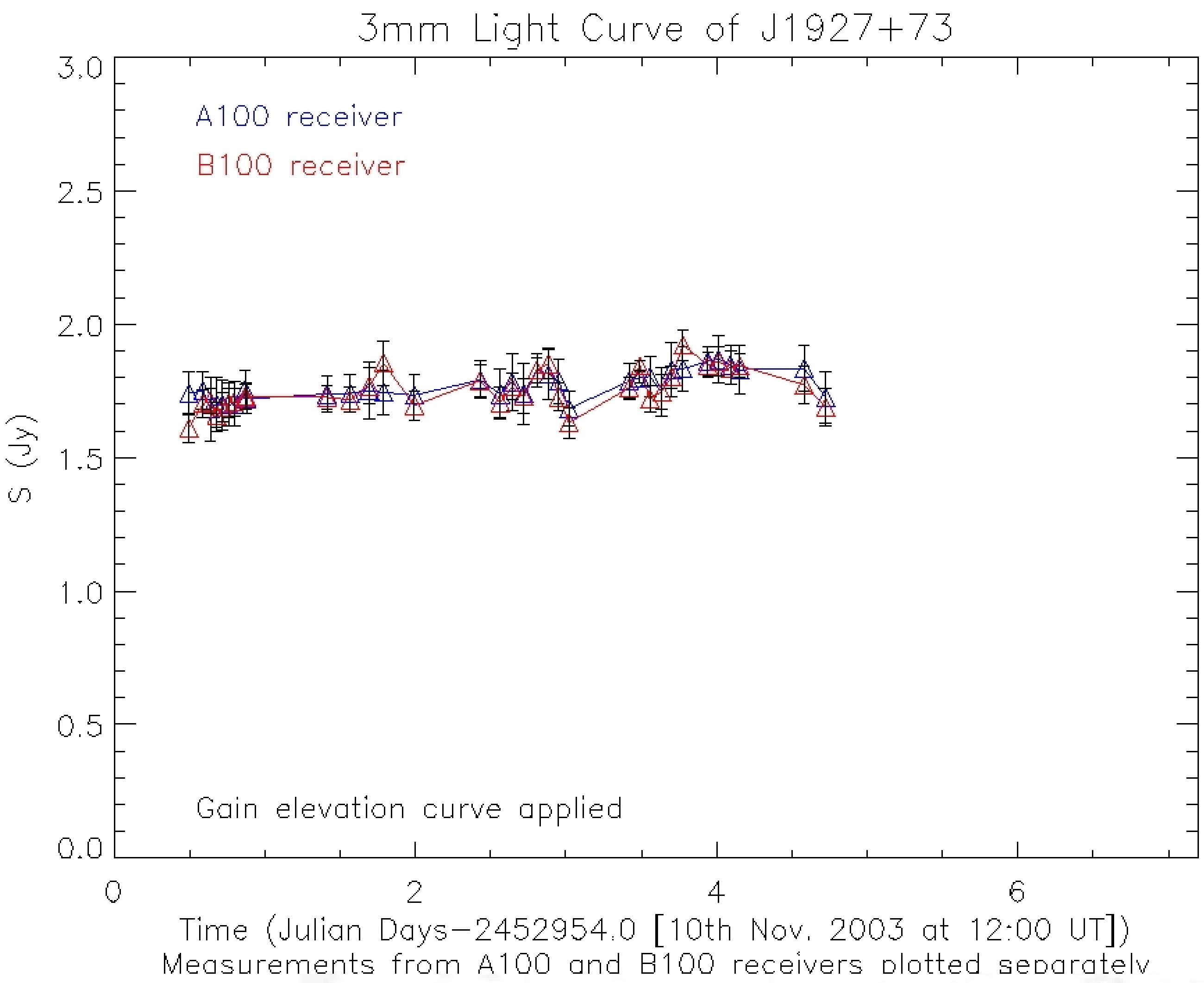

Data reduction: Systematic effects correction

(S(A100)+S(B100))/2

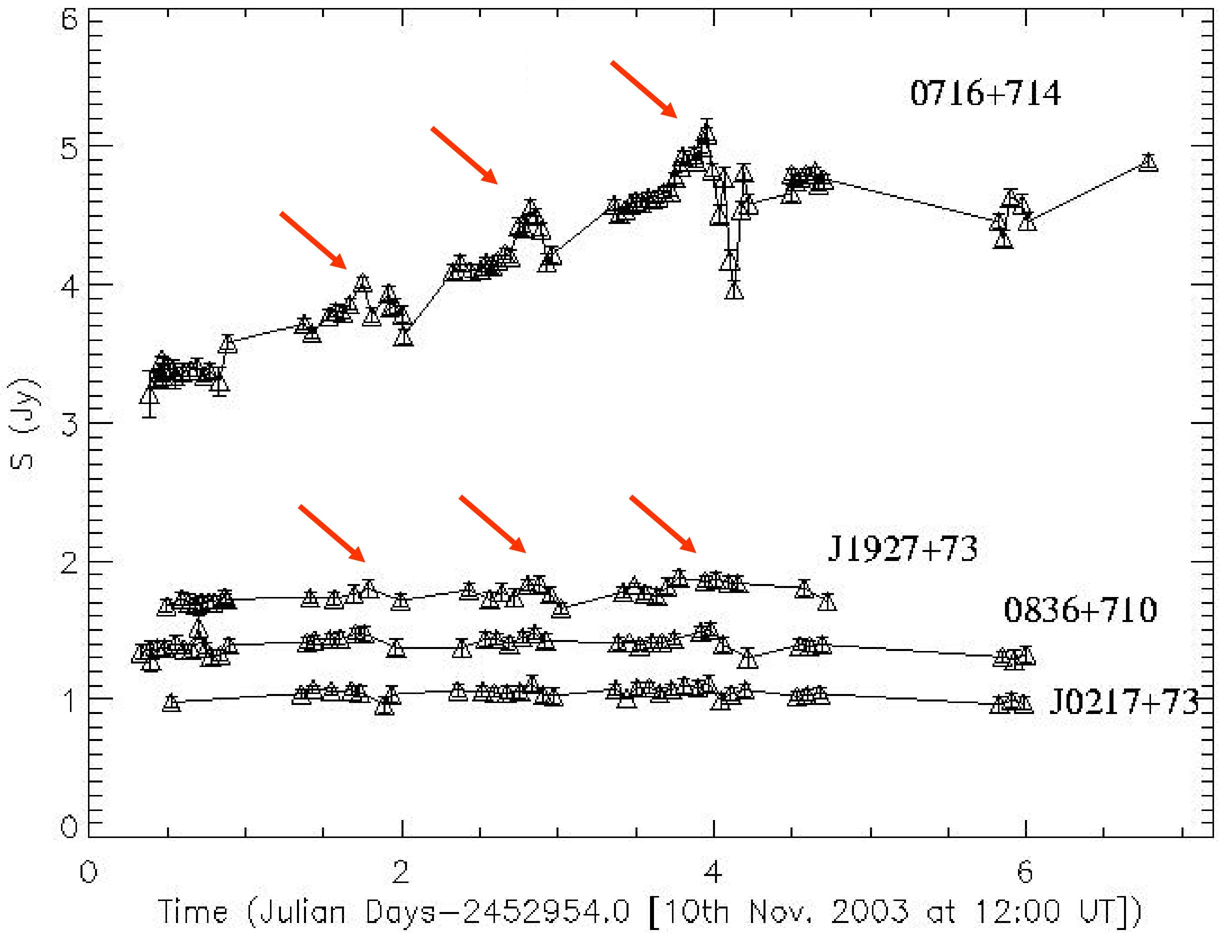

Data reduction: Systematic effects correction

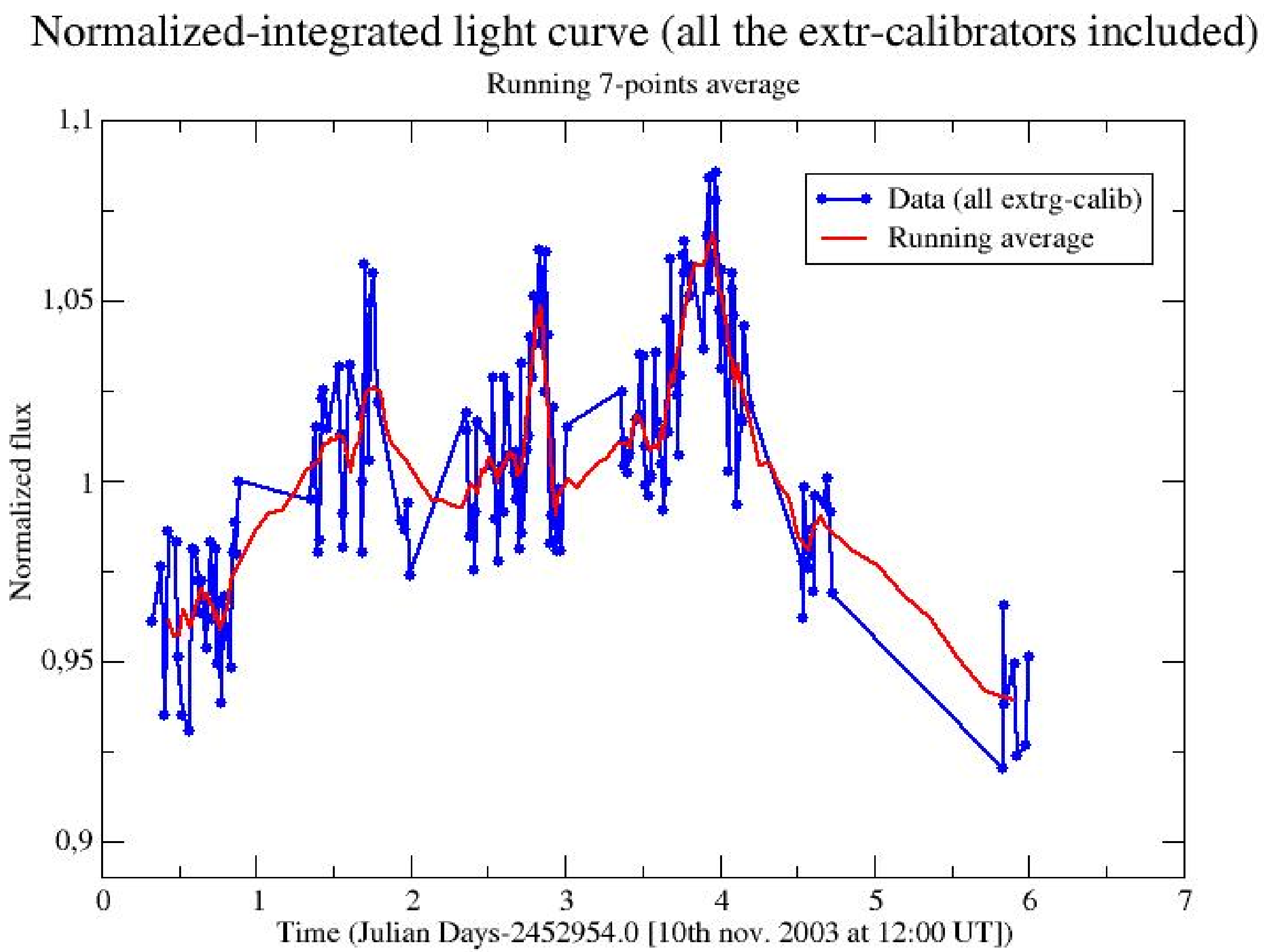

Data reduction: Systematic effects correction

(S(A100)+S(B100))/2

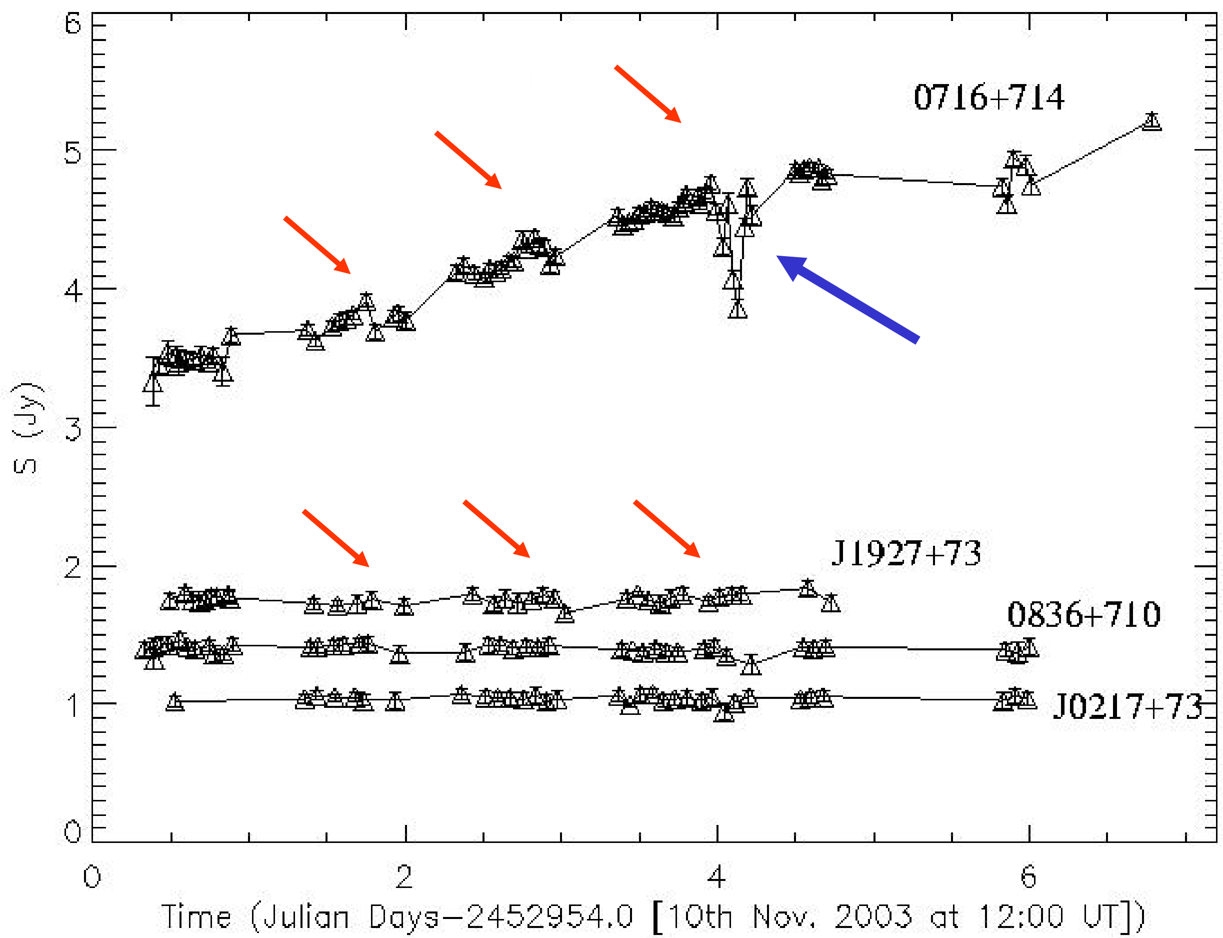

Data reduction: Systematic effects correction

Normalized light curves

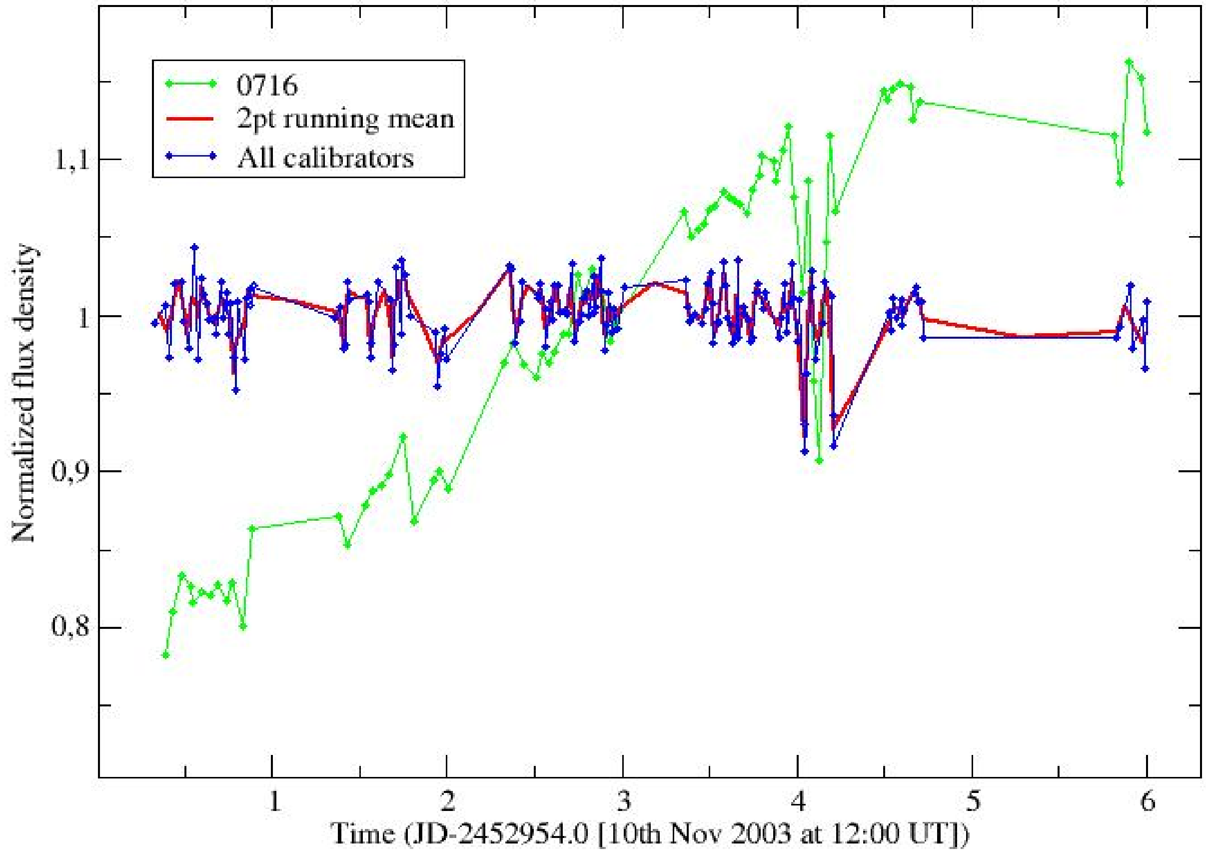

2 points running mean allow to remove short time systematic effects

Data reduction: Systematic effects correction

Normalized light curves

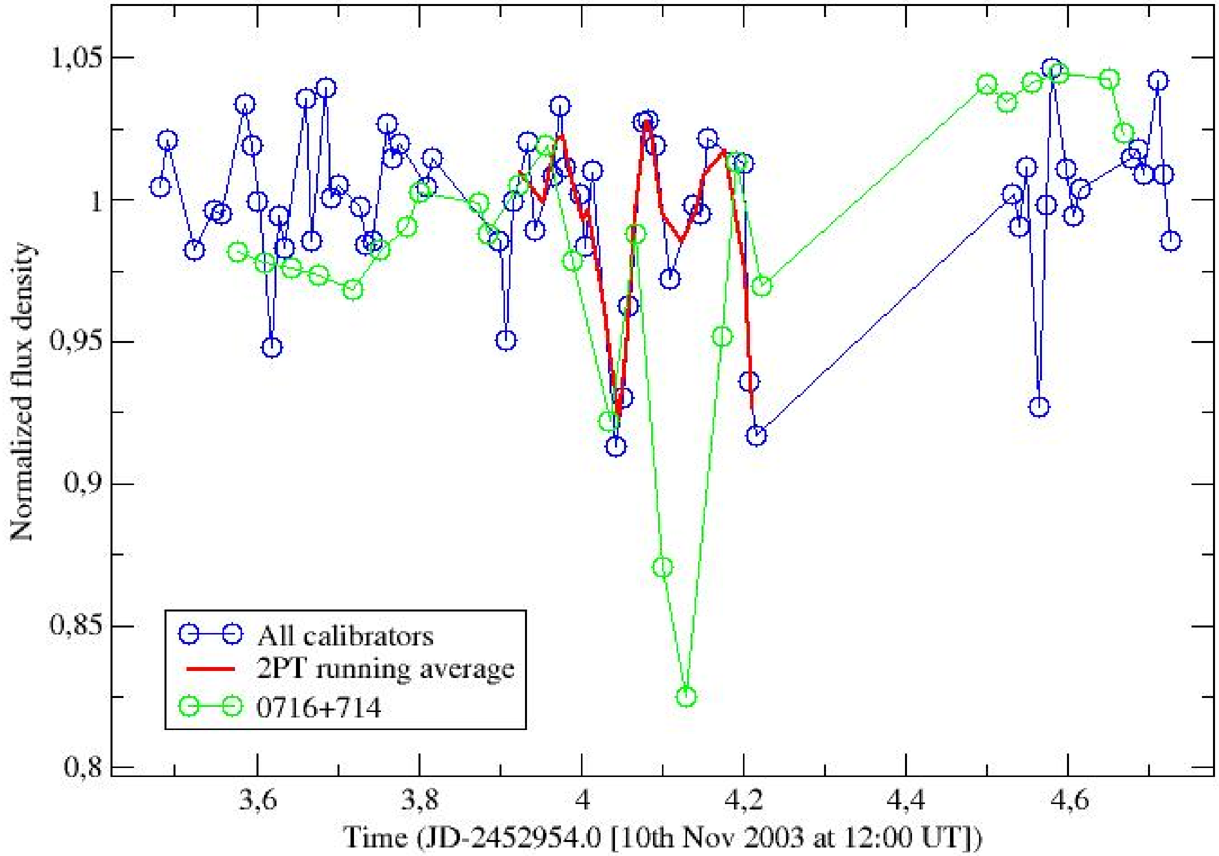

Part of the strong emission dip of 0716+714 will be corrected, but not all

Data reduction: Systematic effects correction

Normalized light curves

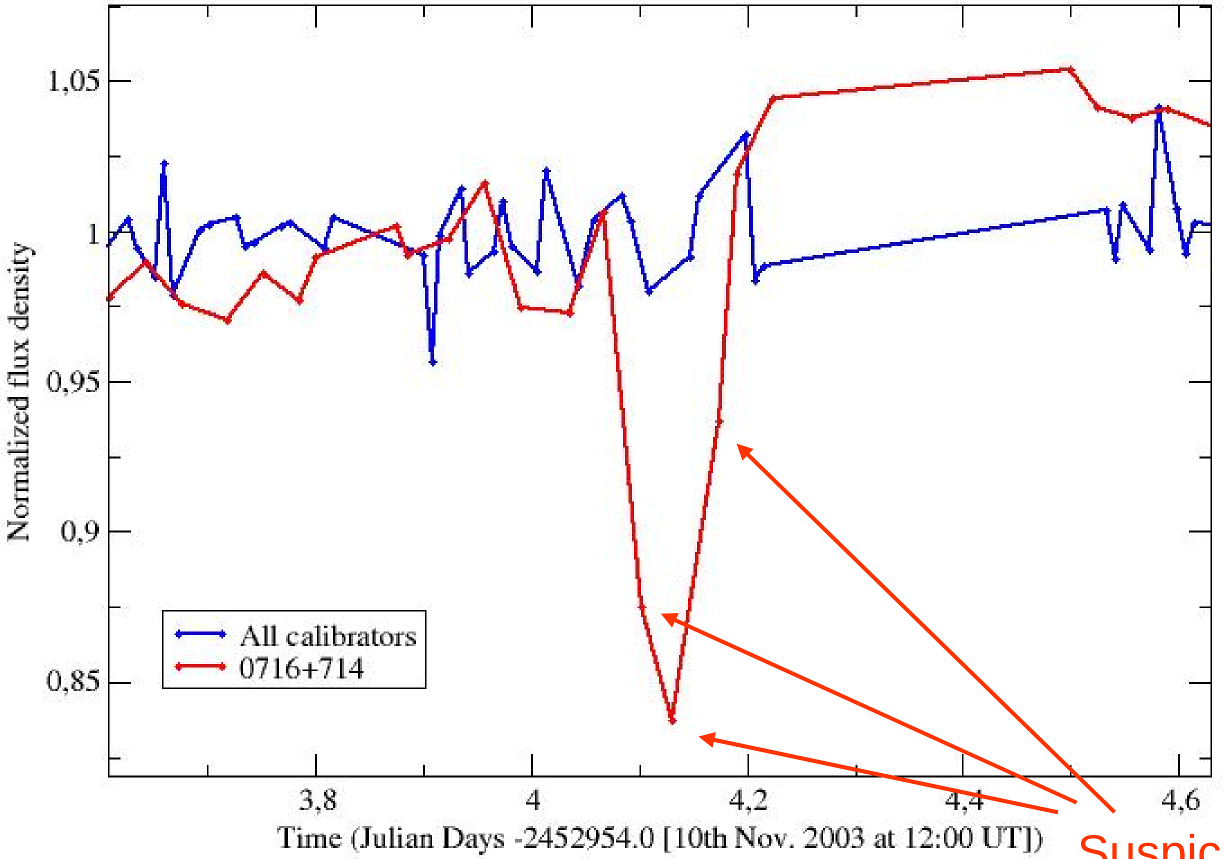

Suspicious to be bad measurements

Results

Present state of the 0716+714 light curve

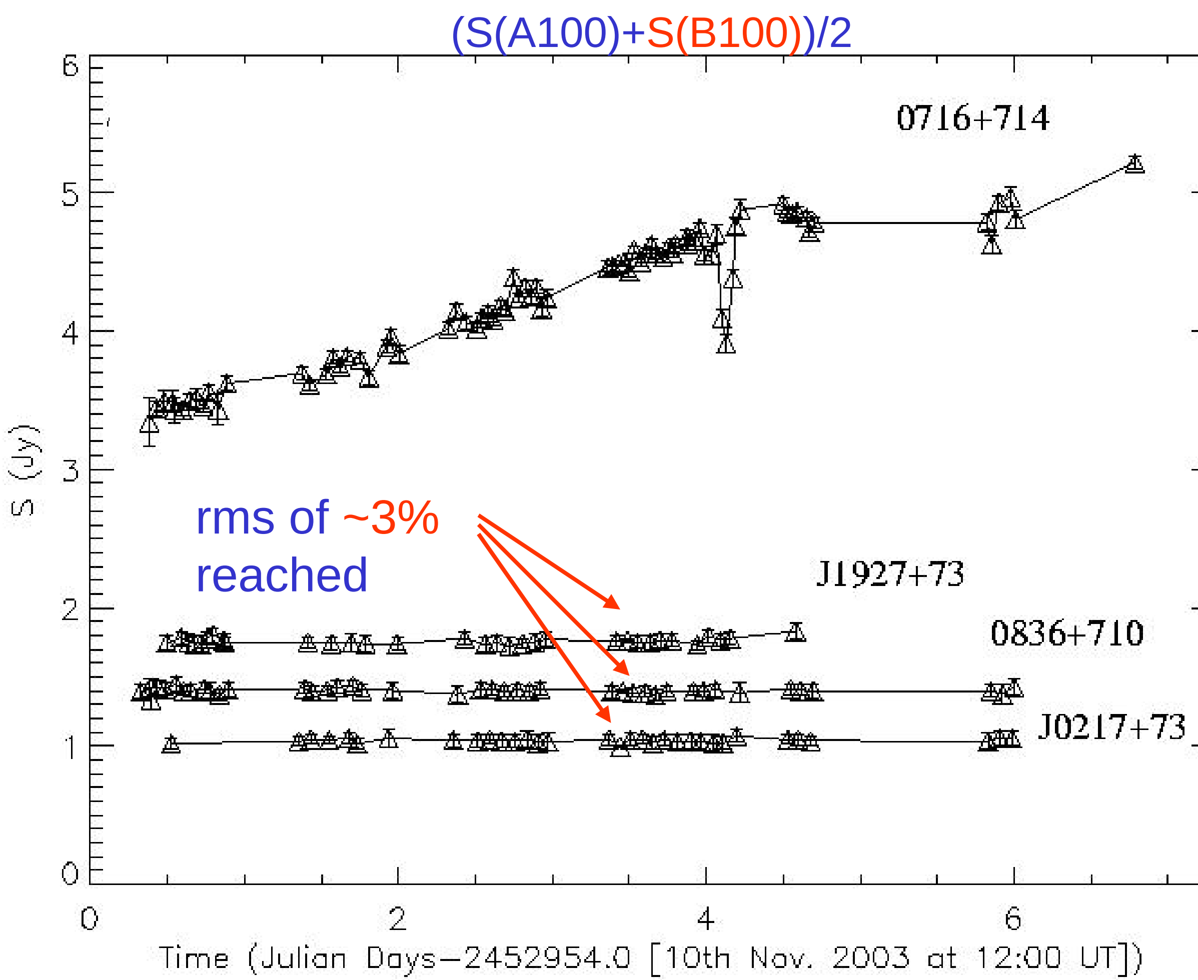

Results

sinus patterns of ∥ and ⊥ polarizations produced by receivers polarization plane rotation (due to Earth rotation)

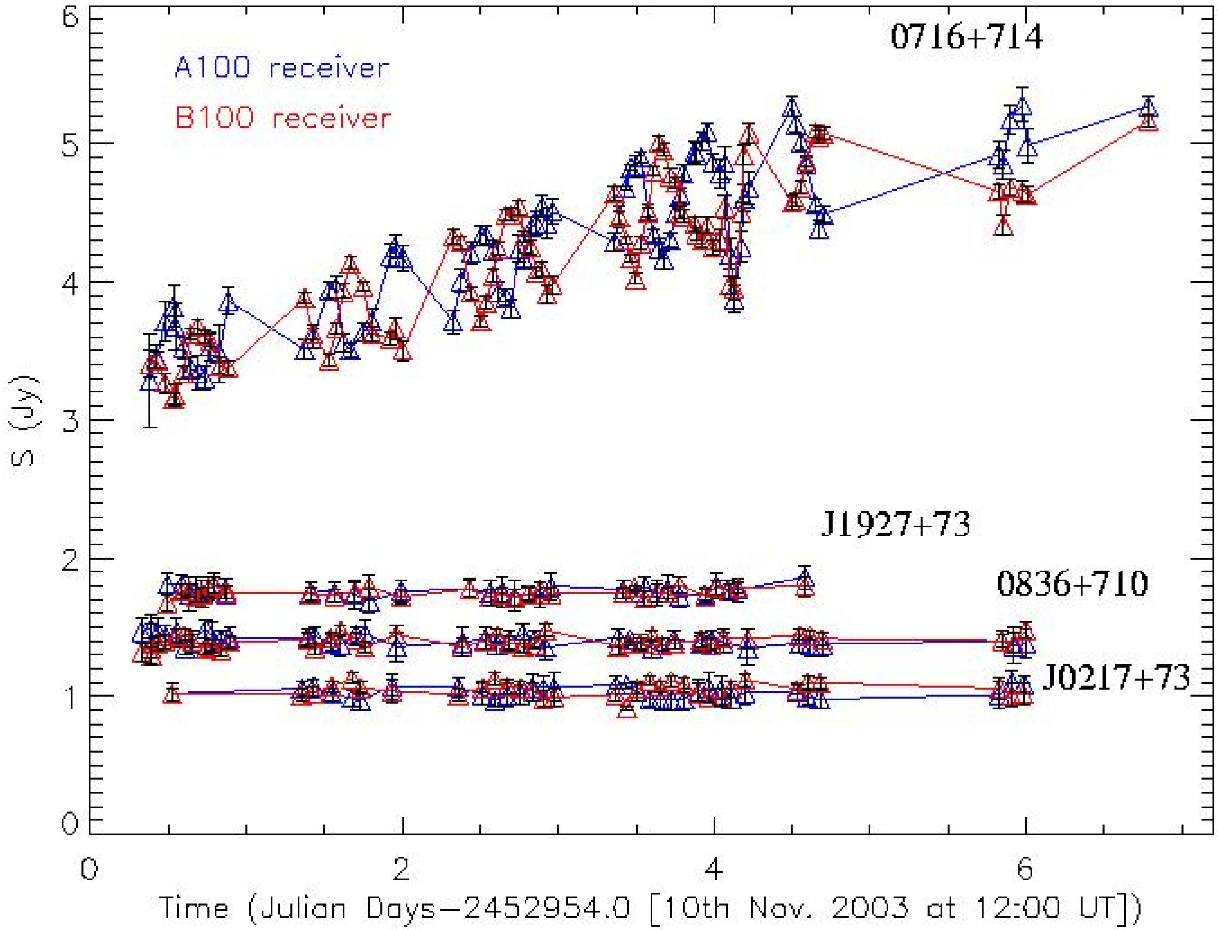

Polarization analysis

Reflects variability, but proper way to represent polarization is vs. P.A.

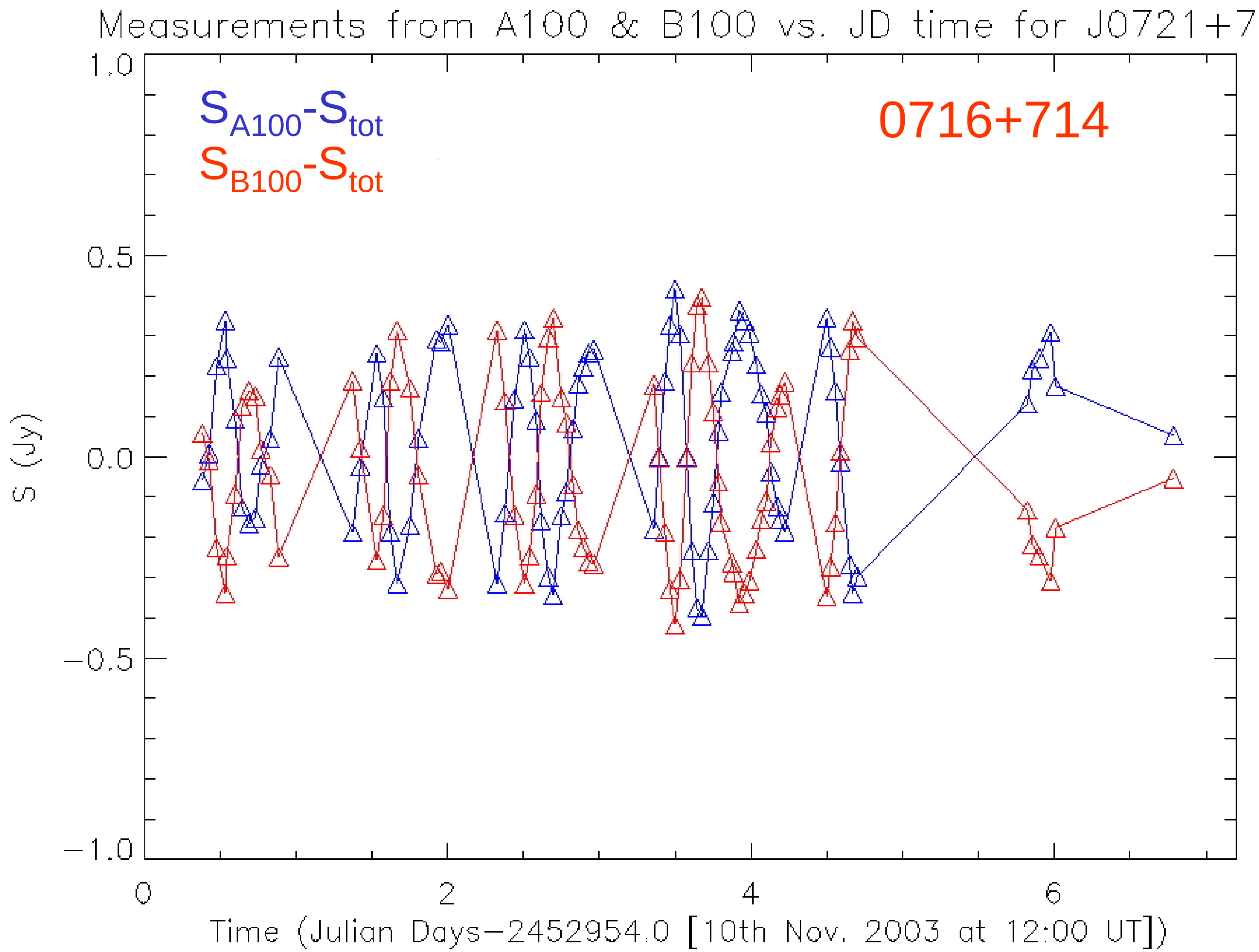

Results

ELV angle removed to account for the elevation rotation of the Nasmyth mirror in the receiver cabin

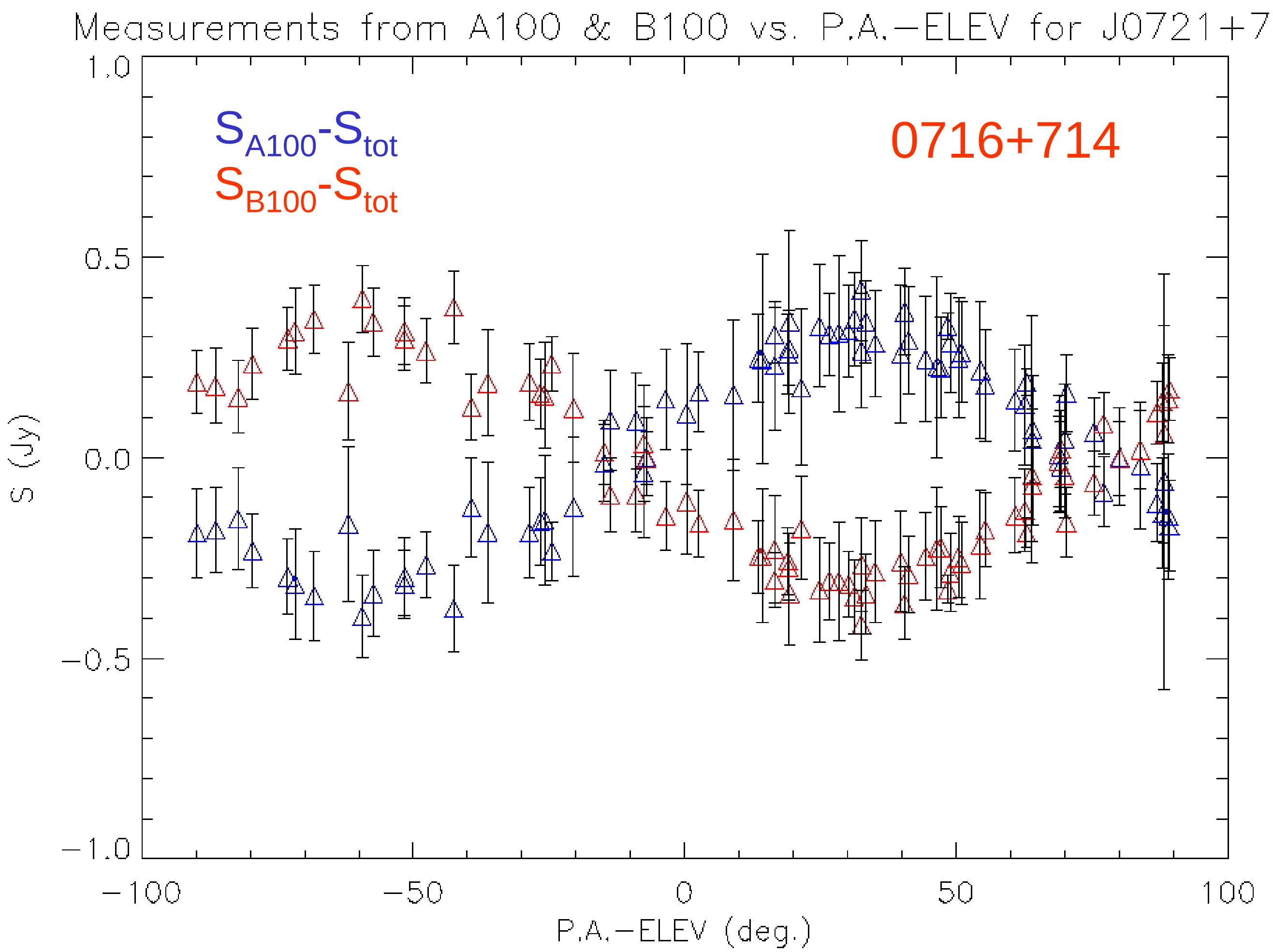

Data from all the observing time span folded in [-90^0,90^0] range

Polarization analysis

1st day

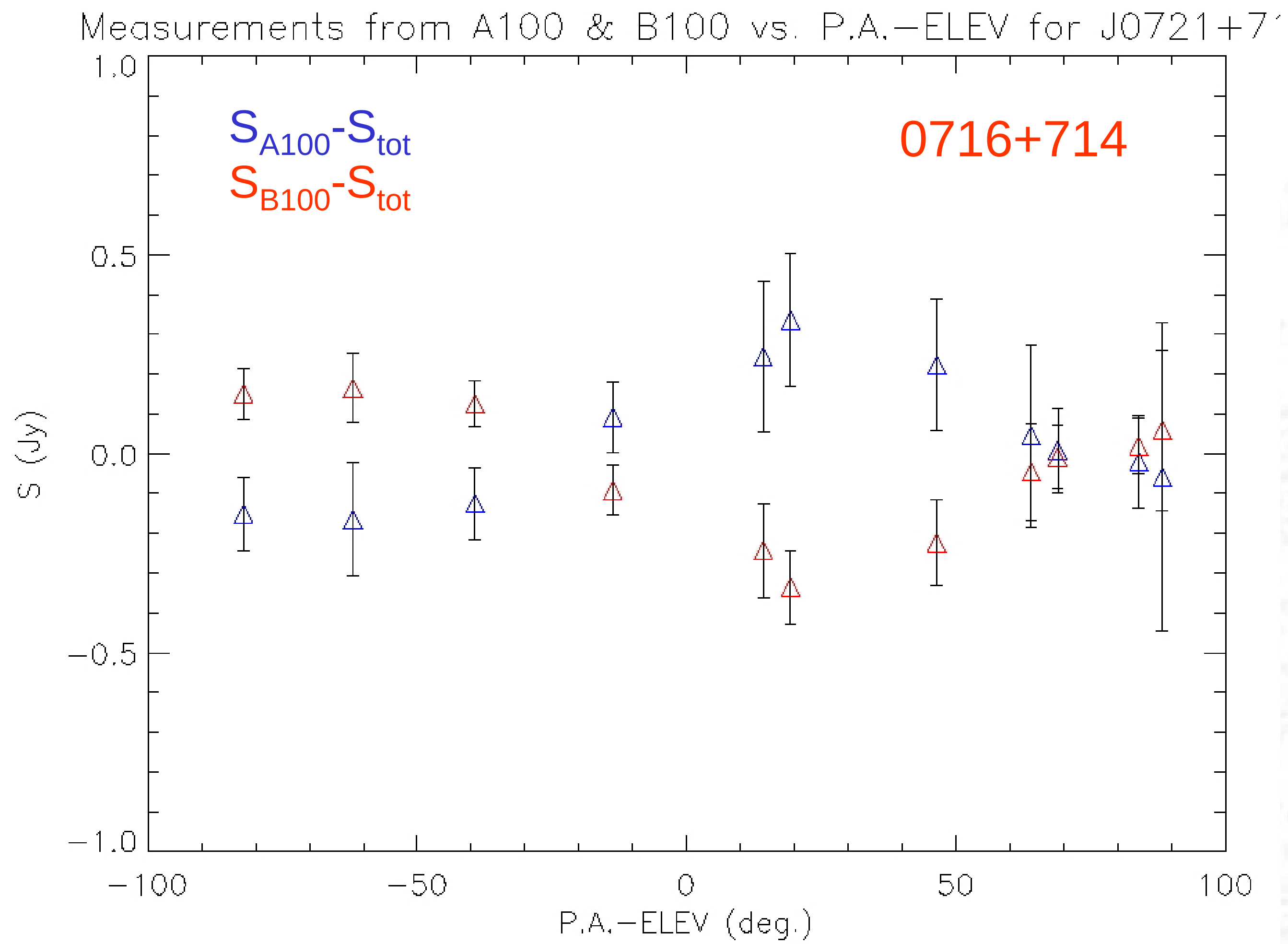

Polarization analysis

2nd day

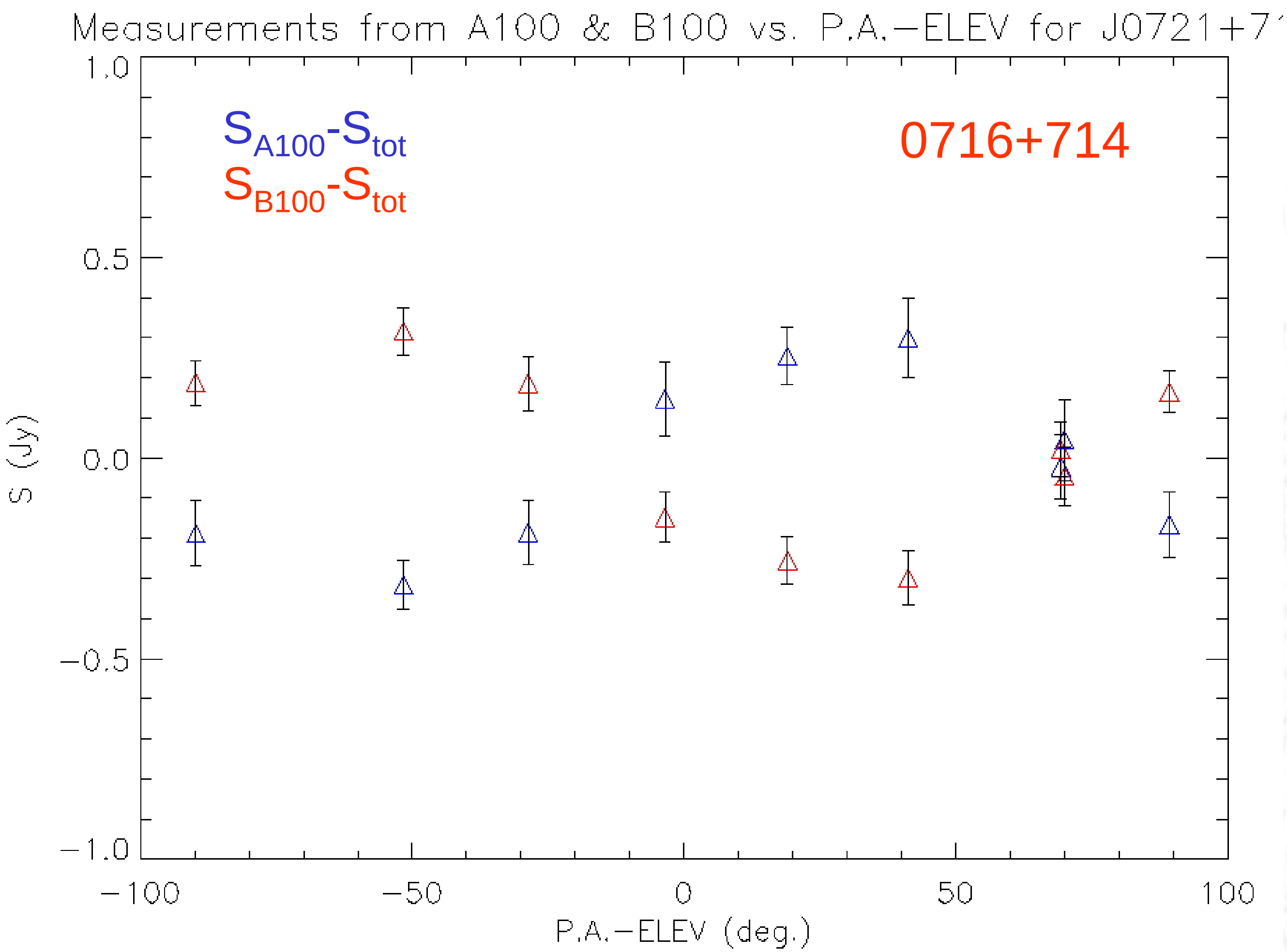

Polarization analysis

3rd day

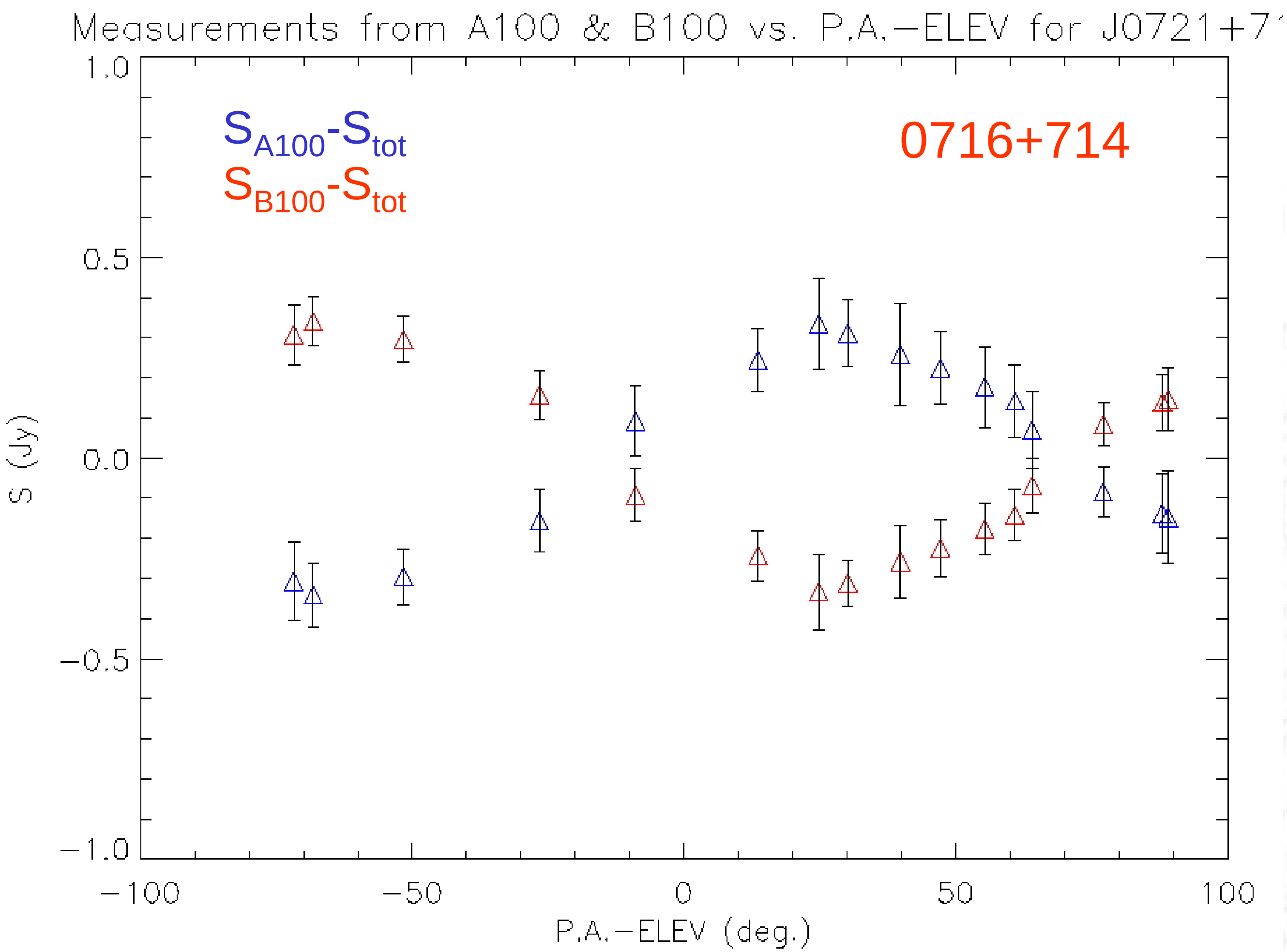

Polarization analysis

4th day

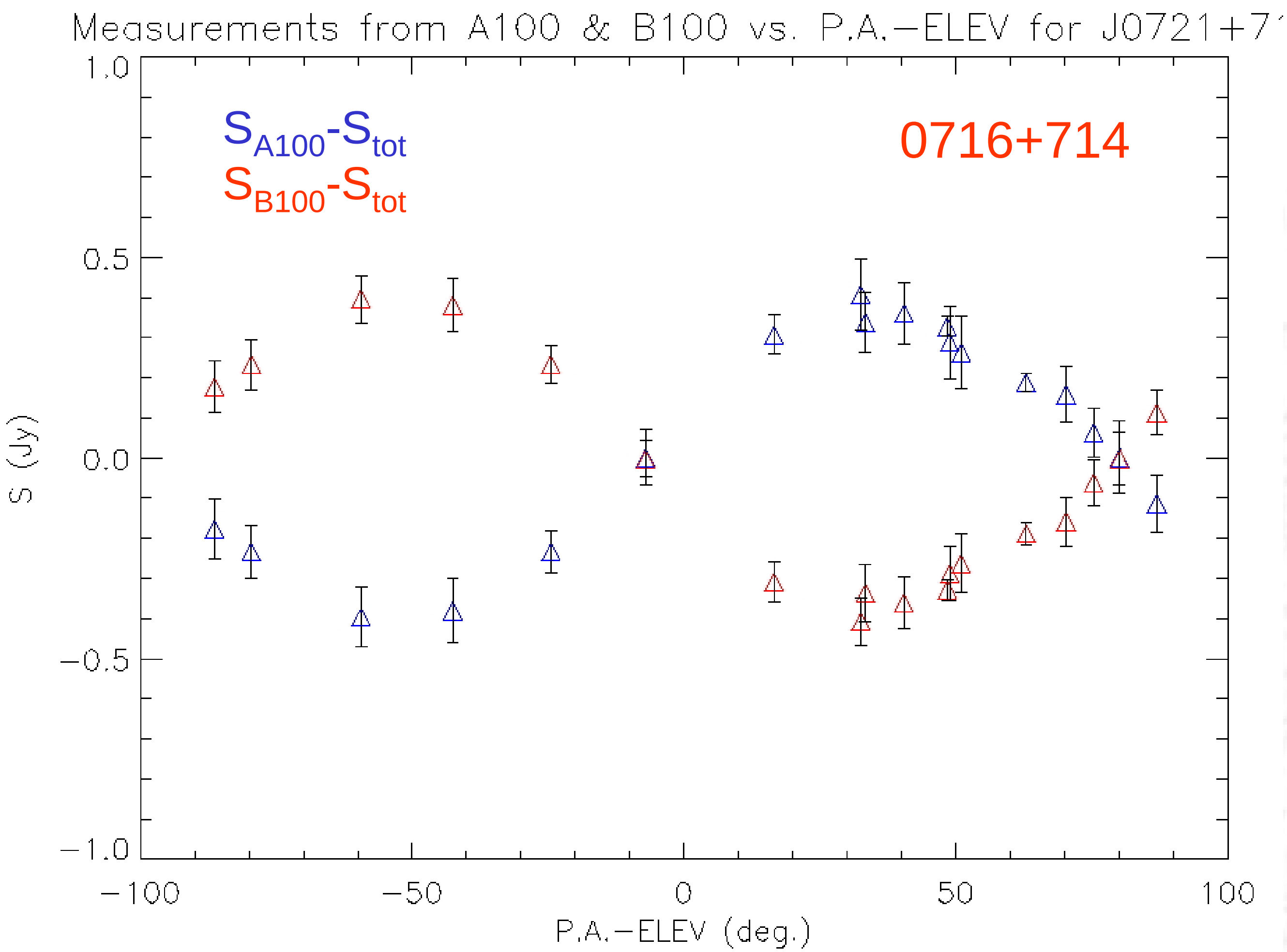

Results

SUMMARY:

- Improved the initial technical goal of reaching a 5% accuracy in flux density measurements. rms~3% obtained
- The data does not seem to present a clear IDV type 2 pattern
- Total flux of 0716+714 increased by ~1.5 Jy in 4 days
- Source is found to be polarized by ~15% (P≃0.8 Jy)
- It presents evidences of polarization variability over 4 days

Future work

- Computation of a more accurate K to Jy conversion factor and S_{tot} scalling

- Further analysis to ensure the nature of the emission dip

- Complete the polarization analysis

- Reduction and analysis of the 1.3mm data

Emmanouil (Manolis) Angelakis
Max-Planck-Institut für Radioastronomie

Elimination of Foreground Sources in the CBI Fields: Status Report

In collaboration with:
MPIfR: A. Kraus , T. Krichbaum, A. Zensus
CALTECH: A. Readhead, T. Pearson, R. Bustos, R. Reeves

Supported by the ENIGMA network

Outline

- Project Description:

Abstract
The Cosmic Background Imager
The Problem
The Solution

- Current Status:

Fields Coverage
Tools Development from Scratch
Problems-Solutions

- First Results:

Flux Distribution
Spectral Indices Distribution
Resume

- Future Plans

Abstract

We are observing **6000 point sources** from the NVSS (NRAO VLA SKY SURVEY at 1.4 GHz) catalogue at **10.45** and **4.85 GHz** (3 and 6 cm respectively) in order to determine their **spectral indices** and subsequently set ourselves able to answer the question whether these sources **contaminate the CMB (~30 GHz) data observed with the Cosmic Background Imager**.

The Cosmic Background Imager (CBI)

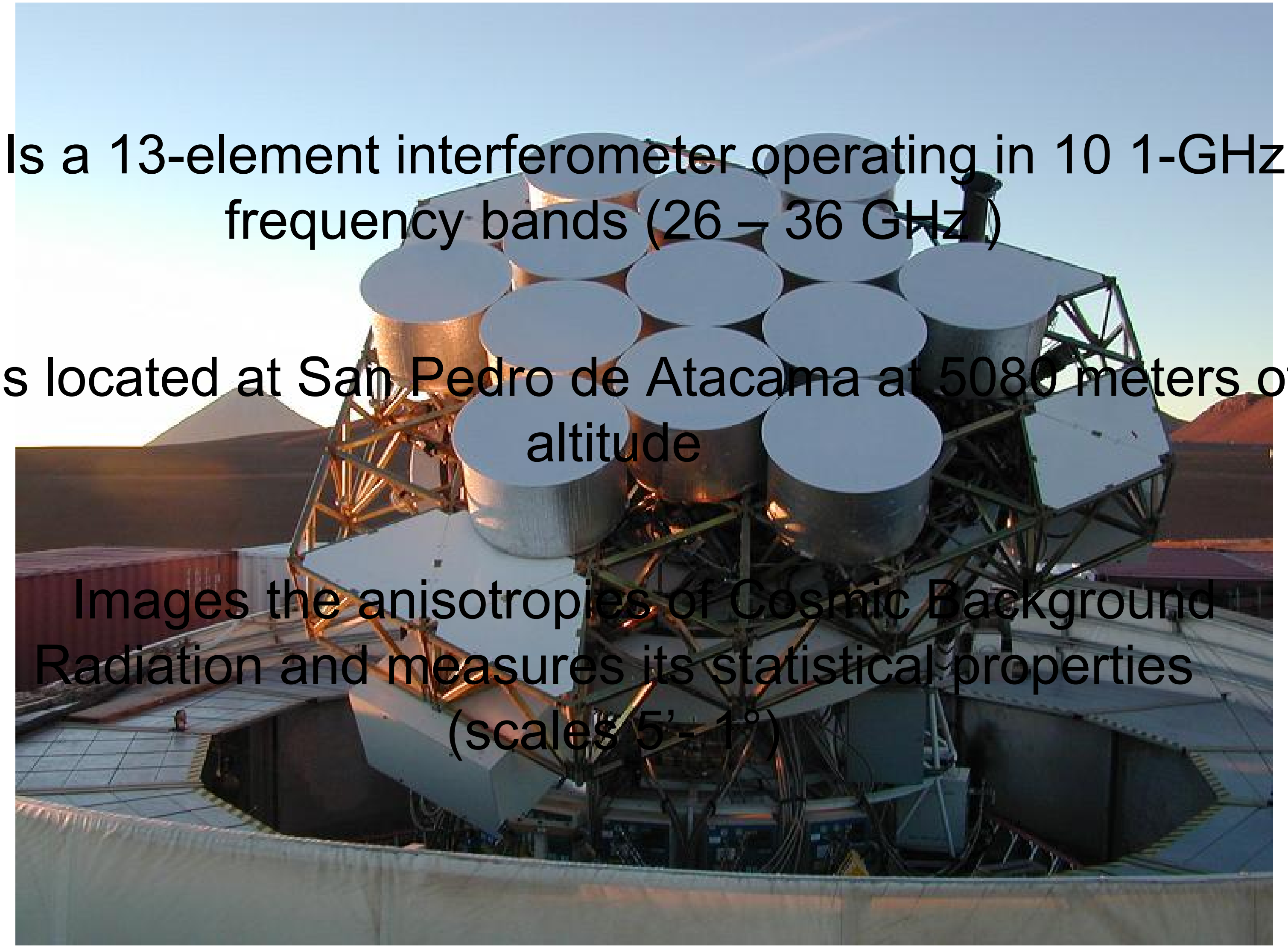

Is a 13-element interferometer operating in 10 1-GHz frequency bands (26 – 36 GHz)

Is located at San Pedro de Atacama at 5080 meters of altitude

Images the anisotropies of Cosmic Background Radiation and measures its statistical properties (scales 5’- 1°)

The Cosmic Background Imager (CBI)

Observes within 4 “windows” separated by 6h in RA covering a sky area of roughly 160 deg^2 in total

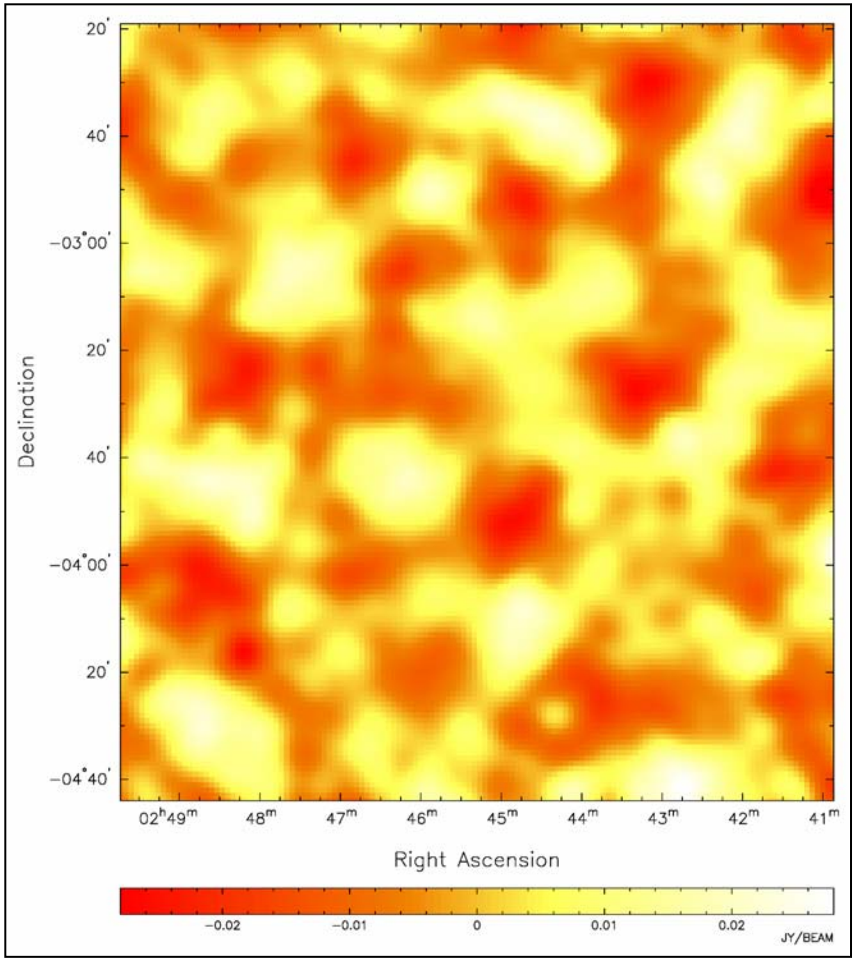

The Problem

Contamination by foreground sources and subsequently unnecessary "holes" in images throwing away 10-20% of the data

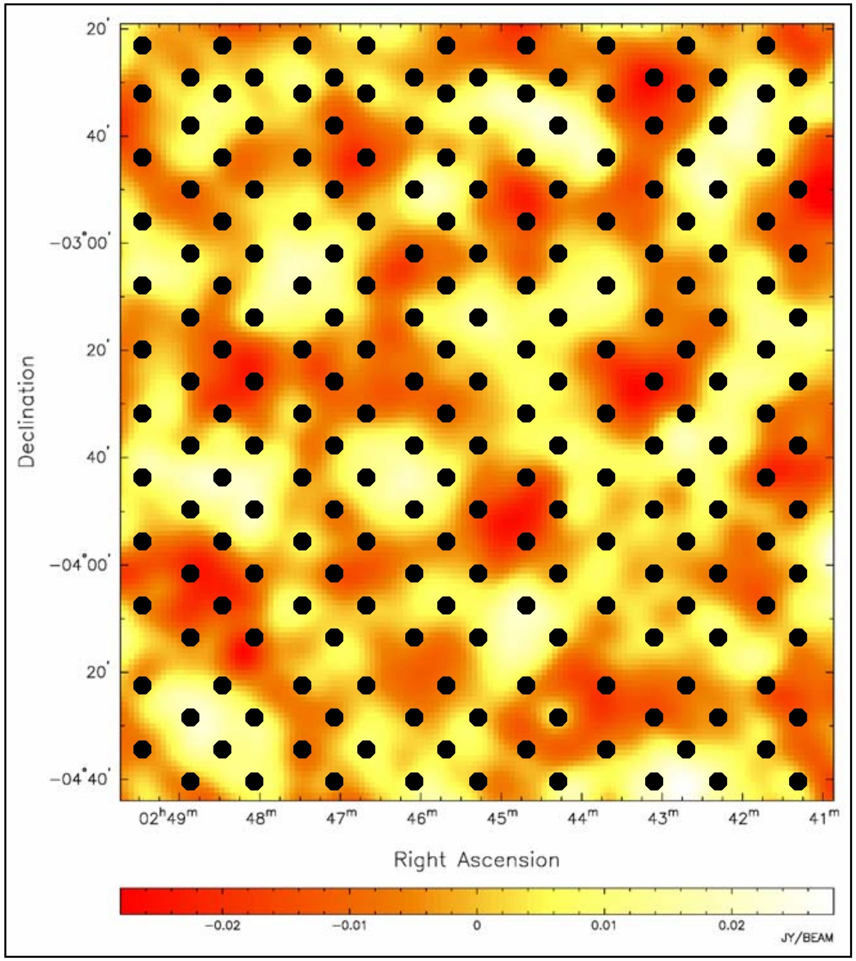

The Solution

Identify those sources and verify that they are NOT bright enough to “distort” the CMB image in the frequency range of the CBI

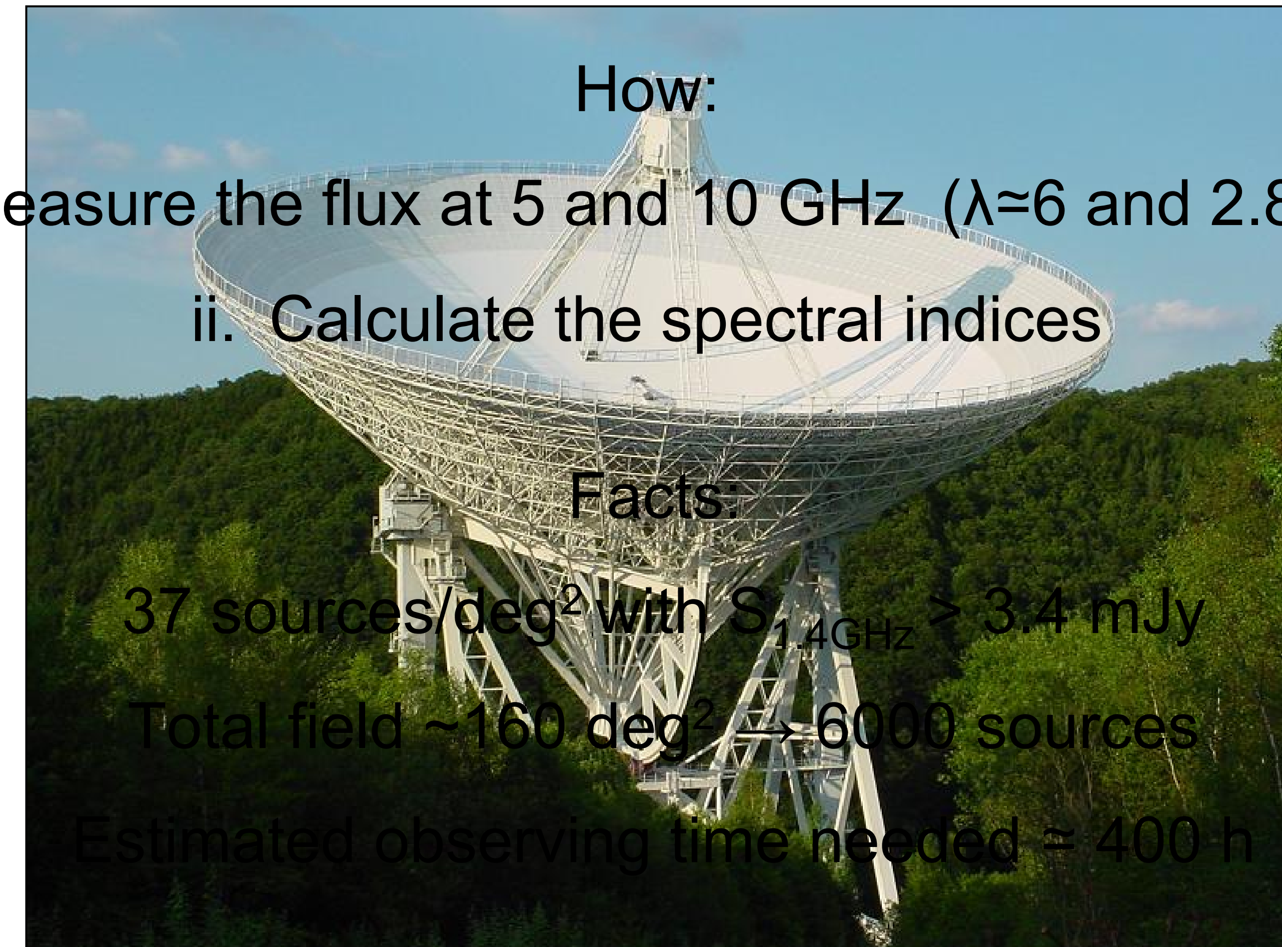

How:

i. Measure the flux at 5 and 10 GHz (λ≃6 and 2.8 cm)

ii. Calculate the spectral indices

Facts:

37 sources/deg^2 with $S_{1.4GHz}$ > 3.4 mJy

Total field ~160 deg^2 → 6000 sources

Estimated observing time needed ≃ 400 h

The Observing Method

The "ON-ON" method is applied:

Always one of the two horns is "on-source" for the subtraction of the atmospheric effects

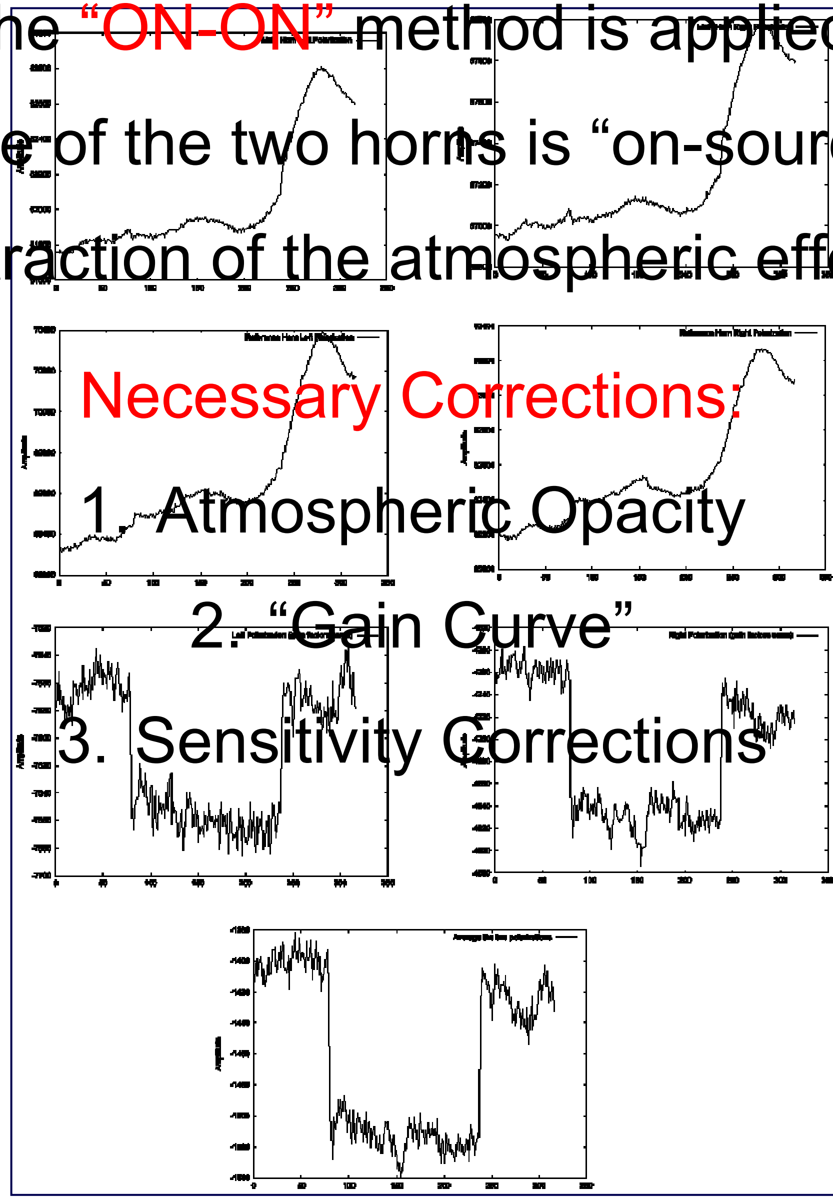

Necessary Corrections:

1. Atmospheric Opacity
2. "Gain Curve"
3. Sensitivity Corrections

Problems-Solutions

1. Weather

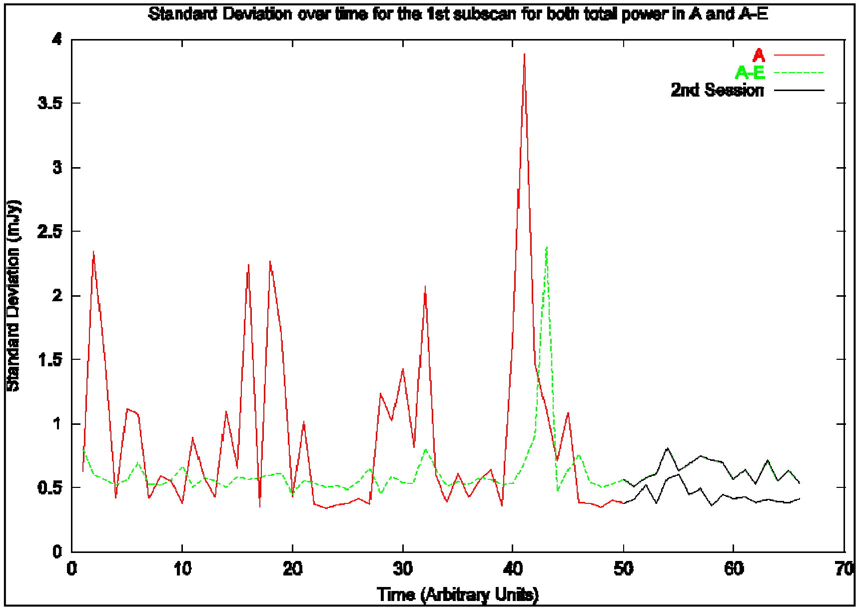

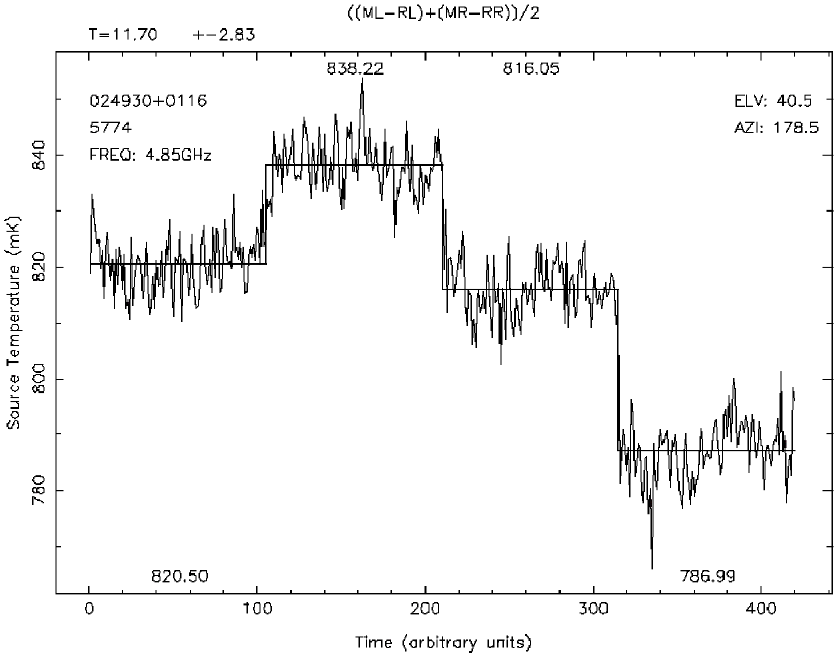

Problems-Solutions

2. Confusing Sources:

Its is estimated that almost 50% of sources may be confused!

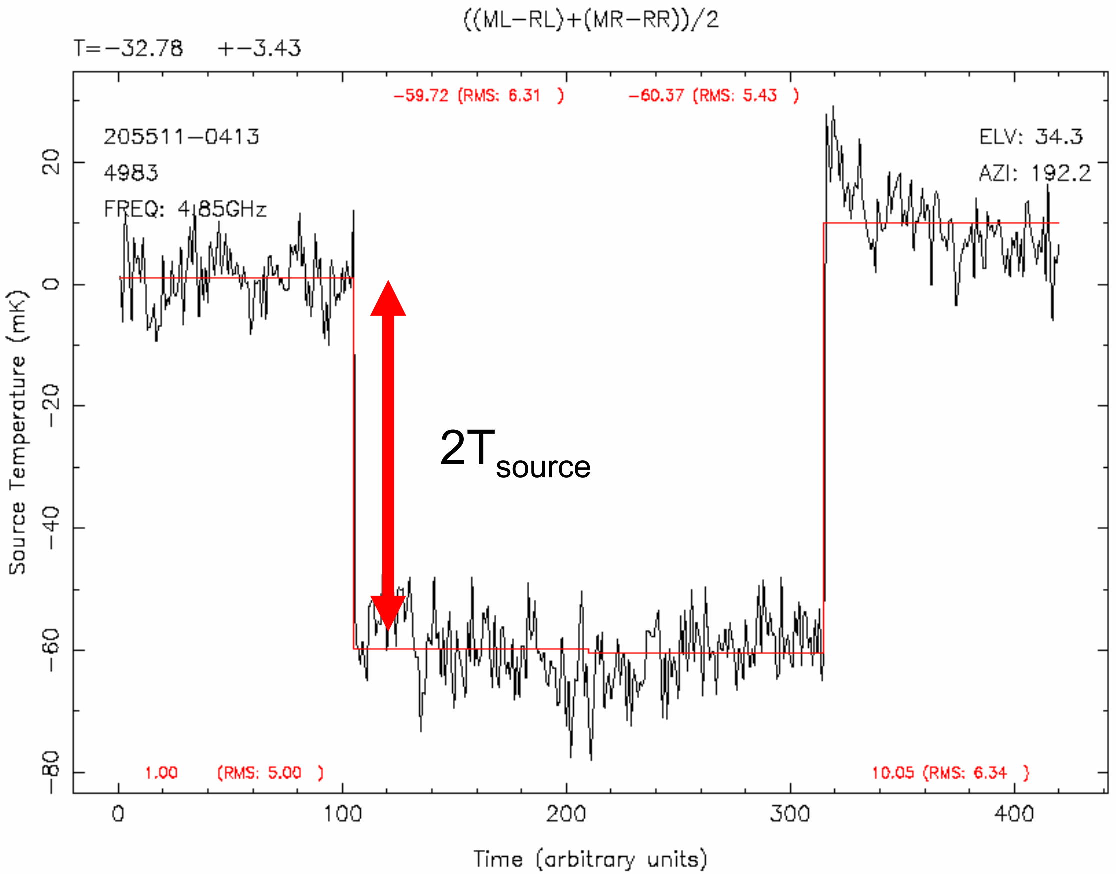

Problems-Solutions

3. Different T_{sys} for different channels:

Not accurate subtraction of atmospheric effects!

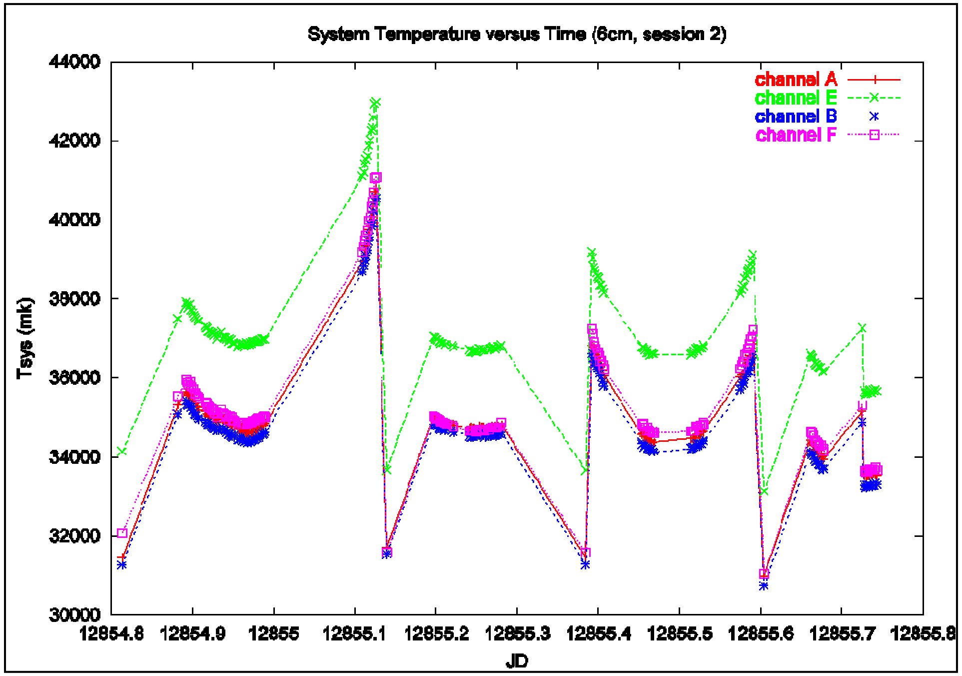

4. Unstable T_{cal}:

May fabricate a non-existing detection or hide away a real one

5. Different Sensitivity for different channels

Problems-Solutions

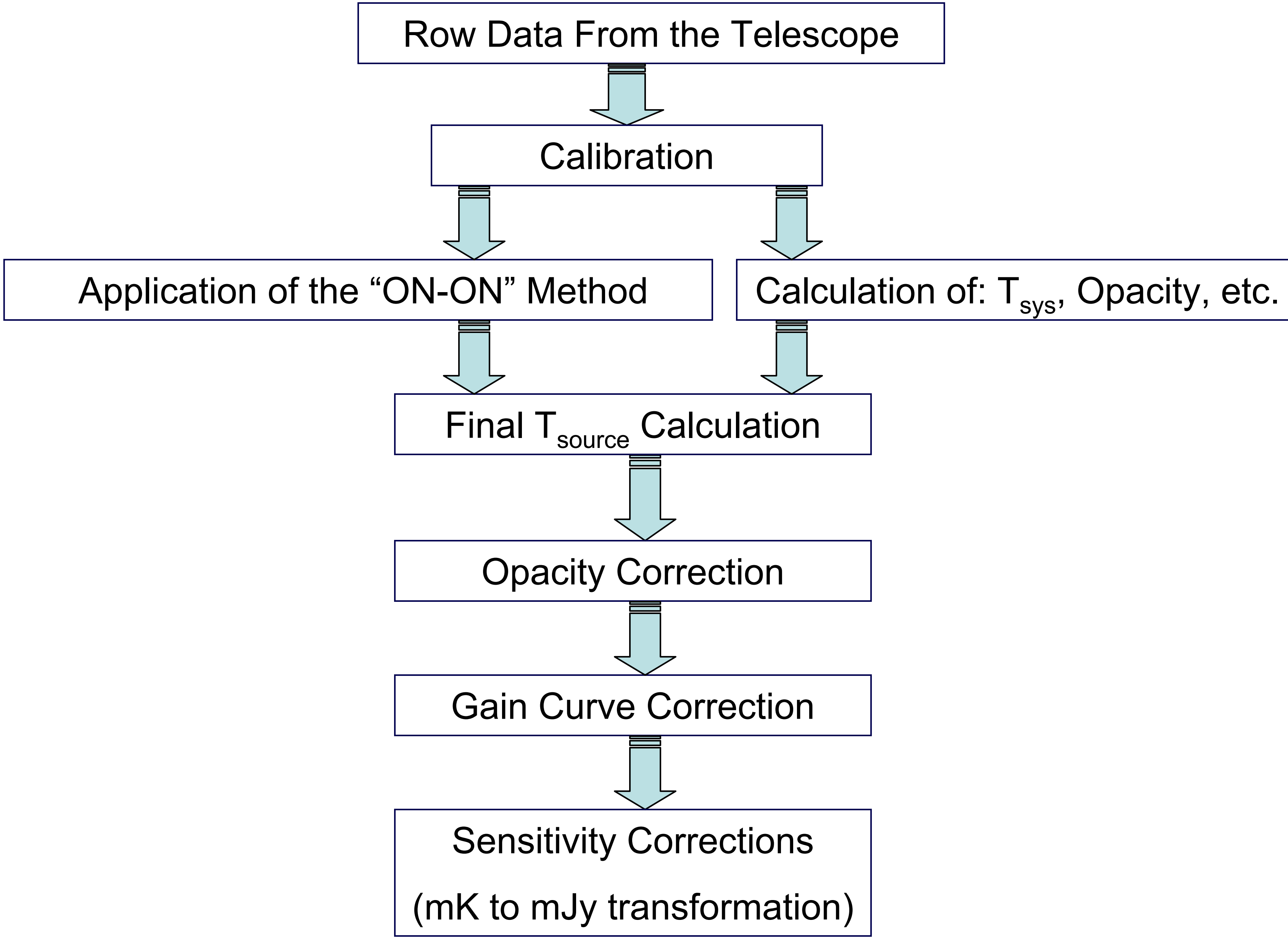

Fields Coverage

- To be observed
- Already observed

Coverage at 3cm **Coverage at 6cm**

2-hours field

8-hours field

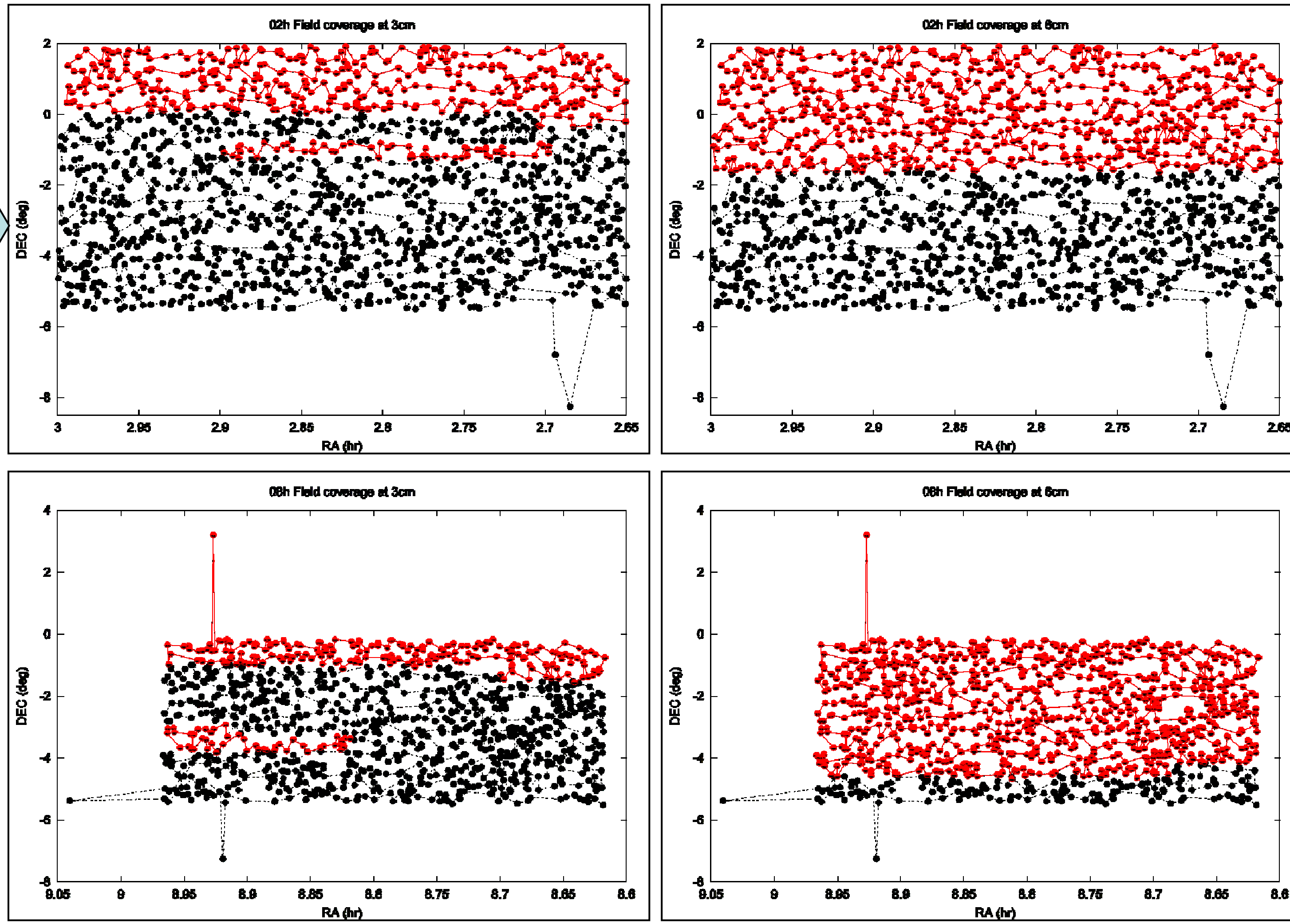

Fields Coverage

- To be observed
- Already observed

Coverage at 3cm

Coverage at 6cm

14-hours field

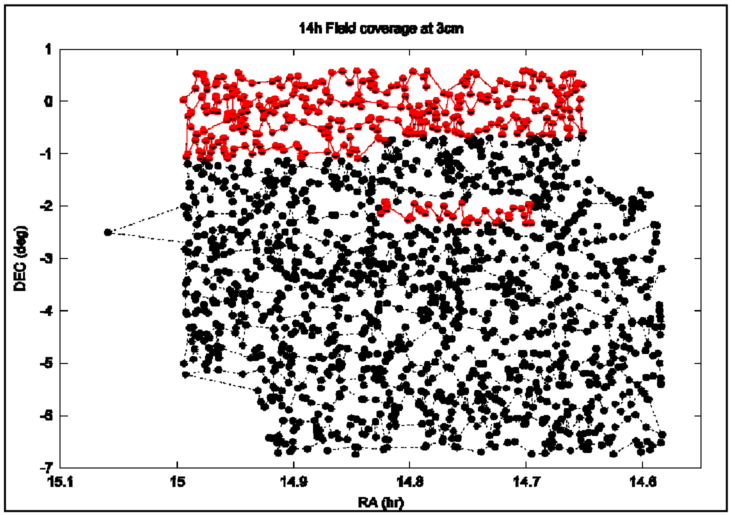

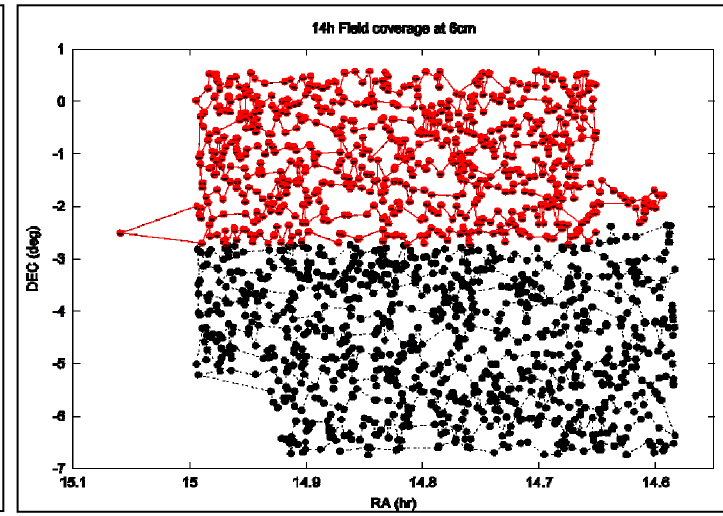

20-hours field

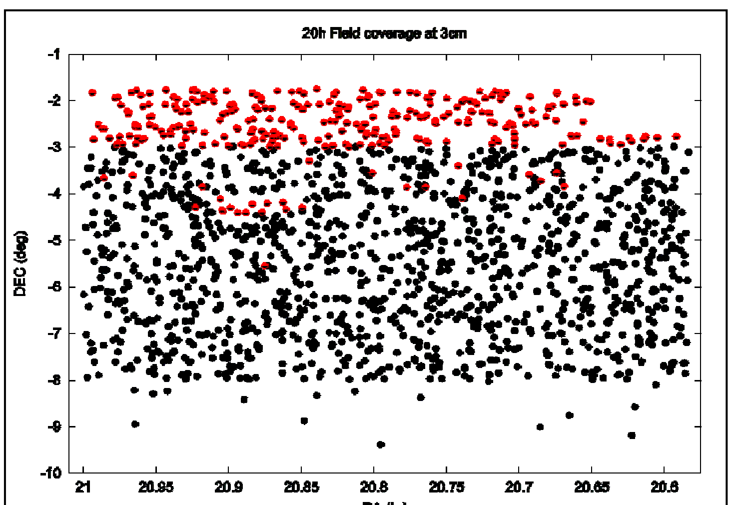

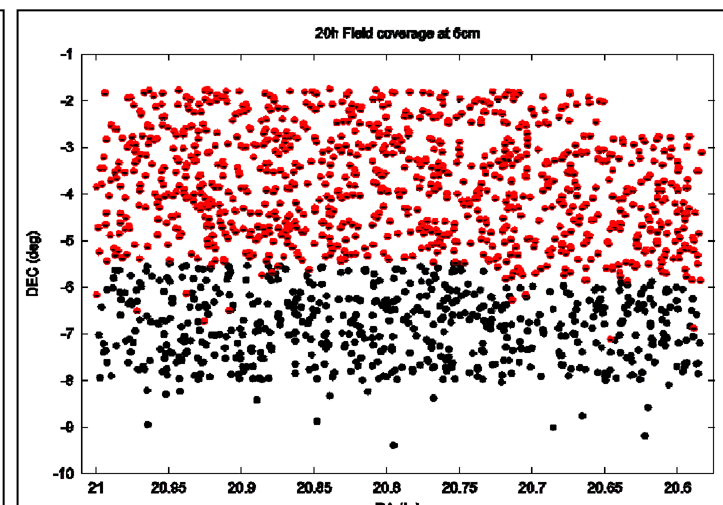

Flux Distribution (preliminary)

~10%

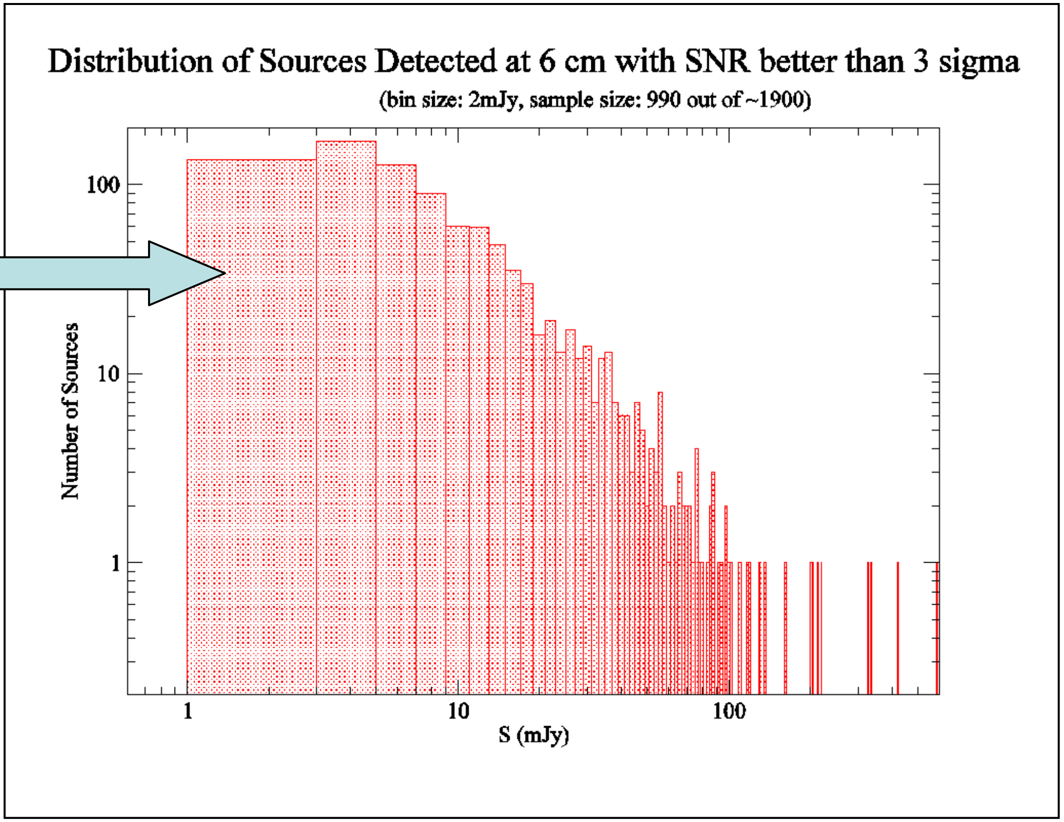

6 cm (4.85 GHz)

Flux Distribution (preliminary)

~17%

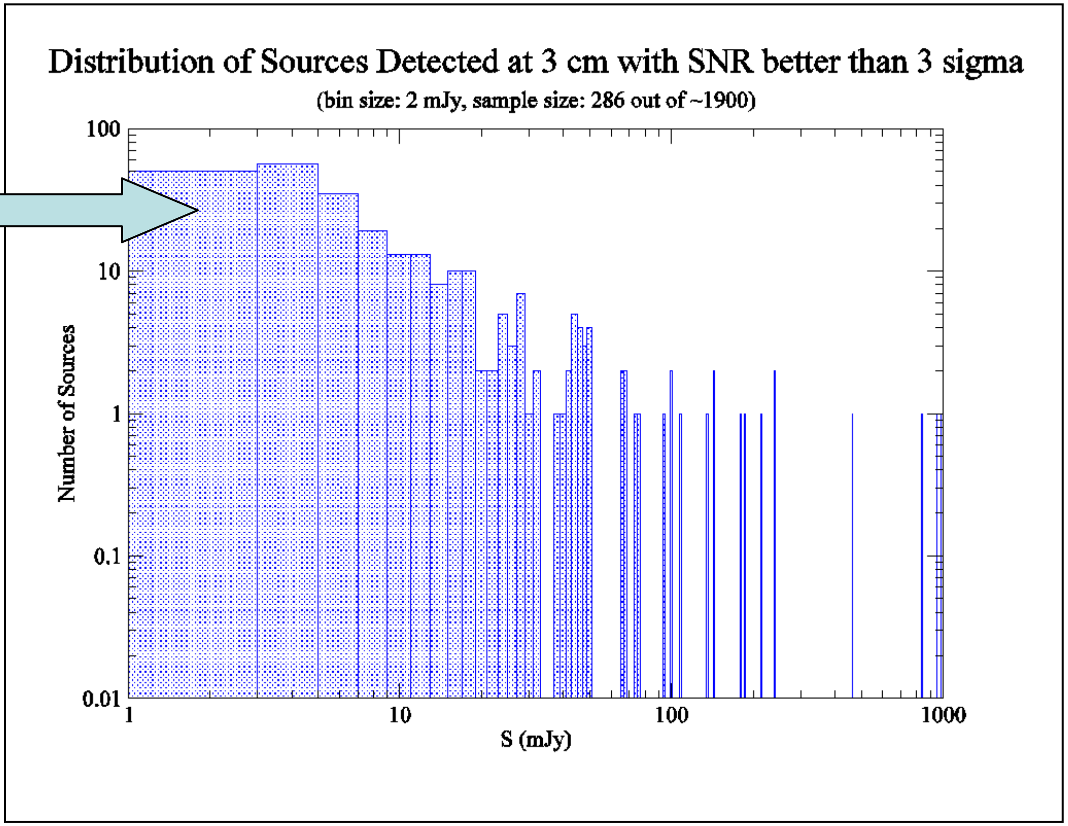

3 cm (10.45 GHz)

Spectral Index Distribution (preliminary)

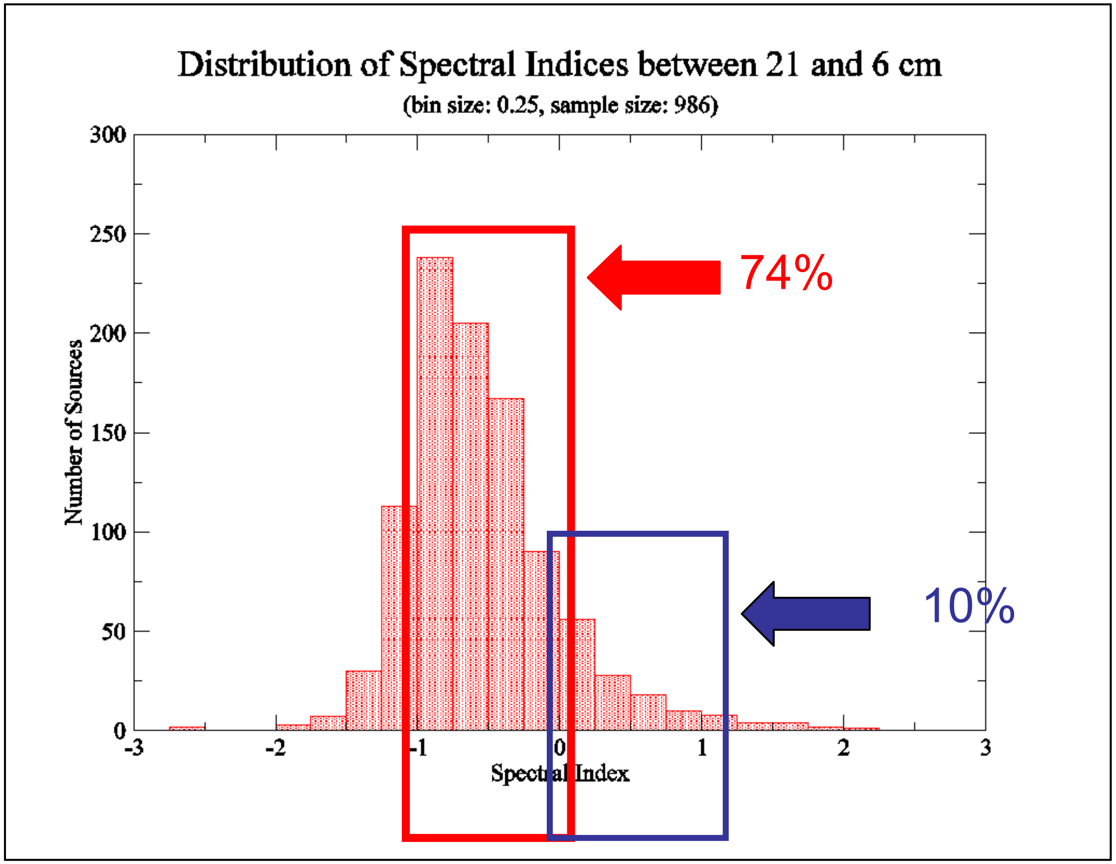

Between 21 and 6 cm

Spectral Index Distribution (preliminary)

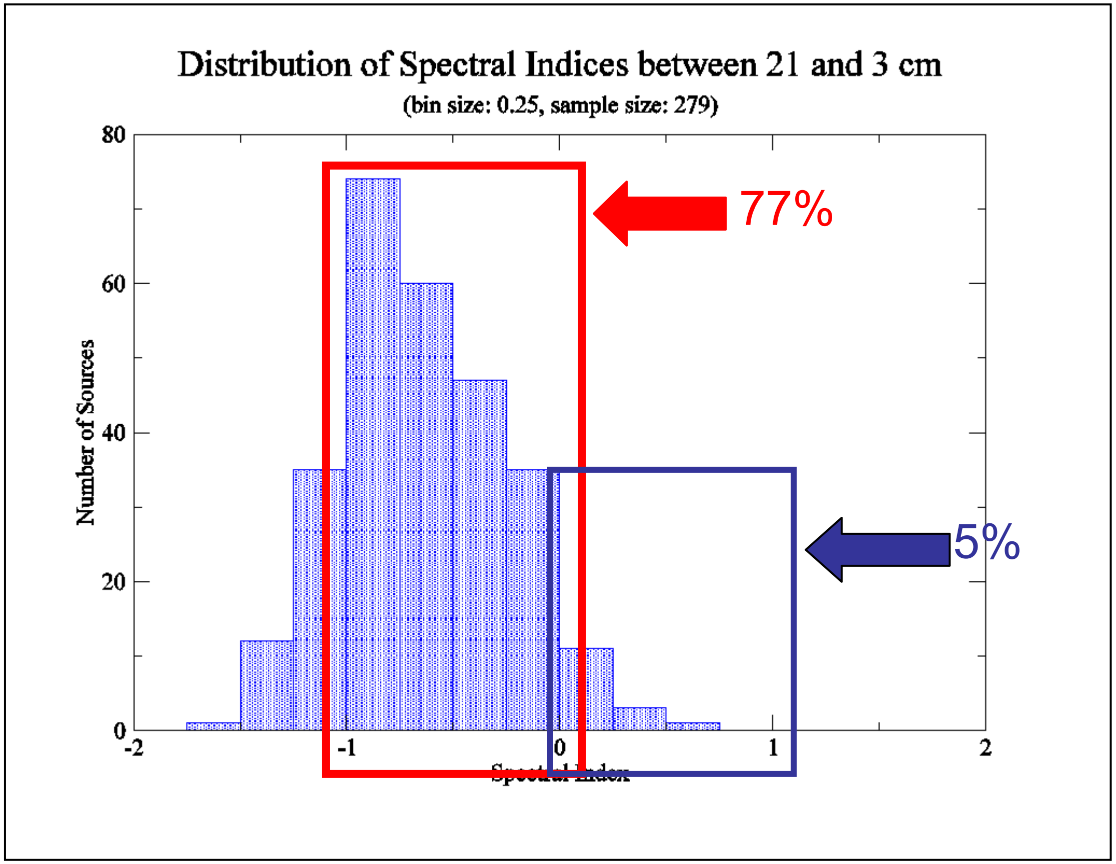

Between 21 and 3 cm

Spectral Index Distribution (preliminary)

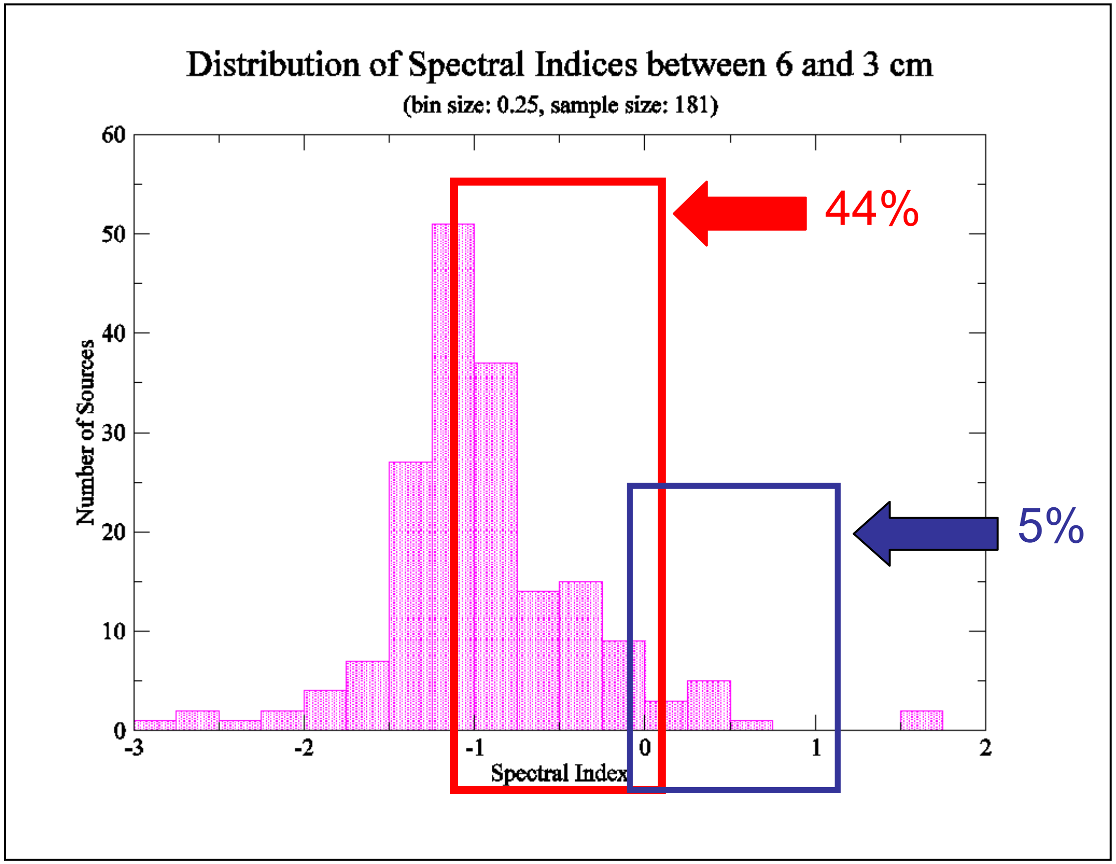

Between 6 and 3 cm

Resume

- The ambition of reaching 1-3 mJy seems approachable
- Most sources display a “steep” spectrum (~75%)
- Significant number of sources display a “flat” or “inverted” (~10%) spectrum being possible candidates for variability studies

Immediate Future Plans

- Completion of the observations and data reduction
- Detailed study of the stability of the system (repeatability)
- Development of sophisticated algorithms to check the confusion problem
- Speculations on possible extensions of the project to a more cosmological orientation
- New proposal submission
- Data Publication within summer 2004
- On-line database development

Thanks

Planck Extragalactic Foreground Sources:

the Metsähovi/Tuorla Quasar Research Team

Anne Lähteenmäki
Metsähovi Radio Observatory

Our team

- Anne Lähteenmäki, coordinator – Metsähovi
- Esko Valtaoja – Tuorla
- Merja Tornikoski – Metsähovi
- Mikko Parviainen, Ilona Torniainen – Metsähovi

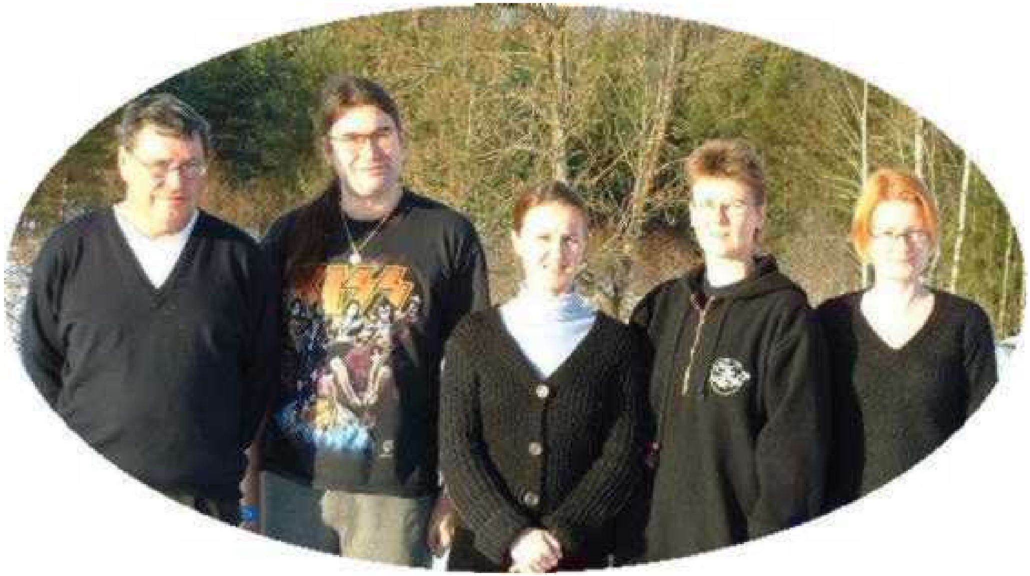

Proposals for Planck Science 2001

- The Astrophysics of Quasars and BL Lac Objects (AL + Core Team)
- Phenomenology of Radio Sources (Core Team)
- Extreme GPS and Other Strongly Inverted-Spectrum Radio Sources (Core Team)
- Statistical Properties of Radio Sources (Core Team)
- Follow-up of Unusual Real-time and ERCSC Objects with Herschel

Anne Lähteenmäki
Metsähovi Radio Observatory

Planck Extragalactic Working Group WG 6

- Quick Detection System
- Pre-launch catalog: data collection (+ follow-up), surveys, construction, theoretical analysis
  - BL Lac & GPS objects, faint quasars, variability
- Modelling, Analysis and Statistical Tools
- Follow-up with Herschel
- Simulations

Variable sources

Anne Lähteenmäki
Metsähovi Radio Observatory

Why are new source samples urgently needed?

- Source selection for mm-studies often based on (few-epoch) low-frequency catalog data
- Many interesting sources or even source populations are excluded from mm-studies!

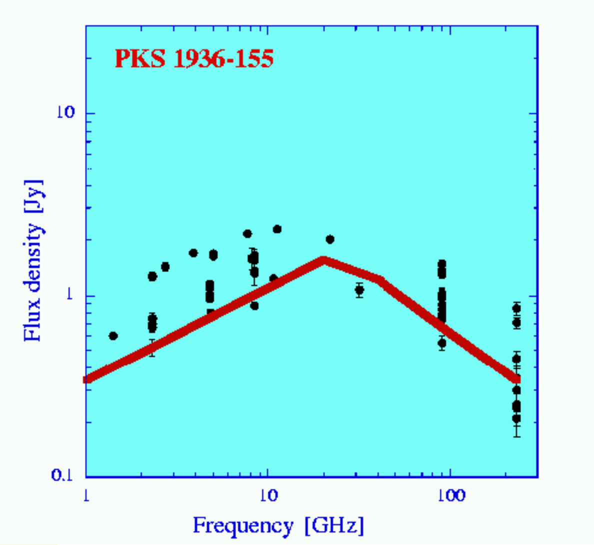

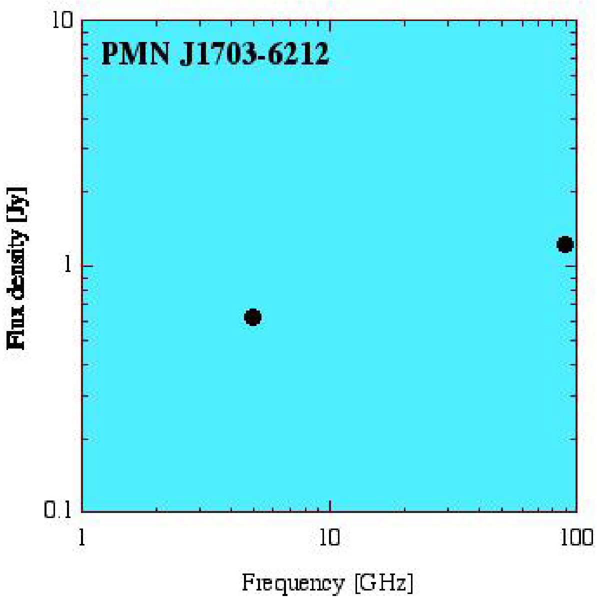

Anne Lähteenmäki
Metsähovi Radio Observatory

One data point is not enough! (Or even four…)

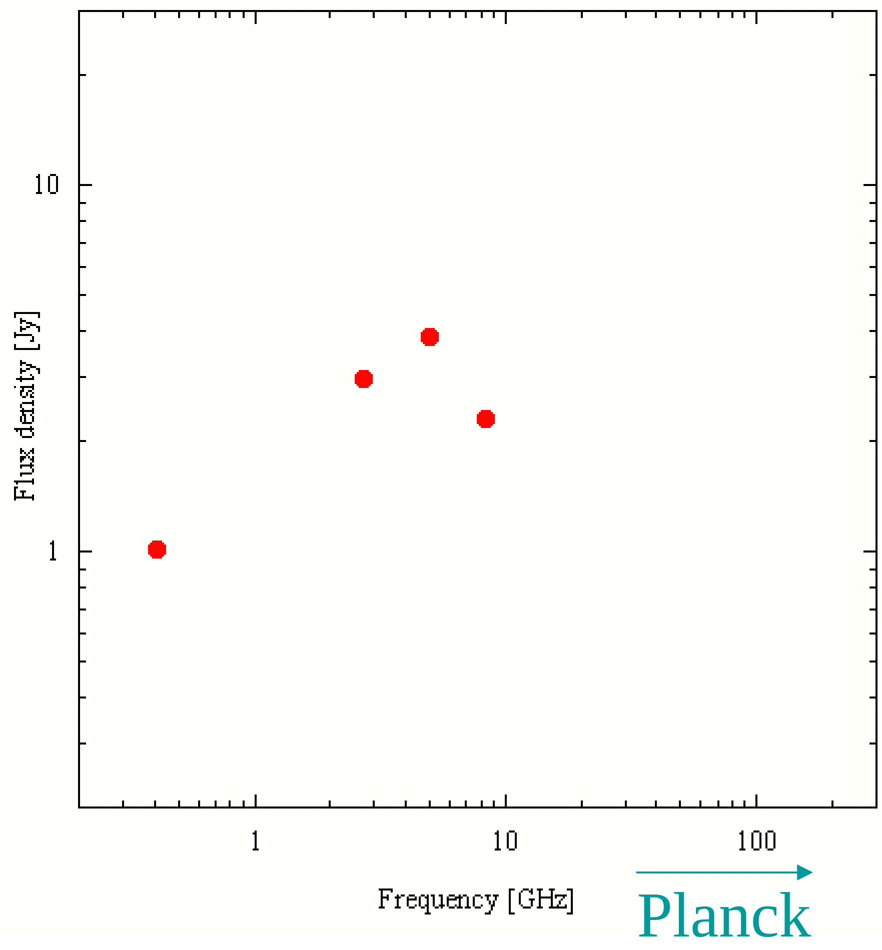

Anne Lähteenmäki
Metsähovi Radio Observatory

One data point is not enough!

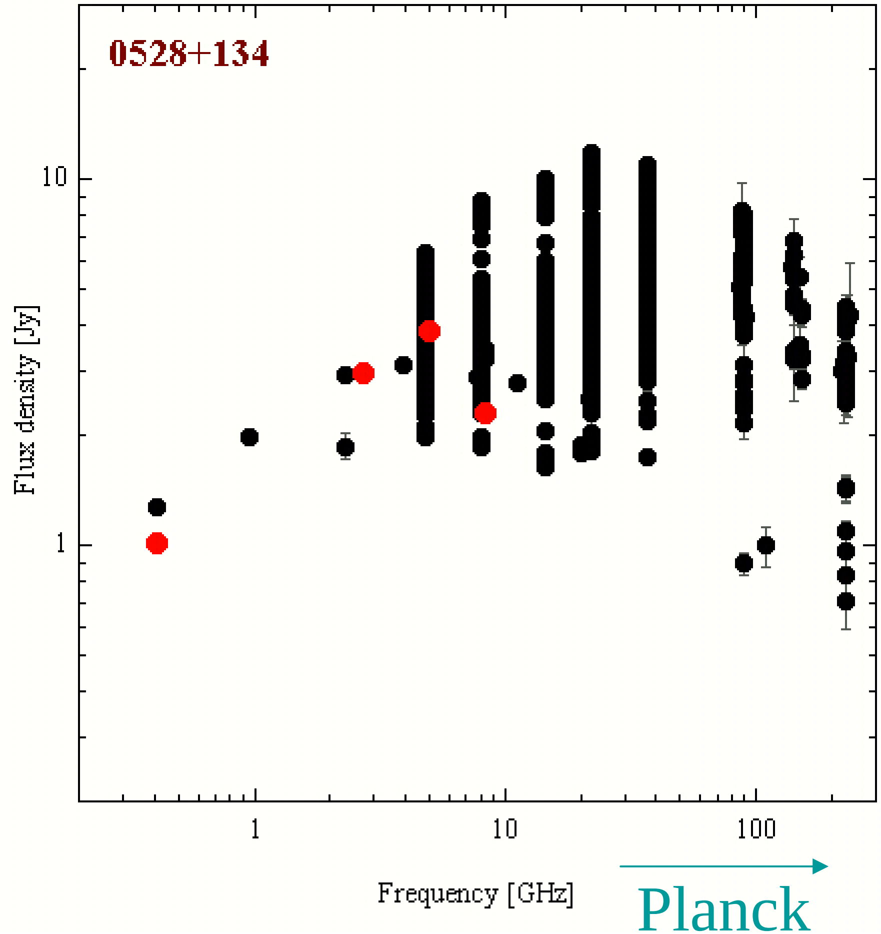

Anne Lähteenmäki
Metsähovi Radio Observatory

Dedicated observing programmes: GPS sources

- Observed every other week since Nov 2001
- Only very few genuine convex spectra but lots of sources with spectra that can sometimes (during flares) be inverted
  - Tornikoski et al. 2001
  - Torniainen 2002 MSc Thesis
  - Torniainen et al. in preparation

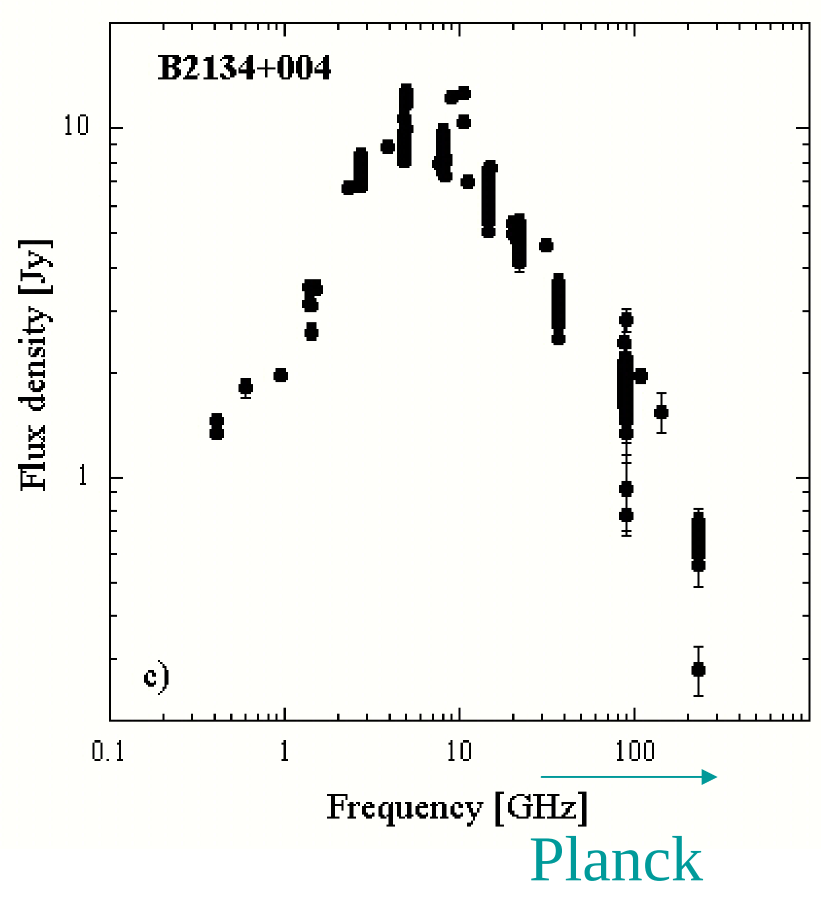

Anne Lähteenmäki
Metsähovi Radio Observatory

Dedicated observing programmes: “Bona fide” GPS sources

- Very few retain the convex shape in long term monitoring

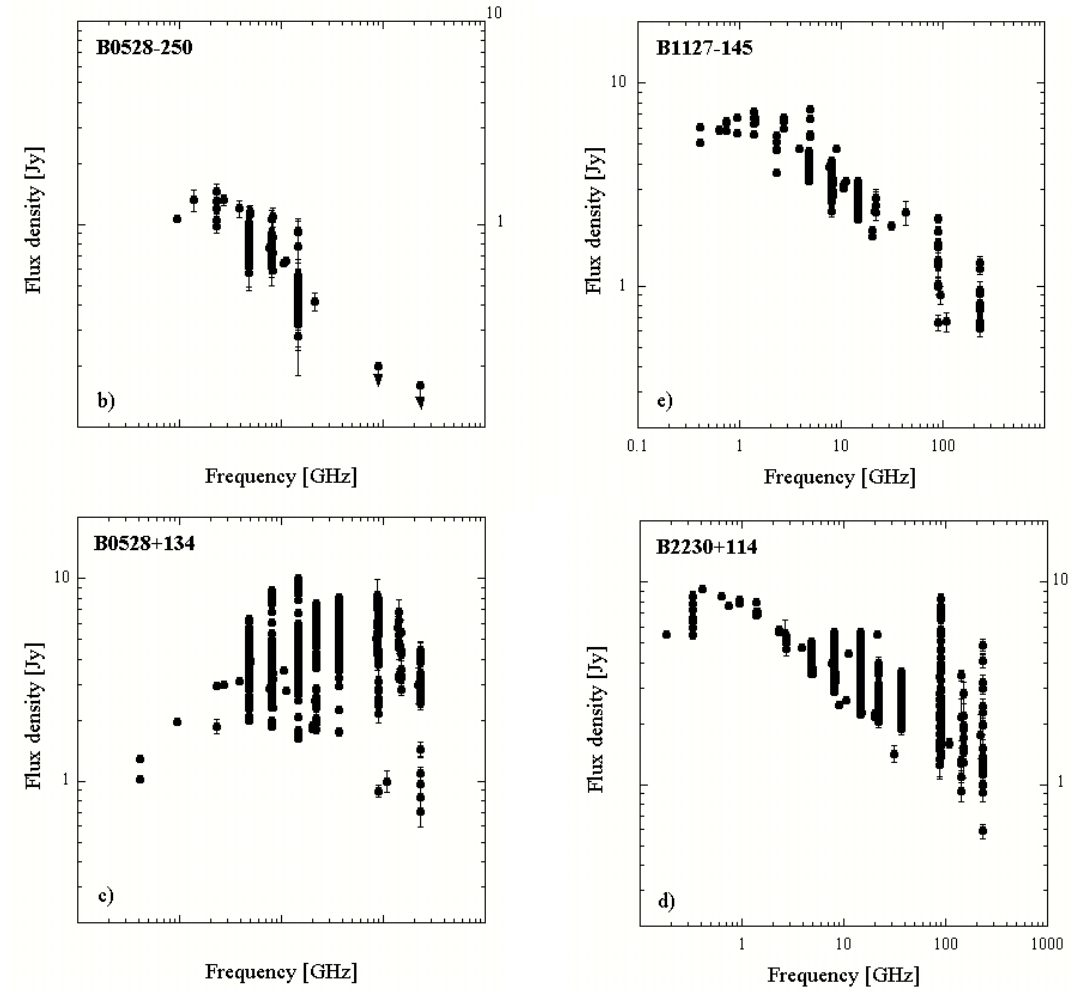

Anne Lähteenmäki
Metsähovi Radio Observatory

Dedicated observing programmes: GPS sources

- Lots of sources with inverted spectra during flaring
- Significant variability — time between the two 90 GHz points is 14 yrs
- during quiescent state spectra remain flat or falling

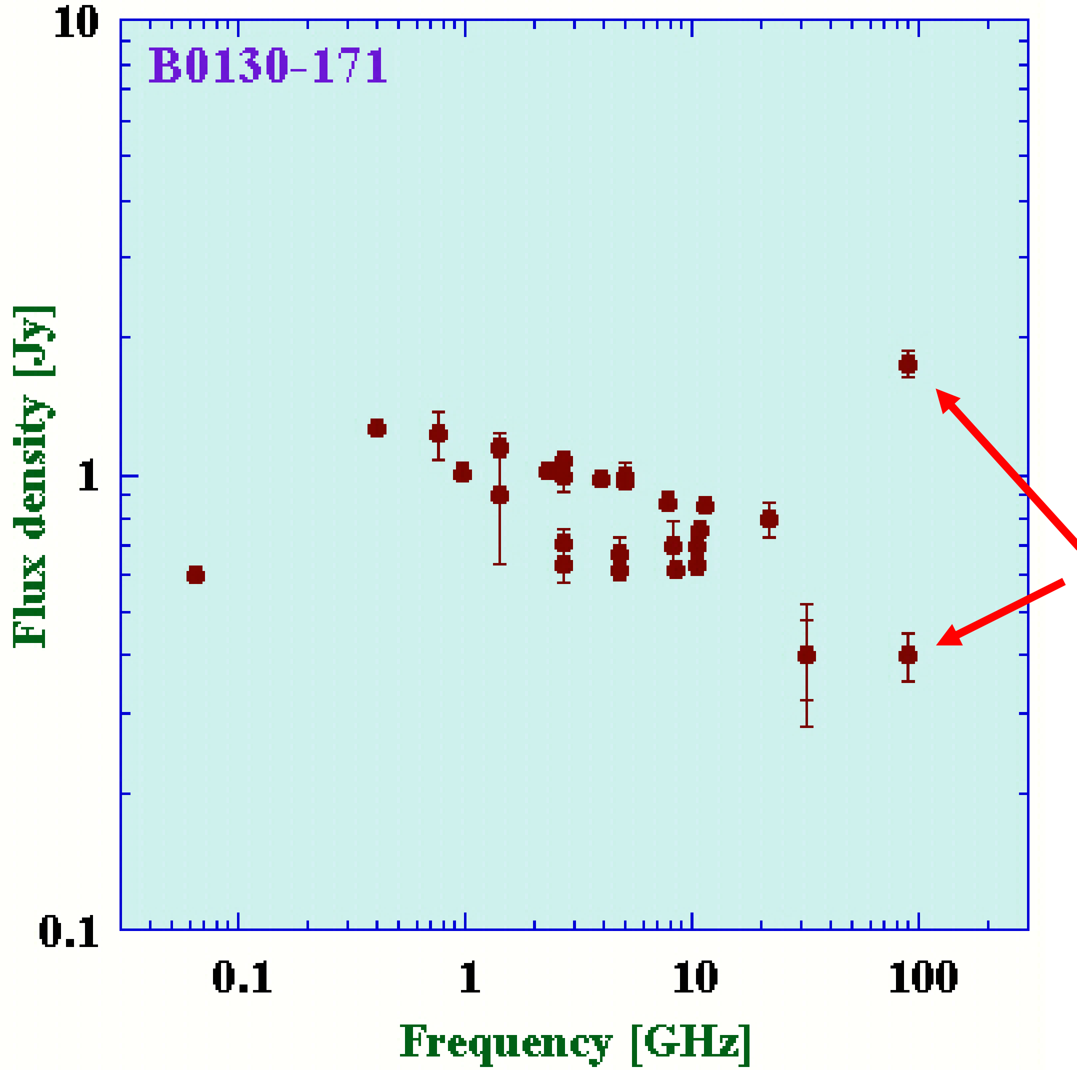

Anne Lähteenmäki
Metsähovi Radio Observatory

Dedicated observing programmes: BL Lac Objects

- Also X-ray selected and intermediate BLOs
  - usually considered weak at radio frequencies
- Autumn 2003: ~400 (almost 100%) observed
- More than 1/3 of all BLOs detected AND ~1/3 of X-ray & intermediate BLOs

➡ Planck should be able to observe 1/3 as well !

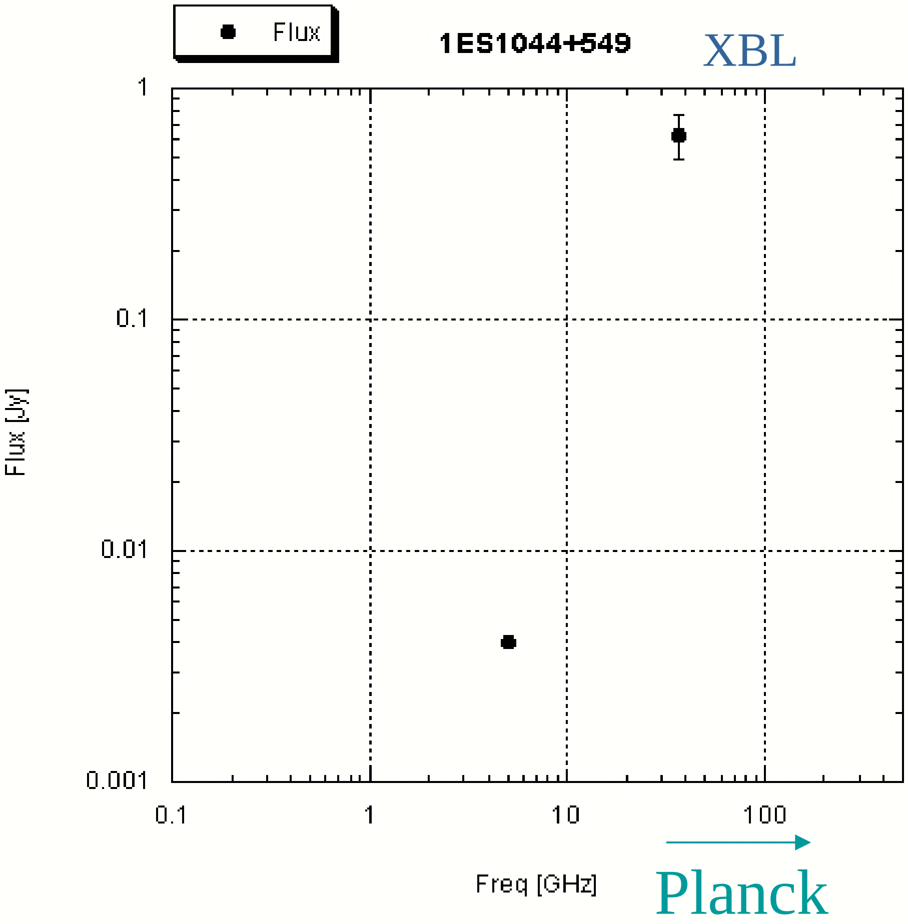

Anne Lähteenmäki
Metsähovi Radio Observatory

Dedicated observing programmes: WMAP sources

- WG 6 joint effort to observe the unidentified or multiple identification WMAP extragalactic foreground sources
- Several identifications achieved

WMAP036

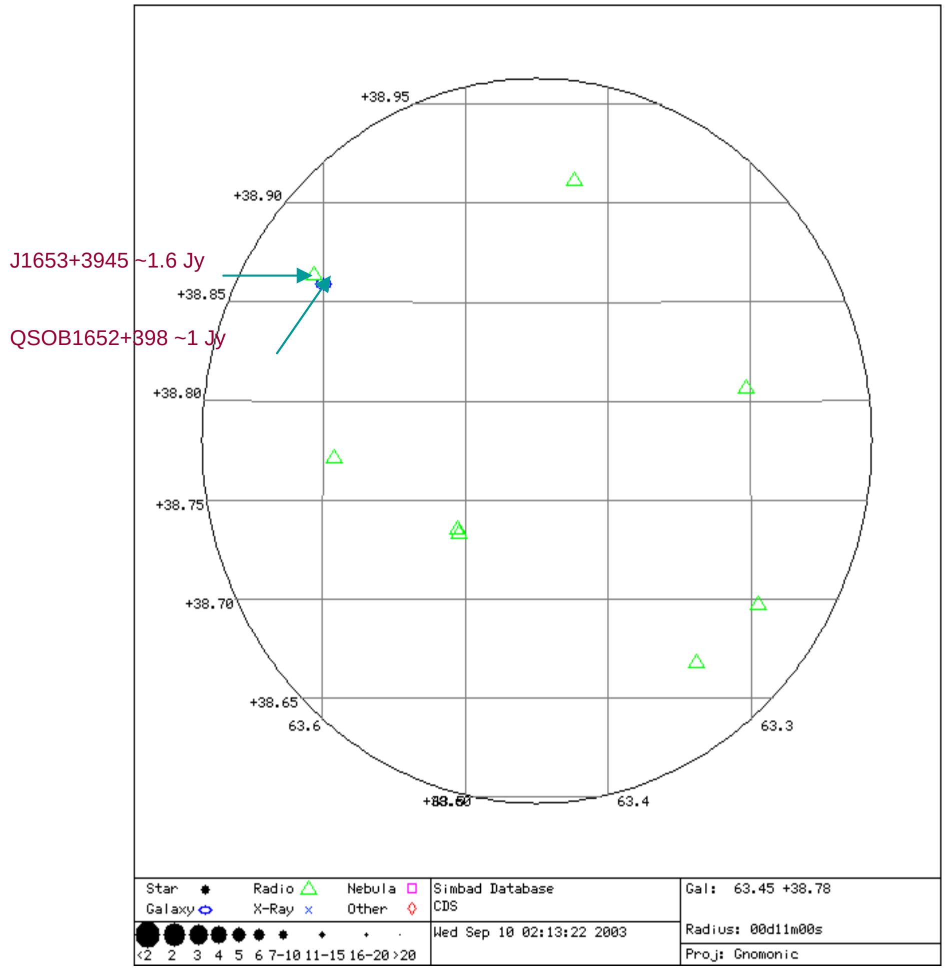

Anne Lähteenmäki
Metsähovi Radio Observatory

Dedicated observing programmes: RATAN-600

- A joint observing programme with Special Astrophysical Observatory and other Russian institutes
- Simultaneous spectra 1 - 22 GHz
- Successful observing runs Autumn 2003 and Spring 2004 —and more to come

Anne Lähteenmäki
Metsähovi Radio Observatory

Variability analysis and statistics...

Is it possible to predict what, when, how often ?

⇒ *Educated guesses*

- 22 & 37 GHz Metsähovi data: variability timescales for 85 sources
  - fastest flares for HPQs and BLOs 10 to 400 days; median 60 and 90 days, respectively
  - fastest flares for LPQs and GALs 50 to 1000 days; median approx. 120 days for both

Anne Lähteenmäki
Metsähovi Radio Observatory

...Variability analysis and statistics

- 90 & 230 GHz SEST data
  - 22 & 37 GHz approach not applicable
  - at 90 GHz, a random observation is likely to see a source in a quiescent or intermediate state
  - activity timescale 3.6 years (for about 4 months)
  - flare timescale 2.6 years (depends on the definition of a flare)

Anne Lähteenmäki
Metsähovi Radio Observatory

Quick Detection System parameters

Emphasis mostly on “surprising” events & sources

1. New flaring objects

   $S_{cur} > k * S_{max}$ or $S_{cur} > k * (S_{max} - S_{min})$;

   S_{max}, N small; different k categories

   Includes objects that are expected to be very faint:

   XBLs, TeV sources etc.

2. Inverted spectrum-sources

   $\alpha > \alpha_{convex}$; S_1, S_2 relatively simultaneous; $\alpha_{convex} \approx 0.5 – 1.0$

3. Fast events

   S_{prev} @ $t_x << S_{cur}$; t_x relatively small

4. Strong events in well-known sources

   As in 1. or $S_{cur} \in$ “top 1/5” etc.

Anne Lähteenmäki
Metsähovi Radio Observatory

QDS structure

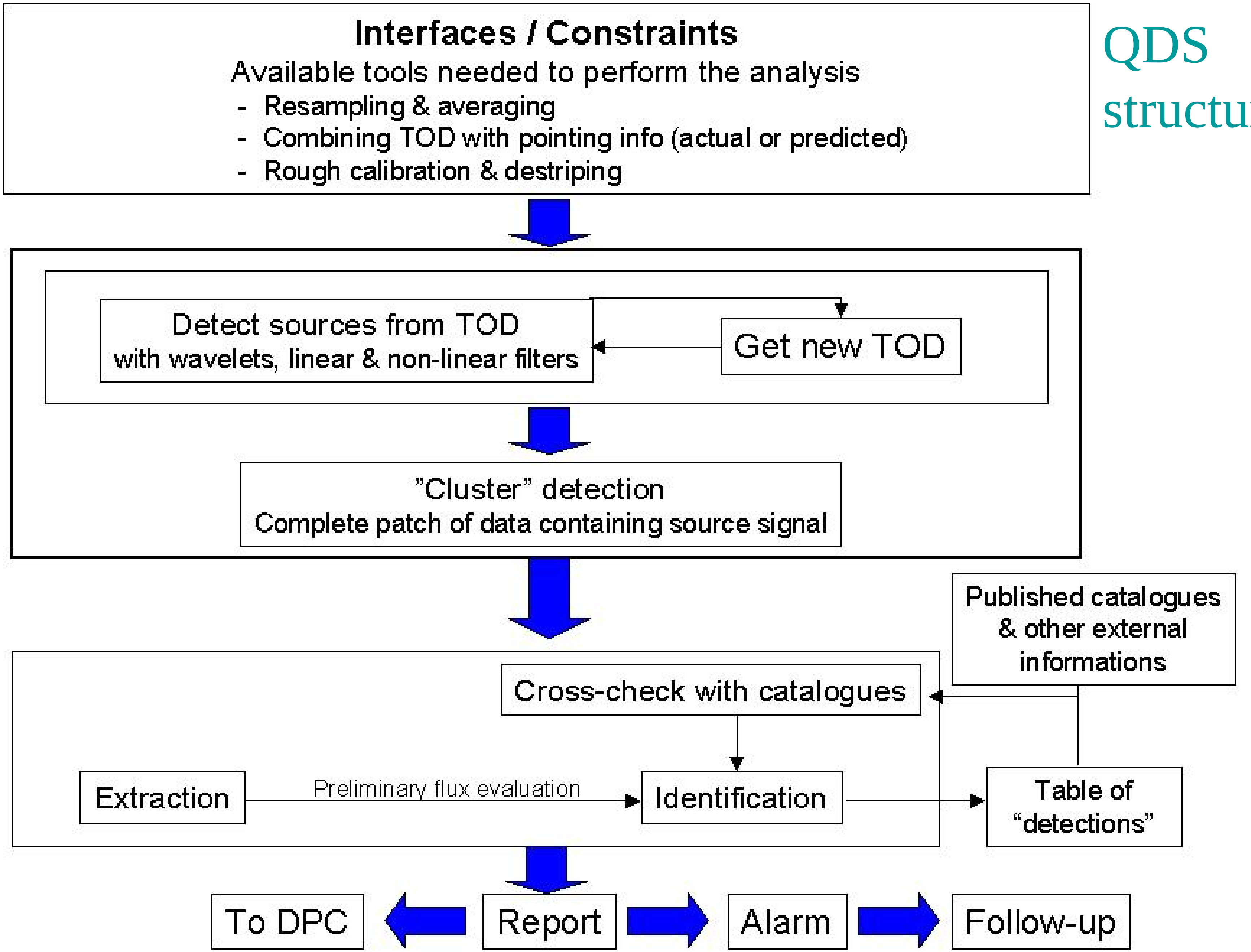

Future: Planck launch scheduled for Feb 2007

- Observations & theory until and after launch
- Herschel follow-up: 2004
- Quick Detection System: approx. 2004, will be in a continuous state of flux until and after launch
- Simulations, modelling, tools: 2004/2005
- Pre-launch Catalog: Feb 2006, updated regularly
- QDS operations & data analysis: 2007 ➔
- ERCSC & final data analysis: mid-2008 ➔

Anne Lähteenmäki
Metsähovi Radio Observatory

Correlation between the X-ray and gamma-ray activity of the high-enery peaked BL Lac objects

Krzysztof Katarzyński[1,2],
Gabriele Ghisellini[2], Fabrizio Tavecchio[2], Laura Maraschi[2]

[1]Osservatorio Astronomico di Brera (OAB, Italy),
[2]Nicolaus Copernicus University -
Toruń Centre for Astronomy (TCfA, Poland)

Introduction

- a few examples of the correlation between the X-ray and TeV activity:

$$\boxed{F_{\mathrm{TeV}}(t) \propto F^{x}_{\mathrm{X-ray}}(t)}$$

  observed in Mrk 421 and Mrk 501
- simple time dependent SSC modeling (no radiative cooling, no crossing time effects)
- estimations for a basic correlations
- correlations around the $\nu F(\nu)$ peaks
- impact of the radiative cooling for the correlation
- light crossing time effect - how it can modify the correlation

Mrk 421 - March 18-25, 2001

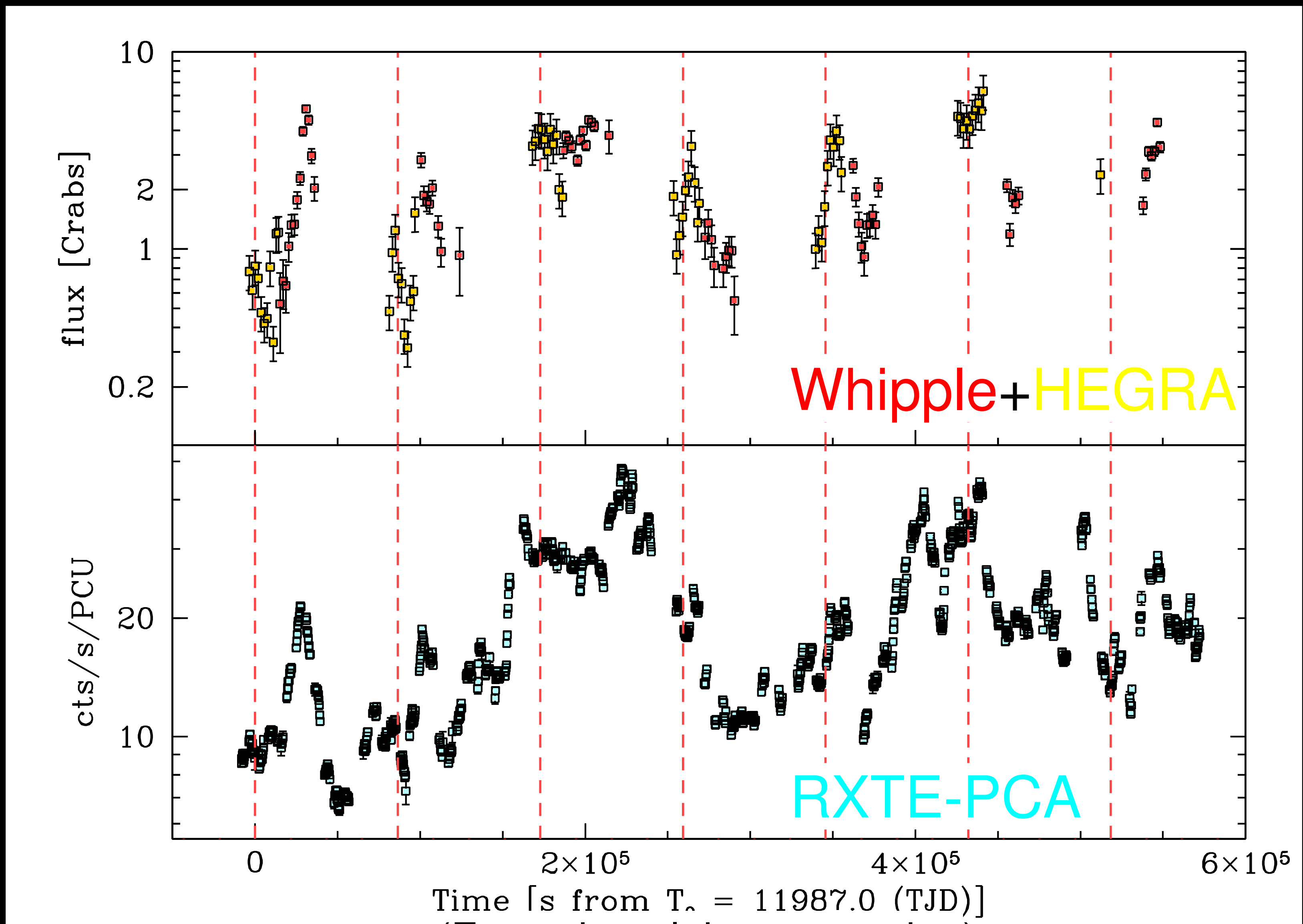

(Fossati et al. in preparation)

Mrk 421 - March 18/19, 2001

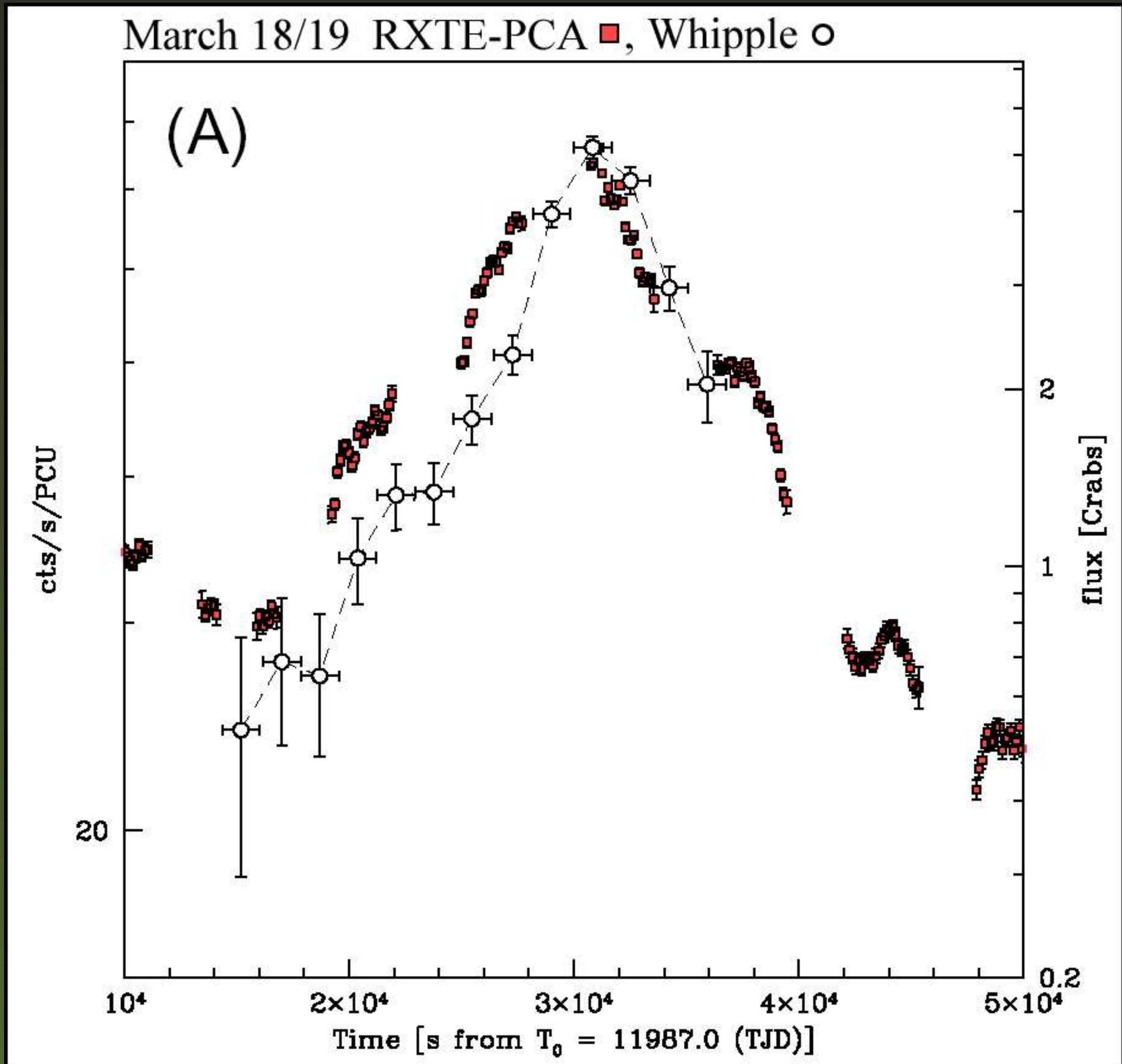

Mrk 421 - Correlation for March 18/19

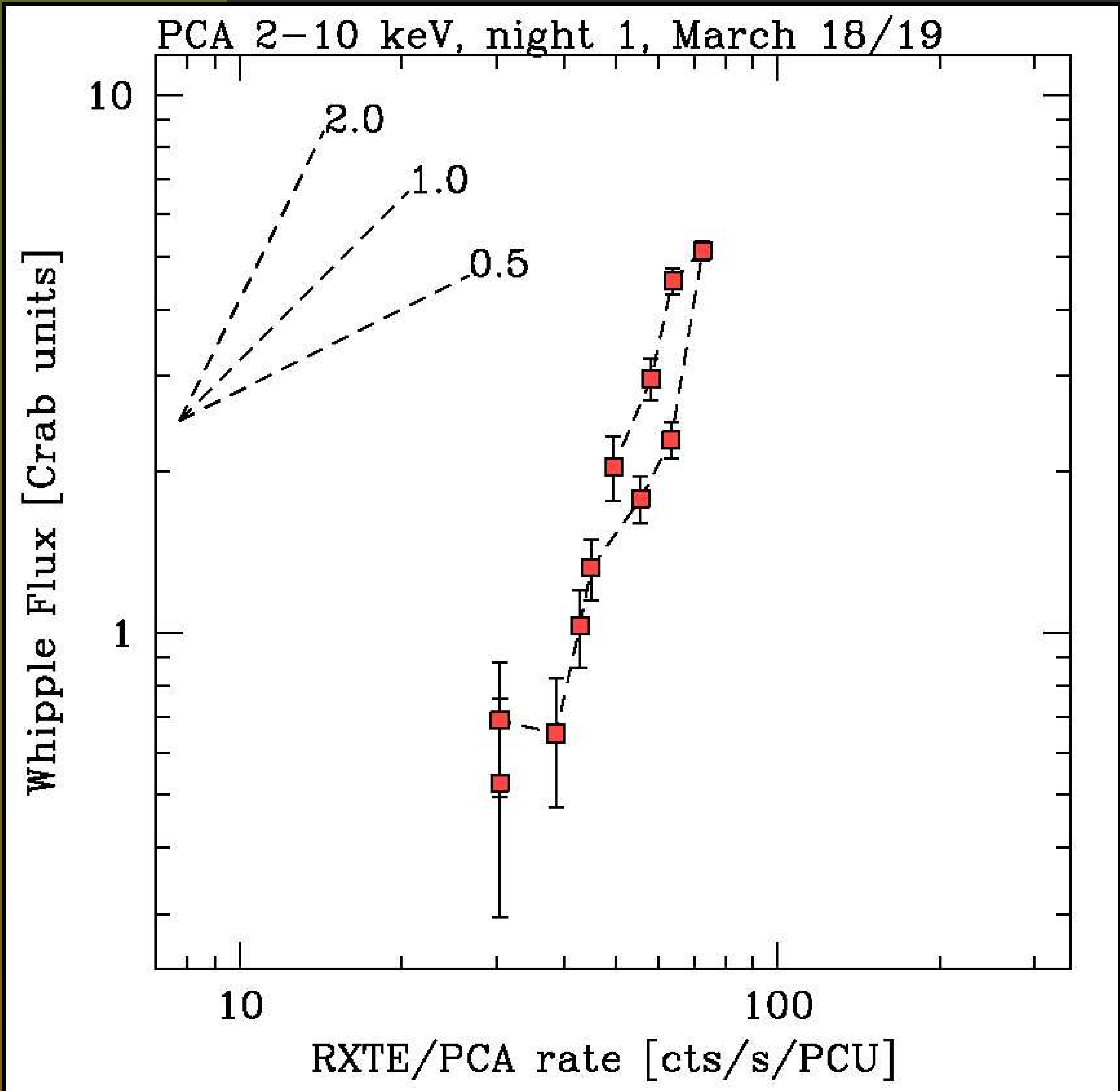

$$F_{\mathrm{TeV}} \propto F^{x}{}_{\mathrm{X-ray}}$$

$$x \simeq 2$$

Mrk 421 - Correlation for March 22/23

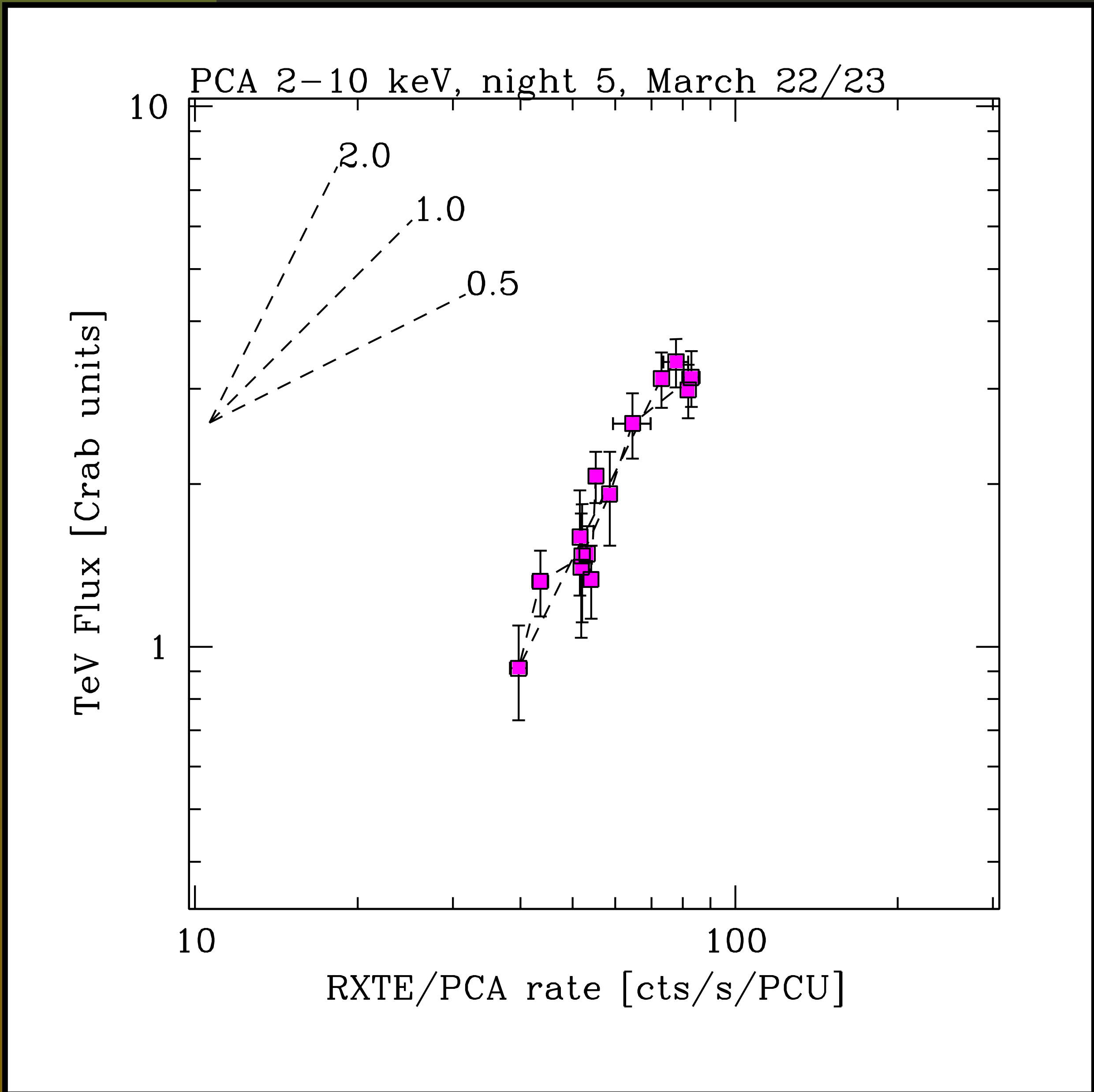

$$F_{\rm TeV} \propto F^{x}{}_{\rm X-ray}$$

$$x \simeq 2$$

Mrk 421 - February, 2000

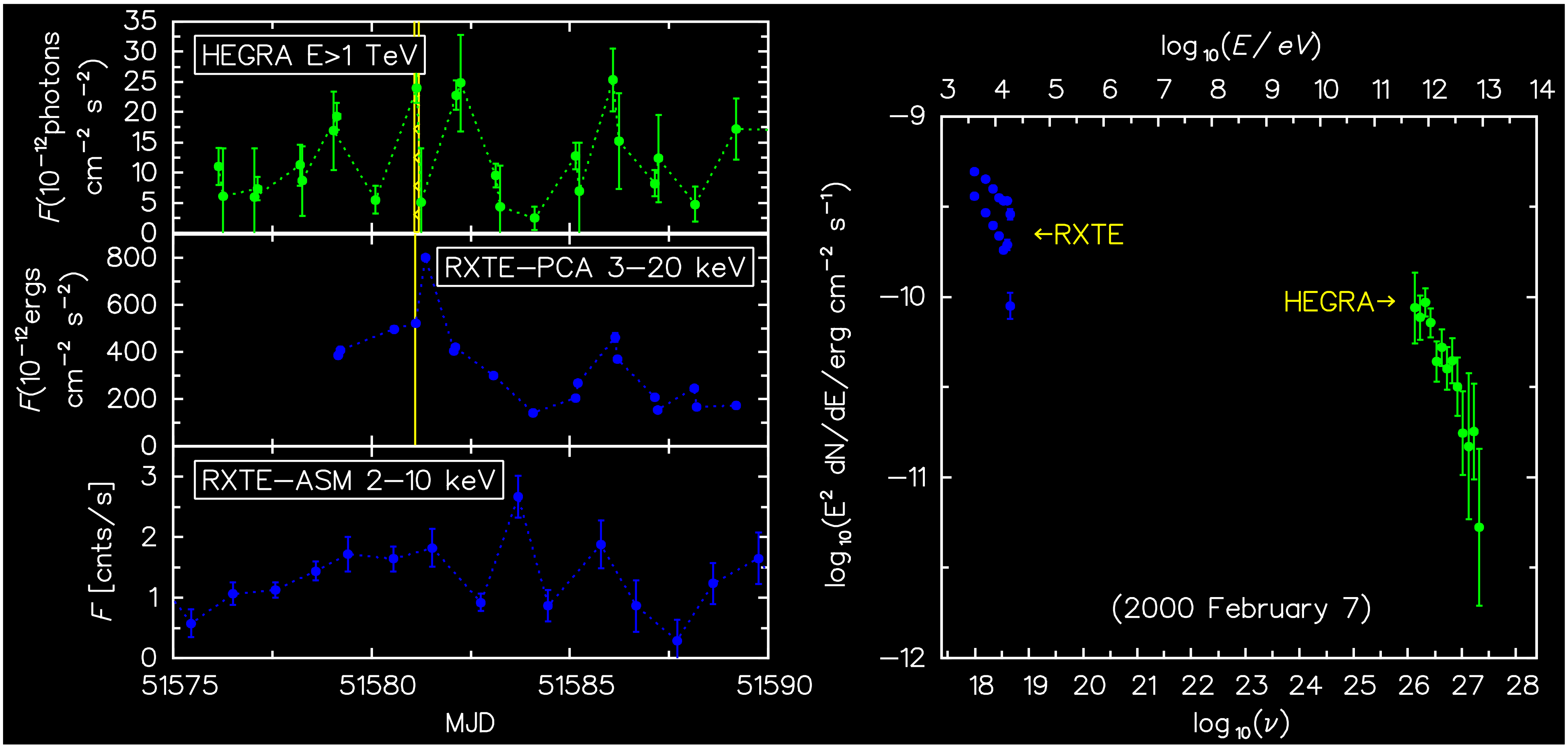

(Krawczynski et al. 2001)

Mrk 421 - Correlation for February, 2000

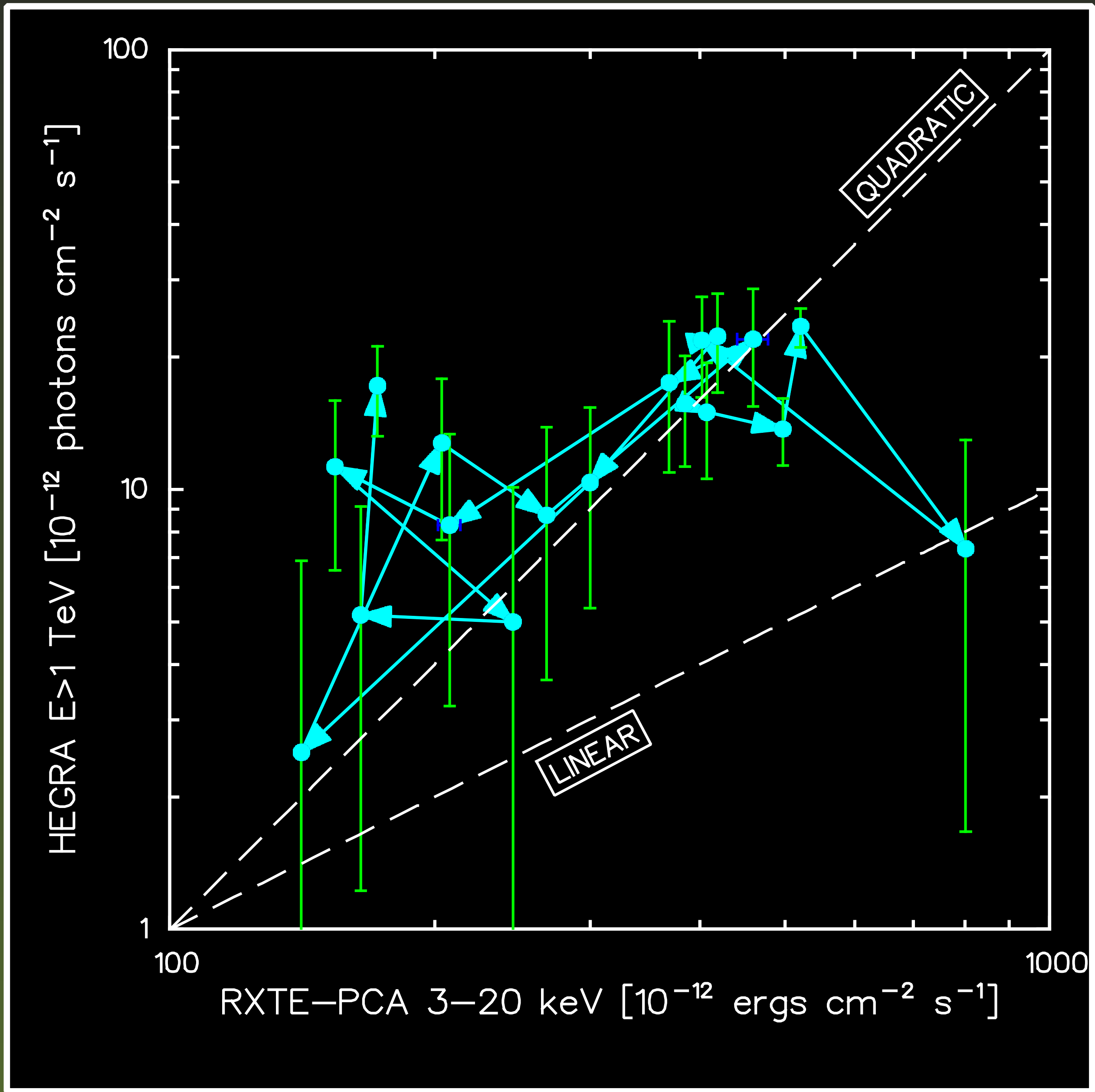

OAB-Italy

Mrk 501 - April, 1997

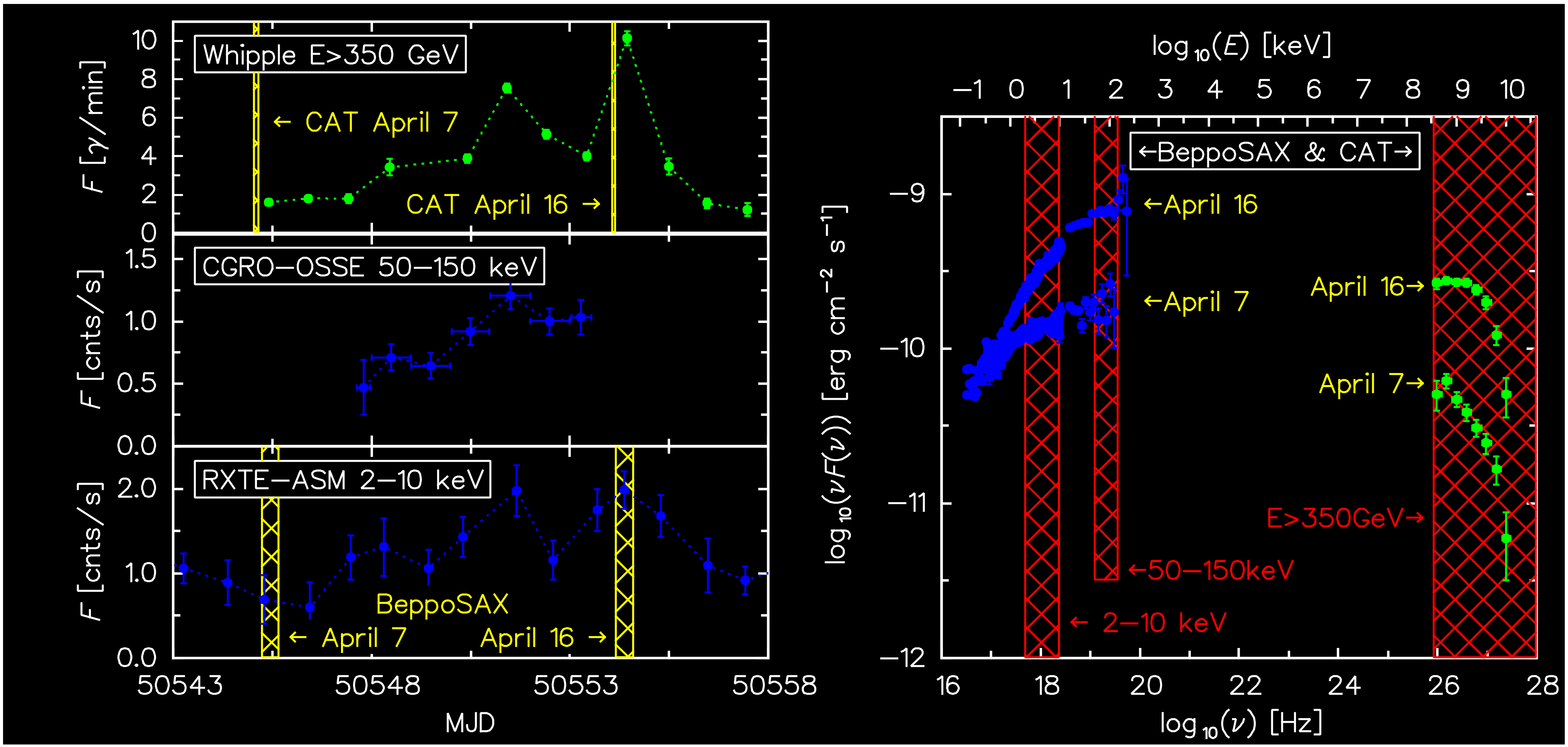

(Catanese et al. 1997, Pian et al. 1998, Djannati-Atai et al. 1999)

Mrk 501 - Correlation for April, 1997

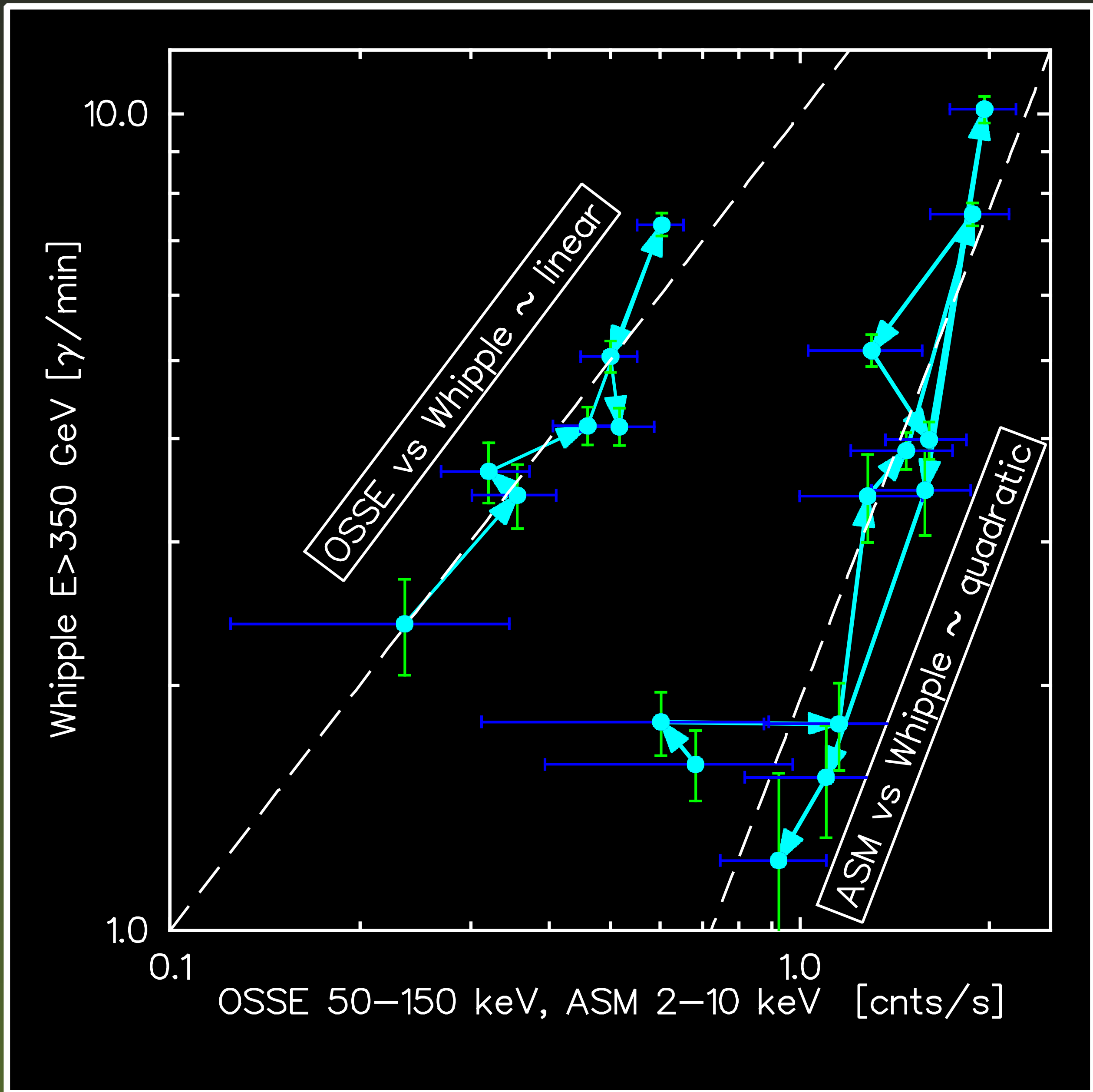

OAB-Italy

A simple Time Dependent SSC modeling

- homogeneous spherical source which may expand or collapse
- no radiative cooling (true only if $t_{cool} \gg R/c$)
- no light crossing time effects for the radiation field inside the source and for the observed emission as well (true only if the evolution is slow (a flare rising/decay time $\gg R/c$)
- as much as possible separation in description of the physical processes (to simulate for example the expansion of the source without the adiabatic losses)

TD-SSC - basic assumptions

The evolution of the source radius:

$$R(t) = R_0 \left(\frac{t_0}{t} \right)^{-r_\mathrm{e}},$$

where R_0 is the initial radius.

The evolution of the magnetic field intensity inside the source:

$$B(t) = B_0 \left(\frac{t_0}{t} \right)^{m},$$

where B_0 is the initial magnetic field intensity.

TD-SSC - electron spectrum

The initial ($t = t_0$) electron energy distribution:

$$N_{\rm e}^0(\gamma) = \begin{cases} K_1 \gamma^{-n_1}, & \gamma_{\rm min} \le \gamma \le \gamma_{\rm brk}^0 \\ K_2 \gamma^{-n_2}, & \gamma_{\rm brk}^0 < \gamma \le \gamma_{\rm max} \end{cases},$$

is approximated by a broken power law.

The evolution of the electron energy spectrum:

$$N_{\rm e}(\gamma, t) = \min \left\{ N_{\rm e}^1(\gamma, t), N_{\rm e}^2(\gamma, t) \right\},$$

is described by a minimum of two power law functions,

TD-SSC - electron spectrum

where the functions are given by:

$$N_{\mathrm{e}}^{1}(\gamma,t) = K_{\mathrm{e}}^{1}(t)\gamma^{-n_1}; \qquad N_{\mathrm{e}}^{2}(\gamma,t) = K_{\mathrm{e}}^{2}(t)\gamma^{-n_2}$$

$$K_{\mathrm{e}}^{1}(t) = K_1 \underbrace{\left(\frac{t_0}{t}\right)^{r_{\mathrm{a}}(n_1-1)}}_{\text{adiabatic heating/cooling}} \times \underbrace{\left(\frac{t_0}{t}\right)^{3r_{\mathrm{d}}}}_{\text{density increase/decrease}},$$

$$K_{\mathrm{e}}^{2}(t) = K_2 \underbrace{\left(\frac{t_0}{t}\right)^{r_{\mathrm{a}}(n_2-1)}}_{\text{adiabatic heating/cooling}} \times \underbrace{\left(\frac{t_0}{t}\right)^{3r_{\mathrm{d}}}}_{\text{density increase/decrease}},$$

r_{a} describes the adiabatic losses and r_{d} describes the decrease of the electron density.

TD-SSC - evolution of the elec. spectrum

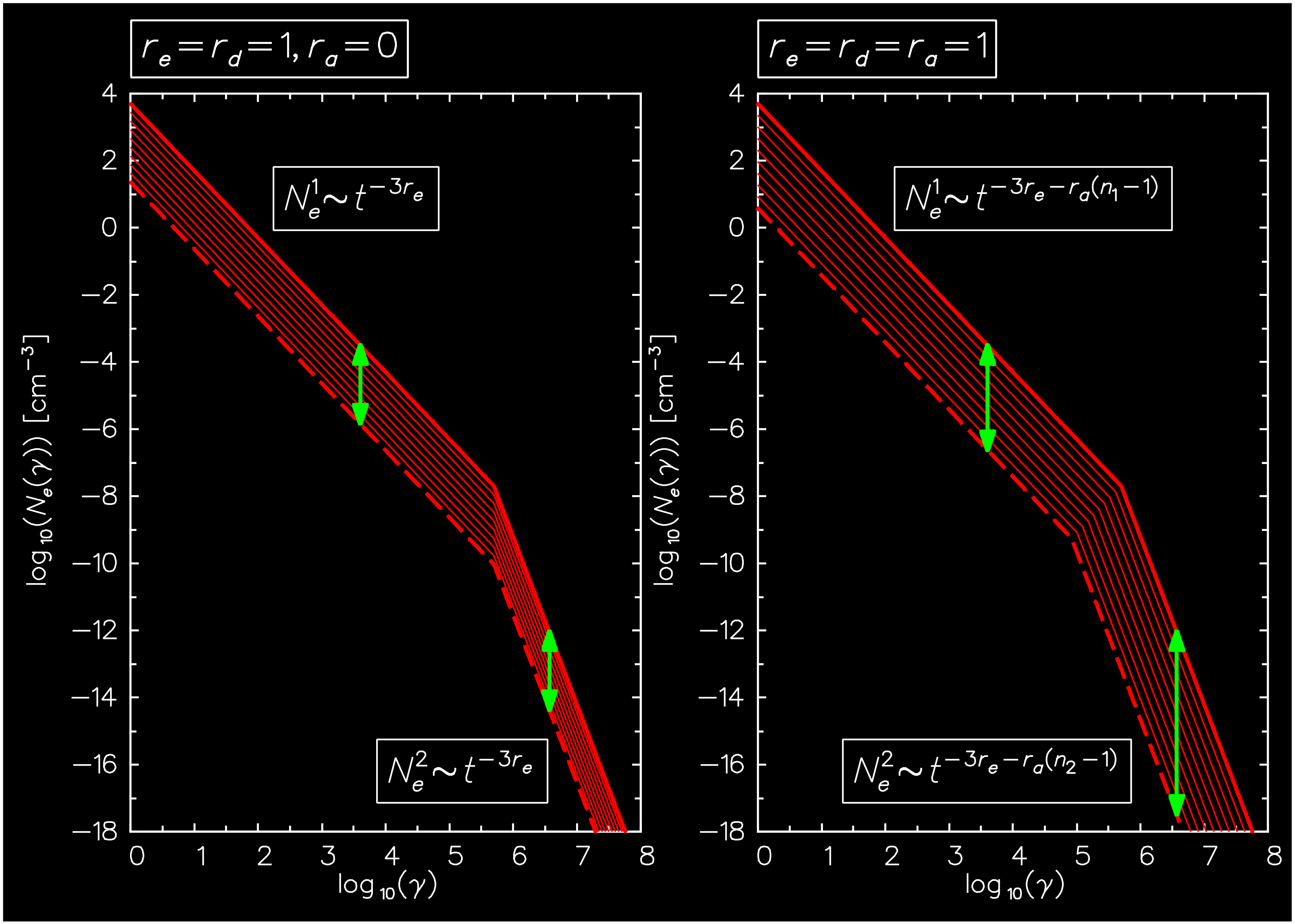

OAB-Italy

TD-SSC - synchrotron emission coefficient

The evolution of the emission coefficient is defined by:

$$\boxed{j_{\rm s}(t) \propto K_{\rm e}(t) B(t)^{m(\alpha+1)}, \quad \alpha = (n-1)/2,}$$

which gives:

$$j_{\rm s}^1(t) \propto K_1 B_1 \left(\frac{t_0}{t}\right)^{3r_{\rm d}+r_{\rm a}(n_1-1)+m(\alpha_1+1)} \quad \text{for} \quad \gamma \leq \gamma_{\rm brk},$$

$$j_{\rm s}^2(t) \propto K_2 B_2 \left(\frac{t_0}{t}\right)^{3r_{\rm d}+r_{\rm a}(n_2-1)+m(\alpha_2+1)} \quad \text{for} \quad \gamma > \gamma_{\rm brk},$$

where $B_1 = B_0^{\alpha_1+1}$ and $B_2 = B_0^{\alpha_2+1}$.

TD-SSC - synchrotron intensity

If we neglect the electron self-absorption then the evolution of the intensity of the synchrotron emission can be approximated by:

$$\boxed{I_{\rm s}(t) \propto R(t) j_{\rm s}(t)} \propto R(t) K_{\rm e}(t) B(t)^{m(\alpha+1)},$$

which gives:

$$I_{\rm s}^{1}(t) \propto R_0 K_1 B_1 \left(\frac{t_0}{t}\right)^{-r_{\rm e}+3r_{\rm d}+r_{\rm a}(n_1-1)+m(\alpha_1+1)},$$

$$I_{\rm s}^{2}(t) \propto R_0 K_2 B_2 \left(\frac{t_0}{t}\right)^{-r_{\rm e}+3r_{\rm d}+r_{\rm a}(n_2-1)+m(\alpha_2+2)}.$$

TD-SSC - synchrotron flux

The evolution of the synchrotron flux is described by:

$$\boxed{F_{\rm s}(t) \propto R(t)^2 I_{\rm s}(t)} \propto R(t)^3 K_{\rm e}(t) B(t)^{m(\alpha+1)},$$

which gives:

$$F_{\rm s}^1(t) \propto R_0^3 K_1 B_1 \left(\frac{t}{t_0}\right)^{s_1},$$
$$s_1 = 3r_{\rm e} - 3r_{\rm d} - r_{\rm a}(n_1 - 1) - m(\alpha_1 + 1),$$

$$F_{\rm s}^2(t) \propto R_0^3 K_2 B_2 \left(\frac{t}{t_0}\right)^{s_2},$$
$$s_2 = 3r_{\rm e} - 3r_{\rm d} - r_{\rm a}(n_2 - 1) - m(\alpha_2 + 1),$$

TD-SSC - inv. Compton emission

The Inverse Compton (IC) emission coefficient is approximated by:

$$\boxed{j_{\rm c}(t) \propto K(t) I_{\rm s}(t)} \propto K(t) R(t) j_{\rm s}(t) \propto K(t)^2 R(t) B(t)^{m(\alpha+1)}.$$

However, we assume that the IC radiation in the Thompson limit ($j_{\rm c}^1$) is produced by the electrons with $\gamma \leq \gamma_{\rm brk}$ ($K_{\rm e}^1$) and the synchrotron radiation field which is described by $I_{\rm s}^1$. This gives:

$$F_{\rm c}^1(t) \propto R_0^4 K_1^2 B_1 \left(\frac{t}{t_0}\right)^{c_1},$$

$$c_1 = 4r_{\rm e} - 6r_{\rm d} - 2r_{\rm a}(n_1 - 1) - m(\alpha_1 + 1),$$

TD-SSC - inv. Compton emission

We assume that the IC emission in the Klein-Nishina regime is generated mostly by the the electrons with $\gamma \leq \gamma_{\rm brk}$ ($K_{\rm e}^2$) and the synchrotron radiation field which is described by $I_{\rm s}^1$. This gives:

$$F_{\rm c}^2(t) \propto R_0^4 K_1 K_2 B_1 \left(\frac{t}{t_0}\right)^{c_2},$$

$$\begin{aligned} c_2 &= 4r_e - 6r_d - r_a(n_1 - 1) - r_a(n_2 - 1) \\ &- m(\alpha_1 + 1). \end{aligned}$$

TD-SSC - an example of the modeling

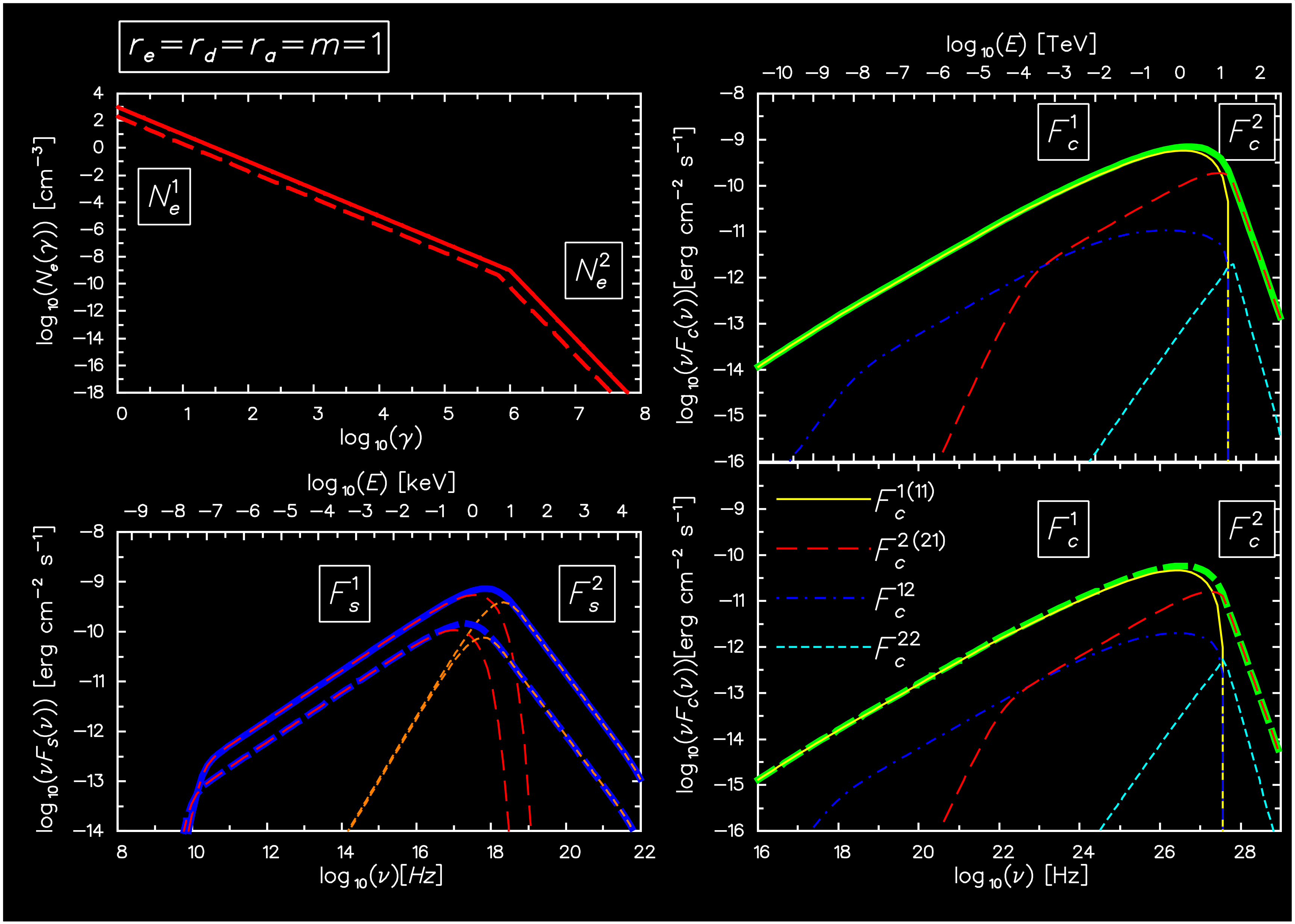

TD-SSC - four basic correlations

we have four basic evolutions:

- $F_{\rm s}^1 \propto t^{s_1}$ for the synch. rad. before the $\nu F_{\rm s}(\nu)$ peak
- $F_{\rm s}^2 \propto t^{s_2}$ for the synch. rad. above the $\nu F_{\rm s}(\nu)$ peak
- $F_{\rm c}^1 \propto t^{c_1}$ for the IC emission before the $\nu F_{\rm c}(\nu)$ peak
- $F_{\rm c}^2 \propto t^{c_2}$ for the IC emission above the $\nu F_{\rm c}(\nu)$ peak

which give four basic correlations:

$$F_{\rm c}^1 \propto (F_{\rm s}^1)^{\rm c_1/s_1} \qquad F_{\rm c}^2 \propto (F_{\rm s}^1)^{\rm c_2/s_1}$$

$$F_{\rm c}^1 \propto (F_{\rm s}^2)^{\rm c_1/s_2} \qquad F_{\rm c}^2 \propto (F_{\rm s}^2)^{\rm c_2/s_2}$$

TD-SSC - four basic correlations

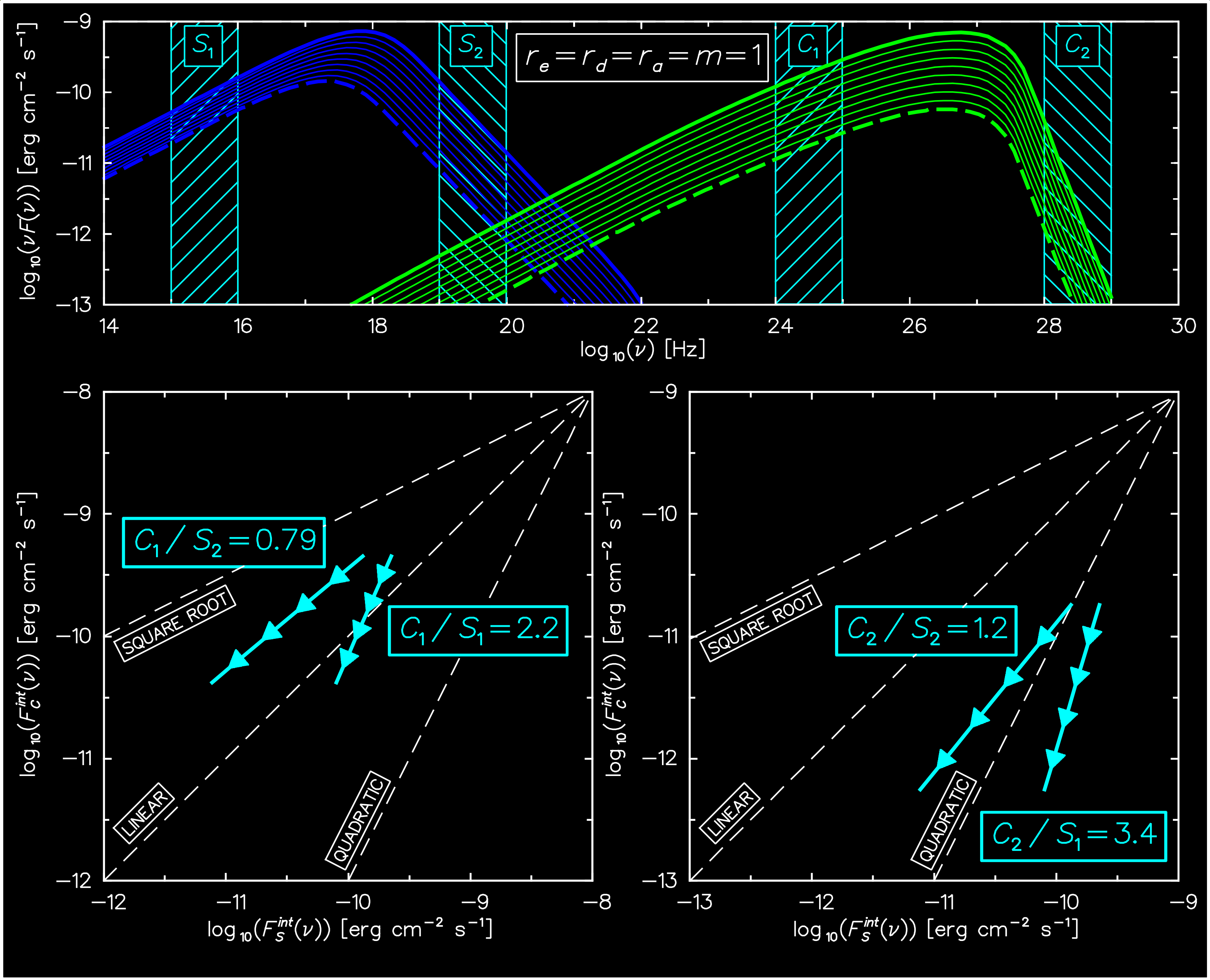

TD-SSC - basic estimations

	r_e	r_d	r_a	m	c_1/s_1	c_1/s_2	c_2/s_1	c_2/s_2
a	1	0	0	0	1.333	1.333	1.333	1.333
b	0	1	0	0	2	2	2	2
c	1	1	0	0	inf	inf	inf	inf
d	1	1	1	0	4	1	7	1.75
e	1	1	1	1	2.2	0.786	3.4	1.214
f	0	0	0	1	1	0.5	1	0.5
g	0	1	1	0	2	1.143	2.75	1.571
h	0	1	1	1	1.727	0.950	2.273	1.250
i	1	1	0	1	2.332	1.167	2.333	1.167
j	1	0	0	1	1.667	inf	1.667	inf
k	0	1	0	1	1.667	1.250	1.667	1.250
l	1	1	1	2	1.75	0.7	2.5	1

TD-SSC - correlations around the peaks

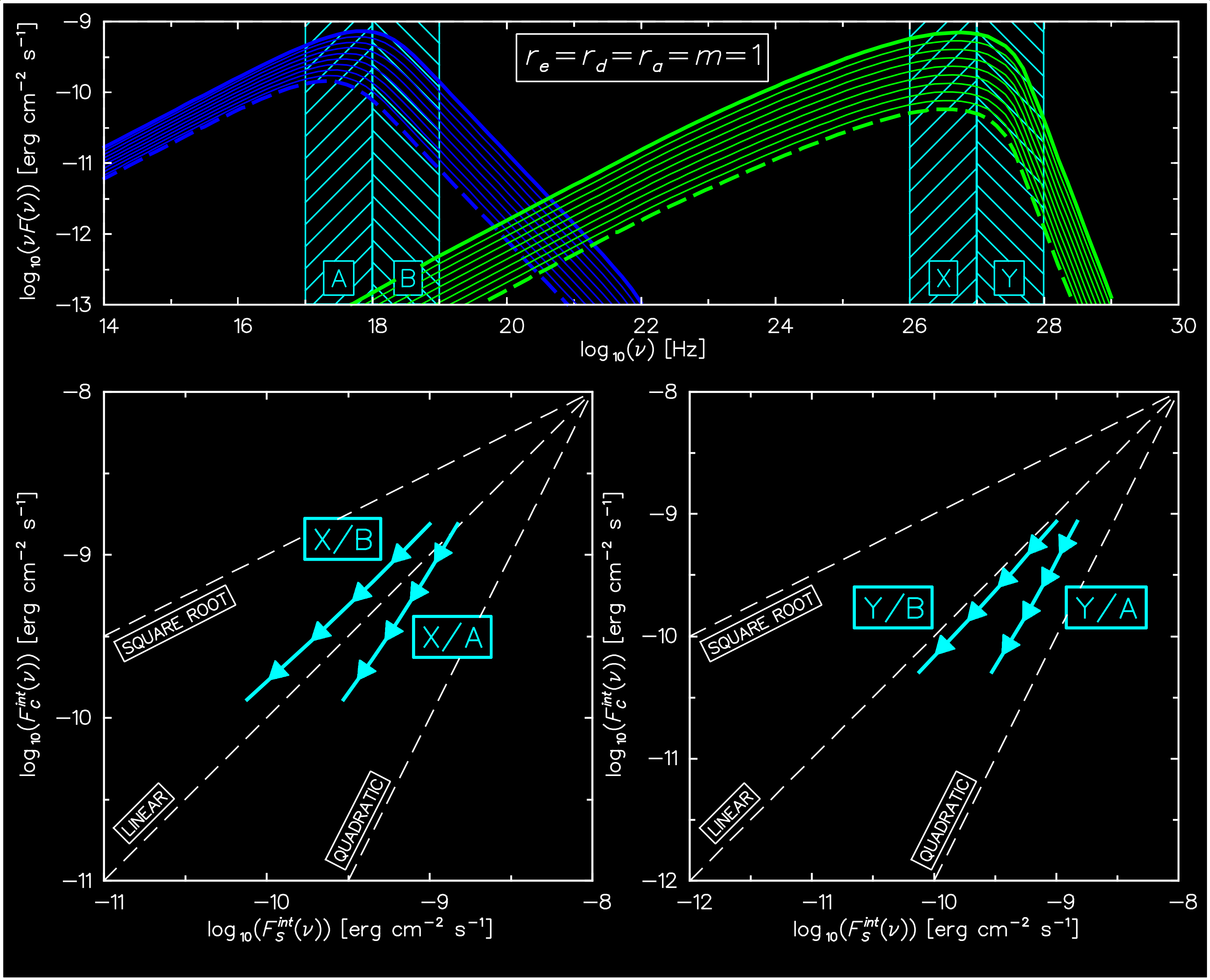

OAB-Italy

TD-SSC - impact of the radiative cooling

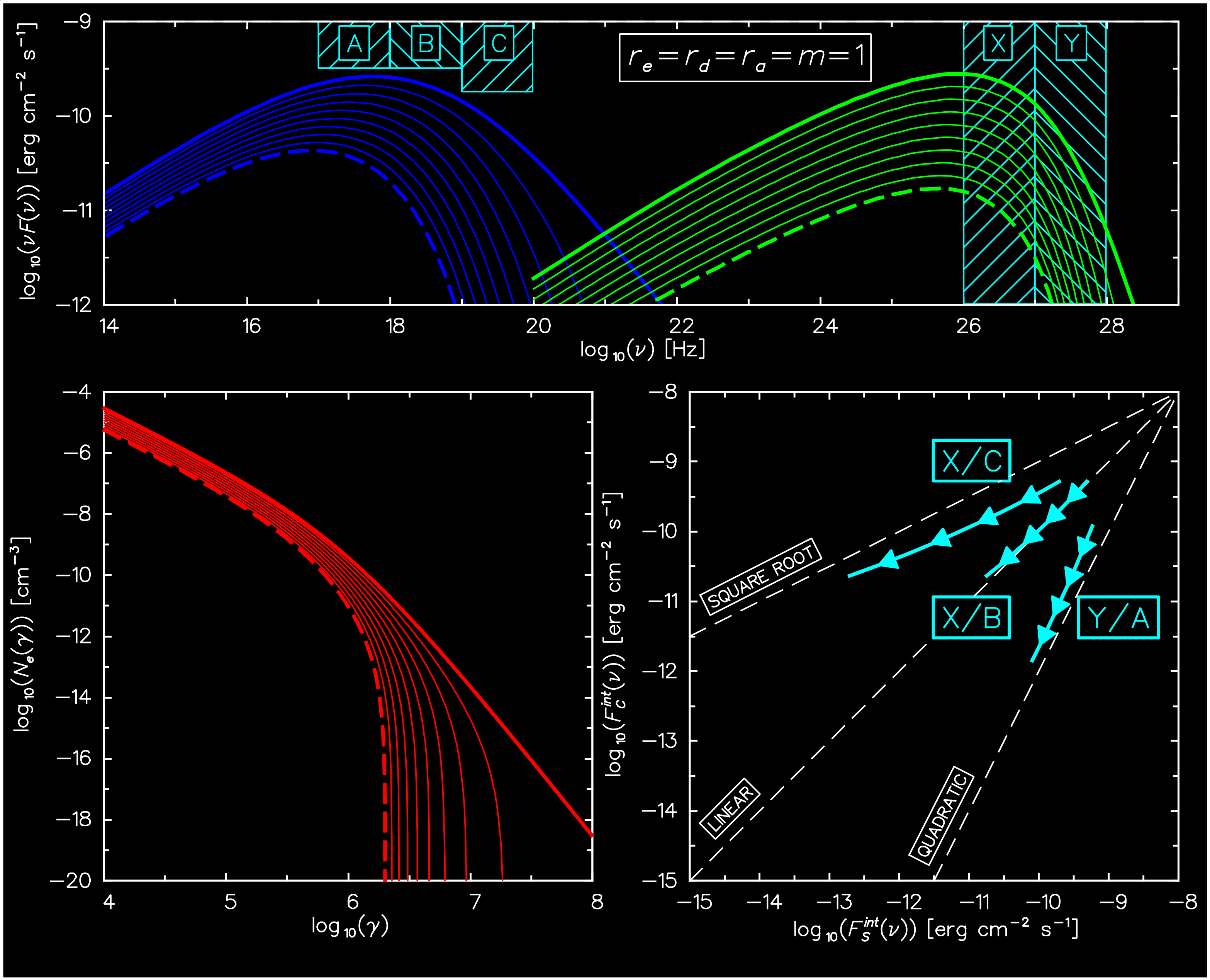

OAB-Italy

Light Crossing Time Effect (LCTE)

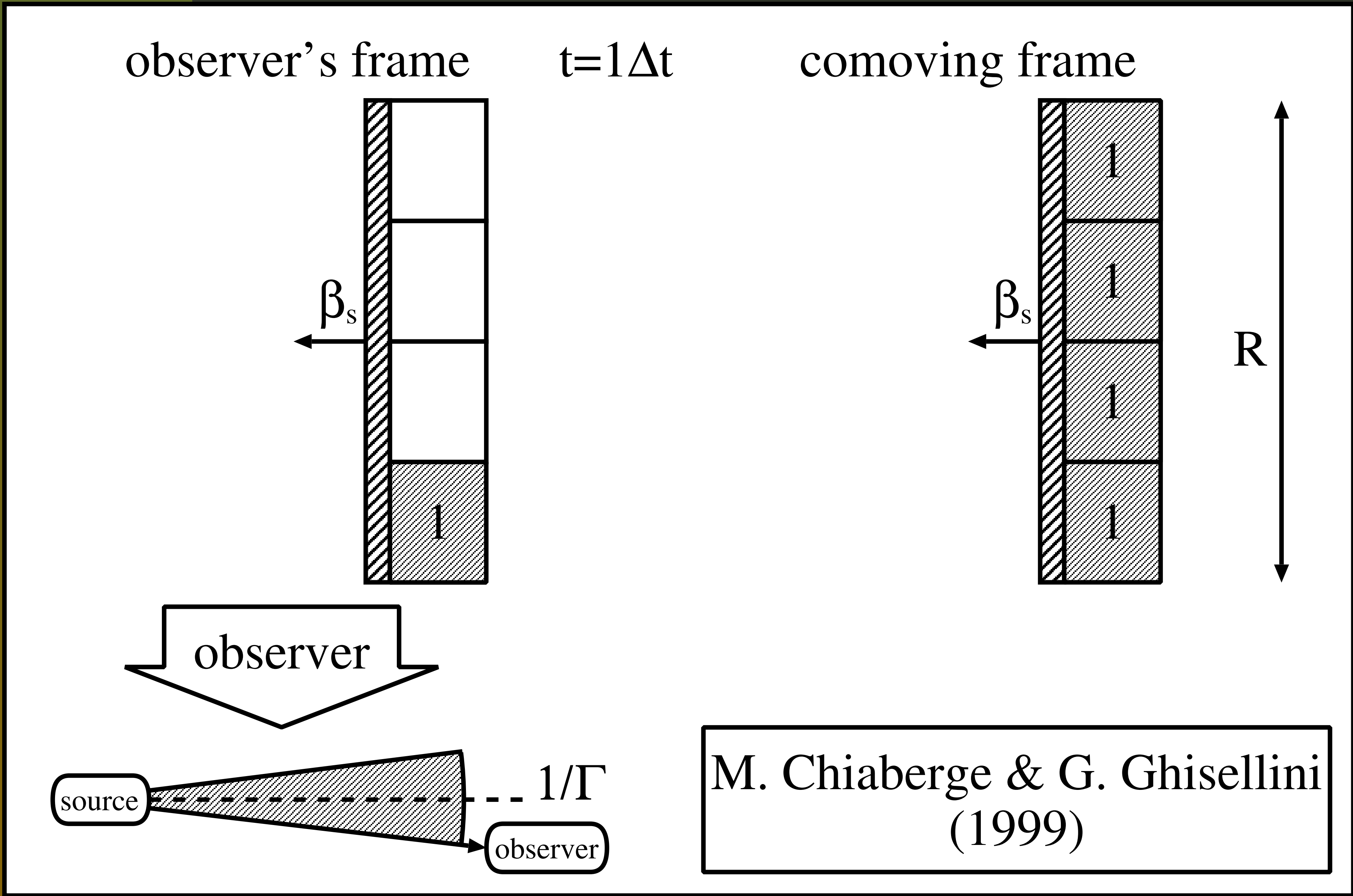

Light Crossing Time Effect (LCTE)

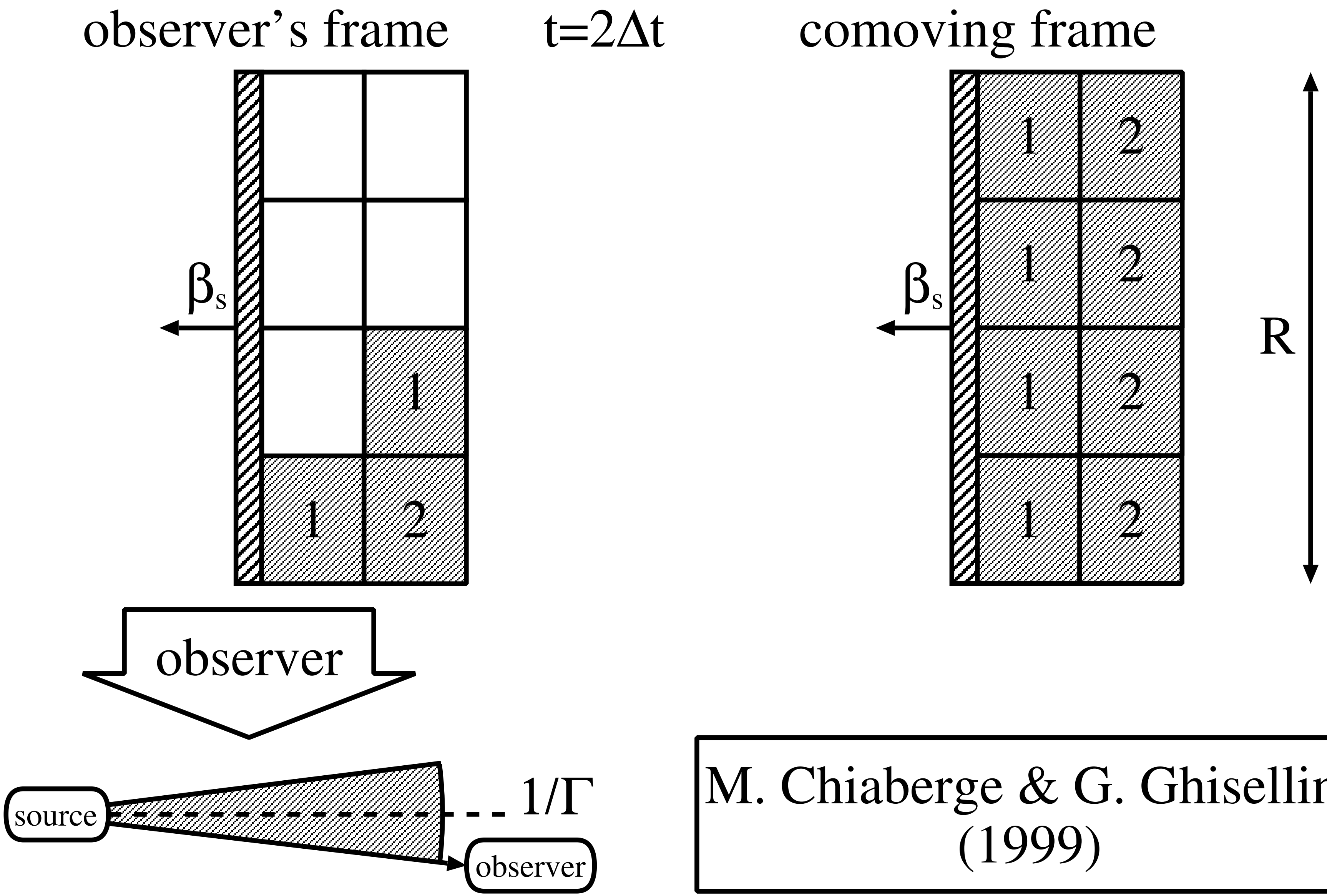

M. Chiaberge & G. Ghisellini (1999)

Light Crossing Time Effect (LCTE)

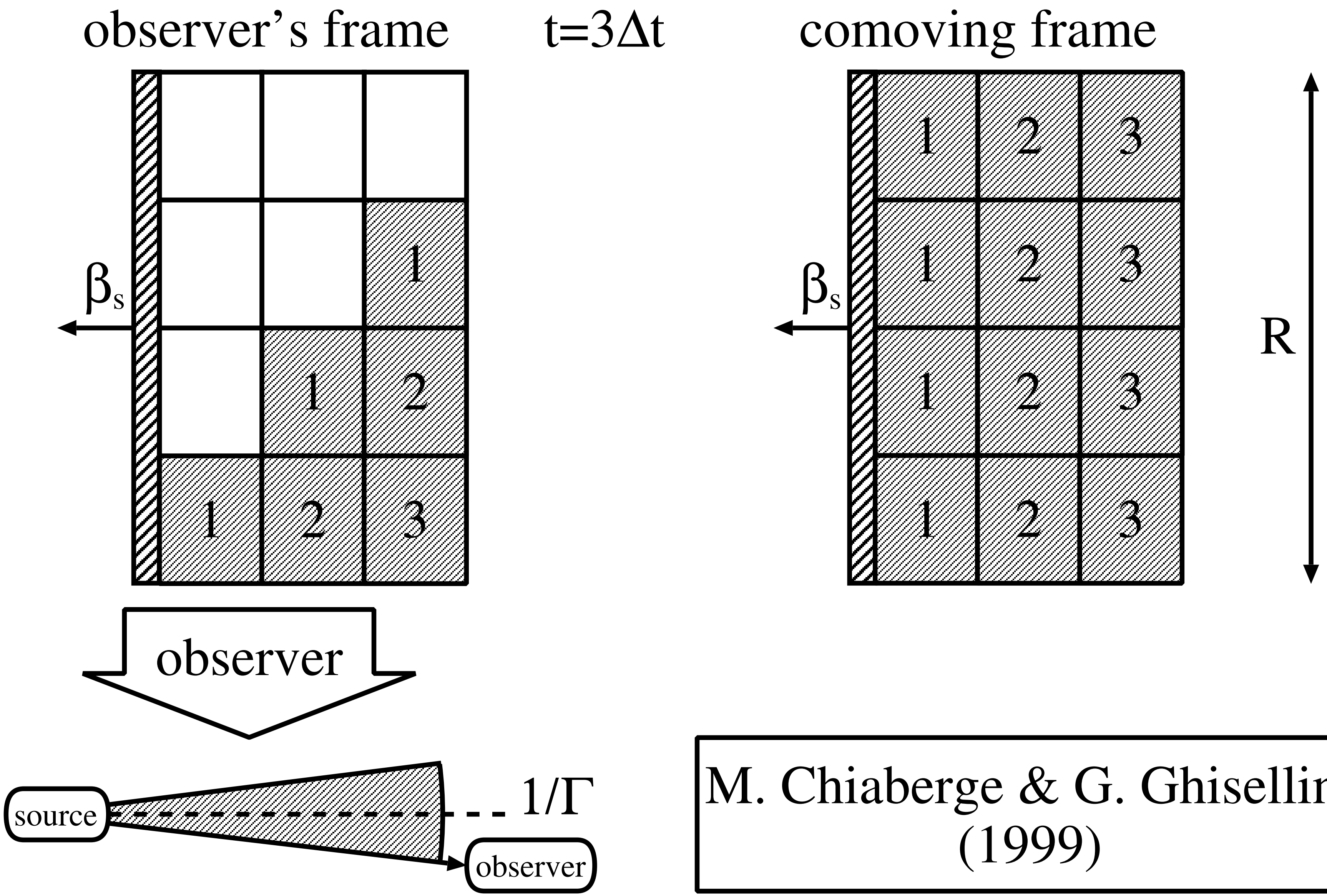

M. Chiaberge & G. Ghisellini (1999)

Light Crossing Time Effect (LCTE)

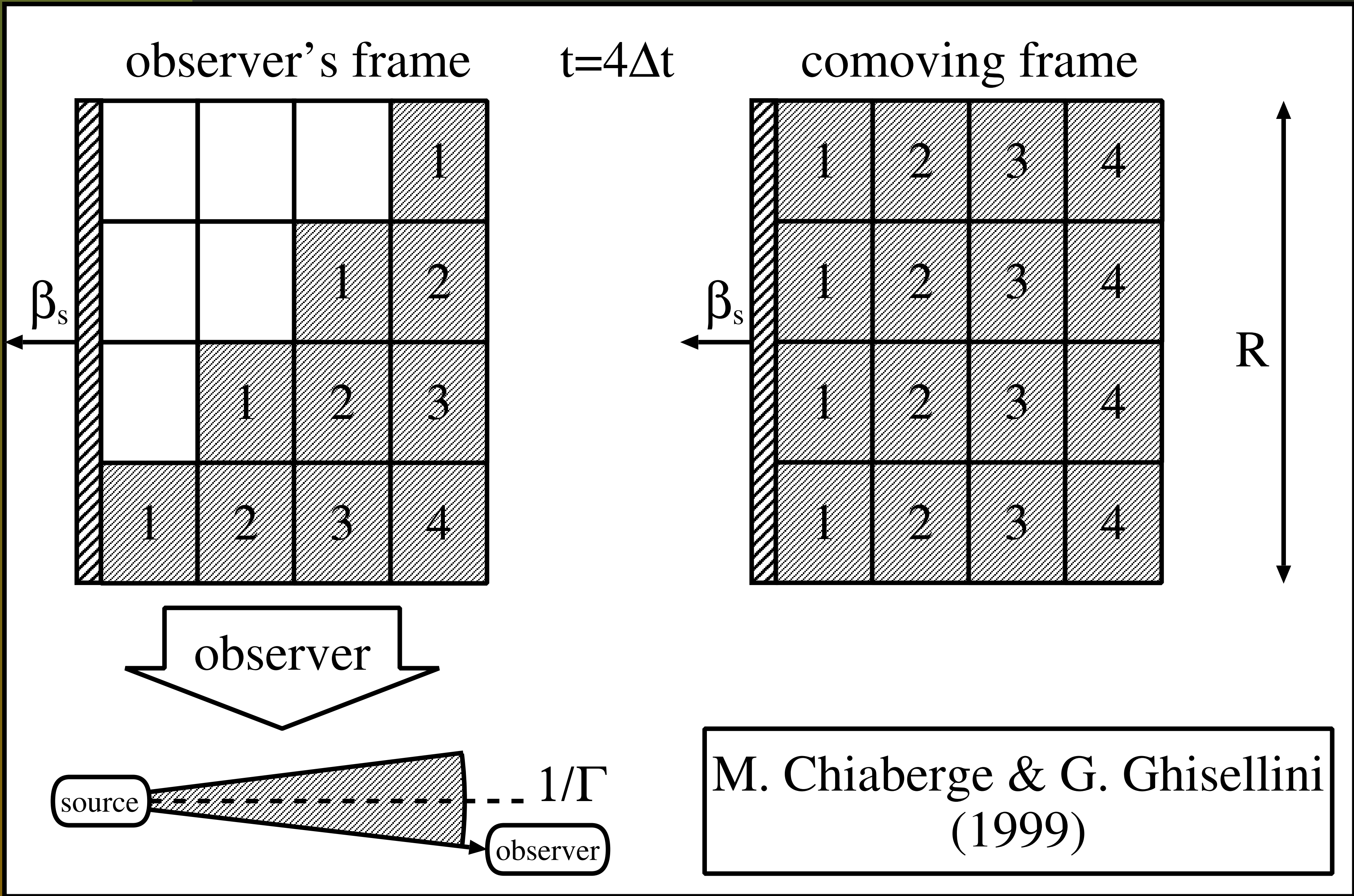

Light Crossing Time Effect (LCTE)

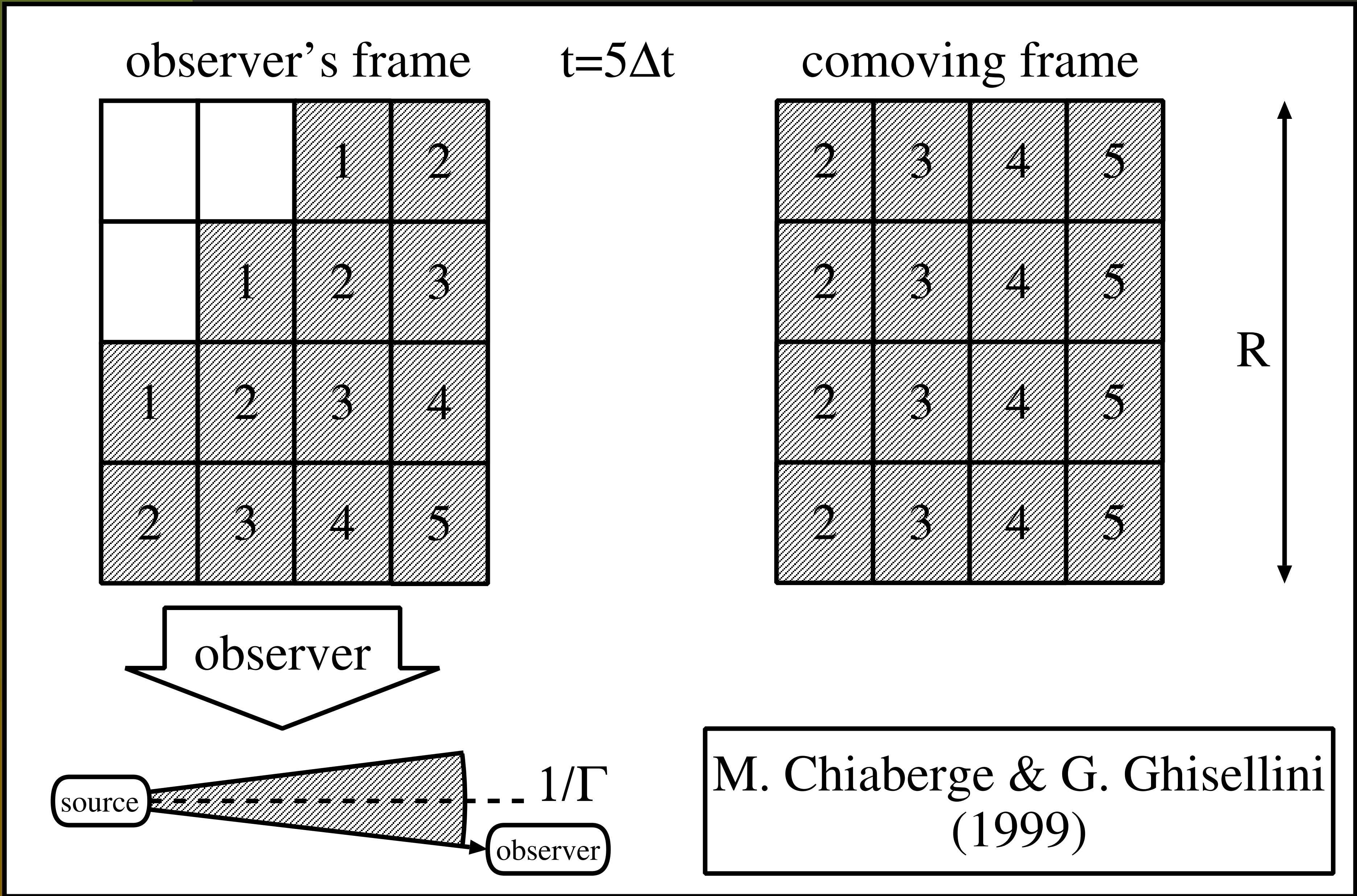

Light Crossing Time Effect (LCTE)

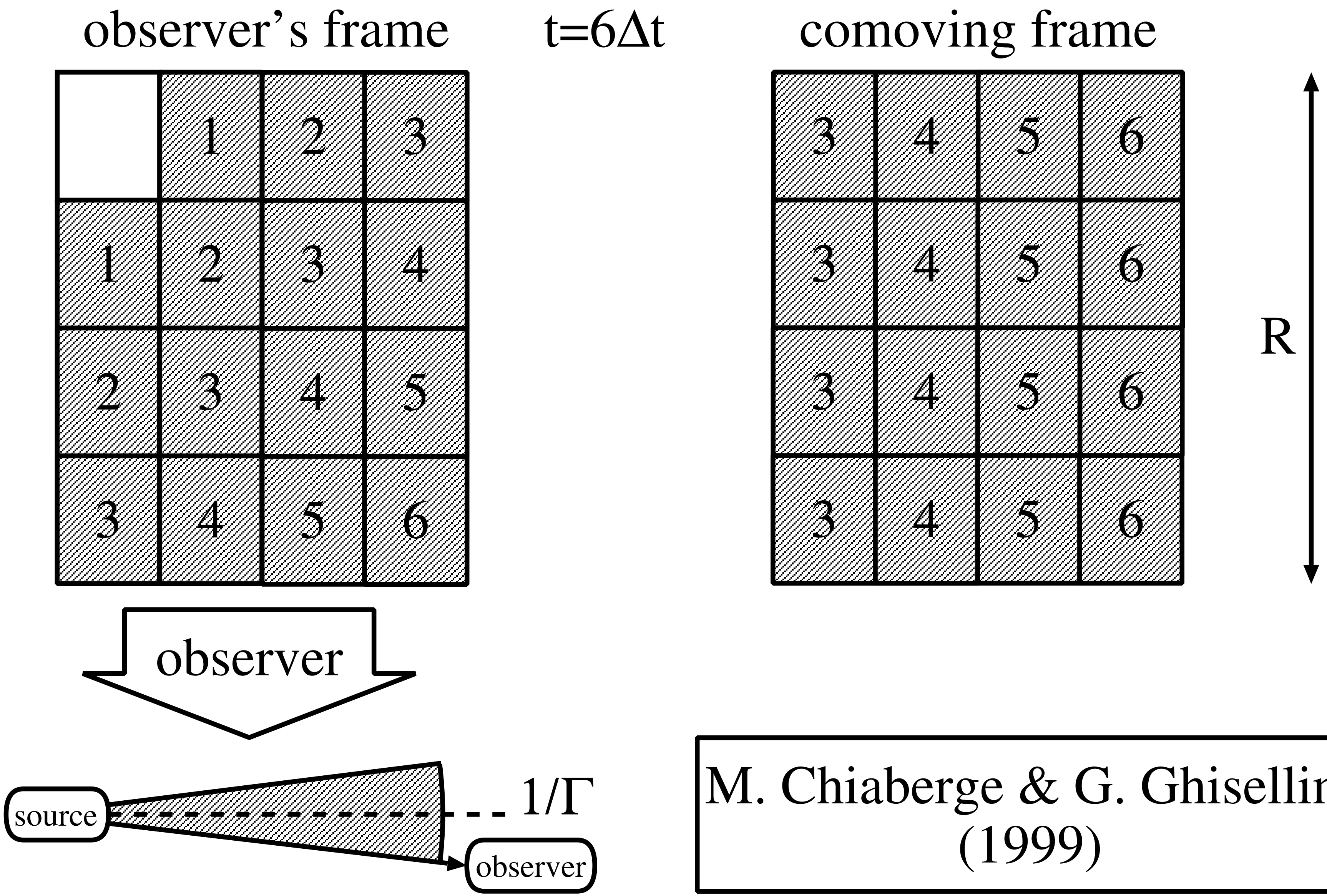

M. Chiaberge & G. Ghisellini (1999)

Light Crossing Time Effect (LCTE)

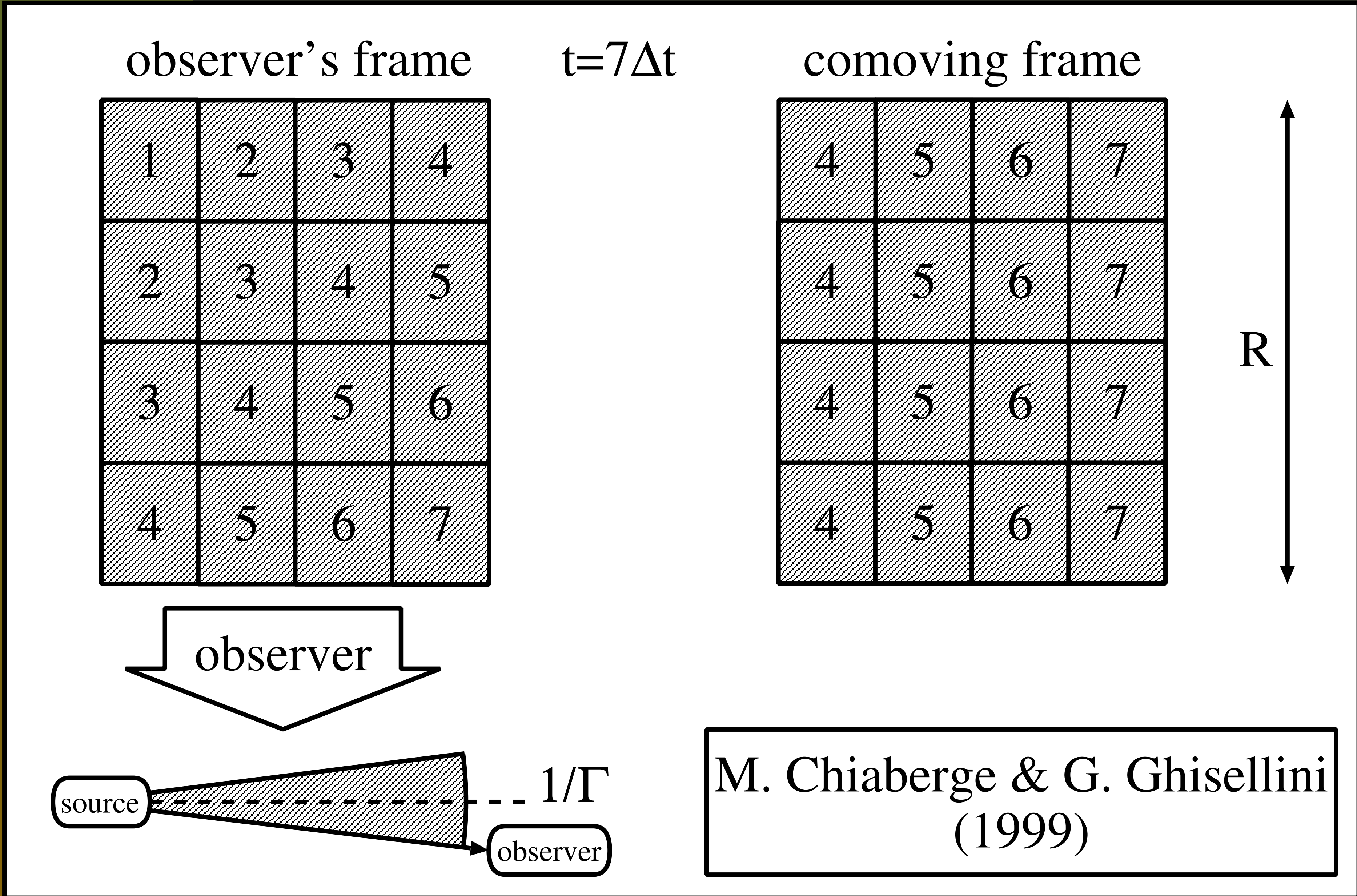

LCTE - constant emission of a single cell

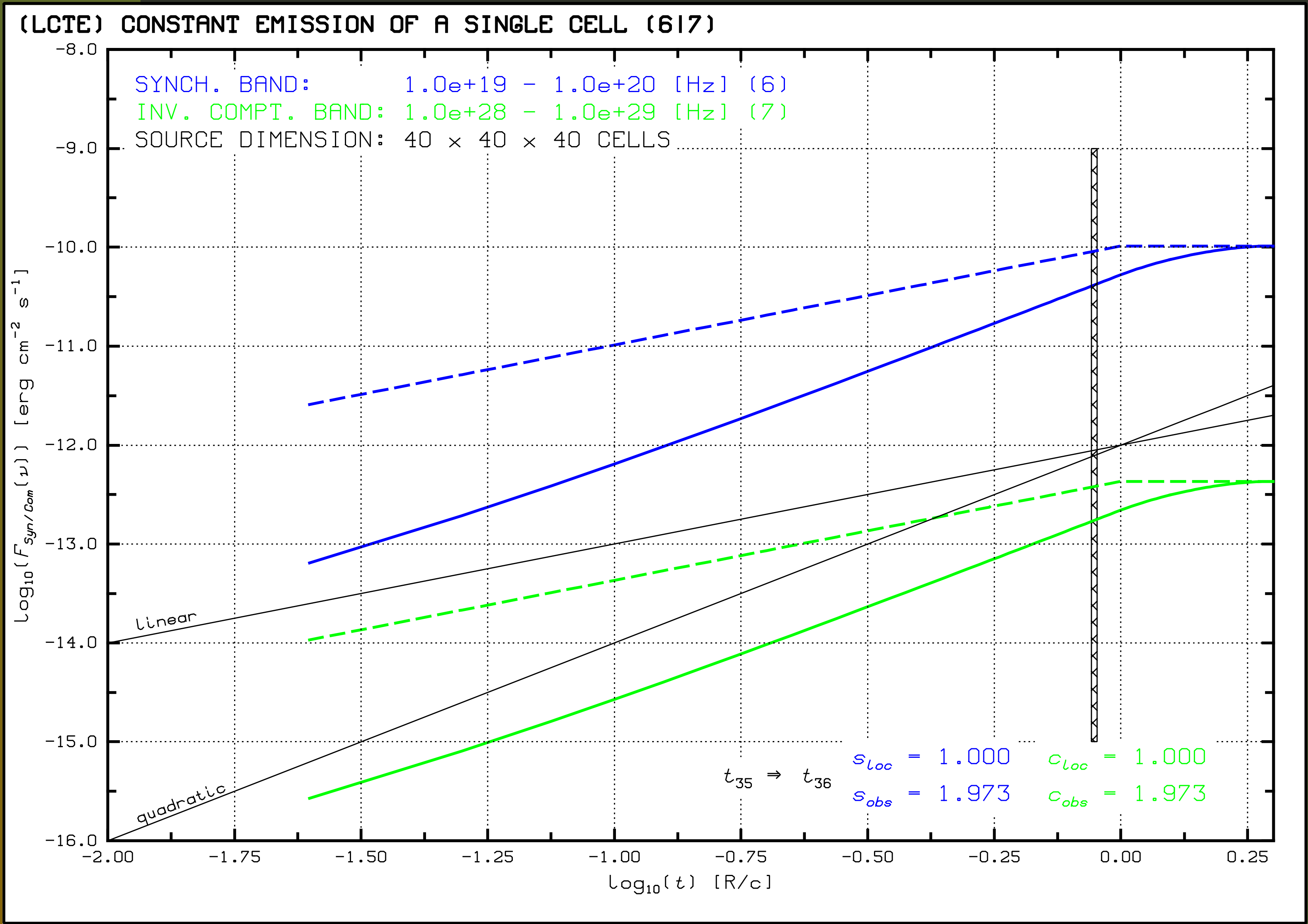

LCTE - very fast decay of a single cell

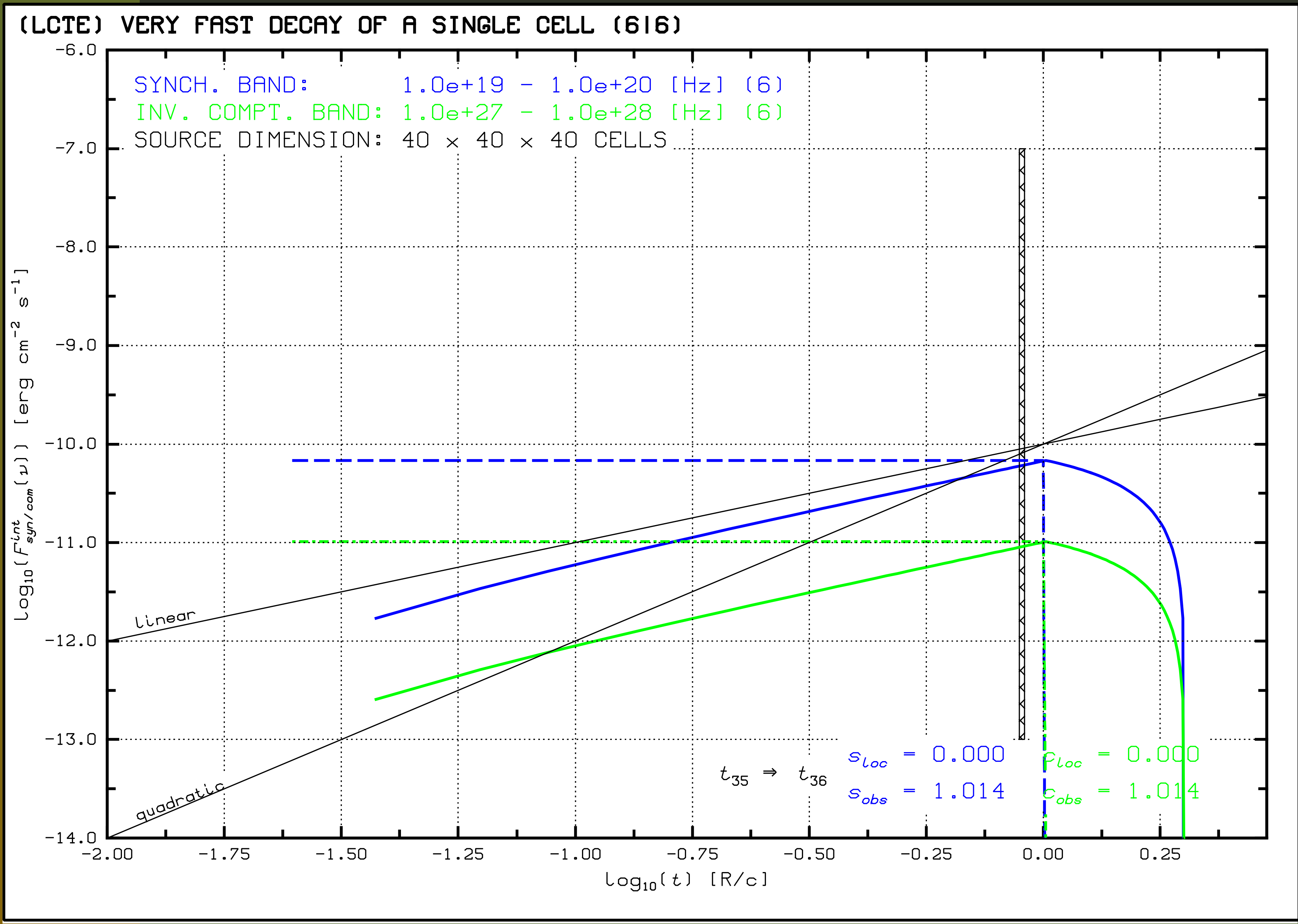

LCTE - the "plus one" formula

If the flux in the comoving frame is given by:

$$F_{\rm src} \propto t^{x}$$

then in the observer's frame we see:

$$F_{\rm obs} \propto t^{x+1}.$$

This indicate that in the comoving frame the evolution of the IC emission must much faster than the evolution of the synchrotron emission to explain the quadratic correlation. For example:

$$\begin{aligned} F^{\rm IC}_{\rm src} &\propto t^{c=3}, \qquad F^{\rm Syn}_{\rm src} \propto t^{s=1}, \\ F^{\rm IC}_{\rm obs} &\propto t^{c=4}, \qquad F^{\rm Syn}_{\rm obs} \propto t^{s=2}, \\ F^{\rm IC}_{\rm obs} &\propto \left(F^{\rm Syn}_{\rm obs}\right)^{c/s=2}. \end{aligned}$$

Conclusions

- a simple TD-SSC model can explain the linear or quadratic correlation during the rising phase of a flare
- the model suggest that in most cases we should observe the linear correlation during the decay phase of a flare
- there is problem with the quadratic correlation observed in the decay phase of the flare
- the impact of the radiative cooling is stronger for the X-ray emission than for the TeV radiation, therefore this process may destroy possible quadratic or even linear correlation
- if LCTE is important then the IC emission must vary much stronger in the comoving frame than the X-ray radiation

References

- Catanese, M., Bradbury, S., M., Breslin, A., C., et al. 1997, ApJ , 487, L143
- Djannati–Atai, A., Piron, F., Barrau, A., et al., 1999, A&A, 350, 17
- Krawczynski, H., Sambruna, R., Kohnle, A., et al., 2001, ApJ , 559, 187
- Pian, E., Vacanti, G., Tagliaferri, G., et al., 1998, ApJ , 492, L17
- Tavecchio, F., Maraschi, L., & Ghisellini, G., 1998, ApJ , 509, 608

Flaring characteristics in XTE studies for MKN421

Dimitrios Emmanoulopoulos

Dr. J.Papadakis

Prof.S.Wagner

ENIGMA meeting Jerisjärvi, Finland 26-28 April 2004

Landessternwarte Heidelberg

ENIGMA

Overview

- Short Reminder of our previous work
- Spectral Analysis
- Basic Motivation of this Study
- Conclusions

Light Curves-Characteristic Time Scale

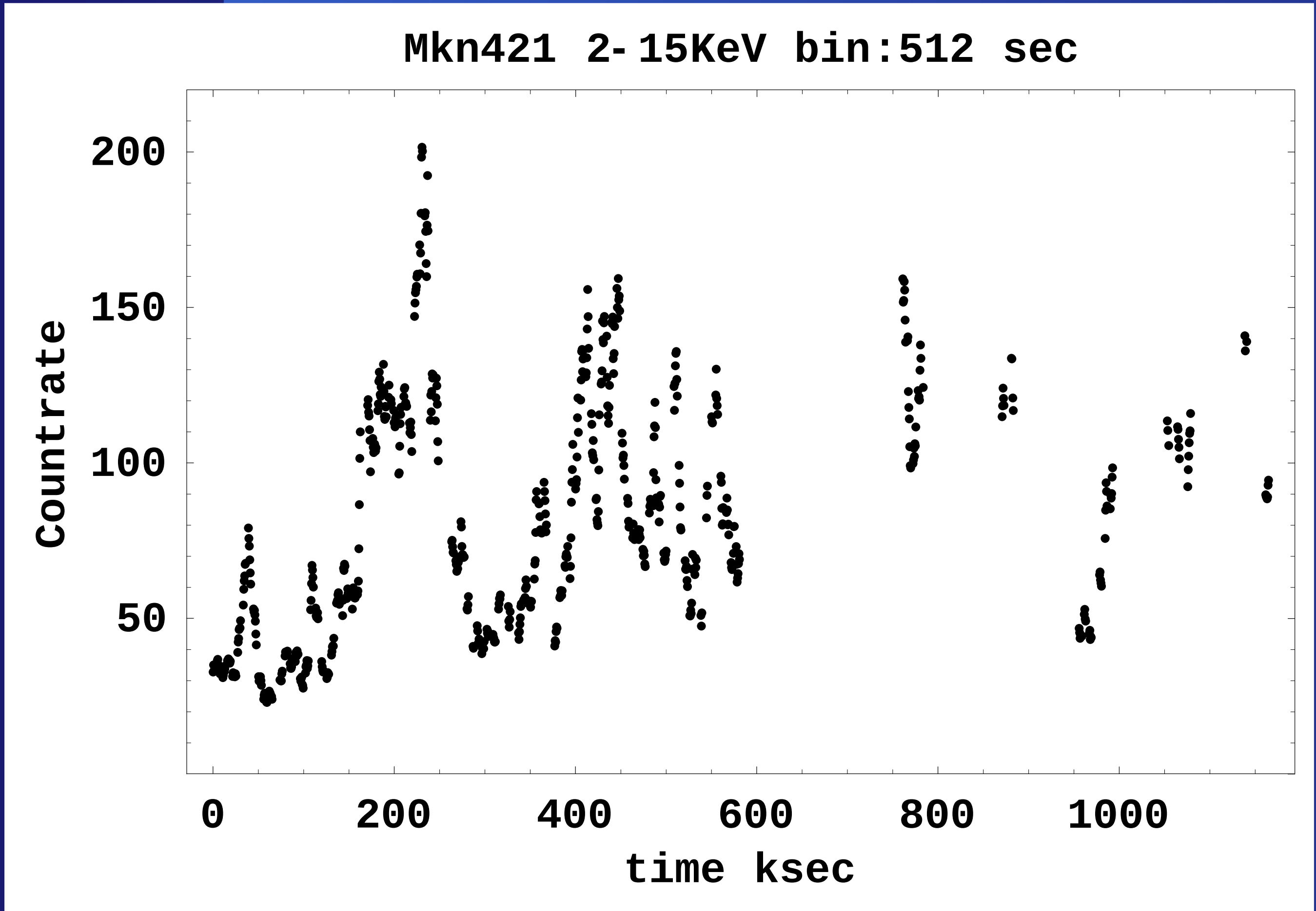

Light Curves-Characteristic Time Scal

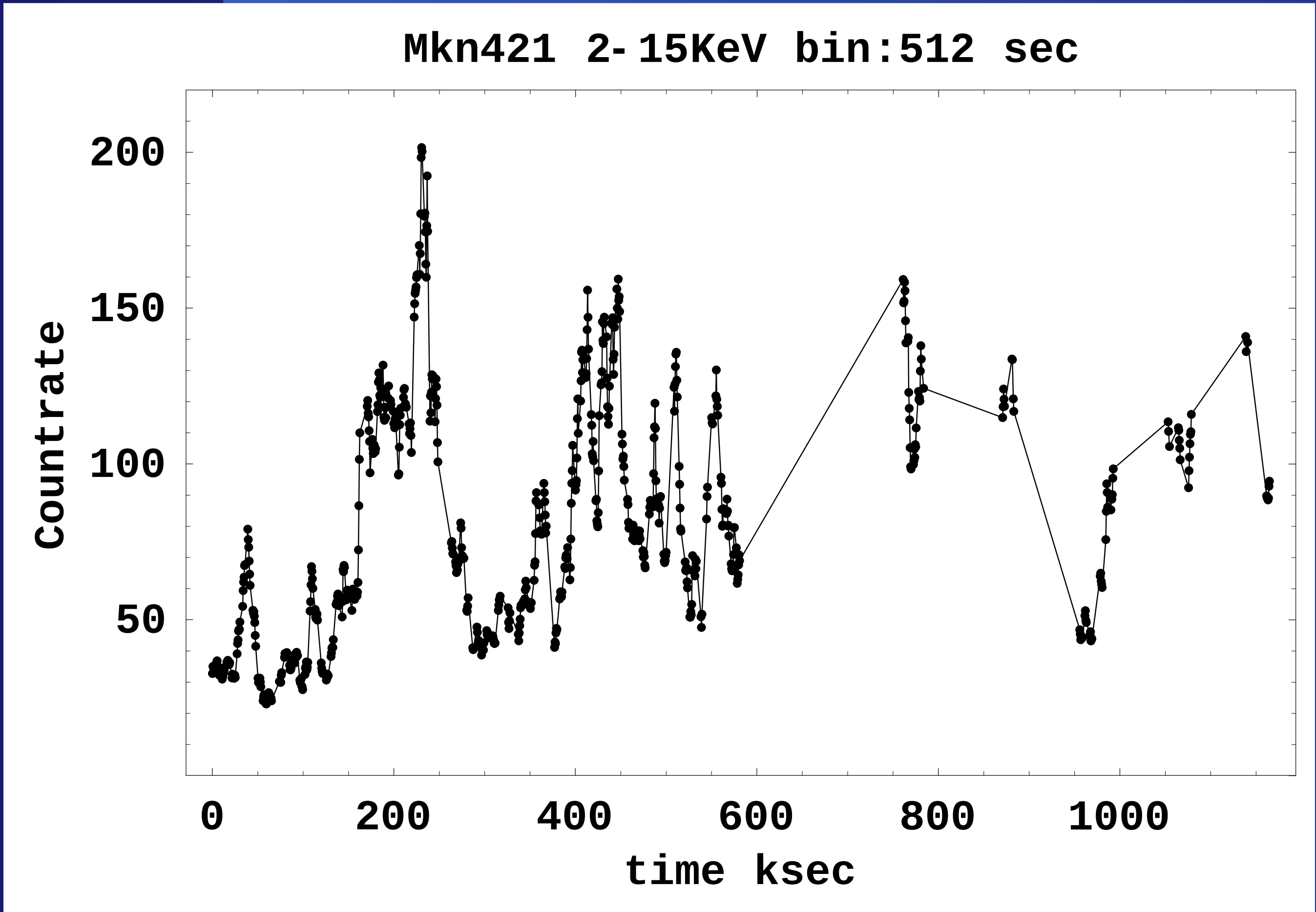

Light Curves-Characteristic Time Scal

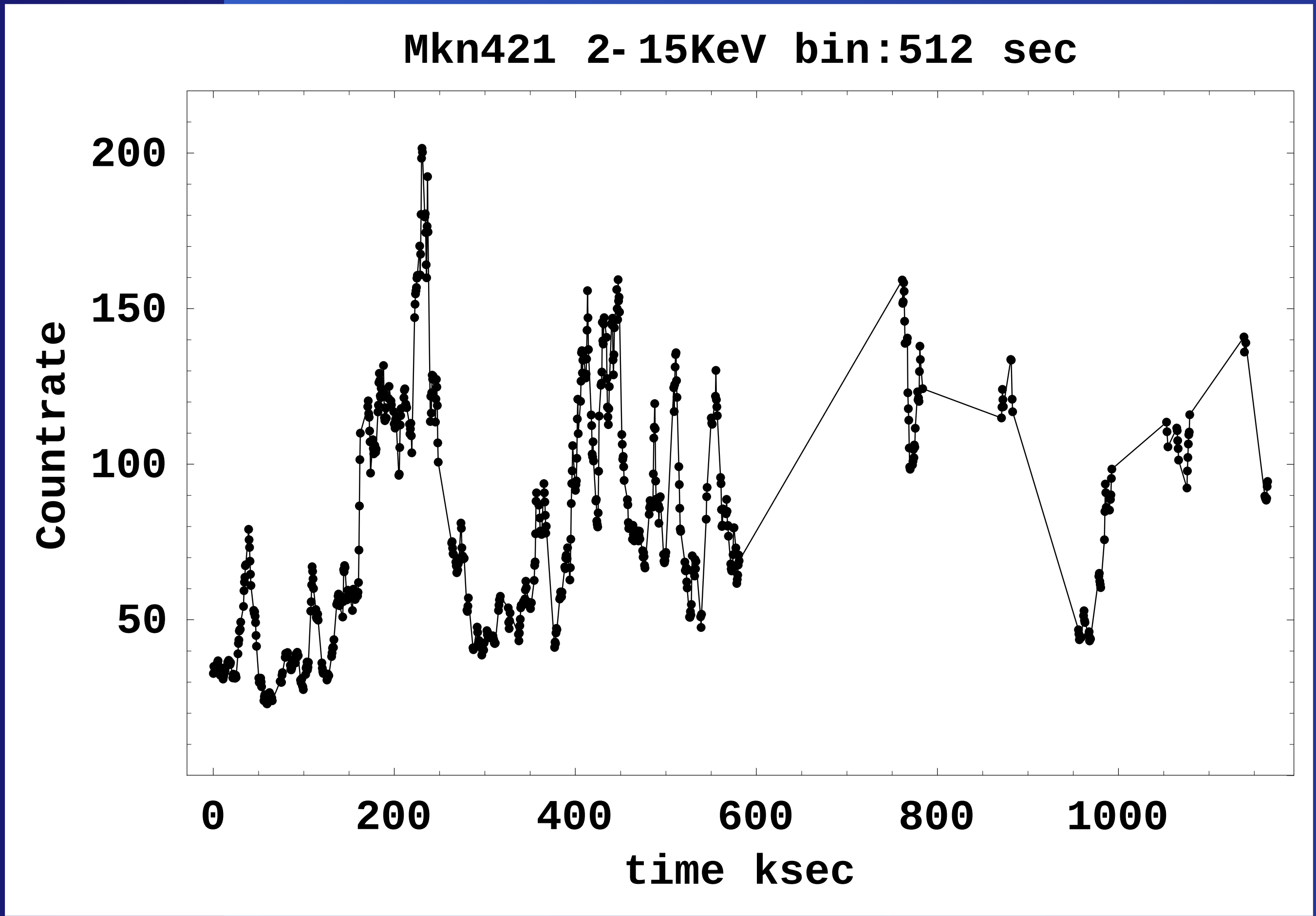

- Two well defined daily flares $\sim$1 day
- The daily flares show substructure with time scales of 4ksec
- Additional variabili between the large flares

Light Curves-Characteristic Time Scal

Structure Function Analysis [10-15keV]

Light Curves-Characteristic Time Scale

Structure Function Analysis [10-15keV]
(Simonetti et al. Ap.J. 296,1985)

$$S_x(\lambda) = \frac{1}{N(\lambda)} \sum_{n=1}^{N} w(i)\, w(i+\lambda) \left[x(t+\lambda\Delta t) - x(t)\right]^2$$

where

$$N(\lambda) = \sum w(i)\, w(i+\lambda)$$

Light Curves-Characteristic Time Scal

Structure Function Analysis [10-15keV]

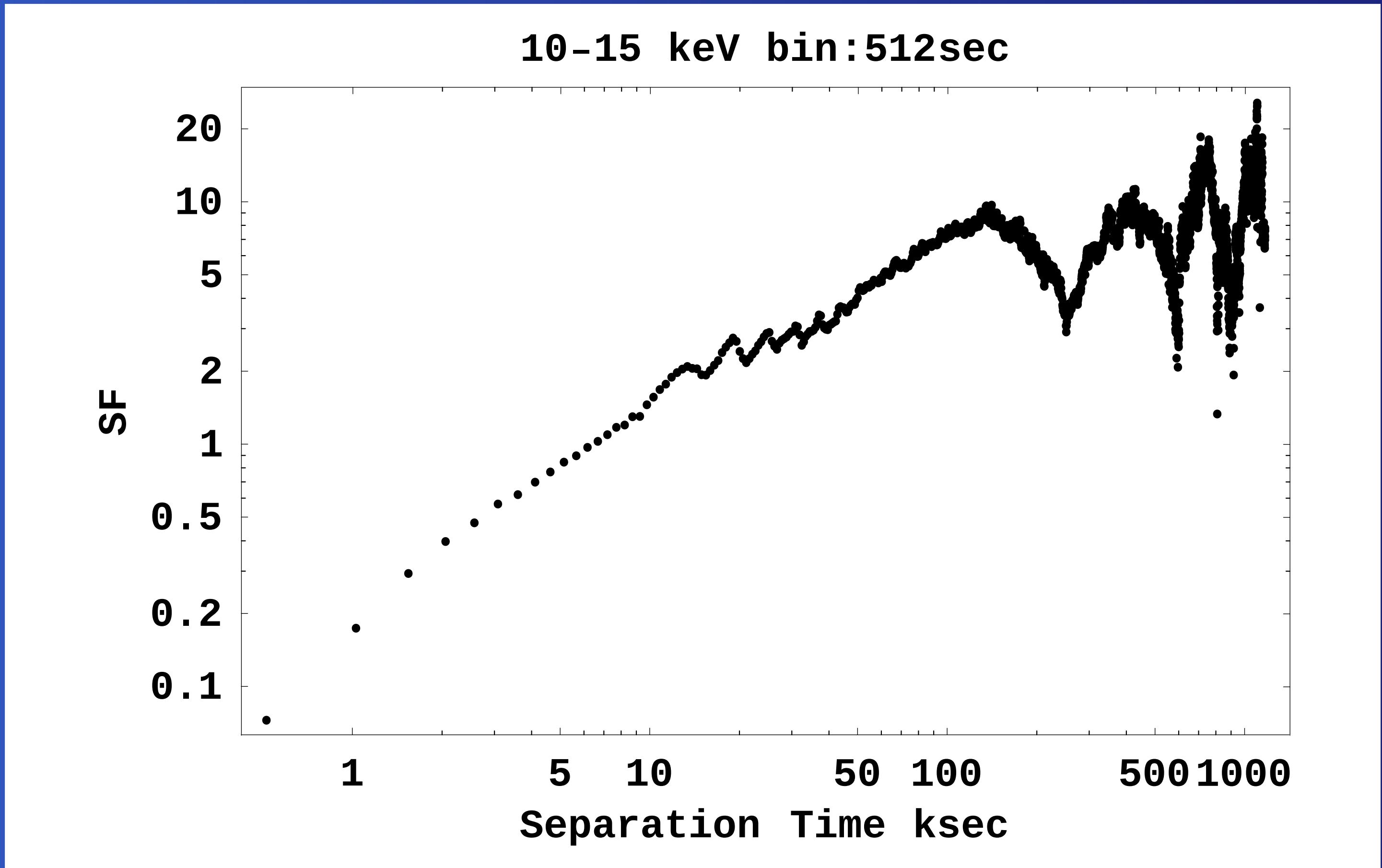

Light Curves-Characteristic Time Scal

Cross Correlation Function (CCF) [2-5 vs 10-15keV]

Light Curves-Characteristic Time Scal

Cross Correlation Function (CCF) [2-5 vs 10-15keV]
(Edelson and Krolik ApJ,333,1988)

$$CCF(\tau) = \frac{\sum_{i=1}^{N} \left(x_i(t) - \overline{x(t)} \right) \cdot \left(y_i(t+\tau) - \overline{y(t)} \right)}{N\sqrt{\sigma_x^2 - e_x^2}\sqrt{\sigma_y^2 - e_y^2}}$$

Light Curves-Characteristic Time Scal

Cross Correlation Function (CCF) [2-5 vs 10-15keV]

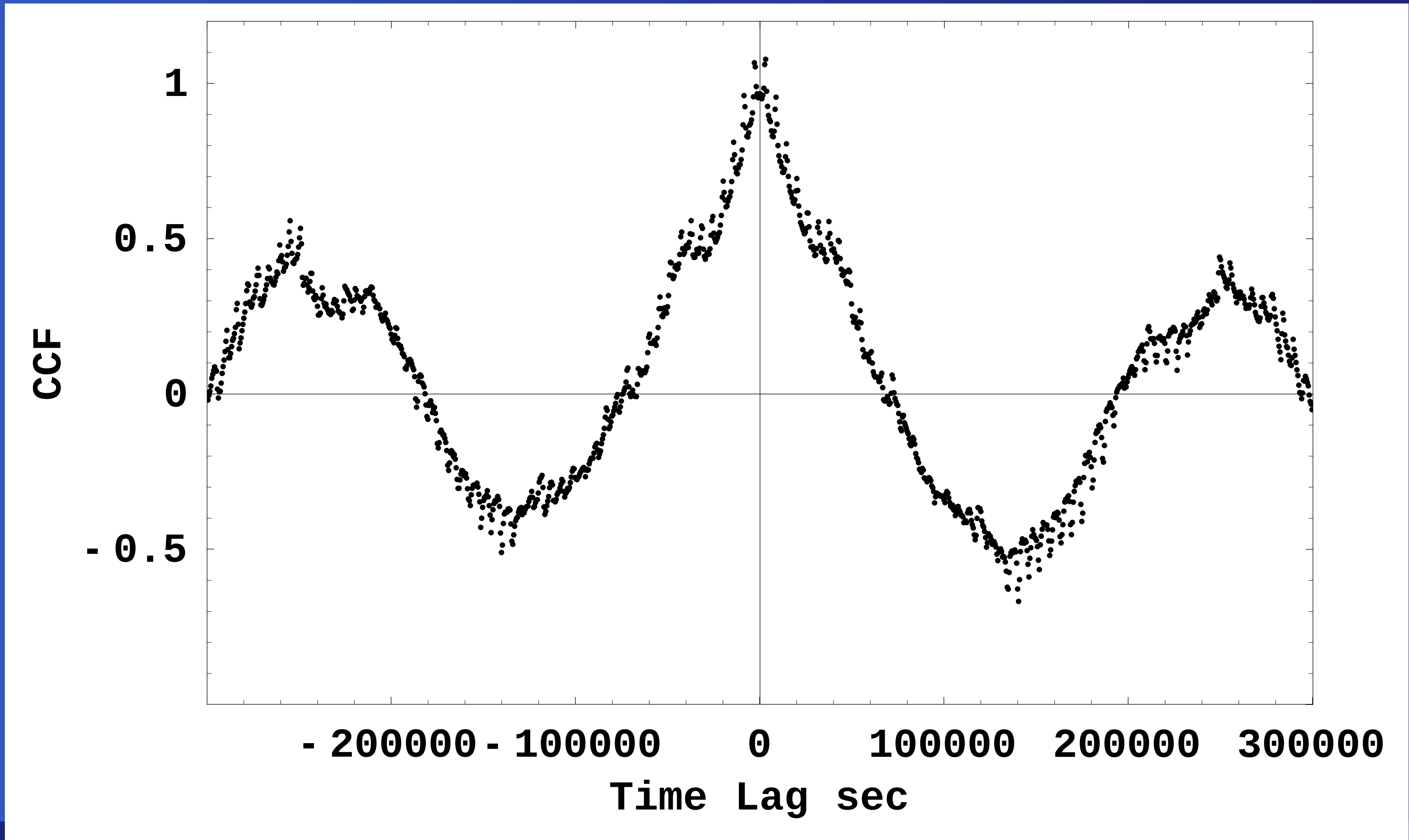

Spectral Analysis

The first flare 0-327ksec

Spectral Analysis

The first flare 0-327ksec

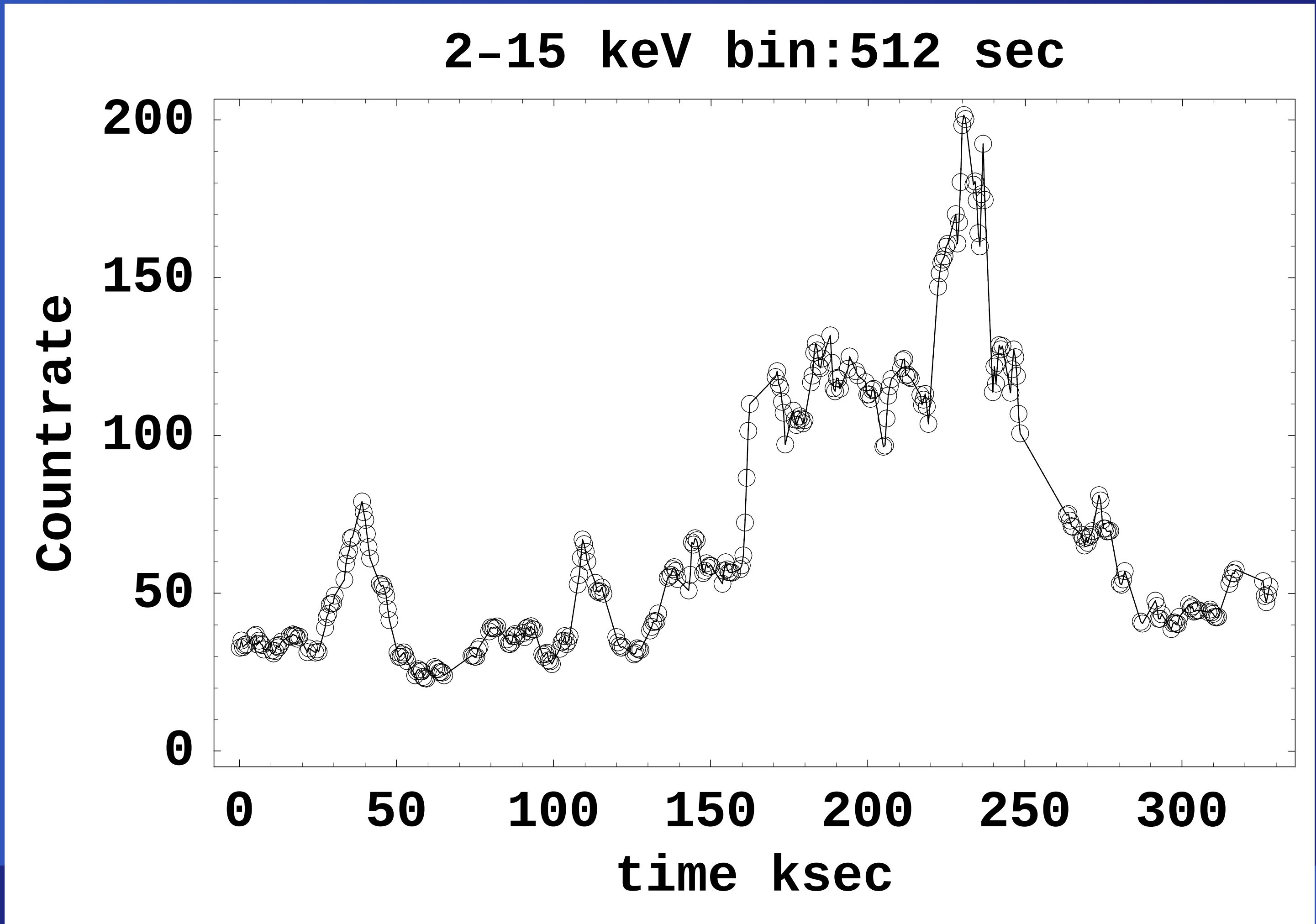

Spectral Analysis

The spectral model

Spectral Analysis

The spectral model

$$A\left(E\right) = \begin{cases} k\left(\frac{E}{1keV}\right)^{-\Gamma_1} & E \leq E_{break} \\ kE_{break}^{\Gamma_2-\Gamma_1}\left(\frac{E}{1keV}\right)^{-\Gamma_2} & E \geq E_{break} \end{cases}$$

Component for the photo electric absorption.

$$M\left(E\right) = e^{-n_H\sigma(E)}$$

$\sigma(\epsilon)$ is the photoelectric cross section

$n_H = 0.0166 \cdot 10^{22}\frac{atoms}{cm^2}$

Spectral analysis

The energy break E_{break}

Spectral analysis

The energy break E_{break}

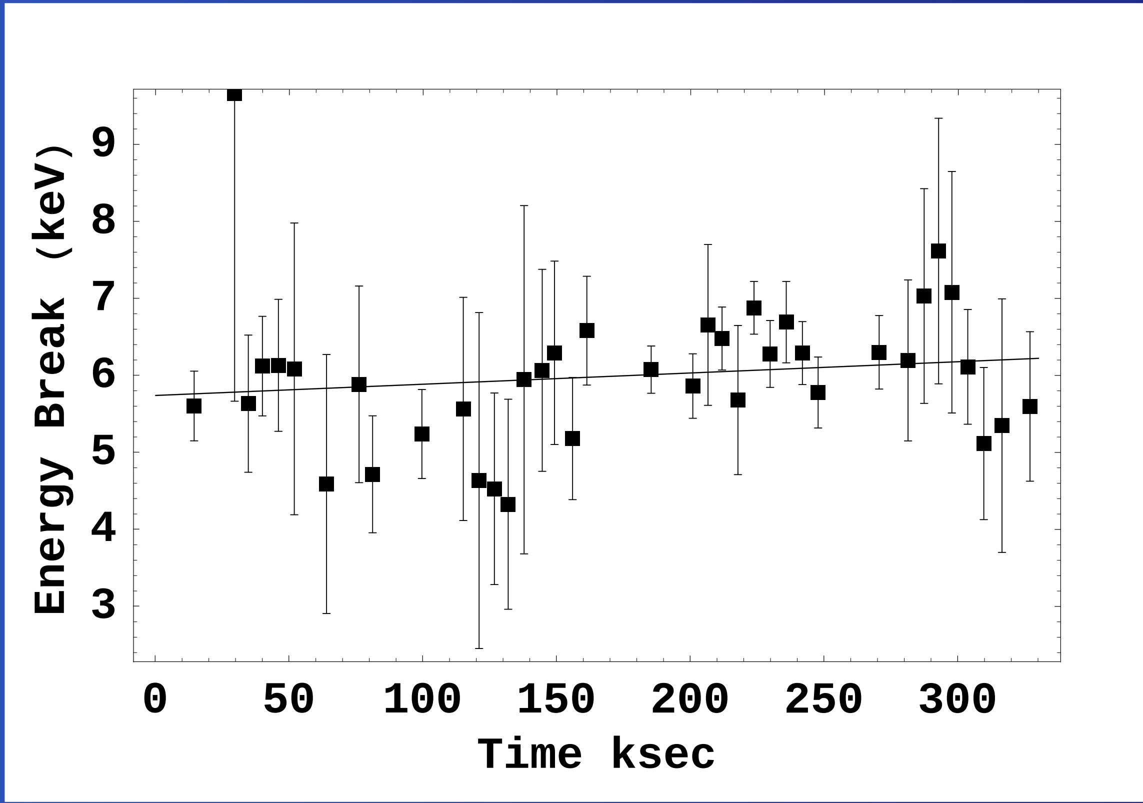

Spectral analysis

The energy break E_{break}

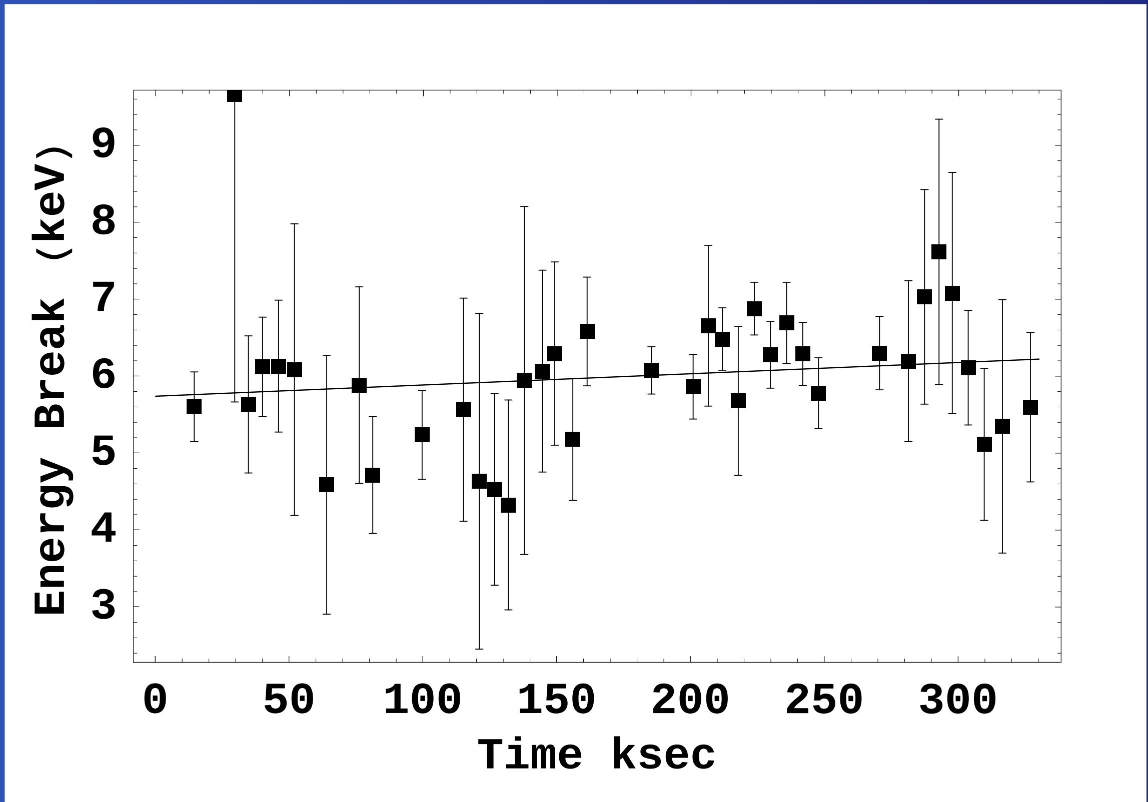

$$E_{break} = (6.01 \pm 0.14) keV$$

Spectral analysis

Flux

Spectral analysis

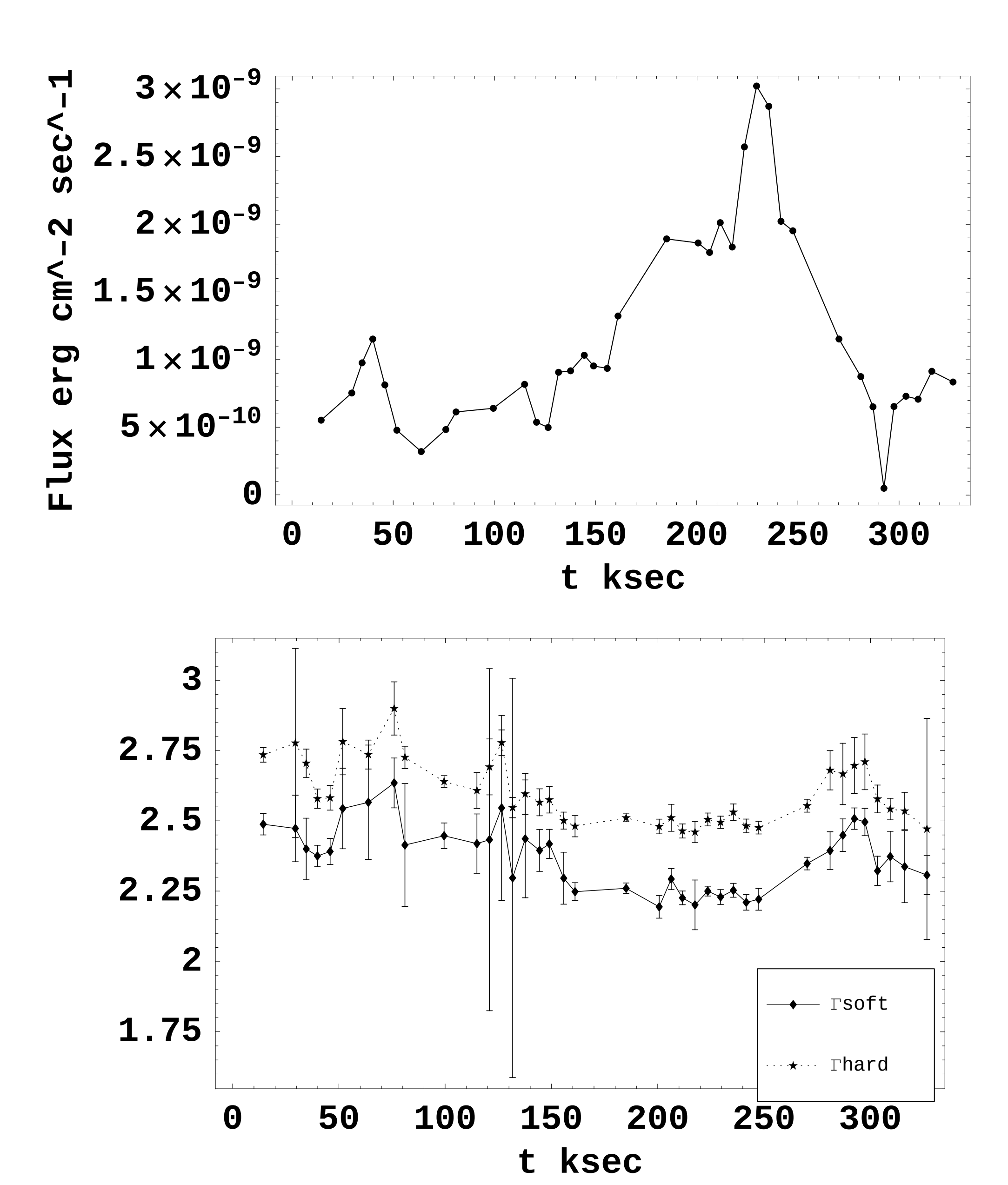

Spectral analysis

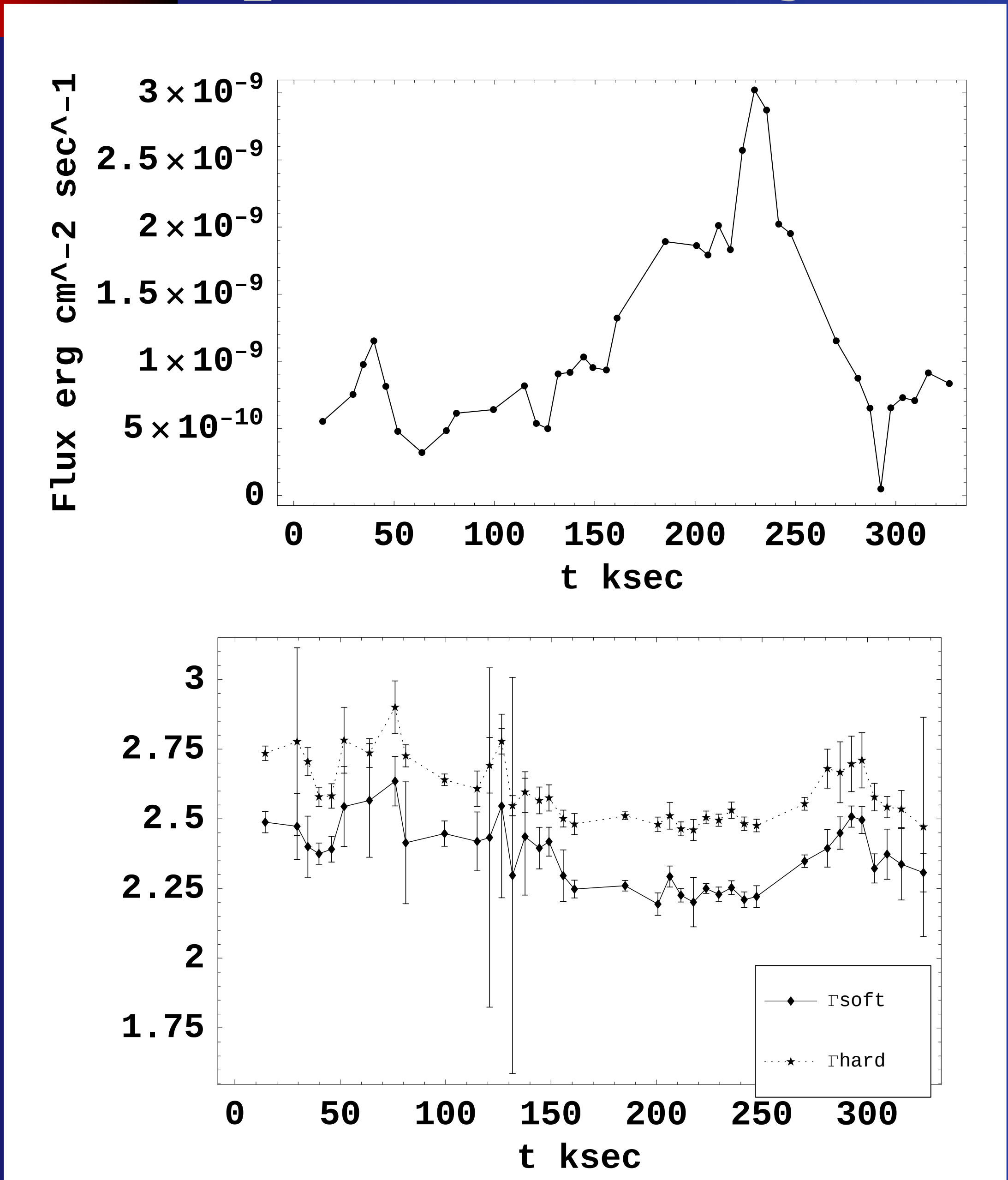

- As the flux ↑ both spectra indices ↓
- The flare around 240ksec doesn't provoke any change to the spectral indices

Spectral analysis

Spectral Time Variations

Spectral analysis

Spectral Time Variations

The CCF between $\frac{2-4keV}{4-5keV}$ and $\frac{7-10keV}{10-30keV}$

Spectral analysis

Spectral Time Variations

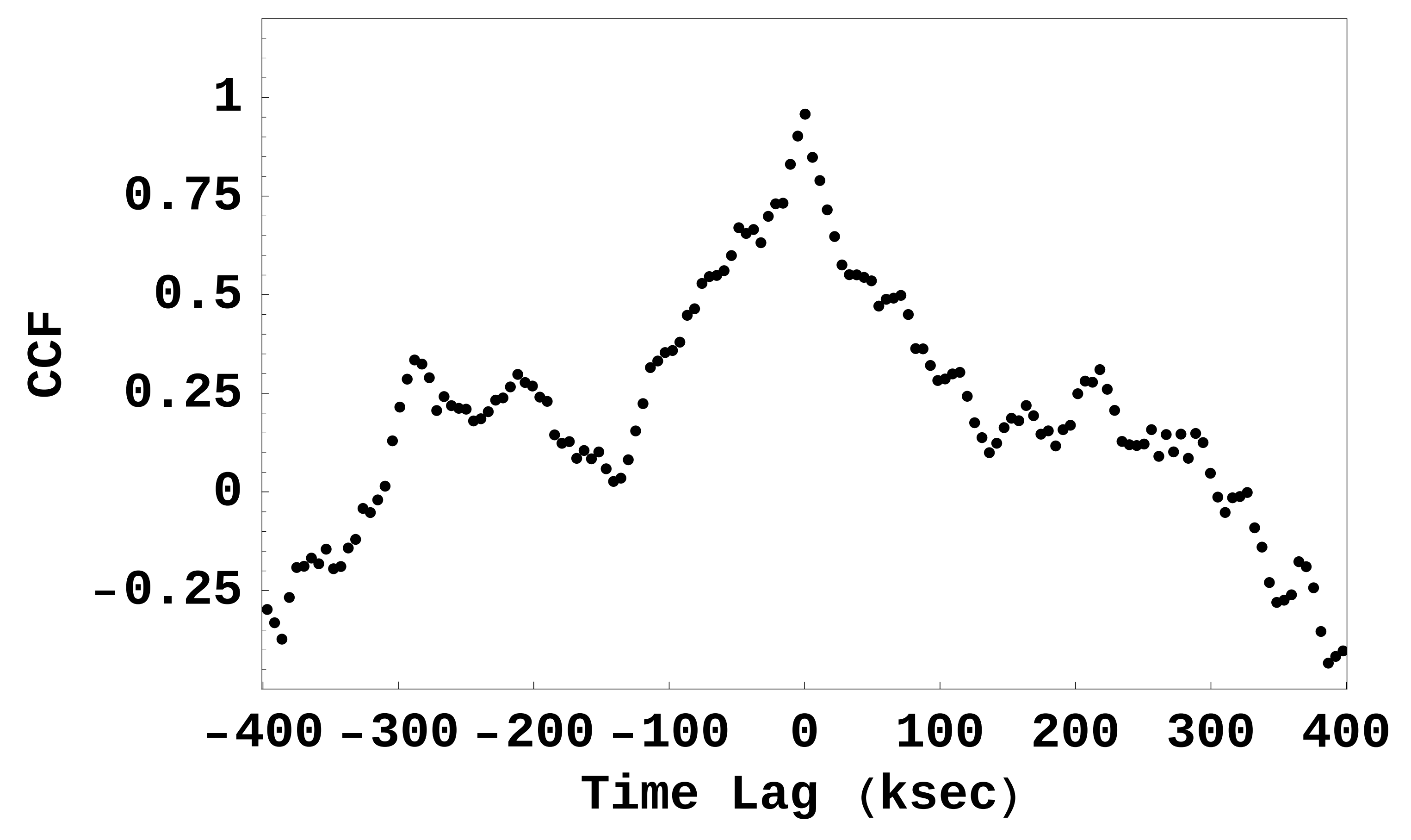

CCF $\frac{2-4keV}{4-5keV}$ $\frac{7-10keV}{10-30keV}$

Spectral analysis

Spectral Time Variations

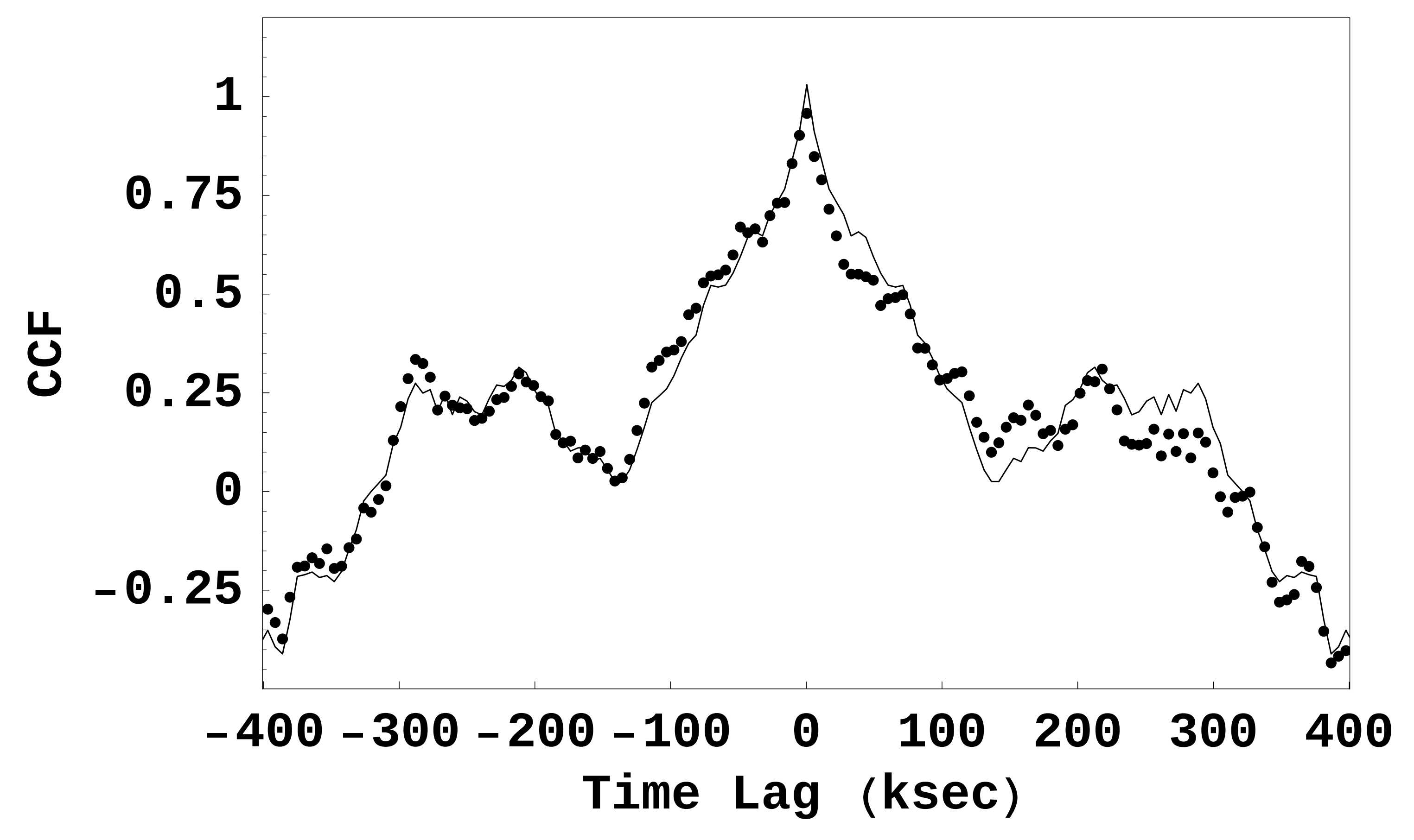

CCF $\frac{2-4keV}{4-5keV}$ $\frac{7-10keV}{10-30keV}$

&

ACF $\frac{2-4keV}{4-5keV}$

Spectral analysis

Spectral analysis

Spectral analysis

Spectral analysis

The “Softness Ratio” (2-4)keV/(4-5)keV vs (2-5)KeV

Spectral analysis

Spectral analysis

The “Softness Ratio” (2-4)keV/(4-5)keV vs (2-5)KeV

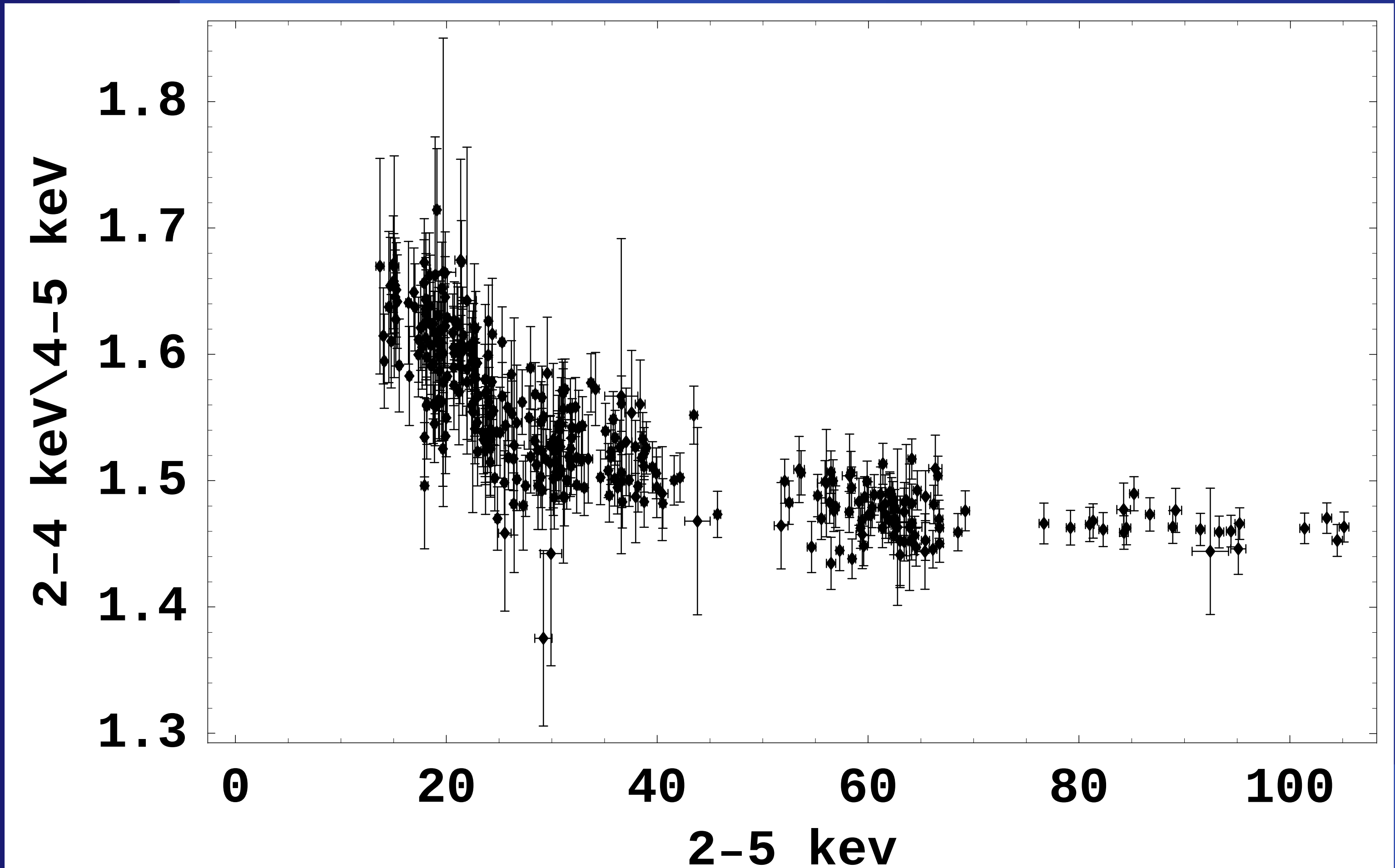

Spectral analysis

Spectral analysis

The “Softness Ratio” (2-4)keV/(4-5)keV vs (2-5)KeV

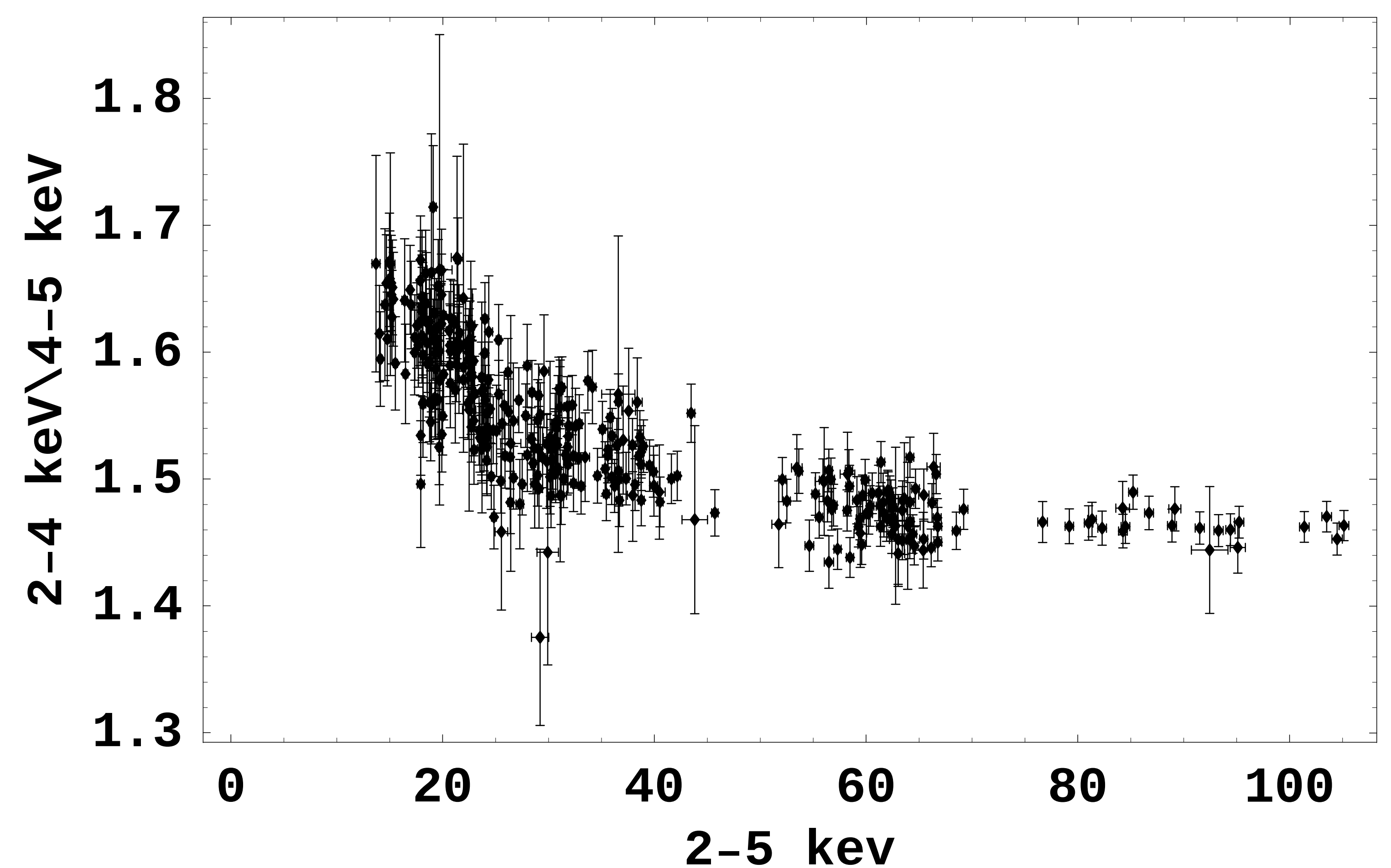

Large value of fluxes ⇒ No signifi- cant spectral changes

Spectral analysis

Spectral analysis

Spectral analysis

Spectral analysis

The “Softness Ratio” (2-4)keV/(4-5)keV vs time ksec

Spectral analysis

Spectral analysis

The “Softness Ratio” (2-4)keV/(4-5)keV vs time ksec

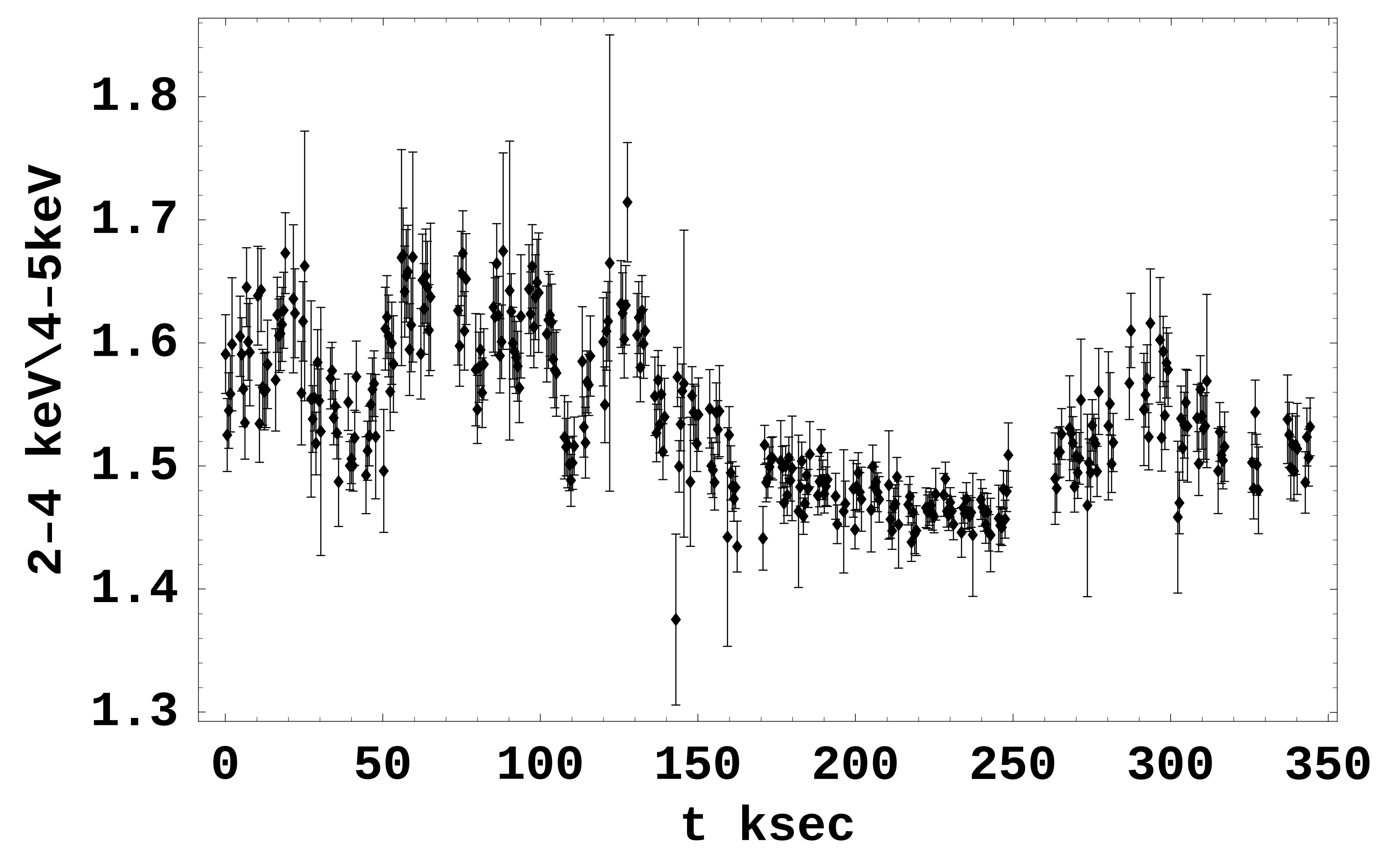

Spectral analysis

Spectral analysis

The "Softness Ratio" (2-4)keV/(4-5)keV vs time ksec

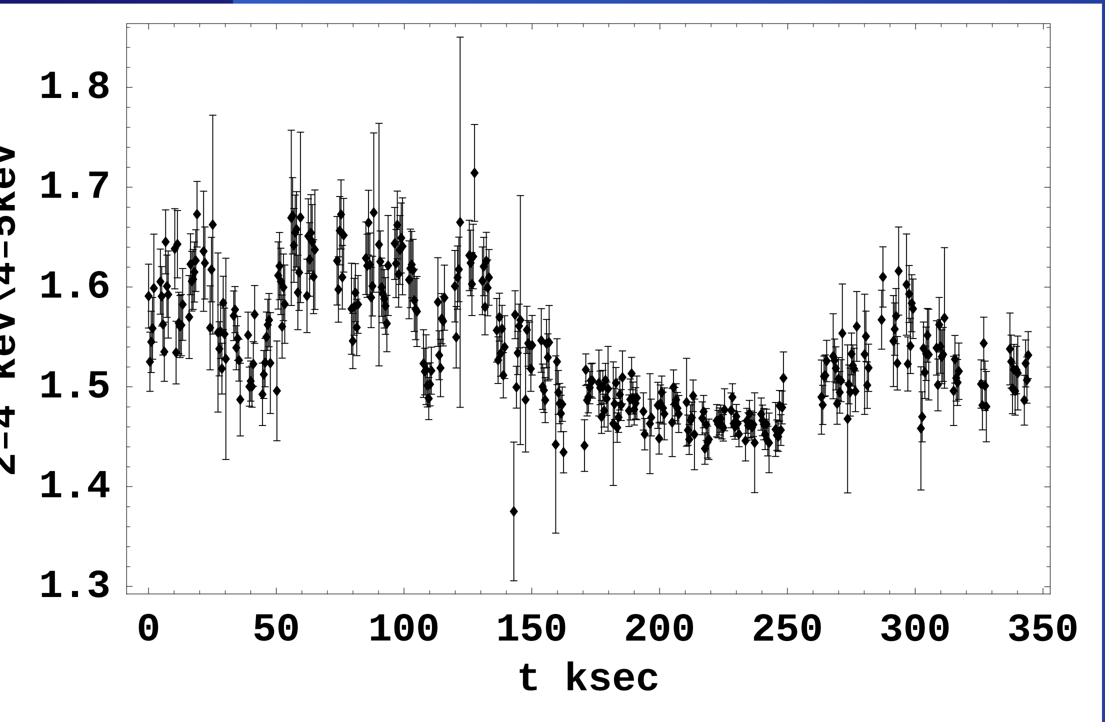

Spectral analysis

Spectral analysis

The "Softness Ratio" (2-4)keV/(4-5)keV vs time ksec

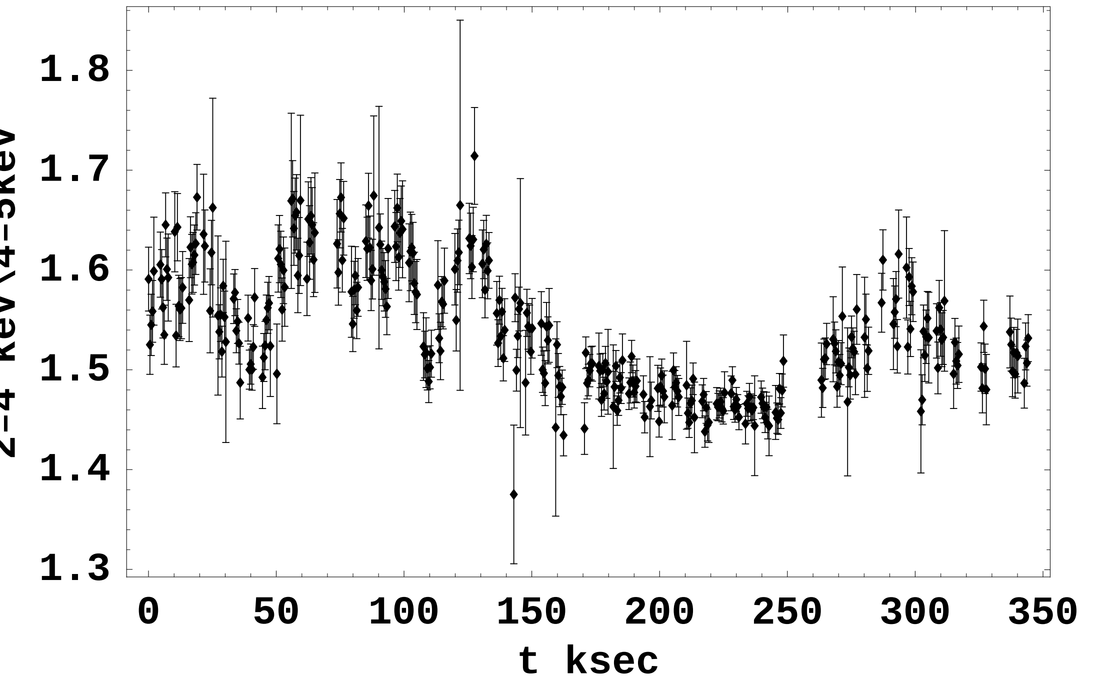

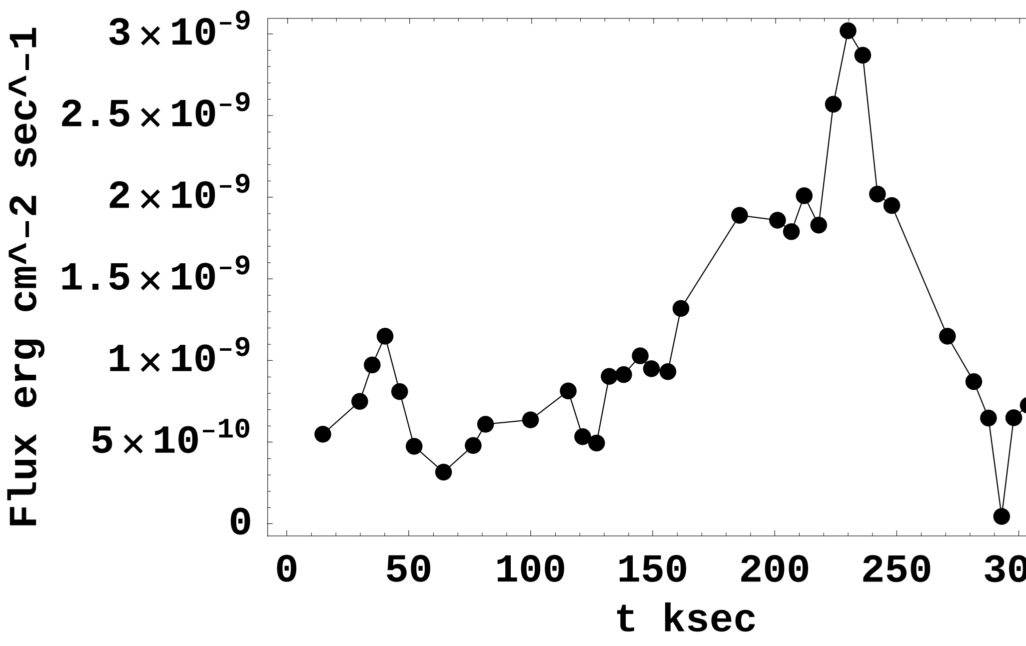

Spectral analysis

Spectral analysis

Spectral analysis

Spectral analysis

The flare between (100-120)ksec

Spectral analysis

Spectral analysis

The flare between (100-120)ksec

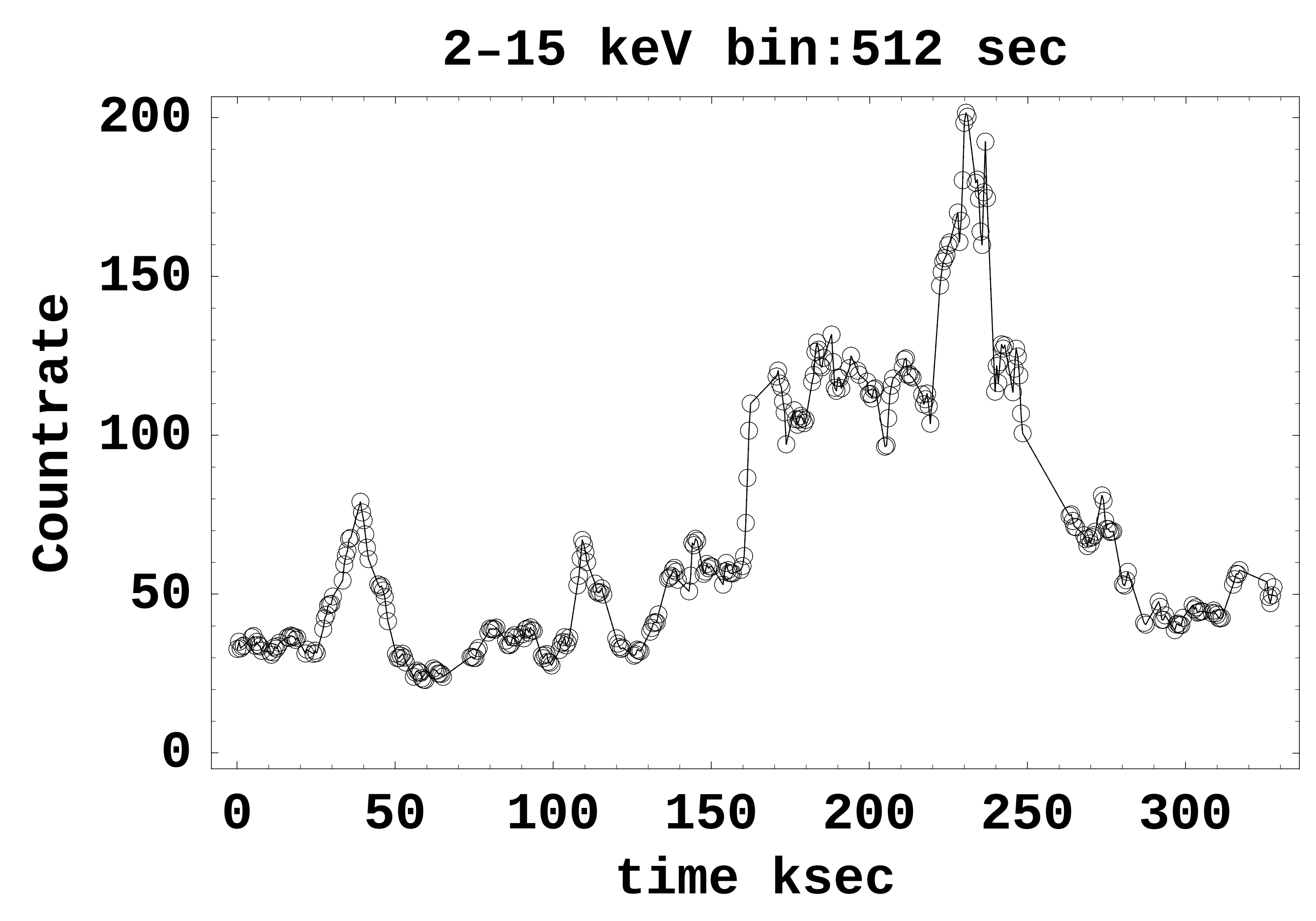

Spectral analysis

Spectral analysis

The flare between (100-120)ksec

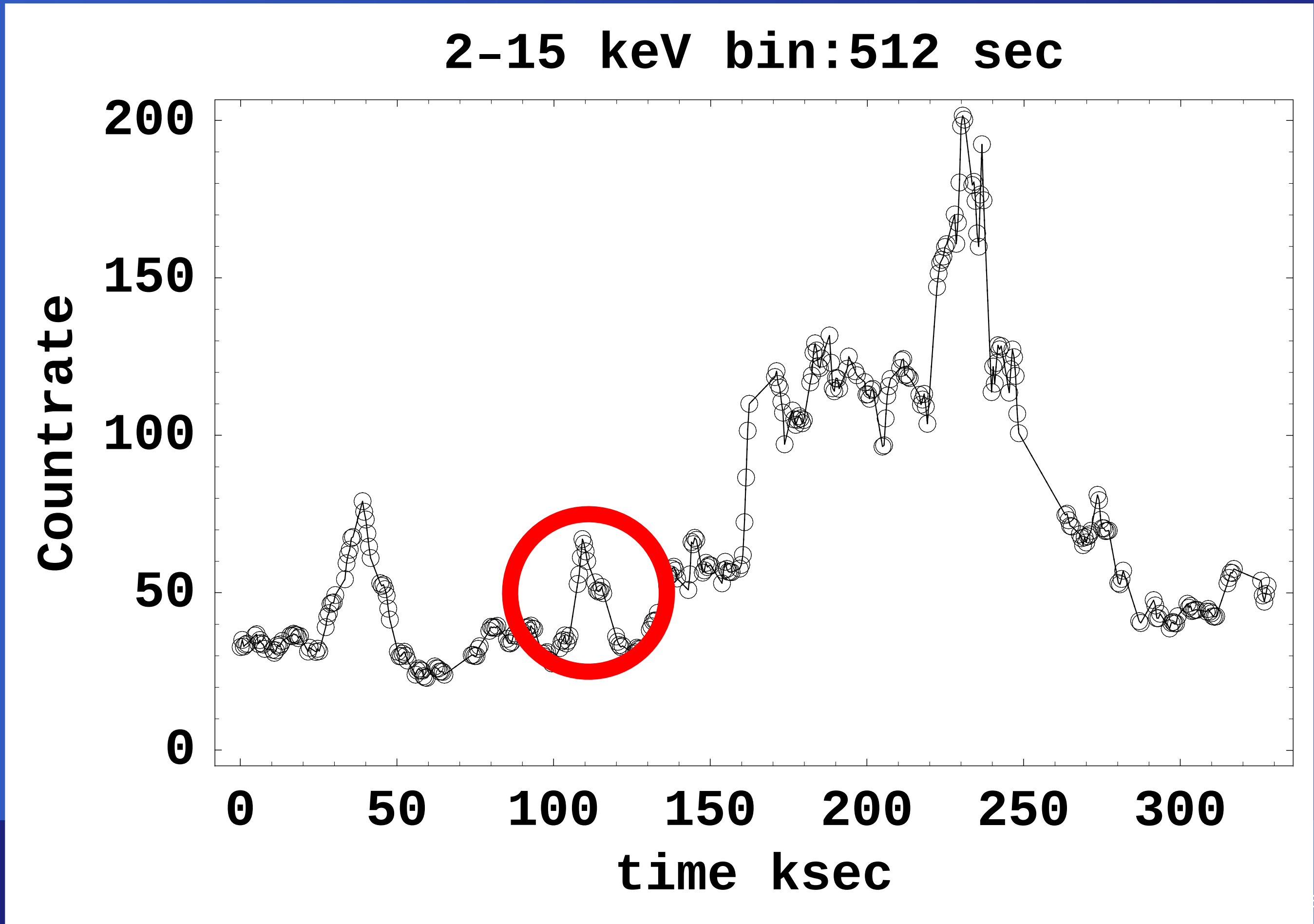

Spectral analysis

Spectral analysis

The flare between (100-120)ksec

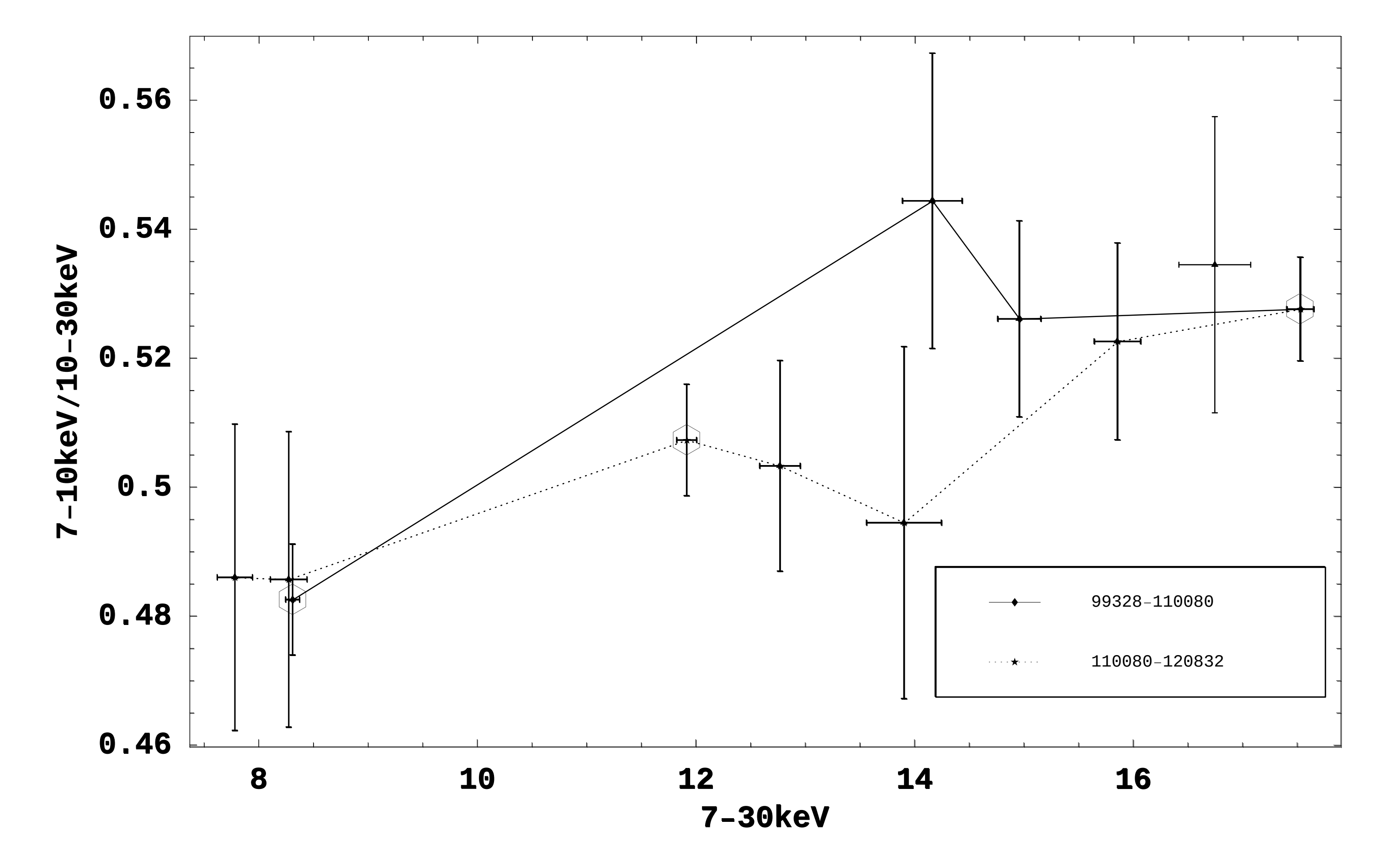

Spectral analysis

Spectral analysis

The flare between (100-120)ksec

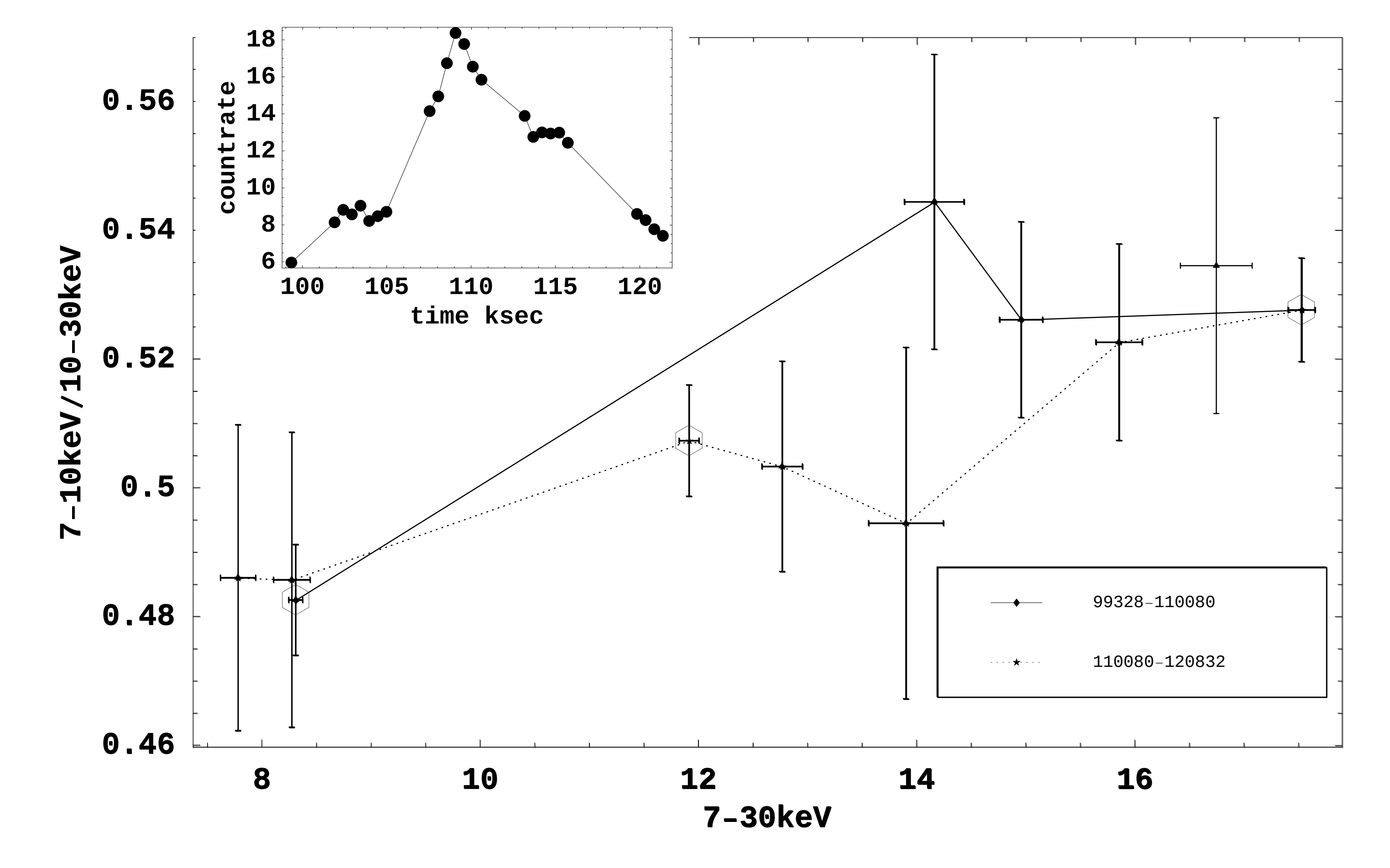

Spectral analysis

Spectral analysis

The flare between (100-120)ksec

Spectral analysis

Spectral analysis

The flare between (100-120)ksec

- The spectrum hardens during phases of rising flux and softens during phases of falling flux

Spectral analysis

Spectral analysis

The flare between (100-120)ksec

- The spectrum hardens during phases of rising flux and softens during phases of falling flux
- The formation of a “Clockwise”Loop is a signature of synchrotron cooling (Kirk et al.A&A 333 1998), in a ‘homogeneous’ synchrotron model

Spectral analysis

Spectral analysis

The flare between (100-120)ksec

- The spectrum hardens during phases of rising flux and softens during phases of falling flux
- The formation of a “Clockwise”Loop is a signature of synchrotron cooling (Kirk et al.A&A 333 1998), in a ‘homogeneous’ synchrotron model
- Similar behavior found by (Takahashi et al. Apj 470 1996).

Spectral analysis

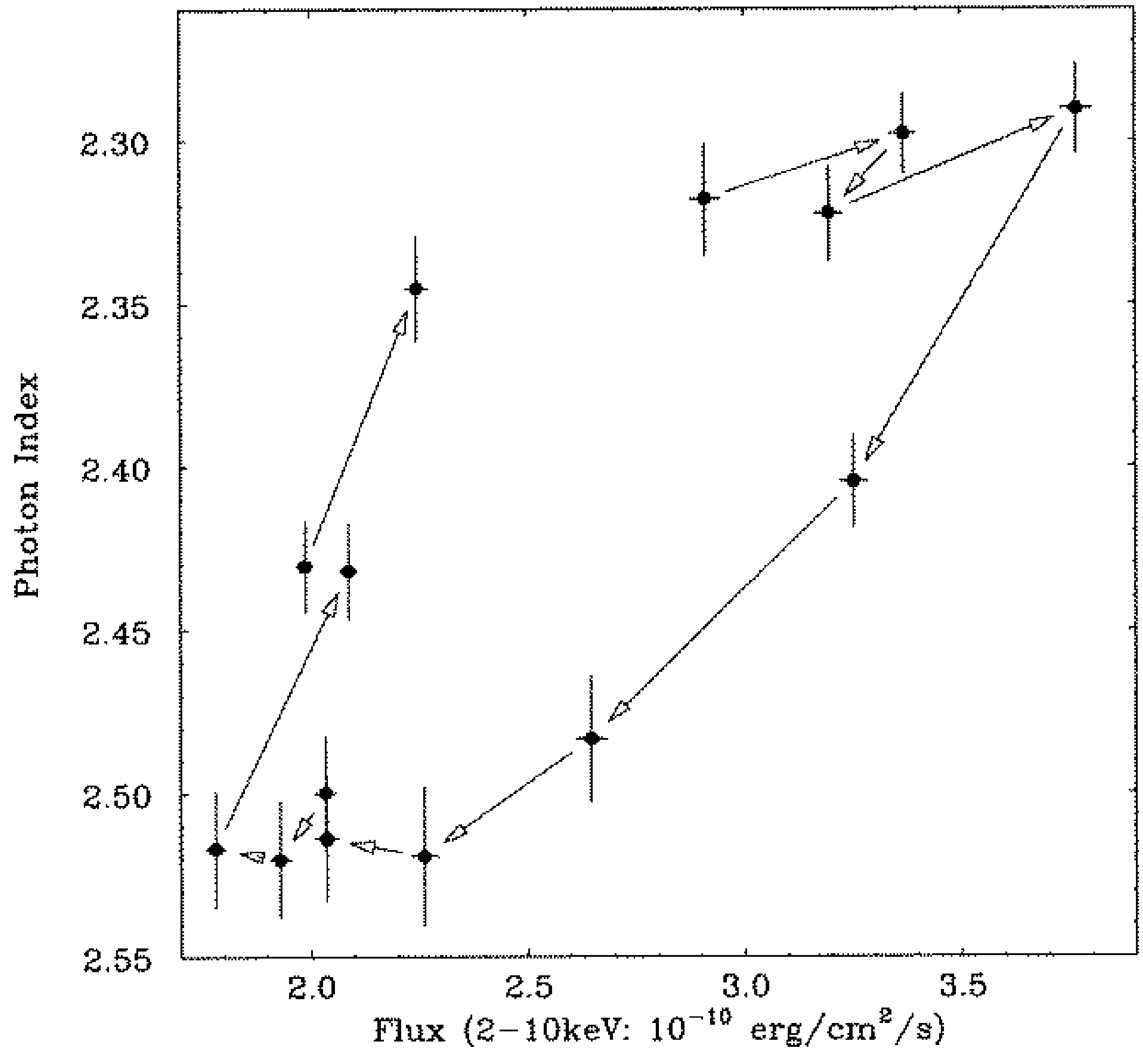

Spectral analysis

Spectrum of MKN421

Spectral analysis

Spectrum of MKN421

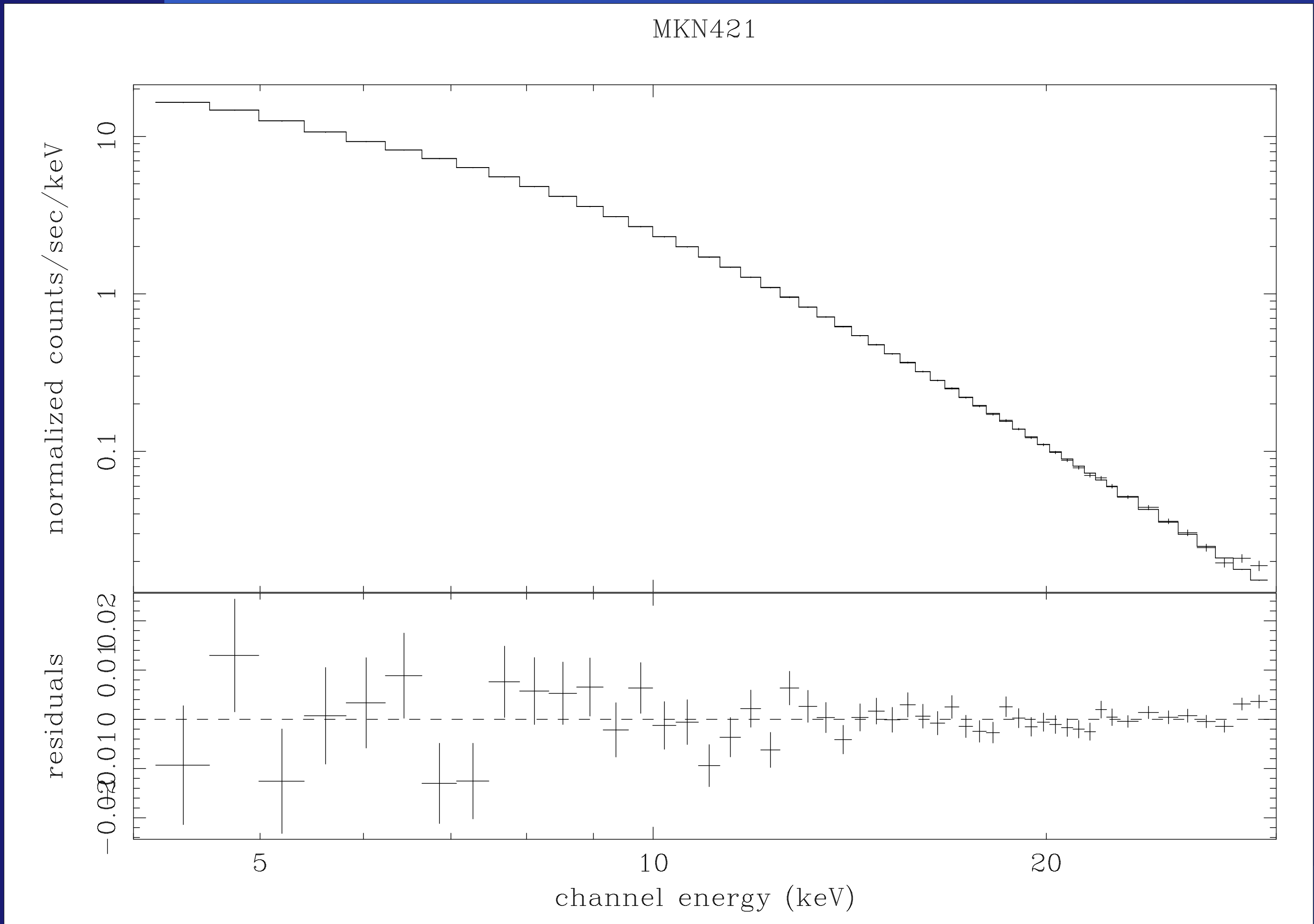

Spectral analysis

Spectrum of MKN421

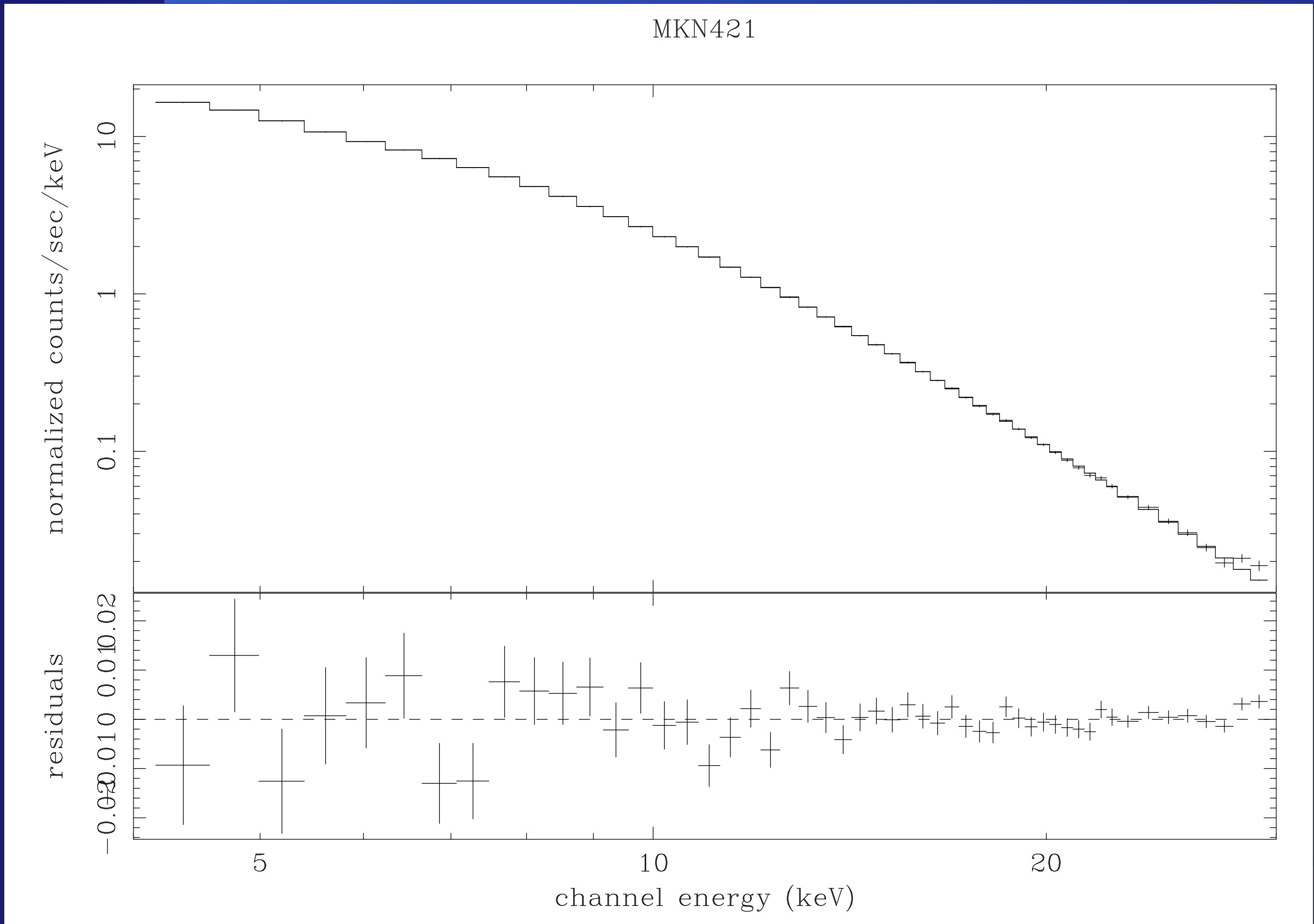

$$a_1 = 2.244^{+0.004}_{-0.005}$$

$$E^{keV}_{1Break} = 6.421^{+0.1}_{-0.1}$$

$$a_2 = 2.408^{+0.009}_{-0.006}$$

$$E^{keV}_{2Break} = 11.58^{+0.}_{-0.}$$

$$a_3 = 2.537^{+0.016}_{-0.018}$$

$$\chi^2/dof$$

$$62.17/45$$

Conclusions

- Big flares doesn’t provoke any change to the spectral index

Conclusions

- Big flares doesn’t provoke any change to the spectral index
- Spectral variations show a characteristic trend around 40ksec

Conclusions

- Big flares doesn't provoke any change to the spectral index
- Spectral variations show a characteristic trend around 40ksec
- The Synchrotron Cooling Process controls the spectral shape

Conclusions

- Big flares doesn't provoke any change to the spectral index
- Spectral variations show a characteristic trend around 40ksec
- The Synchrotron Cooling Process controls the spectral shape
- Are these characteristics temporal or typical for MKN421 ?
  Investigation through ASM data

Conclusions

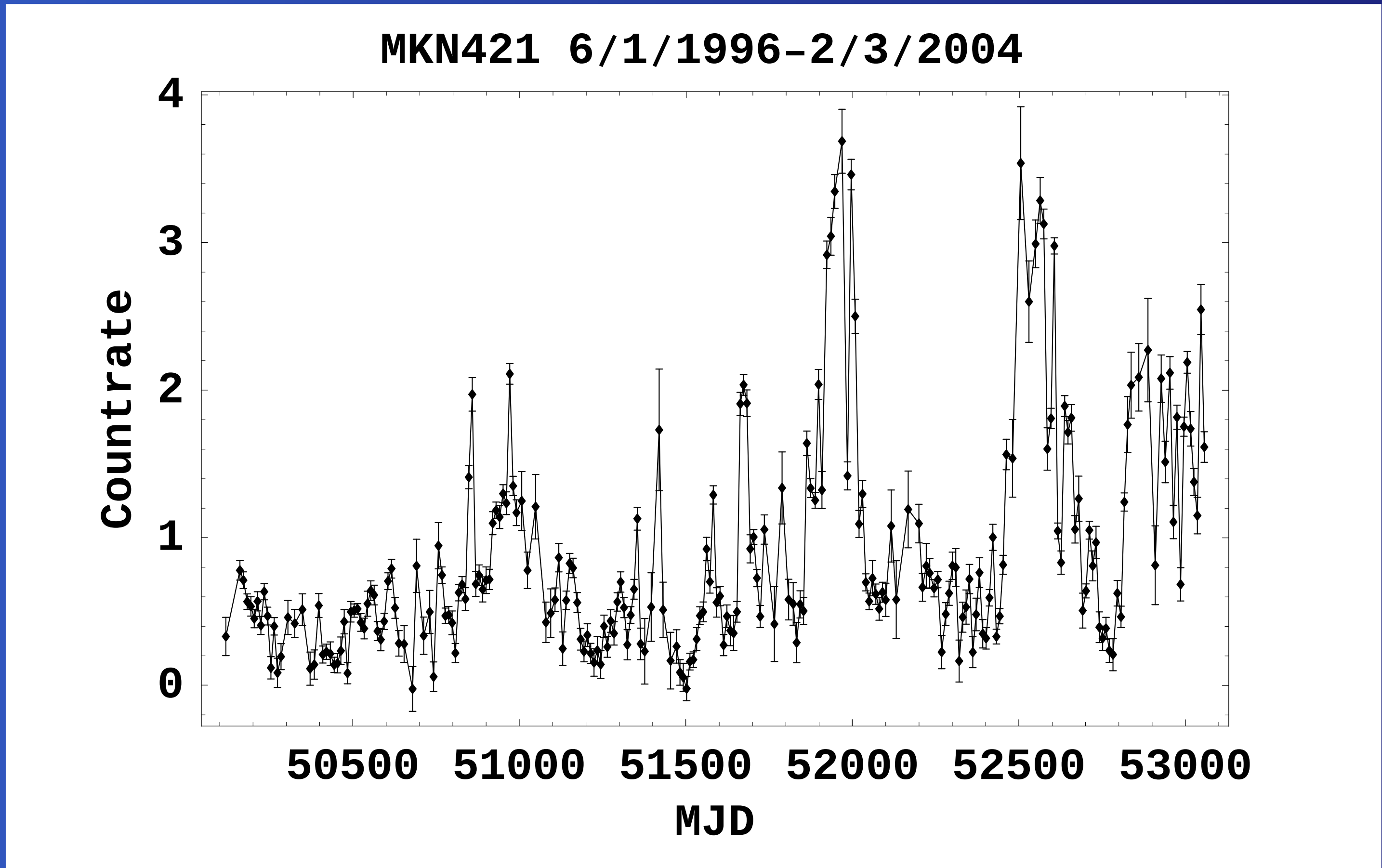

Thank you very much for your attention!

Determination of Doppler Motions using X-Ray Jets

ENIGMA Meeting
Jerisjärvi, Finland
26 April 2004

Peter Strub

Landessternwarte Heidelberg

The role of relativistic motion in jets

- VLBI (pc) scales: Superluminal motion
- Large (kpc) scales:
  -> only accessible with indirect methods
  (based on Doppler beaming characteristics)
  -> enormous impact on acceleration mechanism

Large scale X-Ray jets

- Chandra observations:
  -> kpc-scale jets are common

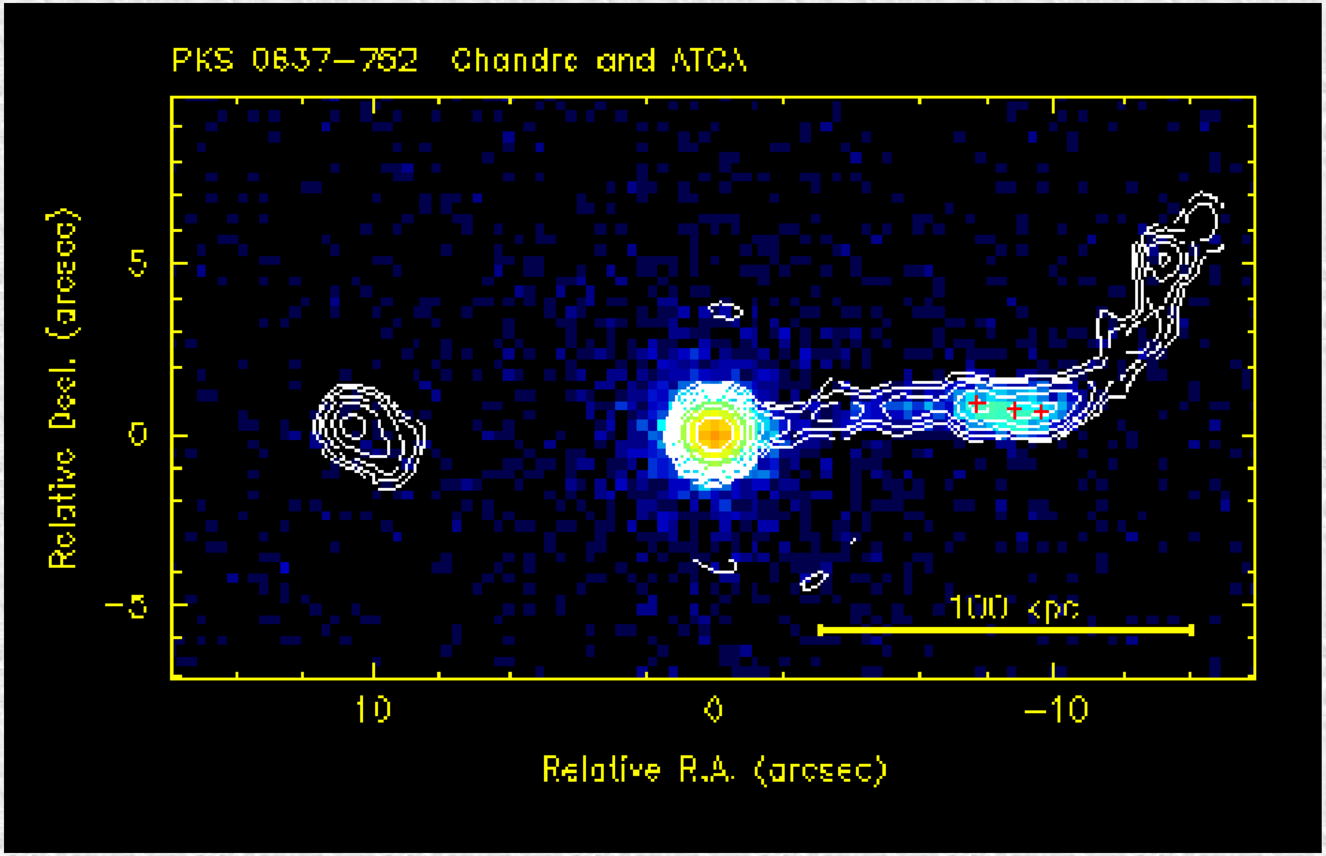

Chartas et al., 2000

Modelling X-Ray jets

- Typical current model:
  - Single blob (-> 1-zone)
  - EC/CMB
  - equipartition
  - 10
- Many ambiguities

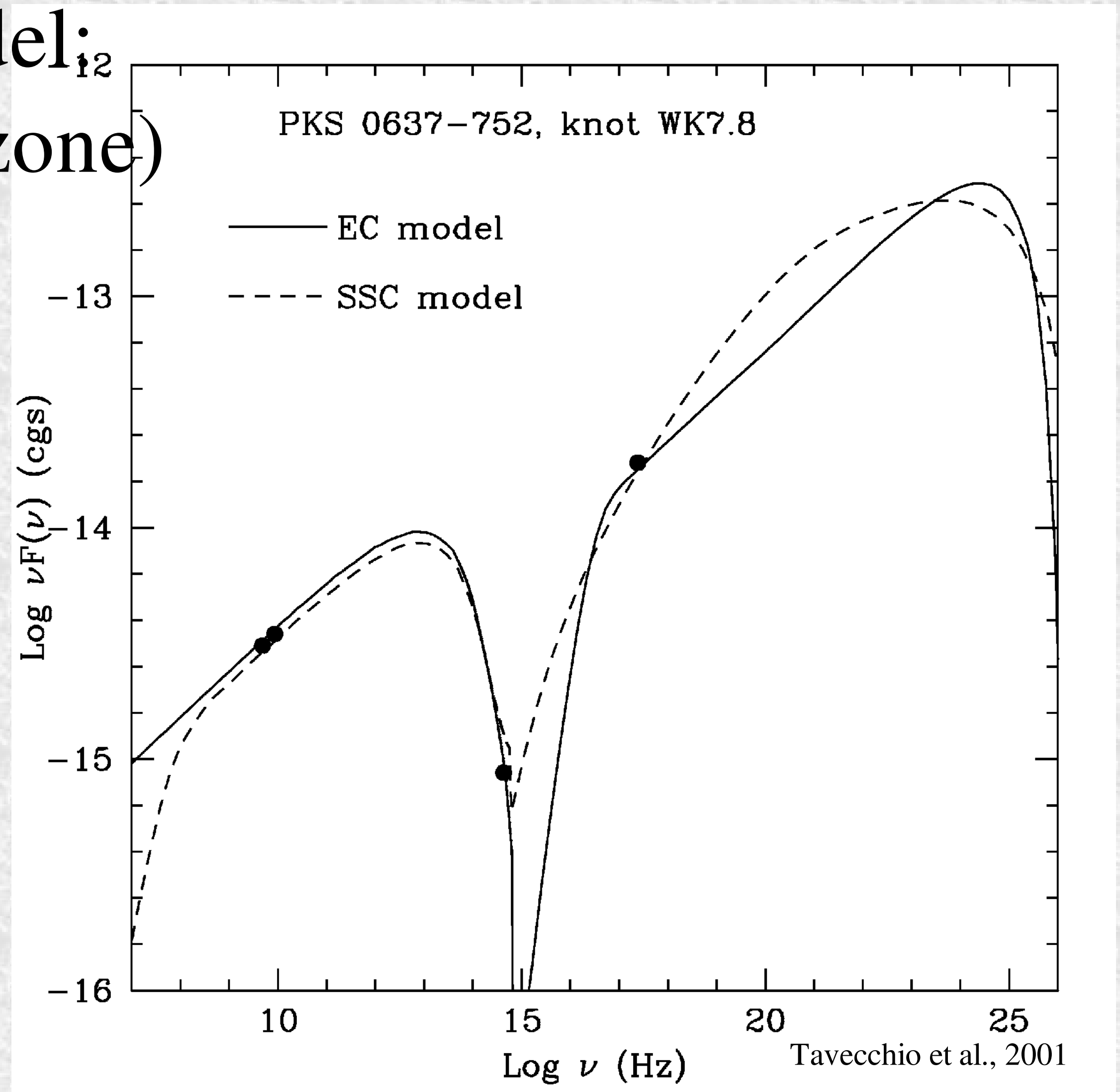

X-ray jets: Indicators for relativistic motion?

- Ratio between Synchro- & EC/CMB-component:
  - -> Synchro: B x n
    EC/CMB: n
  - -> Synchro Beaming: 1/
    EC/CMB:
    CMB enhanced by ²

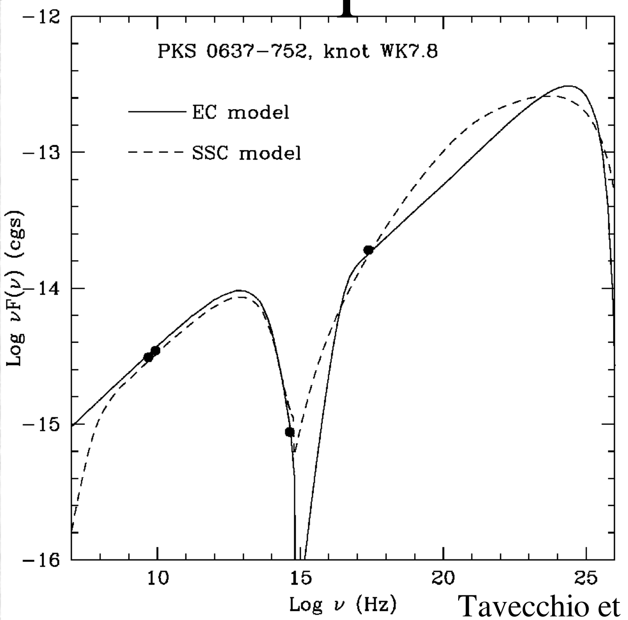

Tavecchio et al., 2001

- Model ambiguous
  -> even if other mechanisms can be ruled out

- One way to ensure EC/CMB dominates X-rays:
  High redshifts -> CMB density $\sim(1+z)^4$

Can be measured independently?

- No, not on large (kpc) scales!
- Assuming symmetric jet:
  jet-counterjet ratio depends only on
- BUT: Symmetry cannot be tested
  -> only accessible statistically in large sample

- examine sample of high-z jets with different jet-counterjet ratios
- 3 X-Ray jets known at z>2
  3 more proposed for next Chandra AO

Example: 7C 1745+6227 (z=3.9)

- 19ks Chandra observation
- Core 1000cts,
  Jet 220cts
- Jet-Counterjet:
  Radio (HS): 8
  Radio (Jet): >= 8
  X-Ray (Jet): >30
- SED model still to be examined in detail

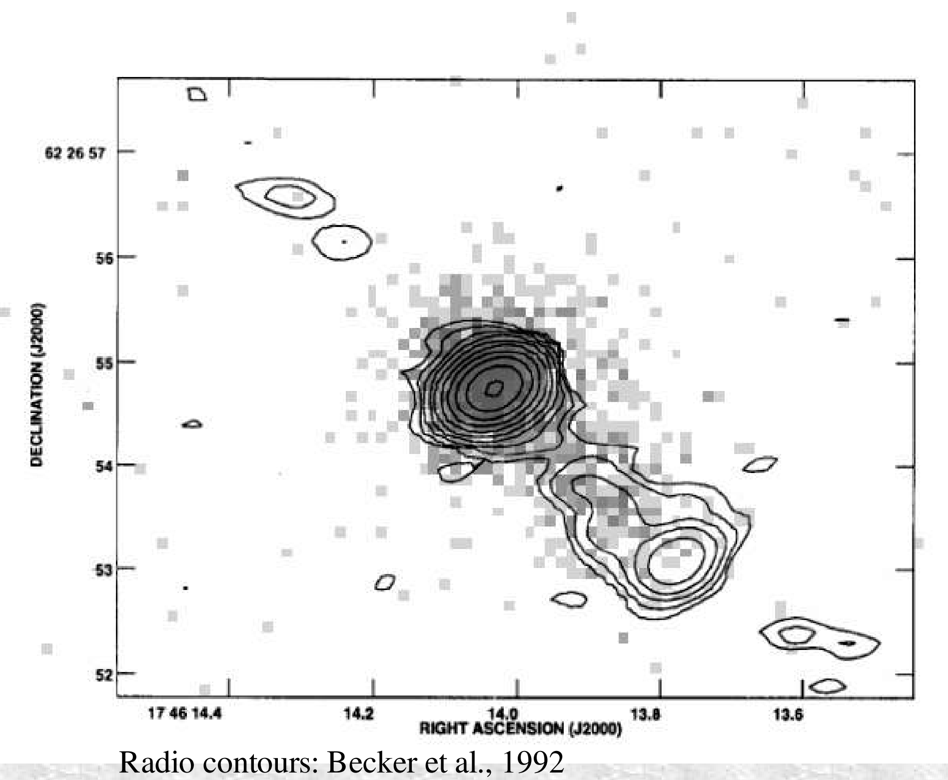

Radio contours: Becker et al., 1992

Conclusions

- X-Ray jets detectable at high z
- Likely to be EC/CMB
- If jets are sufficiently symmetric:
  -> unique handle on crucial point of
  beaming & equipartition
- More jets needed for meaningful statistical analysis

Variations of Source Structure and Flux

with the ENIGMA Team at the MPIfR in Bonn

introduction

Ivan Agudo
Emmanouil Angelakis
Uwe Bach
Silke Britzen
Krisztina Gabanyi
Simone Friedrichs
Violetta Impellizzeri
Matthias Kadler
Jens Klare
Thomas Krichbaum
Eduardo Ros
Bong Won Son
Arno Witzel
Anton Zensus

Rapid Radio Flux-density variations in 0716+714: Intraday Variability (IDV)

Correlated

Radio-

optical

Variability =>

Intrinsic origin

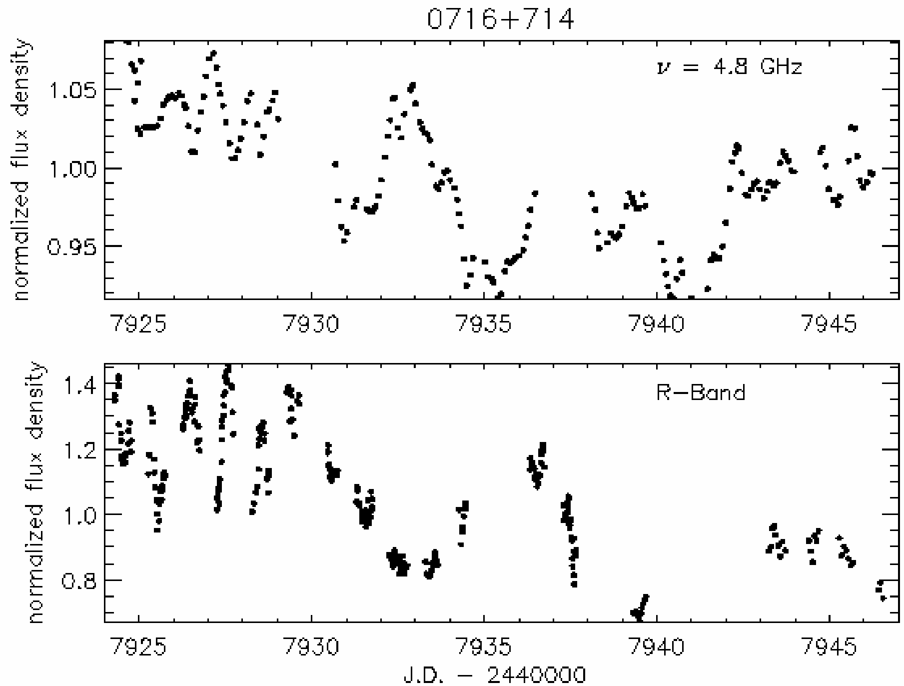

Wagner & Witzel ARA&A 1995

Slow mode

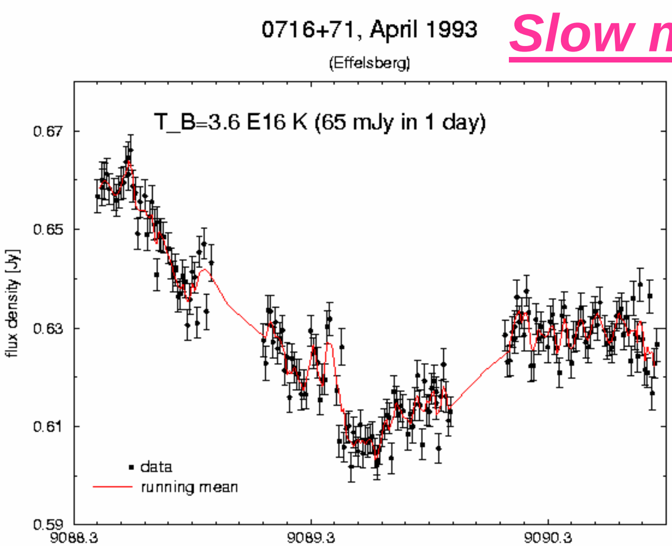

Fast mode

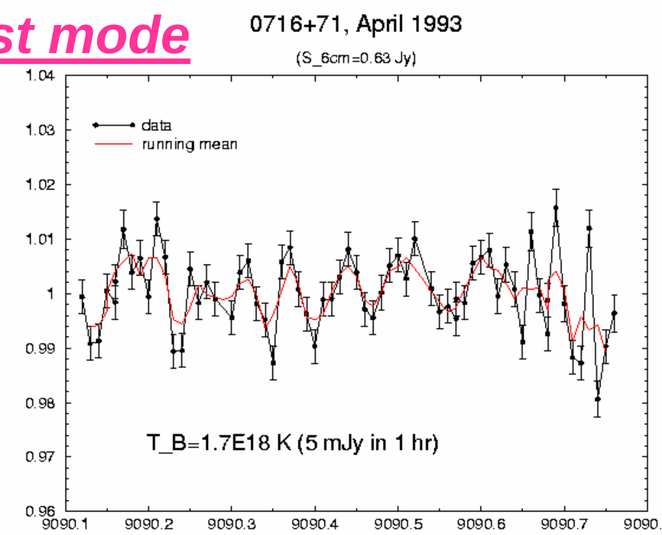

„Jets have a knotty problem!“

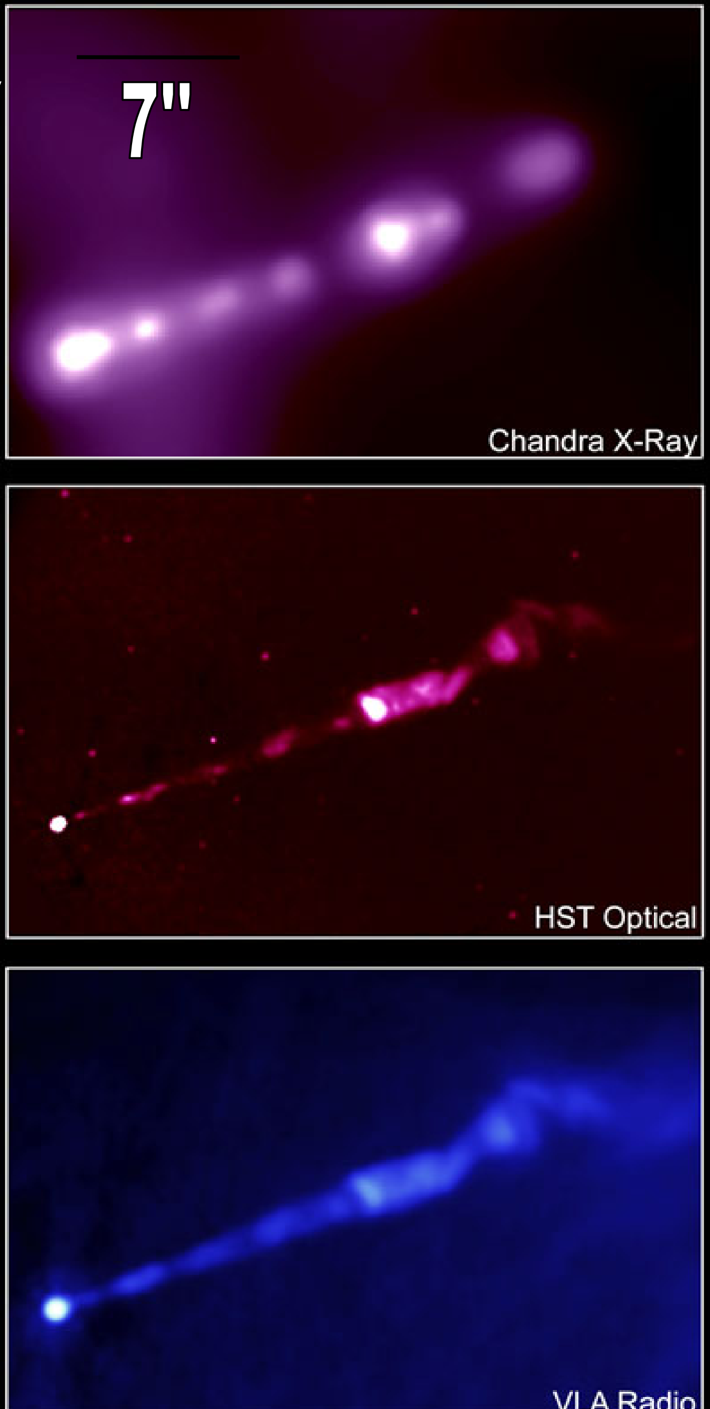

Proper motion

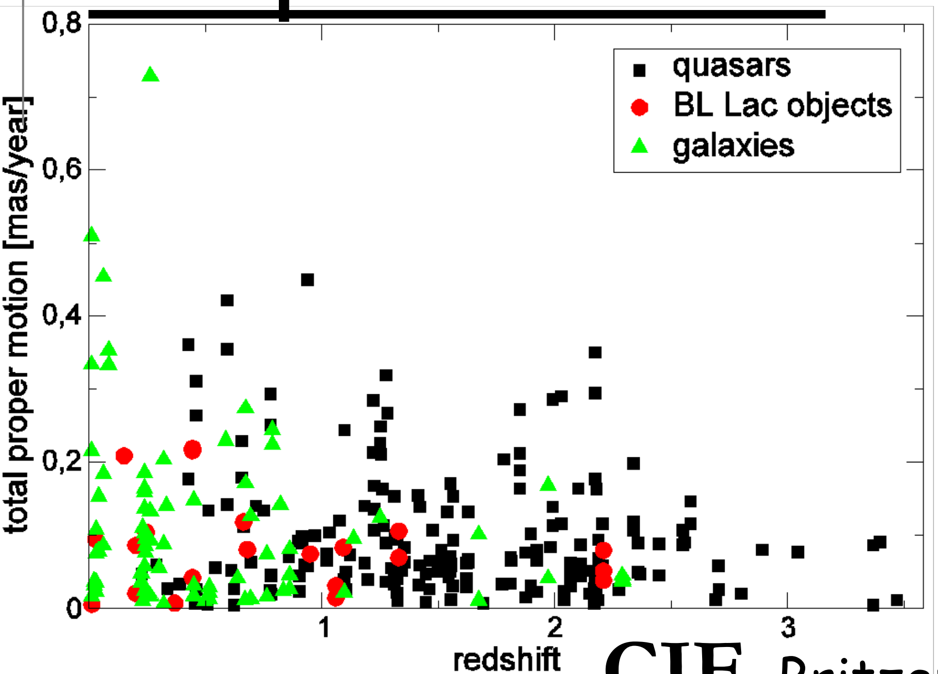

Apparent velocities

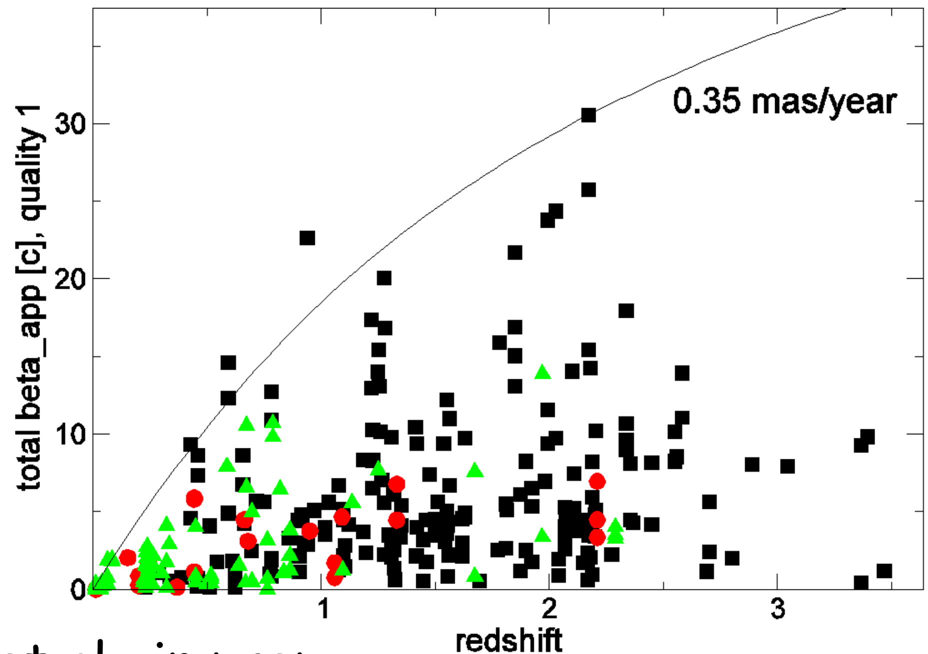

CJF, Britzen et al., in prep

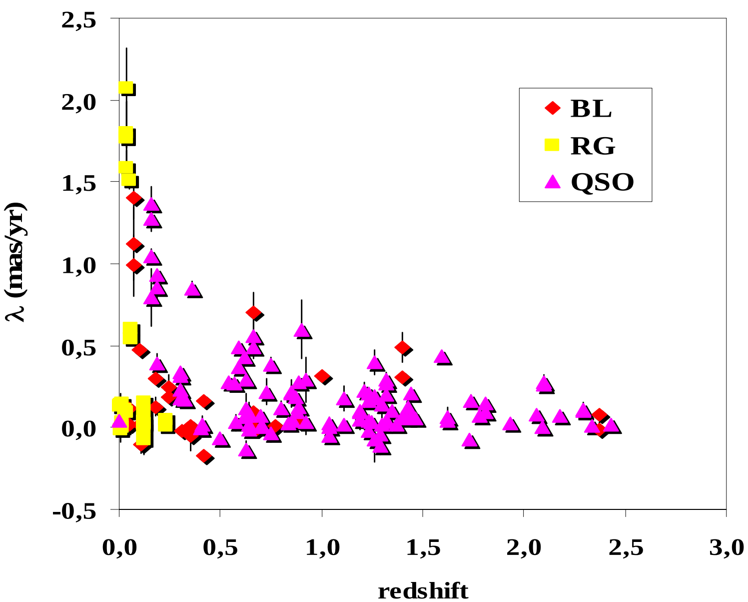

2 cm survey

Kellermann et al.
submitted

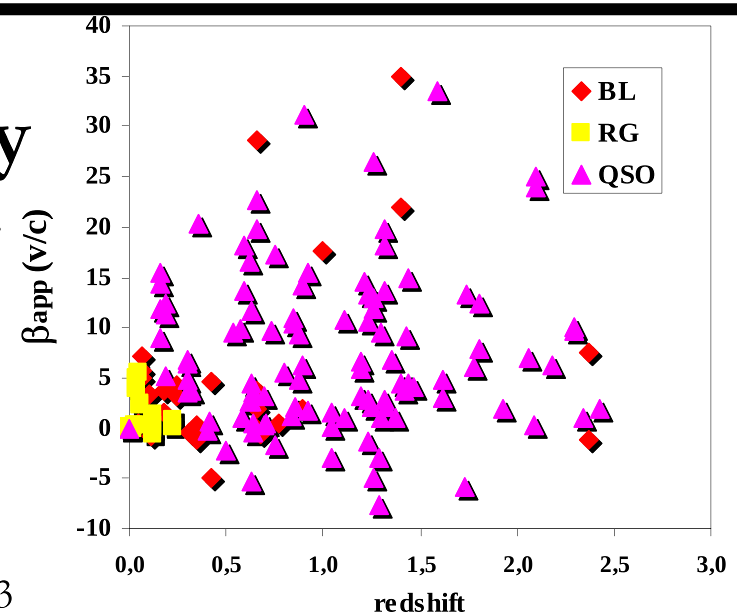

H0=65, □ m=0.3

Variations of Source Structure and Flux

Apparent superluminal motion for different optical classes (CJF)

CJF, Britzen et al., in prep

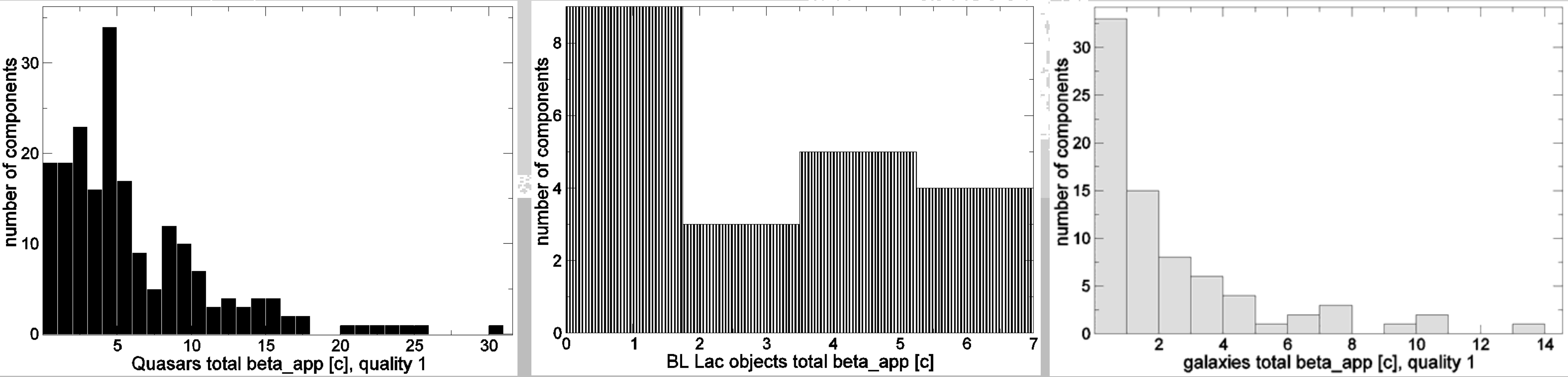

- **Apparent motions:**
  - Quasars (4.48 +/- 4.20c)> BL Lac Objects (3.11 +/- 2.78c) > Radio Galaxies (1.24 +/- 1.87c) => in agreement with unification scenarios
  - mainly acceleration, broad range of velocities within jets
  - Slower apparent velocities than in 2cm-survey (Kellermann et al., subm.) => increase in apparent velocitiy with frequency of the survey (see also Jorstad et al.): no final explanation yet!!

Correlation: Large-scale Radio Structures & ROSAT-detection?

0

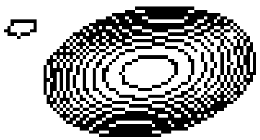

CJF, Britzen et al., in prep

5

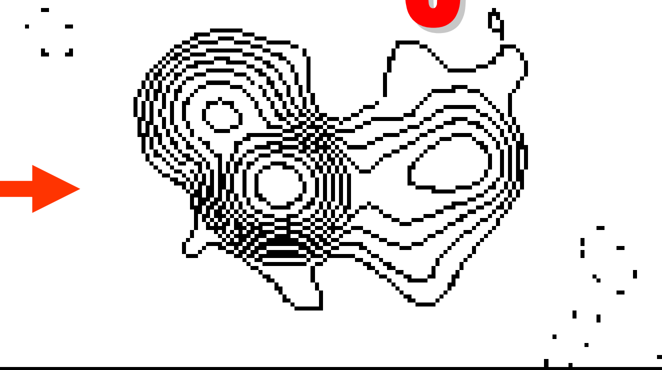

0 : point-like, no extended kpc-scale structure
5: komplex extended kpc-scale structure

Table 4: The table lists the numbers of objects with the complexity factors describing the kpc-scale structure. The numbers are given for the sample of CJF sources detected by *ROSAT* and for then non-detections.

	0	1	2	3	4	5
detected by *ROSAT*	45	11	28	25	20	16
not-detected by *ROSAT*	72	11	38	14	1	1

Variations of Source Structure and Flux

EGRET detected CJF-subsample

EGRET name	radio source IAU name	Radio detected	z	optical class	β_{app} [c]	*ROSAT* detected	PA [deg]	VLA complexity	curvature pc-scales [deg]
3EG J0222+4253	0219+428	√	0.444	B	4.28	√	8	2	20
3EG J0721+7120	0716+714	√	~0.3	B	1.44	√	75	5	16
3EG J0808+4844	0804+499?	poss. Id.	1.43	HPQ	5.02	√	55	2	32
3EG J0845+7049	0836+710	√	2.172	Q	13.96	√	7	3	22
3EG J0917+4427	0917+449?	poss. Id.	2.180	Q	8.17	√	20	4	23
3EG J0952+5501	0954+556	√	0.901	HPQ		√	95	4	13
3EG J0958+6533	0954+658	√	0.368	B	0.16	√	85	2	58
3EG J1104+3809	MRK 421	√	0.031	B	0.19	√	13	4	13
3EG J1635+3813	1633+382	√	1.814	LPQ	5.18	√	86	4	30
	MRK 501	√	0.033663	B	0.31	√	83	4	56
3EG J1738+5203	1739+522	√	1.375	HPQ	11.44	√	106	2	44
3EG J2202+4217	BL Lacertae	√	0.069	B	2.66	√	30	4	34
3EG J2352+3752	2346+385?	poss. Id.	1.032	Q	5.62	√	66	2	16
3EG J2358+4604	2351+456	√	1.992	LPQ	14.91		88	2	39

Apparent velocities higher for gamma-bright Quasars than for complete CJF

„ „ slower „ „ BL Lac Objects than for complete CJF

More misaligned objects

Stronger curvature

CJF, Britzen et al., in prep

Variations of Source Structure and Flux

0716+714: Measured speeds of 5 c to 16 c are atypically fast for a BL Lac object!!!

$z = 0.3$, $H_0 = 71\ \mathrm{km\,s^{-1}\,Mpc^{-1}}$, $\Omega_m = 0.3$ and $\Omega_\lambda = 0.7$.

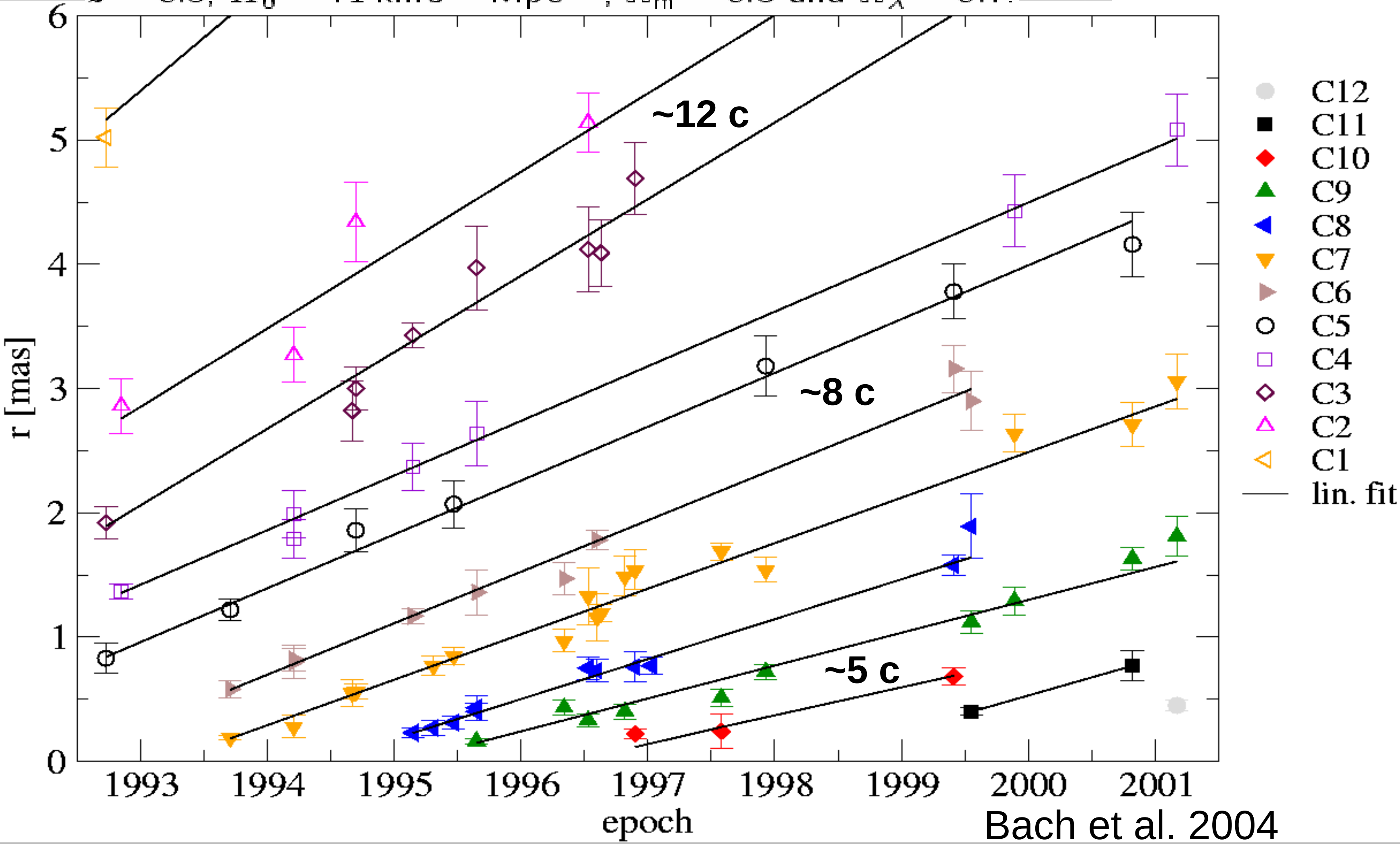

Variations of Source Structure and Flux

0716+714: Comparison between VLBI and Effelsberg Fluxes (5 GHz)

Array	Part	I [mJy]	P [mJy]	χ [°]
		29 Sep 2000		
VLBI	Core	520.3 ± 26.9	12.1 ± 1.3	49.4 ± 4.1
	Jet	56.0 ± 4.7	7.4 ± 0.8	-10.8 ± 5.6
Eb		763.2 ± 6.9	21.4 ± 2.6	23.4 ± 2.1
		4 Oct 2000		
VLBI	Core	499.3 ± 26.1	11.8 ± 1.3	40.7 ± 4.0
	Jet	54.8 ± 6.3	7.3 ± 0.8	-11.2 ± 7.8
Eb		735.7 ± 16.2	21.6 ± 2.6	18.6 ± 2.2
		5 Oct 2000		
VLBI	Core	503.9 ± 25.4	6.5 ± 1.1	52.7 ± 5.2
	Jet	54.7 ± 6.0	7.5 ± 0.8	-9.5 ± 7.4
Eb		740.2 ± 14.6	15.7 ± 1.1	13.3 ± 2.5

Bach et al., in prep

Bach et al., in prep

Variations of Source Structure and Flux

0716+714: Polarisation Variability on October 4

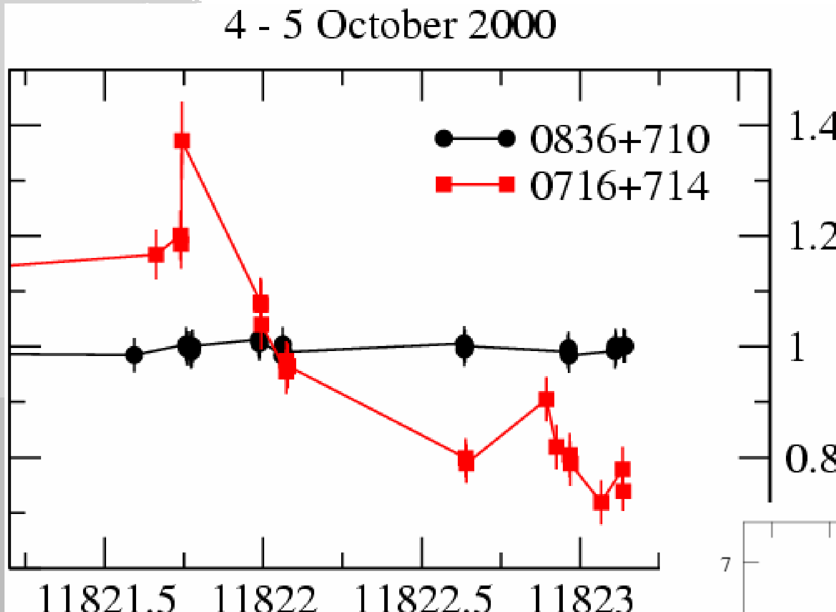

Bach et al., in prep
Bach et al., in pre

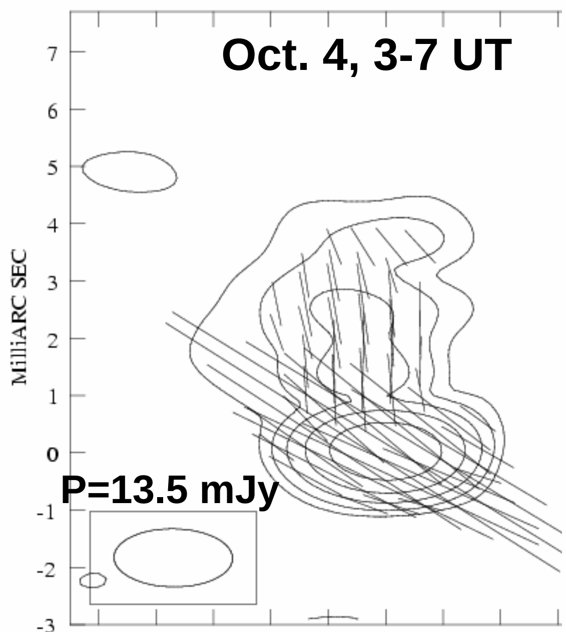

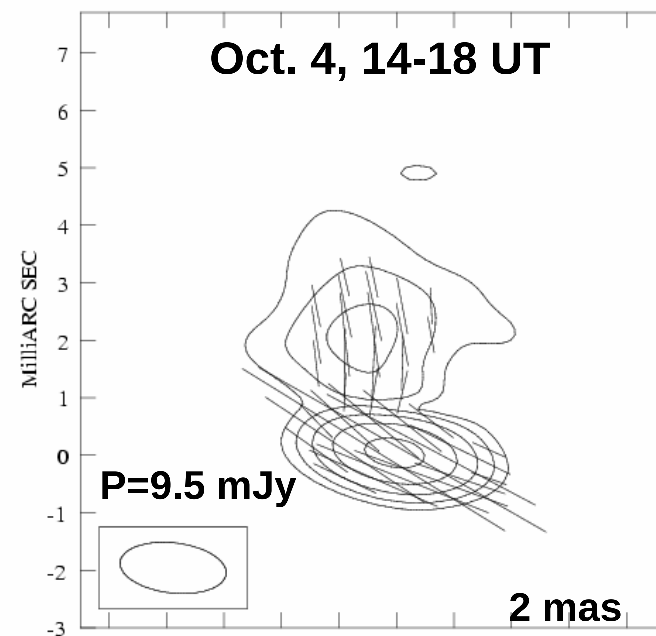

Binary Black Hole Systems (1)

X-ray:

„Chandra makes first positive I.D. of active Binary Black hole“

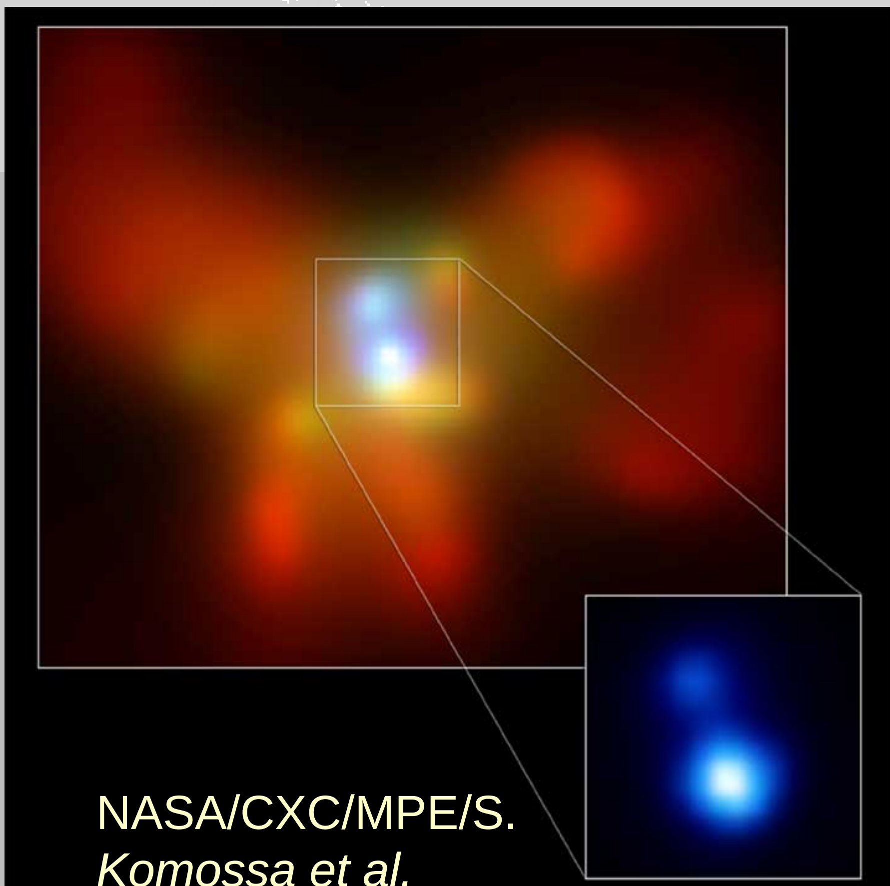

Radio (VLBI) & Optical: 3C345

Presence of a supermassive binary black hole in 3C345 explains:

1. **observed helical trajectories of the jet components**

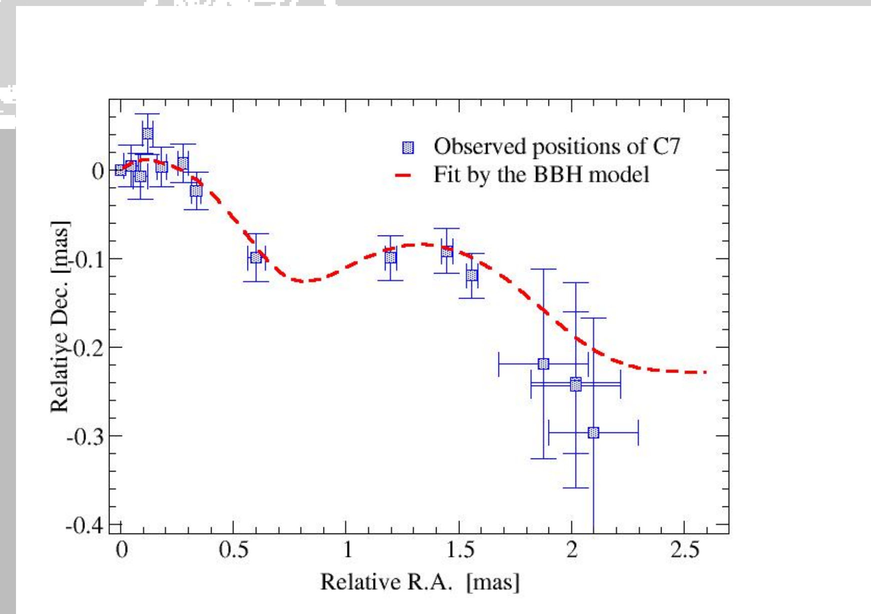

Lobanov & Roland

Parameters of BBH in 3C345
$M_1 = 1\cdot 10^9\,\mathrm{M_{sol}}, \quad M_2 = 5\cdot 10^8\,\mathrm{M_{sol}}$
$a_{maj} = 0.63\mathrm{pc}\ (0.13\,\mathrm{mas}), \quad e = 0.1$
$P_{orb} \approx 170\,\mathrm{years}, \ P_{prec} \approx 2500\ \mathrm{years}$

Binary Black Hole Systems (2)

Radio (VLBI) & Optical: 3C345

2. **flux density changes of the jet components**

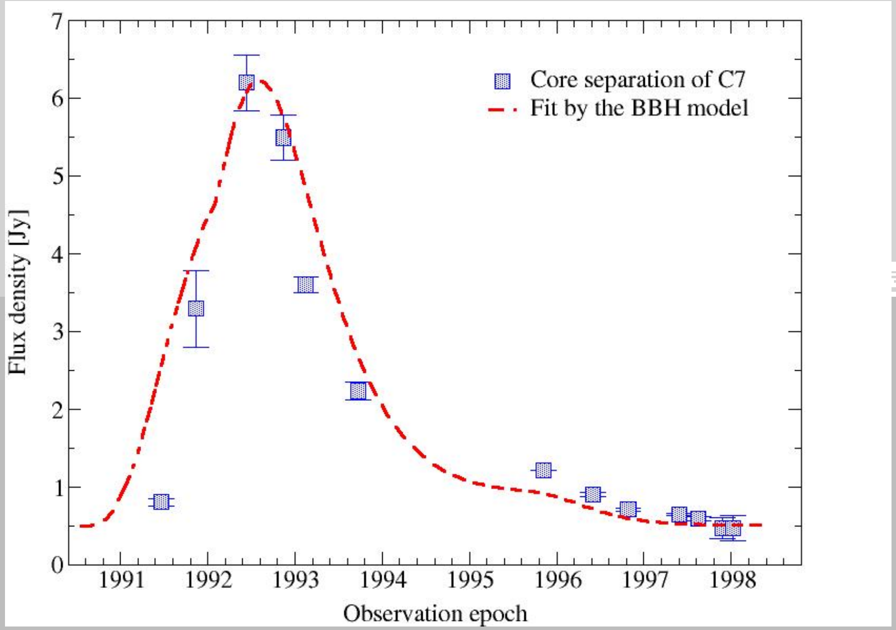

3. **optical variability**

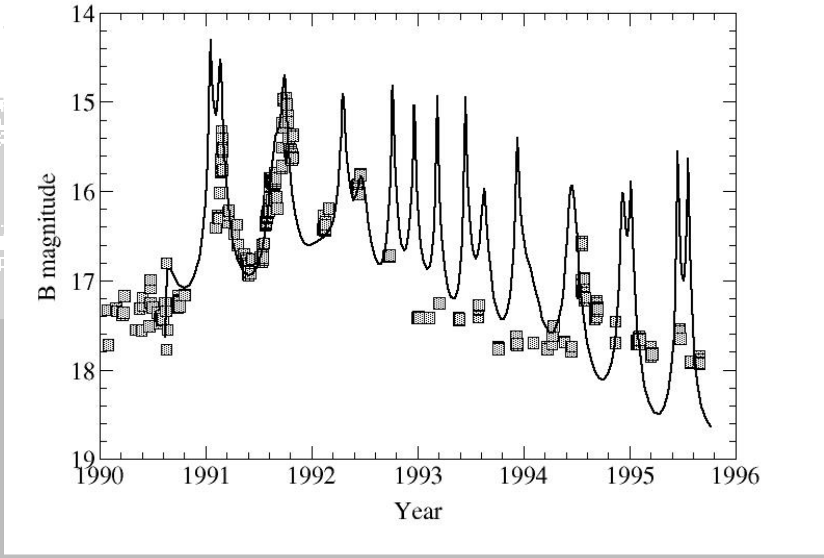

4. **morphology and evolution of the jet**

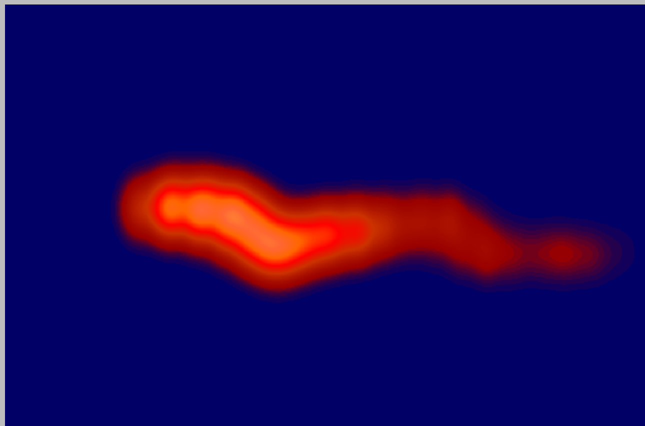

The Binary Black Hole System provides a new paradigm for understanding the dynamics and emission in parsec-scale jets in AGN. Further examples: e.g., PKS 0420-014 (*Britzen et al., 2000, 2001*), Mrk501(*Villata et al. 1999*).

Lobanov & Roland

VSOP Polarization Observations of the IDV Source 0954+658

Simone Friedrichs
T. P. Krichbaum
U. Bach
S. Britzen
A. Witzel
J. A. Zensus

Max-Planck-Institut
für
Radioastronomie

BL Lac 0954+658

Mildly superluminal radio source with helical jet
z = 0.368
IntraDay Variable (IDV) source type 2
Systematic timelags at radio-bands, possible optical-radio correlation (Wagner et al.)
Extreme Scattering Event (ESE, Fiedler et al.)
Very rapid ESE (Cimo et al., in prep.)

Aim of the Experiment

Search for structural changes with regard to IDV

Search for variation in total flux and polarization properties in the core and in the jet on VLBI (sub-mas) scales

Variations in the core or in the jet?

Observation

- Space VLBI at 5 GHz, ground array: VLBA + EB
- Highest resolution imaging of the inner VLBI jet
- A ~ λ/D
- 4 Epochs: 16, 20 – 22 October 2000

VSOP: VLBI Space Observatory Programme

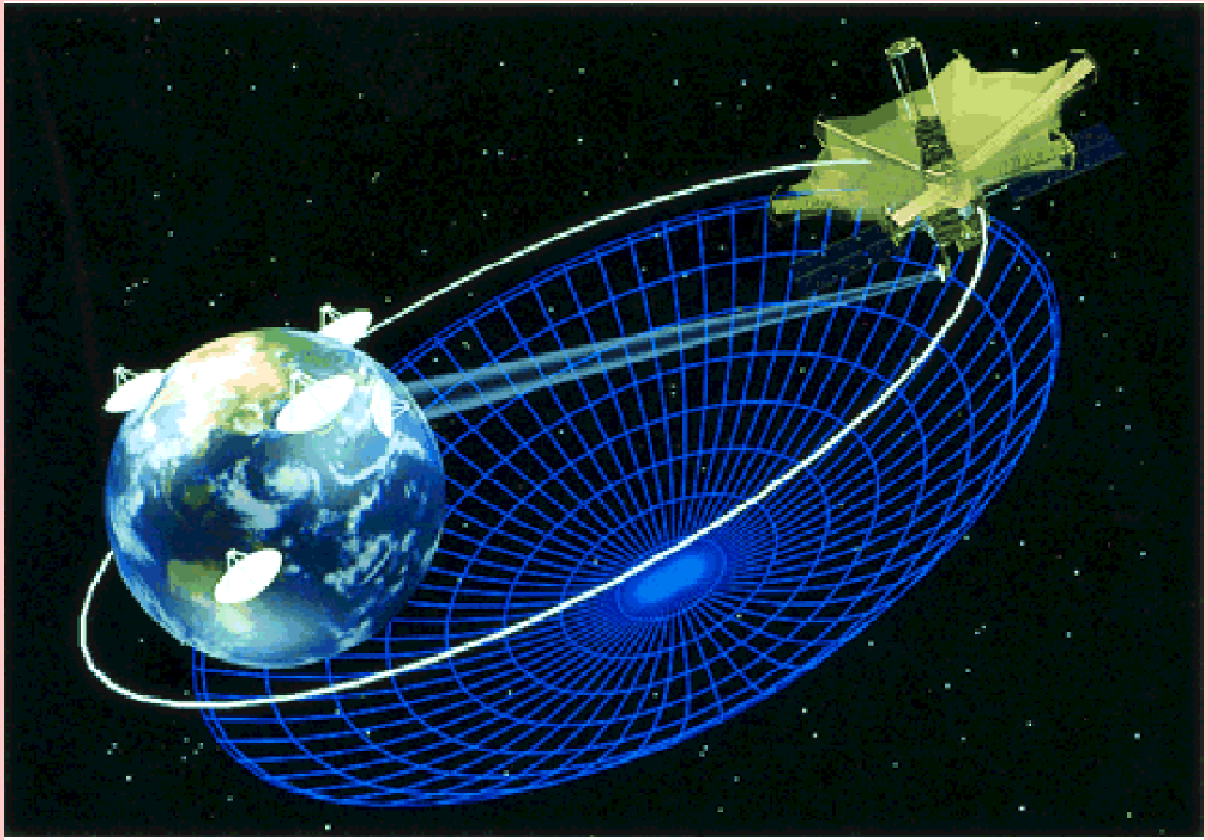

- Diameter 8 m
- Orbital period 6.3 h
- Observing frequencies: 5 GHz and 1.6 GHz
- Elliptical orbit
- Apogee 21.000 km

Zoom with VSOP into the inner jet

2 mas

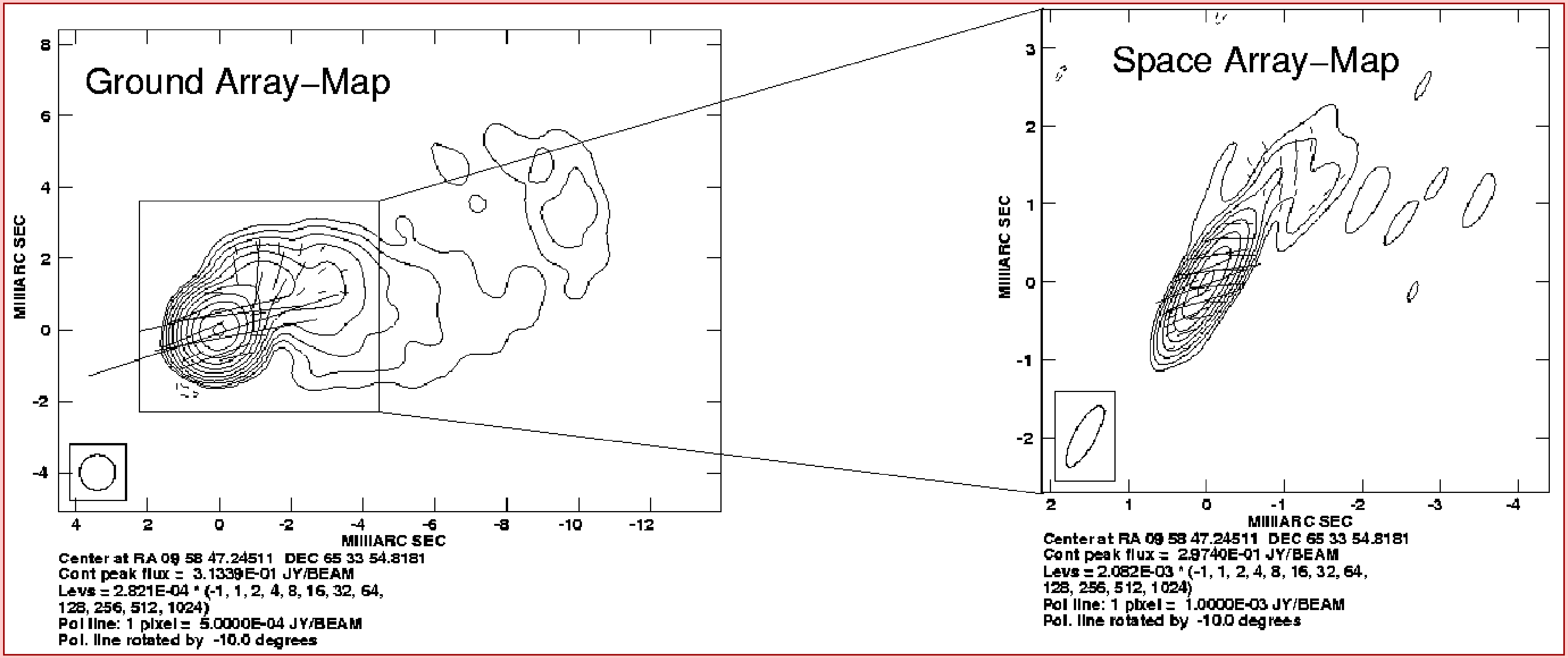

uv–coverage with SVLBI

16-10-00

20-10-00

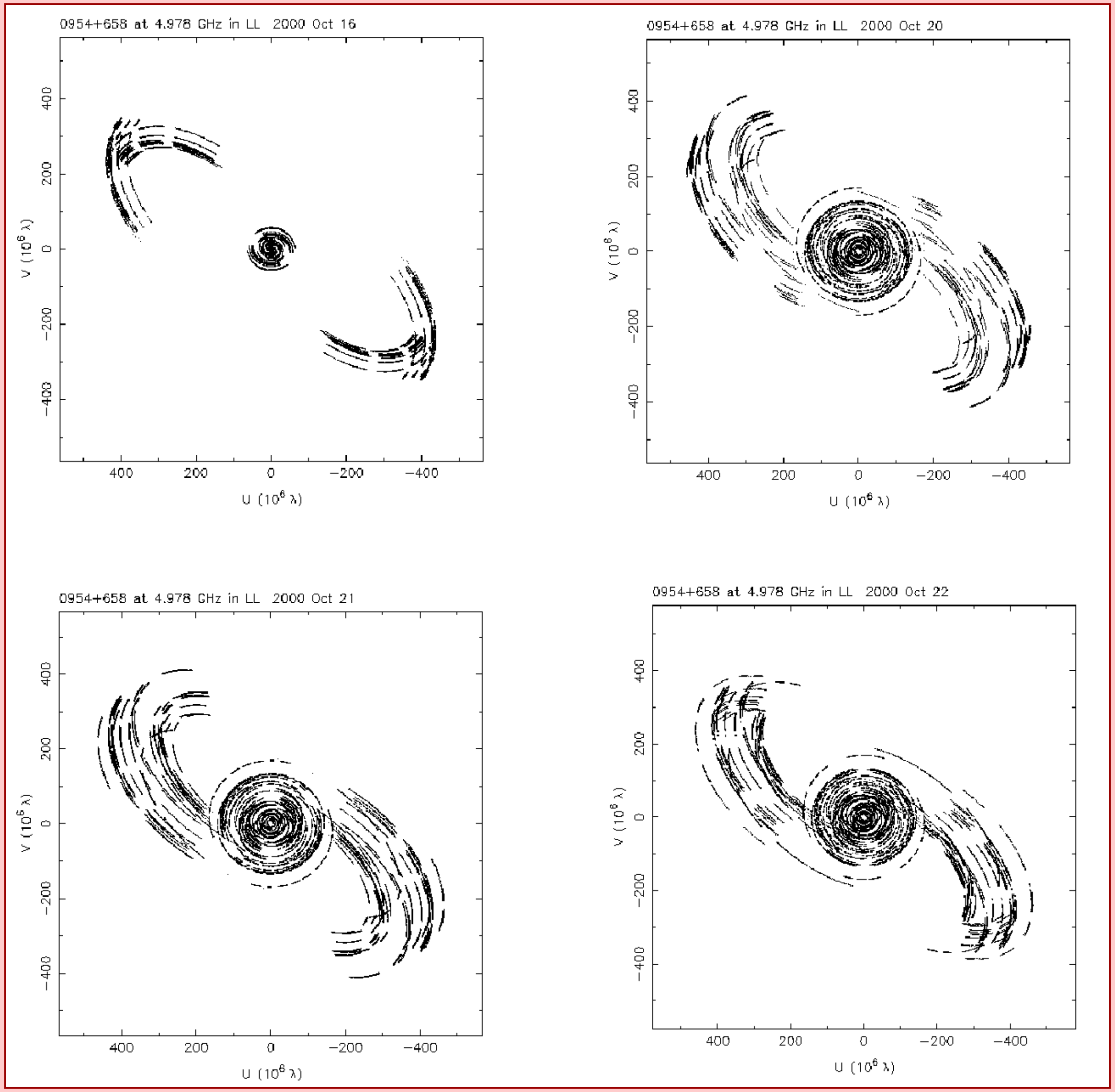

21-10-00

22-10-00

Maps of total and polarized intensity

Beamsize ~ (1 x 0.5) mas
Peakflux in mJy/beam

Epoch	I_{core} [mJy]	I_{jet} [mJy]	ΣI [mJy]	I_{EB} [mJy]
1	332 ± 33	31 ± 3	363	
2	363 ± 36	46 ± 5	409	437
3	379 ± 38	49 ± 5	428	436
4	373 ± 37	50 ± 5	423	[456]

Epoch	P_{core} [mJy]	P_{jet} [mJy]	m_{core} [%]	m_{jet} [%]
1	8.5 ± 0.9	1.1 ± 0.1	2,5	5
2	10.8 ± 1.1	2.9 ± 0.3	3	6,5
3	9.9 ± 1.0	2 ± 0.2	2,6	4,1
4	11.8 ± 1.2	3.2 ± 0.3	3,2	6,4

Epoch	PA_{core} [°]	PA_{jet} [°]
1	75 ± 12	-29 ± 12
2	90 ± 12	-34 ± 12
3	89 ± 13	-35 ± 13
4	88 ± 10	-37 ± 10

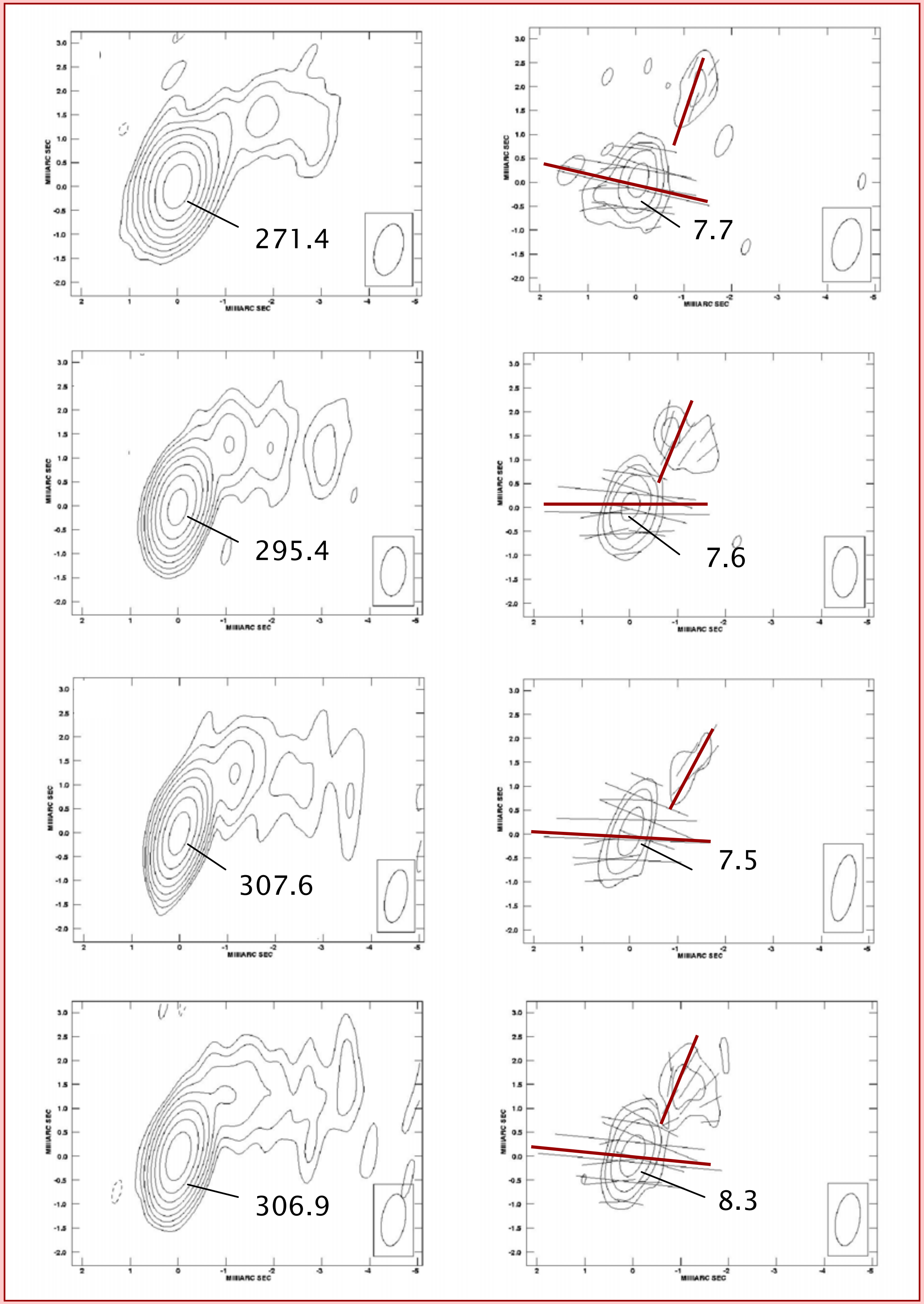

Polarization maps

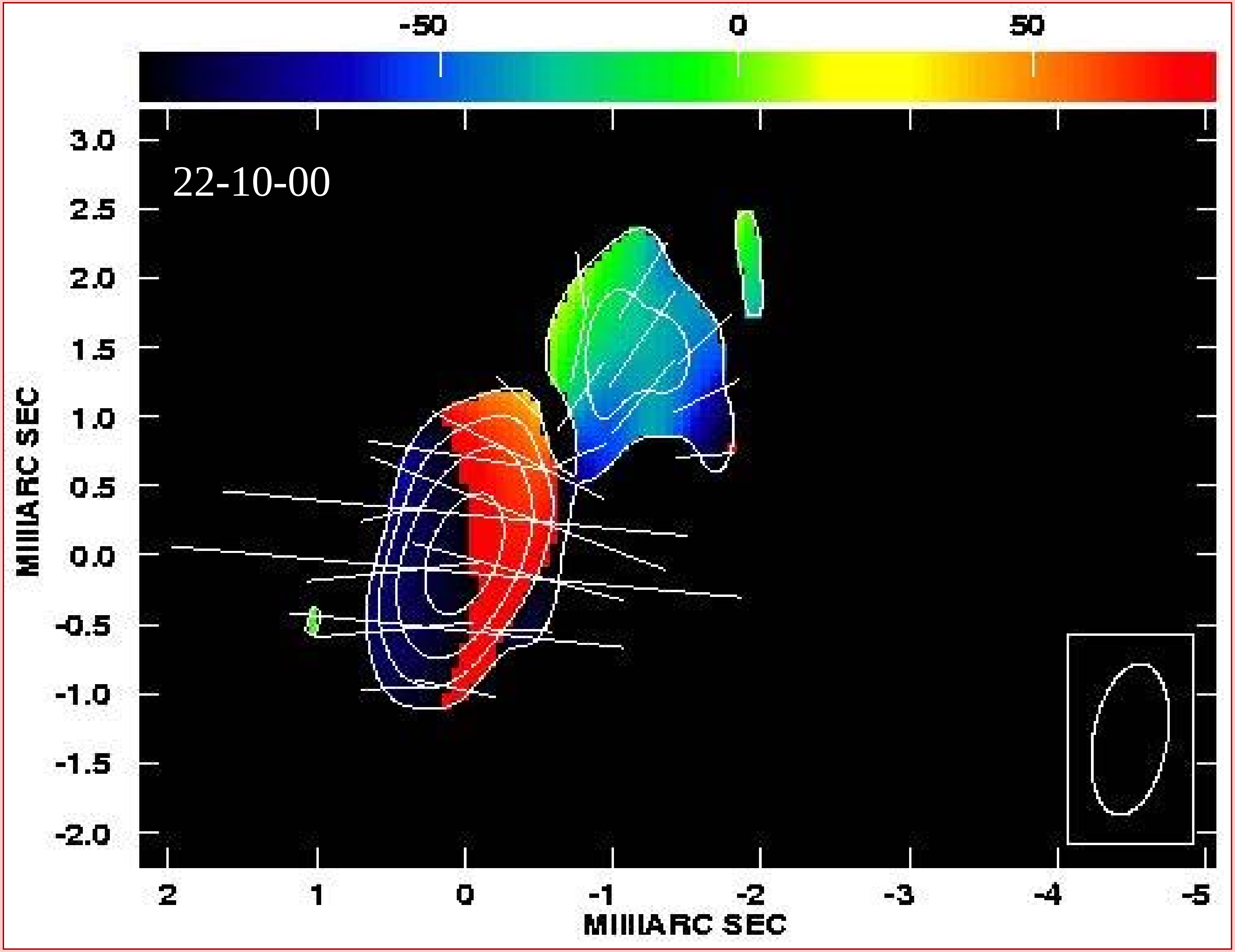

High-resolution maps of total and polarized intensity

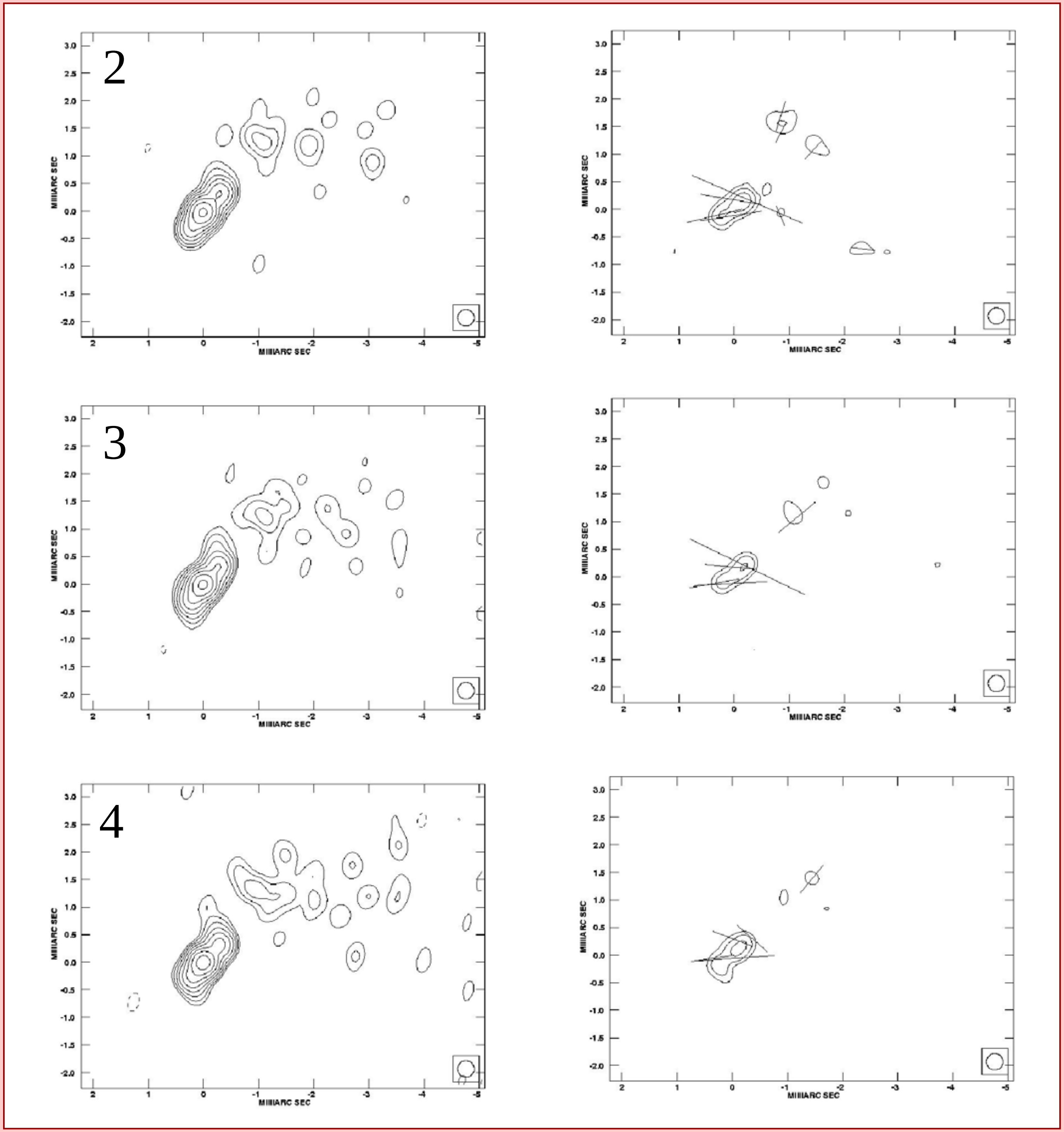

beamsize (0.3 x 0.3) mas

High-resolution polarization maps

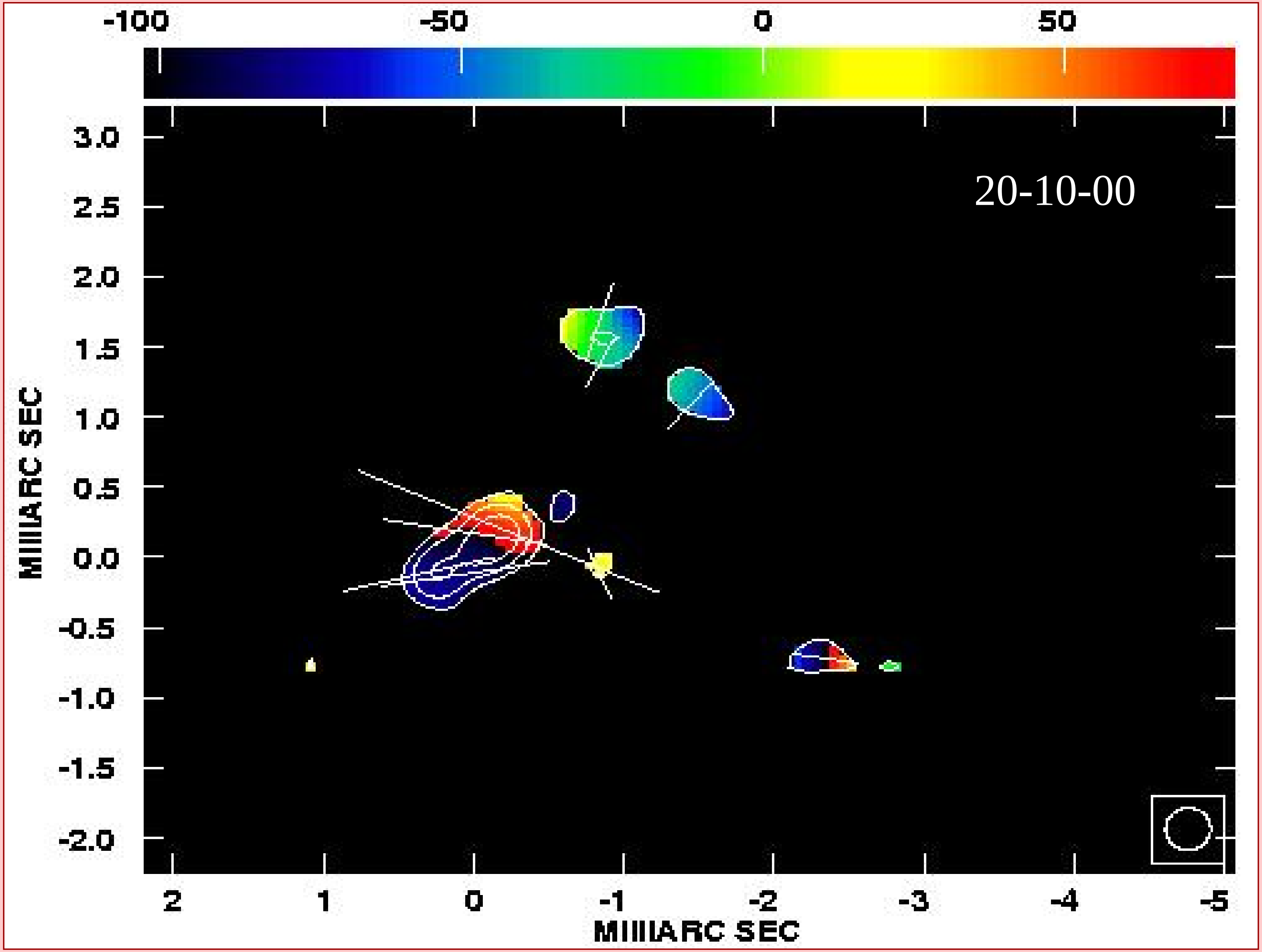

Intensity profiles of the high-resolution maps

Epoch	I_{core} [mJy]	$I_{0.5\,mas}$ [mJy]	P_{core} [mJy]	$P_{0.5\,mas}$ [mJy]
2	302.5 ± 30	66 ± 6.6	3.9 ± 0.4	6.8 ± 0.7
3	313 ± 31	71 ± 7.1	3.6 ± 0.4	6.7 ± 0.7
4	310 ± 31	68.5 ± 6.9	3.8 ± 0.4	7.5 ± 0.8

Epoch	Σ I [mJy]	Σ P [mJy]
2	368.5	10,7
3	384	10,3
4	378.5	11,3

Epoch	m_{core} [%]	$m_{0.5\,mas}$ [%]	PA_{core} [°]	$PA_{0.5\,mas}$ [°]
2	1,3	10,3	-84 ± 12	63 ± 12
3	1,1	9,4	-86 ± 13	57 ± 13
4	1,2	11	-85 ± 10	57 ± 10

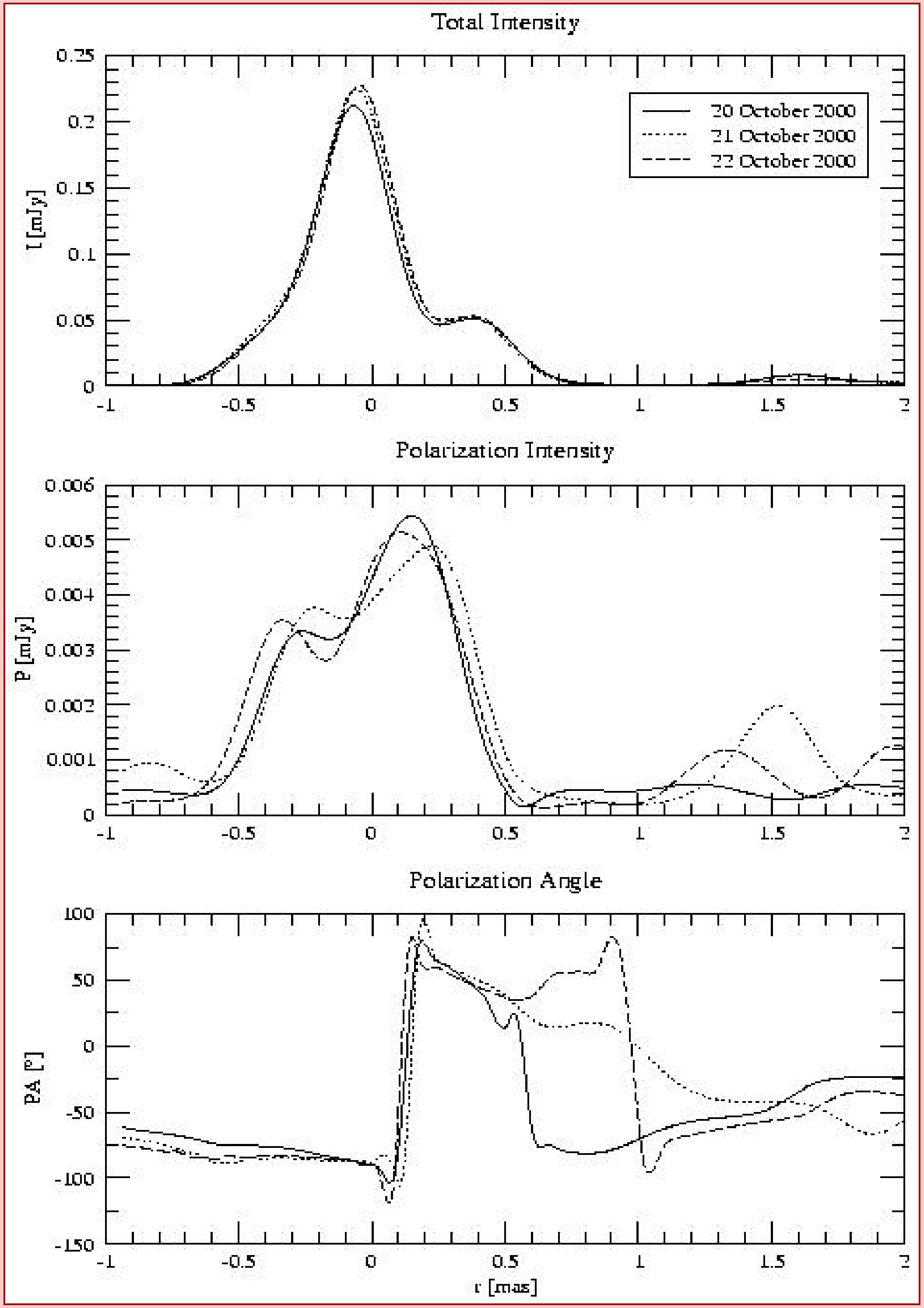

Parametrization with Gaussian components

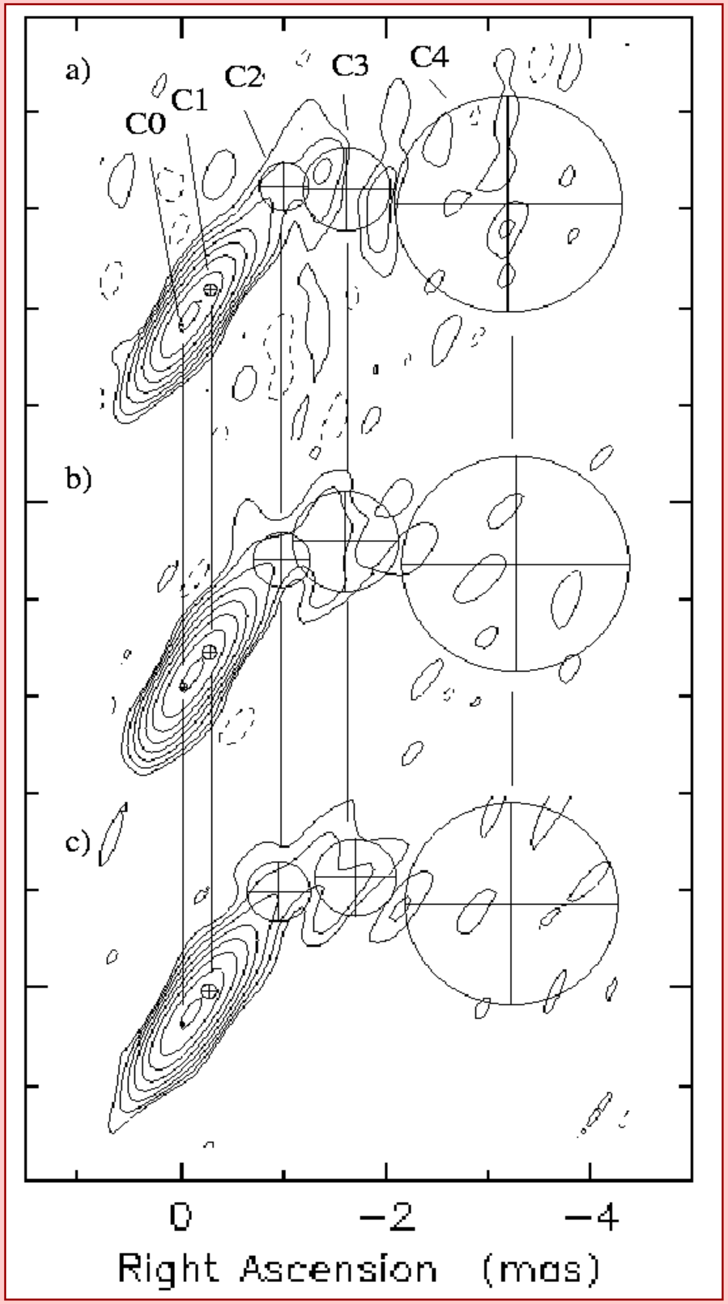

0954+658 model fit components C0 to C5

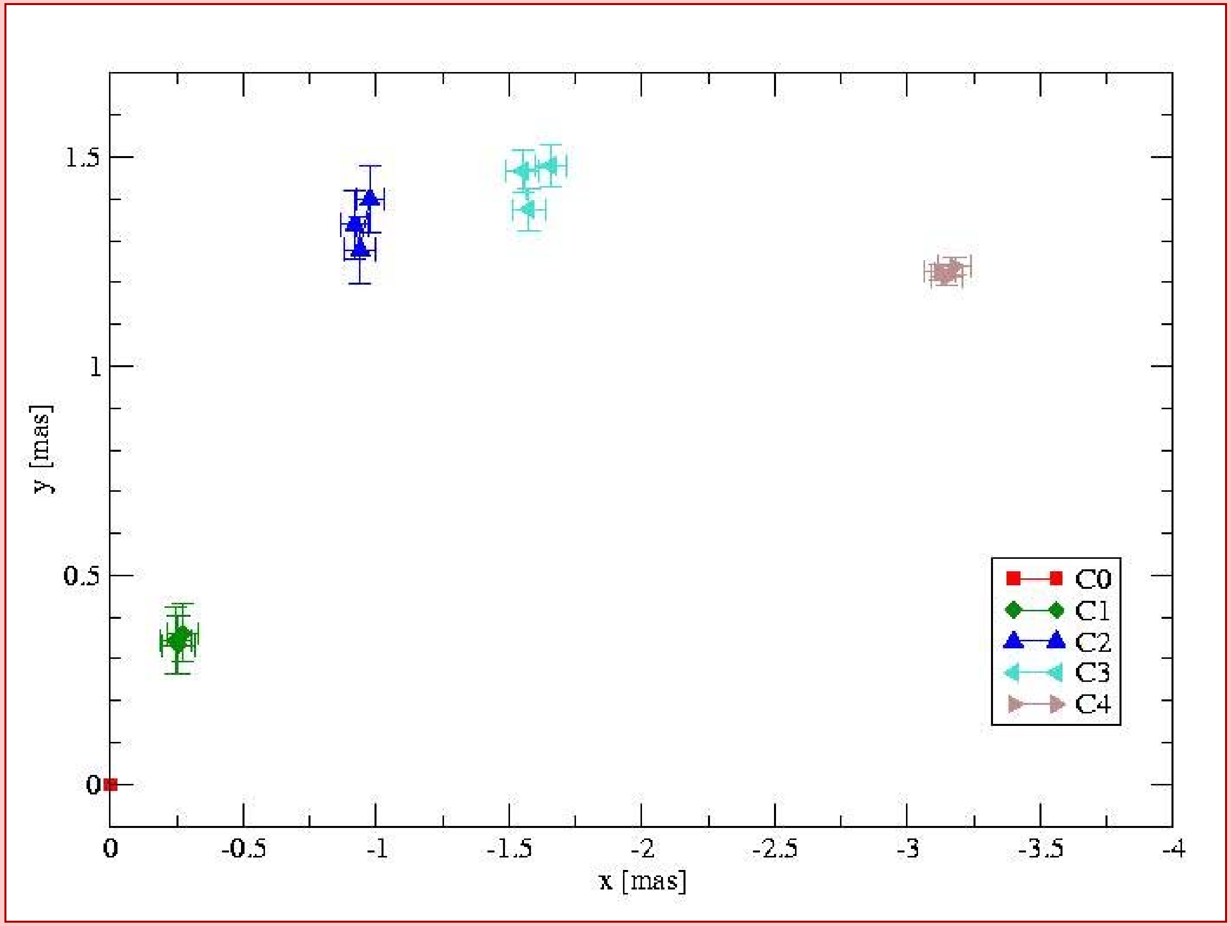

Long-term kinematic studies

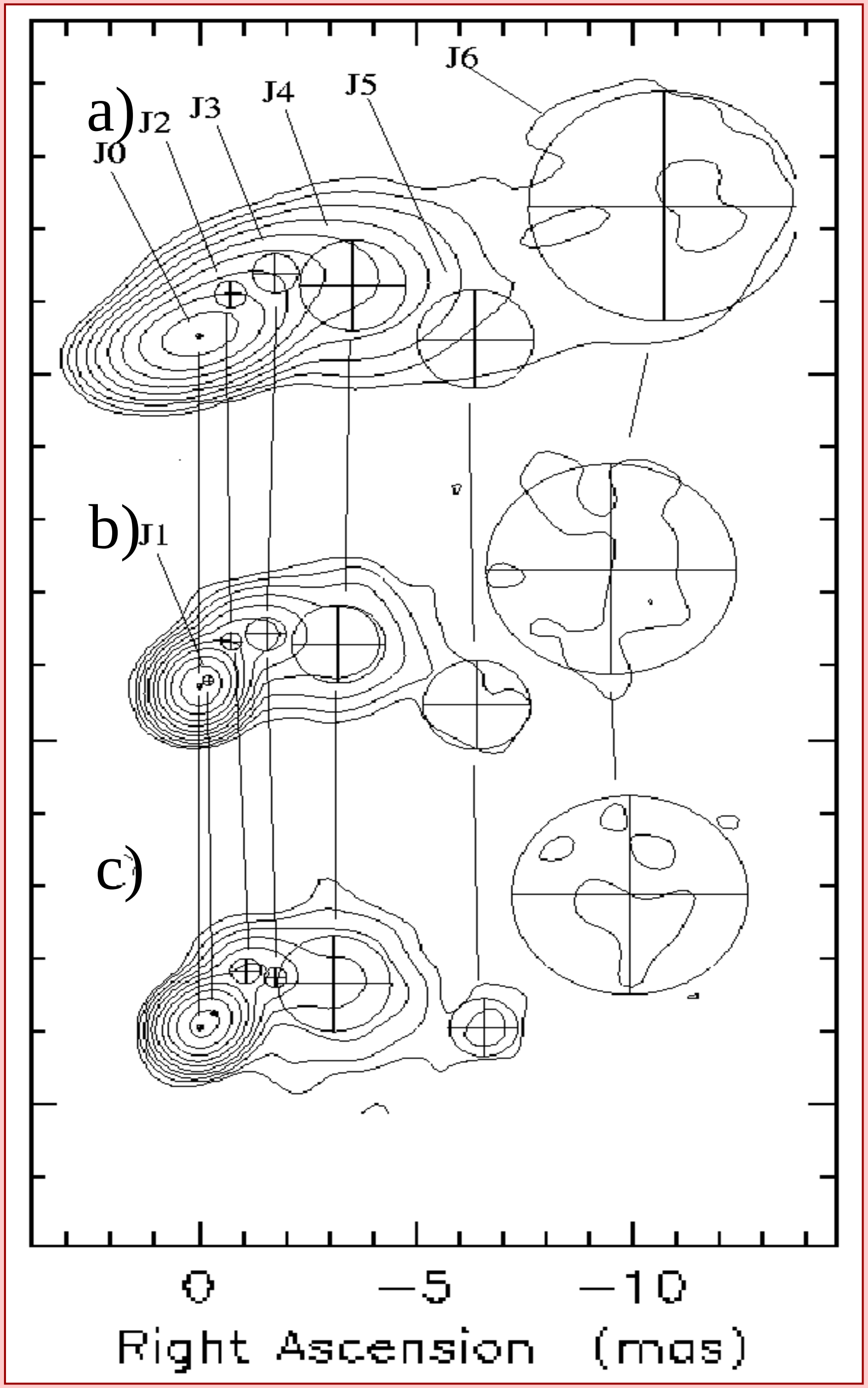

5 GHz VLBI observations from
a) 20-11-1999,
b) 06-03-2000 and
c) 20-11-2000

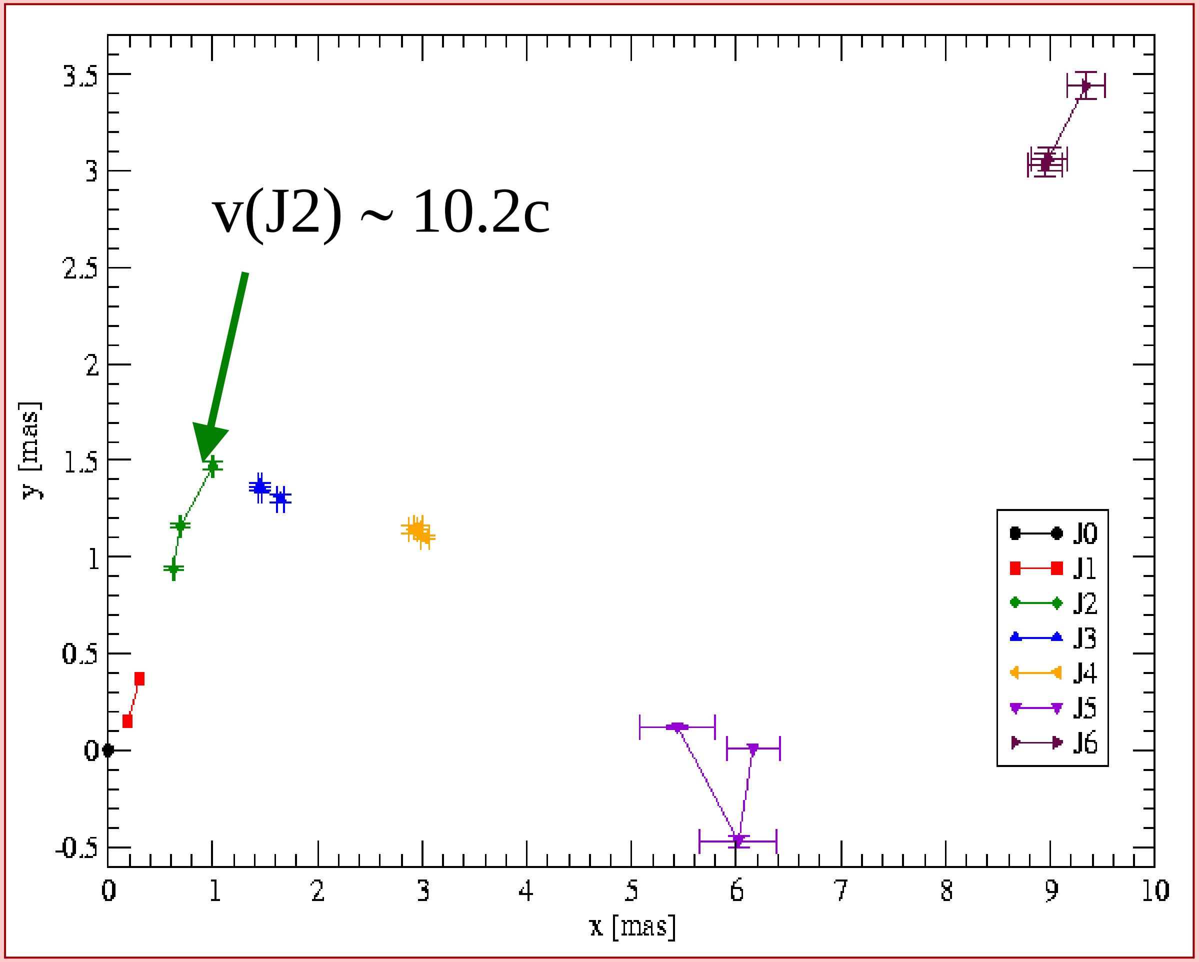

Summary

- No changes in total and polarized intensity between the observed epochs (within a few days), no changes in the PA

- Detection of superluminal (10c) component at 0.8 mas

- Space array maps show multi-component structure of the EVPA in the core region

- High-resolution maps resolve core region into two to three components in total intensity and in polarization intensity

- Inner jet higher polarized (6 %) than core (3 %)

- EVPA follows the strongly bent helical jet axis

- EV perpendicular to jet ridge line suggesting magnetic field parallel to jet axis

- New jet component ejected between November 1999 and March 2000

Update on the VLBA campaign observations

Tuomas Savolainen
Tuorla observatory

VLBI

- Provides the best obtainable angular resolution in astronomy (0.08 mas at 3 mm with the VLBA, 0.05 mas with the global array)
- Excellent tool for investigating blazar jets:
  - Compact emission => high brightness temperatures
  - Possible to follow changes in the jet structure (superluminal motion)
- Most of the past VLBI observing campaigns have been done using only one or two frequencies

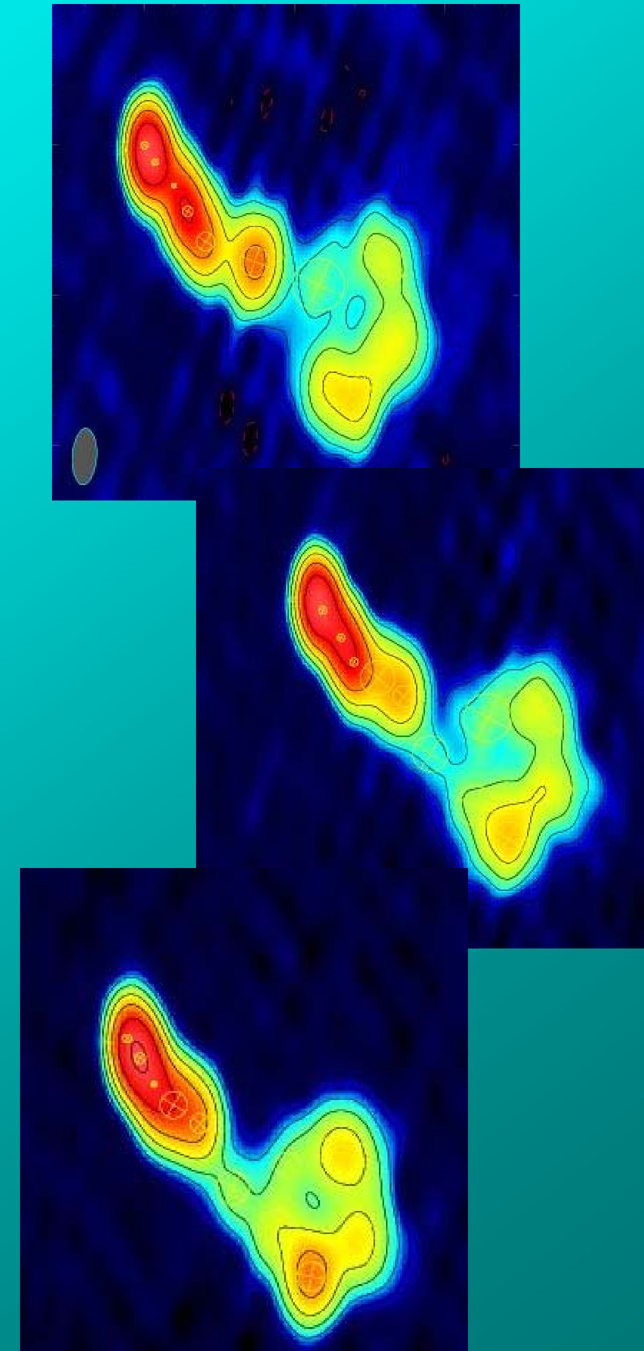

Possibilities of multi-frequency polarimetric VLBI monitoring as a part of large multi-frequency campaigns (e.g. ENIGMA campaings)

- VLBA monitoring allows several physical parameters of the jet to be constrained: Γ,θ,D
  - –From β_{app} we can directly obtain a lower limit for Lorentz factor Γ and an upper limit for the angle between the jet and our line of sight θ.
  - – If suitable variability data exists, it is possible to estimate a variability brightness temperature. $T_{b,Var} \propto D^3$, while the VLBI brightness temperature, $T_{b,VLBI} \propto D$. Hence, by combining VLBI and variability data, it is possible to get the Doppler factor of the source (but remember errors...)
  - –If we know β_{app} and D, it is possible to solve for Γ and θ.
- VLBI data can provide constraints on parameters that are important for the SED modelling.

• An example from 3C 273: apparent superluminal speed of $6.0h^{-1}c$ was measured for a component, ejected just before the INTEGRAL pointing in January 2003

=> $\Gamma_{min} = 8.5$ and $\theta_{max} = 13.7^{o}$ (for H_0 = 71 km/s/Mpc)

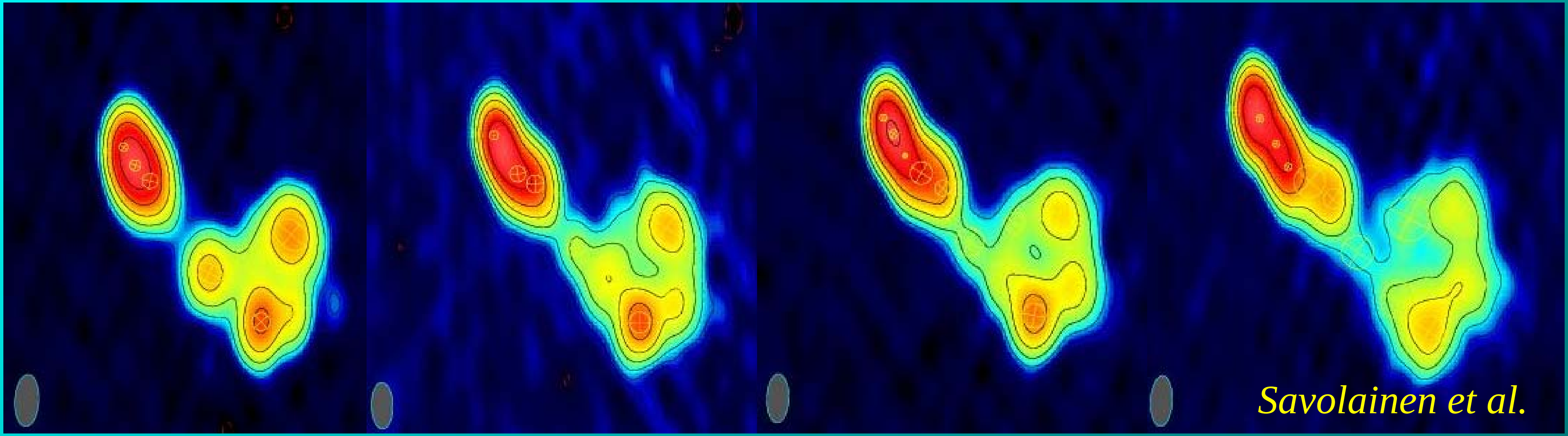

- Multi-frequency = multi-scale

  ⇒Better view of the source structure

- Spectral index maps and possibly ν_{max}-maps

PKS 2136+141 at different frequencies and in different scales

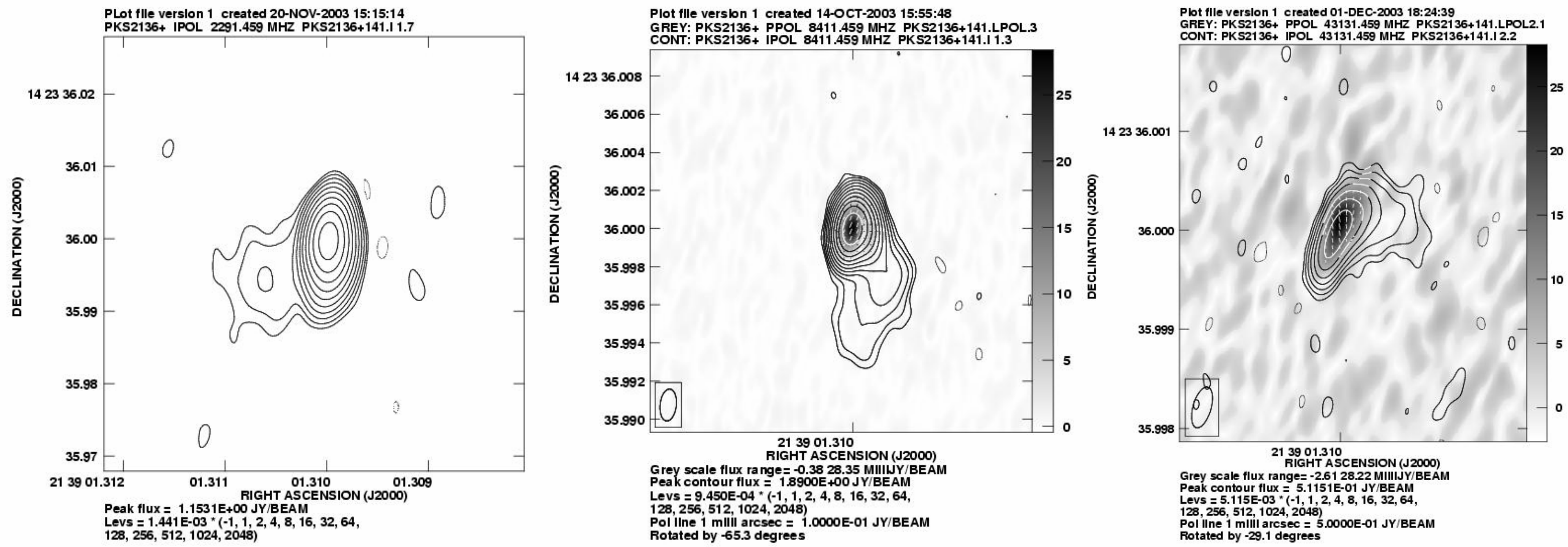

Savolainen et al., in preparation

Spectra of individual components

3C 273 observed with the VLBA on the 28th of February 2003. The map shows the inner 2 mas portion of the jet at 43 GHz.

Savolainen et al., in preparation

1) Description and evolution of the synchrotron spectra of individual components

=> Direct test for the shocked jet models

2) Order of magnitude estimate of the magnetic field strength, by using the spectral turnover and VLBI size, may be possible

VLBI polarimetry

- Potentially powerful diagnostic tool to investigate the physical properties of the jet
- Traditionally VLBI polarimetry has been difficult, but high performance level of the VLBA has changed this in the last ten years
- Usually VLBI polarimetry has been done at rather low frequencies => problem with Faraday rotation (RMs of several thousands measured for quasars, Zavala&Taylor 2003)

Multi-frequency VLBI polarimetry

- Allows one to correct EVPA for Faraday rotation => reveals intrinsic magnetic field direction!

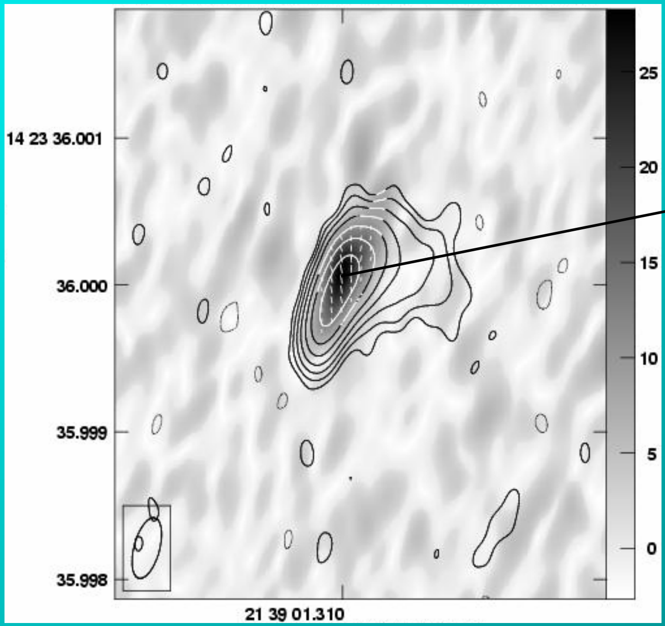

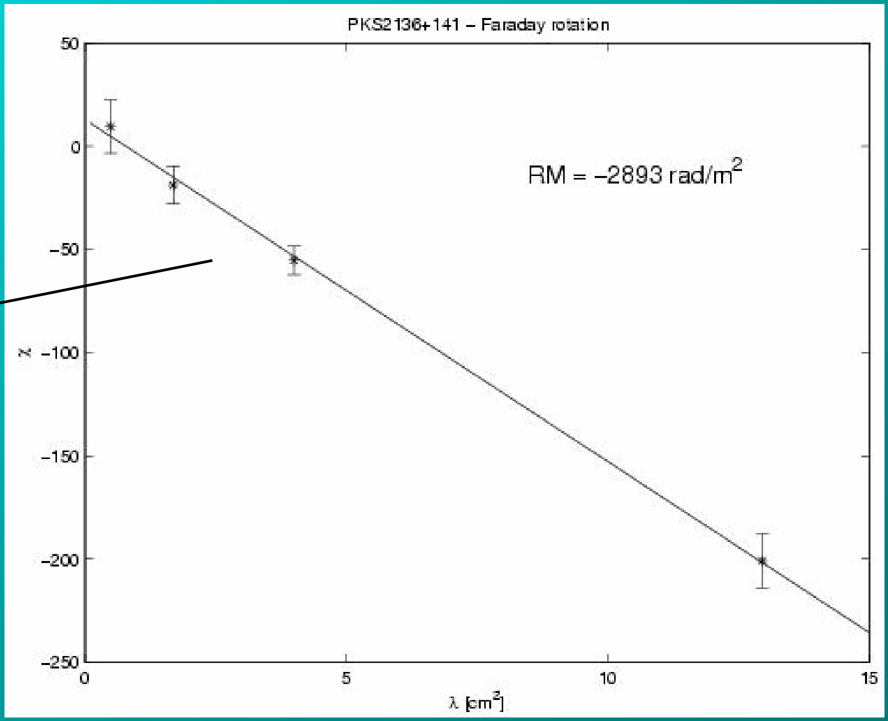

Savolainen et al., in preparation

- Fractional polarization as a function of frequency:
  - Strong suppression of polarization at lower frequencies in some sources (e.g. GPS/HFP)

• Intrinsic effect (synchrotron self-absorption)?
• Faraday depolarization by differential rotation along the line of sight within the source?
• Faraday depolarization by differential rotation across the beam size?

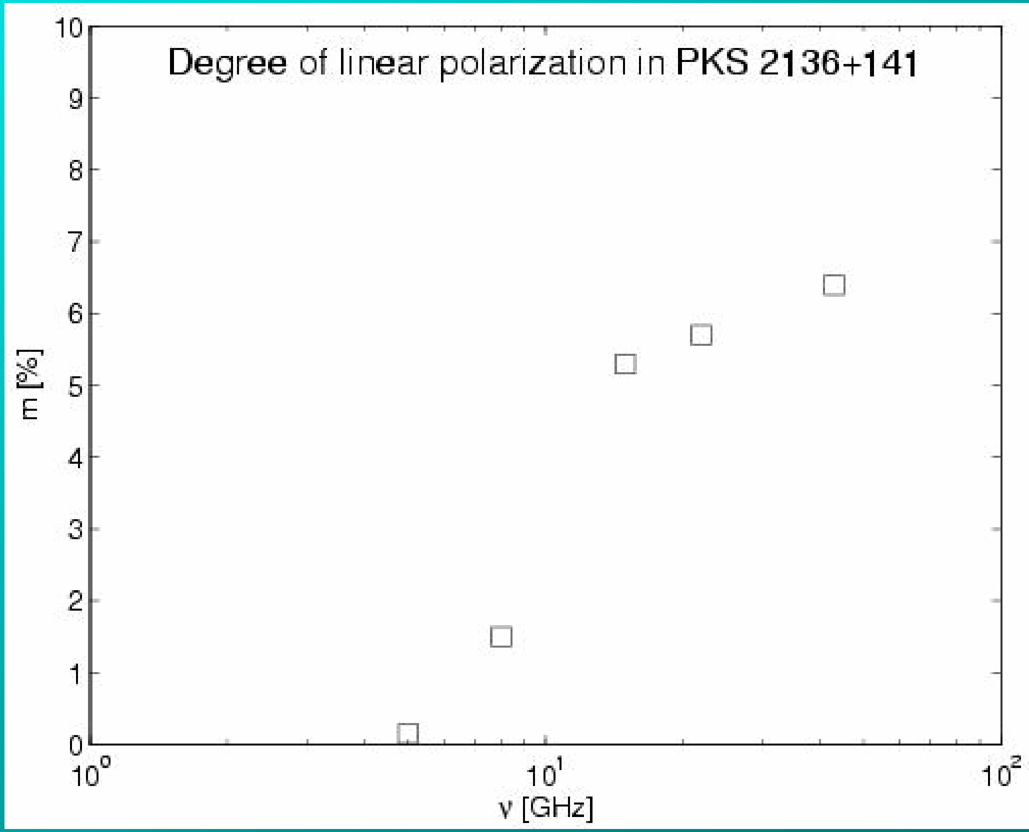

Savolainen et al., in preparation

Ongoing ENIGMA-related campaigns

- Multi-frequency VLBA observations of 3C66A, AO0235+164 and 0716+714
- A lot of VLBA time obtained by the Tuorla group (262 hours altogether) and by the Bonn group
- Anticipated results:
  - Multi-frequency maps at several epochs + spectral index maps
  - Description of component proper motions
  - Constraints for Γ, θ, D
  - Evolution of the spectra of individual components
  - Linear polarization corrected for Faraday rotation
  - Degree of linear polarization as a function of frequency for individual components

3C 66A

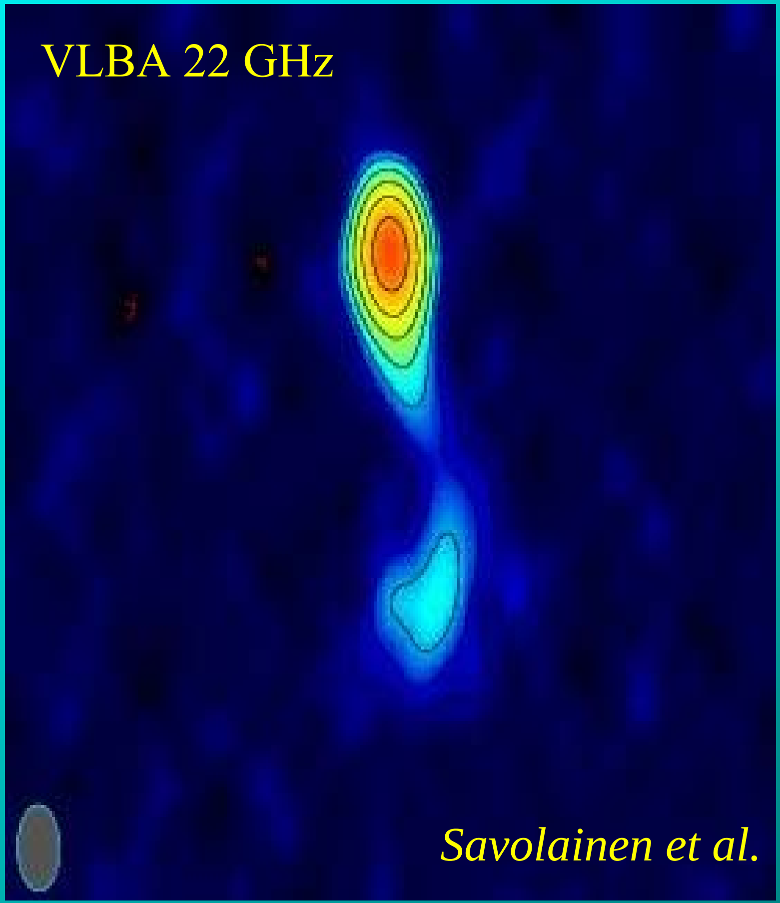

- 3C 66A is a highly variable intermediate BL Lac object showing high levels of optical and radio polarization and superluminal speeds up to $19h^{-1}c$
- Large multi-frequency campaign including RXTE and WEBT started in September 2003 (PI: M. Böttcher)

- 72 hours of VLBA time granted (9 epochs, high priority), observations are running (PI: T. Savolainen)
- Source has been observed on Oct 10, Oct 30, Dec 18 and Jan 28, next observation is in the dynamic queue waiting to be scheduled
- We have requested time interval of 45 days between the observations for the rest of the campaign

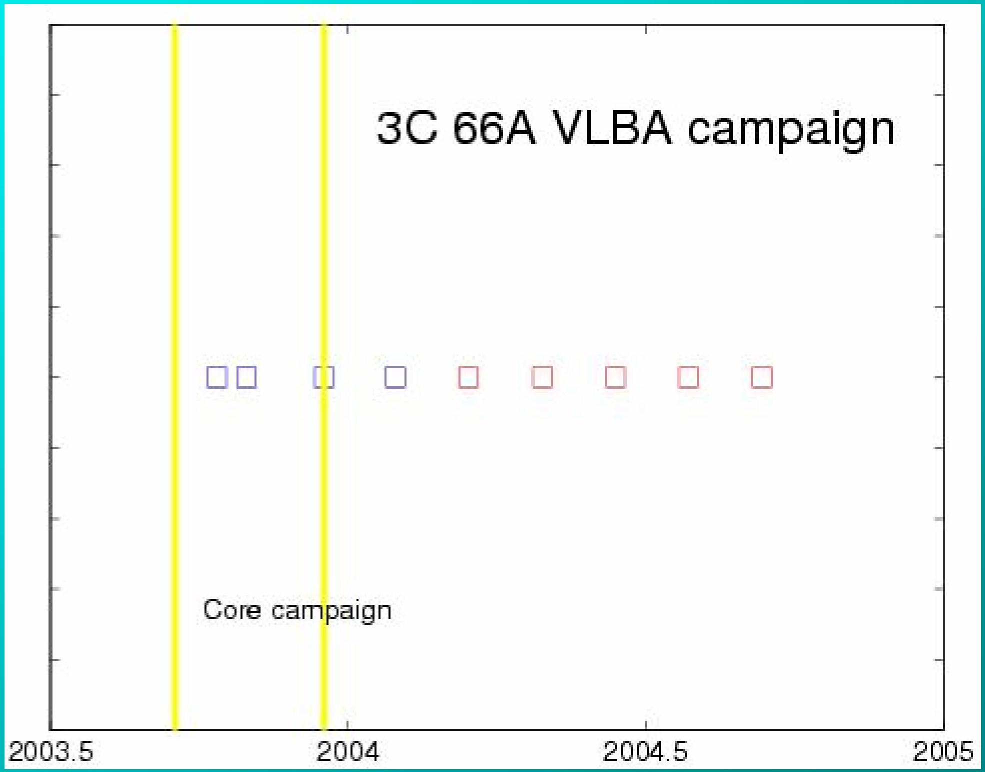

Blue squares: Observed
Red squares: Expected epochs in future

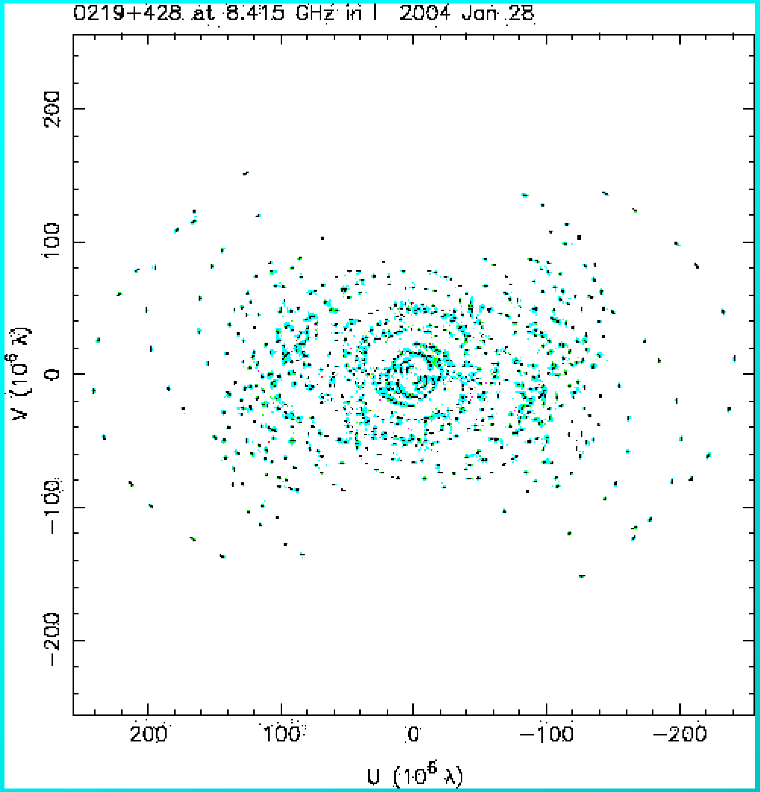

- Frequencies used: 2, 5, 8, 22, 43 and 86 GHz
- Polarization calibrators: 3C 454.3, 0420-014 (also fringe finder) and OJ287

AO0235+164

- Highly variable blazar, possibly showing a 5-yr periodicity in its optical light curve
- Large ongoing multi-frequency campaign including XMM-Newton and WEBT (PI: C. Raiteri)
- 135 hours of VLBA time granted (15 epochs, high priority), observations are running (PI: K. Wiik)
- Source has been observed on Jan 10 and Feb 17, next observation is in the dynamic queue waiting to be scheduled
- Frequencies used: 2, 5, 8, 15, 22, 43 and 86 GHz
- Polarization calibrators: 3C 454.3, 0420-014 and OJ 287

- Complicated structure: 7mm VLBA images reveal bent trajectories towards position angles –30º **and** +10º (Jorstad et al. 2001)
- Variable EVPA: from χ=39º to χ=110º at 5GHz (Gabuzda et al. 1989)
- Large superluminal speeds: up to 30 $h^{-1}c$
- Proposed helical jet model (Ostorero et al. 2004)

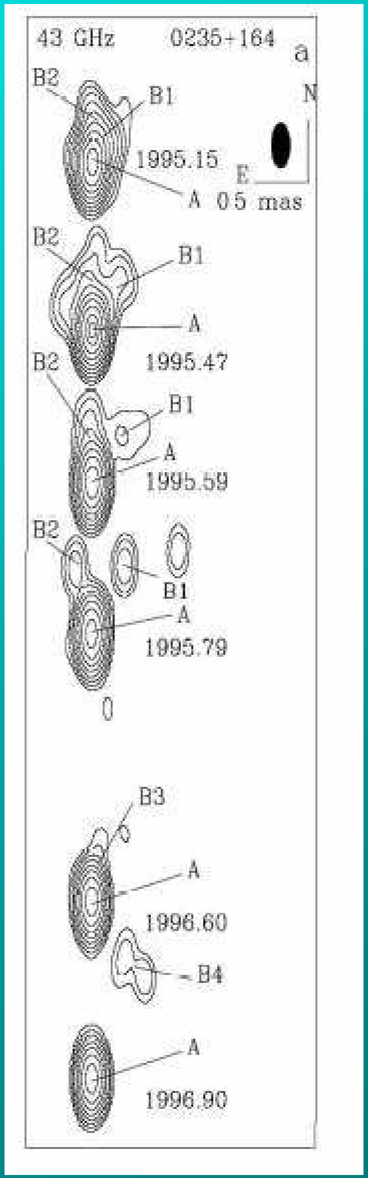

Jorstad et al. 2001

0716+714 in outburst

- IDV source
- Large outburst in late 2003
  - Multi-frequency campaign was activated
  - INTEGRAL observed source in November
- New brightening in March
  - Historical maximum at optical (R=12.1)!
  - INTEGRAL (Pian) and RXTE TOOs

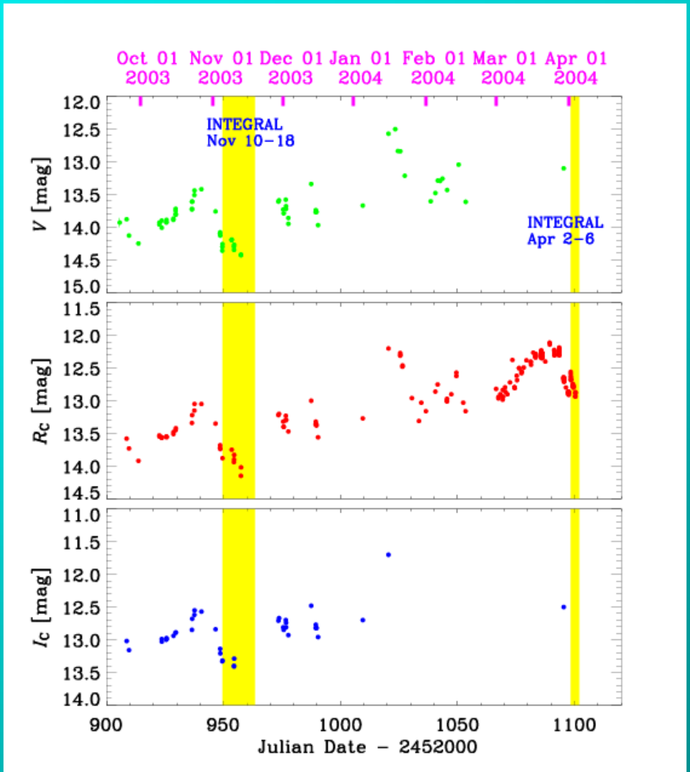

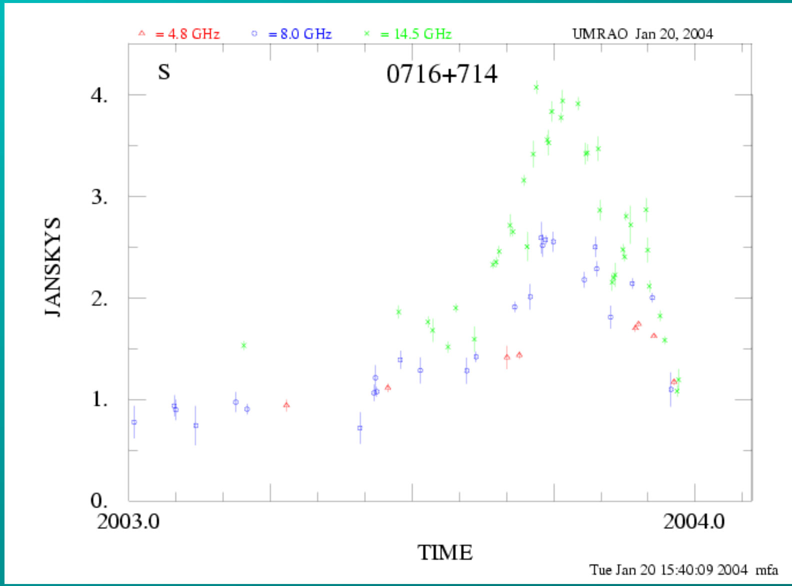

Optical data by WEBT and radio data by UMRAO

VLBA campaign of 0716+714

- On the 6th of November, a VLBA TOO at 3mm by Wiik et al. (10 hours, BW73)
- On Nov 11-16, VLBA TOO by Krichbaum et al. (BK106) – concurrent with the INTEGRAL
- 5-epoch VLBA follow-up by Wiik et al. (BW72)
  - multi-frequency (1.6, 5, 22, 43 and 86 GHz) + polarimetry
  - first epoch on Feb 10, next one is in the queue
- Global 3mm VLBI session by Bach et al. on April and October 2004
- Proposed 12-epoch follow-up with the VLBA after BW72 by Friedrichs et al.

The Overview from Apostolos Mastichiadis can be found in the following link:
http://www.to.astro.it/blazars/proc_t21.html

Task 6: The power of jets

⓿ What is the power of jets?
❶ How to transform bulk kinetic energy of jets into radiation?
❷ The relationship of jet power and accretion power
❸ The origin of FRI-FRII dichotomy

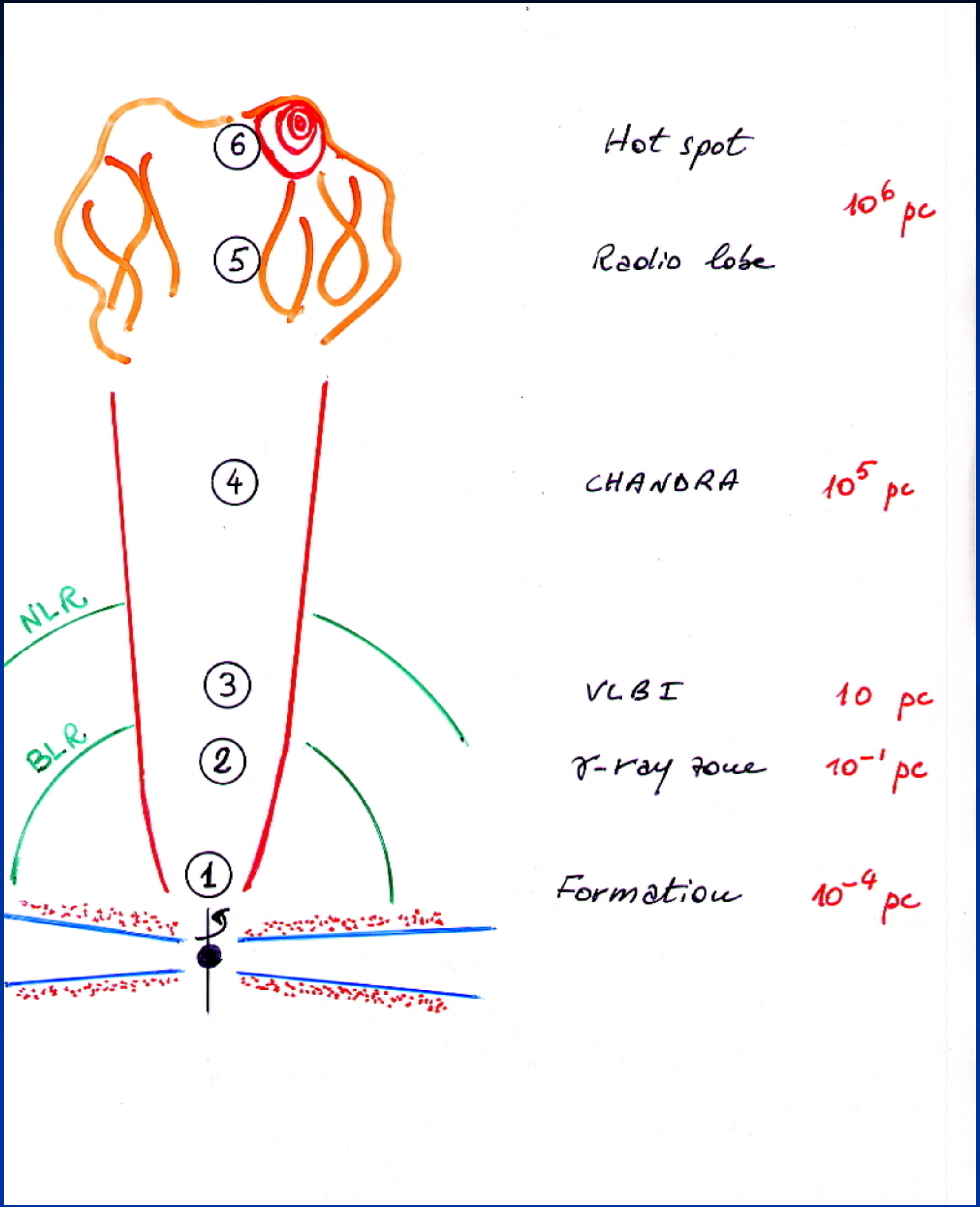

Equal power at all scales?

"Adiabatic jets"?

Is number of particles conserved?

Jet vs disk power

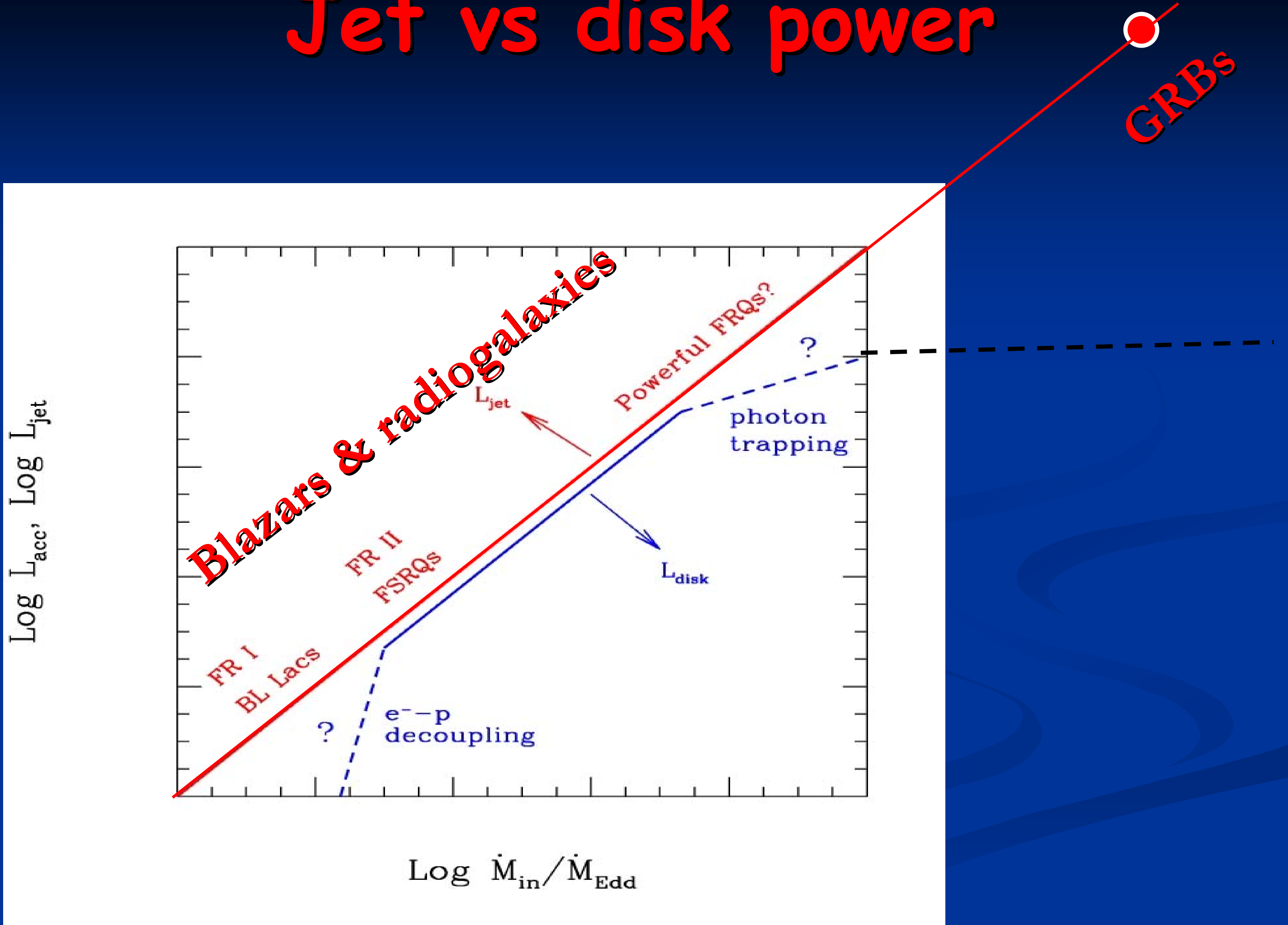

Structured jets: fast spine + slow layer

GG, Tavecchio & Chiaberge

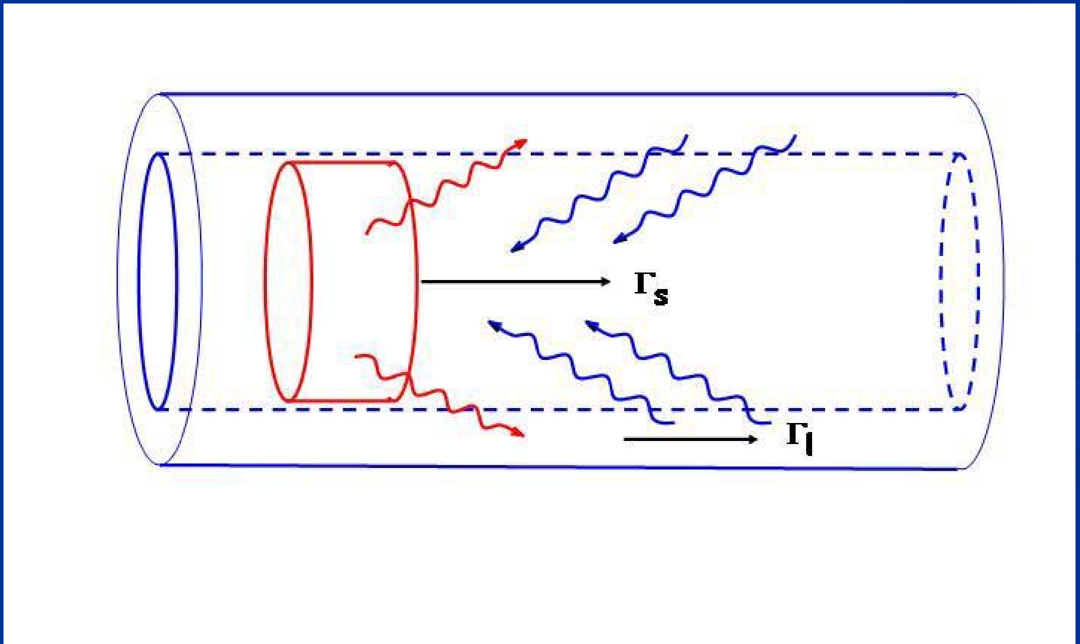

TeV BL Lacs

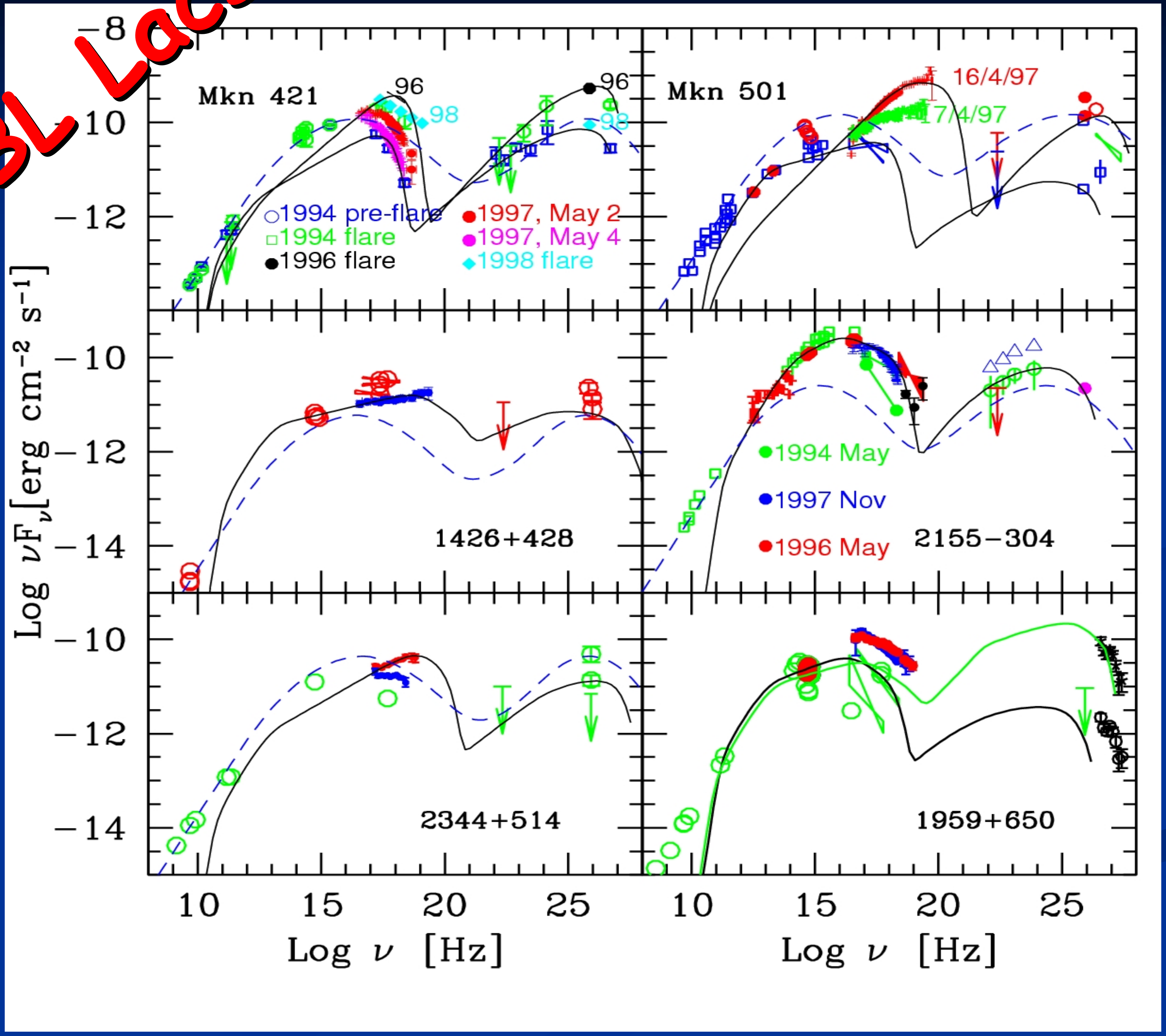

Mkn 421
96
98
96
98
1994 pre-flare
1994 flare
1996 flare
1997, May 2
1997, May 4
1998 flare
Mkn 501
16/4/97
17/4/97
1426+428
2155−304
1994 May
1997 Nov
1996 May
2344+514
1959+650
Log νF_ν[erg cm^-2 s^-1]
Log ν [Hz]

Fitting TeV BL Lacs with one-zone SSC we find:

The smallest B-fields wrt equipartion with emitting electrons (B~0.01-0.1 G)

The fastest jets in the γ-ray emission region (Γ~20-40)

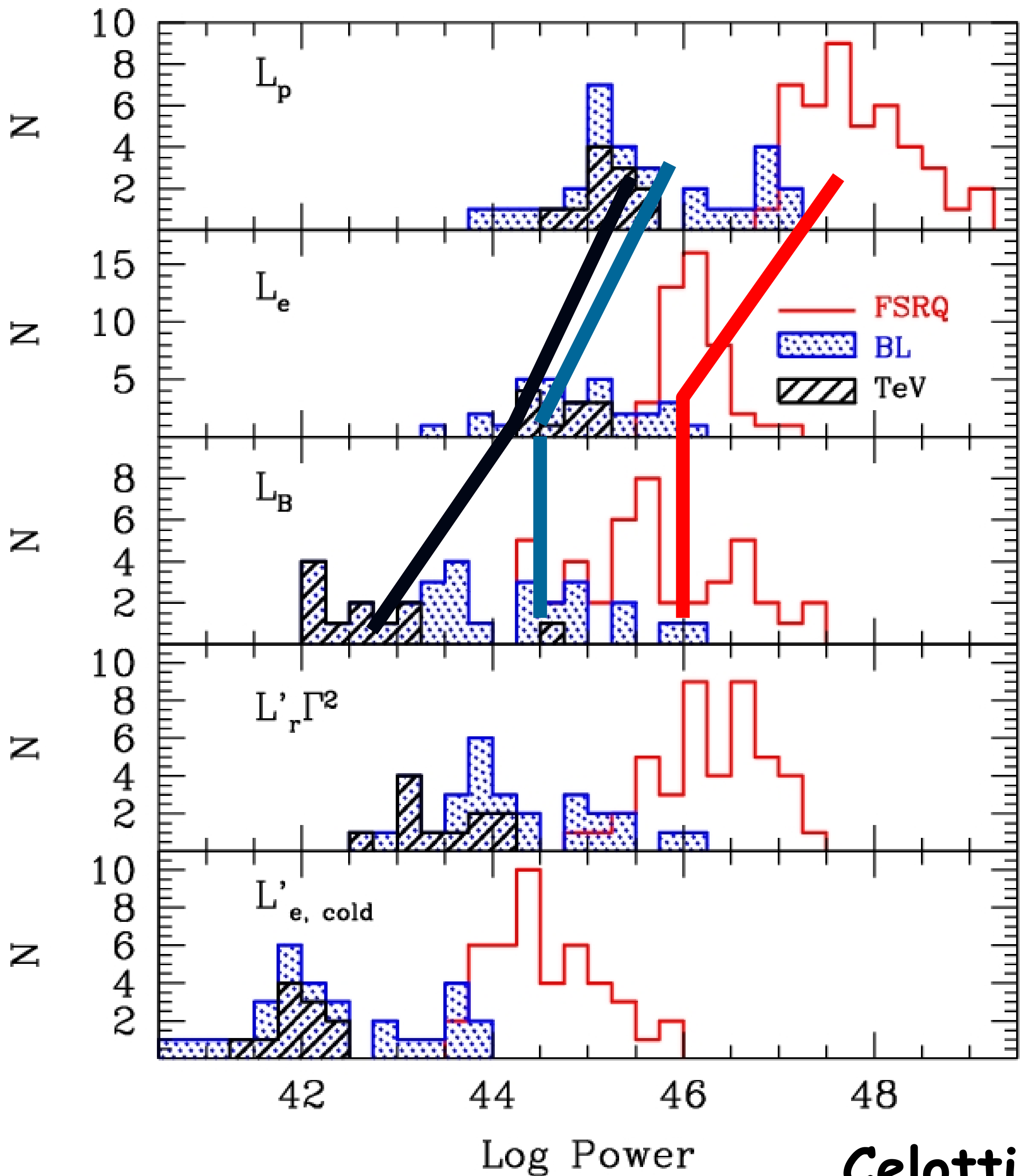

Protons (1 proton per emitting e-)

Relat. Electrons

B-field

Radiation

Cold elecrons

Celotti & GG in prep

Subluminal motion for all TeV sources?

Piner & Edwards, 2004, ApJ, 600, 115

Mkn 421	$\beta_{app} \sim 0.04 – 0.18 (+-0.06)$
Mkn 501	$\beta_{app} \sim 0.05 – 0.54 (+-0.15)$
1959+650	$\beta_{app} \sim 0$
2155-304	$\beta_{app} \sim 4.4 (+-2.9)$
2344+514	$\beta_{app} \sim 0 – 0.5 (+-0.5)$

Limb bri… ?

Giroletti et al. 2004, ApJ, 600, 127

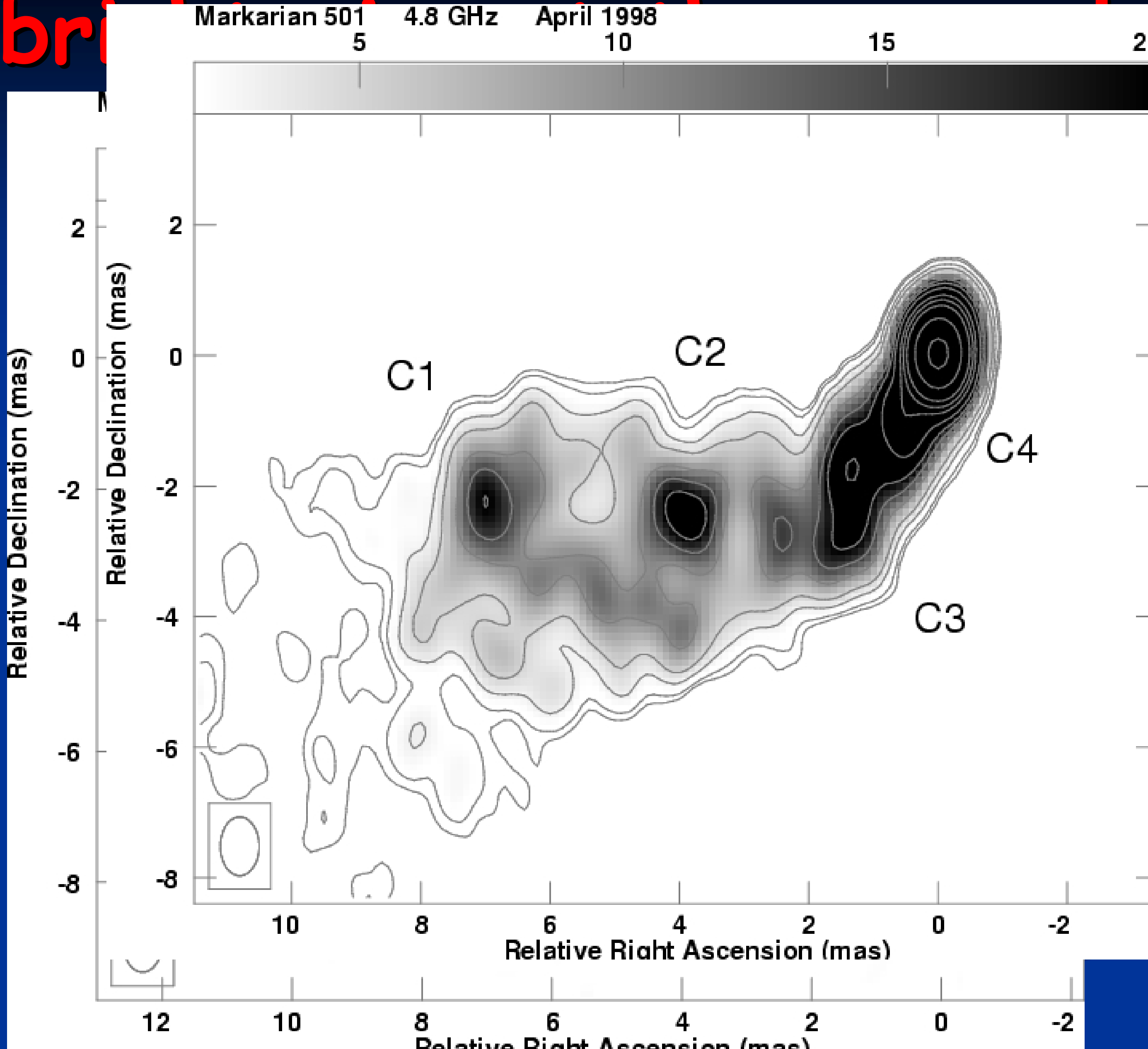

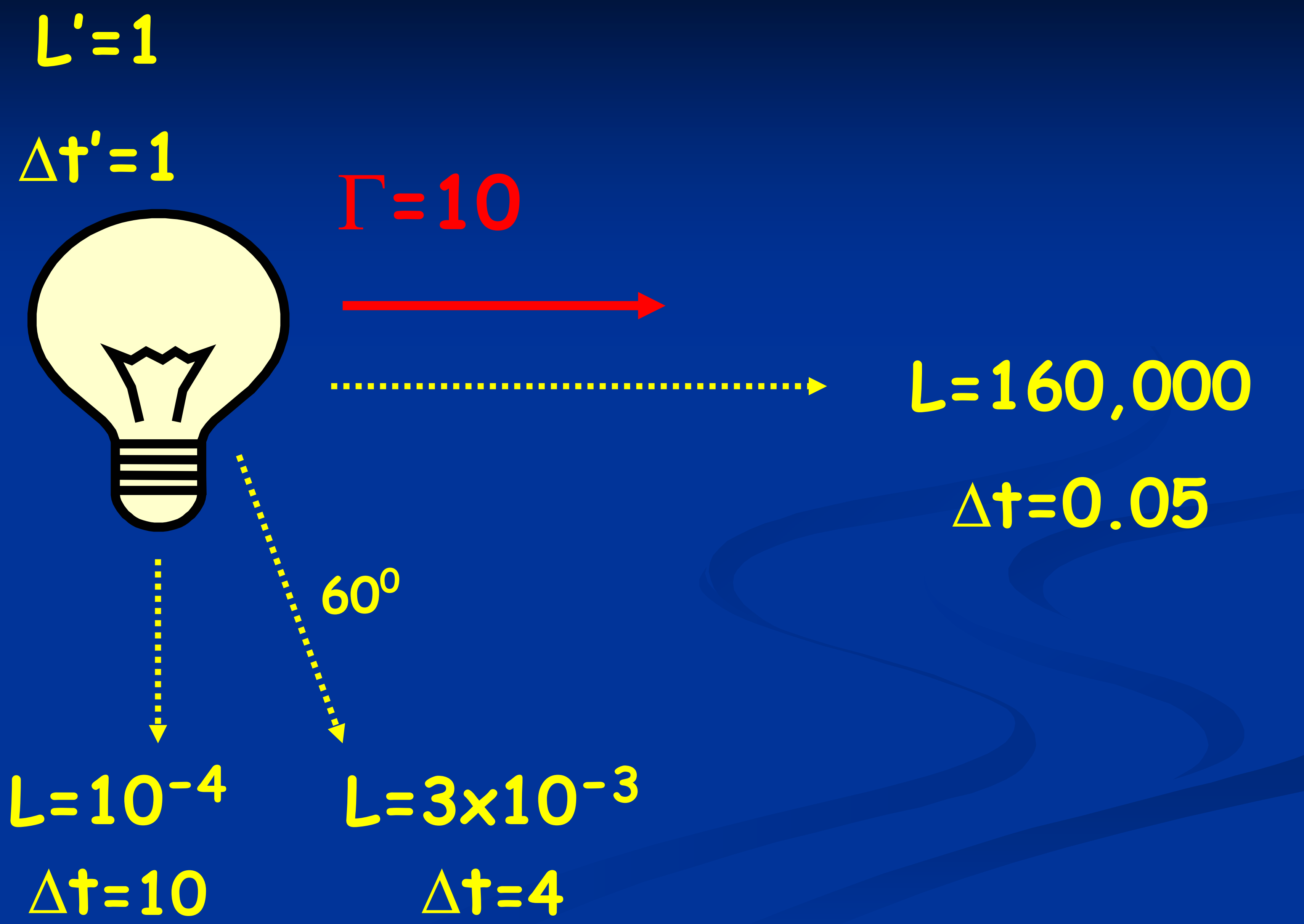

L'=1
Δt'=1
Γ=10
L=160,000
Δt=0.05
60⁰
L=10⁻⁴
Δt=10
L=3x10⁻³
Δt=4

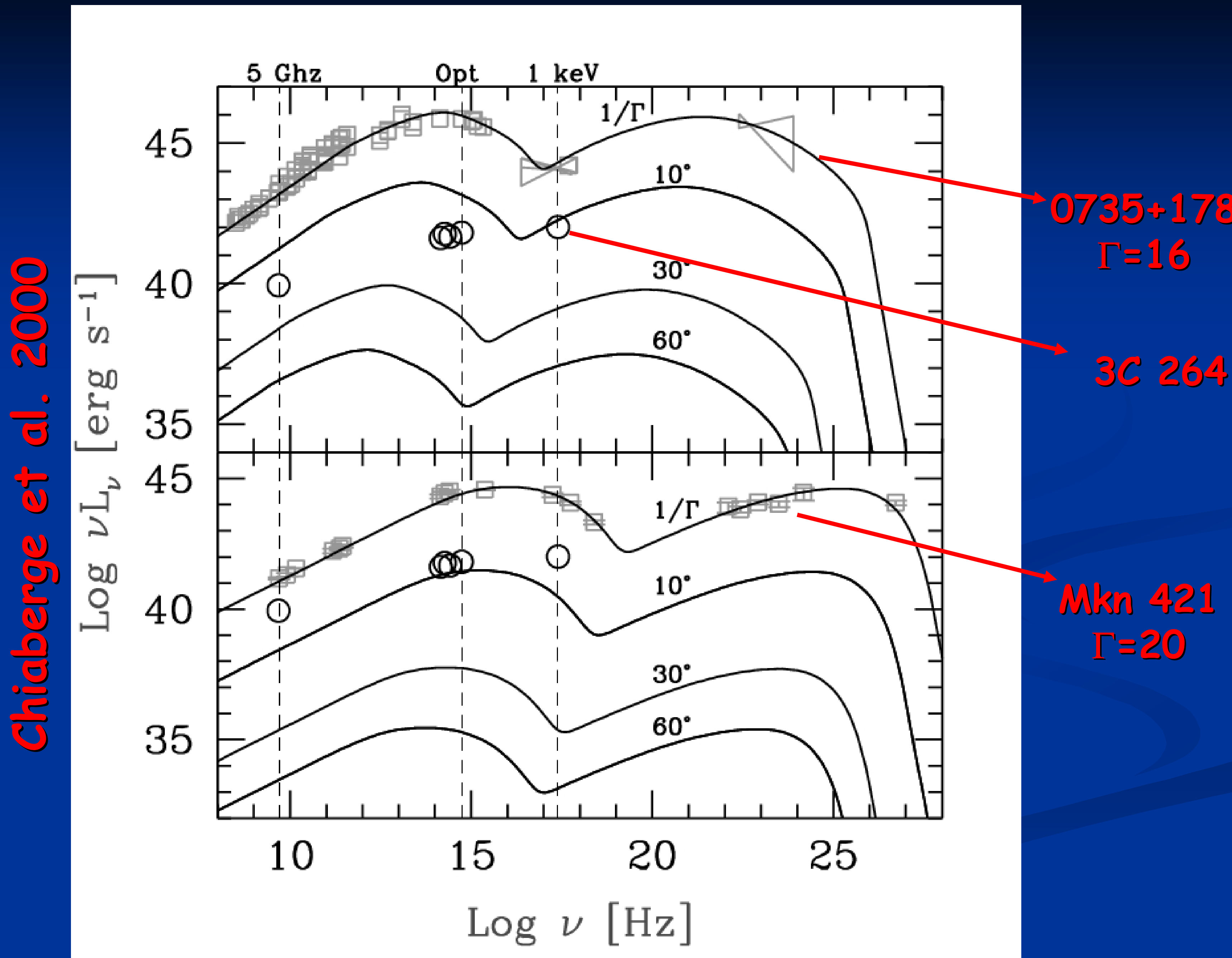

Chiaberge et al. 2000
5 Ghz
Opt
1 keV
1/Γ
10°
30°
60°
45
40
35
Log νL_ν [erg s^-1]
10
15
20
25
Log ν [Hz]
0735+178
Γ=16
3C 264
Mkn 421
Γ=20

BL Lacs at large viewing angles are not FR I… debeaming must be less than thought before…

Chiaberge et al. 2000

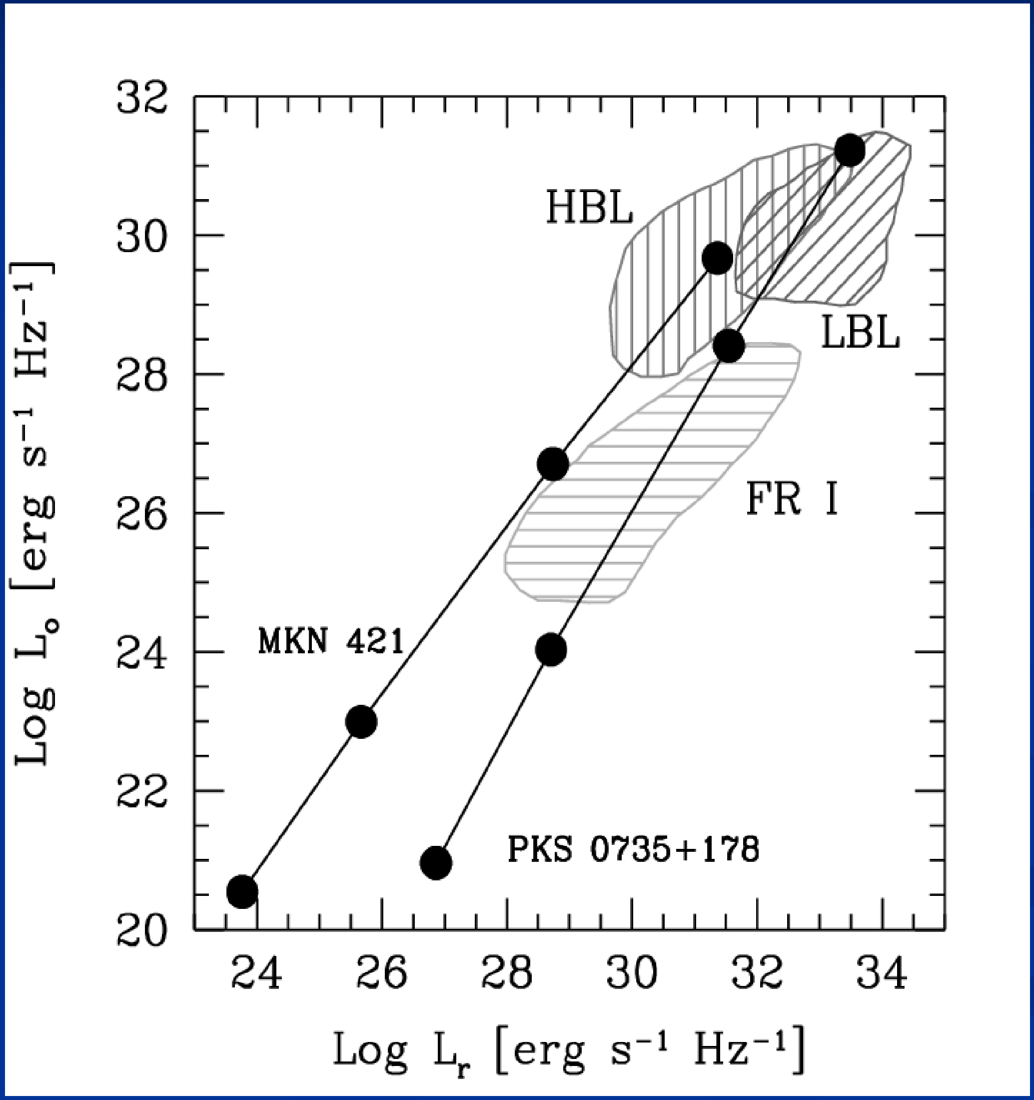

Cospatial fast spine & slow layer

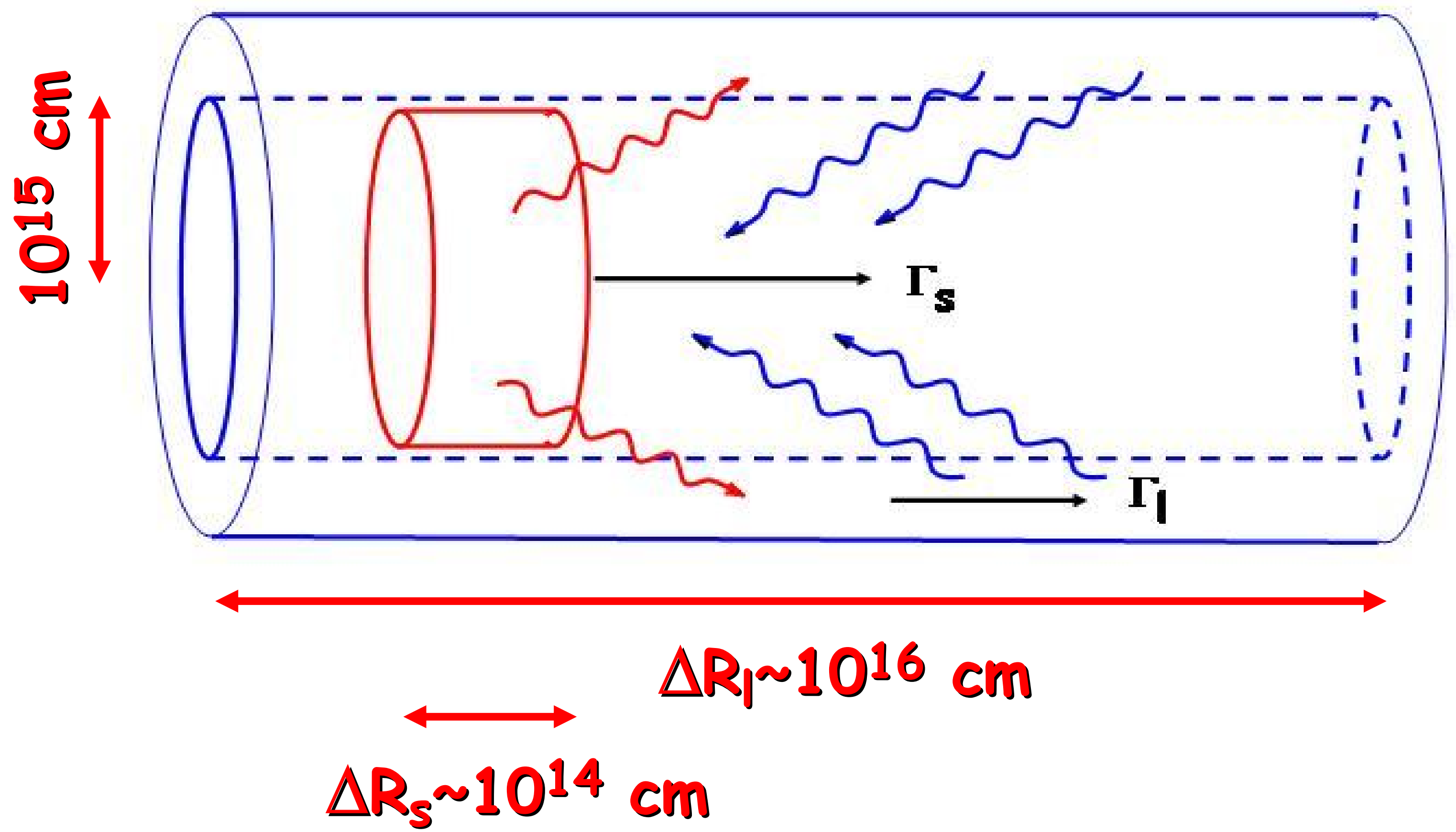

More seed photons for both

- $\Gamma' = \Gamma_{layer}\Gamma_{spine}(1-\beta_{layer}\beta_{spine})$
- The spine sees an enhanced U_{rad} coming from the layer
- Also the layer sees an enhanced U_{rad} coming from the spine
- The IC emission is enhanced wrt to the standard SSC model

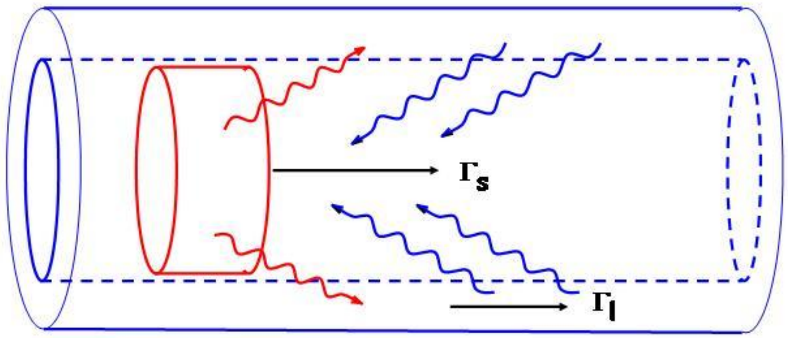

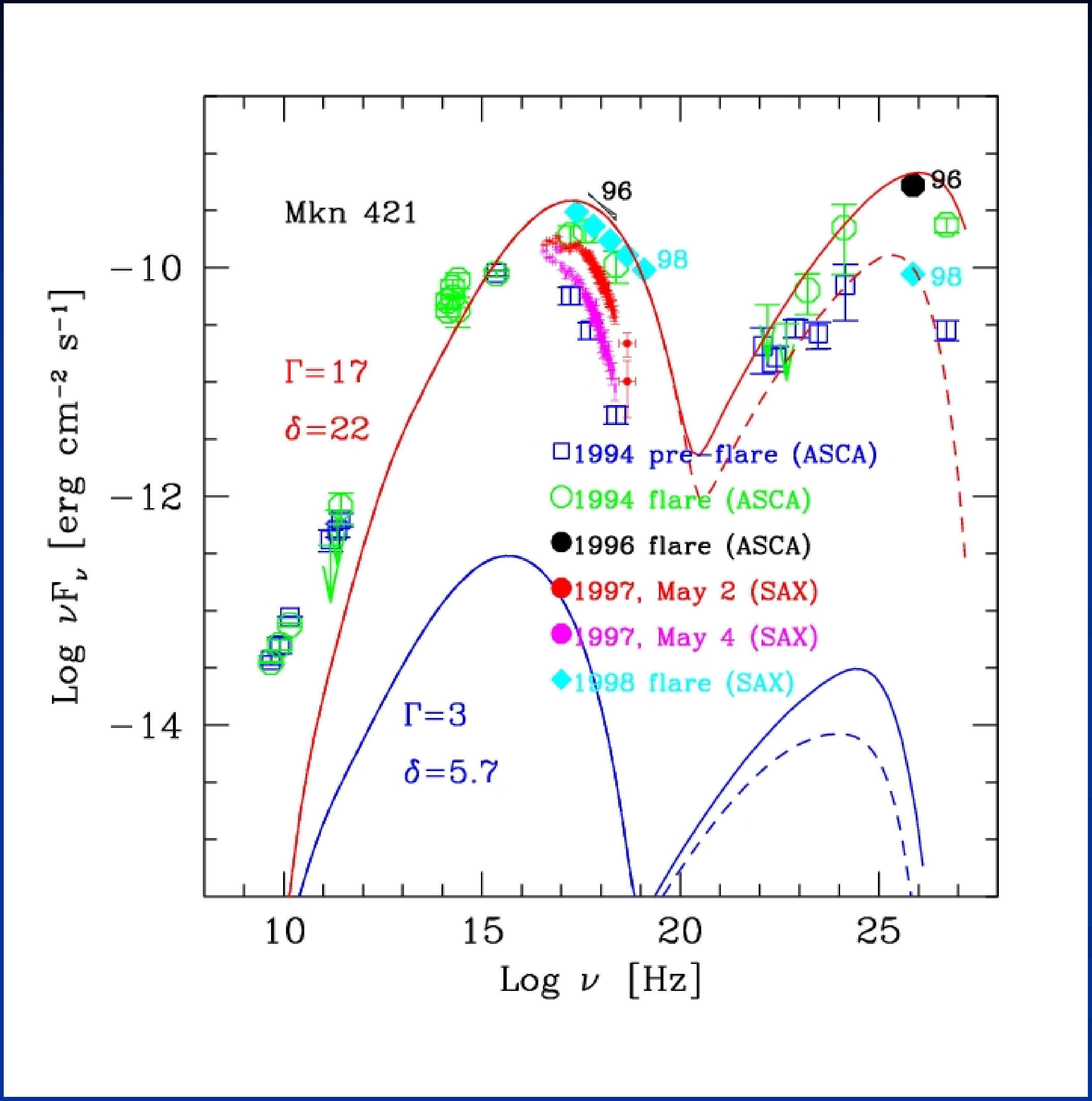

$B=1.1\ G$

$L_B \sim L_e \sim L_p \sim 10^{43}$

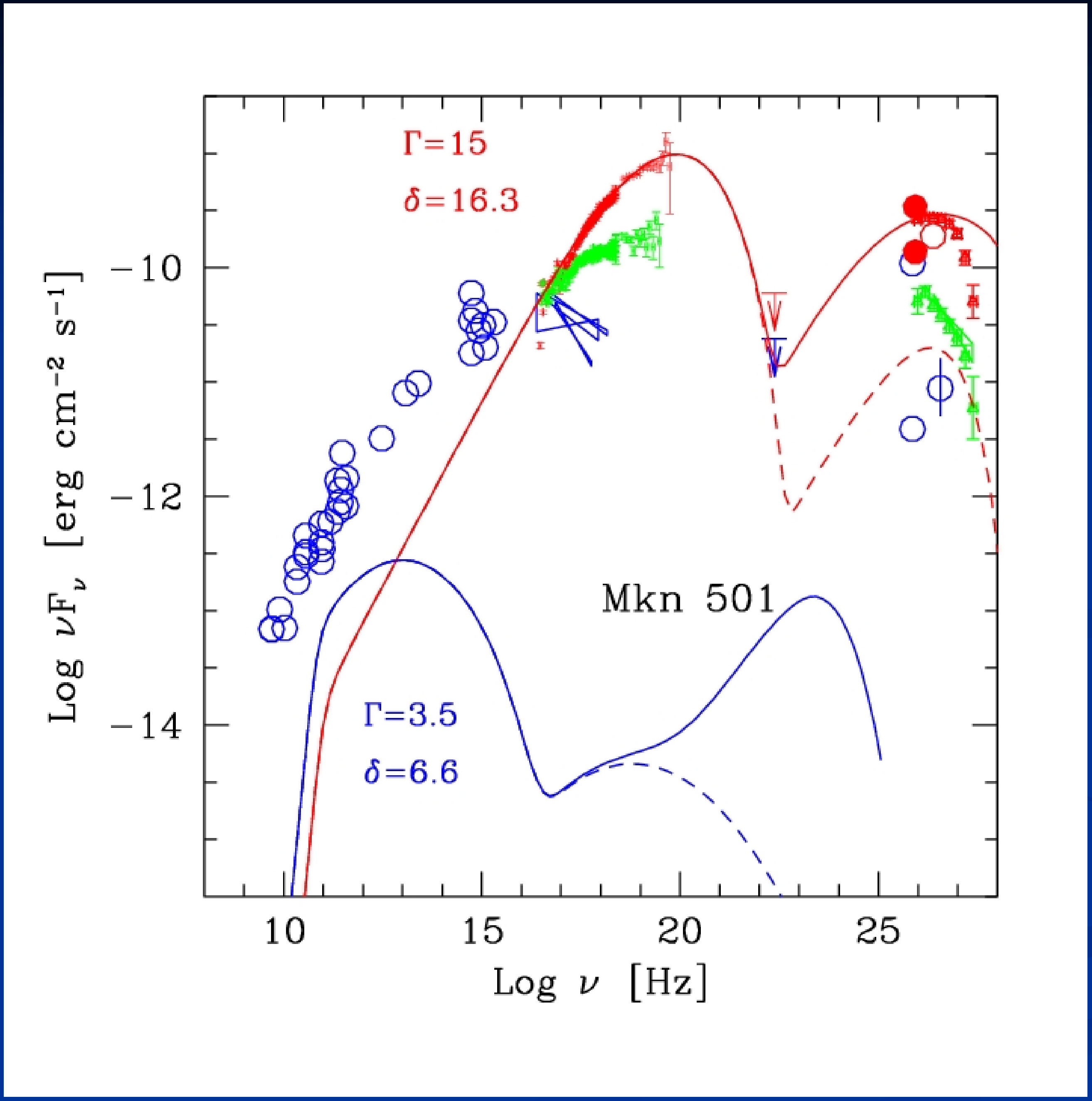

$B=1.3\ G$

$L_e=4\times10^{42}$

$L_B=1\times10^{43}$

$L_p=2\times10^{43}$

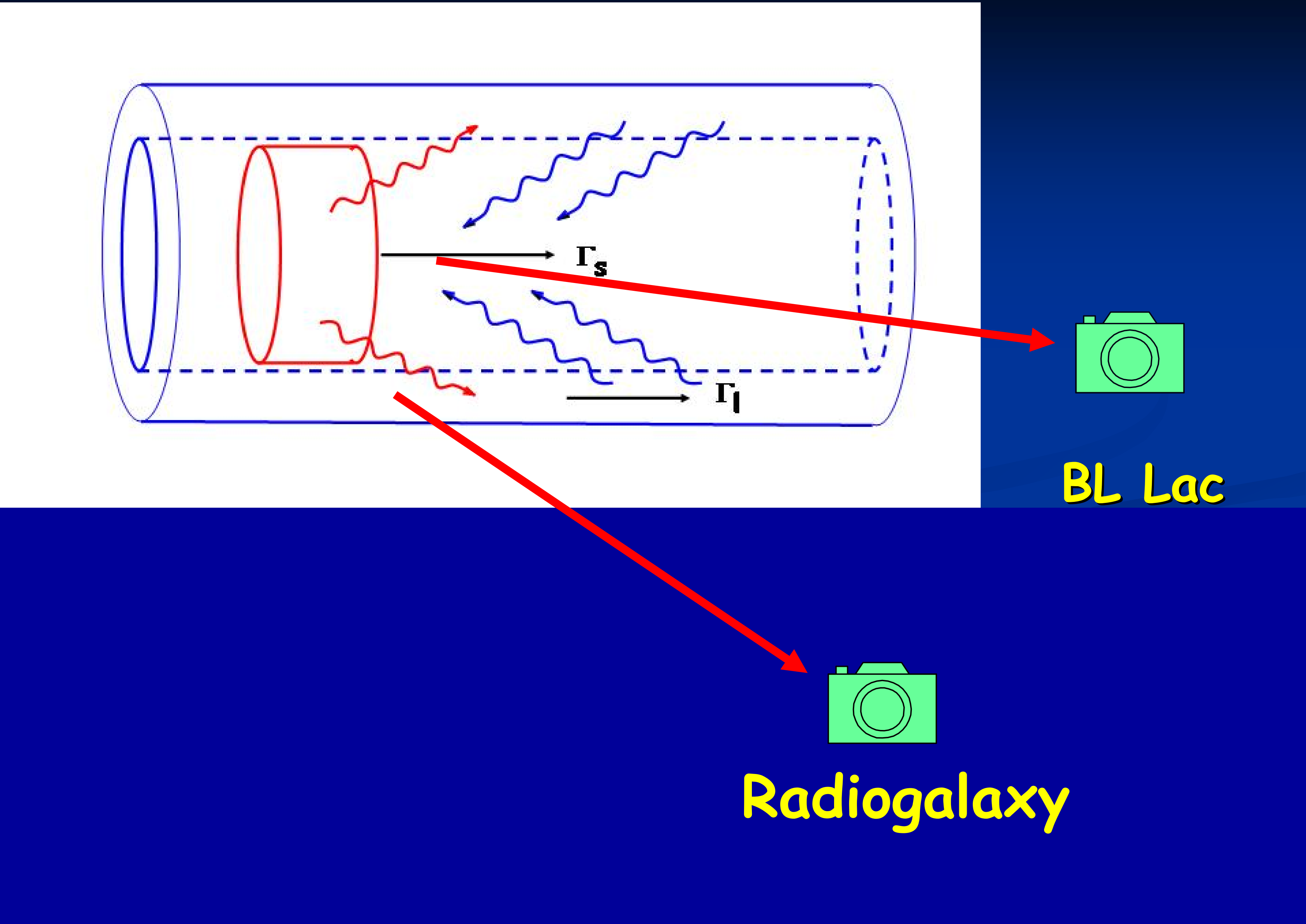
Γ_s
Γ_l
BL Lac
Radiogalaxy

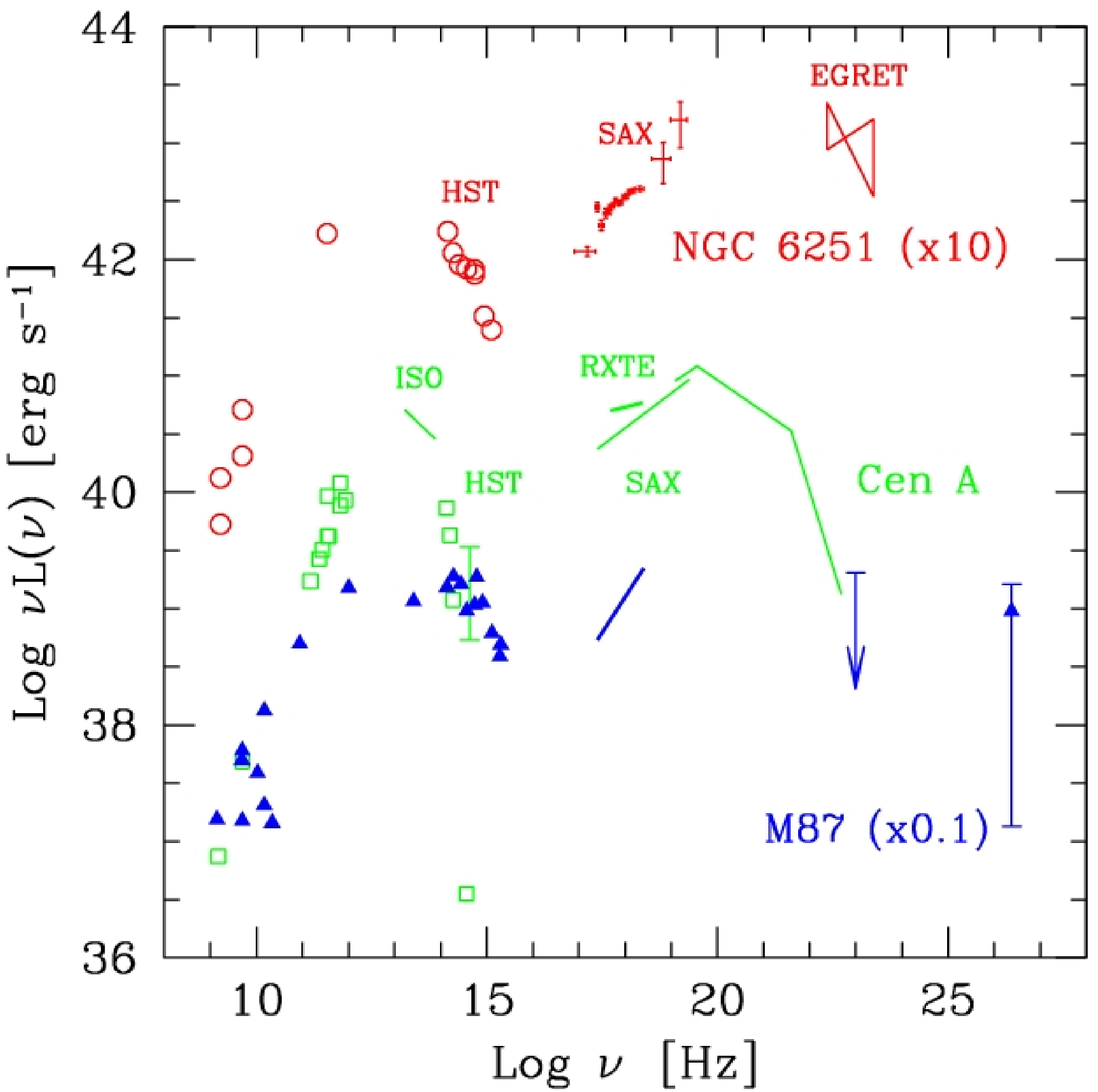

44
42
40
38
36
10
15
20
25
Log ν [Hz]
Log νL(ν) [erg s⁻¹]
EGRET
SAX
HST
NGC 6251 (x10)
ISO
RXTE
HST
SAX
Cen A
M87 (x0.1)

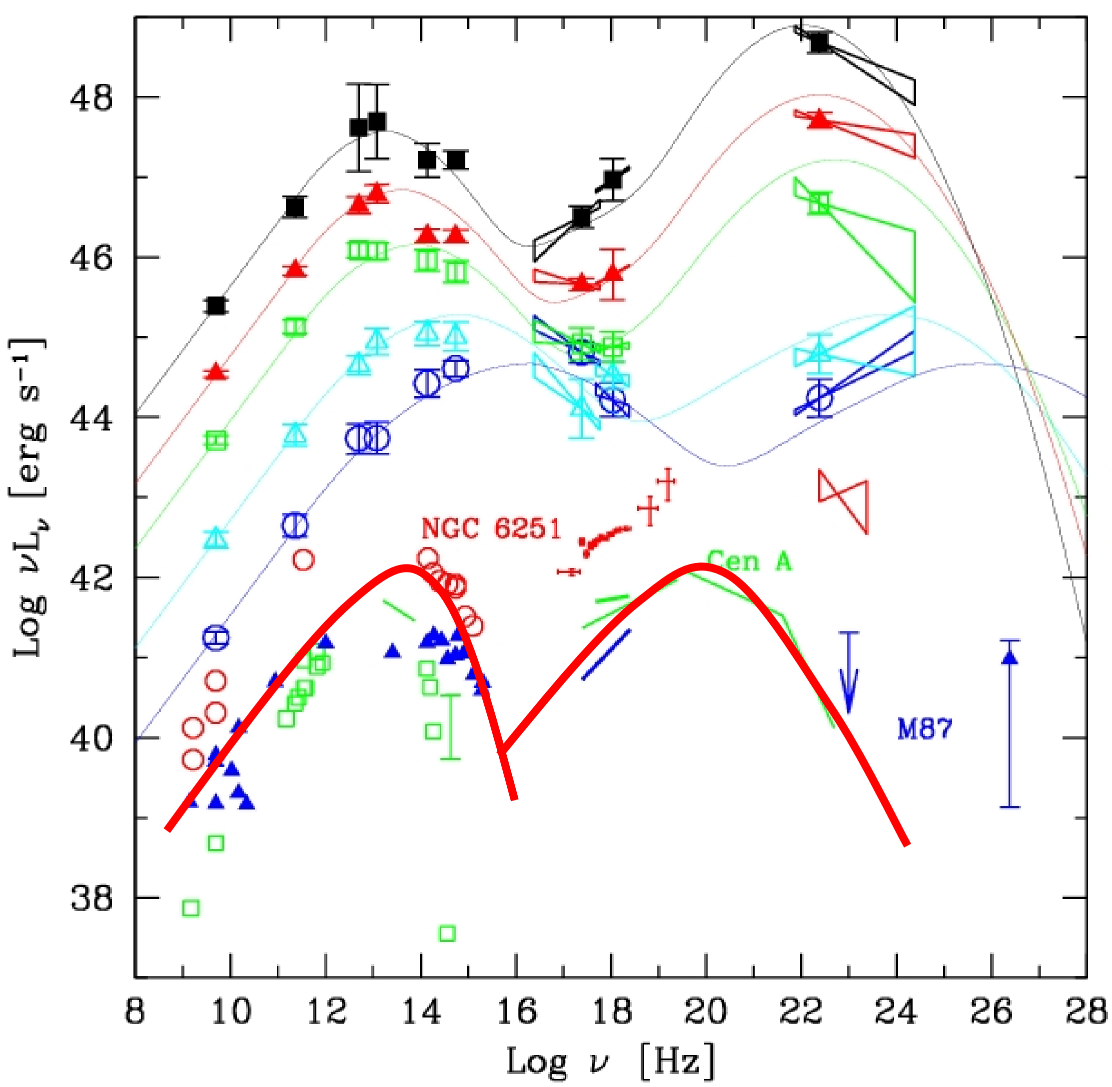

48
46
44
42
40
38
Log νLν [erg s⁻¹]
8
10
12
14
16
18
20
22
24
26
28
Log ν [Hz]
NGC 6251
Cen A
M87

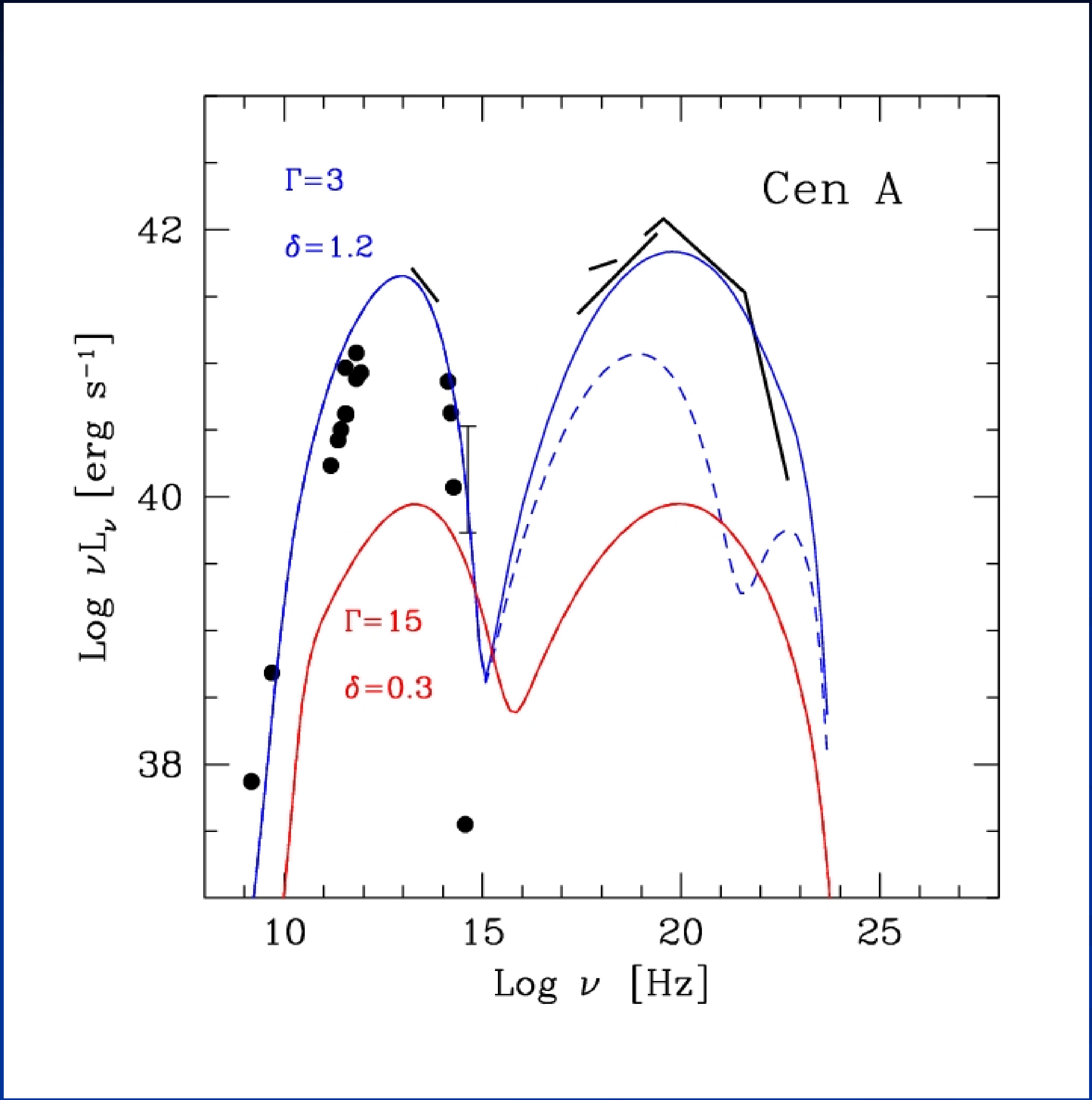

Layer:

B=2 G

L_B~3x10^{41}

L_e~8x10^{41}

L_p~4x10^{42}

R=10^{16} cm

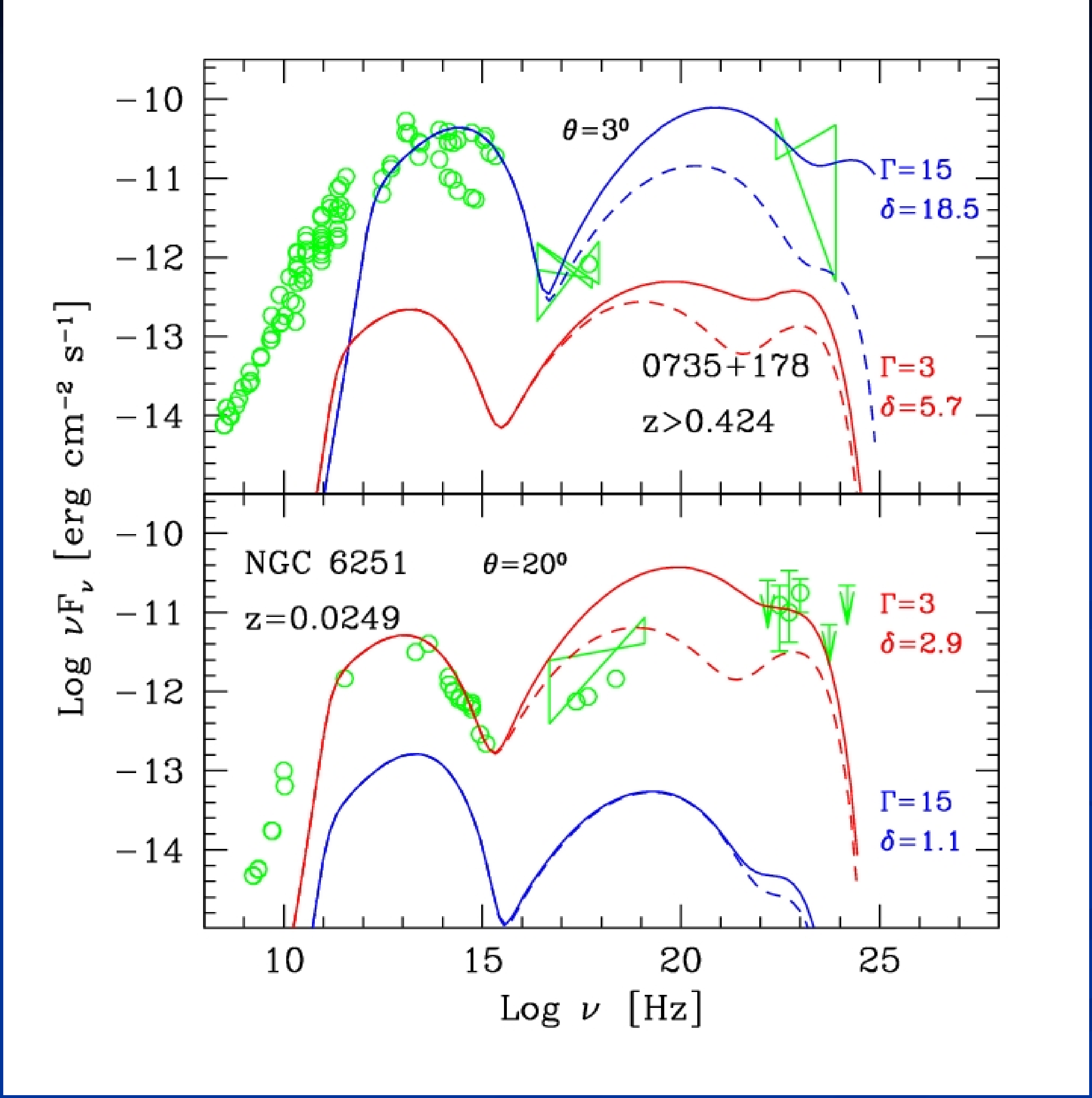

0735+178

B=5 G

$L_B \sim L_e \sim 6\times10^{44}$

$L_p \sim 7\times10^{45}$

NGC 6251

B=1.8 G

$L_B=4\times10^{41}$

$L_e=2\times10^{42}$

$L_p=2\times10^{43}$

Having increased the B-field, we need fewer electrons to do the radiation we see

The jet is lighter

It is easier to make it decelerate

Synchro and SSC

K

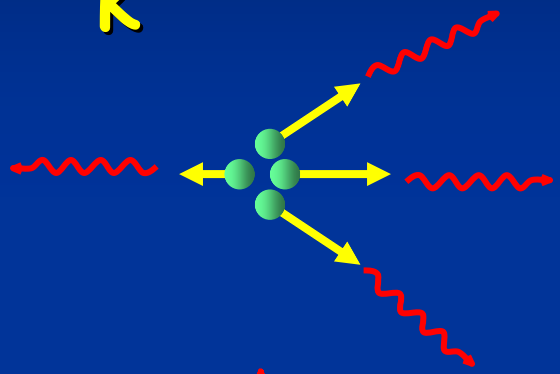

In K there is a loss of momentum…

K'

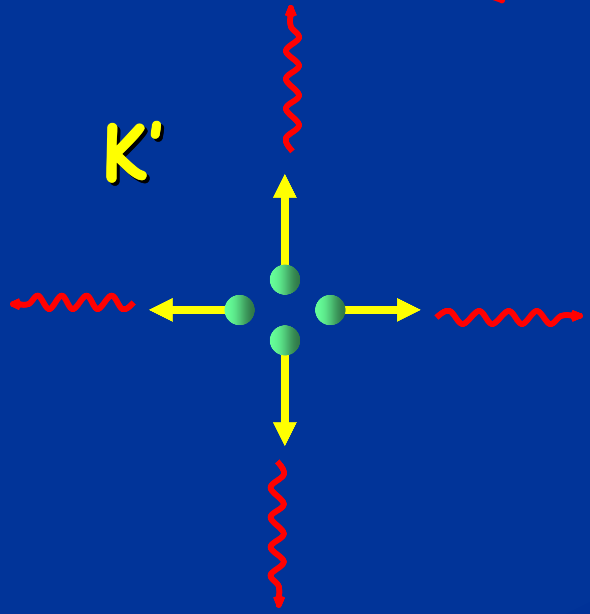

And in K'? no, but the mass $\langle\gamma\rangle m_e$ decreases.

Γ_{bulk} remains the same

External Compton: the rocket

K

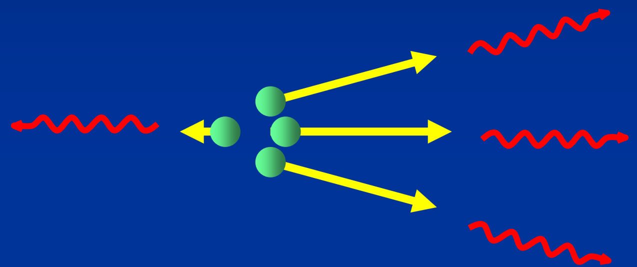

more collimated than before

K'

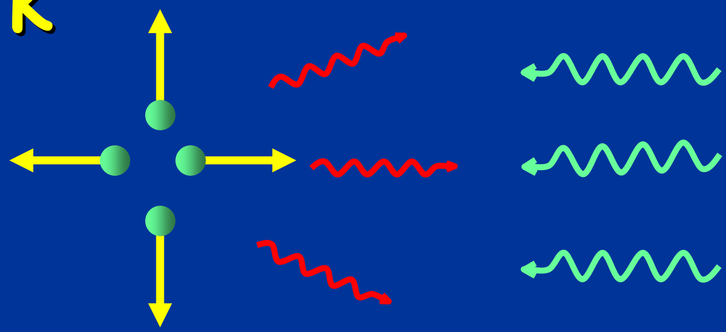

Anisotropic! Loss of momentum ⟹ recoil

Important when $\langle\gamma\rangle m_e \sim m_p$

Γ_{bulk} decreases

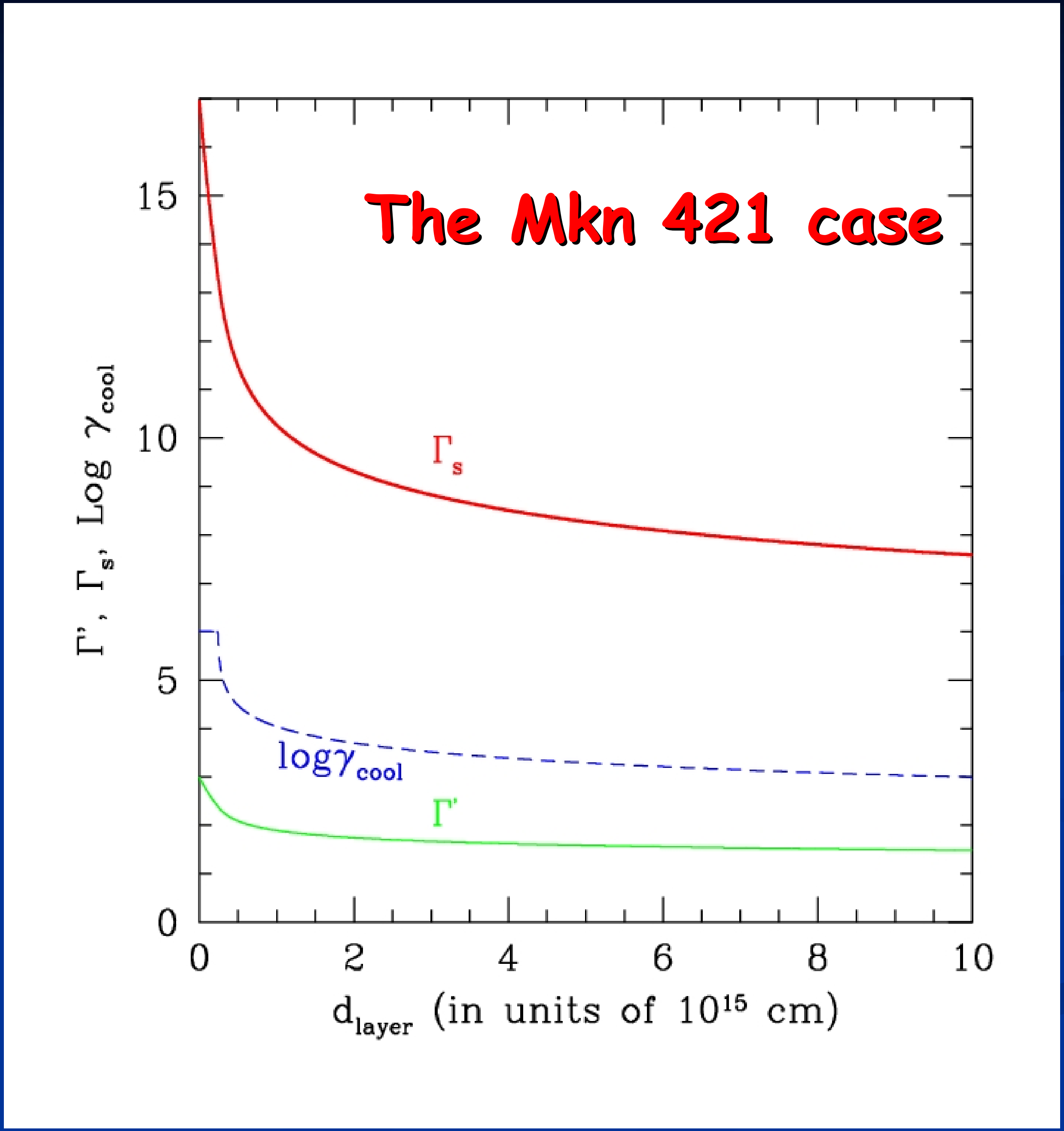
The Mkn 421 case
Γ', Γ_s, Log γ_{cool}
15
10
5
0
Γ_s
$\log\gamma_{cool}$
Γ'
0
2
4
6
8
10
d_{layer} (in units of 10^{15} cm)

Conclusions

- Observations suggest that jets of TeV BL Lacs decelerate, and there is a hint of spine+layer.
- IF they are cospatial, there is an important radiative interplay between the spine and the layer.
- More seeds, more IC, more collimation, more B.
- Less electrons, less protons, less inertia.
- Early interaction of the walls of the jet with ISM produces the layer, Compton rocket can decelerate the spine.

High energy peak is getting large

Mkn 501

1959

Mkn 421

1426

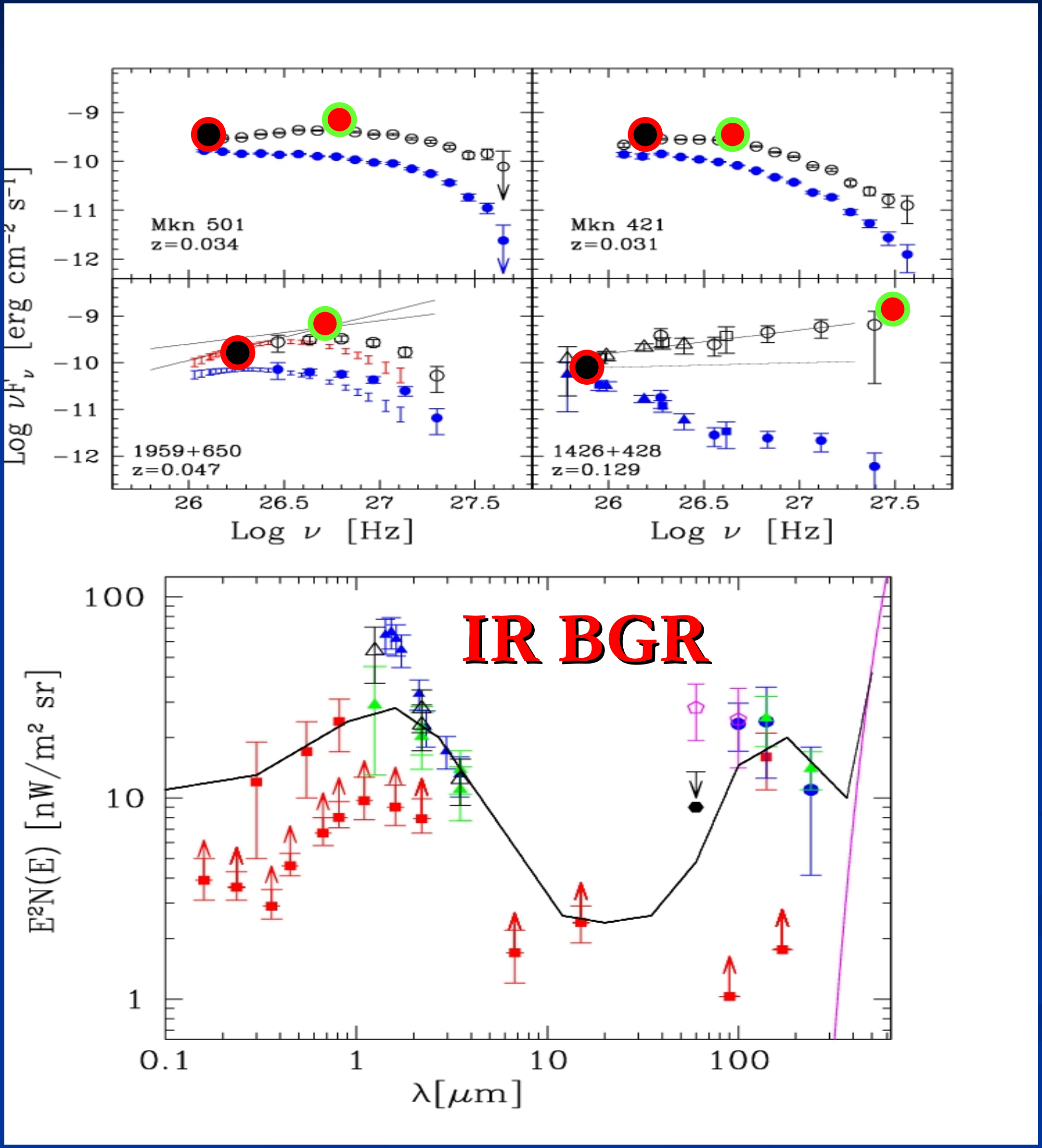

Costamante et al. 2003

Why δ>20?

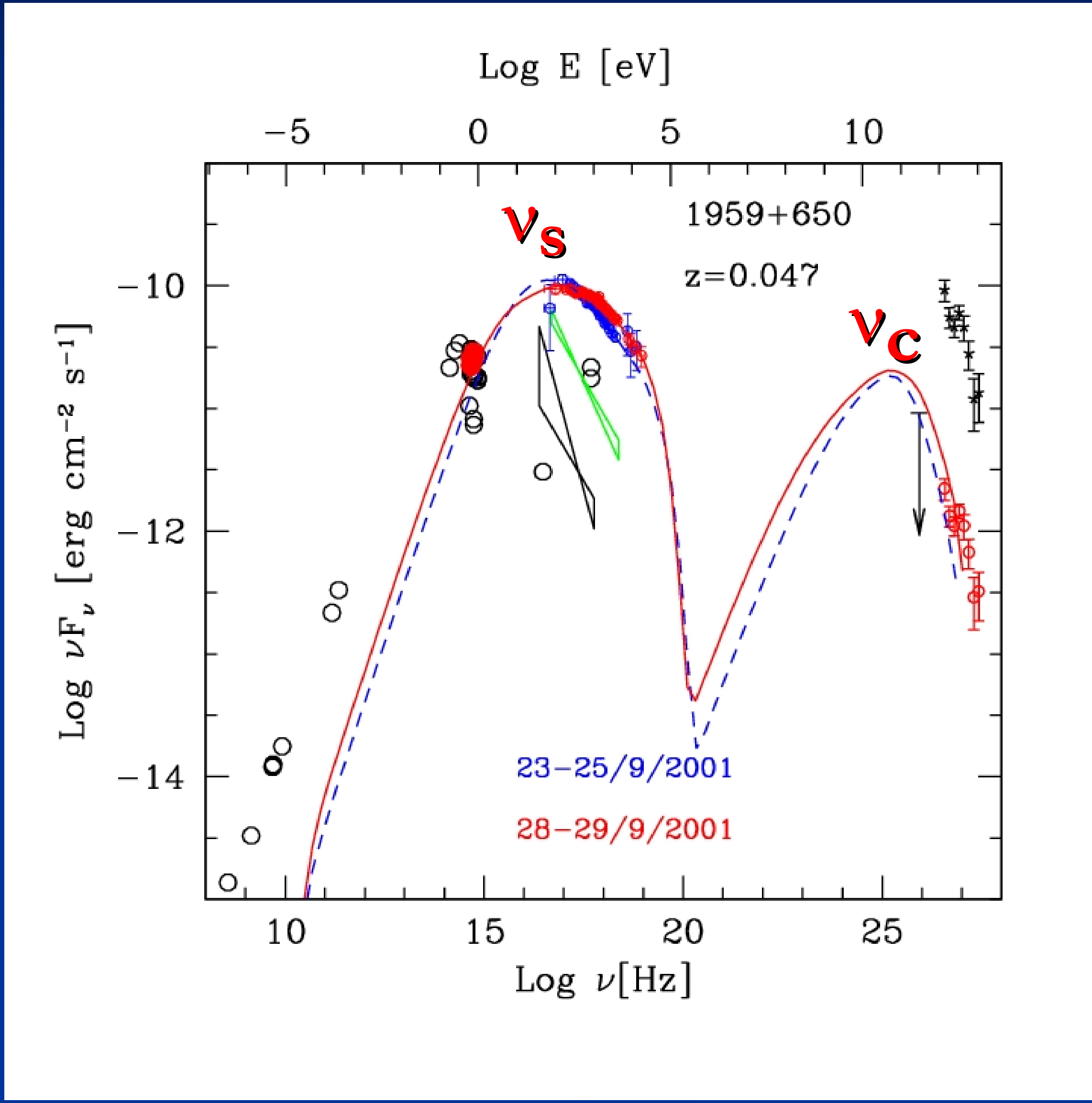

$\nu_c/\nu_s \sim \gamma^2$

$\nu_s \sim \gamma^2 B\delta$

$\Rightarrow B\delta \sim \gamma^{-2}$

$L_c/L_s \sim L_s/(B^2\delta^6)$

$\sim L_s\gamma^4/\delta^4$

$\Rightarrow$ $\delta \sim \nu_c^{1/2}$

K-N: the same

Decelerating the entire jet

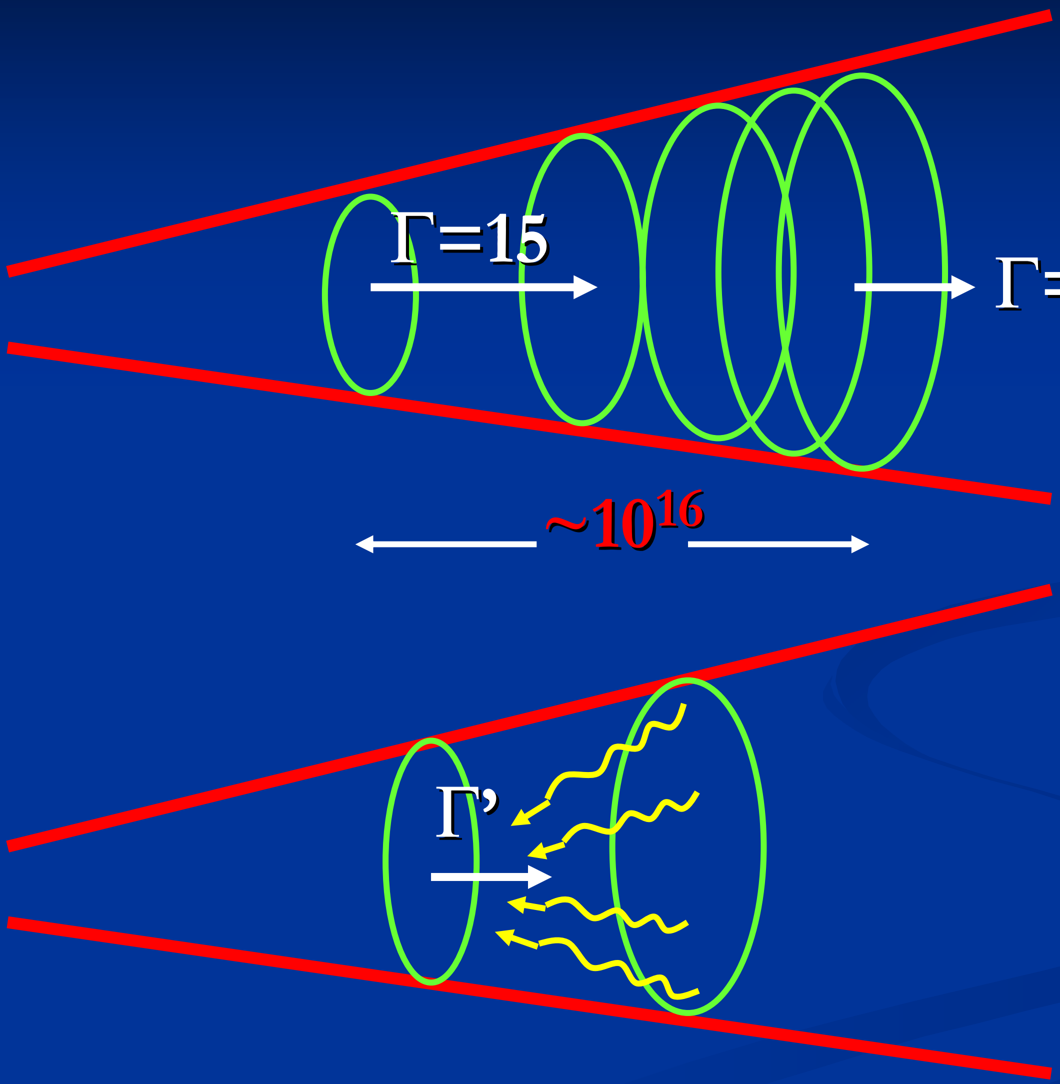

Georganopoulos & Kazanas 2003

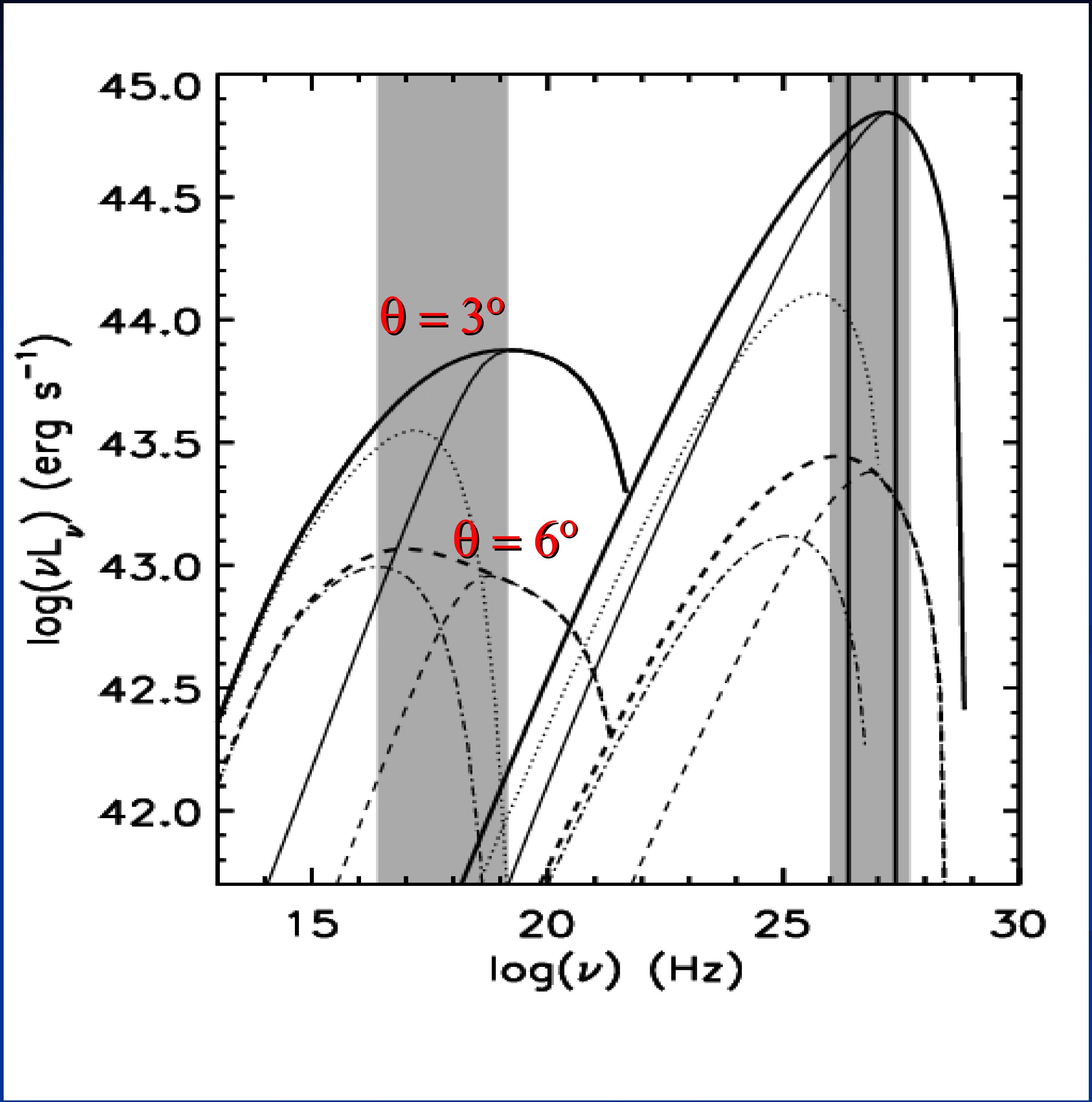

Georganopoulos & Kazanas 2003

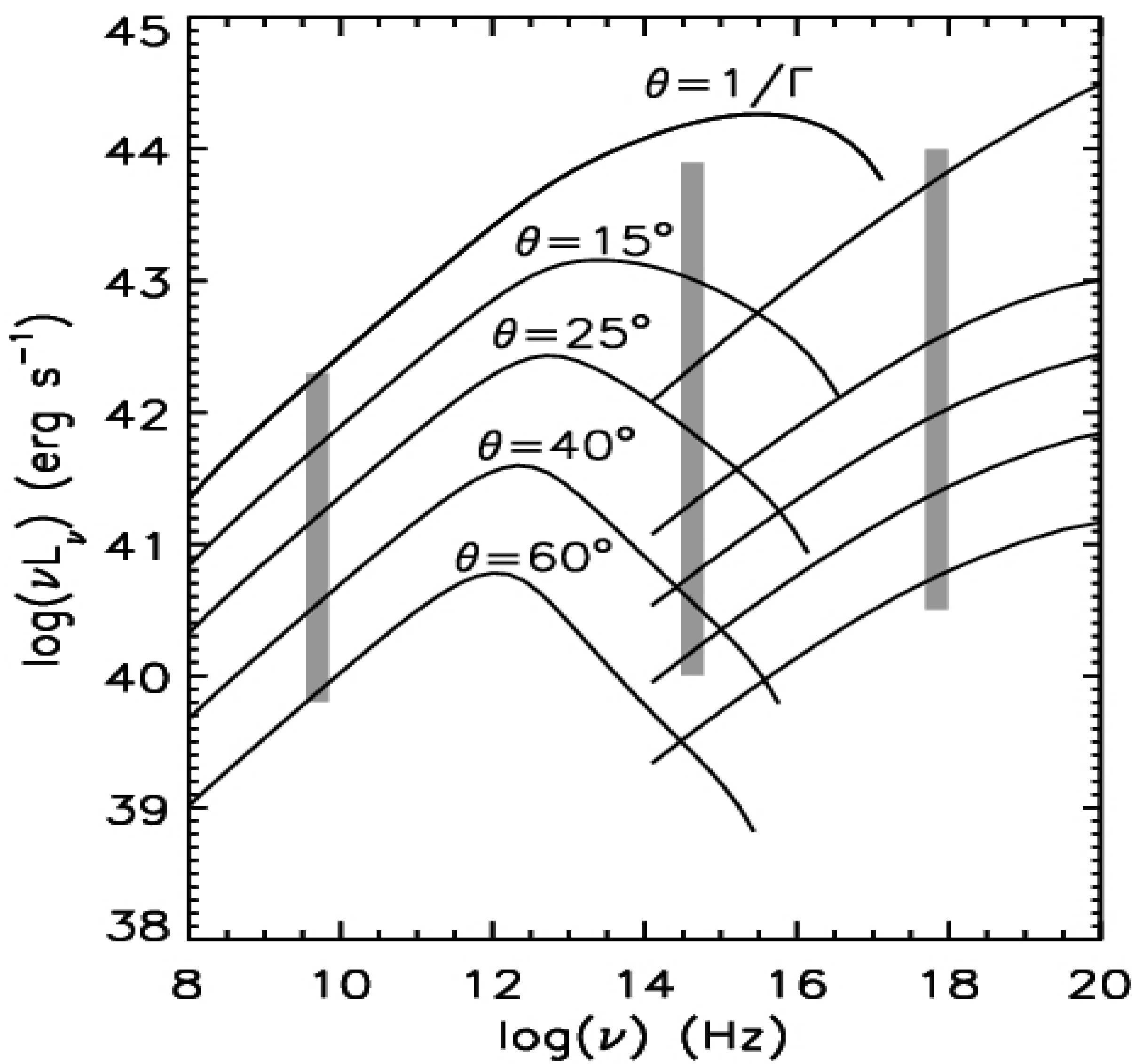

Georganopoulos & Kazanas 2003

Giroletti et al: spine + layer: Mkn 501

R_{core} (pc)	θ	Γ_{spine}	δ_{spine}	Γ_{layer}	δ_{layer}
10^{-3}-0.03	4	15	15	?	?
0.03-0.15	10	15	4	10	5
0.15-7	15	15	2	3	5
7-20	15-20	15	1-2	3	3-4
20-30	25	3-10	1-2	2	2.5
50	25	1.25	1.8	1.1	1.5

Jorstad et al. 2001

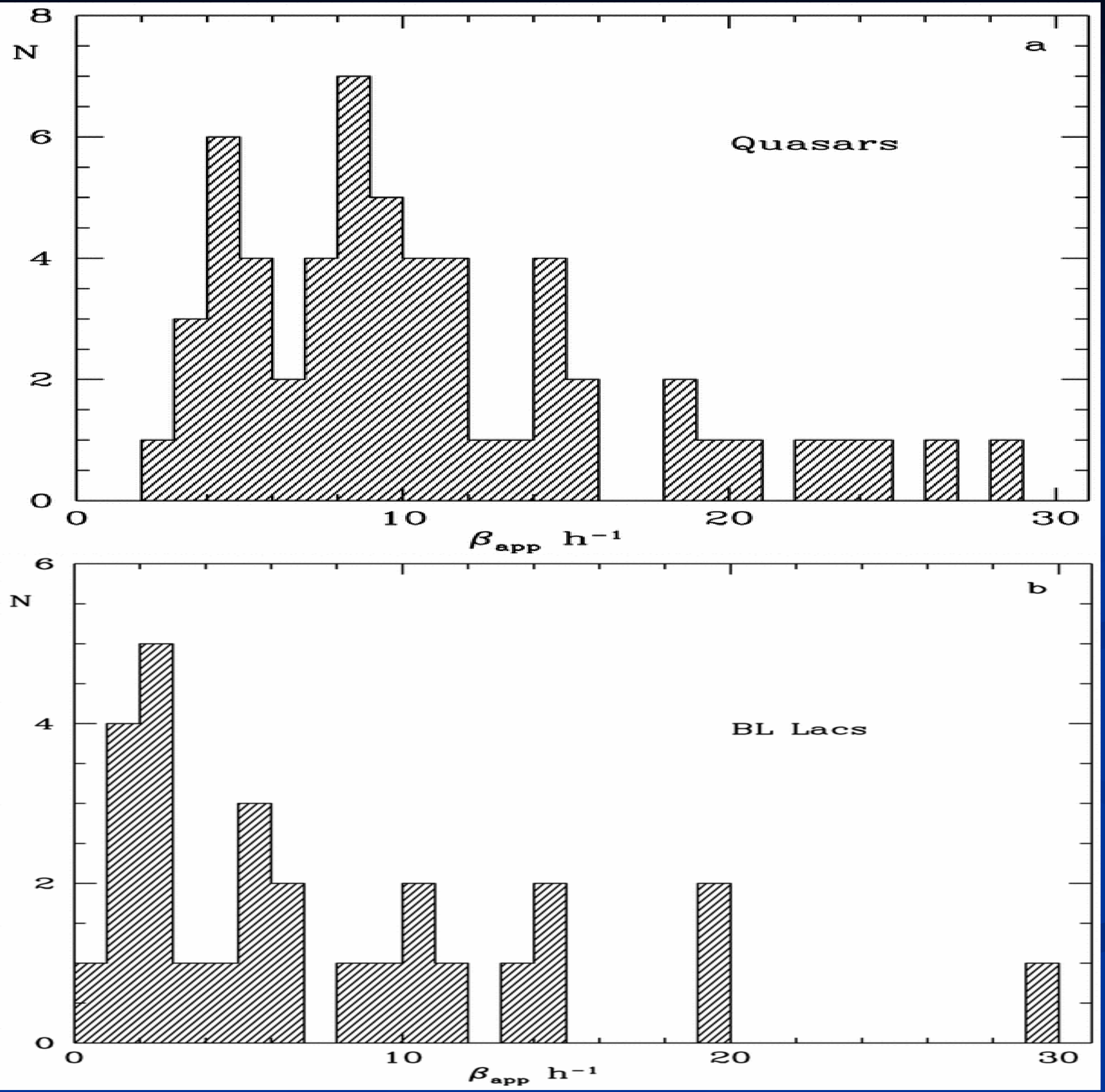

Beamed emission form TeV jets

Dimitrios Emmanoulopoulos

Prof.Stefan Wagner

ENIGMA meeting Jerisjärvi, Finland 26-28 April 2004

Landessternwarte Heidelberg

ENIGMA

Overview

- Prominent TeV sources?
- Doppler boosting factor and pair-production
- The case of MKN421 and PKS2155-304

Prominent TeV sources

The best sources for TeV emission are the "Extreme BL Lacs "

Prominent TeV sources

The best sources for TeV emission are the "Extreme BL Lacs "

General characteristics

Prominent TeV sources

The best sources for TeV emission are the "Extreme BL Lacs "

General characteristics

- Flat radio spectra ($a_R < 0.5$)

Prominent TeV sources

The best sources for TeV emission are the “Extreme BL Lacs ”

General characteristics

- Flat radio spectra ($a_R < 0.5$)
- The spectra steepen in the in the IR and Optical region

Prominent TeV sources

The best sources for TeV emission are the "Extreme BL Lacs "

General characteristics

- Flat radio spectra ($a_R < 0.5$)
- The spectra steepen in the in the IR and Optical region
- Rapid and large amplitude flux variation in the Radio, Optical, X-Ray bands

Prominent TeV sources

The best sources for TeV emission are the “Extreme BL Lacs ”

General characteristics

- Flat radio spectra ($a_R < 0.5$)
- The spectra steepen in the in the IR and Optical region
- Rapid and large amplitude flux variation in the Radio, Optical, X-Ray bands
- Emission lines are absent or very weak

Prominent TeV sources

Why we choose these sources?

Prominent TeV sources

Why we choose these sources?

Among all Blazars they have the highest Synchrotron Peak Frequencies

$\Longrightarrow$ many energetic electrons

Prominent TeV sources

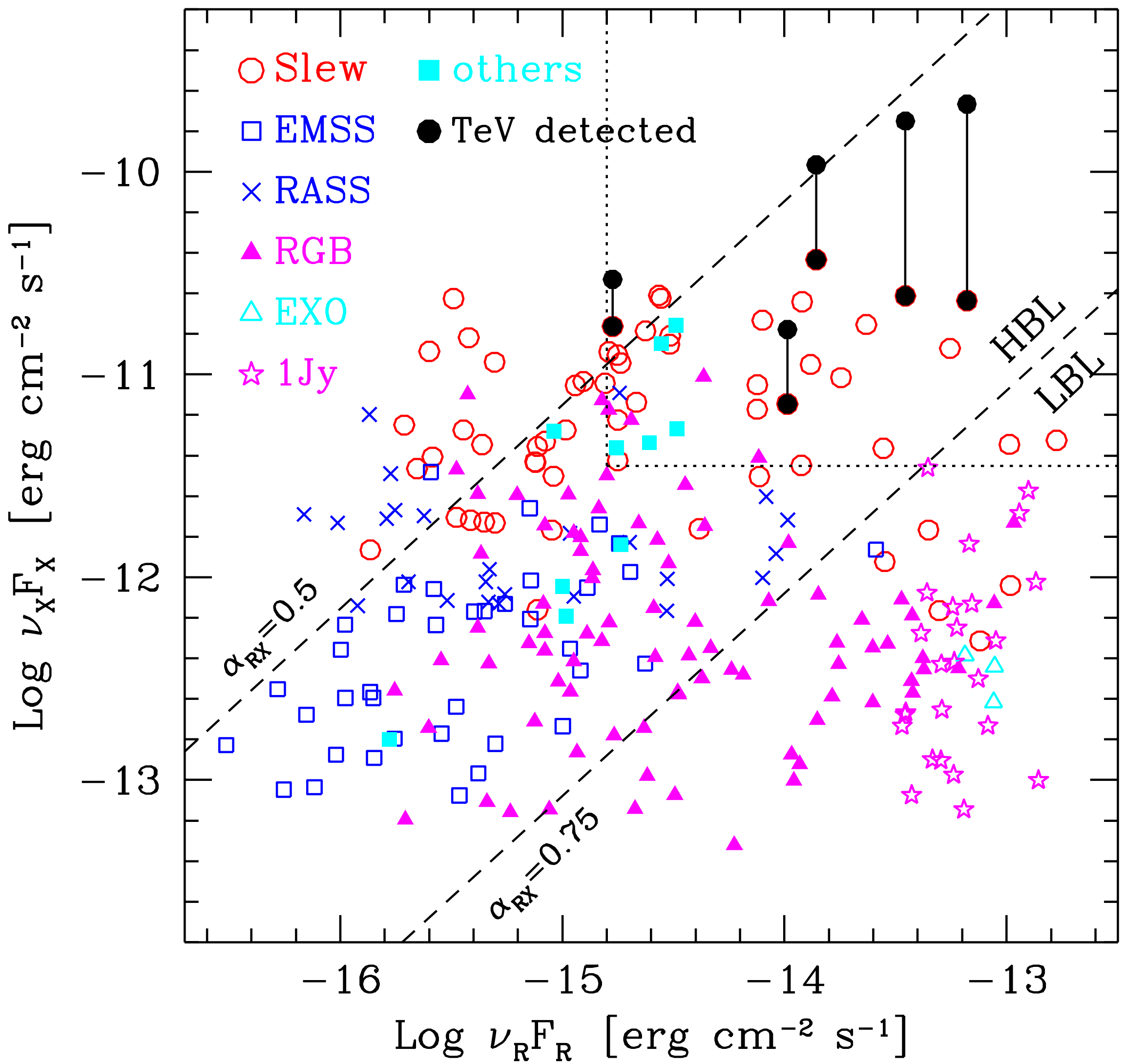

Constamante et al.

A&A 384,2002

Prominent TeV sources

Why we choose these sources?

Low values of a_{RX}

Prominent TeV sources

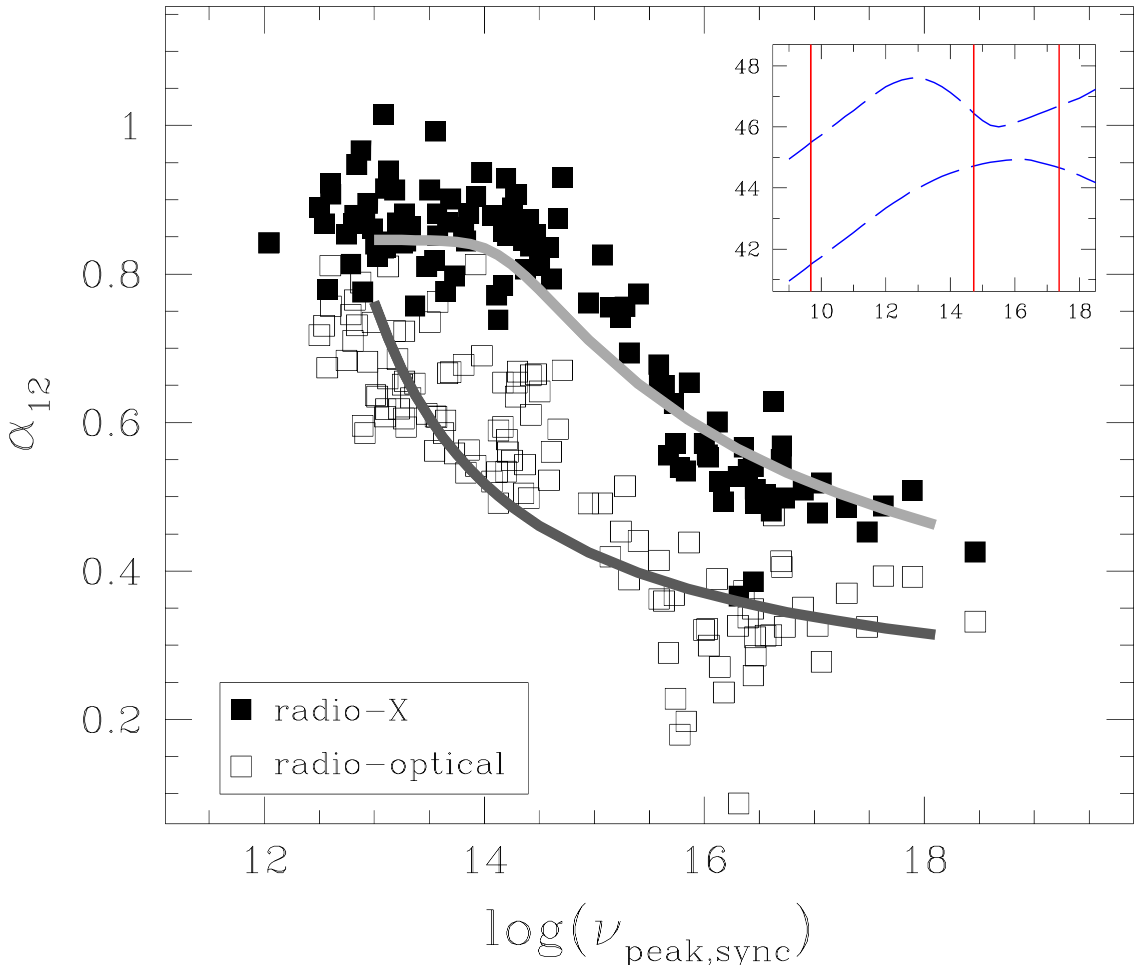

Fossati et al. 1998

Prominent TeV sources

Why we choose these sources?

Brightest sources in X-ray

and

Radio band

Prominent TeV sources

Why we choose these sources?
Brightest sources in X-ray
and
Radio band

The Interpretation

Prominent TeV sources

Why we choose these sources?

Brightest sources in X-ray

and

Radio band

$$TeV \longrightarrow \left\{ \begin{array}{ll} & \text{more energetic electrons} \\ \nu_{peak} \uparrow & \text{less seed photons} \\ & \text{K -- N restrictions} \\ & \text{less energetic electrons} \\ \nu_{peak} \downarrow & \text{abundance of seed photons} \\ & \text{not efficient scattering} \end{array} \right\}$$

Prominent TeV sources

Why we choose these sources?
Brightest sources in X-ray
and
Radio band

Ideal ν_{peak}

$$h\nu_{peak} \leq \frac{mc^2}{\gamma_{peak}}$$

Doppler factor and pair-production

For a constant velocity source, the proper size R of the emitting region is equal to:

$$R = \frac{\delta}{1+z} c\Delta t$$

Doppler factor and pair-production

For a constant velocity source, the proper size R of the emitting region is equal to:

$$R = \frac{\delta}{1+z} c\Delta t$$

(Bassani et al.A&A 161 1986)

Doppler factor and pair-production

For a constant velocity source, the proper size R of the emitting region is equal to:

$$R = \frac{\delta}{1+z} c\Delta t$$

The optical depth for a photon of energy ϵ_2 to cross a region of radius R filled with photons of energy ϵ_1:

Doppler factor and pair-production

For a constant velocity source, the proper size R of the emitting region is equal to:

$$R = \frac{\delta}{1+z} c \Delta t$$

The optical depth for a photon of energy ϵ_2 to cross a region of radius R filled with photons of energy ϵ_1:

$$\tau_{\gamma\gamma} = \frac{R}{4\pi} \int d\epsilon_1 n_0 \epsilon_1^{-a} \int d\Omega (1 - \cos\theta) \sigma_{\gamma\gamma} \left[\frac{\epsilon_1 \epsilon_2}{m_e^2 c^4} (1 - \cos\theta) \right]$$

Doppler factor and pair-production

For a constant velocity source, the proper size R of the emitting region is equal to:

$$R = \frac{\delta}{1+z} c\Delta t$$

The optical depth for a photon of energy ϵ_2 to cross a region of radius R filled with photons of energy ϵ_1:

$$\tau_{\gamma\gamma} = f(\epsilon, z, a, \delta, \Delta t)$$

Doppler factor and pair-production

For a constant velocity source, the proper size R of the emitting region is equal to:

$$R = \frac{\delta}{1+z} c\Delta t$$

The optical depth for a photon of energy ϵ_2 to cross a region of radius R filled with photons of energy ϵ_1:

$$\tau_{\gamma\gamma} = \underbrace{Const}_{z,a} \times F_{\epsilon_1} \times (\epsilon_1 \cdot \epsilon_2)^a \times \delta^{-(4+2a)} \times \Delta t^{-1}$$

Doppler factor and pair-production

Interaction of TeV γ-rays with IR photons

Doppler factor and pair-production

Interaction of TeV γ-rays with IR photons

$$\frac{E_{TeV}E_{IR}}{m_e^2c^4}(1-\cos\theta) \geq 1 \Rightarrow E_{IR} \sim 0.5E_{TeV}^{-1}$$

Doppler factor and pair-production

Interaction of TeV γ-rays with IR photons

$$\tau_{\gamma\gamma} = Const \times F_{E_{IR}} \times (E_{TeV} \cdot E_{IR})^a \times \delta^{-(4+2a)} \times \Delta t^{-1} > 1 \Rightarrow$$

Doppler factor and pair-production

Interaction of TeV γ-rays with IR photons

$$\delta \geq \left[Const \times F_{\epsilon_{IR}}^{-1}(\epsilon_{TeV} \cdot \epsilon_{IR})^{-a} \times \Delta t\right]^{-\frac{1}{4+2a}}$$

Doppler factor and pair-production

Interaction of TeV γ-rays with IR photons

$$\delta \geq \left[Const \times F^{-1}_{\epsilon_{IR}} (\epsilon_{TeV} \cdot \epsilon_{IR})^{-a} \times \Delta t\right]^{-\frac{1}{4+2a}}$$

1Tev γ rays $\xrightarrow{Target\ Photons}$ 0.5eV or 2.2μm

Doppler factor and pair-production

Interaction of TeV γ-rays with IR photons

$$\boxed{\delta \geq \left[Const \times F^{-1}_{\epsilon_{IR}} (\epsilon_{TeV} \cdot \epsilon_{IR})^{-a} \times \Delta t\right]^{-\frac{1}{4+2a}}}$$

1Tev γ rays $\overset{Target\ Photons}{\longrightarrow}$ 0.5eV or 2.2μm

For the case of MKN421

Doppler factor and pair-production

Interaction of TeV γ-rays with IR photons

$$\delta \geq \left[Const \times F_{\epsilon_{IR}}^{-1} (\epsilon_{TeV} \cdot \epsilon_{IR})^{-a} \times \Delta t\right]^{-\frac{1}{4+2a}}$$

1Tev γ rays $\xrightarrow{Target\ Photons}$ 0.5eV or 2.2μm

For the case of MKN421

$\Delta t \sim$ 4ksec-1Day

$F_{IR} \simeq$ 0.063 Jy Schwartz et al.229,1979

a$\sim$ 0.92

Doppler factor and pair-production

Interaction of TeV γ-rays with IR photons

$$\delta \geq \left[Const \times F^{-1}_{\epsilon_{IR}} (\epsilon_{TeV} \cdot \epsilon_{IR})^{-a} \times \Delta t\right]^{-\frac{1}{4+2a}}$$

1Tev γ rays $\xrightarrow{Target\ Photons}$ 0.5eV or 2.2μm

For the case of MKN421

$$\delta \sim 13 - 7$$

Doppler factor and pair-production

Interaction of TeV γ-rays with IR photons:

$$\delta \geq \left[Const \times F_{\epsilon_{IR}}^{-1} (\epsilon_{TeV} \cdot \epsilon_{IR})^{-a} \times \Delta t\right]^{-\frac{1}{4+2a}}$$

1Tev γ rays $\stackrel{Target Photons}{\longrightarrow}$ 0.5eV or 2.2μm

For the case of PKS2155-304

Doppler factor and pair-production

Interaction of TeV γ-rays with IR photons:

$$\delta \geq \left[Const \times F_{\epsilon_{IR}}^{-1} (\epsilon_{TeV} \cdot \epsilon_{IR})^{-a} \times \Delta t\right]^{-\frac{1}{4+2a}}$$

1Tev γ rays $\xrightarrow{Target Photons}$ 0.5eV or 2.2μm

For the case of PKS2155-304

$\Delta t \sim$ 4ksec-1Day
$F_{IR} \simeq$ 0.031 Jy
a$\sim$ 0.5

Doppler factor and pair-production

Interaction of TeV γ-rays with IR photons:

$$\boxed{\delta \geq \left[Const \times F_{\epsilon_{IR}}^{-1} (\epsilon_{TeV} \cdot \epsilon_{IR})^{-a} \times \Delta t\right]^{-\frac{1}{4+2a}}}$$

1Tev γ rays $\xrightarrow{TargetPhotons}$ 0.5eV or 2.2μm

For the case of PKS2155-304

$$\delta \sim 21$$

Doppler factor and pair- production

Why we have so BIG differences?

Doppler factor and pair- production

Why we have so BIG differences?

- Different sources (different redshifts,different spectral indices)

Doppler factor and pair- production

Why we have so BIG differences?

- Different sources (different redshifts,different spectral indices)
- 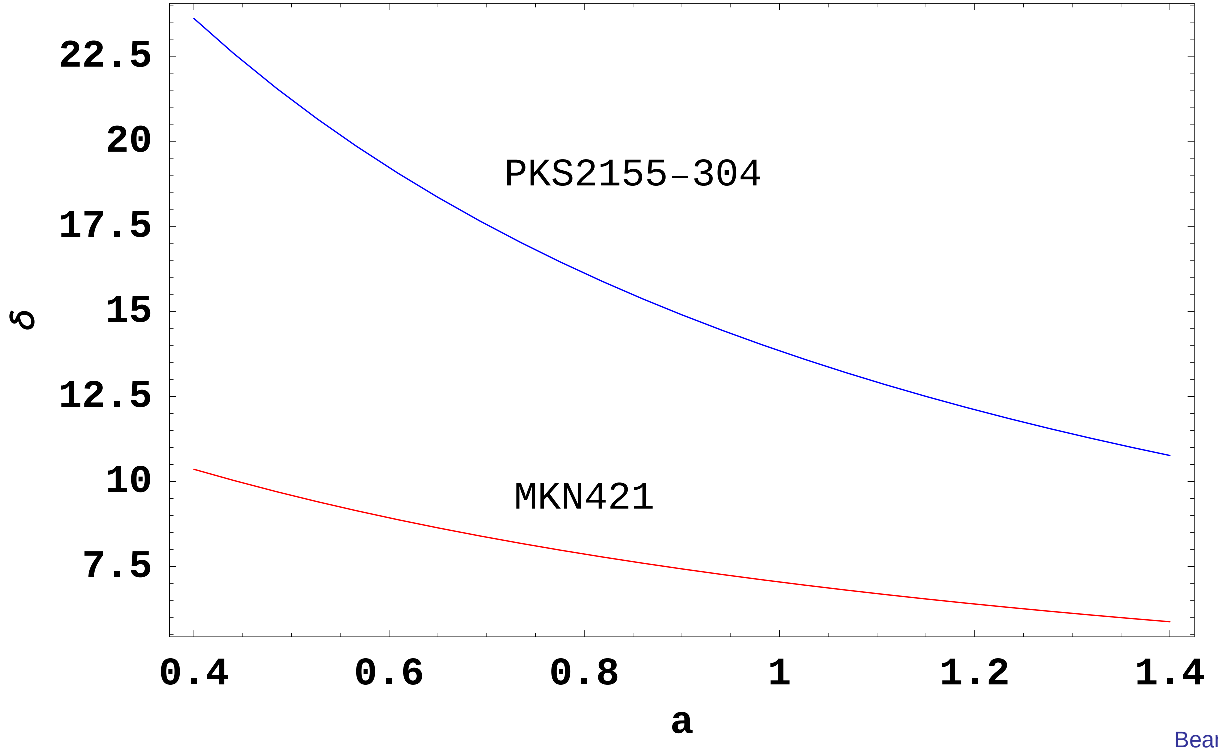

Doppler factor and pair- production

Why we have so BIG differences?

- Different sources (different redshifts,different spectral indices)
- Determination of a characteristic time Δt which indicates the size of the source

Doppler factor and pair-production

Why we have so BIG differences?

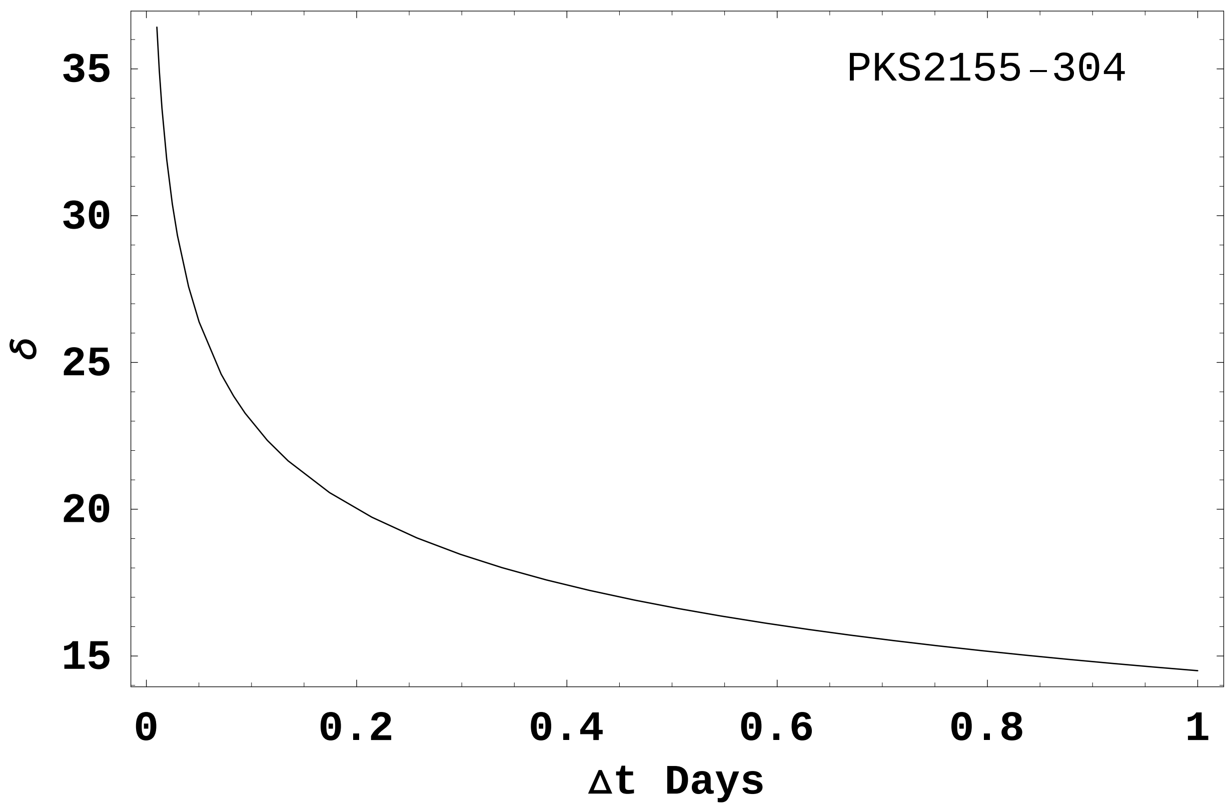

Doppler factor and pair-production

Why we have so BIG differences?

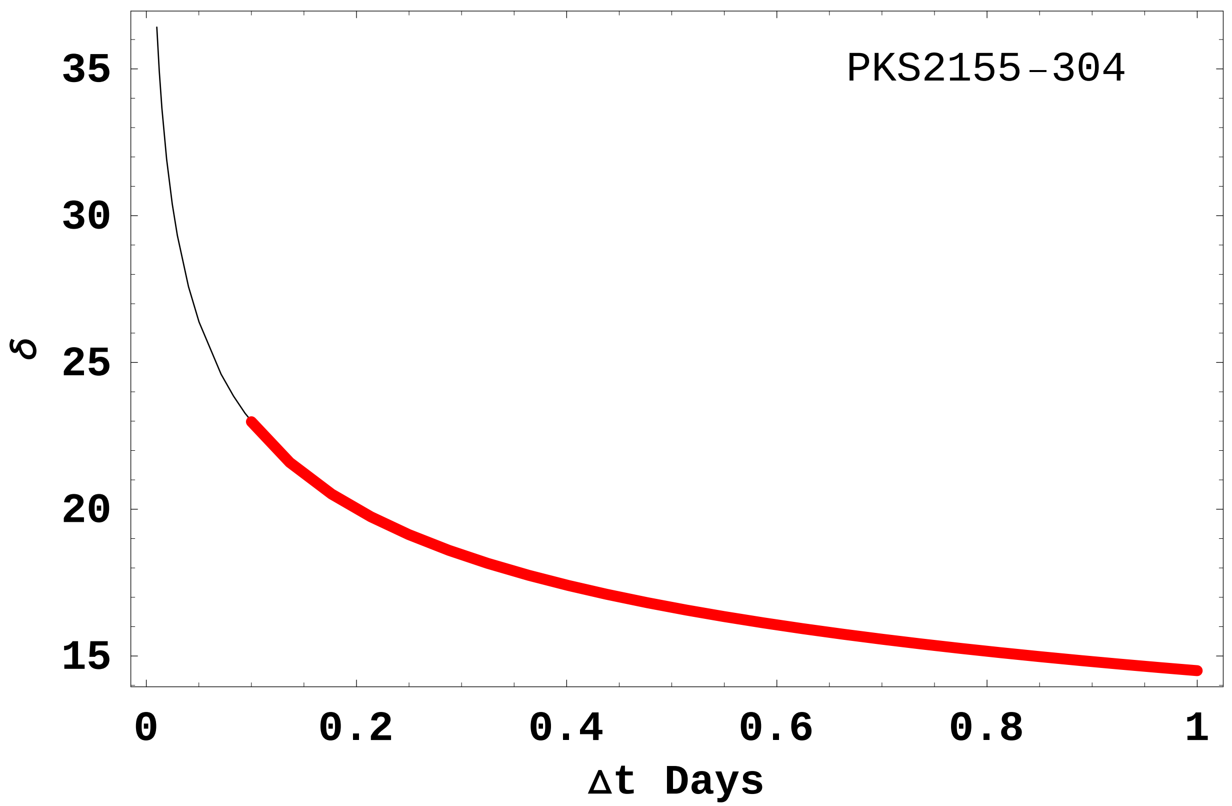

Doppler factor and pair-production

Why we have so BIG differences?

- Different sources (different redshifts,different spectral indices)
- Determination of a characteristic time Δt which indicates the size of the source
- The value of δ may represent a specific region in the jet $\longrightarrow$ Not applicable for the whole jet

Doppler factor and pair-production

Why we have so BIG differences?
(e.g. NGC 1265)

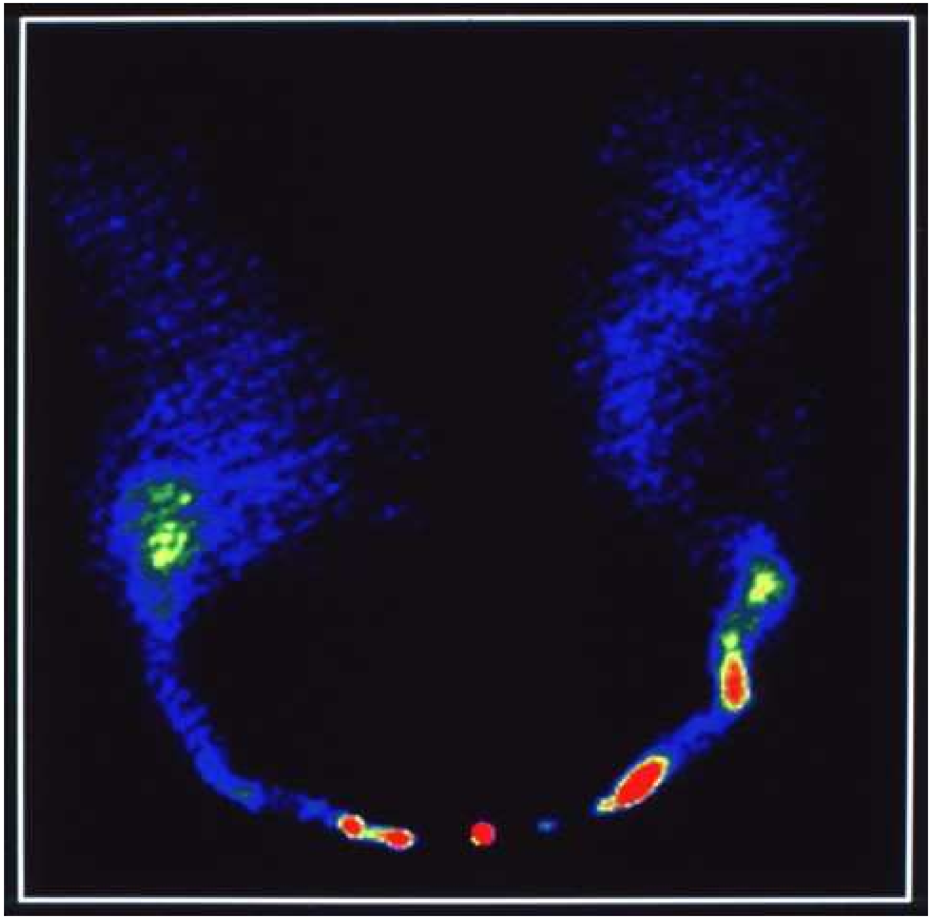

Conclusions

- The transparency of γ-rays in pair-production does not depend on the emission mechanism

Conclusions

- The transparency of γ-rays in pair-production does not depend on the emission mechanism
- The basic assumption is that the TeV photons are situated in the same volume with the target photons

Conclusions

- The transparency of γ-rays in pair-production does not depend on the emission mechanism
- The basic assumption is that the TeV photons are situated in the same volume with the target photons
- The only direct way to investigate the validity of this assumption is through

MultiFre quency Variability

Conclusions

- The transparency of γ-rays in pair-production does not depend on the emission mechanism
- The basic assumption is that the TeV photons are situated in the same volume with the target photons
- The only direct way to investigate the validity of this assumption is through

  MultiFrequency Variability
- Simultaneous TeV-X ray observations from the HESS Collaboration and RXTE for PKS 2155-304

Conclusions

PRELIMINARY results for the campaign of November 2003

Conclusions

PRELIMINARY results for the campaign of November 2003

XTE – HESS light curves

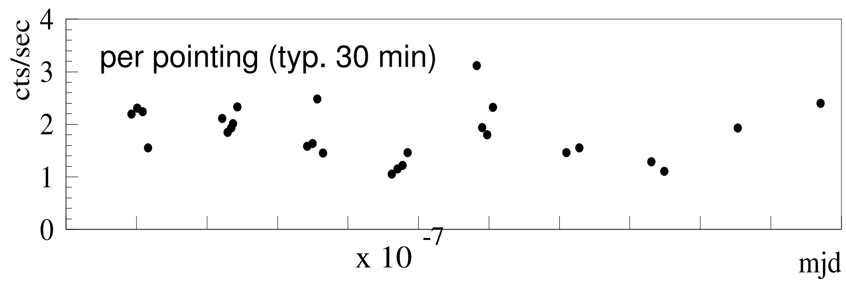

XTE light curve

2–10 keV, only one PCU

H.E.S.S. light curve

threshold at > 165 GeV

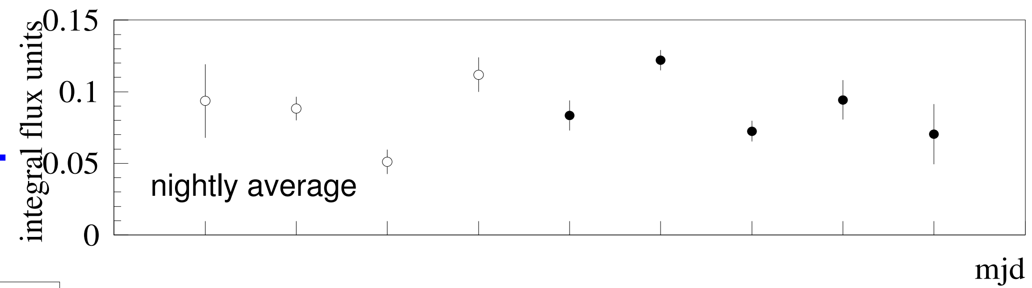

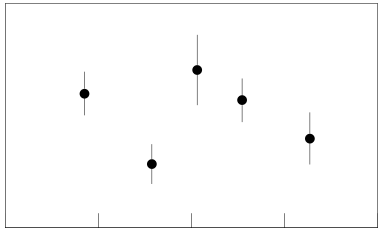

run basis (20 min)

Thank you very much for your attention!

Jet Formation from MHD Accretion Flows

José Gracia, IASA, Athens
K. Tsinganos, Univ of Athens
N. Vlahakis, Univ of Athens
A. Mastichiadis, Univ of Athens

- Why?
- What?
- How?

Why?

[nice jet/BH/disc picture here]

- jet originates from accretion flow/black hole system
- accretion flow and BH will likely imprint their signature on jet:
  - density and magnetic field variations ($\delta\rho, \delta\vec{B}$), typical timescales ($\Delta t$)
  - BH *spin*
- missing link: *jet formation region*

What?

- So far no *convincing* jet from accretion flow in the literature
  $\rightarrow$ *jet formation!*
- Do magnetic fields play a role? Which?
  - collimation: "hoop stress"? 2D versus 3D
  - acceleration: Poynting flux
  - where? from M87: $< 100 R_S$
  - topology: large scale vs turbulent
    origin?
    back currents? MRI
    stability?
- Role of BH spin?
  Blandford-Znajek process converts *rotational energy to Poynting flux*

How? Numerical Simulations

MHD eqs can be stated as:

$$\frac{\partial \vec{U}}{\partial t} + L(\vec{U}) = S$$

where $\vec{U} = (\rho, \vec{B}, \vec{v}, e)$ is the interesting physical quantity and L an operator acting on $\vec{U}$ like a derivative $\frac{\partial \vec{U}}{\partial x}$, etc.

- overlay computational domain with grid
  $\rightarrow (\rho_k, \vec{B}_k, \vec{v}_k, e_k)$
- update at discrete time intervals Δt
  $\rightarrow t^n$

How? Numerical Simulations 2

- finite differencing: replace continous derivative by discrete difference

$$\frac{\partial}{\partial x}U(x_k) = \lim_{\delta x \to 0} \frac{\Delta U(x_k)}{\delta x}$$

$$\approx \frac{U_{k+1} - U_{k-1}}{2\Delta x}$$

$$\frac{\partial}{\partial t}U(t^n) \approx \frac{U^{n+1} - U^n}{\Delta t}$$

- problems:
  initial conditions $\leftarrow$ *analytical models*
  boundary conditions $\leftarrow$ *think!*
  Δt limits $\leftarrow$ *resources*

The WEBT/ENIGMA Campaign on AO 0235+16

C.M. Raiteri, M. Villata

(INAF-Osservatorio Astronomico di Torino, Italy)

for the 0235 collaboration

The campaign started on July 1, 2003

The source showed noticeable variability, but was faint for most of the time (R > 17.5 in the optical band; F < 2 Jy in the radio band)

Last optical datum: April 7, 2004 by Tapio Pursimo $R \approx 18$

Last radio datum: April 11, 2004 by Harri Teräsranta

F = 1.84 Jy at 37 GHz

No outburst detected up to now…but we are still inside the predicted period…!

First XMM pointing

All the XMM instruments observed the source on January 18, 2004

The X-ray pointing lasted 30000 sec

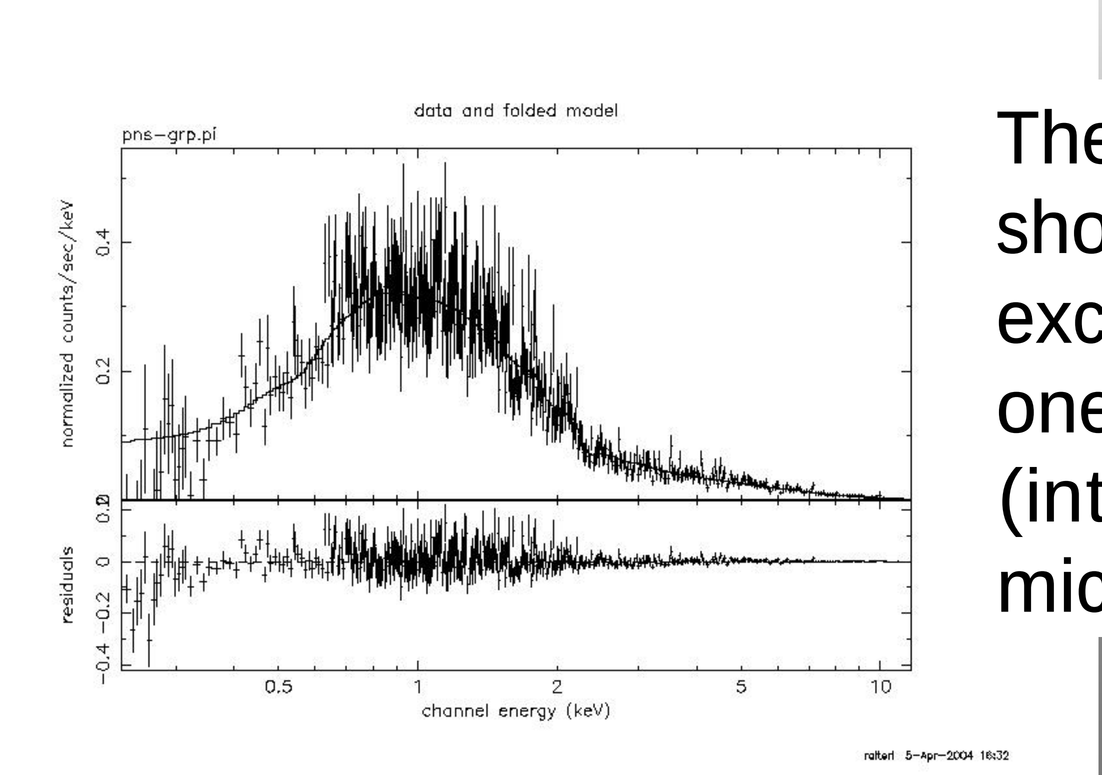

The X-ray spectrum shows absorption in excess to the Galactic one, as expected (intervening galaxy → microlensing candidate!)

First XMM pointing

The Optical Monitor was able to measure the source in the bands V B U W1

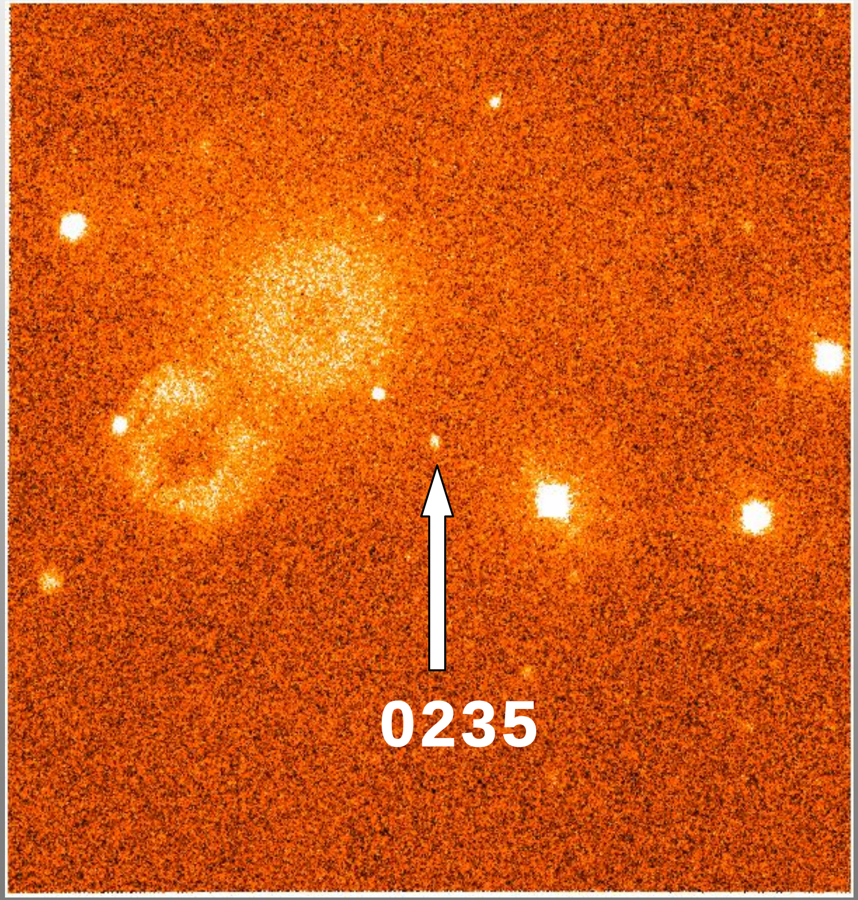

OM image of the AO 0235+16 field in the W1 band (λ=291 nm) with 5000 sec exposure time

Ground-based optical observations suffered from source faintness as well as for terrible weather in most countries!

Dense radio monitoring was possible at Effelsberg!!!

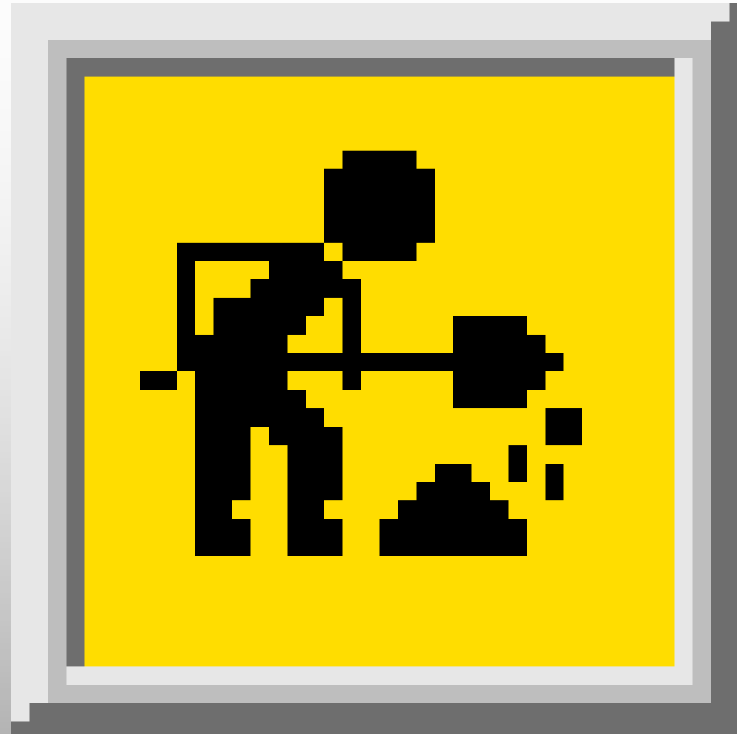

More details at the IV ENIGMA Meeting in Perugia...

The campaign restarts after solar conjunction!!!!!

Radio observations will start again in mid May

Optical observations will be possible from July

ESO-NTT spectra will be taken in August-September

TNG spectra will possibly be taken in the period August 2004-January 2005 (proposal just submitted)

VLBA observations will go on (one observation was done on January 9)

The next two XMM pointings will occur in the time windows July 30 – August 7, 2004, and January 13-21, 2005

ENIGMA CAMPAIGN ON S5 0716+71:

OVERVIEW OF OPTICAL-IR OBSERVATIONS

Luisa Ostorero(*) *& Stefan Wagner*(*)

on behalf of the 0716 optical-IR collaboration

(*)*Landessternwarte Heidelberg, Germany*

3rd ENIGMA Meeting - Jerisjärvi (Finland), April 26-28, 2004

Organization of the optical-infrared campaign

- ***INTEGRAL pointing*** **~500 ksec**

  Nov 10 – Nov 18, 2003

- ***Core campaign:*** **Nov 06 - Nov 20**

  *** BVRI observations: beginning/end of the night**

  *** BRI sequences during the night (R-only for small telescopes)**

- ***Extended campaign:*** **Oct 08 - Nov 05 ; Nov 20 - Dec 20**

  *** BVRI observations**

Unexpected events

- **Brightnening in the radio band before the INTEGRAL pointing:**

  historical maximum !

- **Brightnening in the optical band after the INTEGRAL pointing:**

  historical maximum (March 24, 2004: R=12.1) !

⇒ ***RXTE TOO:*** **1st proposal on March 25, accepted**
2 observations performed on March 27 and 28/29

Δ t ~ 5 ksec

⇒ ***INTEGRAL TOO (PI: E.Pian) :*** **April 02-06, 2004**

Δ t=280 ksec

Preliminary

Optical light curves

INTEGRAL pointing: core campaign (Nov 06-20,2003)

RXTE TOO: Mar 27, 28-29, 2004

INTEGRAL ToO: (Apr 02-06,2004)

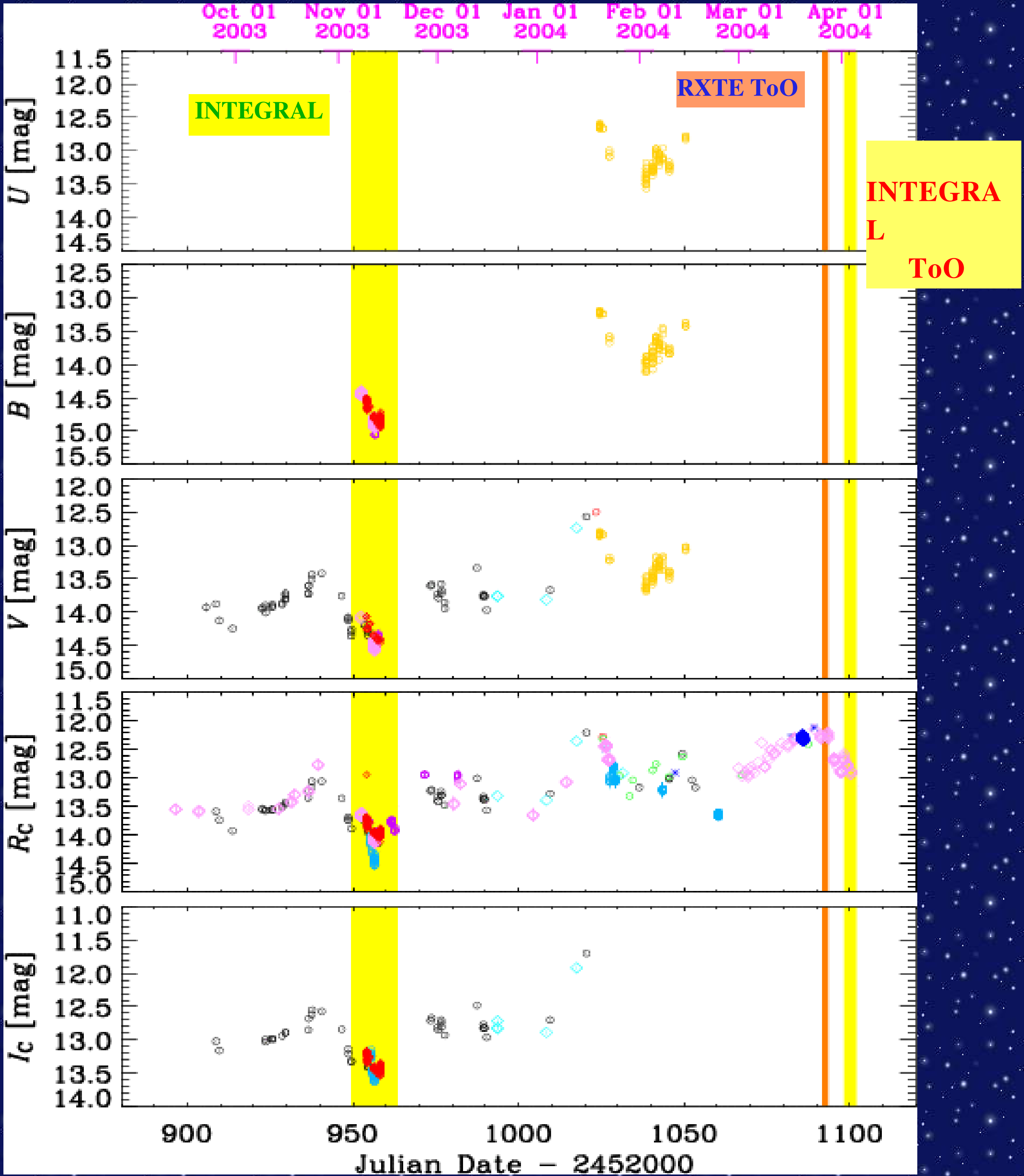

Zoom: INTEGRAL core campaign

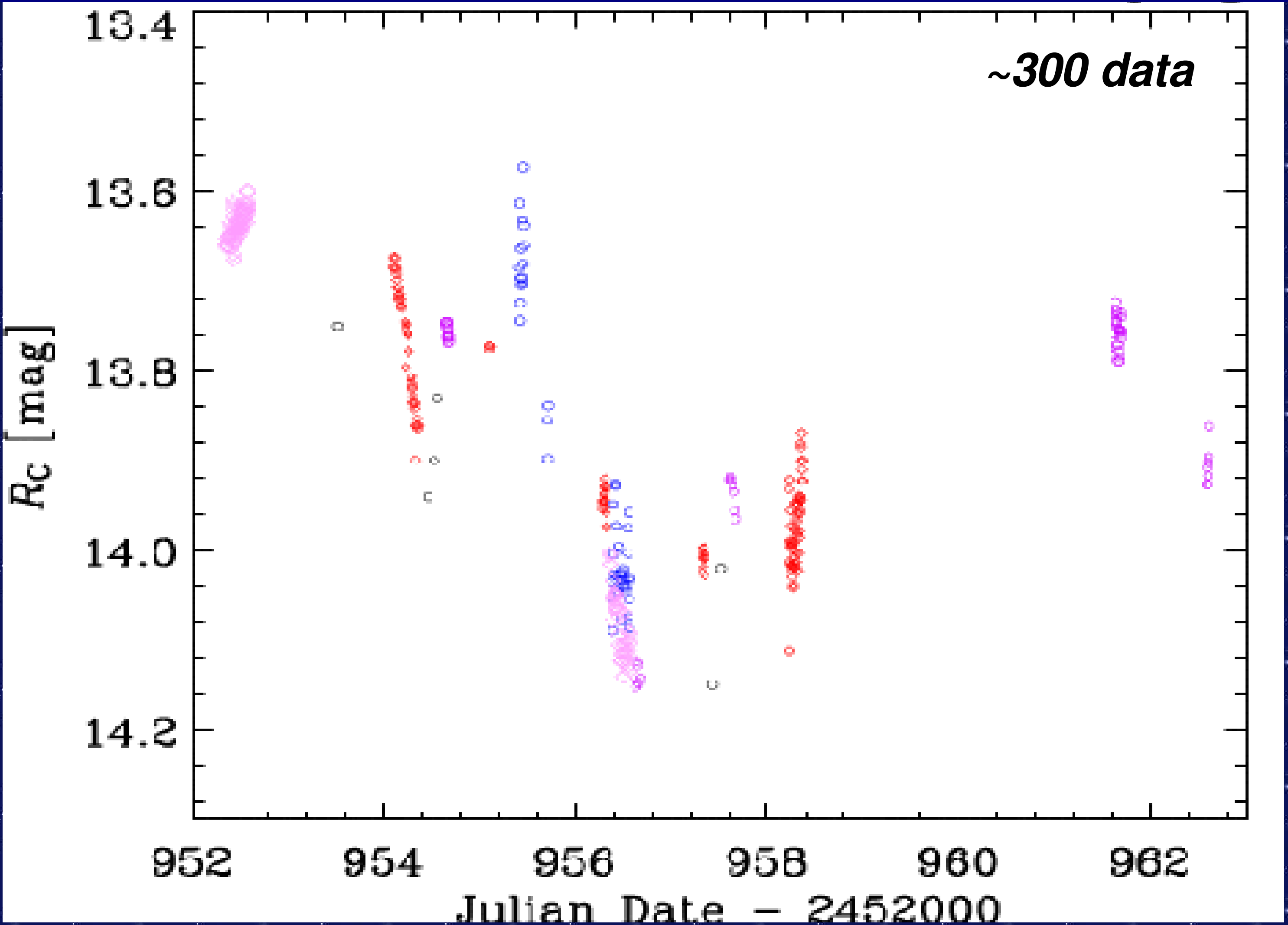

Expected >3000 Rc data points for the core campaign